



GEOSCIENCE BC SUMMARY OF ACTIVITIES 2009





GEOSCIENCE BC SUMMARY OF ACTIVITIES 2009

© 2010 by Geoscience BC.

All rights reserved. Electronic edition published 2010.

This publication is also available, free of charge, as colour digital files in Adobe Acrobat® PDF format from the Geoscience BC website: <http://www.geosciencebc.com/s/DataReleases.asp>.

Every reasonable effort is made to ensure the accuracy of the information contained in this report, but Geoscience BC does not assume any liability for errors that may occur. Source references are included in the report and users should verify critical information.

When using information from this publication in other publications or presentations, due acknowledgment should be given to Geoscience BC. The recommended reference is included on the title page of each paper. The complete volume should be referenced as follows:

Geoscience BC (2010): Geoscience BC Summary of Activities 2009; Geoscience BC, Report 2010-1, 270 p.

ISSN 1916-2960 Summary of Activities (Geoscience BC)

Cover photo: Bryan Hardel at camp near Mt. Bolton, east of Kitimat, overlooking the Kitimat River

Photo credit: Geoffrey Pignotta, 2009

Foreword

Geoscience BC is pleased to present the results of ongoing and recently completed geoscience projects and surveys in this, our third edition of the *Geoscience BC Summary of Activities*. The volume is divided into three sections, and contains a total of 25 papers, making this our largest volume so far. Industry consultants and contractors, university-based researchers and government geoscientists working on Geoscience BC-funded projects in British Columbia prepared most of the papers.

The first section contains two papers on the QUEST-South Project, Geoscience BC's major mineral exploration initiative in 2009. Like the QUEST (2007) and QUEST-West (2008) projects before it, QUEST-South combines regional geochemical surveys and reanalysis with airborne geophysics, but focuses on BC's southern interior. Results for the QUEST-South project will be released in early 2009.

The second section contains seventeen papers on mineral exploration-related partnership projects supported by Geoscience BC, including geochemical, surficial geology, mapping, mineral deposit and data compilation projects. The papers range from preliminary reports after a first field season to final reports highlighting project end results. The papers are organized roughly by project type and location to allow the reader to quickly identify papers of interest.

The third section contains six papers on hydrocarbon-related partnership projects supported by Geoscience BC. Three papers focus on central British Columbia's Nechako Basin, which has been the main focus of Geoscience BC's oil and gas program since 2005. The final three papers focus on northeastern BC, including a paper highlighting a Geoscience BC-Industry partnership initiative in the Horn River Basin.

All papers are also available on Geoscience BC's website (www.geosciencebc.com), and readers are encouraged to visit the website for additional information on all Geoscience BC projects, including project abstracts, posters and presentations, previous *Summary of Activities* or *Geological Fieldwork* articles, and final datasets.

Acknowledgments

Geoscience BC would like to thank all authors of the *Summary of Activities* papers, including project proponents, graduate students and Geoscience BC staff, for their contributions to this volume. Geoscience BC would also like to thank RnD Technical for their work in editing and assembling the volume.

Christa Sluggett, M.Sc.
Project Geologist and Communications Co-ordinator
Geoscience BC
www.geosciencebc.com

Contents

QUEST-South Projects

Simpson, K.A.: QUEST-South geophysics: new airborne gravity survey in southern British Columbia (parts of NTS 093A, B, 092H, I, O, P, 082A, E)..... 1

Jackaman, W. and Reichheld, S.A.: QUEST-South geochemical database upgrades - new survey and sample reanalysis data, southern British Columbia (NTS 082E, L, M, 092H, I, J, O, P)..... 7

Minerals Projects

Heberlein, D.R.: Comparative study of partial and selective extractions of soils over blind porphyry copper-gold mineralization at Kwanika and Mount Milligan, central British Columbia (NTS 093N/01, /19): fieldwork, soil conductivity and pH results..... 11

Bouzari, F., Hart, C., Barker, S. and Bissig, T.: Porphyry indicator minerals (PIMs): exploration for concealed deposits in south-central British Columbia (NTS 092I/06, 093A/12, 093N/01, /14) 25

Sacco, D.A., Ward, B.C., Maynard, D., Geertsema, M. and Reichheld, S.: Terrain mapping, glacial history and drift prospecting in the northwest corner of McLeod Lake map area (part of NTS 093J), central British Columbia..... 33

Ferbey, T.: Quaternary geology and till geochemistry of the Nadina River map area (NTS 093E/15), west-central British Columbia..... 43

Bissig, T., Vaca, S., Schiarizza, P. and Hart, C.: Geochemical and physical variations in the Late Triassic Nicola Arc and metallogenic implications, central British Columbia (NTS 092P, 093A, N): preliminary results..... 49

Mitchinson, D.E. and Bissig, T.: Enhancing geophysical interpretation and mineral deposit modelling through knowledge of physical rock properties: magnetic susceptibility studies for porphyry deposits in the QUEST and QUEST-West areas (NTS 93E, K, N) 53

Mortensen, J.K. and Chapman, R.: Characterization of placer- and lode-gold grains as an exploration tool in east-central British Columbia (NTS 093A, B, G, H) . . . 65

Norris, J.R., Hart, C.J.R., Tosdal, R.M. and Rees, C.: Preliminary study of the magmatic evolution, mineralization and alteration of the Red Chris copper-gold porphyry deposit, northwestern British Columbia (NTS 104H/12W) 77

Byrne, K., Tosdal, R.M. and Simpson, K.A.: Coherent and clastic rocks in the Southwest Zone alkalic porphyry copper-gold system, Galore Creek, northwestern British Columbia (NTS 104G) 87

Pignotta, G.S., Mahoney, J.B., Hardel, B.G. and Meyers, J.L.: Volcanic facies, deformation and economic mineralization in Paleozoic strata of the Terrace-Kitimat area, British Columbia (NTS 103I) 105

Smith, J.L. and Arehart, G.B.: Isotopic investigation of the Adanac porphyry molybdenum deposit in north-west British Columbia (NTS 104N/11): final project report..... 115

Höy, T.: Geology of the Deer Park map area, southeastern British Columbia (NTS 082E/08) 127

Canil, D.: Ultramafic intrusions, detailed geology and geobarometry of the Jurassic Bonanza Arc in the Port Renfrew region, southern Vancouver Island (NTS 092C)..... 141

Ruks, T., Mortensen, J.K. and Cordey, F.: New Results of Geological Mapping and Micropaleontological and Lead Isotopic Studies of Volcanogenic Massive Sulphide-Hosting Stratigraphy of the Middle and Late Paleozoic Sicker and Buttle Lake Groups on Vancouver Island, British Columbia (NTS 092B/13, 092C/16, 092E/09, /16, 092F/02, /05, /07) 149

Cadell, W.M. and Mulligan, G.: Development of a Google Earth query tool for wider dissemination of British Columbia data to the geoscience community 171

Barlow, N.D., Flower, K.E., Sweeney, S.B., Robinson, G.L. and Barlow, J.R.: QUEST and QUEST-West Property File: analysis and integration of Property File's Industry File documents with British Columbia's MINFILE (NTS 093, 094A, B, C, D, 103I)..... 175

Owsiacki, G. and Payie, G.: MINFILE update of the QUEST project area, central British Columbia (parts of NTS 093A, B, G, H, J, K, N, O, 094C, D)..... 189

Oil and Gas Projects

Hayward, N. and Calvert, A.J.: Near-surface volcanic rocks in the southeastern Nechako Basin, south-central British Columbia (parts of NTS 092N, O, 093B, C): interpretation of the Canadian Hunter seismic reflection surveys and first-arrival tomographic inversion 203

Smithyman, B.R. and Clowes, R.M.: Improved near-surface velocity models from the Nechako Basin seismic survey, south-central British Columbia (parts of NTS 093B, C, F, G), part 1: traveltimes inversions . 227

Cassidy, J.F., Kim, H., Idowu, O., Kao, H., Dosso, S., Frederiksen, A., Mercier, J-P., Bostock, M., Frassetto, A. and Zandt, G.: Passive source seismic studies of the sediments, crust and mantle beneath the Nechako Basin, south-central British Columbia (NTS 092O, 093B, C, F, G) 235

Hayes, B.J.R.: Horn River Basin aquifer characterization project, northeastern British Columbia (NTS 094I, J, O, P): progress report 245

Golding, M.L., Ferri, F., Mortensen, J.K., Zonneveld, J-P. and Orchard, M.J.: Biostratigraphic and sedimentological studies of natural gas-bearing Triassic

strata in the Halfway River map area (NTS 094/B), northeastern British Columbia: progress report 249

Henderson, C.M., Zubin-Stathopoulos, K., Dean, G., Spratt, D. and Chau, Y.P.: Tectonic history, biostratigraphy and fracture analysis of upper Paleozoic and lowest Triassic strata of east-central British Columbia (NTS 093I, O, P): preliminary report 259

QUEST-South Geophysics: New Airborne Gravity Survey in Southern British Columbia (Parts of NTS 093A, B, 092H, I, O, P, 082A, E)

K.A. Simpson, Geoscience BC, Vancouver, BC, simpson@geosciencebc.com

Simpson, K.A. (2010): QUEST-South geophysics: new airborne gravity survey in southern British Columbia (parts of NTS 093A, B, 092H, I, O, P, 082A, E); in Geoscience BC Summary of Activities 2009, Geoscience BC, Report 2010-1, p. 1–4.

Introduction

Geoscience BC's QUEST-South Project builds on the successful QUEST and QUEST-West exploration geoscience projects. The QUEST-South Project is focused on the Quesnel Terrane, south of Williams Lake, and will provide new geoscience information over an area of 130 000 km². This region of the province has been explored and mined for decades and remains one of the most actively explored and prospective areas for discovery of new Cu, Mo and Au resources in British Columbia.

Phase 1 of the QUEST-South Project includes regional geochemical surveys and a regional airborne gravity survey over an area extending south from Williams Lake to the Canada–United States border and west from Revelstoke to Pemberton (Figure 1). This paper describes the new regional airborne gravity survey undertaken in 2009. The QUEST-South regional geochemical surveys are described in Jackaman and Reichheld (2010).

Phase 2 of the project will involve adding value to the regional datasets, integrating all available data for QUEST-South area and, where necessary, the acquisition of additional new data. This phase of the project may include geophysical and geochemical modelling, deposit specific studies, data compilations, mapping and other research-oriented studies all aimed at providing industry with new geoscience information to help target their exploration efforts in this highly prospective region of BC.

Airborne Gravity Survey

The QUEST-South airborne gravity survey was undertaken by Sander Geophysics Limited using their airborne inertially referenced gravimeter (AIRGrav; Sander et al., 2004). The survey covers ~45 000 km² with a total of 25 010 line km flown. Sander Geophysics Limited used two fixed-wing aircraft to fly the survey (Figure 2). The survey was flown at 2 km line spacing in an east-west orientation

with 20 km north-south tie lines. The flights were flown at a nominal height of 200 m (above ground level) on a shallow preplanned surface smoothly draped over the topography. The survey crossed two zones, UTM zones 10 and 11, and as such the survey lines turned to accommodate the change in orientation of the UTM grid. The terrain varied from relatively flat topography in the north to mountainous in the central and southern portions of the survey (Figures 1, 3, 4).

Summary

The QUEST-South airborne gravity survey will seamlessly join with the QUEST survey in the north (Barnett and Kowalczyk, 2008; Sander Geophysics Limited, 2008). With the addition of this new QUEST-South survey, 91 000 km² covering 890 km along strike of the Quesnel Terrane has been surveyed by Geoscience BC. This provides high quality airborne gravity data to the exploration community to enhance discovery success. The QUEST-South airborne gravity data will be made available through Geoscience BC's website (<http://www.geosciencebc.com/s/DataReleases.asp>) in early 2010.

Acknowledgments

The digital elevation model in Figure 1 was prepared by K. Shimamura and F. Ma created the final figure. The manuscript benefited from reviews by P. Kowalczyk and C. Sluggott.

References

- Barnett, C.T. and Kowalczyk, P.L. (2008): Airborne electromagnetic and airborne gravity in the QUEST Project area, Williams Lake to Mackenzie, British Columbia (parts of NTS 093A, B, G, H, J, K, N, O; 094C, D); in Geoscience BC Summary of Activities 2007, Geoscience BC, Report 2008-1, p. 1–6, URL <<http://www.geosciencebc.com/s/DataReleases.asp>> [November 2009].
- Canadian Council on Geomatics (2004): Canadian digital elevation data; Natural Resources Canada, GeoBase®, URL <<http://www.geobase.ca/geobase/en/data/cded/description.html>> [October 2004].
- Jackaman, W. and Reichheld, S.A. (2010): QUEST-South geochemical database upgrades; new survey and sample reanalysis data (NTS 082E, L, M, 092H, I, J, O, P), southern British Columbia; in Geoscience BC Summary of Activities 2009, Geoscience BC, Report 2010-1, p. 5–10.

Keywords: *airborne gravity, regional geophysics, Quesnel Terrane, QUEST-South Project*

This publication is also available, free of charge, as colour digital files in Adobe Acrobat® PDF format from the Geoscience BC website: <http://www.geosciencebc.com/s/DataReleases.asp>.

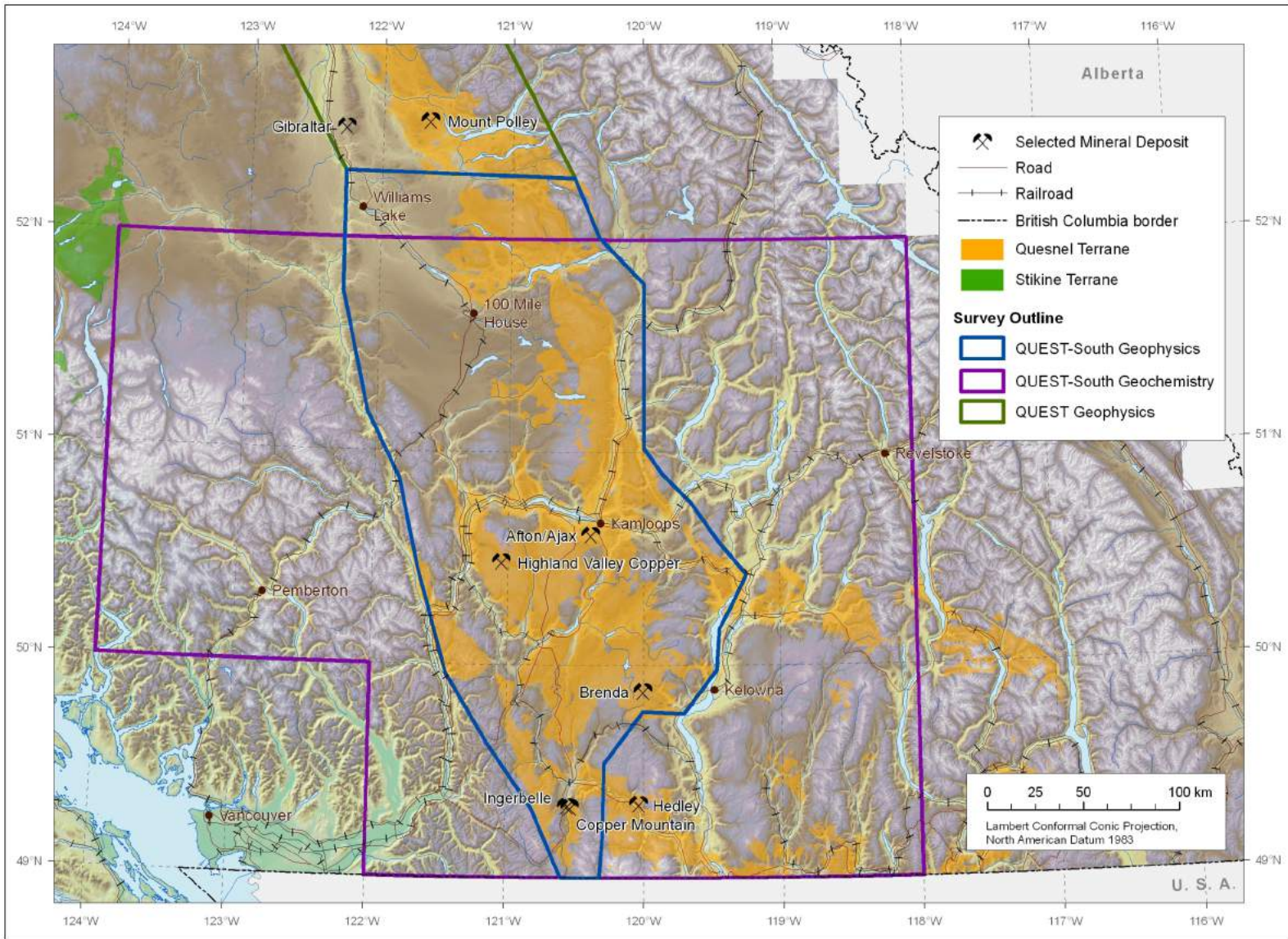


Figure 1. Location of Geoscience BC's QUEST-South geophysical and geochemical surveys. The green outline to the north shows the area of the adjoining QUEST geophysical surveys. Data from Canadian Council on Geomatics (2004), Massey et al. (2005), Natural Resources Canada (2007) and MINFILE (2009).



Figure 2. The two aircraft used in the QUEST-South airborne gravity survey, southern British Columbia, by Sander Geophysics Limited. Photo courtesy of A. MacLeary, Sander Geophysics Limited.



Figure 4. Mountainous terrain from the southern part of the survey area, southern British Columbia. Photo courtesy of G. Smith, Sander Geophysics Limited.



Figure 3. Relatively flat topography in the northern part of the survey area near 100 Mile House, southern British Columbia. Photo courtesy of G. Smith, Sander Geophysics Limited.

Massey, N.W.D., MacIntyre, D.G., Desjardins, P.J. and Cooney, R.T. (2005): Digital geology map of British Columbia: whole province; BC Ministry of Energy, Mines and Petroleum Resources, GeoFile 2005-1.

MINFILE (2009): MINFILE BC mineral deposits database; BC Ministry of Energy, Mines and Petroleum Resources, URL <<http://minfile.ca>> [November 2009].

Natural Resources Canada (2007): Atlas of Canada base maps; Natural Resources Canada, Earth Sciences Sector, URL <<http://geogratis.gc.ca/geogratis/en/option/select.do?id=138>> [November 2007].

Sander, S., Argyle, M., Elieff, S., Ferguson, S., Lavoie, V. and Sander, L. (2004): The AIRGrav airborne gravity system; Australian Society of Exploration Geophysicists–Petroleum Exploration Society of Australia, Airborne Gravity 2004 Workshop, Abstracts, URL <http://www.sgl.com/technicalpapers/AIRGrav_airborne_grav_sys.pdf> [November 2009].

Sander Geophysics Limited (2008): Airborne gravity survey, Quesnellia region, British Columbia; Geoscience BC, Report 2008-08, 121 p., URL <<http://www.geosciencebc.com/s/DataReleases.asp>> [November 2008].

QUEST-South Geochemical Database Upgrades: New Survey and Sample Reanalysis Data, Southern British Columbia (NTS 082E, L, M, 092H, I, J, O, P)

W. Jackaman, Noble Exploration Services Ltd., Sooke, BC, wjackaman@shaw.ca

S.A. Reichheld, Consultant, Sooke, BC

Jackaman, W. and Reichheld, S.A. (2010): QUEST-South geochemical database upgrades: new survey and sample reanalysis data, southern British Columbia (NTS 082E, L, M, 092H, I, J, O, P); in Geoscience BC Summary of Activities 2009, Geoscience BC, Report 2010-1, p. 5–10.

Introduction

The QUEST-South Project is the third of a series of large-scale regional geochemical studies that have been sponsored by Geoscience BC since 2007 (Figure 1). Each of these projects (QUEST, QUEST-West and QUEST-South) has included a number of important initiatives such as infill sampling and the reanalysis of archived sediment pulps. Project results have significantly improved the availability of existing geochemical data for each of the study areas and have made a major contribution of new data to the provincial geochemical dataset. Covering a total area of over 275 000 km², over 5000 drainage sediment samples have been collected and 20 000 sediment samples from previous surveys have been reanalyzed using current laboratory methods. The work not only produced a vast array of geochemical information, it also complements other geoscience initiatives, such as airborne geophysical surveys funded by Geoscience BC that are also aimed at promoting and stimulating exploration interest in the project areas.

Located in southern BC, the QUEST-South Project includes a compilation of existing data, new infill sampling and reanalysis of archived samples. Stream-based sampling and the collection of basal till samples have been conducted in order to improve overall sample site coverage of parts of the study area. In addition, reanalysis work has targeted over 9000 sediment samples that had been saved from previous surveys completed in the late 1970s and early 1980s. The availability of this new geochemical information for over 10 000 samples will represent the largest single infusion of data to the provincial geochemical database since its inception in the 1970s. Results of the work will help stimulate mineral exploration as well as complement other geoscience research and data mining activities

Keywords: mineral exploration, geochemistry, multi-element, reconnaissance, reanalysis, stream sediment, stream water, basal till, Thompson Plateau

This publication is also available, free of charge, as colour digital files in Adobe Acrobat® PDF format from the Geoscience BC website: <http://www.geosciencebc.com/s/DataReleases.asp>.

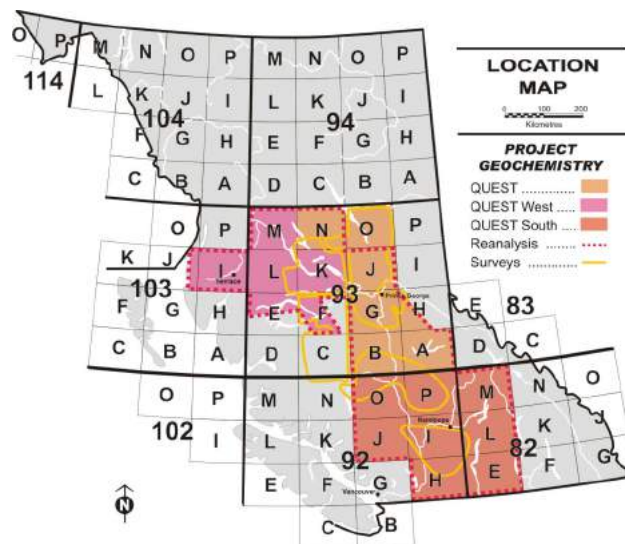


Figure 1. Location of the QUEST, QUEST-West and QUEST-South Project areas, British Columbia.

for an area that is considered to have potential for future mineral deposit discoveries.

QUEST-South Project Area

The QUEST-South Project includes NTS 1:250 000 map sheets 082E, L and M plus 092H, I, J, O and P (Figure 2). Covering over 120 000 km², the area extends south from the Fraser Plateau and contains a large part of the Thompson Plateau, the Okanagan and Shuswap highlands and parts of the Coast, Cascade and Monashee mountain ranges. Examples of several distinct physiographic features can be found in the region such as rugged mountains, heavily forested rolling hills and semi-arid grasslands. The communities of Kamloops, Merritt, Princeton, Lillooet, Kelowna and Vernon are located in the area as well as expanses of private land, cattle ranches and rangeland, Indian reserves and designated park land. Relatively recent expanded highway development, cattle farming and logging activities have increased the local road network, providing improved access to many parts of the survey area.

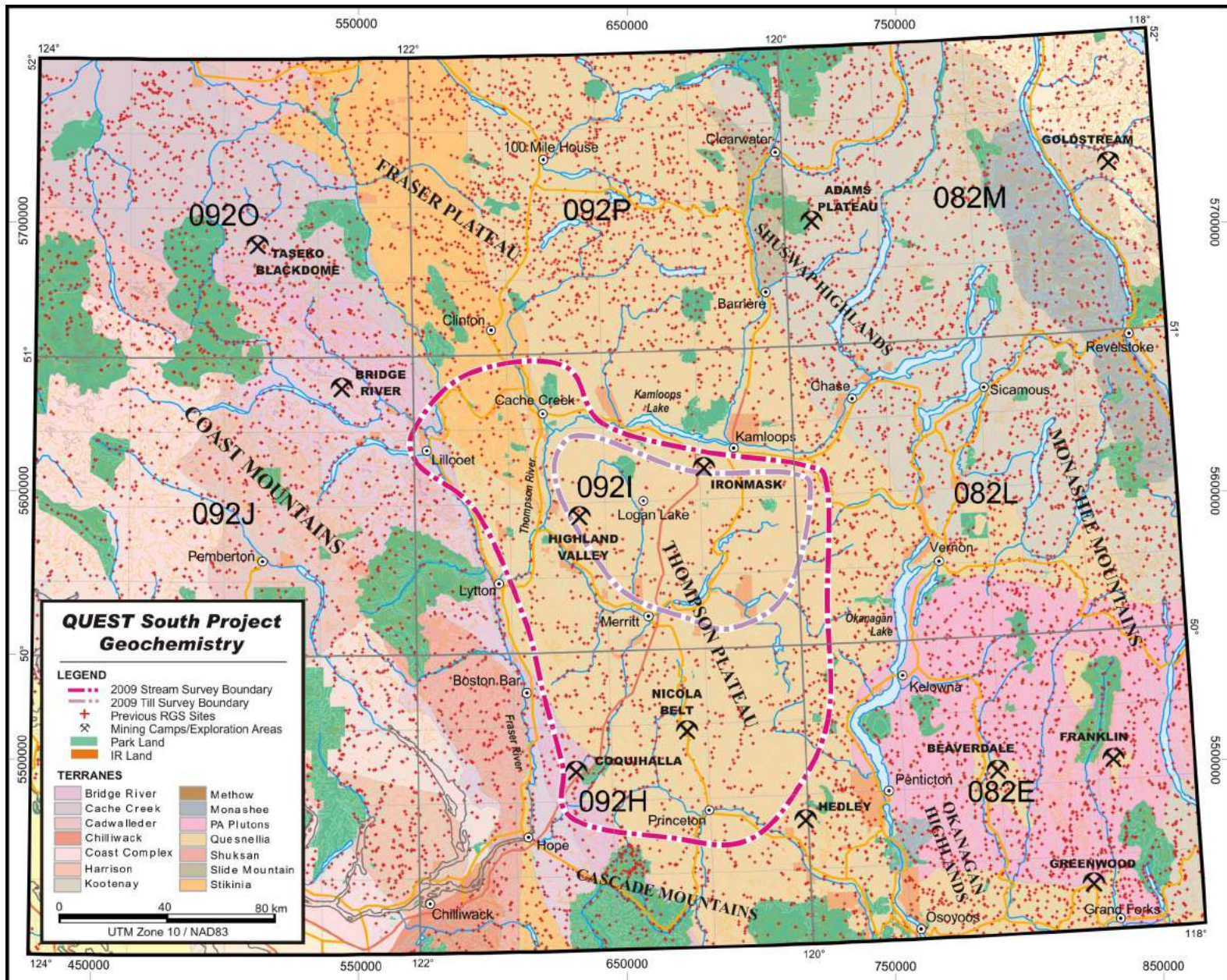


Figure 2: Detailed map of the QUEST-South study area, southern British Columbia.

The infill sampling work was contained within the boundaries of the overall project area and covers a 14 000 km² area primarily focused on the Thompson Plateau. This area is characterized by a gently rolling upland of low relief (Figure 3) that averages between 1200 and 1500 m, and in areas of more resistant rock, heights of over 1800 m are common (Holland, 1976). The higher elevations of the plateau include late Tertiary erosion surfaces that have been cut by the Thompson, Similkameen and Okanagan rivers and their tributaries. Other important hydrological features include Okanagan and Kamloops lakes.

Underlying the region are a number of prospective geological environments including the Quesnel and Stikine terranes. According to Holland (1976), the area contains a very diverse range of rocks that include stocks of granitic rock that have intruded sedimentary and volcanic formations of Paleozoic age as well as flat-lying early Tertiary lavas that blanket large areas of the older rock. The region was occupied by Pleistocene ice and a thick mantle of drift cover, and other evidence of glacial processes, can be noted throughout most of the region (Bobrowsky et al., 2002).

The region has a history of successful exploration and mining that has been influenced by a number of notable mineral deposits. Currently there are over 3200 known mineral occurrences that include several significant operating and past-producing, precious- and base-metal mines as well as prospects (MINFILE, 2009). Of the 533 listed producing and past-producing mines, the porphyry Cu±Mo±Au Highland Valley copper mine (MINFILE 092ISW012; MINFILE, 2009) is recognized as one of the largest copper mining and concentrating operations in the world and has produced more than 2.8 Mt of copper concentrate since the early 1960s.

Regional geochemical surveys were first completed in the study area in 1977, 1978, 1980 and 1982 as part of the Na-



Figure 3. Typical gently rolling topography of the Thompson Plateau region, British Columbia.

tional Geochemical Reconnaissance (NGR) and BC Regional Geochemical Survey (BCRGS) programs. The government-funded work included the collection of stream-sediment and water samples from a total of 8071 stream-based sample sites. In the early 1990s, archived sediment pulps from these surveys were reanalyzed by instrumental neutron activation analysis (INAA) and results for gold and a range of pathfinder metals and rare earth elements was added to the provincial database (Lett, 2005).

QUEST-South Sample Reanalysis

Drainage sediment pulps from previous government-funded surveys completed in the study area are currently stored at facilities in Ottawa, ON, and maintained by Natural Resources Canada (NRCAN). Samples are stored in plastic vials organized by NTS map sheet designation and in order of sample identification numbers. Opportunely, the archive also includes original analytical duplicate and control reference samples that can be used to monitor and assess the accuracy and precision of any subsequent analytical work. On average, up to 30 g of the -80 mesh (180 µm) sediment fraction is available, but in some cases samples may be missing or there is insufficient material remaining in the storage vials.

After obtaining permission to access the archive from NRCAN, sample materials from the QUEST-South study area were retrieved in May 2009. A 1–2 g portion of each sediment sample was carefully extracted from storage containers (Figure 4). Material from each vial was independently split and transferred to a Ziploc® bag labelled with the sample's original unique identification number. Once secured for shipping, the recovered material was delivered to ALS Chemex (North Vancouver, BC). At the lab, each sample was analyzed for 37 elements by inductively coupled plasma–mass spectrometry (ICP-MS) using an aqua-regia digestion. A complete list of the elements and associated detection levels are provided in Table 1.



Figure 4. Sample recovery of sediment pulps from archive storage facility in Ottawa, Ontario.

Table 1. List of elements and associated detection levels from inductively coupled plasma–mass spectrometry (ICP-MS) analysis using an aqua–regia digestion, QUEST-South Project areas.

Element	Detection levels	Units
Aluminum	0.01 to 25	%
Antimony	0.02 to 10 000	ppm
Arsenic	0.1 to 10 000	ppm
Barium	0.5 to 10 000	ppm
Bismuth	0.01 to 10 000	ppm
Boron	10 to 10 000	ppm
Cadmium	0.01 to 2000	ppm
Calcium	0.01 to 40	%
Chromium	0.5 to 10 000	ppm
Cobalt	0.1 to 10 000	ppm
Copper	0.01 to 10 000	ppm
Gallium	0.05 to 10 000	ppm
Gold	0.2 to 100	ppb
Iron	0.01 to 50	%
Lanthanum	0.2 to 10 000	ppm
Lead	0.01 to 10 000	ppm
Magnesium	0.01 to 30	%
Manganese	1 to 50 000	ppm
Mercury	5 to 100	ppb
Molybdenum	0.01 to 10 000	ppm
Nickel	0.1 to 10 000	ppm
Phosphorus	0.001 to 5	%
Potassium	0.01 to 10	%
Scandium	0.1 to 10 000	ppm
Selenium	0.1 to 1000	ppm
Silver	2 to 100	ppb
Sodium	0.001 to 10	%
Strontium	0.2 to 10 000	ppm
Sulphur	0.01 to 10	%
Tellurium	0.01 to 500	ppm
Thalium	0.02 to 10 000	ppm
Thorium	0.1 to 10 000	ppm
Titanium	0.001 to 10	%
Tungsten	0.05 to 10 000	ppm
Uranium	0.05 to 10 000	ppm
Vanadium	1 to 10 000	ppm
Zinc	0.1 to 10 000	ppm

QUEST-South Infill Stream Drainage and Till Surveys

The 2009 QUEST-South infill sampling program covered approximately 14 000 km² and focused on a region that had received relatively limited coverage during earlier geochemical surveys (Figure 2). In parts of the study area, original sample site density was found to be less than one site per 20 km². To address this deficiency, the target survey area offered many opportunities to access new stream sample sites (Figure 5) and basal till sites (Figure 6).

Adhering to standards outlined by Ballantyne (1991) and used by the NGR and BCRGS programs, truck-supported stream-based sample collection was carried out from June to September 2009. A total of 800 stream-sediment and water samples were systematically acquired. The samples were collected from the active stream channel of first and second order drainages not previously sampled and from original sites where archived material was found to be missing. Field observations regarding location, sample information and site characteristics were recorded for each site. In addition, to assist follow-up activities, a tag was placed at each sample site that identified the project and unique sample site number.

To further augment the geochemical coverage of parts of the study area, basal till samples were also collected from 200 sites at an average density of one site per 4 km² over a 1000 km² area. Consideration of this sample media was motivated by orientation studies completed in the region by Bobrowsky et al. (2002), which concluded that the combi-



Figure 5. A typical second order stream, southern British Columbia.



Figure 6. A typical roadcut basal till sample site, southern British Columbia.

nation of basal till availability, a relatively thin overburden cover and a uniform ice-flow direction provided for an ideal sampling environment for reconnaissance-scale till geochemistry exploration programs.

In general, the collection of basal till samples was based on procedures developed during previous British Columbia Geological Survey (BCGS) and Geological Survey of Canada till programs conducted in the Canadian Cordillera (Levson, 2001). As part of this previous work, detailed surficial geological mapping and studies of ice-flow history are often conducted prior to the sampling program. Designed to provide preliminary and timely geochemical information for the study area, it was decided to forgo detailed Quaternary studies and proceed with the regional sampling of basal till as a complement to stream-based work as well as promoting the use of this sampling technique. It is strongly suggested that more comprehensive Quaternary research should be completed in order to properly interpret resulting till geochemical data.

Estwing Geo/Paleo Picks™ were used to expose undisturbed basal till material identified at roadcut exposures. The target material typically consisted of dense, matrix-supported, silt- and clay-rich, dark grey to brown diamicton with subrounded to subangular clasts. At each site, approximately 3 kg of the basal till material was collected at an average depth of 1.0 m. Field data was recorded on BCGS field data forms and a tag was placed at each sample site that identified the project and unique sample site number.

At Eco Tech Laboratory Limited (Kamloops, BC) the dried stream-sediment samples were sieved to –80 mesh (<177 µm) and basal till samples were sieved to –230 mesh (<62.5 µm). To monitor and assess accuracy and precision of analytical results, control reference material, analytical duplicate and field duplicate samples were included in each block of 20 samples. The sample pulps will be analyzed for base and precious metals, pathfinder elements and rare earth elements by ICP-MS and INAA. Loss-on-ignition and fluorine content will also be determined for stream and till material. Fluoride content, conductivity and pH will be determined for the raw streamwater samples.

Data Release

Results of the reanalysis work are scheduled to be released to the public in January 2010 and the new infill survey results will be published in the late spring 2010. Prior to the release, project data will be carefully checked for analytical quality using inserted blind duplicate samples and control reference material. When the information is determined to be complete and accurate, the reanalysis data will be digitally merged with sample site location information, analytical results and field observations from the original survey's digital data reports and the new infill analytical data will be

compiled with its associated field information. The release packages will be made available from the Geoscience BC and BCGS websites and will include detailed descriptions of the work. The survey data will be distributed in a variety of digital formats. Project results will outline a number of exploration opportunities including prospective regional trends as well as individual sample anomalies. In combination with other geoscience information, careful assessments of the data will generate increased mineral tenure acquisition and encourage more detailed follow-up investigations.

Project Summary

Adding value to the BC geochemical database has been one of the primary objectives of Geoscience BC's QUEST initiatives and other geochemical survey work. Since 2005, this has been successfully accomplished with the reanalysis of over 20 000 archived sediment pulps, 8800 new drainage sediment and water samples and in excess of 1000 till samples. This compilation of high quality, publically available geochemical information has infused a vast range of new multi-element data into the existing collection.

Recognized as a valuable exploration tool, the ongoing development of the database from a relatively limited analytical suite of elements has been accomplished utilizing a strong adherence to national standards combined with an interest by government agencies to produce and maintain a consistent and up-to-date exploration resource. Although the database remains a work in progress, its current condition is impressive. The collection currently includes close to 70 000 regionally distributed samples, covers close to 70% of BC and sample sites are attributed with up to 70 analytes. Information extracted from the database continues to complement exploration activities and has been successfully used to discover mineral prospects, re-evaluate previously explored regions and investigate newly identified prospective areas.

Acknowledgments

The authors acknowledge M. McCurdy, P. Friske and J. Pinard of NRCan and R. Lett and D. Lefebure of the BCGS for their assistance with the reanalysis work; E. Jackaman, S. Webb, J. Dimock and R. Grainger for their contributions to the field program; T. Ferbey of the BCGS for his insights into basal till sampling; and the many services located in the communities of Merritt, Princeton, Ashcroft and Lytton. This project is being funded by Geoscience BC.

References

- Ballantyne, S.B. (1991): Stream geochemistry in the Canadian Cordillera: conventional and future applications for exploration; *in* Exploration Geochemistry Workshop, Geological Survey of Canada, Open File 2390, p. 6.1–6.7.

- Bobrowsky, P.T., Cathro, M.S. and Paulen, R.C. (2002): Quaternary geology reconnaissance studies (0921/02 and 07), southern British Columbia; *in* Geological Fieldwork 2001, BC Ministry of Energy, Mines and Petroleum Resources, Paper 2002-1, p. 397–401.
- Holland, S.S. (1976): Landforms of British Columbia: a physiographic outline; BC Ministry of Energy, Mines and Petroleum Resources, Bulletin 48, 138 p.
- Lett, R.E.W. (2005): Regional Geochemical Survey database on CD; BC Ministry of Energy, Mines and Petroleum Resources, GeoFile 2005-17, CD-ROM.
- Levson, V.M. (2001): Regional till geochemical surveys in the Canadian Cordillera: sample media, methods and anomaly evaluation; *in* Drift Exploration in Glaciated Terrain, M.B. McClenaghan, P.T. Bobrowsky, G.E.M. Hall and S.J. Cook (ed.), Geological Society, London, Special Publications 2001, v. 185, p. 45–68.
- MINFILE (2009): MINFILE BC mineral deposits database; BC Ministry of Energy, Mines and Petroleum Resources, URL <<http://minfile.ca>> [November 2009].

Comparative Study of Partial and Selective Extractions of Soils over Blind Porphyry Copper-Gold Mineralization at Kwanika and Mount Milligan, Central British Columbia (NTS 093N/01, /19): Fieldwork, Soil Conductivity and pH Results

D.R. Heberlein, Heberlein Geoconsulting, North Vancouver, BC, dave@hebgeoconsulting.com

Heberlein, D.R. (2010): Comparative study of partial and selective extractions of soils over blind porphyry copper-gold mineralization at Kwanika and Mount Milligan, central British Columbia (NTS 093N/01, 19): fieldwork, soil conductivity and pH results; *in* Geoscience BC Summary of Activities 2009, Geoscience BC, Report 2010-1, p. 11–24.

Introduction

Exploration geochemistry in British Columbia has up to now relied on traditional methods, such as stream sediment and soil geochemistry, to detect metals dispersed mechanically and hydromorphically from outcropping sources. These methods have proven to be highly effective and there has been a long and impressive history of discoveries using them. As exploration maturity increases, however, mining companies are faced with the challenge of exploring more and more in areas of transported cover where traditional geochemical methods are less effective. Much of the central interior of British Columbia is covered by an extensive blanket of glacially derived sediments that completely masks the underlying bedrock. In order to deal with this cover, government, industry and academic institutions have invested heavily in developing airborne and ground geophysical methods to see through the exotic overburden. Unfortunately, geochemical exploration has not evolved as rapidly, despite the availability of a wide range of partial and selective extractions provided by the commercial laboratories. Reasons for this are varied and range from a general lack of understanding by the exploration community of the use and interpretation of these methods to scepticism about their effectiveness. It is only through well documented, nonbiased, comparative field testing of these methods that the exploration community can gain the knowledge and confidence to apply deep-penetrating geochemistry (DPG) to routine exploration programs.

There are relatively few examples of comprehensive comparative studies of DPG methods in BC. Cook and Dunn (2007) evaluated a number of partial leach methods over the 3T's epithermal Au-Ag prospect. They showed that B-horizon soils were more suitable than C-horizon tills for detailed geochemical sampling. Of the methods tested, they

concluded that Mobile Metal Ion (MMI[®]) and Enzyme LeachSM produced superior contrast responses to conventional aqua-regia digestion, although the latter method did detect mineralization in areas of thin cover. Lett and Sandwith (2008) carried out soil orientation surveys to test the effectiveness of a variety of selective and partial extraction methods at the Mouse Mountain, Shilo Lake and Soda Creek properties in the area of the cities of Quesnel and Williams Lake. Their study found that the most anomalous Cu and Au values, reflecting blind Cu-Au mineralization, occur in the C and lower B horizons with an aqua-regia digestion. A discussion of the performance of the various partial and selective extraction methods is still in preparation at the time of writing.

Outside of BC, there have been a number of important studies of DPG in a variety of climatic and physiographic environments. Perhaps the landmark study has been the Deep Penetrating Geochemistry Project, carried out by the Canadian Mining Industry Research Organization (CAMIRO). This study was funded by 26 mining companies, the Ontario Geological Survey and Geological Survey of Canada. Phase I considered movements of elements and ions from buried mineral deposits and nuclear waste facilities in arid and semi-arid environments. It showed that metals and ions can be transported to the surface by advective transport in gases and ground waters (Cameron, 1998; Cameron et al., 2002) and can be effectively detected by partial-extraction methods. In Phase II, a variety of test sites in arid, semi-arid and temperate boreal forest environments were studied. It was found that in all environments partial- and selective-extraction anomalies were detected in soils above buried mineralization (Cameron et al., 2004) and in some cases through appreciable thickness of complex transported cover.

The current study builds upon these important contributions by examining the effectiveness of a variety of partial and selective extractions over two blind porphyry Cu-Au deposits in north-central BC: the Central zone at Kwanika and the MBX-66 zone area at Mount Milligan (Figure 1). Both of these deposits subcrop beneath Quaternary glacial outwash deposits and at least part of the Kwanika Central

Keywords: *deep-penetrating geochemistry, Kwanika, Mount Milligan, copper-gold porphyry, soils, partial extraction, selective extraction, soil pH, conductivity*

This publication is also available, free of charge, as colour digital files in Adobe Acrobat[®] PDF format from the Geoscience BC website: <http://www.geosciencebc.com/s/DataReleases.asp>.



Figure 1. Location of study areas, central British Columbia.

zone lies beneath a post-mineral sedimentary basin. Kwanika is the site of a relatively pristine pine and spruce forest environment while at Mount Milligan the surface has been heavily disturbed by clear-cut logging and drilling activities. These contrasting environments provide a good test for the different methods.

This report documents fieldwork carried out at Kwanika and Mount Milligan projects between August 10 and 21, 2009. It also examines the preliminary results of soil pH and conductivity tests on soil samples from both projects. Results from partial and selective extractions will be the subject of a subsequent report as the analytical results are pending at the time of writing.

This project is funded by Geoscience BC and carried out by the author in partnership with Activation Laboratories Ltd., Acme Analytical Laboratories Ltd., ALS Chemex and SGS Mineral Services.

Benefits to the Mining Industry

Independent, nonbiased studies of commercially available partial and selective extractions are few and far between, particularly in BC. These studies are important as they provide the exploration community with valuable insight into the appropriate sampling strategy and combination of analytical methods for a given environment. Without this type of study, the exploration geologist must rely on information provided by the commercial laboratories, who promote their own methods to see through transported cover. Without knowledge of the relative performance of these methods in different cover environments and for different deposit types, the exploration geologist could choose an inappropriate method on the basis of a laboratory's market-

ing rather than on sound scientific knowledge. This could be an expensive mistake. While all of the methods tested in this study have their merits, it is important to recognize that none of them can be used blindly in all environments. One size does not fit all. This study and others that have preceded it (Cook and Dunn, 2007; Lett and Sandwith, 2008) provide the exploration geologist with the knowledge and tools necessary to make an informed decision and therefore to maximize the benefit of their investment in geochemistry.

Another benefit of this type of study is that it gives mining companies a set of exploration tools and knowledge that helps improve their success rate for exploration projects in covered areas. Deep-penetrating geochemical methods can be used to effectively prioritize drillhole locations to test geophysical targets. Geochemical data can provide an additional layer of information to help discriminate potentially mineralized and barren targets. This reduces drilling risk and protects shareholder value.

Study Areas

Kwanika (Serengeti Resources Inc.)

The Kwanika project is situated in the Omineca Mining Division, approximately 140 km northwest of Fort St. James (55°30'N, 125°18'W; Figure 1). It is accessible by well-maintained Forest Service roads from Fort St. James via the community of Takla Landing. Serengeti Resources Inc., the owner, holds the title to 28 contiguous mineral claims covering an area of 8960 ha (Rennie and Scott, 2009).

The Kwanika Central zone is one of two mineralized centres located at the northern end of the Kwanika property. Together with the Southern zone, it forms a linear, north-trending, Cu-Au porphyry system hosted in several small monzonite intrusions along the western margin of the multiphase Hogem batholith (Rennie and Scott, 2009). Monzonite intrudes diorite, quartz monzonite and granite of the Hogem batholith as well as andesitic volcanic rocks of the Upper Triassic Takla Group. Intrusive and volcanic hostrocks are truncated to the west by the Pinchi fault: a major terrain boundary juxtaposing Cache Creek Terrane rocks to the west.

Mineralization at the Central zone is associated with a strong core of intense, texturally destructive albite alteration associated with a variable multiphase stockwork of quartz veinlets. Surrounding the albitic core is a broad zone of weak to strong, pervasive and fracture-controlled potassic alteration characterized by K-feldspar and secondary biotite (Rennie and Scott, 2009). This alteration grades laterally into propylitic assemblages. Dominant sulphide minerals include pyrite, which is ubiquitous to the deposit, chalcopyrite and bornite. Molybdenite is also commonly present. Supergene enrichment consisting of an upper ox-

ide zone with native copper and a lower sulphide zone with secondary chalcocite occurs on the upper surface of the hypogene mineralization beneath a package of younger conglomerate and sandstone that buries the mineralization to the west. These sedimentary rocks are interpreted to be part of a younger sedimentary basin formed against the Pinchi fault. The eastern part of the deposit subcrops beneath the Quaternary cover.

Surficial Environment

The Kwanika Central zone lies in a broad, flat-bottomed valley containing an extensive cover of glacial till and outwash sediments. Local elevations range from 900 to 1200 m but in the study area itself there is only 40 m of relief. Drilling has shown that the cover varies in thickness from a few metres to over 50 m thick in the immediate deposit area (D. Moore, pers. comm., 2009). Outcrops are rare and only seen in the bottom of the Kwanika Creek valley, which is deeply incised into the Quaternary sequence (Rennie and Scott, 2009). Away from the river valley, the surface is well drained with gently sloping topography. The area is forested with a mixture of lodgepole pine and white spruce as dominant species.

Three types of soil profile are present in the Central zone area. These are for the most part developed on a parent material of cobble-rich sand and gravel. Podzols (Orthic Ferro-Humic; soil nomenclature based on the Canadian System of Soil Classification [Canada Soil Survey Committee, Subcommittee on Soil Classification, 1978]) are the most widespread soil type, occurring on well drained, gen-

tle slopes within the pine and spruce forest. A typical profile (Figure 2) includes a thin LFH horizon consisting of partially decomposed wood, twigs, needles and mosses and a thin (<1 cm) black to dark brown, organic-rich Ah horizon. The organic-rich layers overlie a distinct white to grey or pinkish, sandy textured Ae or Ae_j horizon of variable thickness. Below this, the B horizon is made up of an upper B_f horizon (upper B), enriched with iron oxide, and a lower, medium to chocolate brown, B_c horizon (lower B), which grades into medium to dark grey sand or gravel of the C horizon. Brunisols, the second soil type, are common at the base of slopes that are adjacent to boggy areas (Figure 3). A typical example has a surficial LFH and Ah horizon up to 4 cm thick overlying an undifferentiated olive-brown B_m horizon. The third soil type is represented by Organic soils. These occur in depressions and boggy areas (Figure 4). Profiles consist of an upper thick, peaty O_m horizon that can be tens of centimetres thick, overlying a lower grey or blue-grey C horizon. A mottled B_g horizon was noted at one locality. In all cases, the lower part of the profile is water saturated.

Mount Milligan (Terrane Metals Corp.)

Mount Milligan lies about 100 km east-southeast of Kwanika. It is situated in the Omineca Mining Division, approximately 155 km northwest of Prince George and 95 km west of Mackenzie (55°7.35'N, 124°1.50'W; Figure 1). The principal access is by all-weather Forest Service roads from Mackenzie or by a longer and less maintained logging road from Fort St. James. The property, which is owned by



Figure 2. Typical Podzol profile from the Kwanika Central zone, British Columbia.

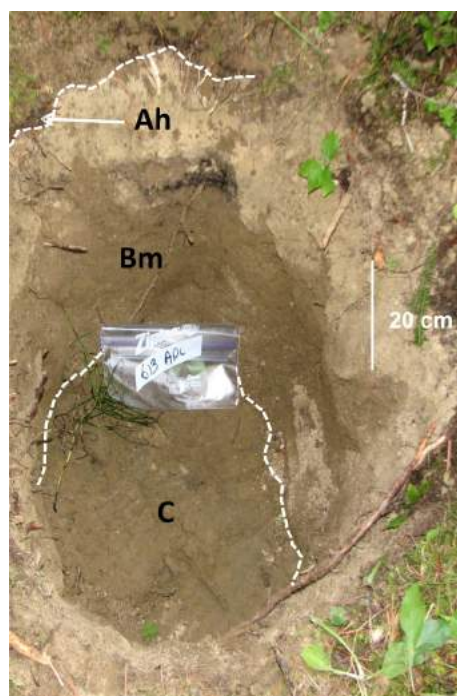


Figure 3. Brunisol from the Kwanika Central zone area, British Columbia.



Figure 4. Organic soil from the Kwanika Central zone area, British Columbia.

Terrane Metals Corp., includes 80 contiguous mineral claims that cover Upper Triassic Takla Group volcanic rocks and associated intrusions that form part of the highly prospective Quesnel Terrane.

There are three known porphyry Cu-Au deposits on the property: the MBX, 66 zone and Southern Star, which together constitute a resource (measured and indicated) of 590.8 million tonnes at 0.193% Cu and 0.352 g/t Au (Mills, 2008). The deposits are classified as belonging to the alkalic suite of porphyry deposits (Panteleyev, 1995). The principal mineralized body is the MBX–66 zone, which lies along the footwall of the west-dipping MBX stock and along the crosscutting Rainbow dike (Figure 5). The gold-dominant 66 zone is distinguished from MBX by higher Au:Cu ratios but, for all intents and purposes, the two deposits are part of a single mineralized system, which is the subject of this study.

Hypogene mineralization at MBX is dominated by chalcocite with lesser bornite and magnetite, associated with intense potassic alteration in the footwall of the stock and adjacent volcanic rocks. In contrast, mineralization at the gold-rich 66 zone occurs with intense albitization and abundant pyrite (Mills, 2008).

Surficial Environment

The MBX and 66 zone lie on the eastern slopes of a northwest-trending ridge of hills, which rises 300–500 m above the elevation of the surrounding plains. The highest point at 1508 m is the summit of Mount Milligan itself, which lies at the northwestern end of the ridge. Drainage patterns along the ridge are dendritic, becoming anastomosing on the surrounding plains where glacially fed, short, meandering streams connect pothole lakes, ponds and swamps (Gravel and Sibbick, 1991). In the vicinity of the mineral deposits, the ridge is divided by a steeply incised east-west valley occupied by Heidi lake, which drains east into King Richard creek (Figure 5).

Quaternary geology mapping by Kerr and Bobrowsky (1991) and Ricker (1991) identified a variety of surficial sediments in the study area (Figure 5). Colluvium derived from tills and bedrock dominates the flanks of the hills to the north and west of the MBX–66 zone area.

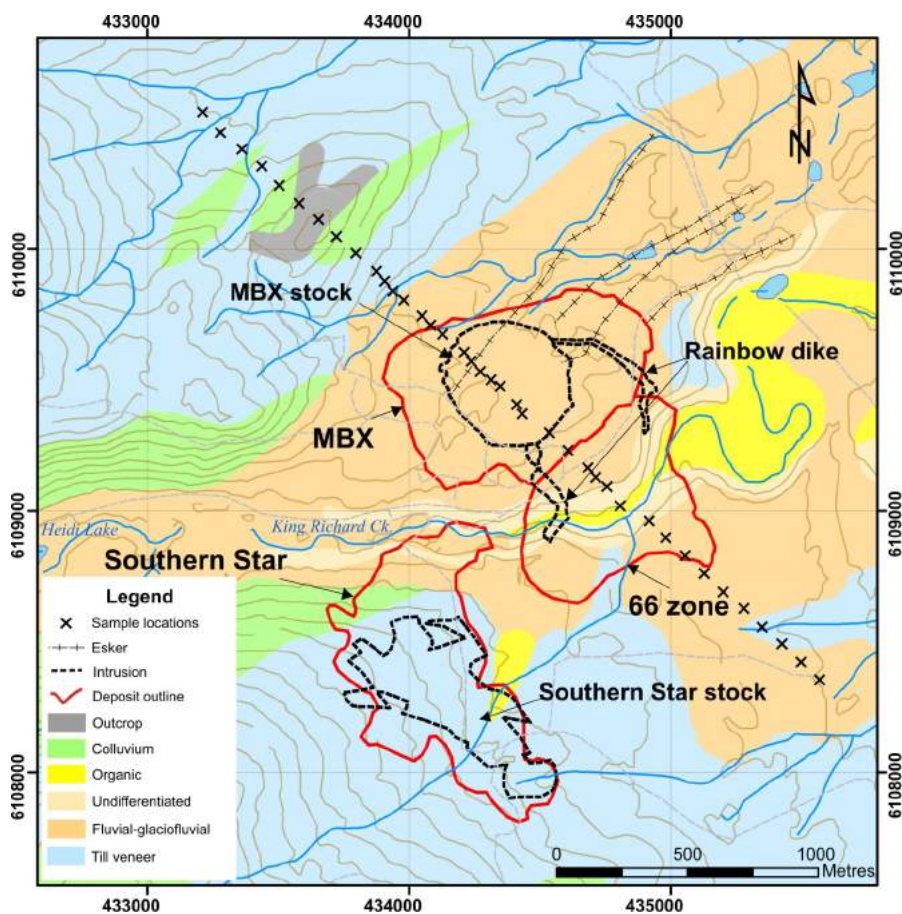


Figure 5. Mount Milligan, study area, British Columbia: sample transect, surficial geology and mineralized intrusions (modified after Ricker, 1991).

Away from the hills, the landscape is blanketed by a veneer of glacial till, which is overlain by a highly variable and complex sequence of glaciofluvial sand and gravel containing cobble- and boulder-rich layers. These deposits form a fan-like feature originating at Heidi lake and spreading out over the MBX-66 zone area to the east (Figure 5). Drilling has shown that the cover thickness is extremely variable, suggesting significant paleotopographic relief (Kerr and Bobrowsky, 1991).

Soils developed on the glaciofluvial deposits are dominantly Orthic Humo-Ferric Podzols. They typically have a thin organic layer made up of a 1–2 cm thick LFH horizon composed of partially decomposed twigs, needles and moss, which overlies a thin, poorly developed, Ah horizon of irregular thickness (0.5–2 cm). The organic-rich layers sit on top of a sandy textured, white, grey or pinkish eluviated Ae horizon or Ae_j horizon (a thin, discontinuous or barely discernible eluviated [Ae] horizon), which may vary from absent to over 10 cm in thickness. A strongly illuviated, red-orange, iron-rich Bf horizon is commonly found beneath the Ae horizon and in some places exceeds 15 cm in thickness. This horizon tends to have a fine silty texture. Bf horizon grades downwards over a few centimetres into a medium to olive brown Bm (an undifferentiated, uniform-coloured B horizon) or transitional BC horizon. Depth to the C horizon may vary from 25 cm over colluvium to 70 cm over sand and gravel. A typical Podzol profile is illustrated in Figure 6.

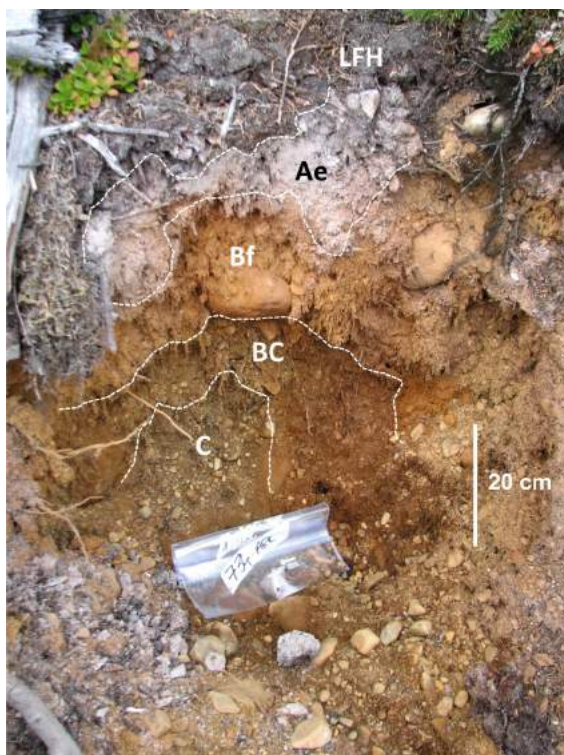


Figure 6. Typical Podzol profile developed on glaciofluvial sediments, Mount Milligan, British Columbia.

Widespread surface disturbance from drill access roads, drill pads and logging activities has resulted in either complete destruction or burial of the original soil profile over large parts of the MBX-66 zone area. Site selection for soil sampling is therefore very important. Where possible, remnant patches of the original surface were identified by the presence of original tree species (white spruce or lodgepole pine). In areas where the profile has been buried, holes were excavated to the original surface or moved to the closest possible location where the original profile is preserved.

As much of the area was clear-cut logged in the 1980s, original tree species are restricted to small enclaves between disturbed areas, water courses or steep slopes. White spruce and lodgepole pine are the dominant species on the well drained flats east of Heidi lake. In the creek valleys, black spruce, balsam poplar and trembling aspen are common. In the clear-cut areas, vegetation is dominated by pioneer shrub species like mountain alder and willow, which form dense thickets between the drill roads.

Sampling and Analyses

There has been much debate in the literature about the appropriate sampling strategy for partial- and selective-extraction geochemistry. Bradshaw et al. (1974) pointed out that “the depth of sampling during a soil program may be very critical as variations with depth can be greater than a factor of 10 within six inches”. A fixed depth interval (10–25 cm below the top of the mineral soil [Mann et al., 1998]), regardless of soil horizon, is recommended by SGS Mineral Services, the purveyor of the MMI leach. Their empirical observations from numerous field studies suggest that the zone of ion accumulation in the soil is a result of equilibrium between capillary rise and evaporation drawing ions upwards and downward leaching by percolating rainwater. Hamilton et al. (2007) conclude that consistent sampling is absolutely necessary for successful selective-extraction geochemical surveys and recommend a strategy of sampling between depths of 10 and 25 cm in mineral soil and below 30 cm in thick organic soil or peat.

Traditional soil sampling in BC has almost exclusively used the –80 mesh fraction of the B horizon. B horizon has been a favoured sampling medium because of the common presence of an illuviated iron- and manganese-oxide-rich Bf horizon that contains elevated metal contents compared to the other parts of the profile (Bradshaw, 1975; Levinson, 1974). It has proven to be an effective sampling medium in residual soil environments.

This study aims to test both the constant depth sampling strategy, with MMI extraction of upper B-horizon soils, as well as horizon-based sampling. Uniform soil profile development over much of the study area means that the upper B horizon occurs at a more or less consistent depth of be-

tween 5 and 15 cm. Upper B horizon samples were collected consistently from this interval.

Sample locations were accurately located using a Garmin GPSMAP® 60CSx handheld GPS receiver. At each site a 50 by 50 cm hole was excavated down to the C horizon to expose the complete soil profile. Each hole was photographed and described using a geochemical coding form and codes proposed by Hoffman (1986), along with the details of the immediate area.

Samples from the Ah, upper B, lower B and C horizons were screened to -12 mesh at the sample site to remove coarse fragments and roots. Where soil moisture precluded screening, coarse fragments were manually removed from the sample. Approximately 500 g of material was placed in 12.7 by 25.4 cm (5 by 10 in.) Hubco Inc. polyester-weave sample bags. Material from the top centimetre of the Ae horizon was tested for soil pH and conductivity. These samples and those for MMI extraction were collected in heavy-duty, polyvinyl chloride (PVC) Ziploc® bags.

Samples were analyzed by a range of proprietary and non-proprietary, selective and partial extractions, as well as by fire assay and super trace (an ALS Chemex proprietary method) for Au. The analytical methods and sampling horizons are summarized in Table 1.

Quality Control

Quality control (QC) measures used in this study include the collection of two types of field duplicates. In each survey area, five sites (about 10%) were randomly selected for field duplicate sampling. Two types of duplicates were col-

lected at these sites: within-hole and between-hole duplicates. Within-hole duplicates are a repetition of the original sampling procedure, collecting another soil sample from the cleaned walls of the soil pit. Between-hole duplicates are taken from a second hole dug as close to the original as possible, usually within 2 m. All duplicate samples were submitted blind to the laboratory.

No standard reference materials were used in this study. The reason for this is the unavailability of suitable matrix-matched materials that are certified for the methods being tested. In order to monitor and mitigate analytical drift, the samples were randomized prior to submission to the laboratory. Randomization has the benefit of distributing the effects of instrumental drift randomly throughout the sample population. It also allows for drift monitoring by plotting the samples in analytical order.

In addition to the field QC procedures, a number of steps were taken at the laboratories to ensure the quality of the analytical results. These include the introduction of analytical standards, blanks and lab duplicates into the sample stream.

Field Analyses

Soil pH

There is a growing body of evidence to indicate that variations in soil pH, or hydrogen ion (H^+) concentration, occur at the surface over buried sulphide mineralization. Smee (1983) proposed a mechanism, based on laboratory experiments and field tests, for the formation of metal anomalies in soils developed on glaciolacustrine clay over massive sulphides in the Abitibi Belt, northern Quebec. His work

showed that H^+ released as a byproduct of sulphide oxidation at the water table diffuses to the surface to form detectable acidic anomalies, and that pH sensitive elements like Ca, Sr, Mg, Fe and Mn in a boreal forest environment (i.e., slightly oxidizing to reducing) become redistributed in response to the pH shift.

Smee (1997, 1998) proposed a similar model for ion transport and indirect anomaly formation for arid environments. Results from a multicompany sponsored orientation survey at the Marigold gold deposit in Nevada (Smee, 1998) showed that Ca concentration, in all weak leaches tested, displayed a distinctive rabbit-ear or double-peak response with the peaks occurring over the edges of the mineralization. The ratio of weak leach Ca (e.g., acetic acid or hydroxylamine

Table 1. Sample media and analytical methods, Kwanika and Mount Milligan, British Columbia.

	Soil horizon	Ah	Ae	Upper B	Lower B	C	Other
Analytical method							
Sodium pyrophosphate		X					
Field pH/conductivity			X**				
Aqua-regia digestion		X		X	X	X	
Cold aqua-regia digestion				X			
Hot hydroxylamine HCl				X			
Cold hydroxylamine HCl				X			
De-ionized water				X			
Ionic Leach				X			
Bioleach				X			
Enzyme Leach SM				X			
Soil Gas Hydrocarbons SM				X			
Super trace gold				X			
Loss-on-ignition		X					
Mobile Metal Ion®-multielement							X*

* Sampled at constant depth typically from lower part of upper B and upper part of lower B horizons.

** Sampled from top centimetre of Ae horizon or top of mineral soil (Bf or Bm horizon depending on the profile type).

HCl) to aqua-regia digested Ca showed clear residual anomalies with the same rabbit-ear form and proposed that two forms of Ca exist in the soil; one of which is easily soluble and spatially related to mineralization and a second less soluble form, which represents background carbonate. Smee (1999) concludes that near-surface Ca over oxidizing mineralization is being remobilized in response to the upward movement of H^+ . Re-precipitation of Ca (carbonate) occurs where pH conditions permit, in other words over the edges of the sulphide body.

More recent work by Hamilton et al. (2004a, b) at the Marsh zone gold prospect and the Cross Lake volcanogenic massive sulphide (VMS) prospect in Ontario shows that similar rabbit-ear patterns occur in H^+ at the surface, above the edges of mineralization. They conclude that pH correlates with oxidation-reduction potential (ORP) and propose that H^+ production is a function of the redox conditions in the overburden column. In an earlier paper, Hamilton (1998) proposed the existence of reduced columns or chimneys in the overburden column above a reduced metal source. Reduction of the overburden column is postulated to occur as a result of upward migration of reduced anionic species between the top of a conductive body and the ground surface. Charge is transferred by the reaction with oxidized cationic species migrating in the other direction. This process results in the formation of an oxidation front that propagates to the surface to form a chimney or column. Within the reduced core of the chimney, oxidation of the underlying mineralization is inhibited thus limiting the amount of H^+ released. At the edges, however, oxidation is enhanced thus promoting H^+ accumulation at the surface over the edges of the underlying mineralization. This process results in a typical rabbit-ear response for H^+ , with a pronounced central low over the reduced chimney, from samples collected at the very top of the mineral soil profile.

The presence of similar patterns in the vastly different environments of Nevada (arid to semi-arid) and northern Ontario (saturated, boreal forest) suggest that a common process is operating in both environments. Regardless of the mechanism, H^+ accumulations (direct response) and redistributed near-surface carbonate (indirect response) should be easily detectable in the field using a simple pH meter and acid bottle. By taking two pH measurements of a 1:1 soil slurry (one without acid and a second with acid), the near-surface H^+ variation and the reactivity of the soil can be readily mapped. In addition to rabbit-ear H^+ peaks over the edges of the mineralization, the remobilized carbonate halo can also be identified. A simple plot of the inverse of the difference between the acidified and non-acidified H^+ concentrations (IDH; Smee, 2009) will highlight the zones of carbonate reprecipitation over the edges of the underlying sulphide body.

Soil Conductivity

Soil conductivity (EC), expressed as micro Siemens per centimetre ($\mu S/cm$), is a useful measurement in exploration geochemistry as it provides an estimation of the soluble anions and cations present in the soil. It has been suggested by various workers (Govett, 1974, 1976; Smee, 1998) that EC variations in surface soils reflect the release of salts and other ionic species as a result of the oxidation of sulphides at depth. Smee (1983) proposed that a special relationship between pH and EC may occur where ions have been mobilized and reprecipitated in response to a change in pH. Therefore a measurement of EC in soils over a sulphide body should show anomalous readings over the flanks of sulphide mineralization. Hamilton (1998) asserts that surficial geochemical anomalies, both rabbit-ear and apical, form above bedrock conductors as a result of strong redox gradients between the top of the conductor and ground surface; a reduced chimney. His model predicts the accumulation of ions at the edges of the reduced chimney as a result of anion movement up and out, and cation movement down and along redox gradients. These zones of ion accumulation should be readily detectable as areas of anomalous soil conductivity.

Results

This section describes the results of the field soil EC and pH measurements carried out at Kwanika and Mount Milligan. Results from the selective and partial extractions will be the subject of a follow-up paper.

Data Quality

Table 2 shows the results of the field duplicate samples for the soil pH and conductivity measurements, expressed as average percent relative standard deviations or RSD%. RSD% values for the pH and acidified pH are below 10% indicating that the results are highly reproducible. It is interesting to note that the RSD% values for the between-hole duplicates are actually slightly lower than for the within-hole duplicates. The reason for this is unclear. These results show that there is little variation in the soil pH values over distances of a few metres from a sample site.

Conductivity measurements have a higher uncertainty than the pH measurements with RSD% values ranging from 18.77 to 32.72%. Once again the between-hole values are marginally lower than those from the same hole; an observation that is not easily explained.

Table 2. Average percent relative standard deviations (RSD%) for field duplicates, Kwanika and Mount Milligan, British Columbia.

	Kwanika			Mount Milligan		
	Acidified			Acidified		
	pH	pH	Conductivity	pH	pH	Conductivity
Within hole	9.24%	2.97%	32.72%	4.62%	5.69%	23.71%
Between hole	7.10%	2.82%	18.77%	4.31%	3.09%	19.85%

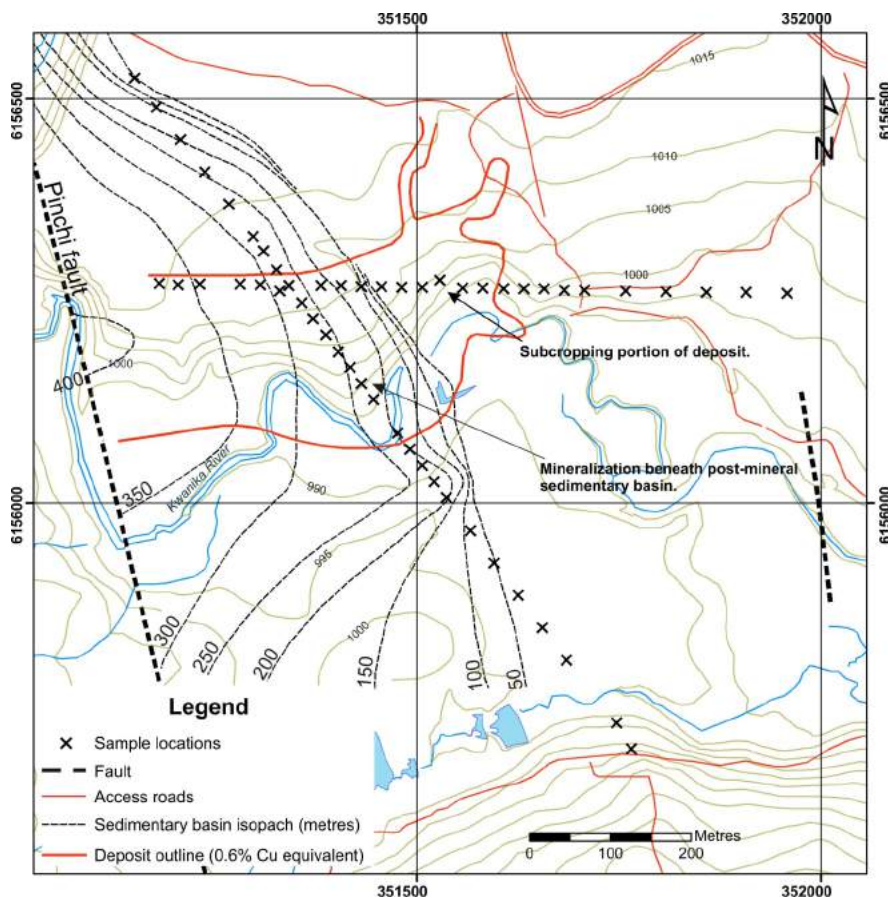


Figure 7. Location map showing the soil profile transects at the Kwanika Central zone, British Columbia.

Kwanika Survey

Two transects of soil profiles (52 samples) were sampled across the Central zone (Figure 7). The east-west transect, which comprises 24 sample sites, passes over the portion of the deposit that subcrops beneath the Quaternary cover. The transect extends from the Pinchi fault in the west to approximately 350 m east of the known mineralization, where drilling indicates that there is no mineralization and background levels exist. A northwest-southeast transect comprising 29 sample sites crosses the portion of the deposit that lies beneath the post-mineral sedimentary basin. In this area, the mineralization is present at a depth of approximately 300 m below surface and is masked by both the post-mineral sedimentary basin and the overlying veneer of Quaternary glacial outwash sediments. The two transects provide different challenges to the DPG methods being tested. Sample sites are spaced at 50 m intervals in inferred background areas and at 25 m intervals over the deposit itself.

Soil pH and conductivity measurements were recorded at the end of each day on material collected from the top centimetre of the mineral soil (usually the top of the Ae or Aej

horizon). This level was chosen based on results presented by Hamilton et. al (2004b) that indicate that the strongest H^+ patterns occur in the uppermost part of the soil profile, or microlayer (Smee, 2009). Conductivity measurements were made on a 1:1 slurry of soil in demineralized water using a VWR International conductivity meter. Measurements of the pH were made on the same slurry using an Oakton® Instruments double junction pHTestr® 30. The instrument was calibrated daily using standard pH buffer solutions at pH 4.00, 7.00 and 10.00. Two pH measurements were taken on each sample: one 20 s after immersion of the electrode into the slurry and a second measurement 20 s after adding one drop of 10% hydrochloric acid and stirring. Measurements of pH were recorded into an Excel spreadsheet and converted to H^+ concentrations. IDH values were also calculated using Smee's (2009) method. Summary statistics for the pH and conductivity measurements are presented in Table 3.

Figure 8 shows profile plots for EC, H^+ , acidified H^+ and IDH along the two transects over the Central zone. Conductivity profiles (Figure 8a) show a relationship to the eastern and southern surface projection of the mineralization as defined by the 0.6% Cu equivalent envelope (Mills, 2008). On the east-west transect, there is an asymmetrical rabbit-ear response slightly offset to the east of the mineralization envelope. The higher contrast peak (11 times the background levels) occurs in the direction of plunge of the mineralization beneath the post-mineral sedimentary basin. An explanation for the apparent offset in the anomaly would be the presence of lower grade subcropping mineralization to the east of the deposit envelope. The strongly anomalous value at the east end of the transect is likely an expression of a prominent north-trending fault zone identified in drillholes to the south of the transect (D. Moore, pers. comm., 2009).

Conductivity values on the northwest-southeast transect show a different pattern. There is a broad but subtle increase in values (over two times the background levels) from north to south over the projection of the mineralization. This culminates in a moderate contrast peak (nine times the background levels) situated directly over the southern edge. There is also an indication of a low-contrast,

Table 3. Summary statistics for soil pH and conductivity measurements, Kwanika and Mount Milligan, British Columbia.

	Kwanika			Mount Milligan		
	Conductivity ($\mu\text{S/cm}$)	pH	Acidified pH	Conductivity ($\mu\text{S/cm}$)	pH	Acidified pH
Number of samples	52	52	52	39	39	39
Minimum	2.7	3.87	2.91	5.2	4.41	2.96
Maximum	36.9	6.07	4.76	30.3	7.66	5.52
Range	34.2	2.2	1.85	25.1	3.25	2.56
Mean	7.72	4.67	3.34	12.58	5.15	3.50
Standard deviation	6.84	0.49	0.46	5.13	0.66	0.60
Variation	46.73	0.24	0.21	26.32	0.43	0.36
Sum	401.50	242.75	173.73	490.60	200.75	136.51
Sum of squares error	5483.05	1145.63	591.24	7171.48	1049.69	491.64
Geometric mean	6.285	4.643	3.314	11.729	5.111	3.458
Median	5.25	4.60	3.18	12.1	5.01	3.27
Mode	3.7	4.00	2.97	12.1	4.46	3.15

rabbit-ear anomaly further to the south. This feature is unexplained.

Hydrogen ion (H^+) profiles are illustrated in Figure 8b. Responses on both transects are relatively noisy but distinct patterns can be seen. On the east-west transect, H^+ values display a general increase over the edges of the mineralization and display a low directly over the centre. While not a classic rabbit-ear response, this pattern is consistent with Hamilton's (1998) model for a reduced overburden column or chimney above sulphide mineralization, which predicts a H^+ low over the mineralized body (Hamilton's [1998] pH measurements were taken at a depth of 25 cm below surface, compared to 7–10 cm in this study). More pronounced lows occur on the northwest-southeast transect. Here, the H^+ response has the form of a double negative or W-shaped profile with the minimum values occurring approximately over the edges of the sulphide body and the central high directly on top of it. The contrasting patterns on the two transects may be an expression of the different depths to the mineralization; i.e., less than 50 m on the east-west transect and approximately 300 m on the northwest-southeast transect.

Negative responses are even more pronounced in the acidified H^+ profiles (Figure 8c). On the east-west transect, a double low or W response is visible slightly to the east of the mineralization envelope. This feature has an antithetic relationship to the conductivity features mentioned above (Figure 8a). Lows are interpreted to be regions where either oxidation of the underlying sulphides is being inhibited by redox conditions in the overburden column, causing a drop in H^+ flux (Hamilton, 1998) or areas of buffering of the acid solution caused by remobilized carbonate (Smee, 1998). A strong negative correlation with conductivity suggests the latter case, where remobilized carbonate is accompanied by other pH sensitive ions in the near surface. A similar W-shaped profile occurs in the acidified H^+ readings on the northwest-southeast transect. The acidified H^+ lows are co-

incident with the edges of the mineralization. Again, there is a strong antithetic relationship with conductivity.

IDH, as mentioned earlier, is a good estimator of the presence of remobilized carbonate. As the inverse of the difference between the acidified and nonacidified H^+ concentrations, high values indicate areas where carbonate has been remobilized and precipitated. Figure 8d shows the IDH profiles for the Kwanika transects. On the east-west transect, there is a very high contrast (66 and 25 times the background levels) asymmetric rabbit-ear response centred slightly east of the projected position of the mineralization. The peaks coincide exactly with the position of the conductivity rabbit-ear response and reinforce the interpretation that they represent redistribution of pH sensitive elements at the surface.

A similar pattern, but with lower contrast, occurs on the northwest-southeast transect. The asymmetrical peaks (13 and 3 times the background levels) fall close to the projected limits of the mineralization. Lower contrast values are likely an expression of the much greater depth to mineralization (>300 m) on this transect.

Mount Milligan Survey

A 3200 m northwest-southeast transect (39 samples) was sampled across the MBX and 66 zone deposits (Figure 5). Samples were spaced at 100 m intervals in background areas at the ends of the transect and at approximately 50 m intervals over the mineralization. Widespread surface disturbance in the deposit area precluded sampling at a regular spacing. Samples were collected from locations that were assessed to have undisturbed profiles. These included roadcuts, exposed roots of first growth trees and isolated enclaves of the original forest preserved between drilling roads. The transect crosses a variety of overburden types, including till and colluvial deposits in the northwest to

glaciofluvial outwash, alluvium and eskers in the centre and southeast (Figure 5).

Soil pH and conductivity measurements were collected using the same procedures employed at Kwanika. Results of the soil EC and pH measurements are shown in Figure 9. EC measurements (Figure 9a) display little contrast between background and mineralized areas. Most of the variation appears to be noise. The only exception being a very subtle peak (2.05 times the background levels) located over

the northwestern boundary of MBX. This feature is barely distinguishable from background values.

Hydrogen ion concentrations (Figure 9b) also display a very low contrast. A subtle, double-peak feature (six and three times the background levels) occurs immediately adjacent to the northwestern boundary of MBX. There is no corresponding peak on the southeastern boundary of the 66 zone, where values are indistinguishable from background levels. A more robust response occurs in the acidified H^+

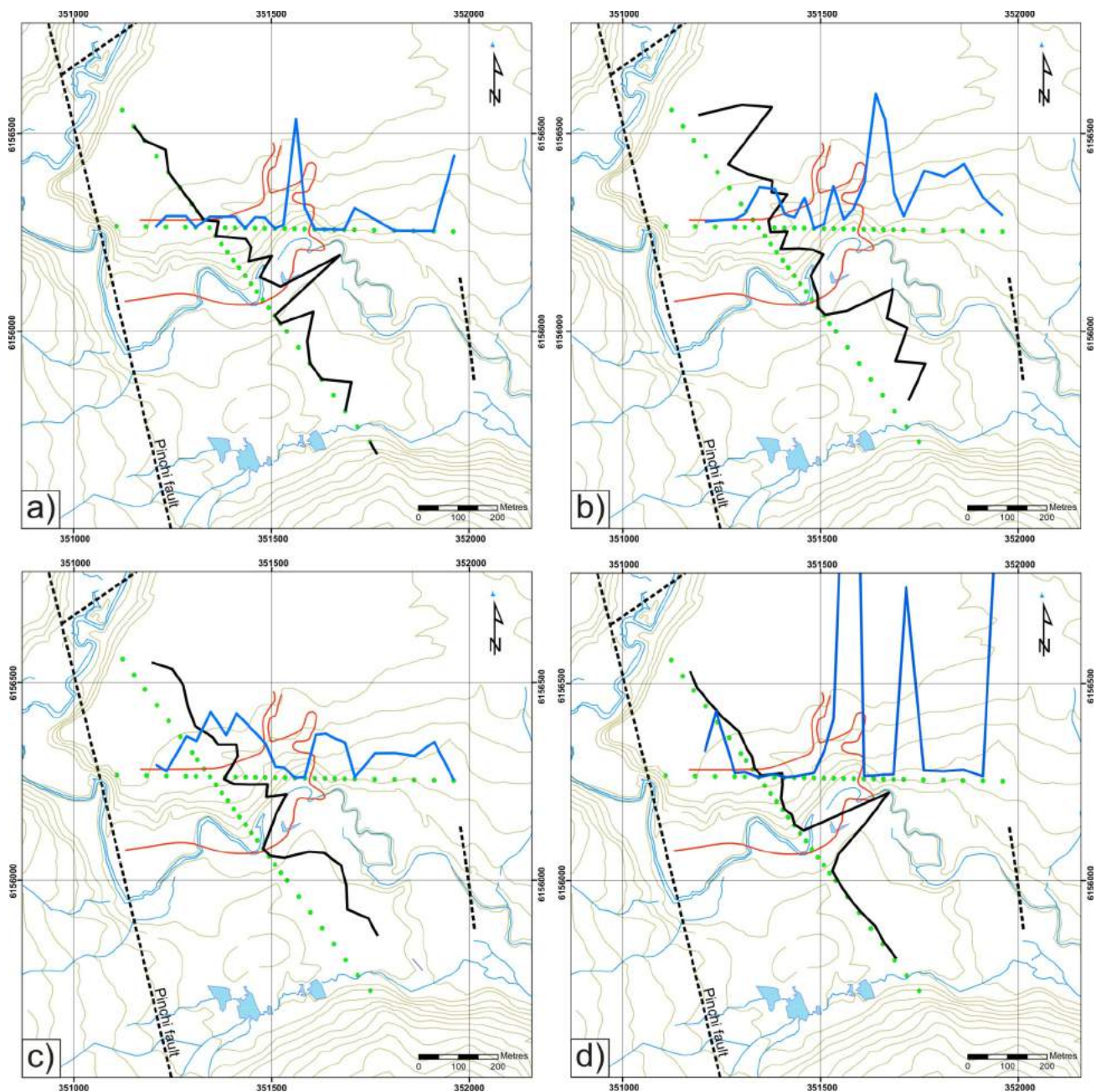


Figure 8. Profiles over the Central zone (red outline), Kwanika, British Columbia: **a)** conductivity; **b)** hydrogen ion concentration; **c)** acidified hydrogen ion concentration; **d)** inverse difference between the acidified and nonacidified hydrogen ion concentrations (IDH).

profile (Figure 9c). Again, the profile is asymmetrical, with the highest values (5.8 times the background levels) occurring adjacent to the northwestern boundary of MBX with no identifiable response on the southeastern boundary of the 66 zone.

The asymmetry of the pH response is highlighted by the IDH profile (Figure 9d). A high-contrast, double-peak feature (39 and 17 times the background levels) can clearly be

seen adjacent to the northwestern boundary of MBX. The peaks show an antithetic relationship with the H^+ profile, strongly suggesting that they are caused by carbonate remobilization in response to changes in the H^+ concentration. Once again there is a lack of a corresponding feature on the southeastern boundary of the 66 zone.

There are two possible explanations for the absence of a rabbit-ear peak on the southeast side of the deposits. As dis-

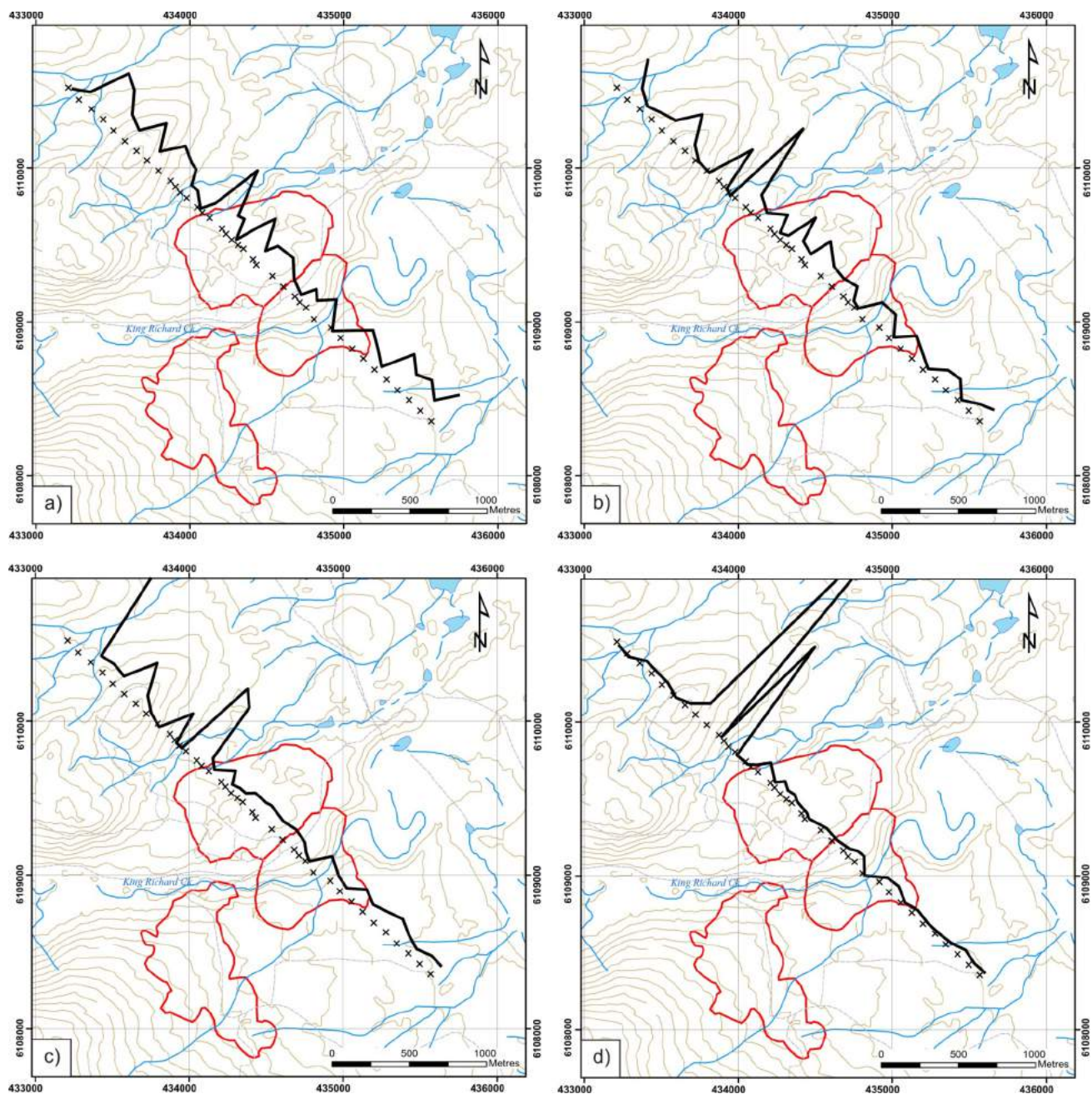


Figure 9. Profiles over the MBX and 66 zone deposits (red outlines) at Mount Milligan, British Columbia: **a)** conductivity; **b)** hydrogen ion concentration; **c)** acidified hydrogen ion concentration; **d)** inverse difference between the acidified and nonacidified hydrogen ion concentration (IDH). Profiles are of response ratios after data levelling to account for overburden type.

cussed earlier, both Smee (1998) and Hamilton's (1998) models predict that there should be an H^+ and IDH peak on both sides of the mineralization. One obvious explanation for the missing peak is surface disturbance. The southeastern boundary of the 66 zone occurs in an area where there has been considerable surface disturbance from road and drill-pad construction. While every effort was made to sample 'pristine' soil profiles, it is possible that the surface is too damaged and the anomaly has been destroyed. The high-contrast, double-peak anomaly on the northwestern boundary of MBX occurs in an area relatively free from disturbance. Another possibility is that the transect does not extend far enough to the southeast to capture the other side of the anomaly. This would be reasonable if there was an extensive zone of low-grade or barren sulphide mineralization extending south of the 66 zone. Drilling southeast of the 66 zone has confirmed the presence of barren pyrite mineralization at depth, however its extent to the south is unknown (D. O'Brien, pers. comm., 2009).

Summary and Conclusions

Part I of this study describes the application and interpretation of soil EC and pH measurements collected over the Kwanika Central zone and the MBX and 66 zone deposits at Mount Milligan. It has been demonstrated that these simple and rapid field measurements appear to detect sulphide mineralization through considerable thicknesses of cover. At Kwanika, the study shows that sulphide mineralization located up to 300 m below the surface has a response consistent with Smee's (1998) model for remobilized and reprecipitated carbonate. IDH patterns define characteristic rabbit-ear anomalies over the edges of the underlying mineralization. At Mount Milligan, a high-contrast IDH anomaly was identified through relatively thin cover immediately adjacent to the northwestern margin of the mineralization. There was no corresponding rabbit-ear response on the southeastern margin of the 66 zone. The lack of a response on the other side might be due to either extensive surface disturbance in that area or the possibility that the sample transect was too short to capture the anomaly. Further work is required to explain this result.

Preliminary conclusions from this study are

Soil pH and EC are low cost, rapid field measurements that appear to effectively detect patterns related to blind sulphide mineralization through considerable thicknesses of transported cover. Blind mineralization can be detected in the field using nothing more sophisticated than a Teflon beaker, demineralized water, an acid drop-per bottle and conductivity and pH meters.

Responses to mineralization in undisturbed areas show classic rabbit-ear patterns with peaks located over or immediately adjacent to the edges of the underlying sulphide mineralization. In temperate boreal forest environments of north-central BC, the signal is strongest in

the IDH, suggesting that carbonate remobilization is occurring in response to subtle changes in pH at the surface.

Both soil EC and pH appear to show a response to mineralization through tens of metres of Quaternary cover at Kwanika, and are able to indicate mineralization through hundreds of metres of post-mineral sediments.

Amplitude of the signal appears to be related to the thickness of the cover. At Kwanika, maximum contrast occurs where the mineralization is subcropping beneath tens of metres of overburden. Where sulphides occur at considerable depth, beneath 300 m of post-mineral sediments and Quaternary cover, contrast is lower but the patterns remain the same.

At Mount Milligan, additional work is required to determine why the southeastern rabbit-ear response is missing. This would involve resampling the southeastern margin of the 66 zone using alternate sample sites and extending the sample transect further to the southeast.

Acknowledgments

Funding for this study was provided by Geoscience BC. The author thanks Acme Analytical Laboratories Ltd., Activation Laboratories Ltd., ALS Chemex and SGS Mineral Services for their generous discounts and contributions to the analytical work. Thanks also go to Serengeti Resources Inc. and Terrane Metals Corp. for allowing access to their sites, for providing food and lodgings during the fieldwork and for their contributions of data. Thanks to C. Dunn and B. Smee for reviewing this manuscript and providing helpful comments and suggestions that greatly enhanced the final product. Finally, thanks to K. Heberlein for her able assistance with the digging and soil sampling.

References

- Bradshaw, P.M.D. (1975): Conceptual models in exploration geochemistry: the Canadian Cordillera and Canadian Shield; *Journal of Geochemical Exploration*, v. 4, no. 1, 223 p.
- Bradshaw, P.M.D., Thomson, I., Smee, B.W. and Larsson, J.O. (1974): The application of different analytical extractions and soil profile sampling in exploration geochemistry; *Journal of Geochemical Exploration*, v. 3, p. 209–225.
- Cameron, E.M. (1998): Deep-penetrating geochemistry; report, Canadian Mining Industry Research Organization (CAMIRO).
- Cameron, E.M., Leybourne, M.I. and Kelley, D.L. (2002): Exploring for deeply-covered mineral deposits: formation of geochemical anomalies in northern Chile by earthquake-induced surface flooding of mineralized groundwaters; *Geology*, v. 30, p. 1007–1010.
- Cameron, E.M., Hamilton, S.M., Leybourne, M.I., Hall, G.E.M. and McClenaghan, M.B. (2004): Finding deeply buried deposits using geochemistry; *Geochemistry: Exploration, Environment, Analysis*, v. 4, p. 7–32.

- Canada Soil Survey Committee, Subcommittee on Soil Classification (1978): The Canadian system of soil classification; Canadian Department of Agriculture, Publication 1646, 164 p.
- Cook, S.J. and Dunn, C.E. (2007): Final report on results of the Cordilleran Geochemistry Project: a comparative assessment of soil geochemical methods for detecting buried mineral deposits – 3Ts Au-Ag prospect, central British Columbia; Geoscience BC, Paper 2007-7, 225 p.
- Govett, G.J.S. (1974): Soil conductivities: assessment of an electrochemical technique; *in* Geochemical Exploration, I.L. Elliott and W.K. Fletcher (ed.), Association of Exploration Geochemists, Special Publication, no. 2, p. 101–118.
- Govett, G.J.S. (1976): Detection of buried and blind sulphide deposits by measurement of H^+ and conductivity of closely spaced surface soil samples; *Journal of Exploration Geochemistry*, v. 6, p. 359–382.
- Gravel, J. and Sibbick, S. (1991): Mount Milligan: geochemical exploration in complex glacial drift; *in* Exploration in British Columbia 1990, BC Ministry of Energy, Mines and Petroleum Resources, Part B, p. 117–134.
- Hamilton, S.M. (1998): Electrochemical mass-transport in overburden: a new model to account for the formation of selective leach geochemical anomalies in glacial terrain; *Journal of Geochemical Exploration*, v. 63, p. 155–172.
- Hamilton, S.M., Hall, G.E.M. and McClenaghan, M.B. (2004a): Redox, pH and SP variation over mineralization in thick glacial overburden. Part II: field investigation at Cross Lake VMS property; *Geochemistry: Exploration, Environment, Analysis*, v. 4, p. 45–58.
- Hamilton, S.M., Cameron, E.M., McClenaghan, M.B. and Hall, G.E.M. (2004b): Redox, pH and SP variation over mineralization in thick glacial overburden. Part I: methodologies and field investigation at the Marsh zone gold property; *Geochemistry: Exploration, Environment, Analysis*, v. 4, p. 33–44.
- Hamilton, S.M., Cameron, E.M., McClenaghan, M.B. and Hall, G.E.M. (2007): Deep penetrating geochemical techniques in exploration (the dos and don'ts); PowerPoint® presentation, Ontario Geological Survey.
- Hoffman, S.J. (1986): Soil sampling; *in* Exploration Geochemistry: Design and Interpretation of Soil Surveys, W.K. Fletcher, S.J. Hoffman, M.B. Mehrtens, A.J. Sinclair and I. Thomson (ed.), Society of Economic Geologists, Reviews in Economic Geology, v. 3, p. 39–76.
- Kerr, D.E. and Bobrowsky, P.T. (1991): Quaternary geology and drift exploration at Mount Milligan (93N/1E, 93O/4W) and Johnny Mountain (104B/6E, 7W, 10W, 11E), British Columbia; *in* Exploration in British Columbia 1990, BC Ministry of Energy, Mines and Petroleum Resources, p. 135–152.
- Lett, R.E. and Sandwith, Z. (2008): Geochemical orientation surveys in the Quesnel Terrane between Quesnel and Williams Lake, central British Columbia (NTS 093A, B, G); *in* Geological Fieldwork 2007, BC Ministry of Energy, Mines and Petroleum Resources, Paper 2008-1, p. 49–60.
- Levinson, A.A. (1974): Introduction to exploration geochemistry; Applied Publishing Ltd., Calgary, 11 p.
- Mann, A.W., Birrell, R.D., Mann, A.T., Humphreys, D.B. and Perdrix, J.L. (1998): Application of the mobile metal ion technique to routine geochemical exploration; *Journal of Geochemical Exploration*, v. 1, p. 87–102.
- Mills, K. (2008): Technical report – feasibility, Mt. Milligan Property - northern BC; unpublished report to Terrane Metals Corp.
- Panteleyev, A. (1995): Porphyry Cu-Au: Alkalic; *in* Selected British Columbia Mineral Deposit Profiles, Volume 1 - Metallics and Coal, D.V. Lefebure and G.E. Ray (ed.), BC Ministry of Energy, Employment and Investment, Open File 1995-20, p. 83–86.
- Rennie, D.W. and Scott, K.C. (2009): Technical report on the Kwanika project, Fort St. James, British Columbia, Canada; unpublished report to Serengeti Resources Inc., Scott Wilson Mining.
- Ricker, K.E. (1991): A preliminary appraisal of the surficial geology of the Mt. Milligan mine site with special reference to tailings impoundment Area A; unpublished report to Placer Dome Inc., January 31, 1991.
- Smee, B.W. (1983): Laboratory and field evidence in support of the electrogeochemically enhanced migration of ions through glaciolacustrine sediment; *in* Geochemical Exploration 1982, G.R. Parslow (ed.), *Journal of Geochemical Exploration*, v. 19, p. 277–304.
- Smee, B.W. (1997): The formation of surficial geochemical pattern over buried epithermal gold deposits in desert environments. Results of a test of partial extraction techniques; *in* Exploration '97, Symposium Volume, Toronto, p. 301–314.
- Smee, B.W. (1998): A new theory to explain the formation of soil geochemical responses over deeply covered gold mineralization in arid environments; *Journal of Geochemical Exploration*, v. 61, p. 149–172.
- Smee, B.W. (1999): The effect of soil composition on weak leach solution pH: a potential exploration tool in arid environments; *Explore*, no. 102, p. 4–8.
- Smee, B.W. (2009): Soil micro-layer, airborne particles and pH: the Govett connection; *in* Proceedings of the 24th International Applied Geochemistry Symposium, Fredericton, 2009, v. 1, p. 91–95.

Porphyry Indicator Minerals (PIMs): Exploration for Concealed Deposits in South-Central British Columbia (NTS 092I/06, 093A/12, 093N/01, /14)

F. Bouzari, Mineral Deposit Research Unit, University of British Columbia, Vancouver, BC, fbouzari@eos.ubc.ca

C.J.R. Hart, Mineral Deposit Research Unit, University of British Columbia, Vancouver, BC

S. Barker, Mineral Deposit Research Unit, University of British Columbia, Vancouver, BC

T. Bissig, Mineral Deposit Research Unit, University of British Columbia, Vancouver, BC

Bouzari, F., Hart, C.J.R., Barker, S. and Bissig, T. (2010): Porphyry indicator minerals (PIMs): exploration for concealed deposits in south-central British Columbia (NTS 092I/06, 093A/12, 093N/01, /14); in Geoscience BC Summary of Activities 2009, Geoscience BC, Report 2010-1, p. 25–32.

Introduction

Resistate minerals, those robust accessory minerals that persist through weathering, have successfully been applied to kimberlite and diamond exploration (e.g., Griffin and Ryan, 1995; Averill, 2001). Although easy to collect in heavy mineral concentrates, these minerals have only rarely been used as exploration tools for other deposit types, including porphyry copper deposits (e.g., Force et al., 1984). The common occurrence of resistate minerals as alteration products in British Columbia porphyry copper deposits suggests that these porphyry indicator minerals (PIMs) could provide a key tool to the increase of exploration targeting success, especially in terrains covered by glacial till.

The Quesnel and Stikine terranes in south-central BC host Late Triassic–Early Jurassic magmatic arcs, which are highly prospective hosts for porphyry Cu (-Mo, Au) deposits. However, exploration success in this area has been limited due to thin, but extensive veneers of till and related glacial sediments, which cover much of the area (Ward et al., 2009), especially in the region between the Mount Milligan and Mount Polley porphyry deposits (Figure 1). Geophysical and geochemical surveys in this region (e.g., Sander Geophysics Limited, 2008; Jackaman et al., 2009; Kowalczyk, 2009) suggest that a broad correlation exists between the geochemical characteristics of these unconsolidated sediments and the underlying bedrock geology (Barnett and Williams, 2009). Therefore, an erosional mineralogical record of the bedrock, and more importantly of potentially mineralized porphyry copper deposits, likely

exists in the glacial sediments, and this signature can be recognized by the resistate mineral population.

The purpose of this research project is to identify the occurrence, types, relative amounts and compositions of PIMs in selected porphyry deposits in order to elucidate important PIM signatures. The main questions are as follows:

What resistate minerals are key indicators for porphyry copper deposits in this region?

What are the characteristic features of these PIMs, particularly their physical appearance?

How extensive and intensive are PIM distribution patterns in surrounding sediments?

How can explorers most effectively and efficiently use PIMs in regional exploration targeting?

The key objectives of the project are therefore to

determine the occurrence and types of resistate minerals in various styles of alteration and mineralization in several central BC porphyry copper-gold deposits to establish a PIM signature;

determine the diagnostic physical parameters and chemical compositions of resistate minerals;

identify important indicator minerals and establish physical properties to distinguish those resistate minerals that are directly associated with porphyry copper-gold deposits; and

establish criteria for use of resistate minerals as an exploration tool in south-central BC.

This study presents a summary of field observations, sampling and preliminary results on contrasting characteristics of apatite crystals associated with mineralized and barren hostrocks at the Highland Valley porphyry copper district. These results suggest that apatite associated with porphyry copper mineralization has distinct physical and chemical properties, which can help to easily distinguish it from apatite associated with barren hostrocks.

Keywords: indicator minerals, porphyry copper deposits, geochemistry

This publication is also available, free of charge, as colour digital files in Adobe Acrobat® PDF format from the Geoscience BC website: <http://www.geosciencebc.com/s/DataReleases.asp>.

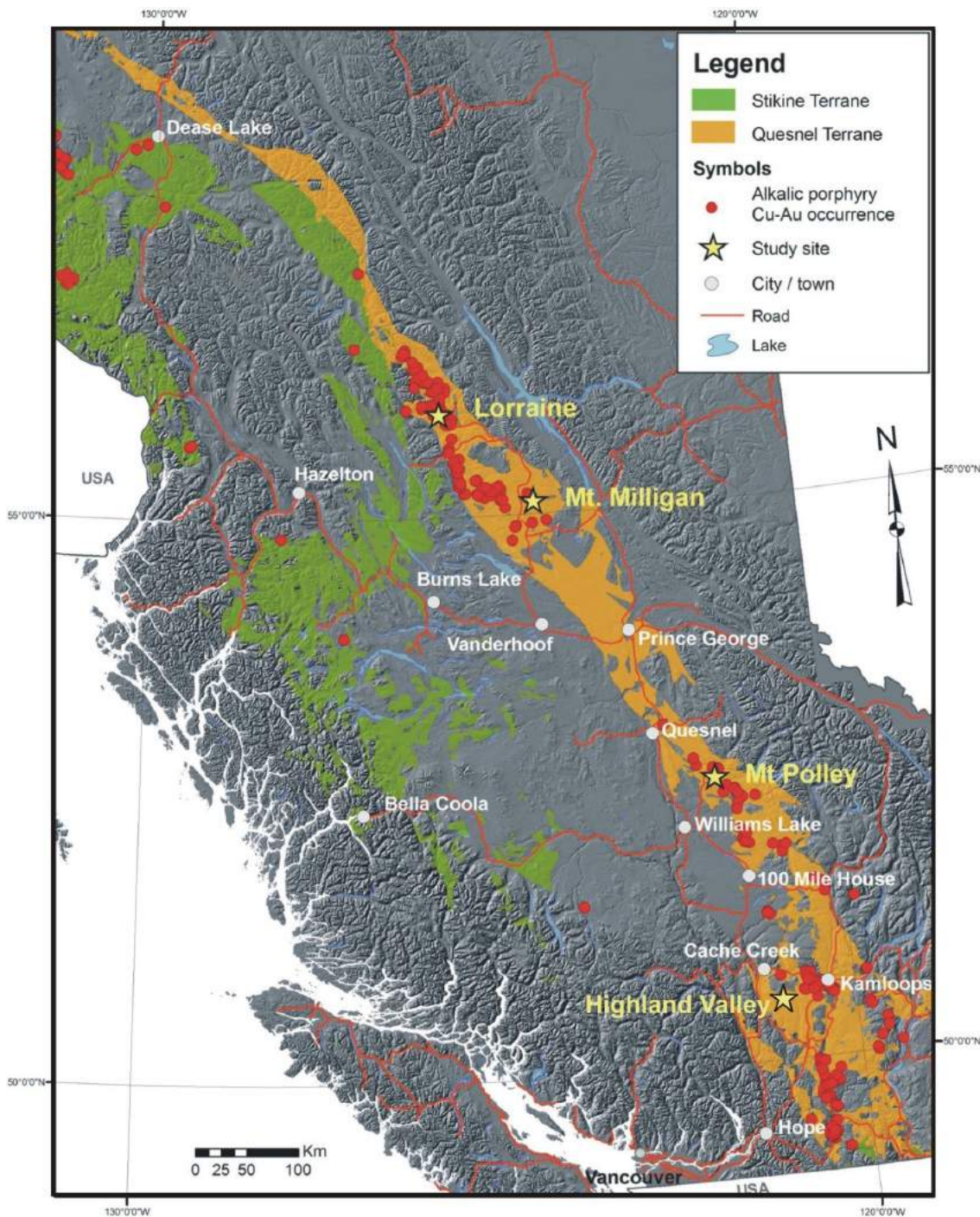


Figure 1. Digital elevation map showing outcrop distribution of Late Triassic and Early Jurassic Quesnel and Stikine terranes of south-central British Columbia (modified from Tosdal et al., 2008) and location of porphyry deposits selected for this study. Note the gap in occurrence of deposits in the area between the Mount Polley and Mount Milligan deposits.

Resistate Minerals in Porphyry Copper Deposits

Resistate minerals have long been known to occur in porphyry copper deposits, both in host intrusions and as hydrothermal alteration products (e.g., Schwartz, 1953; Gustafson and Hunt, 1975; Lang et al., 1995). Apatite, rutile, zircon, titanite, monazite and garnet are common resistate

minerals associated with calcalkaline and alkaline porphyry deposits (Table 1). Tourmaline, dumortierite, andalusite, diaspore and quartz also commonly occur with calcalkaline porphyry deposits. Ore sulphide minerals are unstable and rarely preserved in surficial sediments, but supergene oxidation processes will convert these sulphide minerals into stable, insoluble minerals such as jarosite and turquoise, which can also be used as PIMs.

Table 1. Characteristics of resistate minerals occurring in British Columbia porphyry copper deposits.

Mineral	Density (g/cm ³)	Occurrence in porphyry copper deposits	Characteristic features in porphyry deposits	South-central British Columbia example	References
Rutile	4.2	Occurs in potassic and phyllic zones as alteration product of biotite, ilmenite, titanomagnetite and titanite.	Red color due to high copper content; crystal length:width ratio increases outward from the deposit; grains proximal to the mineralized centre are larger and zoned; abundance and grain size follows the Cu grade; high concentration of V, Ta and Sc; Cr+V:Nb+Ta is high; V-Sb-W-rich rutile defines the Au-rich zone.	Mount Milligan, Babine Lake, Highland Valley	Williams and Cesbron, 1977; Desborough and Sharp, 1978; Czamanske et al., 1981; Harris, 1989; Nelson and Bellefontaine, 1996; Scott, 2005
Apatite	3.2	Occurs with early potassic alteration but records a history of dissolution and precipitation during subsequent alterations.	Fluoresce bright orange color in the ultraviolet; shows complicated history of corrosion and redeposition with a characteristic zoning (Liesegang rings); rings can often be detected 600–1000 m laterally away from the intrusion; commonly displays sulphur-rich cores abruptly changing to sulphur-poor rims; it is chlorine-rich.	Mount Polley, Galore Creek, Lorraine, Granisle	Carson and Jambor, 1974; Williams and Cesbron, 1977; Streck and Dilles, 1998; Tepper and Kuehner, 1999; Belousova et al., 2002; Kempe and Götze, 2002; Bath et al., 2006; Liaghat and Tosdal, 2008
Garnet	~3.9	Occurs in the periphery of porphyry deposits.	Displays zoning and change in composition; Ti-rich andradite commonly reported; hydrothermal titanian andradite can have as much TiSi as igneous varieties, but has zero or negative amounts of TiMg[Fe ³⁺] ₂ .	Mount Polley, Galore Creek, Lorraine	Watson, 1969; Russell et al., 1999; Nixon and Peatfield, 2003
Zircon	4.6	Commonly magmatic, occurring with the host intrusion but few studies report distinct hydrothermal zircon hosted in hydrothermal veins.	Rose zircon commonly reported; hydrothermal, spongy, inclusion-rich zircon may show complex internal textures in which secondary domains cut across primary growth zones; porphyry copper deposits are associated with intrusions with zircon having Ce(IV)/Ce(III)>300 and EuN/EuN* > 0.4.	Mount Milligan, Mount Polley, Ajax	Mortensen et al., 1995; Nelson and Bellefontaine, 1996; Ballard et al., 2002; Hoskin, 2005; Pettke et al., 2005; Schaltegger, 2007
Monazite	~5.1	Commonly magmatic occurring with the host intrusion.	Hydrothermal monazite is characterized by its low ThO ₂ content (0–1 wt. %) and is distinct from that of igneous monazite (3 to >5 wt. %).	Endako	Villeneuve et al., 2001; Schandl and Gorton, 2004
Titanite	~3.5	Commonly magmatic occurring with the host intrusion.	Blond titanite reported.	Mount Milligan, Mount Polley, Copper Mountain	Mortensen et al., 1995; Nelson and Bellefontaine, 1996
Tourmaline	~3	Commonly with transitional phyllic or breccia bodies.	Dravite is more common; associated with or without mineralization.	Megabuck Au-Cu prospect, Highland Valley	Panteleyev et al., 1996; Slack, 1996
Jarosite	~3	Supergene oxidation.	May occur with goetite and/or copper oxides.	Mount Milligan	

Resistate minerals can record salient features of the porphyry system from early magmatic (e.g., zircon) to late hydrothermal (e.g., apatite) and subsequent supergene oxidation stages. Thus, when formed or altered by hydrothermal fluids characteristic of the mineralizing porphyry environments, the physical properties of these minerals may change such that they display unique colour, size and shape characteristics, which can be used as a prospecting tool.

Early work on heavy accessory minerals in porphyry copper deposits mainly focused on the economic exploitation of these minerals (e.g., Czamanske et al., 1981). However, several studies noted the unique physical and chemical features of the resistate minerals associated with various stages of hydrothermal alteration in porphyry copper deposits (Table 1). More recently, chemical and physical properties of apatite and rutile were the subject of studies showing the overall evolution of the hydrothermal system (e.g., Streck and Dilles, 1998; Scott, 2005).

Apatite is a common accessory mineral occurring in various hostrocks and mineral deposits. Trace-element compositions of apatite have been used to recognize the hostrock and degree of fractionation, as well as the oxidation state of the host magma (Tepper and Kuehner, 1999; Belousova et al., 2002). Mariano (1988) and Kempe and Götze (2002) have shown that apatite from mineralization related to alkaline rocks exhibits blue and violet cathodoluminescence due to activation by trace quantities of rare earth element ions (Ce^{3+} , Eu^{2+} , Sm^{3+} , Dy^{3+} and Nd^{3+}), whereas those from P-rich granite show strong Mn^{2+} -activated yellow-greenish luminescence. Apatite from porphyry deposits is Cl-rich and Cl may act as a key component in transporting copper. Williams and Cesbron (1977) noted that apatite of porphyry copper origin displays a characteristic bright orange colour under ultraviolet (UV) light, and shows a complicated history of corrosion and redeposition with characteristic zoning (Liesegang rings). The rings can often be detected up to 600–1000 m laterally away from the intrusion. The composition of these textures is not well known but they may have recorded changes of the hydrothermal system through time and thus have the potential to provide clues to the productivity of the system. Furthermore, Streck and Dilles (1998) demonstrated that zoned apatites from the Yerington batholith, Nevada, have sulphur-rich cores which abruptly change to sulphur-poor rims, indicating that early sulphate-rich magma evolved to sulphate-poor magma via crystallization of anhydrite. Table 1 summarizes key characteristics of the common resistate minerals in porphyry copper deposits.

Geological Setting

Quesnel and Stikine terranes host most of BC's known porphyry copper deposits and are composed of Paleozoic and lower Mesozoic volcanic, sedimentary and plutonic rocks

displaying both oceanic and arc affinities. The Late Triassic–Middle Jurassic porphyry deposits include both calcalkalic and alkalic classes, and show a full range of morphological and depth relationships (McMillan et al., 1995). The Highland Valley (NTS 092I/06), Mount Polley (NTS 093A/12), Mount Milligan (NTS 093N/01) and Lorraine (NTS 093N/14) deposits represent examples of the typical styles and assemblages of porphyry deposits in the Quesnel terrain and were therefore selected for this project (Figure 1).

The Highland Valley Cu-Mo district in southern BC is the largest cluster of porphyry deposits in the region and includes Valley, Lornex, Highmont, Alwin, Bethlehem and JA deposits hosted within the Upper Triassic calcalkaline Guichon Creek batholith (Casselmann et al., 1995). This composite batholith ranges from diorite and quartz diorite at the border to younger granodiorite in the centre, which hosts the mineralization (Figure 2a). Styles and assemblages of alteration and mineralization vary from narrow structurally-controlled mineralized zones (e.g., Alwin) to pervasive stockwork-hosted mineralization (e.g., Valley); coarse secondary muscovite is a major alteration mineral in all deposits commonly accompanying sulphide mineralization (Figure 2b).



Figure 2. Examples of hostrock and alteration from the Alwin mine, Highland Valley, south-central British Columbia: **a)** sample of fresh Bethsaida granodiorite, the main hostrock to mineralization, with characteristic large, rounded quartz phenocrysts and biotite books; **b)** intense green mica alteration and associated chalcopyrite mineralization overprinting the Bethsaida granodiorite.

The alkalic Mount Polley Cu-Au deposit is hosted within Jurassic–Triassic diorite-monzonite intrusions and associated breccia bodies. Alteration-mineralization progresses outward from a higher temperature core of biotite to an intermediate actinolite zone and an outer zone of K-feldspar and albite (Fraser et al., 1995; Logan and Mihalynuk, 2005). Copper and gold values are closely correlated with high magnetite concentrations (Deyell and Tosdal, 2005).

The Middle Jurassic Mount Milligan deposits are hosted by porphyritic monzonite stocks and adjacent volcanic rocks of the Late Triassic Takla Group centred around three main intrusive stocks. The deposit displays a classic zoned alteration-mineralization pattern consisting of a bornite-rich core with potassic alteration surrounded by a pyrite-dominated sulphide halo with propylitic alteration (Sketchley et al., 1995; Jago and Tosdal, 2009).

Farthest to the north, the Lorraine alkalic Cu-Au porphyry deposit is hosted within the Duckling Creek Syenite Complex of the Late Triassic–Cretaceous Hogem batholith, which intrudes the Late Triassic Takla Group volcanic and sedimentary sequences (Nixon and Peatfield, 2003). Mineralization occurs in three zones along strike over a distance of approximately 1.5 km within a northwest-trending corridor dominated by syenitic rocks. Mineralization is characterized by finely disseminated Cu-Fe sulphide minerals in fine-grained K-feldspar biotite rock, biotite pyroxenite and syenitic rocks, and lacks features such as stockwork veining and breccia (Bath and Cooke, 2008). Chalcopyrite and bornite occur as blebs and semi-massive sulphide in pyroxenite (Bishop et al., 1995).

Materials and Methods

Sampling

Because their geology is well documented, Highland Valley, Mount Milligan and Lorraine deposits (Figure 1) were selected for sampling. Samples were selected from different alteration assemblages at different vertical levels to determine and characterize the occurrence of resistate minerals at various depths in a porphyry system. Samples were also collected from unmineralized hostrocks for direct comparison. Overall, 31 samples were collected from Highland Valley (Valley, Bethlehem and Alwin), and 12 samples were collected from Mount Milligan. A total of 13 samples representing Lorraine mineralization and various hostrocks were obtained from a previous study done by the Mineral Deposit Research Unit (MDRU) of the University of British Columbia (Bath and Cooke, 2008). Samples were also collected from Mount Polley Cu-Au and Endako Mo deposits for comparison. Furthermore, it is planned to obtain till and drainage sediments at various locations around at least one of the above study sites.

Methods

An integrated analytical technique is currently employed at MDRU to establish the most valid and cost effective mechanism for characterizing PIMs. Analytical work includes a petrographic study employing optical and cathodoluminescence (CL) microscopy and scanning electron microscopy (SEM) to characterize the abundance and physical properties of various resistate minerals, including shape, size, colour and luminescence. Selected grains are analyzed by electron microprobe for their trace-element composition to test whether there are key chemical features in the PIMs, which are unique to mineralized porphyry copper deposits. Resistate minerals have also been separated to different size fractions using conventional sieve and heavy liquid methods. These samples are currently being studied using a mineral liberation analyzer (MLA), which is an automated scanning electron microscope, to efficiently characterize the physical properties of the resistate minerals. The results of both the MLA and trace-element analysis by laser ablation inductively coupled plasma–mass spectrometry (LA-ICP-MS) will be made available in future presentations and publications.

Cathodoluminescence Microscopy

A Cambridge Image Technology Ltd. MK 4A model cold cathodoluminescence stage mounted on a petrographic microscope was used to study the internal textures of the apatite grains. The samples were irradiated in a vacuum chamber with an electron beam of approximately 15 kV and the current set at 350–500 μ A.

Results

Petrographic observations indicate that apatite, zircon and, to a lesser extent, rutile and titanite are common resistate minerals in the studied deposits. Apatite is by far the most common resistate mineral occurring in a wide range of hostrocks and alteration assemblages. More critically, physical and chemical properties of apatite are significantly different in altered-mineralized rock relative to fresh hostrock largely based on observations from Highland Valley samples.

Apatite in fresh intrusive rocks commonly displays euhedral crystal shape and its hexagonal form is distinctive (Figure 3d). Although small apatite grains surrounded by quartz or feldspar are difficult to recognize under optical microscope, apatite was easily detected by its strong luminescence of yellow to yellow-green in fresh hostrock (Figures 2a, 3a). The yellow luminescence is attributed to excitation by Mn^{2+} (Mariano, 1988; Waychunas, 2002). Some of the apatite grains in fresh granodiorite display yellow-brown luminescence. No major internal structures were observed using either CL or SEM, although some grains show a distinctive narrow brownish luminescence zone near the crystal rim. Apatite in altered granodiorite at Highland Val-

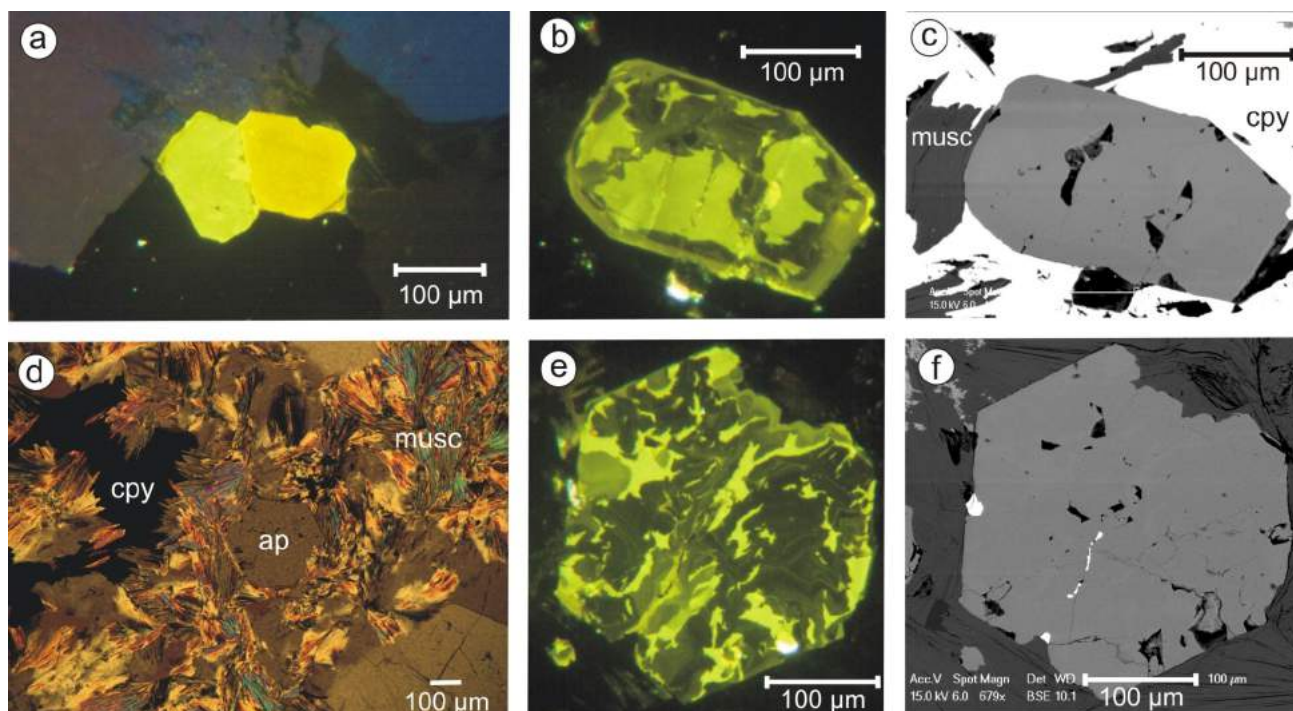


Figure 3. Photomicrographs showing contrasting characteristic features of apatite associated with fresh and altered Bethsaida granodiorite at Alwin mine, Highland Valley, south-central British Columbia: **a**) cathodoluminescence (CL) image showing two primary magmatic apatite grains hosted in fresh granodiorite with strong yellow (right) and yellow-pale green (left) luminescence with no obvious internal texture; **b**) CL image of apatite in altered granodiorite showing green-luminescent phase replaced by dark green- to grey-luminescent phase; **c**) scanning electron microscope (SEM) image of the apatite grain of Figure 3b showing no internal texture; **d**) crossed-polarized image of euhedral apatite (ap) crystal hosted in altered granodiorite with strong muscovite alteration (musc) and associated chalcopyrite (cpy) mineralization; **e**) CL image of the apatite grain of Figure 3d showing replacement of the green-luminescent apatite by a dark green- to grey-luminescent phase generating a 'messy' texture; **f**) SEM image of the apatite grain of Figure 3e showing no internal texture—the very bright phases at the rim and inside the apatite are chalcopyrite, which has formed within a micro-fracture that has an envelope of green to grey-luminescent apatite (see Figure 3e).

ley's Alwin mine looks very similar to that associated with unaltered granodiorite when examined using a polarizing microscope and SEM (Figures 3c, d, f). However, CL microscopy reveals that apatite associated with altered hostrocks displays a unique green luminescence, probably reflecting Fe^{2+} excitation, which is overprinted by a dark complex network and bodies of dark-green to grey-luminescent domains (Figure 3b), producing a characteristic 'messy' texture (Figure 3e). These relationships clearly demonstrate that a darker luminescent phase replaced a brighter, green-luminescent phase possibly contemporaneous with green muscovite alteration and associated copper mineralization.

Conclusions

Apatite is a ubiquitous accessory mineral which occurs in a wide range of hostrocks and commonly incorporates a wide range of trace elements. It is resistant to both late hydrothermal alteration and weathering, making it a robust, easy to collect recorder of mineralization-related alteration. Altered apatite displays yellow-green luminescence probably due to excitation by incorporation of low amounts of Fe^{2+} . Strongly altered apatite shows dark-green to grey lumines-

cence, probably due to the loss of Mn^{2+} , producing a complex texture with remnants of green-luminescent apatite. Preliminary microprobe data suggest that apatite in altered hostrock has lost several trace components such as Mn^{2+} , Cl and S. These results provide the first step towards a better understanding and, ultimately, the use of resistate minerals as indicators for porphyry copper exploration.

Acknowledgments

The authors would like to thank Teck Corporation and Terrane Metals Corp. for allowing access and sampling at their Highland Valley and Mount Milligan deposits, respectively. D. Tosdal provided a field introduction to Highland Valley. Geoscience BC is thanked for its generous financial contribution in support of this project.

References

- Averill, S.A. (2001): The application of heavy indicator mineralogy in mineral exploration, with emphasis on base metal indicators in glaciated metamorphic and plutonic terrain; *in* Drift Exploration in Glaciated Terrain, M.B. McClenaghan, P.T. Bobrowsky, G.E.M. Hall and S.J. Cook (ed.), Geological Society of London, Special Publication 185, p. 69–82.

- Ballard, J.R., Palin, J.M. and Campbell, I.H. (2002): Relative oxidation states of magmas inferred from Ce(IV)/Ce(III) in zircon: application to porphyry copper deposits of northern Chile; *Contributions to Mineralogy and Petrology*, v. 144, p. 347–364.
- Barnett, C. and Williams, P.M. (2009): Using geochemistry and neural networks to map geology under glacial cover; Geoscience BC, Report 2009-3, 26 p.
- Bath, A.B. and Cooke, D. (2008): The importance of biotite for the deposition of sulfides at the Lorraine Cu-Au porphyry deposit, north-central British Columbia; *in* Shallow and Deep-Level Alkalic Deposits, Porphyry Module, K. Simpson and T. Bissig (ed.), Mineral Deposit Research Unit, University of British Columbia, and Centre of Excellence in Ore Deposit Research, University of Tasmania, unpublished report, p. 7.1–7.30.
- Bath, A.B., Logan, J.M. and Kamenetsky, V.S. (2006): Apatite in Cu-sulfide ore from the Mount Polley alkalic porphyry, BC Canada (abstract); 16th Annual V.M. Goldschmidt Conference, *Geochimica et Cosmochimica Acta*, v. 70, no. 18, suppl. 1, p. A40.
- Belousova, E.A., Griffin, W.L., O'Reilly, S.Y. and Fisher, N.I. (2002): Apatite as an indicator mineral for mineral exploration: trace-element compositions and their relationship to host rock type; *Journal of Geochemical Exploration*, v. 76, p. 45–69.
- Bishop, S.T., Heah, T.S., Stanley, C.R. and Lang, J.R. (1995): Alkalic intrusion hosted copper gold mineralization at the Lorraine deposit, north-central British Columbia; *in* Porphyry Deposits of the Northwestern Cordillera of North America, T.G. Schroeter (ed.), Canadian Institute of Mining and Metallurgy, Special Volume 46, p. 623–629.
- Carson, D.J.T. and Jambor, J.L. (1974): Mineralogy, zonal relationships and economic significance of hydrothermal alteration at porphyry copper deposits, Babine Lake Area, British Columbia; Canadian Institute of Mining and Metallurgy, Bulletin, v. 67, p. 110–133.
- Casselman, M.J., McMillan, W.J. and Newman, K.M. (1995): Highland Valley porphyry copper deposits near Kamloops, British Columbia: a review and update with emphasis on the Valley deposit; *in* Porphyry Deposits of the Northwestern Cordillera of North America, T.G. Schroeter (ed.), Canadian Institute of Mining and Metallurgy, Special Volume 46, p. 161–191.
- Czamanske, G.K., Force, E.R. and Moore, W.J. (1981): Some geologic and potential resource aspects of rutile in porphyry copper deposits; *Economic Geology*, v. 76, p. 2240–2256.
- Desborough, G.A. and Sharp, W.N. (1978): Tantalum, uranium, and scandium in heavy accessory oxides, Climax molybdenum mine, Climax, Colorado; *Economic Geology*, v. 73, p. 1749–1751.
- Deyell, C.L. and Tosdal, R.M. (2005): Alkalic Cu-Au deposits of British Columbia: sulfur isotope zonation as a guide to mineral exploration; *in* Geological Fieldwork 2004, BC Ministry of Energy, Mines and Petroleum Resources, Paper 2005-1, p. 191–208.
- Force, E.R., Djaswadi, S., van Leeuwen, T. and Lynd, L.E. (1984): Exploration for porphyry metal deposits based on rutile distribution—a test in Sumatra: a new exploration tool for porphyry deposits in the tropics; United States Geological Survey, Bulletin 1558-A-B.
- Fraser, T.M., Stanley, C.R., Nikic, Z.T., Pesalj, R. and Gorc, D. (1995): The Mount Polley copper-gold alkalic porphyry deposit, south-central British Columbia; *in* Porphyry Deposits of the Northwestern Cordillera of North America, T.G. Schroeter (ed.), Canadian Institute of Mining and Metallurgy, Special Volume 46, p. 609–622.
- Griffin, W.L. and Ryan, C.G. (1995): Trace elements in indicator minerals: area selection and target evaluation in diamond exploration; *Journal of Geochemical Exploration*, v. 53, p. 311–337.
- Gustafson, L.B. and Hunt, J.P. (1975): The porphyry copper deposit at El Salvador, Chile; *Economic Geology*, v. 70, p. 875–912.
- Harris, D.C. (1989): The mineralogy and geochemistry of the Hemlo gold deposit, Ontario; Geological Survey of Canada, Economic Geology Report 38, 88 p.
- Hoskin, P.W.O. (2005): Trace-element composition of hydrothermal zircon and the alteration of Hadean zircon from the Jack Hills, Australia; *Geochimica et Cosmochimica Acta*, v. 69, p. 637–648.
- Jackaman, W., Balfour, J.S. and Reichheld, S.A., (2009): QUEST-West Project geochemistry: field survey and data reanalysis, central British Columbia (parts of NTS 093E, F, J, K, L, M, N); *in* Geoscience BC Summary of Activities 2008, Geoscience BC, Report 2009-1, p. 7–14.
- Jago, C.J. and Tosdal, R.M. (2009): Distribution of alteration in an alkalic porphyry copper-gold deposit at Mount Milligan, central British Columbia (NTS 094N/01); *in* Geoscience BC Summary of Activities 2008, Geoscience BC, Report 2009-1, p. 33–48.
- Kempe, U. and Götze, J. (2002): Cathodoluminescence (CL) behaviour and crystal chemistry of apatite from rare-metal deposits; *Mineralogical Magazine*, v. 66, p. 151–172.
- Kowalczyk, P.K. (2009): QUEST-West geophysics in central British Columbia (NTS 093E, F, G, K, L, M, N, 1031): new regional gravity and helicopter time-domain electromagnetic data; *in* Geoscience BC Summary of Activities 2008, Geoscience BC, Report 2009-1, p. 1–6.
- Lang, J.R., Lueck, B., Mortensen, J.K., Russell, J.K., Stanley, C.R. and Thompson, J.F.H. (1995): Triassic–Jurassic silica-undersaturated and silica-saturated alkalic intrusions in the Cordillera of British Columbia: implications for arc magmatism; *Geology*, v. 23, p. 451–454.
- Liaghat, S. and Tosdal, R. (2008): Apatite chemical composition and textures as a probe into magmatic conditions at Galore Creek porphyry copper-gold deposit, British Columbia (abstract); 18th Annual V.M. Goldschmidt Conference, *Geochimica et Cosmochimica Acta*, v. 72, no. 12, p. A550.
- Logan, J.M. and Mihalyuk, M.G. (2005): Regional geology and setting of the Cariboo, Bell, Springer and Northeast porphyry Cu-Au zones at Mount Polley, south-central British Columbia; *in* Geological Fieldwork 2004, BC Ministry of Energy, Mines and Petroleum Resources, Paper 2005-1, p. 249–270.
- Mariano, A.N. (1988): Some further geological applications of cathodoluminescence; *in* Cathodoluminescence of Geological Materials, D.J. Marshall (ed.), Unwin Hyman, Boston, p. 94–123.
- McMillan, W.J., Thompson, J.F.H., Hart, C.J.R. and Johnston, S.T. (1995): Regional geological and tectonic setting of porphyry deposits in British Columbia and Yukon Territory; *in* Porphyry Deposits of the Northwestern Cordillera of North America, T.G. Schroeter (ed.), Canadian Institute of Mining and Metallurgy, Special Volume 46, p. 40–57.

- Mortensen, J.K., Ghosh, D.K. and Ferri, F. (1995): U-Pb geochronology of intrusive rocks associated with copper-gold porphyry deposits in the Canadian Cordillera; *in* Porphyry Deposits of the Northwestern Cordillera of North America, T.G. Schroeter (ed.), Canadian Institute of Mining and Metallurgy, Special Volume 46, p. 142–158.
- Nelson, J.L. and Bellefontaine, K.A. (1996): The geology and mineral deposits of north-central Quesnellia: Tezzeron Lake to Discovery Creek, central British Columbia; BC Ministry of Energy, Mines and Petroleum Resources, Bulletin 99, 112 p.
- Nixon, G.T. and Peatfield, G.R. (2003): Geological setting of the Lorraine Cu-Au porphyry deposit, Duckling Creek Syenite Complex, north-central British Columbia; *in* BC Ministry of Energy, Mines and Petroleum Resources, Open File 2003-4, 24 p.
- Panteleyev, A., Bailey, D.G., Bloodgood, M.A. and Hancock, K.D. (1996): Geology and mineral deposits of the Quesnel River–Horsefly map area, central Quesnel Trough, British Columbia (NTS 93A/5, 6, 7, 11, 13; 93B/9, 16; 93G/1; 93H/4); BC Ministry of Energy, Mines and Petroleum Resources, Bulletin 97, 156 p.
- Pettke, T., Audétat, A., Schaltegger, U. and Heinrich, C.A. (2005): Magmatic-to-hydrothermal crystallization in the W–Sn mineralized Mole granite (NSW, Australia): part II: evolving zircon and thorite trace element chemistry; *Chemical Geology*, v. 220, p. 191–213.
- Russell, J.K., Dipple, G.M., Lang, J.R. and Lueck, B. (1999): Major-element discrimination of titanium andradite from magmatic and hydrothermal environments: an example from the Canadian Cordillera; *European Journal of Mineralogy*, v. 11, p. 919–935.
- Sander Geophysics Limited (2008): Airborne gravity survey, Quesnellia Region, British Columbia; Geoscience BC, Report 2008-8, 121 p.
- Schaltegger, U. (2007): Hydrothermal zircon; *Elements*, v. 3, p. 51–79.
- Schandl, E.S. and Gorton, M.P. (2004): A textural and geochemical guide to the identification of hydrothermal monazite: criteria for selection of samples for dating epigenetic hydrothermal ore deposits; *Economic Geology*, v. 99, p. 1027–1035.
- Schwartz, G.M. (1953): Geology of the San Manuel copper deposit, Arizona; United States Geological Survey, Professional Paper 256, 65 p.
- Scott, K.M. (2005): Rutile geochemistry as a guide to porphyry Cu-Au mineralization, Northparkes, New South Wales, Australia; *Geochemistry: Exploration, Environment, Analysis*, v. 5, p. 247–253.
- Sketchley, D.A., Rebagliati, C.M. and DeLong, C. (1995): Geology, alteration and zoning patterns of the Mt. Milligan copper-gold deposits; *in* Porphyry Deposits of the Northwestern Cordillera of North America, T.G. Schroeter (ed.), Canadian Institute of Mining and Metallurgy, Special Volume 46, p. 650–665.
- Slack, J.F. (1996): Tourmaline association with hydrothermal ore deposits; *in* Boron: Mineralogy, Petrology and Geochemistry, E.S. Grew and L.M. Anovitz (ed.), Mineralogical Society of America, Reviews in Mineralogy, v. 33, p. 559–643.
- Streck, M.J. and Dilles, J.H. (1998): Sulfur evolution of oxidized arc magmas as recorded in apatite from a porphyry copper batholith; *Geology*, v. 26, p. 523–526.
- Tepper, J.H. and Kuehner, S.M. (1999): Complex zoning in apatite from the Idaho batholith: a record of magma mixing and intracrystalline trace element diffusion; *American Mineralogist*, v. 84, p. 581–595.
- Tosdal, R.M., Jackson, M., Pass, H.E., Rees, C., Simpson, K.A., Cooke, D.R., Chamberlain, C.M. and Ferreira, L. (2008): Hydrothermal breccia in the Mount Polley alkalic porphyry copper-gold deposit, British Columbia; *in* Geoscience BC Summary of Activities 2007, Geoscience BC, Report 2008-1, p. 105–114.
- Villeneuve, M., Whalen, J.B., Anderson, R.G. and Struik, L.C. (2001): The Endako batholith: episodic plutonism culminating in formation of the Endako porphyry molybdenite deposit, north-central British Columbia; *Economic Geology*, v. 96, p. 171–196.
- Ward, B., Maynard, D., Geertsema, M. and Rabb, T. (2009): Ice-flow history, drift thickness and drift prospecting for a portion of the QUEST Project area, central British Columbia (NTS 093G, H [west half], J); *in* Geoscience BC Summary of Activities 2008, Geoscience BC, Report 2009-1, p. 25–32.
- Watson, J.L. (1969): Garnets of the Stikine copper’s Galore Creek porphyry; B.Sc. thesis, University of British Columbia, 34 p.
- Waychunas, G.A. (2002): Apatite luminescence; *in* Phosphates—Geochemical, Geobiological, and Materials Importance, M.L. Kohn, J. Rakovan and J.M. Hughes (ed.), Mineralogical Society of America, Reviews in Mineralogy and Geochemistry, v. 48, p. 710–742.
- Williams, S.A. and Cesbron, F.P. (1977): Rutile and apatite: useful prospecting guides for porphyry copper deposits; *Mineralogical Magazine*, v. 41, p. 288–292.

Terrain Mapping, Glacial History and Drift Prospecting in the Northwest Corner of McLeod Lake Map Area (Part of NTS 093J), Central British Columbia

D.A. Sacco, Department of Earth Sciences, Simon Fraser University, Burnaby, BC, dsacco@sfu.ca

B.C. Ward, Department of Earth Sciences, Simon Fraser University, Burnaby, BC

D. Maynard, Denny Maynard & Associates Ltd., North Vancouver, BC

M. Geertsema, Northern Interior Forest Region, British Columbia Ministry of Forests, Prince George, BC

S. Reichheld, Department of Geography, University of Victoria, Victoria, BC

Sacco, D.A., Ward, B.C., Maynard, D., Geertsema, M. and Reichheld, S. (2010): Terrain mapping, glacial history and drift prospecting in the northwest corner of McLeod Lake map area (part of NTS 093J), central British Columbia; *in* Geoscience BC Summary of Activities 2009, Geoscience BC, Report 2010-1, p. 33–42.

Introduction

Central British Columbia has highly prospective bedrock geology, but mineral exploration activity has been limited in some areas due to the thick cover of surficial deposits. Economic growth in this region has been severely affected by the spread of the mountain pine beetle, therefore funding bodies, such as Geoscience BC, with their QUEST Project, and the federal and provincial governments, are providing financial support for geological projects that will help spur mineral exploration in the impacted areas. Significant knowledge gaps exist in the glacial history of the QUEST Project area and thus pose a considerable hindrance to mineral exploration, in particular when sampling transported sediments for geochemical analysis. Knowledge of the glacial history, specifically the ice-flow history and dominant transport direction, is vital to the interpretation of geochemical survey data from the area. This project is designed to address this knowledge gap by providing a Quaternary framework for a portion of the QUEST Project area, along with data from both regional and detailed till geochemical surveys from which inferences on local, covered, bedrock units can be made.

This ambitious three-year project is currently in year two. The study area comprises NTS map sheets 093G, H (west half) and J. The overall objectives of this three-year program are to provide

- 1) the regional glacial geological framework for NTS map areas 093G, H (west half) and J (i.e., the central portion of the QUEST area; Figure 1);

- 2) a map of approximate drift cover thickness (based on existing surficial geology, soils and landform mapping augmented with reconnaissance field observations) for areas within NTS map area 093J, the southern half of NTS 093G, and the western half of NTS 093H;
- 3) terrain mapping of six 1:50 000 scale map areas (NTS 093J/05, /06, /11, /12, /13, /14);
- 4) regional-scale, major, minor and trace-element till geochemical data (through aqua-regia digestion followed by inductively coupled plasma–mass spectrometry [ICP-MS] and instrumental neutron activation analysis [INAA], gold grain counts and heavy mineral separations) for samples collected within these six sheets; and
- 5) detailed-scale till geochemical data down-ice of two geophysical anomalies, which were interpreted from airborne gravity survey data (Barnett and Kowalczyk, 2008).

This work will help to stimulate mineral exploration activity in beetle-kill-affected areas through the release of new surficial geology and geochemical survey data. It is hoped these data will provide new exploration targets but also provide some geological context for companies to interpret their own geochemical and geological datasets.

The focus of this report is the detailed work carried out in the western half of NTS map area 093J. Fieldwork began in 2008, late June to early July, with the majority of it being completed in 2009, July and August. The 2008 field season concentrated on the collection of striation data for the reconstruction of ice-flow history and assessing the accuracy of the existing soil and landform and surficial geology mapping to be used for drift thickness mapping throughout the project area. Also, detailed-scale till geochemistry sampling occurred in areas down-ice from two geophysical anomalies (described in Ward et al., 2009). The 2009 field season concentrated on the terrain mapping of the six 1:50 000 map areas in NTS 093J, while collecting ice-flow

Keywords: *terrain mapping, drift prospecting, geochemical survey, ice-flow history, striations, heavy minerals*

This publication is also available, free of charge, as colour digital files in Adobe Acrobat® PDF format from the Geoscience BC website: <http://www.geosciencebc.com/s/DataReleases.asp>.

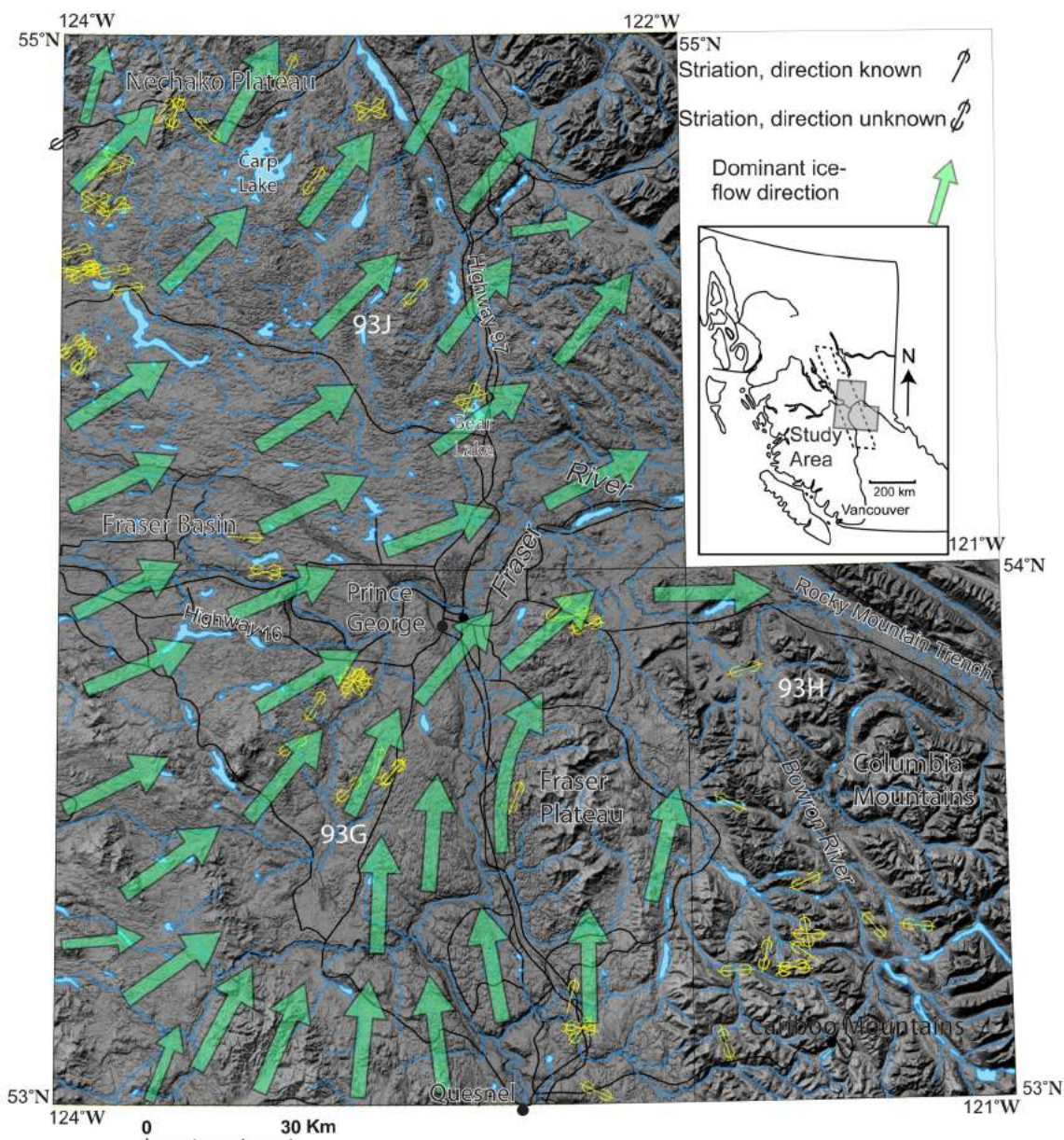


Figure 1. Digital elevation model (DEM) of the study area with ice-flow information. Drumlinized drift is evident throughout most of the study area and is used to interpret dominant ice flow. Striation data is compiled from field observations and existing maps (Tipper, 1971a; Clague, 1998a, b; Paulen, 2000; Blais-Stevens and Clague, 2007). Inset map indicates the location of the study area (shaded area) in relation to British Columbia and the QUEST Project geophysical survey area (dashed line).

data and conducting regional-scale till geochemical sampling for the map areas.

Study Area and Physiography

The study area is situated at the heart of the QUEST Project area (Figure 1). The majority of the study area lies in the relatively low relief area of the Interior Plateau (Holland, 1976; Mathews, 1986), including its subdivisions, the Fraser Basin and Nechako Plateau. It is characterized by glacial lake deposits, drumlinized drift and glaciofluvial outwash and esker deposits. The Cariboo Mountains, located in the southeastern corner, occupy the rest of the area.

Regional Quaternary History

The Cordilleran Ice Sheet has repeatedly covered British Columbia and portions of Yukon, Alaska and Washington over the last two million years (Armstrong et al., 1965; Clague, 1989). At its maximum extent, the Cordilleran Ice Sheet was up to 900 km wide and up to 2000–3000 m thick over the Interior Plateau, closely resembling the present-day Greenland Ice Sheet (Clague, 1989). A more comprehensive history of the Cordilleran Ice Sheet can be found in Jackson and Clague (1991).

The major sources of regional ice that covered the study area advanced from accumulation centres in the Coast, Skeena and Cariboo mountains (Tipper, 1971a, b; Levson and Giles, 1997; Plouffe, 1997, 2000). The study area occurs near the convergence of these three advancing ice fronts, making it difficult to determine which ice centre(s) had the most influence on the study area in the early parts of the Late Wisconsinan. Previously reported ice-flow indicators (Tipper, 1971a; Paulen, 2000), in combination with data from this study, suggest that it was mainly ice from the Coast Mountains to the west and south, and to a lesser extent ice from the Cariboo Mountains, that covered the area. Chronological information on the movement and/or confluence of ice fronts through the study area is limited. Although it is known that ice was advancing out of the Coast Mountains by $28\,800 \pm 740$ BP (sample GSC-95, Clague, 1989), it is not clear when this advance reached the central Interior Plateau. Ice, possibly sourced from the Cariboo Mountains (Paulen, 2000), covered the Bowron Valley sometime after 19.9 Ka (sample AA44045, Ward et al., 2008). According to Bobrowsky and Rutter (1992), ice advancing from the Skeena Mountains into what is now the north arm of Williston Lake occurred sometime after $15\,180 \pm 100$ BP (sample TO-708, Bobrowsky and Rutter, 1992).

Throughout the Interior Plateau, stratigraphic exposures of advance-phase glaciolacustrine, advance-phase glaciofluvial and till deposits suggest that regional ice advances were not necessarily continuous, nor uniform, but were instead interrupted by standstills and possible retreats (Clague, 1989). Evidence of this has been reported in exposures to the south (Tipper, 1971a, b; Clague, 1989; Eyles and Clague, 1991) and west (Plouffe, 1997, 2000) of the study area. Eventually, these ice fronts did coalesce sometime during the Fraser glaciation maximum, forming the Cordilleran Ice Sheet.

Deglaciation is thought to have occurred by downwasting, followed by widespread stagnation throughout much of the interior (Fulton, 1967; Clague, 1989). Initially, ice continued to flow at a subdued rate and eventually downwasting of ice exposed the uplands. Ice was then restricted to the valleys and as it retreated downslope it locally produced ice-dammed lakes, culminating with glacial Lake Fraser around Prince George. Thick deposits of glaciolacustrine silt and clay over large areas are a product of these ice-dammed lakes, such as glacial Lake Fraser. Eventually ice became stagnant and melted in place

resulting in hummocky and kame-and-kettle topography. The deglacial history of the study area will be discussed further in a later section of this paper.

Methods and Results

Terrain Mapping

Terrain mapping for the six 1:50 000 scale map areas in the western half of NTS 093J (093J/05, /06, /11, /12, /13, /14) began this year using standardized mapping methods (Resources Inventory Committee, 1996; Howes and Kenk, 1997). High resolution, 1:40 000 scale, aerial photographs provided 3-D imagery of the entire area upon which the mapping was based. In addition, field checking was carried out to assist in identifying and delimiting the surficial materials occurring within the study area. Good ground access was available throughout most of the map areas enabling detailed fieldwork to be conducted through much of the study area. In addition, GIS software and a variety of digital spatial data were used to create a digital elevation model (DEM) for the map areas from which landforms could be identified and spatial relationships could be observed (Figure 2). Although useful, these models were limited by the resolution of the available elevation data. Map units have been stereoscopically delimited, subdividing the land surface according to the origin and texture of surficial materials and landforms (surface expression) that occur there. Geomorphological processes that have modified the landscape were included on the map and on-site map symbols were used to identify specific landscape features, such as small terrace scarps and meltwater channels.

The final maps, to be completed in early 2011, will use a hybrid surficial geology and terrain map legend. Polygons will be placed into a coloured closed legend, similar to that of a surficial geology map but will include additional terrain information, such as additional surficial materials and

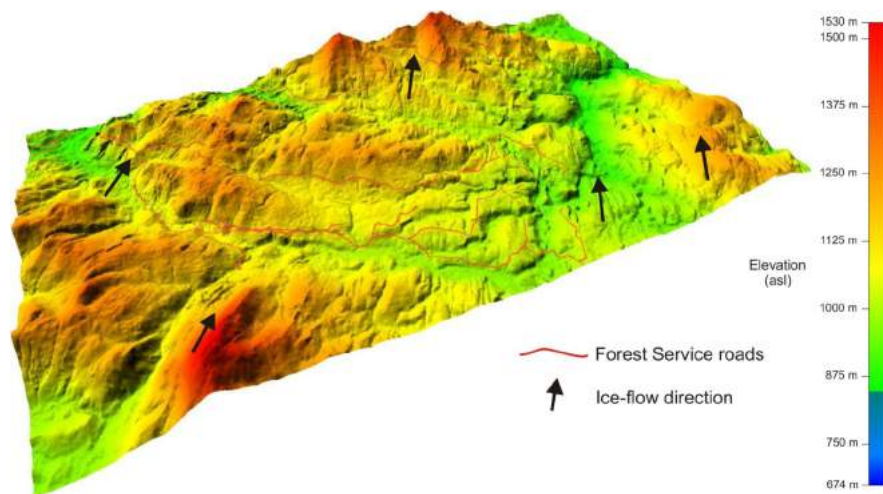


Figure 2. Digital 3-D model for a portion of the northern uplands in NTS 093J/14, central British Columbia, created using GIS software. Model is oriented in the direction of ice flow, illustrated by streamlined rock and drift.

any active geomorphological processes. This will make these maps easier to read yet still retain a more detailed description of the surficial materials and geomorphological processes occurring within individual polygons.

Nature of Surficial Materials

Surficial material of the study area is dominantly composed of till, glaciofluvial and glaciolacustrine sediments. Postglacial materials are also present, including fluvial, eolian, colluvial and organic deposits. Similar surficial units have been described to the west and south of the study area (Tipper, 1971a; Howes, 1977; Paulen, 2000; Plouffe, 2000).

Most of the till in the area is a dense, dark grey, matrix-supported diamicton, characteristics typical of a basal till. Subangular to well rounded, gravel-sized clasts comprise 10–40% of the diamicton and are supported by a sandy silt to silty clay matrix (Figure 3A). In several locations, the till was less dense, more gravelly and supported by a dominantly sand matrix. This facies of till was commonly observed within the top metre of an exposure and is interpreted as ablation till. The surface expression of tills range from fields of ridged, streamlined features (e.g., drumlins) to near-level plains with little or no vertical expression.

Glaciofluvial deposits varied greatly from well sorted sand to poorly sorted gravel that locally was composed of cobble-sized clasts (Figure 3B). These deposits most commonly consist of moderately sorted sandy pebble to pebbly sand granular material and form hummocky or kame-and-kettle topography, esker complexes and systems of terraces and plains. Numerous meltwater channels were observed throughout the study area, often, although not always, spatially associated with glaciofluvial deposits. In the northern portion of the study area, some of these channels crosscut topographic highs and incised valleys while others exist as areally extensive plains, generally draining northward. Farther south, roughly to the southwest of Carp Lake, the main meltwater channels formed in conformance to the southwesterly retreating ice sheet and thus drained somewhat laterally along the northwest-southeast oriented ice front. Present-day underfit streams occupy some of these meltwater channels, and their associated fluvial deposits partially infill the channels.

Glaciolacustrine deposits are generally composed of laminated silt and fine sand with some clay (Figure 3C). They are expressed as plains if they are thick deposits, and blankets or veneers where the material is thinner and the underlying unit controls its surface expression. These sediments cover extensive regions in the southern map sheets (NTS 093J/05, /06) and are less widespread in the north.

Eolian deposits, consisting of dominantly well sorted, fine to medium, wind-blown sand (Figure 3D), occur only lo-

cally but are worthy of mention. These deposits were commonly located near glaciofluvial, and to a lesser extent, glaciolacustrine sediments; the source material for these eolian sediments. The surficial expression of these deposits ranged from veneers to ridges (sand dunes). It is likely that the size of the sediment source correlates with the surface expression of the adjacent eolian deposit (i.e., small sources yield veneers and larger sources yield dunes). Further analysis of the spatial distribution of eolian and glaciofluvial deposits may reveal characteristics of deglacial wind regimes.

Bedrock is prevalent on the uplands in the northern portions of NTS 093J/13 and /14. In the southern map sheets, drift is much thicker and bedrock outcrops occur mainly on isolated topographic highs such as Merton Hill and Mount Prince. Thin mantles of bedrock-derived colluvium and discontinuous till occur in association with the bedrock-dominated terrain.

Ice-Flow History

The ice-flow history of the study area was determined by compiling ice-flow information from existing maps (Tipper, 1971a; Clague, 1998a, b; Paulen, 2000; Blais-Stevens and Clague, 2007), combined with newly conducted aerial photograph interpretation and observations made during the 2008 and 2009 field seasons (Figure 1). In this study area, ice-flow indicators generally consist of macroforms such as drumlins, flutings, crag-and-tail forms and streamlined bedrock ridges. Indicators measured in the field were mainly microflow indicators, such as grooves, striations and rat tails. Further information on these ice-flow indicators and the processes by which they form can be found in Ward et al. (2009).

The ice-flow–indicator data collected in 2009 provides further support to previous interpretations of the dominant ice flow. In most areas, the dominant flow is indicated by macroforms visible in the DEM. In portions of NTS 093H where these macroforms are rare, these data were substituted with the observed microflow indicators. Striations, rat tails and grooves were recorded at 33 sites in 2008 and an additional 23 sites in 2009. Finding microflow indicators was problematic due to the lack of bedrock exposures in the majority of the study area, and the weathered nature of some of the outcrops present. In most cases, striations were only found after sediment, usually till, was scraped, brushed or washed off bedrock surfaces. Where more than one orientation was observed at a site, it was sometimes possible to determine a relative age or timing of ice-flow events by locating crosscutting relationships or by the relative locations of the striated surfaces (Figure 4). For example, if a large groove is present and there are striations within the groove, the groove must be older than the striations. Similarly, by noting the dominant flow of ice

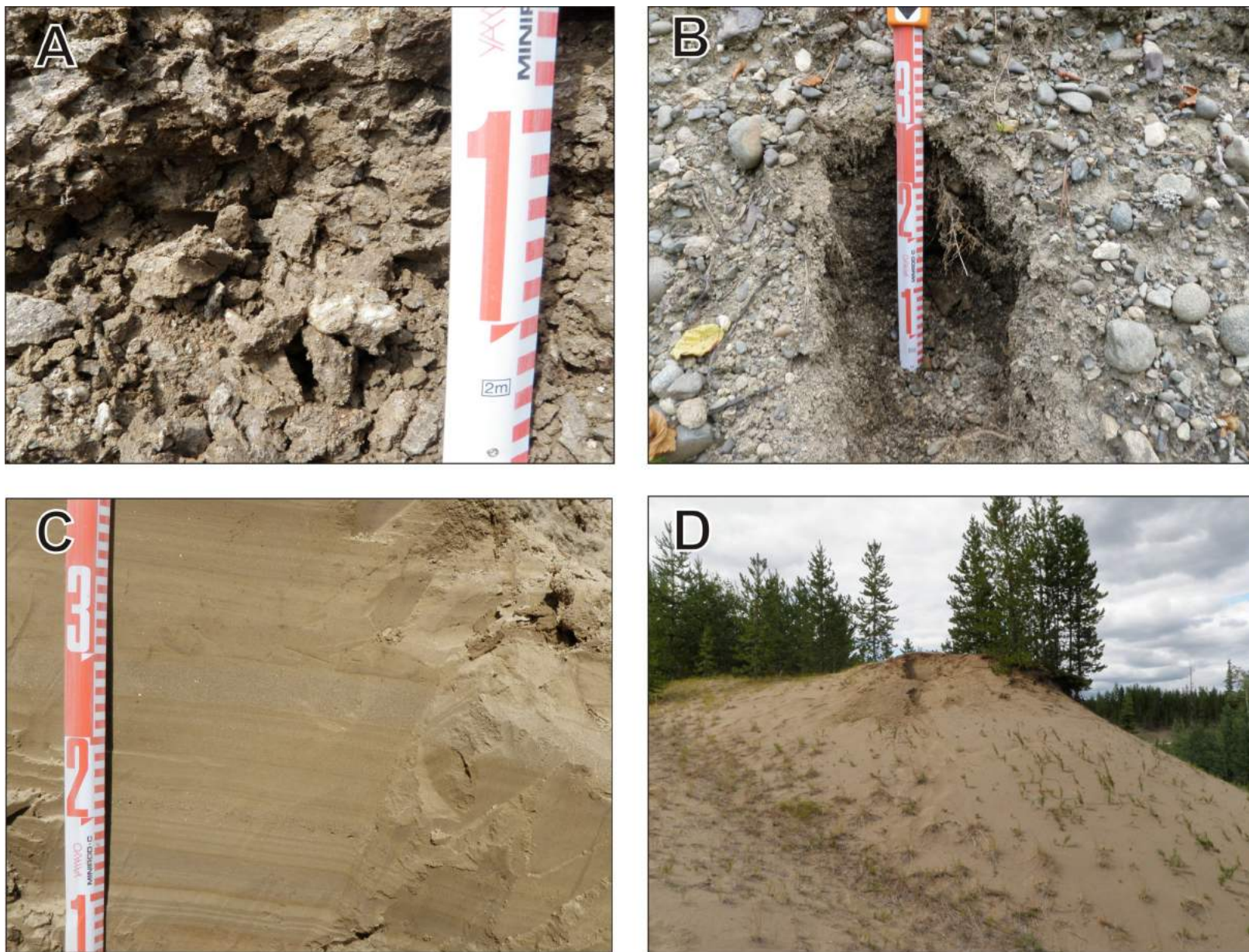


Figure 3. Surficial materials commonly found in the mapped regions of NTS 093J, central British Columbia: **A)** typical dense basal till from sample pit in NTS 093J/13; **B)** moderately sorted gravel from a glaciofluvial terrace; **C)** glaciolacustrine beds of laminated silt, clay and fine sand with some faulting; **D)** eolian dune cut by road construction.

over a bedrock outcrop, striations located on protected surfaces on the lee side (down-ice) of the feature, are likely older. Relative age control, or timing of different ice-flow events, was only possible at a few sites. At most of these sites, orientations of microflow indicators were within $\sim 035^\circ$ of each other, reflecting only minor changes in ice-flow direction, which likely occurred during deglaciation.

Some sites, however, showed dramatic differences in microflow indicator orientations. For example, southwest of Prince George three sets of striations were observed at one field station. The oldest was oriented at 150° , the second oldest at 100° and the youngest at 080° . Based on this chronology, it is possible to infer that ice flowing east from the Coast Mountains reached the area first and produced the oldest striations. The younger striations likely reflect a sequential northerly shift in dominant ice flow as ice from the Cariboo Mountains in the south interacted with ice from the Coast Mountains.

These data are in agreement with existing ice-flow data that suggest easterly flowing ice from the Coast Mountains entered the area first (Plouffe, 2000; Ward et al., 2009). To the south, ice constrained by topographic highs flowed west and northwest from the Cariboo Mountains as well as up the Bowron River valley (Paulen, 2000). The orientations of macroflow and microflow features suggest these two sources interacted south of Quesnel, with ice flow from the west appearing to be dominant. This interaction caused ice from the Cariboo Mountains to be deflected eastward to the southeast of Prince George, along the Fraser Plateau and then into the Rocky Mountain Trench. In the northern section of the study area, the dominant flow changes from east-northeast to northeast, possibly due to the same interaction. Exceptions to this occur locally where flow direction

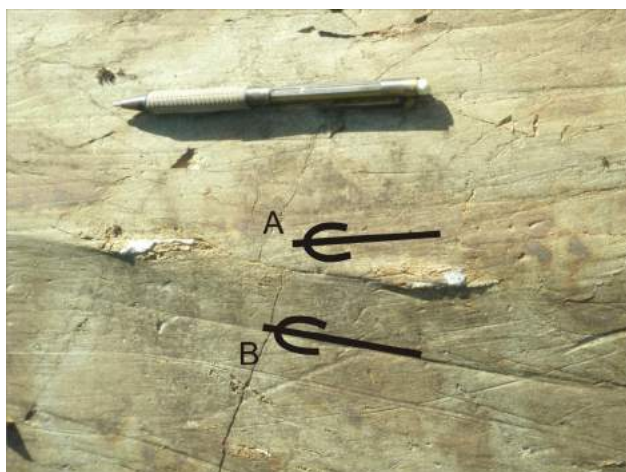


Figure 4. Glacially smoothed bedrock along Highway 16 (central British Columbia) illustrating microflow indicators of two different-aged ice flows. The older flow formed the rat tails (**A**) that are truncated by the younger flow. Rat tails show unidirectional flow and striations (**B**) generally indicate bidirectional flow. Due to the cross-cutting relationship between these two microforms, these striations suggest unidirectional flow.

changes are the result of ice thinning sufficiently enough to be influenced by topography.

Deglaciation

The timing and style of deglaciation in the study area is poorly understood. Based on the distribution of surficial deposits and glacial landforms associated with deglaciation, Fulton (1967) put forth a model of deglaciation for south-central BC. This model can be divided into the following four phases: 1) active ice phase; 2) transitional upland phase; 3) stagnant ice phase; and 4) dead ice phase. This model is the generally accepted model for deglaciation of areas in BC with low to moderate relief, and is a good framework for understanding the deglaciation of the study area. Some physiographic differences in this study area may, however, cause deviations from the general model.

The distribution of glaciofluvial and glaciolacustrine sediments and glacial features, such as meltwater channels and lateral moraines, can be critical to unravelling the deglacial history of an area. Glacial lake sediments in the higher valleys and meltwater channels subparallel to the topography delineate the locations of the ice fronts of the retreating glaciers. In the study area, this retreat appears to have been from east to west. As with many other areas in central BC that have subdued to moderate topography, glaciers in the study area first abandoned the higher elevations and then retreated to the lower areas. Ice-marginal channels were cut along irregular ice fronts as they progressively retreated downslope (a combined result of ice front retreat and downwasting of the ice mass; Figure 5). Hummocky melt-out till, and kettle-and-kame topography associated with deformed glaciofluvial sediments, is limited in the study area. This could indicate that during deglaciation the glaciers that were constrained to valleys remained active longer than Fulton's model would suggest. Further evidence that thinning ice was still active can be seen in striation data from topographically constrained areas. For example, north of Bear Lake, on Highway 97, striations in the valley indicate a north-northeast ice flow that is parallel to the valley walls. This is contrary to the surrounding streamlined features that indicate northeast was the dominant flow direction during times of unconstrained ice flow. The last glacial lake in the area, glacial Lake Fraser, left thick packages of silt and clay sediments in the Prince George region. This lake was the result of ice retreating across the Fraser Valley, but still damming the Fraser River further south. A large esker complex, occupying the Hart Highway area, north of Prince George, indicates the location of a glaciofluvial system that once fed water and sediment into this lake.

Plouffe (2000) offers evidence that similar processes occurred west of the study area with ice retreating east to west with irregular margins that were controlled by topography.

Till Geochemistry

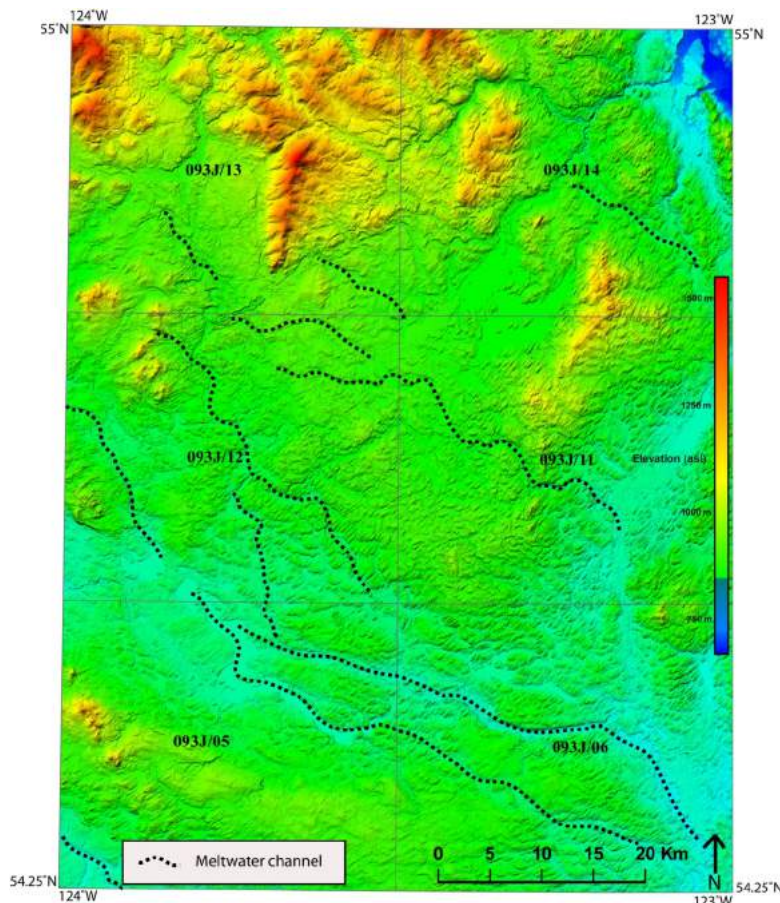


Figure 5. Ice marginal meltwater channels, which crosscut topographic highs, illustrate that ice retreated in a southwesterly direction along an irregular ice front during deglaciation in areas of subdued to moderate topography, central British Columbia.

Plouffe also suggests significant movement during the stagnation phase and a less influential dead ice phase during deglaciation. These differences from Fulton’s original model are likely a result of the increased topography in the north compared to the more subdued southern regions (where the model was developed) where deglaciation was characterized by downwasting, followed by widespread dead ice stagnation.

Postglacial deposits, in particular organic and eolian, can be useful for creating a timeline for, or chronology of, deglaciation. Basal peat, directly overlying glacial sediments, can provide a minimum age of deglaciation. Attempts have been made to find such organic deposits east of the study area, but they appear to be absent, possibly due to the warm dry climate of the early Holocene retarding paludification (Plouffe, 2000). Sand dunes, last active between ice retreat and vegetative colonization, can also provide a minimum age for deglaciation. Six sites were sampled during the 2009 field season for optically stimulated luminescence dating. If successful, these samples will provide an approximate age for when the sand was last exposed to sunlight (i.e., the last time the dunes were active).

Regional-scale till sampling can be carried out to assess the mineral potential of areas covered with drift (Paulen, 2000; Levson 2001). Detailed investigations, when possible, of regional-scale till samples with elevated or anomalous values can help define potentially mineralized zones within covered bedrock units. The preferred sampling medium for till geochemical surveys is basal till, as it is commonly considered a first derivative of bedrock (Dreimanis, 1989; Levson, 2001).

In 2008 and 2009, detailed- and regional-scale till geochemical surveys were conducted respectively. The sampling regime for both included collecting three separate 900 g samples at each sample site for: 1) analysis of the clay-sized fraction by aqua-regia digestion followed by ICP-MS at Acme Analytical Laboratories Ltd. (Vancouver, BC); 2) analysis of the silt- plus clay-sized fraction by INAA at Becquerel Laboratories Inc. (Mississauga, ON); and 3) archiving. In addition, at every 4–5 sites, a >10 kg sample was collected for heavy mineral separation and gold grain counts. These separations and counts are conducted at Overburden Drilling Management Limited (Nepean, ON). The <0.25 mm fraction heavy mineral concentration is sent for INAA determinations. Results from the INAA are used to identify samples with elevated element values and it is from these samples that

heavy minerals are picked and identified.

To quantify the accuracy and precision of these analytical data, a combination of field duplicates, analytical duplicates and reference standards are used. For every 20 samples collected in the field, one field duplicate is collected, one analytical duplicate is split and inserted into the sample sequence at the lab, and one reference standard (either an in-house BCGS standard or a certified Canada Centre for Mineral and Energy Technology [CANMET] standard) is inserted.

In 2008, till samples were collected from a total of 123 sites around two anomalies interpreted from airborne gravity survey data (Saxton Lake and 200 Road anomalies; Figure 6). Geochemical determinations around the Saxton Lake anomaly delineated a potential mineralized zone. Elements related to mineralization, such as Cu, Au, As, Cr and Ni, tend to have higher concentrations in samples down-ice of the anomaly. These results imply that there may be volcanogenic massive sulphide (VMS) mineralization associated with the transition from the high to low magnetic

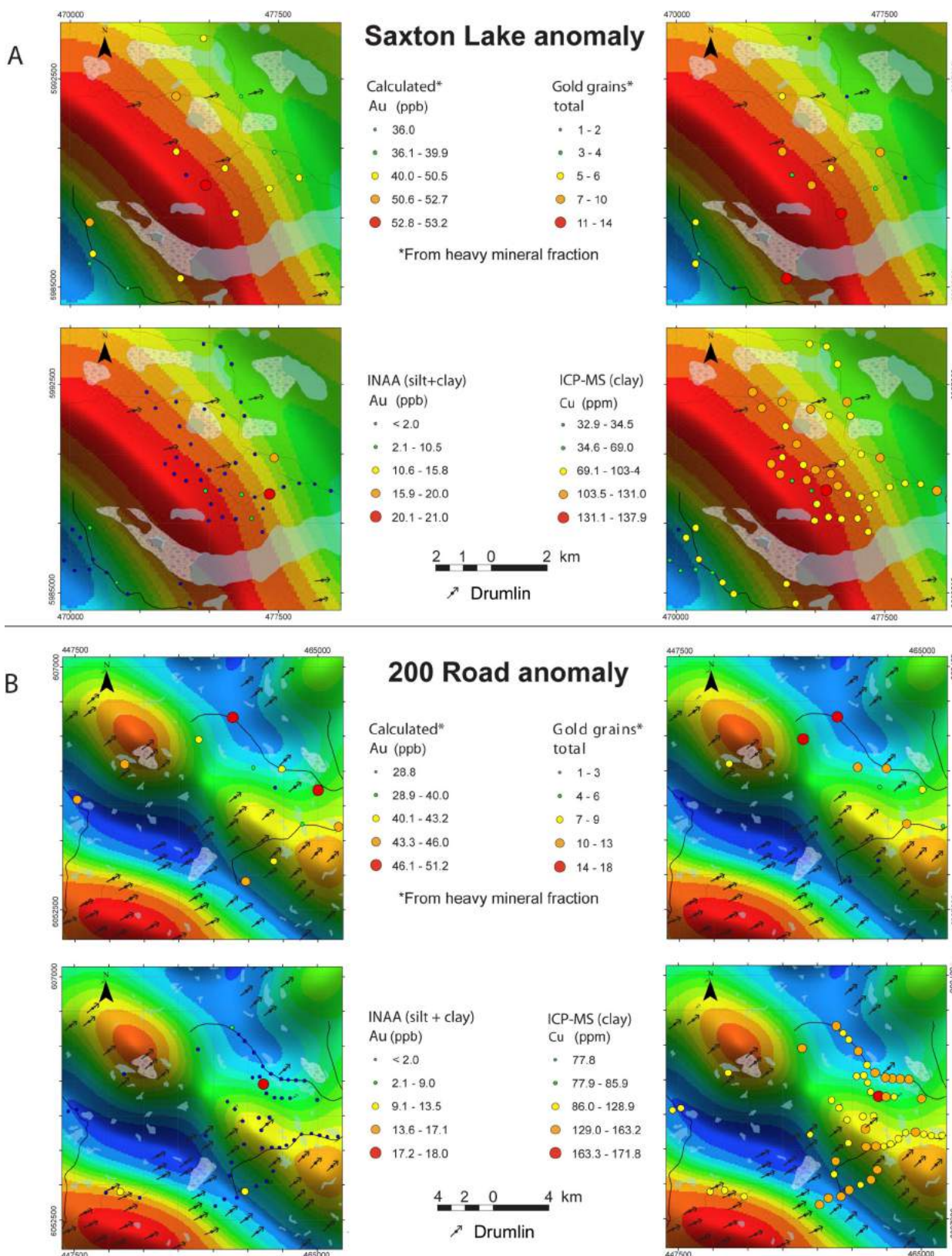


Figure 6. Copper (Cu) and gold (Au) distributions, associated with Saxton Lake (A) and 200 Road (B) linear magnetic anomalies, derived from till geochemical survey analysis. The Saxton Lake example shows elevated Cu values down-ice compared to up-ice of the anomaly. Absolute Cu values are actually higher in the 200 Road area but up-ice values are also high, reducing the contrast of the dispersal plume to the background values. In both examples, instrumental neutron activation analysis (INAA) of Au indicated low values, but gold grain counts and resultant calculated concentrations in the smaller suite of heavy mineral analysis indicate gold is present down-ice of both anomalies. Abbreviation: ICP-MS, inductively coupled plasma–mass spectrometry.

values (Figure 6). Element concentrations in the 200 Road anomaly are more subdued making it more difficult to define any mineralized zones (Figure 6). It should be noted, however, that increases in Cr and Ni are evident on the down-ice side of the geophysical anomaly. More samples were taken in the vicinity of the 200 Road anomaly in 2009 so that background values could be better defined. Road deactivation combined with large areas of eolian deposits limited where sampling could take place. In general, initial geochemical results from till samples collected in 2008 suggest that a detailed till geochemical survey conducted around geophysical anomalies, in areas where there is very little rock outcrop, is an effective way of assessing potential relationships between the geophysical anomalies and metallic mineralization.

In 2009, 670 new till samples were collected at a density of about one sample per 8 km² from NTS 093J/05, /06, /11, /12, /13 and /14 (Figure 7), using the same sampling regime described above. The geochemical analysis of these samples should be available in late 2010. Due to sampling restrictions in Carp Lake Provincial Park, thick surficial deposits (i.e., not basal till) and areas without road access, there were several large regions that could not be sampled thus decreasing the average sampling density. Detailed sampling of any geochemical anomalies may be carried out in 2010 to more accurately delineate new zones of elevated trace-element concentrations.

Future Work

Six 1:50 000 scale terrain maps will be completed in early 2011. These maps will be useful to explorationists following up on till geochemical data conducted as part of this study but also for other geochemical surveys (including their own) conducted within this portion of the QUEST Project area. Also in 2010, regions of the study area that proved difficult to access will be sampled using all-terrain vehicles and foot traverses.

Conclusion

Further progress has been made in the understanding of the glacial geological framework for a portion of the QUEST Project area. This understanding is integral to the interpretation of data from geochemical surveys that use glacially

transported sediments as a sample medium. The initial stages of terrain mapping have been completed for six 1:50 000 scale map sheets. These maps will delineate and describe surficial deposits and landforms occurring within the study area and will be useful for planning and implementing media-specific geochemical surveys. These data, combined with the compilation and collection of ice-flow data, have provided the basis for a more comprehensive understanding of the study area's ice-flow history. This improved understanding can only improve the effectiveness of drift-prospecting programs in the region.

Trace-element geochemistry of till samples collected in the vicinity of two geophysical anomalies suggest that these anomalies may be associated with metallic mineralization. This suggests that detailed till geochemical sampling, combined with an understanding of an area's glacial history, is an effective way to test geophysical anomalies within areas of thick drift and determine if they are in fact related to me-

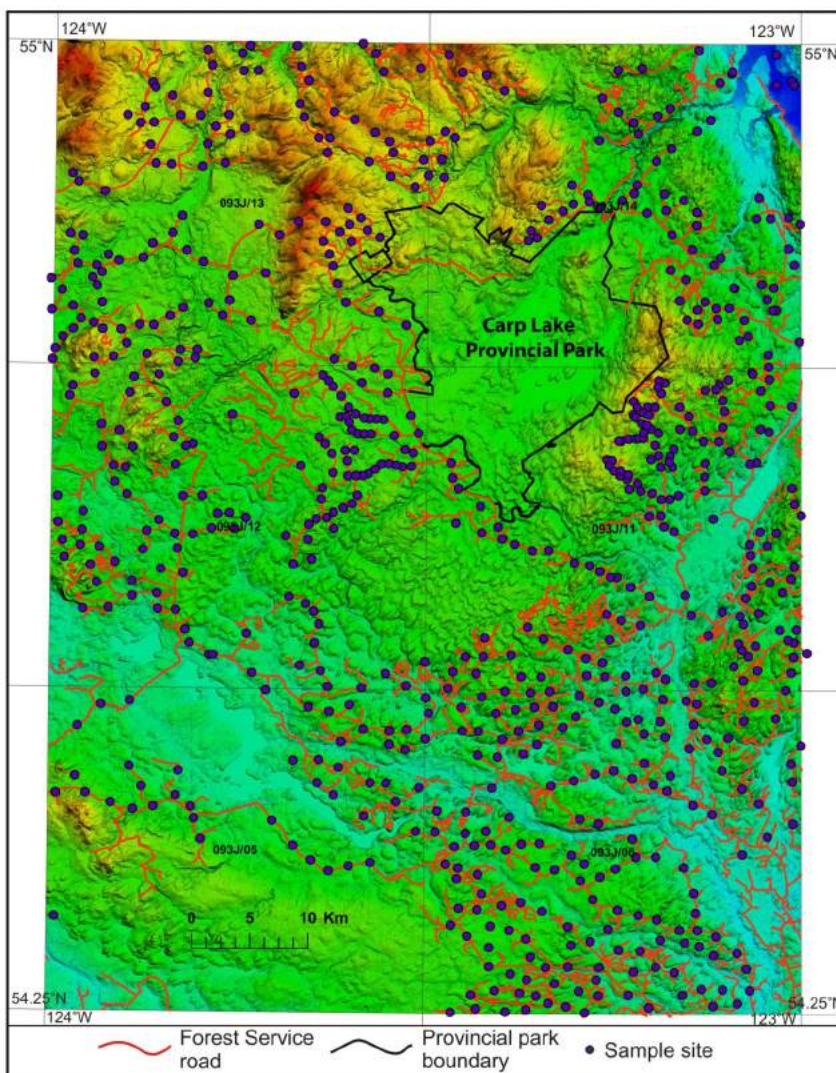


Figure 7. Till geochemical survey sample site distribution in NTS map areas 093J/05, /06, /11, /12, /13 and /14, central British Columbia.

tallic mineralization. Geochemical determinations for 670 new sites are pending for a larger portion of the study area.

Acknowledgments

The majority of funding for this project was provided by Geoscience BC. Additional funding for the heavy mineral analysis and some of the ICP-MS analysis was provided by the Mountain Pine Beetle (MPB) Program under the direction of C. Hutton (GSC, NRCan). Geochemical reference standards were provided by R.E. Lett (BCGS). C. Pennimpede, D. Vis, J. Macdonald, M. Casola and M. Brine provided able assistance in the field. A special thanks to T. Ferbey for his careful review and suggestions on the manuscript.

References

- Armstrong, J.E., Crandell, D.R., Easterbrook, D.J. and Noble, J.B. (1965): Late Pleistocene stratigraphy and chronology in south-western British Columbia and north-western Washington; *Geological Society of America Bulletin*, v. 72, p. 321–330.
- Barnett, C.T. and Kowalczyk, P.L. (2008): Airborne electromagnetics and airborne gravity in the QUEST Project area, Williams Lake to Mackenzie, British Columbia (parts of NTS 093A, B, G, H, J, K, N, O; 094C, D); *in Geoscience BC Summary of Activities 2007*, Geoscience BC, Report 2008-1, p. 1–6.
- Blais-Stevens, A. and Clague, J.J. (2007): Surficial geology, south-eastern portion of the Prince George map area British Columbia; *Geological Survey of Canada, Open File 5274*, scale 1:100 000.
- Bobrowsky, P. and Rutter, N.W. (1992): The Quaternary geologic history of the Canadian Rocky Mountains; *Géographie physique et Quaternaire*, v. 46, p. 5–50.
- Clague, J.J. (1989): Chapter 1: Quaternary geology of the Canadian Cordillera; *in Quaternary Geology of Canada and Greenland*, R.J. Fulton (ed.), *Geological Survey of Canada, Geology of Canada Series*, no. 1, p. 17–96.
- Clague, J.J. (1998a): Surficial geology, Cluculz Lake, British Columbia; *Geological Survey of Canada, Open File 3638*, scale 1:100 000.
- Clague, J.J. (1998b): Surficial geology, West Road (Blackwater) River, British Columbia; *Geological Survey of Canada, Open File 3639*, scale 1:100 000.
- Eyles, N. and Clague, J.J. (1991): Glaciolacustrine sedimentation during advance and retreat of the Cordilleran Ice Sheet in central British Columbia; *Géographie physique et Quaternaire*, v. 45, p. 317–331.
- Dreimanis, A. (1989): Tills: their genetic terminology and classification; *in Genetic Classification of Glacigenic Deposits*, R.P. Goldthwait and C.L. Matsch (ed.), A.A. Balkema, Rotterdam, p. 17–83.
- Fulton, R.J. (1967): Deglaciation studies in Kamloops region, an area of moderate relief, British Columbia; *Geological Survey of Canada, Bulletin 154*, p. 1–36.
- Holland, S.S. (1976): Land forms of British Columbia – a physiographic outline; BC Ministry of Energy, Mines and Petroleum Resources, *Bulletin 48*, 138 p.
- Howes, D.E. (1977): Terrain inventory and Late Pleistocene history of the southern part of the Nechako Plateau; BC Ministry of Environment, *Bulletin 1*, 27 p.
- Howes, D.E. and Kenk, E., editors (1997): Terrain classification system for British Columbia (revised edition); BC Ministry of Environment, *Manual 10 (Version 2)*, 102 p.
- Jackson, L.E. and Clague, J.J. (1991): The Cordilleran Ice Sheet: one hundred and fifty years of exploration and discovery; *Géographie physique et Quaternaire*, v. 45, p. 269–280.
- Levson, V.M. (2001): Regional till geochemical surveys in the Canadian Cordillera: sample media, methods and anomaly evaluation; *in Drift Exploration in Glaciated Terrain*, M.B. McClenaghan, P.T. Bobrowsky, G.E.M. Hall and S.J. Cook (ed.), *The Geological Society, Special Publication*, no. 185, p. 45–68.
- Levson, V.M. and Giles, T.R. (1997): Quaternary geology and till geochemistry studies in the Nechako and Fraser plateaus, central British Columbia; *in Interior Plateau Geoscience Project: Summary of Geological, Geochemical and Geophysical Studies*, L.J. Diakow, P. Metcalfe and J. Newell (ed.), BC Ministry of Energy, Mines and Petroleum Resources, *Paper 1997-2*, p. 121–145.
- Mathews, W.H. (1986): Physiographic map of the Canadian Cordillera; *Geological Survey of Canada, Map 1701A*, scale 1:5 000 000.
- Paulen, R.C. (2000): Appendix VI, ice flow patterns and copper dispersal trains Eureka Property - Hudson Bay Exploration; *in Geological, Geophysical and Geochemical Surveys, Trenching, Drilling Report on the Eureka Property*, G.E. Bidwell, G. Mulligan and R.C. Paulen (ed.), BC Ministry of Energy, Mines and Petroleum Resources, *Assessment Report 26 531*, 88 p.
- Plouffe, A. (1997): Ice flow and late glacial lakes of the Fraser glaciation, central British Columbia; *in Current Research 1997-A*, *Geological Survey of Canada*, p. 133–143.
- Plouffe, A. (2000): Quaternary geology of the Fort Fraser and Manson River map areas, central British Columbia; *Geological Survey of Canada, Bulletin 554*, 62 p.
- Resources Inventory Committee (1996): Guidelines and standards for terrain mapping in British Columbia; *Government of British Columbia*, 216 p.
- Tipper, H.W. (1971a): Glacial geomorphology and Pleistocene history of central British Columbia; *Geological Survey of Canada, Bulletin 196*, 89 p.
- Tipper, H.W. (1971b): Multiple glaciations in central British Columbia; *Canadian Journal of Earth Sciences*, v. 8, p. 743–752.
- Ward, B.C., Geertsema, M., Telka, A.M. and Mathewes, R.W. (2008): A paleoecological record of climatic deterioration from middle to late Wisconsinan time on the interior plateau of British Columbia, Canada; 33rd International Geological Congress, August 6–14, 2008, Oslo, Norway.
- Ward, B., Maynard, D., Geertsema, M. and Rabb, T. (2009): Ice-flow history, drift thickness and drift prospecting for a portion of the QUEST Project area, central British Columbia (NTS 093G, H [west half], J); *in Geoscience BC Summary of Activities 2008*, Geoscience BC, Report 2009-1, p. 25–32.

Quaternary Geology and Till Geochemistry of the Nadina River Map Area (NTS 093E/15), West-Central British Columbia

T. Ferbey, British Columbia Geological Survey, Victoria, BC, travis.ferbey@gov.bc.ca

Ferbey, T. (2010): Quaternary geology and till geochemistry of the Nadina River map area (NTS 093E/15), west-central British Columbia; in *Geoscience BC Summary of Activities 2009*, Geoscience BC, Report 2010-1, p. 43–48.

Introduction

The Tahtsa Lake district has high potential to host new porphyry Cu±Mo and polymetallic vein-style mineralization (including Au). Centred on Tahtsa Lake (approximately 100 km south of Houston, British Columbia; Figure 1), this district, and areas immediately adjacent to it, have a rich mineral exploration history and at present host a producing porphyry Cu-Mo mine (Huckleberry mine) and numerous developed Cu±Mo prospects (e.g., Berg, Lucky Ship; MacIntyre, 1985). This district also hosts epithermal and perhaps volcanogenic massive sulphide-style mineralization, and polymetallic veins, as suggested by past producers such as Equity Silver and Emerald Glacier (MacIntyre, 1985; MacIntyre et al., 2004; Alldrick et al., 2007; Figure 2). Currently there are large areas of unstaked ground within, and adjacent to, the northern portion of the Tahtsa Lake district. Much of this area is covered with glacial drift and continuous bedrock outcrop is limited to the higher peaks and their steep flanks. Till geochemical surveys are an effective method for assessing the metallic mineral potential of areas covered with glacial drift and are ideally suited to assessing the potential for new mineralization in this area. Till geochemical surveys are also well suited for following up on airborne geophysical data recently acquired by Geoscience BC for the QUEST-West Project area (Kowalczyk, 2009), where drift can cover anomalous bedrock.

A two-year Quaternary geology and till geochemistry program is currently underway within the northern portion of the Tahtsa Lake district and adjacent areas (NTS map areas 093E/15, /16, 093L/01, /02; Figure 2). The objectives of this program are to

- 1) characterize and delineate the Quaternary materials that occur in the study area and reconstruct the region's ice-flow history; and
- 2) assess the economic potential of covered bedrock (subcrop) by conducting a till geochemistry survey.

Keywords: *till geochemical survey, trace-element geochemistry, heavy minerals, gold grain counts, porphyry Cu, polymetallic vein, Tahtsa Lake district*

This publication is also available, free of charge, as colour digital files in Adobe Acrobat® PDF format from the Geoscience BC website: <http://www.geosciencebc.com/s/DataReleases.asp>.

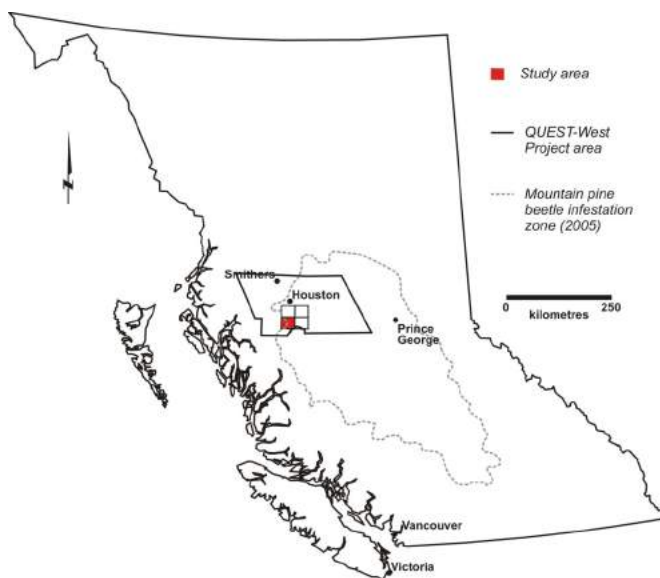


Figure 1. Location of study area in west-central British Columbia.

The study area falls within the mountain pine beetle-impacted zone and Geoscience BC's QUEST-West Project area. The goal of this project is to provide high-quality, regional-scale, geochemical data to the mineral exploration community that will help guide exploration efforts. Integrating interpretations of these data with other geochemical and geophysical data being collected by Geoscience BC in the QUEST-West Project area, and historic data that have been collected by the British Columbia Geological Survey (BCGS) and the Geological Survey of Canada (GSC), will provide a powerful tool for companies exploring in this drift-covered area.

The focus of this paper is surficial geology mapping, and the sampling component of a till geochemical survey, completed within the Nadina River map area (NTS 093E/15) during the 2009 field season.

Study Area

The study area is located in west-central BC, approximately 100 km southwest of Houston, in NTS map area 093E/15 (Figures 1, 2). It is accessible by Forest Service, private and

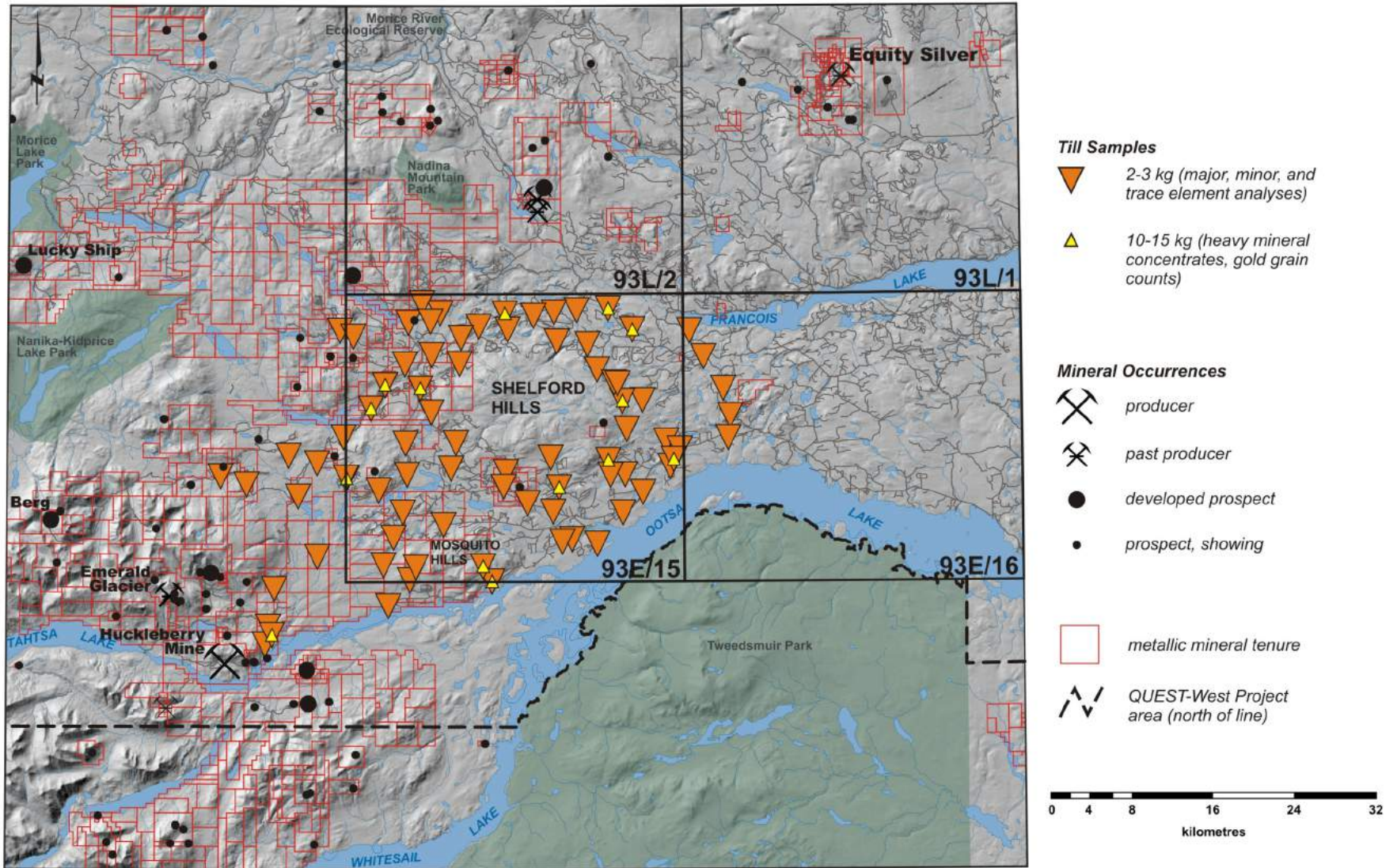


Figure 2. Locations of till samples within the Nadina River map area (NTS 093E/15), British Columbia. Additional samples were collected outside the map area to take into account possible east and/or west transport.

abandoned mine and mineral exploration roads. The majority of the study area is situated in the Nechako Plateau, a subdivision of the Interior Plateau. The Nechako Plateau is an area of low relief with flat or gently rolling topography (Holland, 1976), most of which is covered by a thick package of glacial sediments (Figure 3). Although bedrock outcrop is relatively uncommon, some exposures can be found at the stoss (i.e., up-ice) end of crag-and-tail forms, along lake shorelines, on higher ground within Shelford and Mosquito hills, and on local small-scale erosional remnants that stand above the plateau surface to the west and northwest of Shelford Hills. The very southwest corner of the study area is situated in the Tahtsa Ranges (Holland, 1976), a northwest-trending belt of nongranitic mountains.

Bedrock Geology

The Tahtsa Lake district lies within the Stikine Terrane, just east of the Coast Crystalline Belt (Monger et al., 1991). The west half of the study area is underlain mainly by Early to Middle Jurassic Hazelton Group volcanic and sedimentary rocks (MacIntyre, 1985). In places, these rocks are unconformably overlain by Middle to Late Jurassic Bowser Lake Group marine sedimentary rocks and Early Cretaceous Skeena Group turbidites and local basalt flows. These rocks are in turn unconformably overlain by felsic pyroclastic rocks, felsic flows and younger basaltic flows of the Early to Late Cretaceous Kasalka Group volcanic rocks. Many small- to medium-sized, Late Cretaceous to Early Tertiary stocks have intruded these volcanic piles and sedimentary packages (MacIntyre, 1985). The east half of the study area is dominantly underlain by Late Cretaceous to Tertiary Ootsa Lake Group and Eocene Endako Group volcanic rocks. There is a strong correlation between the location of intrusive rock types (in particular, porphyritic intrusions like those of the Late Cretaceous Bulkley suite) and the locations of Cu, Mo, Au, Pb, Zn and Ag mineralization (Carter, 1981; MacIntyre, 1985).



Figure 3. Subdued topography of the southwest corner of the study area, British Columbia. View is towards the east with Mosquito Hills in the background.

Quaternary Geology

Till is the dominant surficial material type within the study area. In lower valley settings, and on hill flanks, it occurs as thick units (>2 m thick) that typically overlie glacially eroded bedrock. In high elevations, it occurs as thinner veneer units (<1 m thick) that are closely associated, and discontinuous, with colluvium and bedrock. The surface expression of till most often conforms to underlying bedrock topography but also can be streamlined, as seen in the drumlinized and fluted terrain between the south and south-east flank of Shelford Hills and the northern shore of Ootsa Lake.

Glaciofluvial sand and gravel can also be found within the study area. They occur in fan-like features at the mouths of gulleys that head in higher ground such as Shelford and Mosquito hills. They also occur within late-glacial to deglacial drainage systems (now abandoned) as outwash plains and esker-like ridges. Glaciolacustrine and lacustrine sediments only rarely occur within the study area. Thick organic units are, however, common along the shorelines of smaller lakes and in low-lying areas that separate these smaller lakes when they occur in chains.

Ferbey and Levson (2001a, b, 2007) built on previous work by Stumpf et al. (2000) that indicated there was an ice-flow reversal in west-central BC during the Late Wisconsinan glacial maximum. During the onset of glaciation, ice flowed radially from accumulation centres, such as the Coast Mountains, towards central BC. Sometime during the glacial maximum, however, the ice divide over the Coast Mountains migrated east into central BC resulting in an ice-flow reversal. Glaciers were now flowing west across some parts of the western Nechako Plateau (including the study area), over the Coast Mountains and towards the Pacific Ocean. Eastward ice flow resumed once the ice divide migrated back over the axis of the Coast Mountains, and continued until the close of the Late Wisconsinan glaciation.

Evidence for this ice-flow reversal in the Huckleberry mine region is seen in macro-scale glacial landforms (e.g., crag-and-tail forms, roches moutonnées) and micro-scale ice-flow indicators (e.g., rat tails, roches moutonnées) on bedrock outcrop in valley bottoms and at higher elevation sites (i.e., >1500 m asl). This ice-flow reversal is also detectable in trace-element till geochemical data from Huckleberry mine (Ferbey and Levson, 2007).

Previous Work

Directly south and adjacent to the study area, Ferbey and Levson (2001a, b, 2003, 2007) and Ferbey (2004) conducted a detailed study of the Quaternary geology and till geochemistry of the Huckleberry mine region. These studies demonstrate a clear relationship between till samples el-

evated in Cu, Mo, Au, Ag and Zn and the Cu-Mo ore zones at Huckleberry mine and smaller-scale polymetallic vein occurrences on the mine property. Lateral and vertical variability in trace-element concentrations in till at Huckleberry mine provide further evidence for an ice-flow reversal in the region during the Late Wisconsinan glacial maximum (Ferbey and Levson, 2007). These results suggest that interpreting trace-element geochemical data from tills or soils in this region can be complex, in particular when considering transport direction.

Plouffe and Ballantyne (1993), Plouffe (1995), Plouffe et al. (2001) and Levson and Mate (2002) have also conducted till geochemistry surveys to the east of the study area, in NTS map areas 093F and K. Using percentile plots of precious-metal, base-metal, and pathfinder element concentrations, and/or gold grain counts, each of these surveys identifies prospective ground where there are no known mineral occurrences.

Methods

Surficial Geology Mapping and Reconstruction of Ice-Flow History

Surficial geology mapping will be completed for each of the four map sheets in the study area. This mapping will be conducted at 1:50 000 scale using aerial photographs (1:40 000 scale black and white), digital orthophotographs and other available remotely sensed imagery (e.g., Landsat). An integral part of this component is the reconstruction of the region's ice-flow history using macro-scale landforms (e.g., drumlins, flutes, crag-and-tail forms) and outcrop-scale glacial features, such as striations, rat tails and roches moutonnées. Surficial geology mapping will characterize and delineate Quaternary materials occurring within the study area and the reconstructed ice-flow history will be used to determine the transport direction of glacial sediments. The efficiency and effectiveness of till sampling, and interpretation of resultant geochemical data, will be increased by knowing where basal till is likely to occur and the direction it was transported. Surficial geology mapping is currently in progress for NTS map area 093E/15.

Basal Till Sampling

Till geochemical surveys can detect known sources of mineralization and identify new geochemical exploration targets (e.g., Levson et al., 1994; Cook et al., 1995; Sibbick and Kerr, 1995; Plouffe, 1997; Levson, 2002; Ferbey, 2009). Till geochemical surveys are well suited to assessing the mineral potential of ground covered by glacial drift. Basal till, a specific type of drift and the sample medium used in these surveys, is ideal for these assessments as it has a relatively simple transport history, is deposited directly down-ice of its source, and produces a geochemical signa-

ture that is areally more extensive than its bedrock source and therefore, at a regional-scale, can be more easily detected (Levson, 2001). The area under investigation as part of this study is thought to fall within the area affected by the Late Wisconsinan ice-flow reversal (Ferbey and Levson, 2001a, b, 2007). Its influence on the transport direction of basal tills was taken into consideration when designing and implementing the till geochemical survey component of this program.

During the 2009 field season, 2–3 kg till samples were collected at 84 sample sites for major, minor and trace-element geochemical analyses (Figures 2, 4). An additional 16 till samples, each weighing 10–15 kg, were collected for heavy mineral separation and gold grain counts (Figure 2). These larger samples were collected at sites where an adequate amount of sample material was exposed. Given that net transport direction in the study area was likely affected by an ice-flow reversal during the Late Wisconsinan glacial maximum, till samples were collected outside of NTS 093E/15 to take into account possible east and/or west transport of basal till. Till sample density for this survey is one sample per 14 km². For simplicity, areas inaccessible by truck (e.g., Shelford Hills), and areas where till does not occur, were included in this calculation.

Till samples collected for major, minor and trace-element analyses are being sieved, and decanted and centrifuged to produce a silt- plus clay-sized (<0.063 mm) and clay-sized (<0.002 mm) fraction. This sample preparation is being conducted at Acme Analytical Laboratories Ltd. (Vancouver, BC). Heavy mineral samples have been sent to Overburden Drilling Management Limited (ODM; Nepean, ON), where heavy mineral (0.25–2.0 mm) and gold grain (<2.0 mm) concentrates are being produced using a combination of gravity tabling and heavy liquids.

On the 2–3 kg samples, minor and trace-element analyses (37 elements) will be conducted on splits of the silt- plus



Figure 4. Typical sample site in a roadcut, west-central British Columbia. In the foreground is a 2–3 kg sample.

clay- and clay-sized fractions, respectively, by inductively coupled plasma–mass spectrometry (ICP-MS), following an aqua-regia digestion. Major element analyses will be conducted on a split of the silt- plus clay-sized fraction only using inductively coupled plasma–emission spectrometry (ICP-ES), following a lithium metaborate/tetraborate fusion and dilute nitric acid digestion. This analytical work will be conducted at Acme Analytical Laboratories Ltd. (Vancouver, BC).

Also as part of this project, a split of the silt- plus clay-sized fraction will be analyzed for 35 elements by instrumental neutron activation analysis (INAA) at Becquerel Laboratories Inc. (Mississauga, ON). Instrumental neutron activation analyses for elements such as Au, Ba and Cr complement those produced by aqua-regia digestion followed by ICP-MS as they are considered to be a near-total determination and hence more representative of rock-forming and economic mineral geochemistry. Additionally, INAA determinations will be conducted on bulk heavy mineral concentrates produced from the 10–15 kg samples. Heavy mineral picking, scanning electron microscope (SEM) analyses on difficult-to-identify heavy mineral grains, and pebble counts may be conducted on these samples at a later date. Results from INAA will dictate for which samples, if any, these additional and costly analyses are warranted.

Quality Control

Quality control measures for analytical determinations include the use of field duplicates, analytical duplicates and reference standards. For each block of 20 samples submitted for analysis, one field duplicate (taken at a randomly selected sample site), one analytical duplicate (a sample split after sample preparation but before analysis) and one reference standard will be included in INAA and ICP-MS analysis. Reference standards used will be a combination of certified Canada Centre for Mineral and Energy Technology (CANMET) and in-house BCGS geochemical reference materials. Duplicate samples will be used to measure sampling and analytical variability, whereas reference standards will be used to measure the accuracy and precision of the analytical methods.

Upcoming Data Releases and Future Work

Till geochemical data for the Nadina River map area (NTS 093E/15) will be the topic of a combined BCGS Open File and Geoscience BC Report to be released in late spring 2010. This report will present data from the geochemical survey discussed here, including interpretations of these data in the context of metallic mineral exploration and the region's complex ice-flow history.

Field crews will return to the study area during the 2010 summer field season and complete data collection for the Wistaria, Colleymount and Owen Lake map areas (NTS

093E/16, L/01, /02). The methods used to complete this work will be the same as those presented in this report for the Nadina River map area (NTS 093E/15).

Summary

The 2009 field season saw the completion of fieldwork for year one of a two-year Quaternary geology program that is designed to assess the mineral potential of the northern portion of the Tahtsa Lake district and adjacent areas (NTS 093E/15, /16, 093L/01, /02). This study area falls within Geoscience BC's QUEST-West Project area where additional geochemical data have been compiled and collected, mineral occurrence data (i.e., MINFILE, 2009) have been updated, and helicopter-borne time domain electromagnetic and gravity data have been acquired. The focus of this year's work is the Nadina River map area (NTS 093E/15) where 84 samples of basal till, each weighing 2–3 kg, were collected for major, minor and trace-element geochemical analyses, and an additional 16 till samples, each weighing 10–15 kg, were collected for separation and analysis of heavy mineral concentrates and gold grain counts. Ongoing and complementary to this till geochemical survey, is 1:50 000 scale surficial geology mapping and a regional ice-flow study. Given that the study area experienced an ice-flow reversal during the Late Wisconsinan glacial maximum, assessing and quantifying net transport direction of basal till in the study area will be a significant contribution to the understanding of detrital dispersion for the region. An understanding of these variables must exist prior to further investigation of any till samples, collected as part of this study, that are elevated in an element(s) of interest. An assessment of net transport direction will also be of interest to mineral exploration companies working in the area, who are conducting their own surficial sediment geochemistry surveys.

Acknowledgments

This year's program has truly been a collaborative effort and the author would like to gratefully acknowledge Geoscience BC for analytical support; the Smithers Exploration Group (C. Ogryzlo and J. L'Orsa); Northwest Community College (T. Reedy and R. Maurer) for sponsoring a graduate of their Reclamation and Prospecting Program to assist with fieldwork; and Huckleberry Mine Ltd. (B. Mracek, W. Curtis and F. Sayeed) for allowing the field crew to stay at the minesite. R.E. Gawa is thanked for his assistance in the field. The author would also like to thank L.J. Diakow and D.G. MacIntyre for discussions on, and their insight into, local bedrock lithologies. R.E. Lett is thanked for assistance with geochemical reference standards. The author would also like to thank P.L. Ogryzlo for so freely sharing his ideas on porphyry Cu deposits and how and where he believes the next ones will be found.

T.E. Demchuk is thanked for her review of an earlier version of this manuscript.

References

- Alldrick, D.J., MacIntyre, D.G. and Villeneuve, M.E. (2007): Geology, mineral deposits, and exploration potential of the Skeena Group (NTS 093E, L, M; 103I), central British Columbia; *in* Geological Fieldwork 2006, BC Ministry of Energy, Mines and Petroleum Resources, Paper 2007-1, p. 1–17.
- Carter, N.C. (1981): Porphyry copper and molybdenum deposits, west-central British Columbia; BC Ministry of Energy, Mines and Petroleum Resources, Bulletin 64, 150 p.
- Cook, S.J., Levson, V.M., Giles, T.R. and Jackaman, W. (1995): A comparison of regional lake sediment and till geochemistry surveys: a case study from the Fawnie Creek area, central British Columbia; *Exploration Mining Geology*, v. 4, p. 93–101.
- Ferbey, T. (2004): Quaternary geology, ice-flow history and till geochemistry of the Huckleberry mine region, west-central British Columbia; M.Sc. thesis, University of Victoria, 301 p.
- Ferbey, T. (2009): Till geochemical exploration targets, Redstone and Loomis Lake map areas (NTS 93B/04 and 05), central British Columbia; BC Ministry of Energy, Mines and Petroleum Resources, Open File 2009-9, 52 p.
- Ferbey, T. and Levson, V.M. (2001a): Quaternary geology and till geochemistry of the Huckleberry mine area; *in* Geological Fieldwork 2000, BC Ministry of Energy, Mines and Petroleum Resources, Paper 2001-1, p. 397–410.
- Ferbey, T. and Levson, V.M. (2001b): Ice flow history of the Tahtsa Lake – Ootsa Lake region; BC Ministry of Energy, Mines and Petroleum Resources, Open File 2001-8, 1:110 000 scale map.
- Ferbey, T. and Levson, V.M. (2003): Surficial geology of the Huckleberry mine area; BC Ministry of Energy, Mines and Petroleum Resources, Open File 2003-2, 1:15 000 scale map.
- Ferbey, T. and Levson, V.M. (2007): The influence of ice-flow reversals on the vertical and horizontal distribution of trace elements in tills, Huckleberry mine area, west-central British Columbia; *in* Application of Till and Stream Sediment Heavy Mineral and Geochemical Methods to Mineral Exploration in Western and Northern Canada, R.C. Paulen and I. McMartin (ed.), Geological Association of Canada, Short Course Notes 18, p. 145–151.
- Holland, S.S. (1976): Landforms of British Columbia: a physiographic outline; BC Ministry of Energy, Mines and Petroleum Resources, Bulletin 48, 138 p.
- Kowalczyk, P.K. (2009): QUEST-West geophysics in central British Columbia (NTS 093E, F, G, K, L, M, N, 103I): new regional gravity and helicopter time-domain electromagnetic data; *in* Geoscience BC Summary of Activities 2008, Geoscience BC, Report 2009-1, p. 1–6.
- Levson, V.M. (2001): Regional till geochemical surveys in the Canadian Cordillera: sample media, methods, and anomaly evaluation; *in* Drift Exploration in Glaciated Terrain, M.B. McClenaghan, P.T. Bobrowsky, G.E.M. Hall and S.J. Cook (ed.), Geological Society, Special Publication, no. 185, p. 45–68.
- Levson, V.M. (2002): Quaternary geology and till geochemistry of the Babine porphyry copper belt, British Columbia (NTS 93 L/9, 16, M/1, 2, 7, 8); BC Ministry of Energy, Mines and Petroleum Resources, Bulletin 110, 278 p.
- Levson, V.M. and Mate, D.J. (2002): Till geochemistry of the Tetachuck Lake and Marilla map areas (NTS 93F/5 and F/12); BC Ministry of Energy, Mines and Petroleum Resources, Open File 2002-11, 180 p.
- Levson, V.M., Giles, T.R., Cook, S.J. and Jackaman, W. (1994): Till geochemistry of the Fawnie Creek area (93F/03); BC Ministry of Energy, Mines and Petroleum Resources, Open File 1994-18, 40 p.
- MacIntyre, D.G. (1985): Geology and mineral deposits of the Tahtsa Lake District, west-central British Columbia; BC Ministry of Energy, Mines and Petroleum Resources, Bulletin 75, 82 p.
- MacIntyre, D.G., McMillan, R.H. and Villeneuve, M.E. (2004): The mid-Cretaceous Rocky Ridge Formation – important host rocks for VMS and related deposits in central British Columbia; *in* Geological Fieldwork 2003, BC Ministry of Energy, Mines and Petroleum Resources, Paper 2004-1, p. 231–247.
- MINFILE (2009): MINFILE BC mineral deposits database; BC Ministry of Energy, Mines and Petroleum Resources, URL <<http://minfile.ca>> [November 2009].
- Monger, J.W.H., Wheeler, J.O., Tipper, H.W., Gabrielse, H., Harms, T., Struik, L.C., Campbell, R.B., Dodds, C.J., Gehrels, G.E. and O'Brien, J. (1991): Cordilleran terranes (Chapter 8: Upper Devonian to Middle Jurassic assemblages); *in* Geology of the Cordilleran Orogen in Canada, H. Gabrielse and C.J. Yorath (ed.), Geological Survey of Canada, Geology of Canada Series, no. 4, p. 281–327.
- Plouffe, A. (1995): Geochemistry, lithology, mineralogy, and visible gold grain content of till in the Manson River and Fort Fraser map areas, central British Columbia (NTS 93K and N); Geological Survey of Canada, Open File 3194, 119 p.
- Plouffe, A. (1997): Reconnaissance till geochemistry on the Chilcotin Plateau (92O/5 and 12); *in* Interior Plateau Geoscience Project: Summary of Geological, Geochemical and Geophysical Studies (092N, 092O, 093B, 093C, 093F, 093G, 093G), L.J. Diakow, P. Metcalfe and J. Newell (ed.), BC Ministry of Energy, Mines and Petroleum Resources, Paper 1997-2, p. 145–157.
- Plouffe, A. and Ballantyne, S.B. (1993): Regional till geochemistry, Manson River and Fort Fraser area, British Columbia (93K, 93N), silt plus clay and clay size fractions; Geological Survey of Canada, Open File 2593, 210 p.
- Plouffe, A., Levson, V.M. and Mate, D.J. (2001): Till geochemistry of the Nechako River map area (NTS 93F), central British Columbia; Geological Survey of Canada, Open File 4166, 66 p.
- Sibbick, S.J. and Kerr, D.E. (1995): Till geochemistry of the Mount Milligan area, north-central British Columbia; recommendations for drift exploration for porphyry copper-gold mineralization; *in* Drift Exploration in the Canadian Cordillera, P.T. Bobrowsky, S.J. Sibbick, J.M. Newell and P. Matyssek (ed.), BC Ministry of Energy, Mines and Petroleum Resources, Paper 1995-2, p. 167–180.
- Stumpf, A.J., Broster, B.E. and Levson, V.M. (2000): Multiphase flow of the Late Wisconsinan Cordilleran ice sheet in western Canada; *Geological Society of America Bulletin*, v. 112, p. 1850–1863.

Geochemical and Physical Variations in the Late Triassic Nicola Arc and Metallogenic Implications, Central British Columbia (NTS 092P, 093A, N): Preliminary Results

T. Bissig, Mineral Deposit Research Unit, University of British Columbia, Vancouver, BC, tbissig@eos.ubc.ca

S. Vaca, Mineral Deposit Research Unit, University of British Columbia, Vancouver, BC

P. Schiarizza, British Columbia Geological Survey, Victoria, BC

C. Hart, Mineral Deposit Research Unit, University of British Columbia, Vancouver, BC

Bissig, T., Vaca, S., Schiarizza, P. and Hart, C. (2010): Geochemical and physical variations in the Late Triassic Nicola Arc and metallogenic implications, central British Columbia (NTS 092P, 093A, N): preliminary results; *in* Geoscience BC Summary of Activities 2009, Geoscience BC, Report 2010-1, p. 49–52.

Introduction

The Late Triassic Nicola Group marine arc sequence in south-central British Columbia and its northward continuation, the Takla Group, largely define the Quesnel oceanic arc terrane (Figure 1). The terrane hosts most of the alkalic copper-gold deposits and prospects in BC, including Mount Milligan, Lorraine, Mount Polley, Afton/Ajax and Copper Mountain. Additional alkalic porphyry copper-gold deposits, most importantly Galore Creek, occur in the Stikine Terrane, which is generally accepted to represent the continuation of the Quesnel arc (e.g., Nelson and Colpron, 2007). Porphyry copper-gold (\pm silver \pm platinum group element) deposits related to alkalic magmatism are rare globally but well represented in BC. They are scattered over a combined strike length of approximately 1600 km.

Exploration for alkalic porphyry copper-gold deposits in BC is challenging because of poor exposure and locally thick glacial overburden. Moreover, unlike their calcalkalic cousins, alkalic porphyry deposits have more cryptic alteration footprints (e.g., Jensen and Barton, 2000). This project aims to provide new exploration guidelines by looking at along-strike variations in the Quesnel volcanic arc and identifying physical, chemical and volcanological characteristics unique to areas where porphyry copper-gold mineralization is known. Fieldwork initiated in June 2009 and observations presented herein are preliminary.

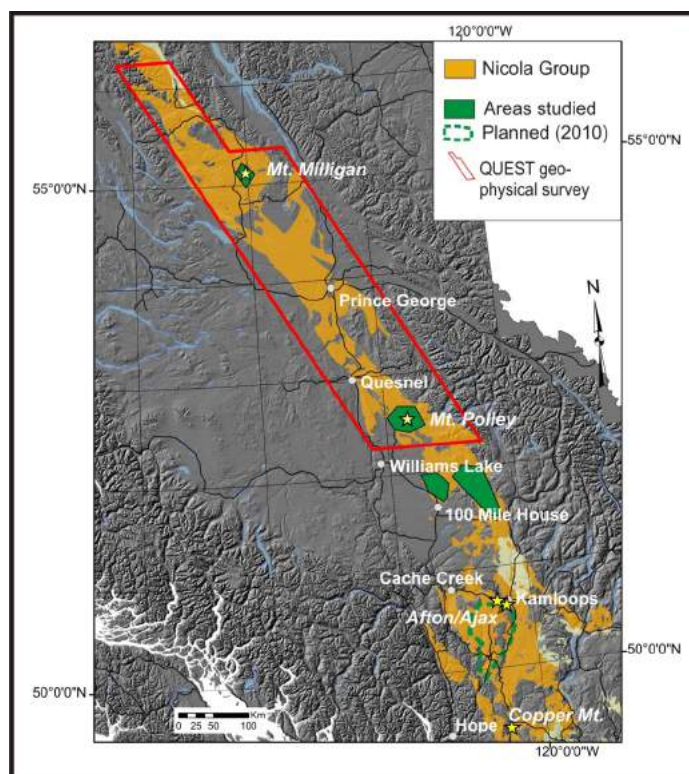


Figure 1. Location of areas studied in 2009 and major alkalic copper-gold porphyry deposits (yellow stars) hosted by the Nicola and Takla groups, which largely define the Quesnel Terrane in central British Columbia. Figure compiled using digital-elevation data from GeoBase (Canadian Council on Geomatics, 2010) with post-processing by K. Shimamura (Geological Survey of Canada); BC Geological Survey MINFILE database (porphyry occurrences; MINFILE, 2010); and the tectonic assemblage map of the Vancouver area (Journey et al., 2000).

Nicola Group

The Nicola arc sequences are dominated by submarine basaltic to andesitic augite \pm plagioclase-phyric lavas and associated volcanoclastic rocks. The Nicola Group derives its name from exposures south of Nicola Lake near Merritt (Dawson, 1879) and has been studied in most detail in

Keywords: Nicola Group, alkalic porphyry, physical properties, basalt, petrochemistry

This publication is also available, free of charge, as colour digital files in Adobe Acrobat® PDF format from the Geoscience BC website: <http://www.geosciencebc.com/s/DataReleases.asp>.

south-central BC, where it has been subdivided into an eastern, central and western belt (e.g., Preto, 1977; Mortimer, 1987). The eastern belt is dominated by distal volcano-sedimentary facies derived from augite-porphyrific basalt and andesite. Compositionally similar proximal deposits, including lavas, occur in the central belt. The western belt consists principally of lavas and volcanoclastic rocks ranging from basalt to rhyolite. Recent and ongoing mapping by the BC Geological Survey (e.g., Schiarizza and Blingh, 2008; Schiarizza et al., 2008) north and east of 100 Mile House subdivides the Nicola Group in that area into a lower volcano-sedimentary unit containing black argillite, limestone and volcanoclastic rocks; a middle unit containing submarine augite-phyric basalt and basalt breccia; and an upper unit containing partially subaerial polymictic volcanoclastic rocks. A common characteristic throughout the entire strike length of the Nicola Group is the presence of augite(\pm plagioclase)-phyric basalt and associated monomictic breccia. Similar rocks are also widespread in the Stuhini and Takla groups, the latter being the northern equivalent of the Nicola Group (e.g., Mortimer, 1987; Nelson and Bellefontaine, 1996; Dostal et al., 1999).

Composition of the Nicola Group Volcanic Rocks

A number of workers (e.g., Barrie, 1993; Lang et al., 1995; Bath and Logan, 2005; Logan and Bath, 2005; Breitsprecher et al., 2007, 2008) have investigated the geochemistry of the Late Triassic and Early Jurassic intrusive rocks of the Nicola Group and its equivalents, many of which have associated porphyry copper-molybdenum and copper-gold mineralization. Mineralized alkalic igneous suites in BC are compositionally varied and range from silica-saturated monzonite (e.g., Mount Milligan; Barrie, 1993; Jago and Tosdal, 2009) to strongly silica-undersaturated monzonite and syenite (Galore Creek; Schwab et al., 2008).

In contrast, the geochemistry of the volcanic hostrocks has received comparatively little attention. Mortimer (1987) identified three compositionally distinct but areally overlapping groups of volcanic rocks between Copper Mountain and the Iron Mask area. Group 1 is shoshonitic and comprises strongly augite-porphyrific basalt, locally analcime bearing, and picrite. Group 2 consists of augite- and plagioclase-phyric basalt and andesite belonging to the low-potassium calcalkaline series, and group 3 is composed of petrographically heterogeneous andesite and basalt of tholeiitic to transitional affinity. Shoshonitic lavas from group 1 are stratigraphically above group 2 and 3 rocks.

Basaltic rocks with shoshonitic affinity have also been reported from the Mount Polley (Logan and Bath, 2005) and Mount Milligan areas (Barrie, 1993); basalt at Mount Polley is locally analcime phyric. Similar geochemical

characteristics suggest a genetic relationship between the alkalic intrusive rocks and the extrusive shoshonitic rocks at Mount Polley, and the latter are thought to be relatively high in the Nicola Group stratigraphic sequence (Logan and Bath, 2005). At Mount Milligan, in contrast, the ca. 186–182 Ma intrusive rocks are significantly younger than the Late Triassic volcanic hostrocks (Mortensen et al., 1995; Nelson and Bellefontaine, 1996).

Fieldwork and Preliminary Observations in 2009

Geochemical sampling concentrated on coherent basalt flows or large clasts from volcanoclastic breccias in four areas (Figure 1): 1) around the Mount Milligan deposit; 2) around the Mount Polley deposit; 3) areas north of 100 Mile House, including exposures near the Lac La Hache porphyry prospect; and 4) exposures east of 100 Mile House and north of Highway 24. The latter area has no known alkalic mineralization. Magnetic susceptibility measurements were routinely taken from coherent and volcanoclastic rocks, and samples from all areas are currently being analyzed for physical properties and whole-rock geochemistry. Although detailed geochronological constraints are scarce, the Late Triassic volcanic hostrocks at Mount Polley, which are constrained between 204 and 201 Ma (Logan and Mihalynuk, 2005), are temporally more closely related to the mineralization than those at Mount Milligan, where mineralization significantly postdates the volcanic rocks.

In the exposures around Mount Polley and the Lac La Hache property, weakly altered coherent volcanic rocks have relatively high magnetic susceptibilities of $35\text{--}85 \times 10^{-3}$ SI units, except where affected by chlorite and epidote alteration. In those cases, magnetite is destroyed and susceptibilities are commonly below 5×10^{-3} SI units (Figure 2A, B). This contrasts with the Mount Milligan area and northeast from Lac La Roche, where relatively unaltered coherent basalt has low magnetic susceptibilities of $0.3\text{--}2 \times 10^{-3}$ SI units. Only two samples from Mount Milligan have high values of $20\text{--}25 \times 10^{-3}$ SI units.

The groundmass and some phenocrysts (possibly former olivine) within volcanic rocks are commonly hematite stained in the Mount Polley and Lac la Hache areas but rare in the other areas studied. Red sandstone and polymict breccias and conglomerates have been mapped near these deposits and are interpreted to have been subaerially deposited (Figure 2; Logan and Bath, 2005; Schiarizza and Blingh, 2008).

Analcime-phyric basalt that is macroscopically identifiable as alkalic in composition has been observed only in the Mount Polley area thus far, but whole-rock geochemistry is expected to provide further insight.

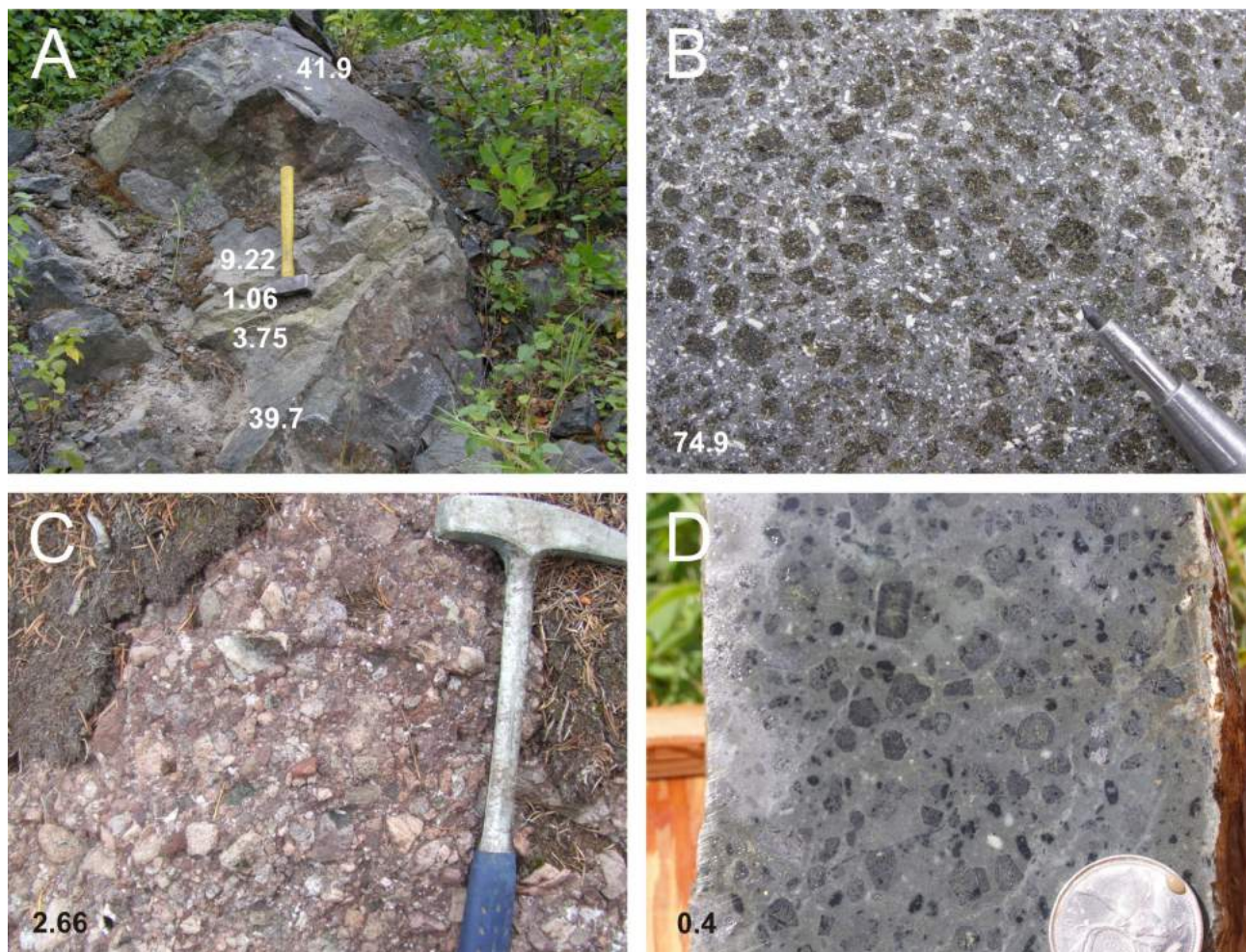


Figure 2. Rock types from the study areas in central British Columbia, showing magnetic susceptibility values ($\times 10^{-3}$ SI units): **a)** basalt with local chlorite and epidote alteration, possibly reflecting pillow margins, northeast of Lac La Hache (UTM Zone 10, 605473E, 5773358N, NAD 83); **b)** coherent pyroxene- and plagioclase-phyric basalt near Mount Polley (UTM 591321E, 5814995N); **c)** possible subaerially deposited volcanoclastic conglomerate, 10 km northeast of Mount Polley, (UTM 582376E, 5827795N); **d)** coherent augite-phyric basalt, 2.5 km south of Mount Milligan (UTM 433079E, 6105548N).

Discussion and Possible Implications

The higher magnetite content of coherent basalt near areas with copper-gold mineralization may indicate that the arc has been more oxidized in those areas compared to elsewhere. Alternatively, there may also be a general evolution from lower to higher magnetite content as the arc evolves and deposits are associated with the stratigraphically higher portions of the arc assemblage.

Highly magnetic volcanic hostrocks in some areas may obscure aeromagnetic signatures of magnetite-rich alteration zones associated with alkalic porphyry copper-gold deposits. However, both distal propylitic and seafloor alteration can introduce epidote and chlorite, and destroy magnetite. Extensive distal propylitic alteration may have the potential for generating distinctive magnetic lows in the periphery of the mineralization. In contrast, where the deposits significantly postdate the host volcanic rocks and where these have low magnetic susceptibility, magnetite introduced

during hydrothermal alteration can be more evident in aeromagnetic data.

Outlook

Despite the limited data available at this point, arc segments hosting mineralization are apparently distinctive based on magnetic susceptibility and distribution of alkalic basalt. Whole-rock geochemistry and additional physical property data from samples of all areas visited will provide further constraints on potentially prospective volcanic rocks. Determination of ferric/ferrous iron ratios will be routinely performed on least-altered coherent volcanic rocks to establish the relationship between magnetic susceptibility and oxidation state of the magmas. Detailed petrographic work will be undertaken to identify the nature and type of magnetite-destructive alteration, which will be crucial for interpreting aeromagnetic signatures around alkalic porphyry copper-gold deposits.

References

- Barrie, C.T. (1993): Petrochemistry of shoshonitic rocks associated with porphyry copper-gold deposits of central Quesnellia, British Columbia, Canada; *Journal of Geochemical Exploration*, v. 48, p. 225–258.
- Bath, A.B., and Logan, J.M. (2006): Petrography and geochemistry of the Late Triassic Bootjack stock (NTS 093A/12), south-central British Columbia; *in Geological Fieldwork 2005*, BC Ministry of Energy, Mines and Petroleum Resources, Paper 2006-1, p. 5–20, URL <<http://www.empr.gov.bc.ca/Mining/Geoscience/PublicationsCatalogue/Fieldwork/Pages/GeologicalFieldwork2005.aspx>> [November 2009].
- Breitsprecher, K., Scoates, J.S., Anderson, R.G. and Weis, D. (2007): Geochemistry of Mesozoic intrusions, Quesnel and Stikine terranes (NTS 082, 092, 093), south-central British Columbia: preliminary characterization of sampled suites; *in Geological Fieldwork 2006*, BC Ministry of Energy, Mines and Petroleum Resources, Paper 2007-1 and Geoscience BC, Report 2007-1, p. 247–257, URL <<http://www.empr.gov.bc.ca/mining/Geosurv/Publications/Fieldwork/2006/toc.htm#GeoscienceBC>> [November 2009].
- Breitsprecher, K., Weis, D. and Scoates, J.S. (2008): Crustal recycling vs. arc maturity, Mesozoic Quesnel terrane intrusive rocks, Canadian Cordillera; *Goldschmidt Conference Abstracts 2008*, *Geochimica et Cosmochimica Acta*, v. 72, p. A113.
- Canadian Council on Geomatics (2010): GeoBase geospatial data portal; Canadian Council on Geomatics, URL <<http://www.geobase.ca>> [November 2009].
- Dawson, G.M. (1879): Preliminary report on the physical and geological features of the southern portion of the interior of British Columbia, 1877; *Geological Survey of Canada, Progress Report*, p. 1877-8, 1879.
- Dostal, J., Gale, V. and Church, B.N. (1999): Upper Triassic Takla Group volcanic rocks, Stikine Terrane, north-central British Columbia: geochemistry, petrogenesis, and tectonic implications; *Canadian Journal of Earth Sciences* v. 36, p. 1483–1494.
- Jago, C.J. and Tosdal, R.M. (2009): Distribution of alteration in an alkalic porphyry copper-gold deposit at Mount Milligan, central British Columbia (NTS 094N/01); *in Geoscience BC Summary of Activities 2008*, Geoscience BC, Report 2009-1, p. 33–48, URL <<http://www.geosciencebc.com/s/SummaryofActivities.asp?ReportID=358404>> [November 2009].
- Jensen, E.P. and Barton, M.D. (2000): Gold deposits related to alkaline magmatism; *in Gold in 2000*, S.G. Hagemann and P.E. Brown (ed.), *Reviews in Economic Geology*, no. 13, p. 279–314.
- Journeay, J.M., Williams, S.P. and Wheeler, J.O. (2000): Tectonic assemblage map, Vancouver, British Columbia–U.S.A.; *Geological Survey of Canada, Open File 2948a*, scale 1:1 000 000, URL <http://apps1.gdr.nrcan.gc.ca/mirage/mirage_list_e.php?id=211051> [November 2009].
- Lang, J.R., Lueck, B., Mortensen, J.K., Russell, J.K., Stanley, C.R. and Thompson, J.F.H. (1995): Triassic–Jurassic silica-undersaturated and silica-saturated alkalic intrusions in the cordillera of British Columbia: implications for arc magmatism; *Geology*, v. 23, p. 451–454.
- Logan, J.M. and Bath, A.B. (2006): Geochemistry of Nicola Group basalt from the central Quesnel Trough at the latitude of Mount Polley (NTS 093A/5, 6, 11, 12), central British Columbia; *in Geological Fieldwork 2005*, BC Ministry of Energy, Mines and Petroleum Resources, Paper 2006-1, p. 83–98, URL <<http://www.empr.gov.bc.ca/Mining/Geoscience/PublicationsCatalogue/Fieldwork/Pages/GeologicalFieldwork2005.aspx>> [November 2009].
- Logan, J.M. and Mihalynuk, M.G. (2005): Regional geology and setting of the Cariboo, Bell, Springer and Northeast Porphyry Cu-Au Zones at Mount Polley, south-central British Columbia; *in Geological Fieldwork 2004*, BC Ministry of Energy, Mines and Petroleum Resources, Paper 2005-1, p. 249–270, URL <<http://www.empr.gov.bc.ca/Mining/Geoscience/PublicationsCatalogue/Fieldwork/Pages/GeologicalFieldwork2004.aspx>> [November 2009].
- MINFILE (2010): MINFILE BC mineral deposits database; BC Ministry of Energy, Mines and Petroleum Resources, URL <<http://www.empr.gov.bc.ca/Mining/Geoscience/MINFILE/Pages/default.aspx>> [November 2009].
- Mortensen, J.K., Ghosh, D.K. and Ferri, F. (1995): U-Pb geochronology of intrusive rocks associated with copper-gold porphyry deposits in the Canadian cordillera; *in Porphyry Deposits of the Northwestern Cordillera of North America*, T.G. Schroeter (ed.), *Canadian Institute of Mining and Metallurgy, Special Volume 46*, p. 142–158.
- Mortimer, N. (1987): The Nicola Group: Late Triassic and Early Jurassic subduction-related volcanism in British Columbia; *Canadian Journal of Earth Sciences*, v. 24, p. 2521–2536.
- Nelson, J.L. and Bellefontaine, K.A. (1996): The geology and mineral deposits of north-central Quesnellia: Tezzeron Lake to Discovery Creek, central British Columbia; BC Ministry of Energy, Mines and Petroleum Resources, *Bulletin 99*, 100 p.
- Nelson, J. and Colpron, M. (2007): Tectonics and metallogeny of the British Columbia, Yukon and Alaskan cordillera, 1.8 Ga to the present; *in Mineral Deposits of Canada*, W.D. Goodfellow (ed.), *Geological Association of Canada, Mineral Deposits Division, Special Publication 5*, p. 755–792.
- Preto V.A.G. (1977): The Nicola Group: Mesozoic volcanism related to rifting in southern British Columbia; *in Volcanic Regimes in Canada*, W.R.A. Baragar, L.C. Coleman and J.M. Hall (ed.), *Geological Association of Canada, Special Paper 16*, p. 39–57.
- Schiarizza, P. and Blingh, J.S. (2008): Geology and mineral occurrences in the Timothy lake area, south-central British Columbia (NTS 092P/14); *in Geological Fieldwork 2007*, BC Ministry of Energy, Mines and Petroleum Resources, Paper 2008-1, p. 191–211, URL <<http://www.empr.gov.bc.ca/Mining/Geoscience/PublicationsCatalogue/Fieldwork/Pages/GeologicalFieldwork2007.aspx>> [November 2009].
- Schiarizza, P., Blingh, J.S., Bluemel, B. and Tait, D. (2008): **Geology and mineral occurrences of the Timothy Lake area**(NTS 092P/14); BC Ministry of Energy, Mines and Petroleum Resources, Open File, 2008-5 1:50 000 scale.
- Schwab, D.L., Petsel, S., Otto, B.R., Morris, S.K., Workman, E.E. and Tosdal, R.M. (2008): Overview of the Late Triassic Galore Creek copper-gold-silver porphyry system, northwestern British Columbia, Canada; *in Ores and Orogenesis: Circum-Pacific Tectonics, Geologic Evolution, and Ore Deposits*, J.E. Spencer and S.R. Tittley (ed.), *Arizona Geological Society, Digest 22*, p. 471–484.

Enhancing Geophysical Interpretation and Mineral Deposit Modelling Through Knowledge of Physical Rock Properties: Magnetic Susceptibility Studies for Porphyry Deposits in the QUEST and QUEST-West Areas (NTS 093E, K, N)

D.E. Mitchinson, Mineral Deposit Research Unit, University of British Columbia, Vancouver, BC, dmitchinson@eos.ubc.ca

T. Bissig, Mineral Deposit Research Unit, University of British Columbia, Vancouver, BC

Mitchinson, D.E. and Bissig, T. (2010): Enhancing geophysical interpretation and mineral deposit modelling through knowledge of physical rock properties: magnetic susceptibility studies for porphyry deposits in the QUEST and QUEST-West areas (NTS 93E, K, N); in Geoscience BC Summary of Activities 2009, Geoscience BC, Report 2010-1, p. 53–64.

Introduction

Knowledge of physical rock properties is necessary for interpretation of geophysical data and maps, and is also essential for constraining geophysical inversion calculations to yield improved three-dimensional (3-D) models of the Earth's subsurface. With recent release by Geoscience BC of a series of geophysical datasets over mineral deposits in west-central British Columbia (Geotech Limited, 2008, 2009; Aeroquest Limited, 2009; Phillips et al., 2009), there is increased interest in improving our understanding of the links between geology and geophysics.

A postdoctoral project was initiated by the Mineral Deposit Research Unit at the University of British Columbia that focuses on understanding the relationships between geology and physical properties in porphyry deposit settings. Study sites for this project include the Mount Milligan copper-gold deposit, the Endako molybdenum mine and the Huckleberry copper-molybdenum mine. These porphyry deposits were surveyed as part of the Geoscience BC QUEST and QUEST-West airborne electromagnetic (EM) and magnetic geophysical surveys (Figure 1). Magnetic susceptibility is the first physical property dataset to be compiled. This report provides a preliminary summary of the characteristic susceptibility ranges for suites of rocks from the three deposits. Data collected from the three deposits reveal three distinct susceptibility distributions. In

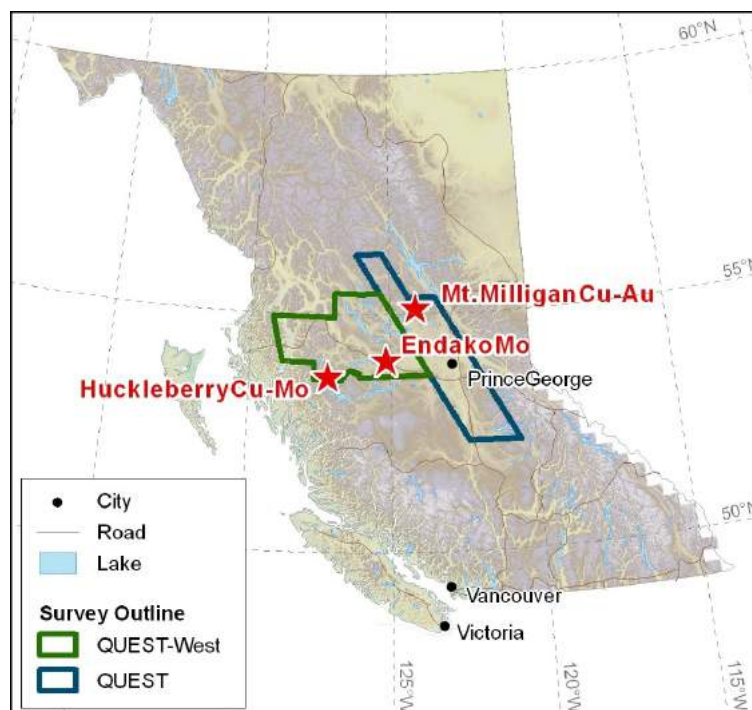


Figure 1. Areas covered by the Geoscience BC QUEST and QUEST-West airborne electromagnetic (EM) and magnetic geophysical surveys of central British Columbia. Smaller scale surveys were completed over several deposits within the larger survey areas, including the three deposits investigated during this study: the Endako, Huckleberry and Mount Milligan deposits (MINFILE, 2010). Base map from Canadian Council on Geomatics (2004) and Natural Resources Canada (2007).

each case, however, the presence or absence of magnetite may help to distinguish prospective versus barren zones, or else enhance geological mapping in these areas of extensive cover and limited outcrop.

Physical Property Measurements

Representative rock samples for each major geological unit and alteration type were collected from each of the three porphyry deposits. Magnetic susceptibility measurements were taken along selected drillholes, and from the collected samples, using a KT-9 Kappameter hand-held susceptibil-

Keywords: QUEST, QUEST-West, Mount Milligan, Endako, Huckleberry, porphyry deposit, physical properties, magnetic susceptibility, geophysical inversion

This publication is also available, free of charge, as colour digital files in Adobe Acrobat® PDF format from the Geoscience BC website: <http://www.geosciencebc.com/s/DataReleases.asp>.

ity probe. The suite of samples was sent to the physical property laboratory of Geological Survey of Canada–Pacific in Sidney, BC for further property measurements. Although these data were not available at the time this paper was written, there is a large enough magnetic susceptibility dataset to gain some preliminary insight into how this physical property relates to geological and mineralization processes at each study site, and how the susceptibility distribution may influence magnetic signatures.

Mount Milligan Susceptibility Trends: Alteration-Related Magnetite Formation

Geology of the Mount Milligan Copper-Gold Deposit

The Mount Milligan deposit occurs within the Quesnel Terrane of central BC. The geology underlying the deposit is dominated by augite-phyric basaltic rocks of the Takla Group (Figure 2), a volcanic package that extends over a significant portion of the Quesnel Terrane. Mineralization is spatially associated with two silica-saturated alkalic monzonite stocks. The stocks are part of a suite of Early Jurassic intrusions known to be related to a number of gold-rich alkalic porphyry copper deposits in north-central BC (Nelson and Bellefontaine, 1996). Although the Mount Milligan deposit is subdivided into two zones, the Main and Southern Star zones, the more well-documented Main zone is the focus of this study. Mineralization occurs predominantly in basaltic volcanoclastic rocks in four subzones (the MBX, WBX, DWBX and 66 zones) surrounding the Main zone monzonite stock, with the MBX and 66 zones having

higher gold grades relative to the others (Sketchley et al., 1995; Jago, 2008). Hydrothermal alteration, thought to be related to ore-bearing fluids, forms near-concentric zones around the monzonite stock (Jago, 2008). Potassic alteration, manifested by biotite and K-feldspar+magnetite, occurs centrally, passing outward into albite+actinolite+epidote alteration (sodic-calcic zone of Jago, 2008) and then into a propylitic alteration assemblage of epidote+albite+chlorite+actinolite+calcite+pyrite. The MBX, WBX and DWBX mineralization is hosted within rocks exhibiting strong potassic alteration. Gold and copper mineralization within the 66 zone is spatially related to a phyllic alteration assemblage that contains chlorite, sericite and iron-rich carbonate. This mineral assemblage is interpreted to have formed from low-temperature magmatic fluids circulating at higher levels within the Mount Milligan porphyry system (Jago, 2008).

Magnetic Susceptibility Data from the Mount Milligan Deposit

In June 2009, the Mount Milligan deposit site was visited and nine drillholes from the 2006–2007 drilling program of Terrane Metals Corp. were examined and sampled (see Figure 2 for location of sampled drillholes). The drillholes were chosen to best sample representative geology and alteration from each of the different mineralized zones, and to sample least-altered rocks. Susceptibility measurements were taken on 65 samples using the KT-9 Kappameter hand-held probe. Terrane Metals Corp. collected downhole susceptibility data for holes drilled in 2006 and 2007, so there is an extensive database that can be used for analysis.

This downhole database will be used to constrain future magnetic inversions for Mount Milligan but is not discussed herein due to an incomplete knowledge of mineralogy of the rocks at the measurement locations. Petrographic work was completed on most of the 65 samples from this study, so there is more control in interpretation of these samples and their associated susceptibility data.

Magnetic susceptibility data from Mount Milligan basaltic volcanic hostrock samples are shown in histograms in Figure 3, and monzonite sample data are plotted in Figure 4. Potassically altered basalt (biotite+K-feldspar; Figure 3) has a range of susceptibilities, but more than half of the samples have susceptibility values $>1 \times 10^{-3}$ SI units, a subset of which have susceptibilities of $>50 \times 10^{-3}$ SI units. Propylitic and albite-altered basalt does not exhibit the very high susceptibilities seen in the potassically altered sample suite, and most samples have susceptibilities of $<10 \times 10^{-3}$ SI units.

Most monzonite samples contain primary magnetite at various stages of destruction or alteration to

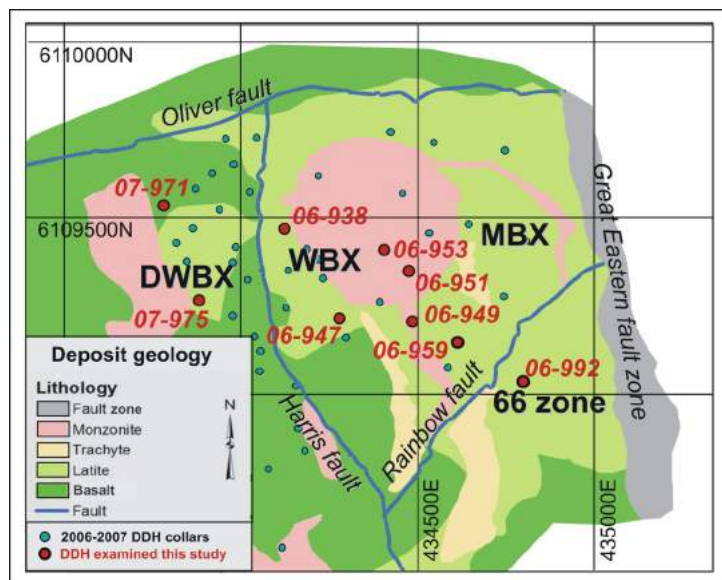


Figure 2. Plan-view geology of the Mount Milligan copper-gold deposit, central British Columbia, showing locations of the four main mineralized zones associated with the 'MBX' monzonite stock. Also shown are the locations of the 2006–2007 drillholes of Terrane Metals Corp. and the holes sampled for this study. Base-map files and collar locations provided by Terrane Metals Corp.

hematite (Figure 5). Monzonite thus typically has moderate susceptibilities on average ($>1 \times 10^{-3}$ SI units; Figure 4), regardless of whether or not it is potassically altered. Secondary magnetite (Figure 5), related to hydrothermal alteration, can further increase the susceptibility. Monzonite samples do not attain the susceptibility values of $>50 \times 10^{-3}$ SI units measured in andesitic samples. This is interpreted to be due to the lower initial iron content of the monzonite rocks, which would prevent magnetite formation, but may also be related to the low permeability of the intrusive rocks, which makes them less conducive to alteration or crystallization of secondary magnetite. Albite alteration of monzonite results in slightly lower susceptibility values (Figure 4).

Discussion

The close spatial relationship between magnetite, biotite and copper mineralization at Mount Milligan has been documented by several workers (Sketchley et al., 1995; Jago, 2008). This relationship is supported by the magnetic highs clearly associated with known mineralized areas on the magnetic map shown in Figure 6. The highest susceptibility measurements collected for this study occur within potassically altered basalt from near the bottom of east-dipping drillholes 07-975 and 07-971, and drillhole 06-959 in the DWBX and MBX zones (Figure 6). Although magnetite veins in a few selected basalt samples crosscut propylitic mineral assemblages, propylitic samples almost always have low susceptibilities. Targeting high-susceptibility rocks (greater than approximately 15×10^{-3} SI units) should therefore locate mainly potassically altered basalt, along with some monzonite (which, due to its role in porphyry formation, is also prospective). Less prospective, propylitically altered rocks could consequently be disregarded.

Basalt samples were collected distally from the Mount Milligan deposit for a regional footprint study of alkalic porphyry deposits (Bissig et al., 2010). From the initial assessment by Bissig et al. (2010) of susceptibility measurements, both high-susceptibility ($>20 \times 10^{-3}$ SI units) and low-susceptibility ($<1 \times 10^{-3}$ SI units), least-altered basaltic volcanic rocks occur within the district. Future petrographic and geochemical work on these distal volcanic samples, and on the more consistently high-susceptibility rocks from the area of the Mount Polley copper-gold deposit, may indicate varying compositions of volcanic rocks throughout the Takla Group and within the laterally equivalent Nicola Group. This preliminary work suggests that it would be important

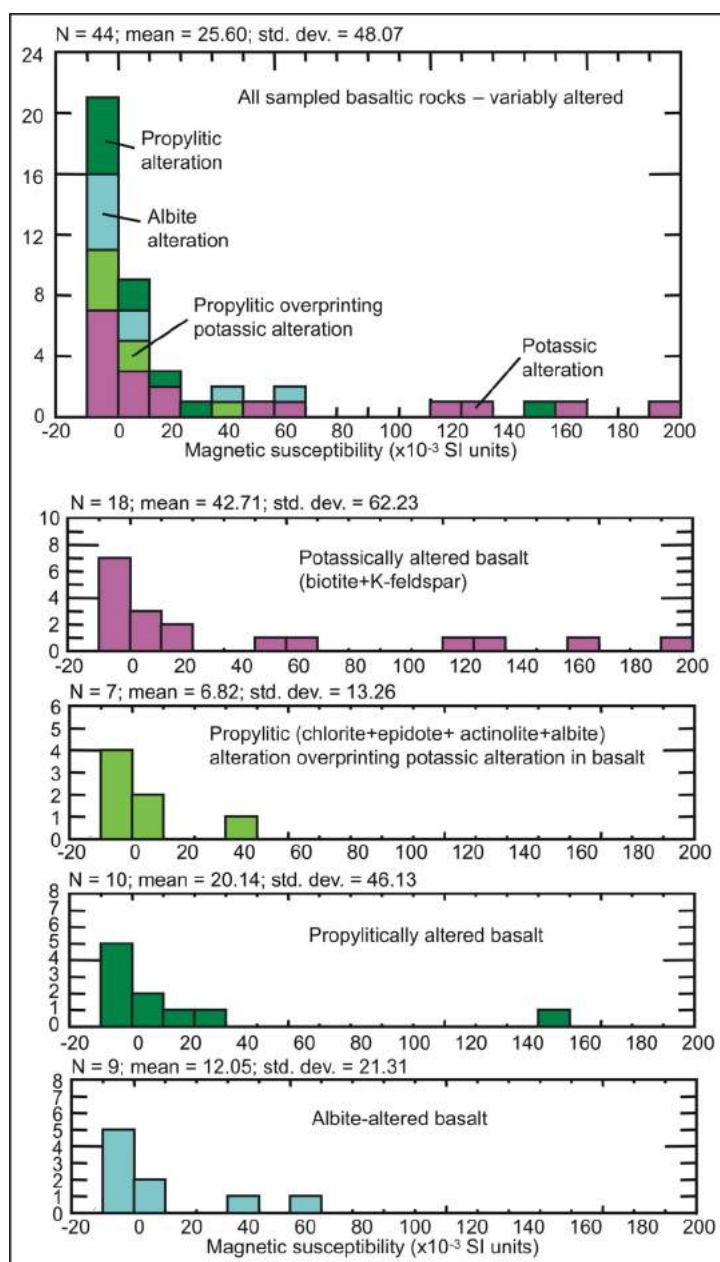


Figure 3. Magnetic susceptibility data for basaltic rock samples taken from drillcore at the Mount Milligan deposit, central British Columbia. Alteration types are shown plotted together in the upper histogram for comparison, and then separately. Abbreviations: N, number of samples; std. dev., standard deviation.

to determine whether or not the volcanic rocks being explored for porphyry copper-gold deposits in this region are magnetite bearing before it is assumed that magnetic highs represent potassic alteration. Least-altered ('background') samples collected during this study from the immediate vicinity of the Mount Milligan deposit are likely weakly altered to inner and outer propylitic mineral assemblages (Jago, 2008). If it is shown that distally these volcanic sequences contain magnetite in their least-altered states, this might mean that, at district scales of exploration, lower susceptibility rocks (indicative of propylitic alteration) should

initially be targeted, within which localized areas of high susceptibility (potassic alteration) would be of interest.

Endako Susceptibility Trends: Alteration-Related Magnetite Destruction

Geology of the Endako Molybdenum Deposit

The Endako molybdenum deposit is located in north-central BC at the boundary between the Cache Creek and Stikine terranes. It is hosted by the Endako quartz monzonite (Figure 7), one of the calcalkaline granitoid phases making up the extensive Upper Jurassic Francois Lake intrusion suite. Bounding granitic intrusive rocks, the Francois Lake granite and the Casey granite, are younger than, and intrude, the Endako quartz monzonite (Bysouth and Wong, 1995). The Casey granite has been dated at an age similar to that of late-stage molybdenite mineralization at Endako (ca. 145 Ma; Villeneuve et al., 2001), and the mineralization closely follows the contact between the two granites, suggesting a linkage between the Casey intrusion and the formation of the deposit.

Molybdenite occurs with quartz in a series of east-northeastward-striking vein systems. Proximal alteration phases include a potassic phase and a quartz-sericite phase, characterized respectively by pink K-feldspar and by quartz-sericite fracture and vein selvages of varying widths (Kimura et al., 1976). Quartz-sericite alteration is documented to be most consistently related to molybdenum mineralization (Selby et al., 2000). Pervasive kaolinite alteration overprints all other alteration phases and is considered to be a late, postmineral alteration stage (Selby et al., 2000).

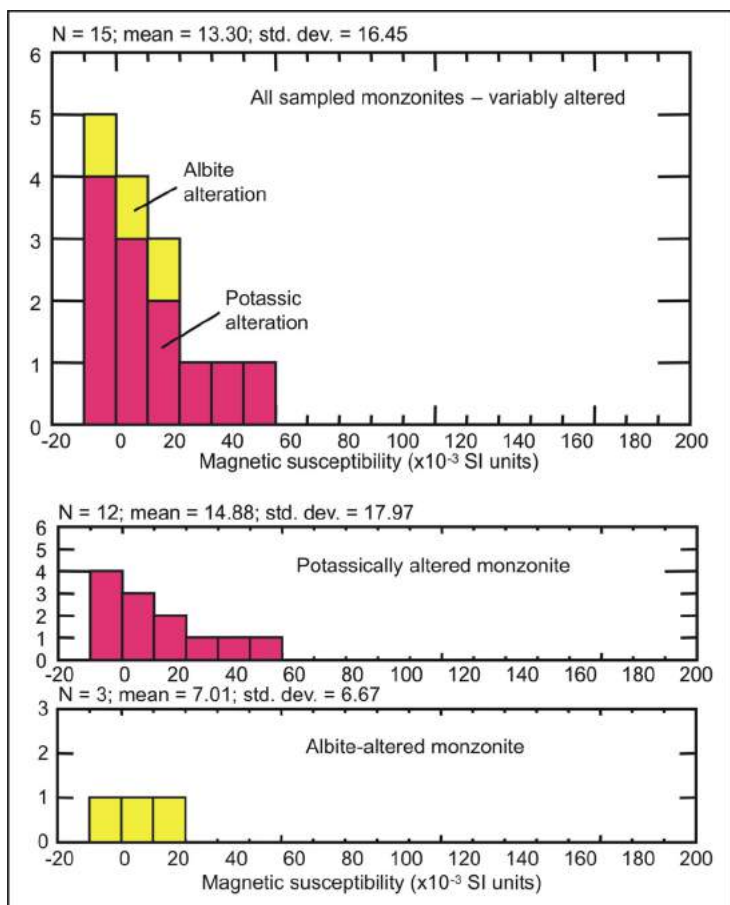


Figure 4. Magnetic susceptibility data for monzonite intrusive rock samples taken from drillcore at the Mount Milligan deposit, central British Columbia. Abbreviations: N, number of samples; std. dev., standard deviation.

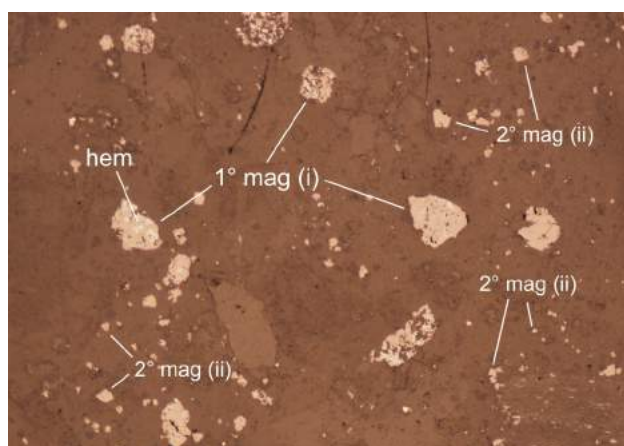


Figure 5. Reflected-light photomicrograph of potassically altered monzonite sample from the Mount Milligan deposit, central British Columbia, showing i) breakdown of primary magnetite (1 mag) to hematite (hem) within monzonite, and ii) subhedral secondary magnetite (2 mag) occurring within the groundmass. Field of view approximately 4 mm.

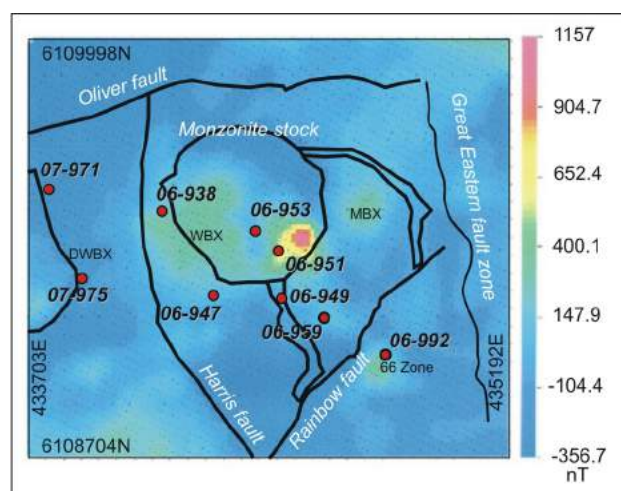


Figure 6. Ground magnetic data over the Mount Milligan deposit, central British Columbia, showing important geological contacts and mineralized zones. Data collected in 1984–1985 by BP Minerals. Abbreviation: nT, nanoteslas.

Magnetic Susceptibility Data from the Endako Deposit

Four drillholes from within and outside the Endako open pits (Figure 7) were examined and 40 representative samples collected of the different granitic units, and of the typical overprinting alteration assemblages. Susceptibility measurements were taken on all samples and also at approximately 1.2 m (4 ft.) intervals along drillcore from two holes, for later incorporation into magnetic-inversion-model calculations. Additionally, a suite of 17 samples was collected from the Endako open pits.

Least-altered Endako quartz monzonite was sampled from the near-surface portion of drillhole 08-35. Susceptibility values, which reflect the presence of accessory magnetite, were relatively consistent along the core, with values around 25×10^{-3} SI units. Some monzonite samples characterized as 'least altered' from other drillcore have low susceptibilities (Figure 8). There is a distinct bimodal distribution in the least-altered sample data, with few samples falling into the gap between 5×10^{-3} and 25×10^{-3} SI units. The lower susceptibility values may be attributed to weak clay alteration of the monzonite. Figure 9 compares a relatively fresh Endako quartz monzonite with a clay-altered monzonite, the associated susceptibility values dropping significantly from 19×10^{-3} to 0.27×10^{-3} SI units.

In order to compare the magnetic susceptibilities of altered quartz monzonite samples, they were grouped based on the predominant or latest apparent alteration phase. All potassically altered samples are overprinted by either later quartz-sericite or kaolinite, and were grouped accordingly. Altered quartz monzonite, regardless of alteration assemblage, is characterized by consistently low susceptibilities (Figure 8), indicating that accessory magnetite is destroyed in association with one or more of the hydrothermal alteration events overprinting it.

Postmineral basalt has generally high susceptibilities. The Casey granite does not appear to contain magnetite and therefore has consistently low susceptibilities (Figure 8).

Discussion

The destruction of magnetite associated with the alteration and mineralization of the Endako quartz monzonite hostrocks results in low susceptibility values. Thus, the use of magnetic and susceptibility data, and related models, may highlight potentially prospective zones within the monzonite. However, late kaolinite alteration, which is not consistently spatially related to mineralization, appears to

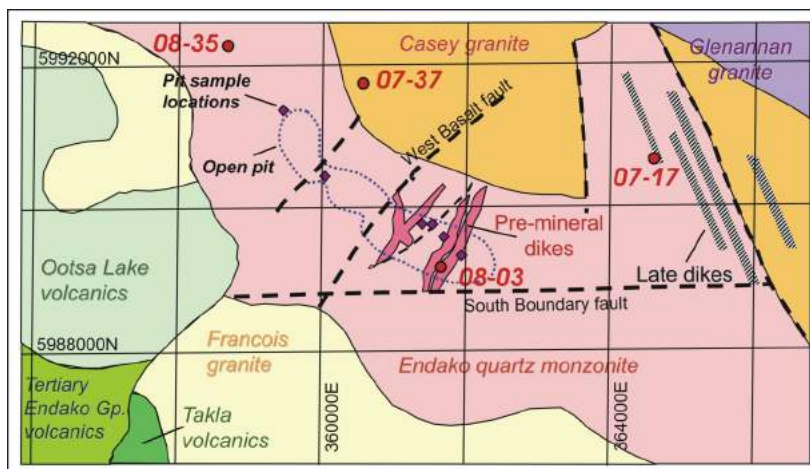


Figure 7. Plan-view geology of the Endako molybdenum deposit (modified from Kimura et al., 1976). The dotted blue line represents the outline of the Endako open pit. Drillholes sampled for this project are indicated by the red circles, and open-pit sample locations are indicated by purple diamonds.

also result in magnetite destruction. This means that not all low-susceptibility monzonite should be assumed to be mineralized.

Magnetic surveys have been useful in outlining the contact between the low susceptibility Casey granite and the Endako quartz monzonite (Figure 10). Modelling susceptibility in the subsurface via magnetic inversion could help to further define the 3-D geometry of this important contact.

Huckleberry Susceptibility Trends: Overprinting Magnetite Constructive and Destructive Events

Geology of the Huckleberry Copper-Molybdenum Deposit

The Huckleberry deposit occurs within the west-central Stikine Terrane. The underlying geology (Figure 11) is dominated by Early to Middle Jurassic Hazelton Group volcanic rocks and Late Cretaceous Bulkley intrusive rocks (Jackson and Illerbrun, 1995). The intrusion of the Bulkley granodiorite resulted in contact metamorphism (hornfels development) in the volcanic rocks of this area, which added biotite, amphibole, chlorite, magnetite, hematite and pyrite to the host andesite (Jackson and Illerbrun, 1995). Mineralization at Huckleberry occurs in proximity to the granodiorite stocks. The Main zone is located on the eastern flank of the western granodiorite stock, and the East zone occurs within and adjacent to the eastern stock (Figure 11).

Copper and lesser molybdenum occur in narrow veins and as fracture coatings within andesitic hostrocks and, to a lesser degree, within granodiorite intrusions. The geological setting of the Huckleberry deposit is similar to that of Mount Milligan, with volcanic rock-hosted mineralization

spatially related to granitic intrusions. The intrusive rocks at Huckleberry, however, are calc-alkalic in nature, as at Endako, and alteration assemblages include sericite and clays, mineral phases that are less typical in alkalic systems (Stanley, 1992). Distal alteration is characterized by chlorite+epidote+pyrite-bearing assemblages. Proximal alteration assemblages include biotite, albite, amphibole, chlorite and sericite. Many of these minerals also occur as alteration selvages to chalcopryite-, pyrite- and molybdenum-bearing veins. Chalcopryite-bearing veins commonly have K-feldspar, albite and/or albite-biotite haloes (Figure 12).

Magnetic Susceptibility Data from the Huckleberry deposit

Susceptibility measurements were taken on 25 samples from two drillholes on the Huckleberry property, one hole intersecting moderately mineralized andesitic volcanic rocks in an area currently being mined immediately north of the Main zone and the other intersecting poorly mineralized, relatively unaltered andesitic rocks in the East zone. Downhole measurements were taken at intervals of approximately 1.2 m (4 ft.). In addition, three samples were collected south of the deposit, and are thought to represent both subaerially and subaqueously deposited andesitic volcanic rocks from outside the influence of the intrusions and mineralizing system.

Magnetic susceptibility data from Huckleberry are compiled in a series of histograms in Figures 13 and 14. Andesitic rocks from outside the main mineralized zones have generally low to moderate susceptibilities ($<50 \times 10^{-3}$ SI units; Figure 13). Near the granodiorite intrusions, susceptibilities are typically $>70 \times 10^{-3}$ SI units and range up to 230×10^{-3} SI units. These high values are attributed to the premineral hornfels development in andesitic hostrocks (during contact metamorphism associated with granodiorite intrusion), which introduced magnetite. Within this high-susceptibility zone, susceptibilities can locally decrease slightly (to $30\text{--}100 \times 10^{-3}$ SI units) where mineralized veins and fractures are associated with albite, K-feldspar and biotite alteration selvages. Since the sample population for propylitically altered and biotite-feldspar-altered andesitic samples is limited (15 samples), it is difficult to demonstrate the slight shift in susceptibility that occurs. However, by looking at the distributions of susceptibility data for each of the drillholes, one from a

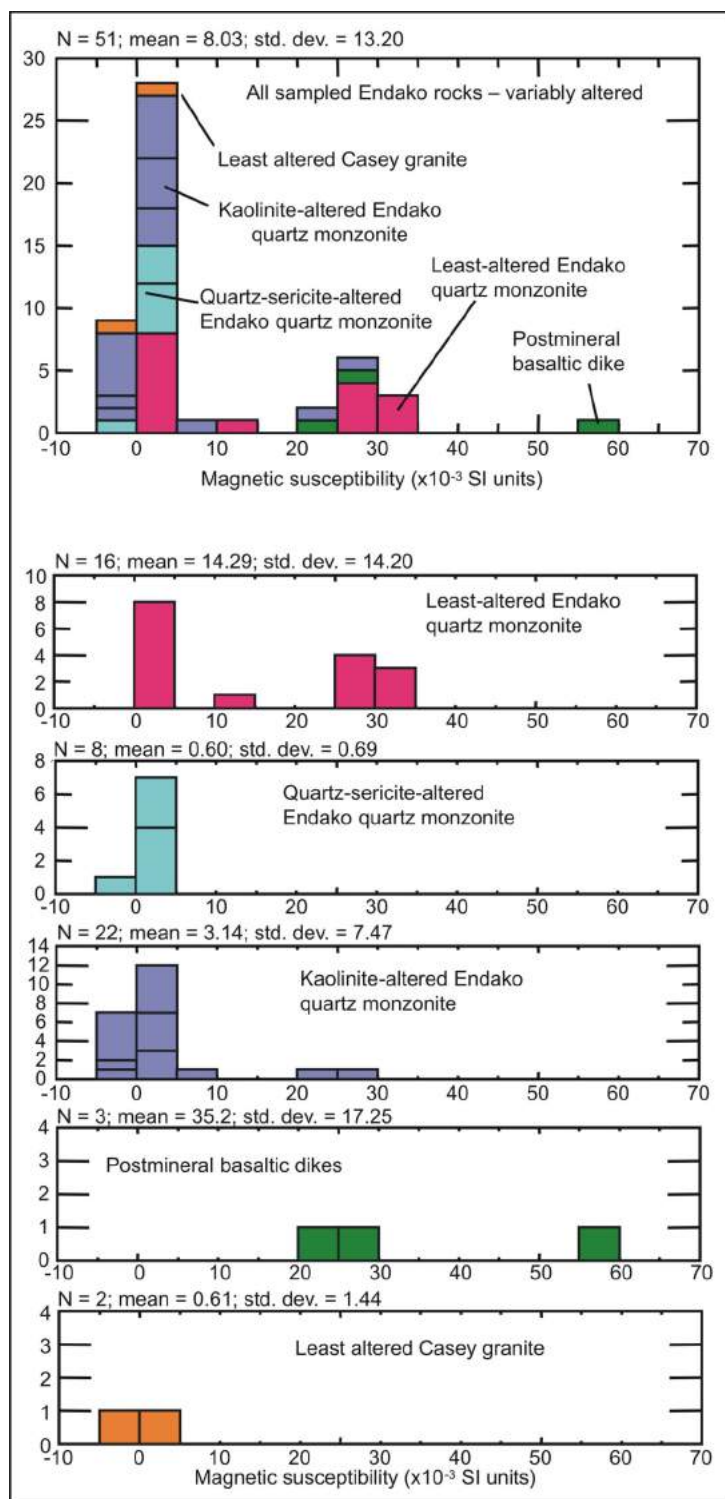


Figure 8. Magnetic susceptibility data from samples of monzonite, granite and basalt dikes taken from drillcore at the Endako molybdenum deposit, central British Columbia. Samples are shown plotted together in the upper histogram for comparison and then separately.

more strongly mineralized area than the other, a slight shift in susceptibility is apparent (Figure 15).



Figure 9. Comparison of least-altered Endako quartz monzonite (i) with weakly kaolinite (kaol)-altered Endako quartz monzonite (ii), Endako molybdenum deposit, central British Columbia. The susceptibility drops significantly between samples, from 19×10^{-3} SI units (least-altered sample on left) to 0.27×10^{-3} SI units (kaolinite-altered sample on right).

Neither of the two granodiorite stocks was intersected in the two drillholes examined, but nine samples were randomly collected from drillcore stacked at the Huckleberry core repository. From the small sample suite collected, weakly biotite-altered Main zone granodiorite is moderately susceptible ($\sim 25\text{--}40 \times 10^{-3}$ SI units), with susceptibility decreasing to around zero with increasing K-feldspar, sericite and clay alteration (Figure 14). The East zone granodiorite was mineralized and therefore mined in addition to the mineralized andesite. This granodiorite has lower susceptibilities ($\sim 1 \times 10^{-3}$ SI units) but also exhibits

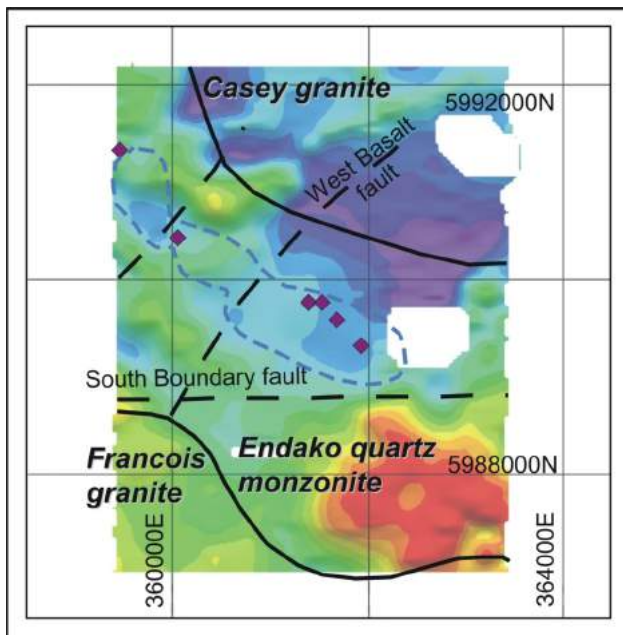


Figure 10. Total magnetic intensity data over the Endako molybdenum deposit, central British Columbia, showing outlines of the open pit (blue dashed line), open-pit samples (purple diamonds), geological contacts (black solid lines) and faults (black dashed lines). Data collected by Aeroquest Limited (2009) as part of the Geoscience BC QUEST-West initiative.

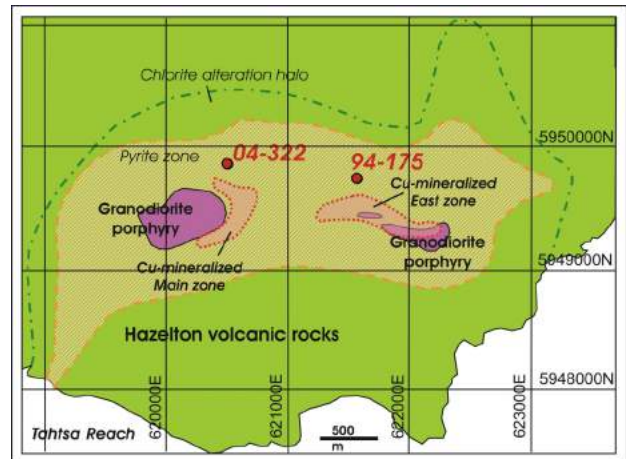


Figure 11. Plan-view geology and alteration of the Huckleberry mine area (modified from Jackson and Illerbrun, 1995), central British Columbia, showing the two mineralized zones, Main and East, and related granodiorite intrusive rocks. Drillholes examined for this study are indicated by red dots.

variable degrees of overprinting clay, sericite and K-feldspar alteration.

Discussion

Magnetite-destructive albite and K-feldspar alteration appears to be quite localized, perhaps because of the poor permeability of the very competent hornfels rocks. The applicability of magnetic and susceptibility data in the Huckleberry area to target mineralized veining and fracture zones could therefore be limited. It may not be possible, using geophysics or geophysical inversion, to separate the moderate-susceptibility albite- and K-feldspar-altered andesite from the high-susceptibility hornfels andesite.

Figure 16 shows magnetic data collected over the Huckleberry deposit for the Geoscience BC QUEST-West project. The mineralized zones appear to lie within magnetic lows,



Figure 12. Quartz-chalcopyrite vein with a bleached, K-feldspar-bearing alteration selvage crosscutting andesitic and granodioritic rocks from the Main zone of the Huckleberry copper-molybdenum deposit, central British Columbia.

which likely represent footprints of the relatively low susceptibility granodiorite, possibly combined with proximal magnetite-destructive alteration. If these lows on the magnetic map are related to granodiorite, it is possible that the western intrusive unit extends farther to the west.

The extent of the broad magnetic high over the area may represent the extent of hornfels development. More regional samples are needed to determine if hornfels development is indeed the cause of strong susceptibility in the Huckleberry mine area. If the Telkwa volcanic rocks are normally magnetite poor, then it may be possible to explore for magnetite-rich hornfels zones within them using magnetic data and modelling. This might help to locate other unexposed Bulkley intrusive rocks in the area and, with subsequent fine-scale geophysics applied, it may be possible to detect variations related to hydrothermal alteration within these thermal haloes.

Summary of Findings

This study was successful in gaining further insight into the magnetic susceptibility characteristics of rocks in a range of porphyry settings in central BC. Both alkaline and calcalkaline systems were considered, and intrusion- and volcanic-hosted porphyry deposits were assessed.

Formation of secondary magnetite in association with potassic alteration, like that occurring at the Mount Milligan deposit, is common within the known alkalic porphyry systems hosted by the Quesnel Terrane (Nelson and Bellefontaine, 1996), and local magnetic anomalies in andesitic rocks should be considered for exploration targeting. Initial regional volcanic rock studies by Bissig et al. (2010), however, indicate that not all basaltic volcanic rocks within the equivalent Takla and Nicola groups are low susceptibility. Magnetic data may not be as useful for targeting copper-gold, porphyry-related, magnetite-bearing potassic alteration if hosting volcanic sequences contain primary magnetite and already have high susceptibilities.

As demonstrated for Endako, it is important to understand the physical properties of regional least-altered hostrocks. Understanding that the Endako granite is a magnetic body makes it possible to use geophysics to map the contact between it and other granites, and to target areas of magnetite-destructive alteration within it.

More data must be collected for background susceptibility of distal Telkwa volcanic rocks to determine if their geophysical signatures differ from volcanic rocks that exhibit

hornfels development and are potentially mineralized. Other porphyry deposits near Huckleberry, occurring in spatial association with stocks related to the Bulkley intrusive suite, also exist within contact-metamorphosed volcanic rocks (MacIntyre, 1985). Understanding physical property variations between rocks with and without hornfels development, and within hornfels zones, may help to localize mineralization related to Bulkley intrusions.

The data collected and general trends observed will be useful in helping to understand magnetic data collected over areas that are along strike from mineralization, or over geologically similar settings. The data can also be used to help

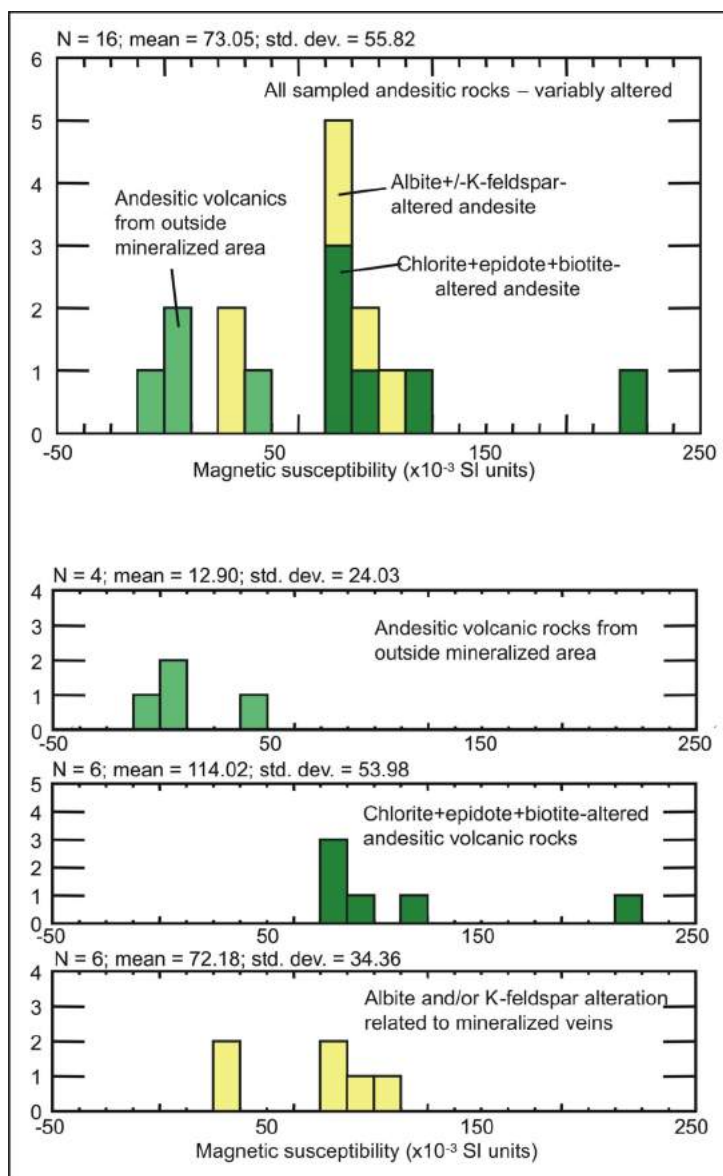


Figure 13. Magnetic susceptibility data for samples of andesitic rocks taken from drillcore at the Huckleberry copper-molybdenum deposit, central British Columbia. Samples are shown plotted together in the upper histogram for comparison, and then separately.

geologically constrain magnetic inversions in these districts.

Future Work

Continued Physical Property Analysis

Density, conductivity and chargeability measurements on representative rocks from each of the three deposits are being taken at the physical property laboratory of Geological Survey of Canada–Pacific in Sidney, BC. The resulting data will help relate the rocks to other geophysical datasets collected.

Petrographic analysis on Endako and Huckleberry rocks will confirm alteration assemblages, and help identify processes causing magnetite formation and destruction. X-ray diffraction analyses, using the Rietveld method, may be carried out to quantify abundances of specific minerals, such as magnetite and sulphides, that control physical properties. From this, it will be possible to identify whether there are direct relationships between alteration or mineralization and physical property data, making it feasible to use such data as a proxy for alteration or mineralization.

Geophysical Inversion

Three-dimensional (3-D) electromagnetic (EM) inversions on the Mount Milligan geophysical data collected during the Geoscience BC QUEST project are ongoing at the Geophysical Inversion Facility of the University of British Columbia. As part of future work, EM and magnetic inversions will be performed over the Endako and Huckleberry deposits using data collected during the QUEST-West initiative. With an improved understanding of physical property characteristics of rocks in central BC porphyry deposit settings, geophysical inversion models in these, or similar, settings can be constrained in an informed way. Interpretations of the 3-D inversion results will also consequently be more informed.

Physical property ranges determined to identify hostrocks, mineralization or prospective alteration can potentially be queried within 3-D physical property models produced from inversion. This type of querying can be especially powerful when multiple inversion models are queried in combination. For example, it may be possible in the Endako deposit area to separate low-susceptibility nonmineralized kaolinite-altered areas from prospective low-susceptibility rocks by considering conductivity or chargeability models.

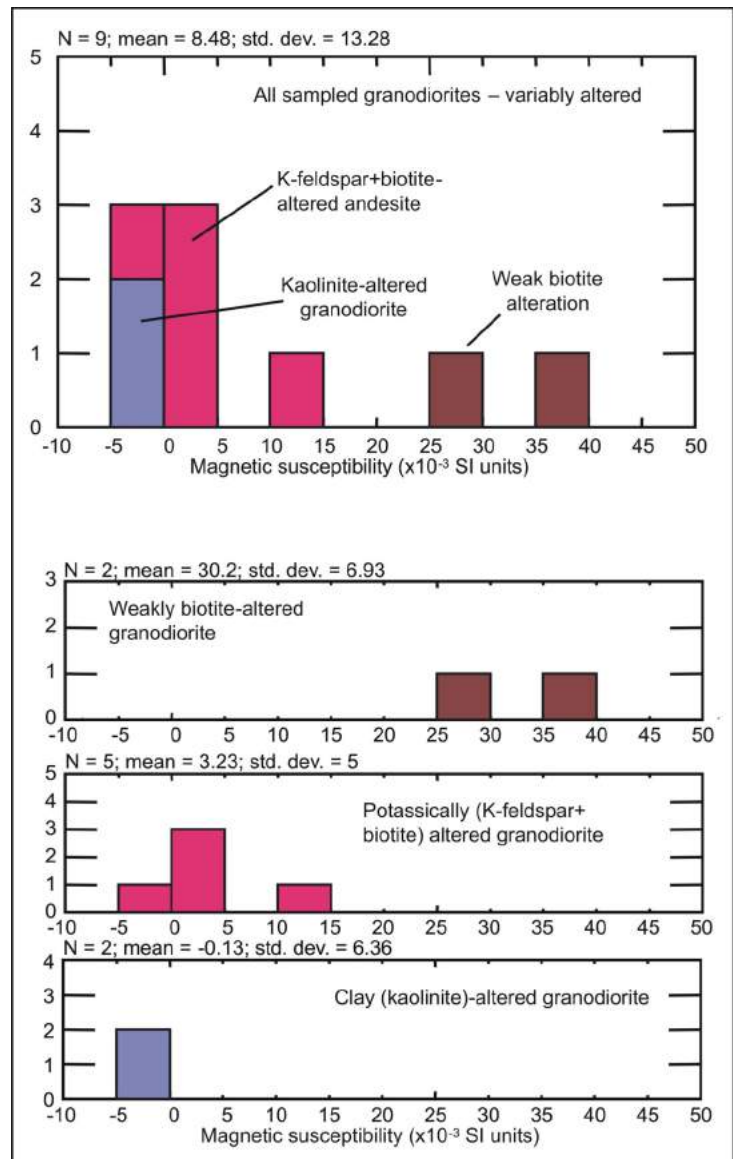


Figure 14. Magnetic susceptibility data for samples of granodiorite taken from drillcore at the Huckleberry copper-molybdenum deposit.

With continued physical property data compilation for the range of mineral deposit settings in BC, increased quantitative data become available for assessment alongside geological and geochemical data. Use of multiple datasets and quantitative criteria for mineral exploration will help to narrow down and improve confidence in selected regional- and local-scale exploration targets.

Acknowledgments

The authors gratefully acknowledge Geoscience BC and the Mineral Deposit Research Unit, University of British Columbia for funding this project. Thanks go to

Terrane Metals Corp., Endako Mines and Huckleberry Mines Ltd. for access to their properties, drillcore and data, and for logistical support;

D. O'Brien, D. Labrenz and S. Espinosa from Terrane Metals Corp. for ongoing correspondence with the authors on the Mount Milligan deposit and associated data;

J. Schroff, and F. Sayeed, head geologists at the Endako and Huckleberry mines, respectively, for discussions on the geological and geophysical characteristics of these two porphyry deposits;

P. Ogryzlo, former head geologist for Huckleberry Mines Ltd. for providing background information on the geology of the Huckleberry mine area;

P. Wojdak (Regional Geologist, BC Ministry of Energy Mines and Petroleum Resources) for discussions on the geology and alteration of central BC mineral deposits, and for access to sample collections from mineral deposits encompassed within the Geoscience BC QUEST and QUEST-West areas;

C. Barnett for assembling a collection of useful geological and geophysical maps prior to the authors' fieldwork at the Endako and Huckleberry mines; and

F. Ma of Geoscience BC compiled Figure 1 of this report, using an elevation model prepared by K. Shimamura of the Geological Survey of Canada.

References

- Aeroquest Limited (2009): Report on a helicopter-borne AeroTEM[®] system electromagnetic and magnetic survey; Geoscience BC, Report 2009-6, 28 p., URL <<http://www.geosciencebc.com/s/2009-06.asp>> [November 2009].
- Bissig, T., Vaca, S., Schiarizza, P. and Hart, C. (2010): Geochemical and physical variations in the Late Triassic Nicola Arc and metallogenetic implications, central British Columbia (NTS 092P, 093A, N): preliminary results; *in* Geoscience BC Summary of Activities 2009, Geoscience BC, Report 2010-1, p. 49–52.
- Bysouth, G.D. and Wong, G.Y. (1995): The Endako molybdenum mine, central British Columbia: an update; *in* Porphyry Deposits of the Northwestern Cordillera of North America, T.G. Schroeter (ed.), Canadian Institute of Mining and Metallurgy, Special Volume 46, p. 697–703.
- Canadian Council on Geomatics (2004): Canadian digital elevation data; Natural Resources Canada, GeoBase[®], URL <<http://www.geobase.ca/geobase/en/data/cded/description.html>> [October 2004].
- Geotech Limited (2008): Report on a helicopter-borne versatile time domain electromagnetic (VTEM) geophysical survey: QUEST Project, central British Columbia (NTS 93A, B, G, H, J, K, N, O and 94C, D); Geoscience BC, Report 2008-4, 35 p., URL <<http://www.geosciencebc.com/s/2008-04.asp>> [November 2009].
- Geotech Limited (2009): Helicopter-borne z-axis Tipper electromagnetic (ZTEM) and aeromagnetic survey, Mt. Milligan test block; Geoscience BC, Report 2009-7, 51 p., URL

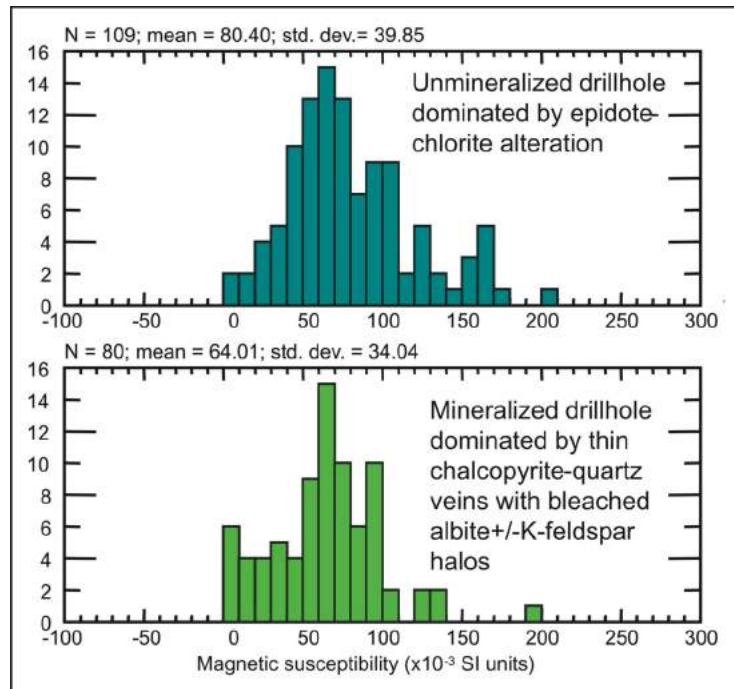


Figure 15. Comparison of susceptibility measurements taken along a poorly mineralized drillhole from near the East zone and measurements taken in a mineralized drillhole from the Main zone, Huckleberry copper-molybdenum deposit, central British Columbia. A slight decrease in average susceptibility values is apparent.

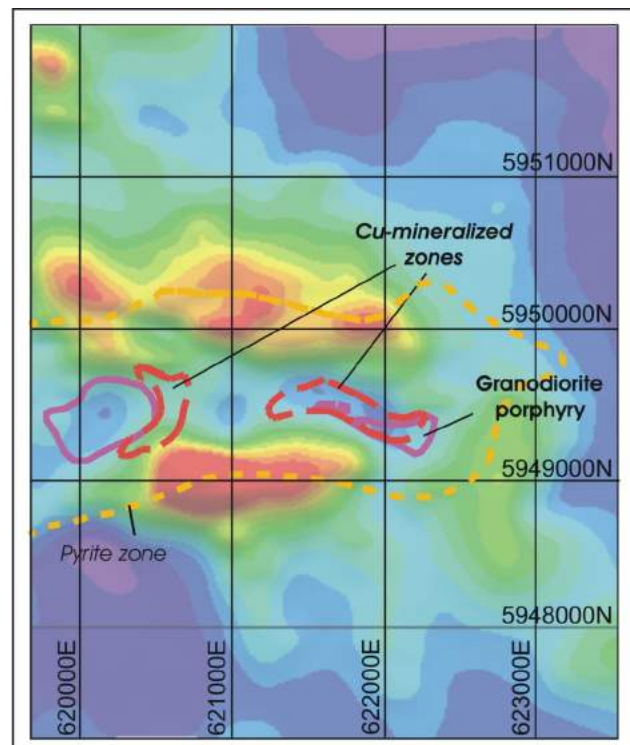


Figure 16. Total magnetic intensity data over the Huckleberry copper-molybdenum deposit, central British Columbia. Outlines of the mineralized zones (red), geological contacts (pink) and pyrite halo (orange) are shown. Data collected by Aeroquest Limited (2009) as part of the Geoscience BC QUEST-West initiative.

- <<http://www.geosciencebc.com/s/2009-07.asp>> [November 2009].
- Jackson, A. and Illerbrun, K. (1995): Huckleberry porphyry copper deposit, Tahtsa Lake district, west-central British Columbia; *in* Porphyry Deposits of the Northwestern Cordillera of North America, T.G. Schroeter (ed.), Canadian Institute of Mining and Metallurgy, Special Volume 46, p. 313–321.
- Jago, C.P. (2008): Metal- and alteration-zoning and hydrothermal flow paths at the moderately-tilted, silica-saturated Mount Milligan Cu-Au alkalic porphyry deposit: M.Sc. thesis, University of British Columbia, 210 p.
- Kimura, E.T, Bysouth, G.D. and Drummond, A.D. (1976): Endako; *in* Porphyry Deposits of the Canadian Cordillera, A. Sutherland Brown (ed.), Canadian Institute of Mining and Engineering, Special Volume 15, p. 444–454.
- Macintyre, D.G. (1985): Geology and mineral deposits of the Tahtsa Lake district, west-central British Columbia: BC Ministry of Energy, Mines and Petroleum Resources, Bulletin 75, 82 p., URL <<http://www.empr.gov.bc.ca/Mining/Geoscience/PublicationsCatalogue/BulletinInformation/BulletinsAfter1940/Pages/Bulletin75.aspx>> [November 2009].
- MINFILE (2010): MINFILE BC mineral deposits database; BC Ministry of Energy, Mines and Petroleum Resources, URL <<http://minfile.ca>> [November 2010].
- Natural Resources Canada (2007): The atlas of Canada base maps; Natural Resources Canada, Earth Sciences Sector, URL <<http://geogratis.cgdi.gc.ca/geogratis/en/option/select.do?id=138>> [November 2007].
- Nelson, J. L. and Bellefontaine, K.A. (1996): The geology and mineral deposits of north-central Quesnellia, Tezzeron Lake to Discovery Creek, central British Columbia; BC Ministry of Energy, Mines and Petroleum Resources, Bulletin 99, 112 p., URL <<http://www.empr.gov.bc.ca/Mining/Geoscience/PublicationsCatalogue/BulletinInformation/BulletinsAfter1940/Pages/Bulletin99.aspx>> [November 2009].
- Phillips, N., Nguyen, T.N.H. and Thomson, V. (2009): QUEST Project: 3D inversion modelling, integration, and visualization of airborne gravity, magnetic, and electromagnetic data, BC, Canada (NTS 93A, 93B, 93G, 93H, 93J, 93K, 93N, 93O, 94C, 94D); Geoscience BC, Report 2009-15, 79 p., URL <<http://www.geosciencebc.com/s/2009-15.asp>> [November 2009].
- Selby, D., Nesbitt, B.E., Muehlenbachs, K. and Prochaska, W. (2000): Hydrothermal alteration and fluid chemistry of the Endako porphyry molybdenum deposit, British Columbia; *Economic Geology*, v. 95, p. 183–202.
- Sketchley, D.A., Rebagliati, C.M. and DeLong, C. (1995): Geology, alteration, and zoning patterns of Mount Milligan copper-gold deposits; *in* Porphyry Deposits of the Northwestern Cordillera of North America, T.G. Schroeter (ed.), Canadian Institute of Mining and Metallurgy, Special Volume 46, p. 650–665.
- Stanley, C.R. (1992): Porphyry copper-gold systems of British Columbia; University of British Columbia, Mineral Deposit Research Unit, Annual Technical Report—Year 1, p. 13.2–13.30.
- Villeneuve, M, Whalen, J.B., Anderson, R.G. and Struik, L.C. (2001): The Endako batholith: episodic plutonism culminating in formation of the Endako porphyry molybdenite deposit, north-central British Columbia; *Economic Geology*, v. 96, p. 171–196.

Characterization of Placer- and Lode-Gold Grains as an Exploration Tool in East-Central British Columbia (NTS 093A, B, G, H)

J.K. Mortensen, Department of Earth and Ocean Sciences, University of British Columbia, Vancouver, BC, jmortensen@eos.ubc.ca

R. Chapman, University of Leeds, United Kingdom

Mortensen, J.K. and Chapman, R. (2010): Characterization of placer- and lode-gold grains as an exploration tool in east-central British Columbia (NTS 093A, B, G, H); in Geoscience BC Summary of Activities 2009, Geoscience BC, Report 2010-1, p. 65–76.

Introduction

The famous Cariboo gold rush in east-central British Columbia was triggered by the discovery of rich placer-gold deposits on several creeks in the Likely and Wells–Barkerville areas (Figure 1) between 1859 and 1862. This area has subsequently yielded an estimated 2.5 to 3 million ounces (80–96 tonnes) of placer gold (e.g., Levson and Giles, 1993), which represents roughly half of BC’s total historic placer-gold production. Numerous gold-bearing orogenic quartz veins and associated pyritic mantos were discovered in medium-grade metamorphic rocks of the Barkerville Terrane in the Wells–Barkerville area (Figure 1) soon after placer mining began, and have since produced approximately 1.2 million ounces (38.3 tonnes) of gold. Although these lode deposits were probably the source of much of the placer gold in the immediate area (e.g., Johnston and Uglow, 1926), the ultimate bedrock source(s) of much of the placer gold elsewhere in this part of BC has (have) still not been conclusively identified. Other styles of lode gold known to be present in this region include vein-hosted and disseminated gold in low-grade metasedimentary units of the Quesnel Terrane (e.g., Spanish Mountain and Frasergold deposits) and these occurrences, together with those in the Wells–Barkerville area, are referred to as the ‘Cariboo gold district’ (CGD; Rhys et al., 2009; Figure 1). Farther to the west, volcanic strata and intrusive rocks of the Quesnel Terrane (Figure 1) host porphyry Cu-Au and skarn Au deposits such as Mount Polley and QR, respectively, and potentially other styles of lode-gold mineralization. Active mineral exploration is ongoing in this area and in similar rocks along strike to the north. Airborne geophysical surveys and parallel silt and lake-sediment geochemical studies carried out as part of the QUEST Project by Geoscience BC cover much of the CGD

and initial results of the new work have already generated an increased level of exploration activity in this region.

A study by Rhys et al. (2009) of orogenic gold in the CGD, which comprises the Wells–Barkerville mining camp and vicinity in the Barkerville Terrane, and the Spanish Mountain and Frasergold deposit areas in the Quesnel Terrane (Figure 1), has provided an improved understanding of the nature and age of orogenic gold mineralization throughout much of the CGD and, in particular, has shed new light on the structural controls on mineralization in various parts of the CGD and relationships between the various styles of lode-gold mineralization.

Attempting to match the alloy composition of placer-gold grains determined using an electron microprobe with compositions of known lode occurrences in the same vicinity (‘geochemical fingerprinting’) has previously been used as an exploration tool in many localities, including the Cariboo district (e.g., McTaggart and Knight, 1993; Knight et al., 1999a; Townley et al., 2003; Chapman, 2007). Over the past several years, a much more comprehensive approach for examining the relationships between placer and lode gold has been developed, based on extensive work in the Klondike gold district in western Yukon and in several other localities worldwide (e.g., Chapman and Mortensen, 2006; Mortensen et al., 2006). In this study of relationships between placer and lode gold, a number of different tools were used to determine not only the major-element but also the trace-element compositions of gold from placers and their potential lode sources using both electron microprobe and laser ablation inductively coupled plasma–mass spectrometry (ICP-MS) methods. Other analyses focused on examining and characterizing the mineral-microinclusion suites present within placer and lode gold and carrying out quantitative studies of the evolution of the shapes of placer-gold grains as they are transported in an alluvial-fluvial environment. Use of this much broader array of tools to resolve the problem of relationships between placer and lode gold in a particular region has led to the development of considerably more unique fingerprints for placer gold, which makes it possible to more closely match placer-gold grains with very specific lode sources. In addition, work

Keywords: Cariboo gold district, gold, placer, lode, composition, exploration

This publication is also available, free of charge, as colour digital files in Adobe Acrobat® PDF format from the Geoscience BC website: <http://www.geosciencebc.com/s/DataReleases.asp>.

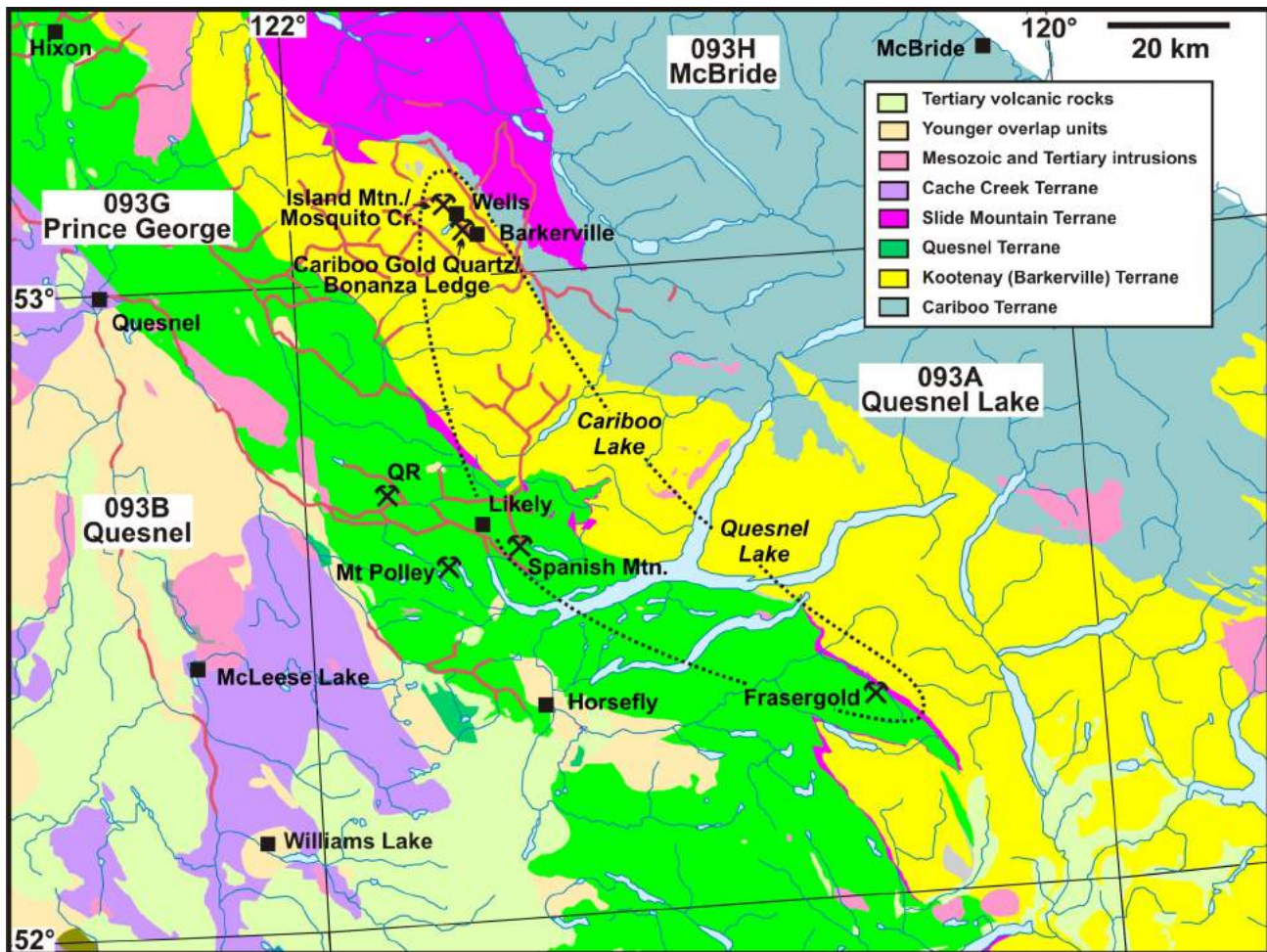


Figure 1. Regional geology of the study area in east-central British Columbia, showing locations of the Cariboo gold district (dotted black line), significant known lode-gold and Cu-Au deposits (mine symbols), and significant placer streams (red lines).

done on the evolution of the shapes of gold grains during transport (Crawford, 2007) shows great promise in producing realistic and relatively precise estimates of the distance a particular set of placer-gold grains has travelled from its lode source. The results of these studies have direct applicability to gold exploration programs. Specific questions that can be addressed using this approach include

How many individual populations of gold (presumed to be derived from different lode sources) are present within a single sample of placer gold based on the sample's alloy composition and/or shape?

What is the most probable style of lode-gold mineralization from which each population was derived, compared to established global compositional fingerprints for gold from different styles of mineralization?

What distance has each compositional population travelled on the basis of average grain shape?

Based on a single sample of placer gold from near the outlet of a drainage basin, one can then evaluate

- what style(s) of lode gold are present within that drainage basin;

- how far down the drainage system each population of gold in the sample has travelled after liberation from its source; and
- whether the alloy compositions and shapes of all of the placer-gold grains can be entirely explained by derivation from known lode sources in the drainage basin or, alternatively, whether other lode sources contributed to the placer.

In the latter case, it is also possible to speculate on the style of mineralization which remains to be discovered in situ. However, numerous complicating factors must be considered in any interpretation, including

- Has the area been glaciated or not, and if so, what is the exact nature of the unconsolidated material from which the placer gold was derived (e.g., fluvial, glaciofluvial or till) and what was the direction of glacial transport?
- Are the host sediments first-cycle deposits or have they potentially been reworked following drainage reversals or modifications?

Despite these potential complications, characterization of placer gold has been used effectively to guide lode exploration

tion in many parts of the world, including the Klondike district in Yukon (e.g., Knight et al., 1999a, b; Chapman and Mortensen, 2006; Mortensen et al., 2006), Great Britain and Europe (Chapman, 2007; Chapman et al., 2009), and the Otago Schist belt in New Zealand (Youngson and Craw, 1995). This type of information can be obtained at an early stage in a reconnaissance exploration program, at a relatively low cost.

Research Goals

The current project involves a one-year reconnaissance study of placer- and lode-gold compositions from a large area in east-central BC, including both the CGD and a large region to the west and northwest (Figure 1). This study builds directly on earlier work in the area by McTaggart and Knight (1993; discussed below). A total of approximately 1600 placer-gold grains were collected from 34 separate localities during 2009; together with a large number of additional placer- and lode-gold samples from other sources, these samples will be used to constrain relationships between placer and lode gold in the study area. The main goals of the project are to develop more unique microgeochemical ‘fingerprints’ for each of the known lode-gold occurrences in the region based on major- and trace-element geochemistry and mineral-microinclusion suites, as well as to evaluate the distribution and likely source(s) of gold with similar signatures in as many placer deposits in the region as possible. It is expected that the work will validate this approach to the study of relationships between placer and lode gold in east-central BC and provide a preliminary assessment of the nature of, and potential for, undiscovered lode sources within the study area. These outcomes will have direct implications for ongoing mineral exploration in this part of BC. Results of this study could later be applied on a regional basis to help with reconnaissance of the less well-explored area to the northwest, which was recently investigated by airborne geophysical and geochemical surveys as part of Geoscience BC’s QUEST and QUEST-West projects. Placer-gold deposits are known to be widely distributed throughout this large region; however, few if any significant gold (or gold-bearing) lode sources have been identified thus far. A detailed study of the placer gold in various deposits could provide valuable insights into what style(s) of lode source contributed to each placer deposit, and some indication of their location.

Regional Geological Setting

The study area is underlain by parts of five main terranes (Figure 1). Bedrock in most of the northern and eastern parts of the area comprises metamorphic rocks of the Barkerville Terrane and the structurally overlying Cariboo Terrane. Both the Barkerville and Cariboo terranes in the northern part of the area have been overthrust by mainly mafic volcanic rocks of the Slide Mountain Terrane. The

southwestern margin of the Barkerville Terrane is structurally overlain by Middle and Late Triassic volcanic and sedimentary rocks of the Quesnellia Terrane (Figure 1). Still farther to the southwest are mafic volcanic rocks and associated pelagic sedimentary units of the Cache Creek Terrane. A variety of intermediate to felsic intrusions of Mesozoic to Early Tertiary-age plutons occur throughout the area. Parts of the study area are overlain by Tertiary and younger sedimentary and volcanic cover (Figure 1).

Placer-gold deposits in the study area have been described by Levson and Giles (1993). East-central BC was strongly glaciated during the Pleistocene and surficial deposits include a wide range of glacial materials, and alluvial-fluvial deposits from both pre- and postglacial streams. The placer geology in some portions of the study area is further complicated by the fact that several different drainage systems are superimposed on one another and the exact position of the older drainage systems is not well understood. Placer gold in portions of the study area occurs as placer deposits derived directly from relatively local lode sources, but also as deposits that have been reworked from older stream deposits (in some cases still preserved in raised channels, as in the Spanish Mountain area; Figure 1), as deposits dispersed within glacial deposits, and in postglacial streams that may in part be reworking gold from glacially dispersed older placer deposits (e.g., the Hixon area; Figure 1; Levson and Giles, 1993). Interpretation of relationships between placer and lode gold in the study area is therefore not straightforward. Placer gold in major drainages is likely to have a more complex origin than that of placer gold near the headwaters of streams, where there is a greater likelihood that the gold is a primary deposit eroded directly from a local lode source.

Lode- and Placer-Gold Deposits in East-Central BC

The study area covers a variety of known lode-gold occurrences, including both orogenic gold-vein systems in the CGD (comprising the Wells–Barkerville mining camp, together with the Spanish Mountain and Frasersgold deposits, and several other areas of gold prospects along and adjacent to placer-gold-bearing creeks in this area), and porphyry Cu-Au deposits, such as Mount Polley, and other intrusion-related deposits, such as the QR skarn Au deposit (Figure 1). Several distinct, but probably related, styles of orogenic gold mineralization have been recognized in the CGD (Rhys et al., 2009). Gold-bearing extensional quartz (\pm carbonate) veins, in some cases associated with dextral shear zones, hosted by low- to medium-grade phyllite and schist are the most typical style of lode gold within the Barkerville Terrane. This style of mineralization occurs in many localities within the immediate Wells–Barkerville area as well as the Yanks Peak area north of Cariboo Lake (Figure 1), and was the main type of ore mined at the Mos-

quito Creek, Island Mountain and Cariboo Gold Quartz mines in the Wells area. Gold-bearing pyritic replacement ('manto-style') mineralization also occurs in the Wells area, where it accounted for roughly one third of the lode production. The other two main centres of orogenic gold mineralization in the CGD comprise quartz (\pm carbonate) veins and vein breccias hosted by Middle to Late Triassic, low-grade, phyllitic metasedimentary rocks that make up the structurally lower portion of the Quesnellia Terrane, which has been thrust northeastward over the Barkerville Terrane. This style of mineralization is currently being explored in the Spanish Mountain deposit southeast of Likely and in the Frasergold deposit, which is approximately 50 km east of Horsefly (Figure 1). Some gold at the Spanish Mountain deposit also occurs with pyrite disseminated within the host phyllite. Published BC MINFILE descriptions of small lode-gold occurrences northeast of Hixon, in the northwestern corner of the study area (Figure 1), indicate that the mineralization may be similar to that at Spanish Mountain.

Historic and current placer-gold workings are present throughout much of the western part of the study area, and the main currently held placer properties are shown on Figure 1. The fact that placer deposits are present in the immediate vicinity of all of the main known lode-gold sources in the region means this area is ideal for evaluating the relationships between placer gold and the various styles of lode gold, and for developing well-characterized microchemical signatures for each type of lode deposit.

Previous Gold Compositional Studies in East-Central BC

A compositional study of placer- and some lode-gold deposits and occurrences in the Cariboo area of east-central BC was carried out by McTaggart and Knight (1993), mainly with funding from the BC Geological Survey. They analyzed gold from a total of 47 placer-gold samples from throughout the region, as well as 18 lode-gold samples (a total of some 3700 individual analyses). Most of the placer samples had been donated from active placer operations set on major placer streams, although a small proportion of samples had been collected in the middle or upper reaches of streams. They also did a limited amount of scanning electron microscope (SEM) work to characterize features such as the presence and nature of high-fineness rims on placer grains (fineness = $(\text{Au}/[\text{Au} + \text{Ag}] * 1000)$), but the study was based mainly on major- and minor-element concentrations determined using an electron microprobe. Although a very large amount of analytical data was generated by the study, no detailed analysis or interpretation of the data was ever completed and preliminary conclusions were not sufficiently detailed to provide specific constraints for future exploration in the region.

McTaggart and Knight (1993) recognized several distinct compositional populations for placer and lode gold in the region, based mainly on calculated fineness and, to a lesser extent, on measured Hg content of the Au. Their main conclusions about these compositional populations were

relatively high-fineness (900–950) gold was characteristic of quartz veins in the Wells–Barkerville mining camp and of most of the placers in that area, and farther to the west;

gold in pyritic replacement-style deposits in the Wells–Barkerville mining camp has considerably lower fineness (850–875), is typically much finer-grained than gold in quartz veins in the same area and has been only rarely seen in placer deposits;

gold from the Proserpine and Warspite quartz-vein occurrences southeast of Barkerville has a somewhat different composition, with samples from these lodes yielding measured fineness values of 830–890, which indicates that their composition more closely resembles that of the replacement-style mineralization in the main Wells–Barkerville mining camp; and

lode gold from quartz veins in the Spanish Mountain deposit area and placer gold in streams in the Likely area nearby have distinctly lower fineness values (750–810) than the lode deposits and associated placers farther east in the Barkerville Terrane.

2009 Placer Sampling

A total of 34 new placer-gold samples were collected during the 2009 field season, using gold pans and a portable test sluice. Sampling in 2009 was hampered by relatively high-water conditions during the fieldwork (Figures 2a, b). Placer sampling in east-central BC is also made difficult by the preponderance of low-gradient streams, deep overburden and current paucity of active placer operations allowing ready access to gold-bearing gravel deposits. Despite these obstacles, an excellent suite of placer-gold samples was obtained from sites throughout the CGD and other scattered localities farther to the west and northwest.

Preliminary Results

Samples obtained during the 2009 field season are currently being prepared for analysis. However, analysis of bulk lode-gold samples from the CGD, which were collected during field studies of orogenic gold in the area (Rhys et al., 2009), and gold grains in polished thin sections (K. Ross, unpublished petrographic studies, 2008) has been completed. In addition, the entire dataset generated by the McTaggart and Knight (1993) study has been digitized and this data is currently being re-evaluated and re-interpreted in light of recent re-interpretations (Rhys et al., 2009) of the nature and distribution of orogenic gold in the CGD. The entire suite of gold samples previously studied by



Figure 2. Collecting placer-gold samples in east-central British Columbia, using **A)** panning methods and **B)** a portable test sluice and hand pump.

McTaggart and Knight (1993) has been re-examined using SEM and energy dispersive spectroscopy (EDS) methods to identify and quantify the mineral-microinclusion suites present in each sample.

Figures 3a and b show lode- and placer-gold compositional data from the Wells–Barkerville area of the CGD. Cumulative percentile plots are used to portray the compositional range(s) of the various samples, instead of the simple histograms used by McTaggart and Knight (1993). This method

allows straightforward interrogation of data from individual samples; for example, the data for the Burns Mountain lode sample in Figure 3a shows three distinct compositional populations corresponding to ‘steps’ in the cumulative percentile plot for Ag from this sample at 10, 12 and 15–17% Ag. These relatively subtle variations in composition are nearly impossible to recognize using simple histogram representations of the data. In addition, when using cumulative percentile plots data from a large number of samples can be plotted on the same diagram (e.g., Fig-

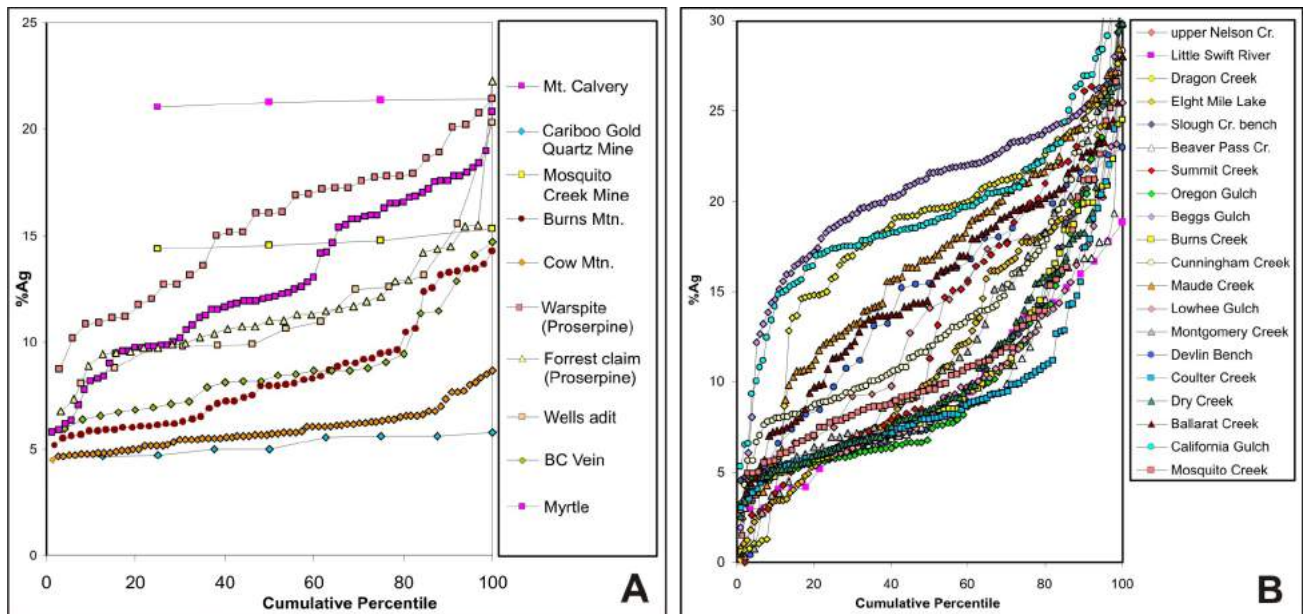


Figure 3. Compositions of **A)** lode gold and **B)** placer gold from the Wells–Barkerville area of the Cariboo gold district, in east-central British Columbia, expressed as cumulative percentile plots of Ag contents. Specific lode occurrences are veins that were sampled by McTaggart and Knight (1993).

ure 3b), which allows direct comparison of the compositional signatures from various sources.

Preliminary results and sampling strategies for specific parts of the study area are discussed in detail below.

Wells–Barkerville Area

Figure 4 presents the simplified geology of the Wells–Barkerville area, showing the locations of the main mines and other significant lode-gold occurrences. Also shown are the locations of placer- and lode-gold samples from the McTaggart and Knight (1993) study, as well as new placer- and lode-gold samples collected during this study. The data for lode gold from various occurrences in the Wells–Barkerville mining camp in Figure 3a clearly shows significant and recognizable differences between the compositions of gold from various lode sources in this area. By comparing the compositions of placer gold in streams in the vicinity of these lode sources, one can immediately begin to evaluate the contribution of gold from the different lode sources into individual placer deposits. Current work focuses on assessing the compositional data from lodes and

placers in terms of past drainage patterns in the area, and specifically attempting to determine whether all of the gold in each placer sample could have been derived entirely from known lode occurrences within that drainage system or whether there are other, still undiscovered lode sources to be found. The McTaggart and Knight (1993) dataset is too limited for most of the drainages to be able to make definite conclusions about this; because most of these samples came from active placer operations in main-trunk streams, they are likely to show mixed compositional signatures resulting from the presence of gold from more than one lode source. Placer sampling during 2009 focused on samples from nearer to the heads of streams, where gold is likely to be derived from a single lode occurrence or group of related occurrences.

An example of how the placer and lode compositional data can be used to constrain the source(s) of gold in a specific placer deposit is shown in Figure 5, which compares the compositional range of a sample of placer gold from the middle reaches of Cunningham Creek (in the southeastern part of the area shown in Figure 4) with that of gold from the Hibernia lode occurrence approximately 5 km upstream

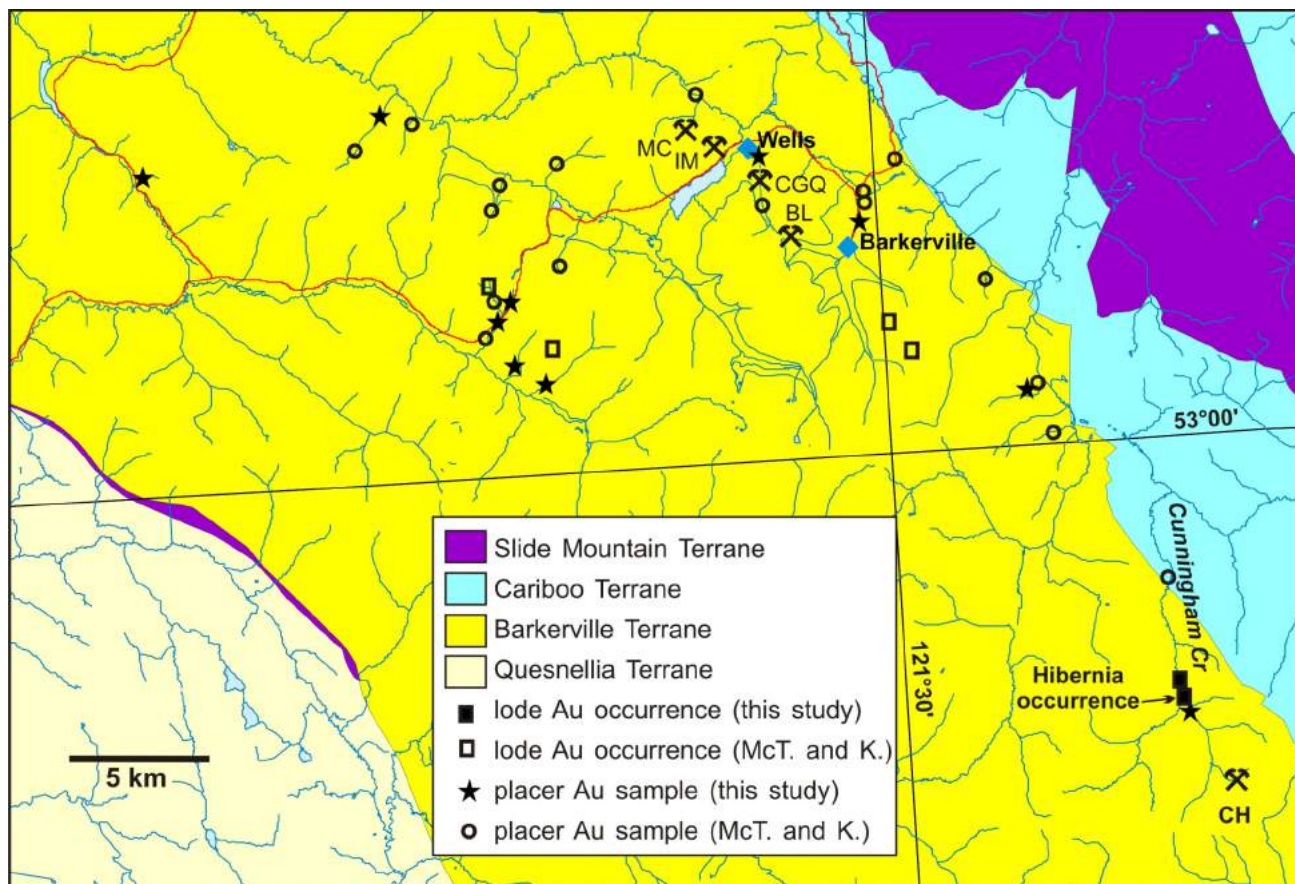


Figure 4. Simplified geology of the Wells–Barkerville and Cunningham Creek areas, east-central British Columbia, showing previous (McTaggart and Knight, 1993) and new (this study) lode- and placer-gold sampling localities. Past-producing gold mines and significant lode occurrences include Mosquito Creek mine (MC), Island Mountain mine (IM), Cariboo gold quartz mine (CGQ), Bonanza Ledge deposit (BL) and Cariboo Hudson mine (CH).

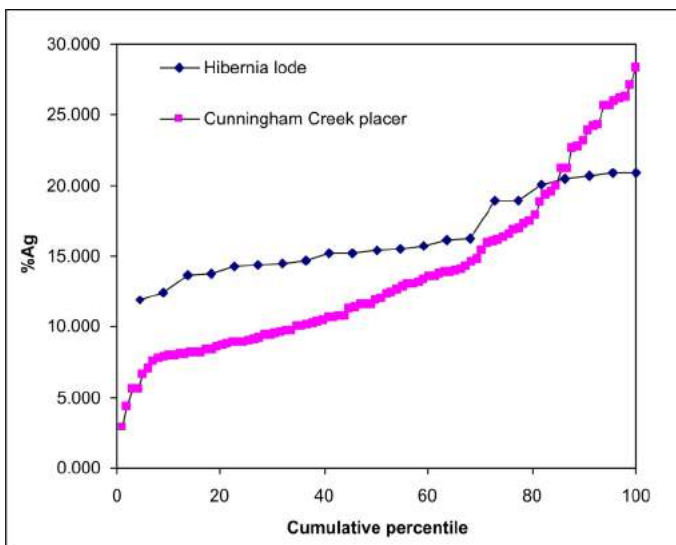


Figure 5. Comparison of compositions of gold from the Hibernia lode on upper Cunningham Creek (this study) with a placer-gold sample from the middle reaches of Cunningham Creek (data from McTaggart and Knight, 1993), east-central British Columbia.

from the placer locality. Gold in the Hibernia lode shows a narrow range of compositions (possibly two separate populations) between 12 and 20% Ag. Although a substantial portion of the gold in the Cunningham Creek placer sample gives compositions that are similar to gold from the Hibernia lode, more than half of the placer sample comprises gold with Ag contents that differ significantly from the Hibernia lode. This indicates either that there is greater compositional diversity in the Hibernia and related vein systems than is indicated by this single sample or that other undiscovered lode sources contributed gold to the placer deposit.

Likely–Cariboo Lake Area

Figure 6 presents the simplified geology map of the Likely–Cariboo Lake area, showing the locations of the Spanish Mountain deposit and the Midas adit in the Yanks Peak area north of Cariboo Lake (lode

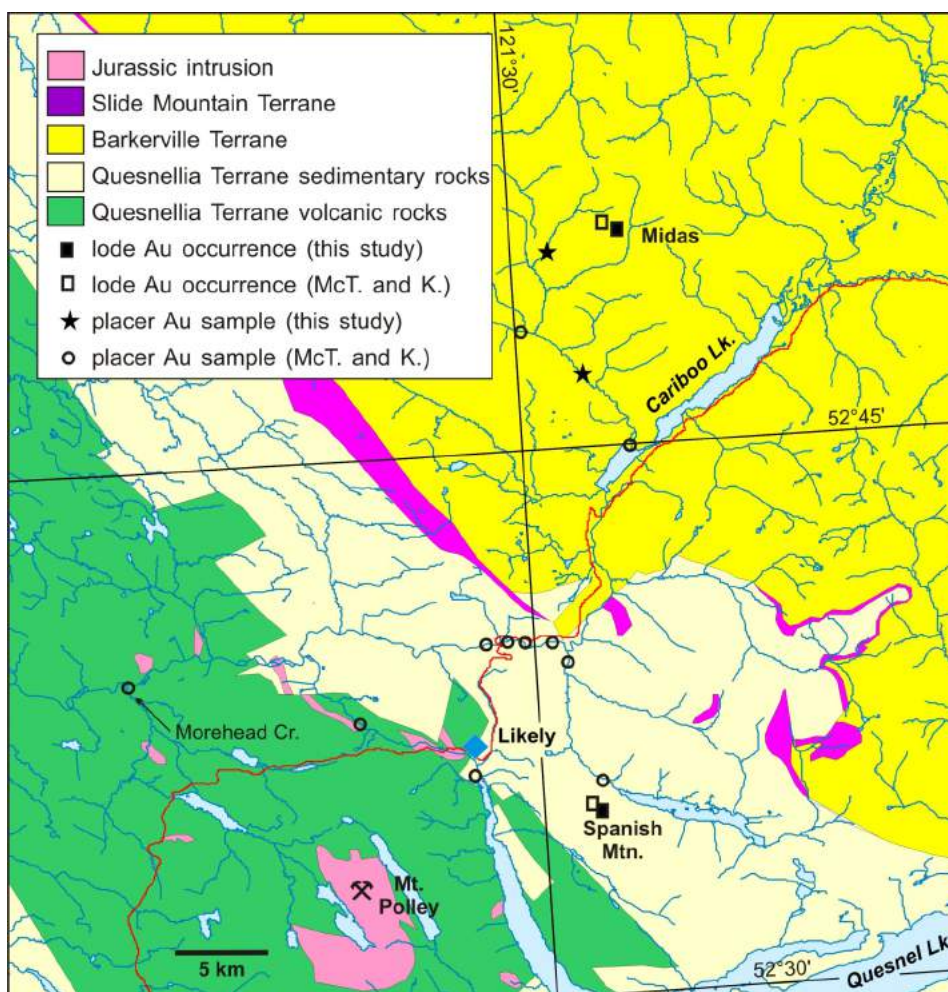


Figure 6. Simplified geology of the Likely–Cariboo Lake area, east-central British Columbia, showing previous (McTaggart and Knight, 1993) and new (this study) placer- and lode-gold occurrences.

samples), as well as previous and new placer sampling localities.

The compositional data for lode occurrences (Figure 7) demonstrates the very limited range of compositions (13–14% Ag) from the Midas vein occurrence in the Barkerville Terrane, as compared to that of veins in the Spanish Mountain deposit (18–27% Ag). Most of the placer-gold grains analyzed in the two Spanish Creek placer samples (data from McTaggart and Knight, 1993) yielded expected compositions, consistent with having been derived from Spanish Mountain veins; however, approximately 30% of the grains yielded much lower Ag contents, which suggests that they are more similar in composition to lode gold from the Cow Mountain area (including the Cariboo Gold Quartz mine; Figure 3a). It appears likely that a component of Barkerville Terrane gold, more specifically a Cow Mountain-Cariboo Gold Quartz-type component, has been incorporated into the Spanish Creek placer, perhaps via an earlier west- or southwest-directed drainage system.

Frasergold Area

A significant lode-gold resource has been established at the Frasergold deposit, approximately 52 km east of Horsefly. The geology of this area is shown in Figure 8.

Gold-bearing veins at the Frasergold deposit are hosted within the same package of Quesnellia Terrane, Middle to Late Triassic, phyllitic sedimentary rocks as that which hosts the Spanish Mountain deposit; however, veins at Frasergold are the product of an earlier veining event than that at Spanish Mountain (Rhys et al., 2009). The composition of lode gold at Frasergold is also distinctly different from that at Spanish Mountain, although this is based on a limited number of analyses (Figure 7). Gold grains at Frasergold have Ag contents of 26–34%, whereas those from several different veins at Spanish Mountain range from 18–27% Ag. This suggests that it may be possible to discriminate between early Frasergold-type vein systems and later Spanish Mountain-type veins on the basis of the alloy composition.

There are no currently active placer leases anywhere in the area shown in Figure 8; however, anecdotal information indicates that some placer deposits are known in the area (the Frasergold deposit was discovered by tracing placer gold up the MacKay River). Of the three placer-gold samples col-

lected from the Frasergold area (Figure 8), two come from small tributaries draining into the MacKay River from the slope on which the Frasergold deposit was located and the third is from the MacKay River itself, at a point approximately 8 km downstream from the deposit. These three samples should provide an excellent representation of the range of gold compositions in the Frasergold deposit and associated occurrences in the area. Rhys et al. (2009) pointed out that two other mineral occurrences in the area (Kusk and Tep 1 [or Forks], MINFILE 093A 061 and 093A 092, respectively; MINFILE, 2009; Figure 8) closely resemble the Frasergold deposit in terms of hostrocks, as well as style of mineralization and alteration. This correlation could be further tested by comparing the composition of gold obtained from veins, local placers or heavy-mineral samples in these two occurrences with that of the gold at the Frasergold deposit.

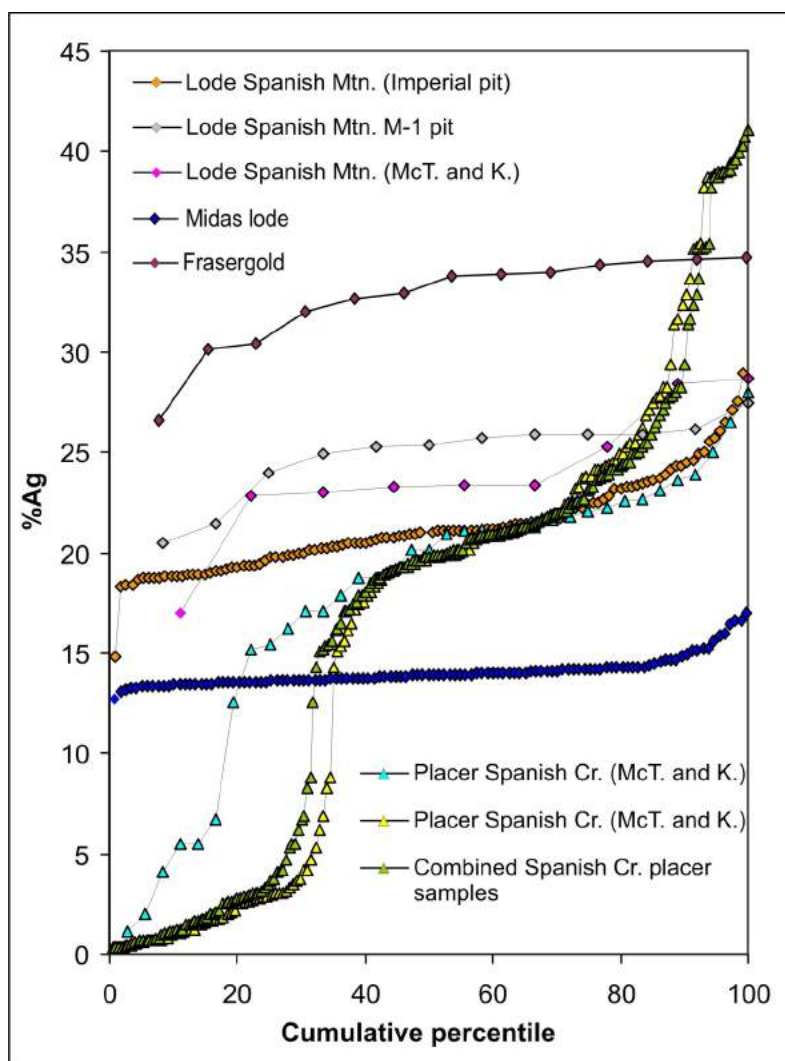


Figure 7. Compositional ranges from gold in veins at the Spanish Mountain deposit, the Midas adit (Yanks Peak area north of Cariboo Lake), east-central British Columbia, and the Frasergold deposit, east-central British Columbia, and two separate placer samples from the Spanish Creek placer immediately downstream from the Spanish Mountain deposit (data from McTaggart and Knight, 1993).

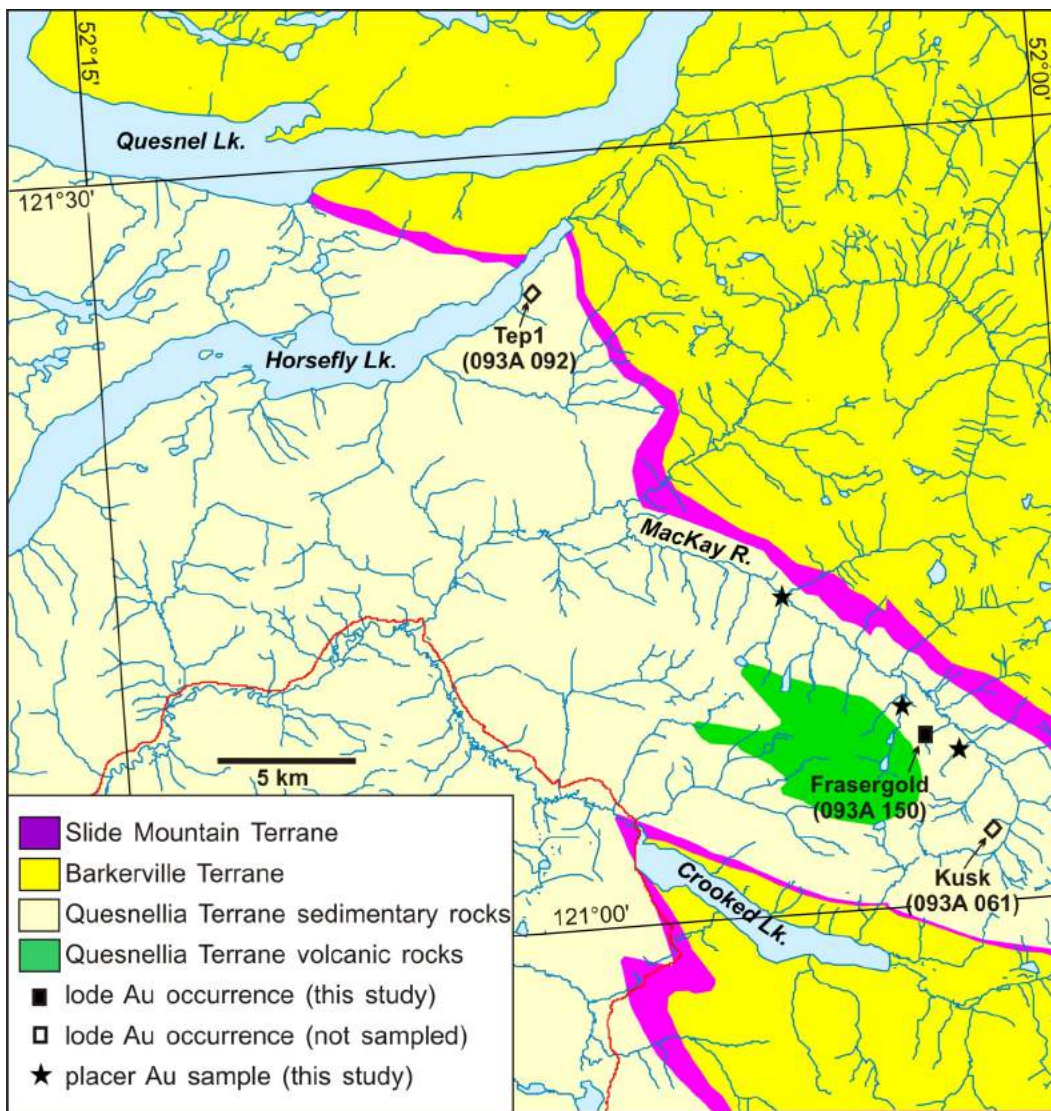


Figure 8. Simplified geology of the Quesnel Lake–Crooked Lake area, east-central British Columbia, showing the location of the Frasersgold deposit and two geologically similar occurrences (Kusk and Tep 1), and placer-gold samples collected during 2009.

Hixon Area

Placer deposits have been mined on Hixon Creek and its tributaries in the extreme northwest corner of the study area (Figure 1) for many years. The geology of the Hixon area is shown in Figure 9, together with the locations of placer- and lode-gold occurrences, currently valid placer leases in the area, and the locations of a placer sample previously collected by McTaggart and Knight (1993) and one collected during this study.

The nature of the lode source(s) from which gold in the Hixon Creek placer deposits was derived has not been resolved. Several lode occurrences immediately upstream from the Hixon Creek placer are hosted within the same Middle to Late Triassic black phyllite package that hosts the Spanish Mountain and Frasersgold deposits to the southeast, or in greenstones that are interpreted to be part of the

Triassic volcanic package of Quesnellia. This includes the Quesnel Quartz occurrence (MINFILE 093G 015), which produced a small amount of gold in the 1930s, and the Cayenne occurrence (MINFILE 093G 014). Both of these occurrences comprise quartz-vein systems in foliated schist and greenstone of the Quesnellia Terrane (Allan, 1984; MINFILE, 2009). The Pioneer occurrence (MINFILE 093G 013), situated on an upstream tributary into Hixon Creek (Figure 9), comprises quartz veins within Triassic black phyllite of Quesnellia. Although it was mined on a very small scale for Pb, Zn and Ag in the 1920s, the veins are also anomalous for gold, which indicates they resemble those at Spanish Mountain. An alternative interpretation of the origin of the placer gold on Hixon Creek might be that it is derived from presently unrecognized epithermal-vein occurrences in the area. This is a possibility because the relatively high Ag contents of most of the gold analyzed from

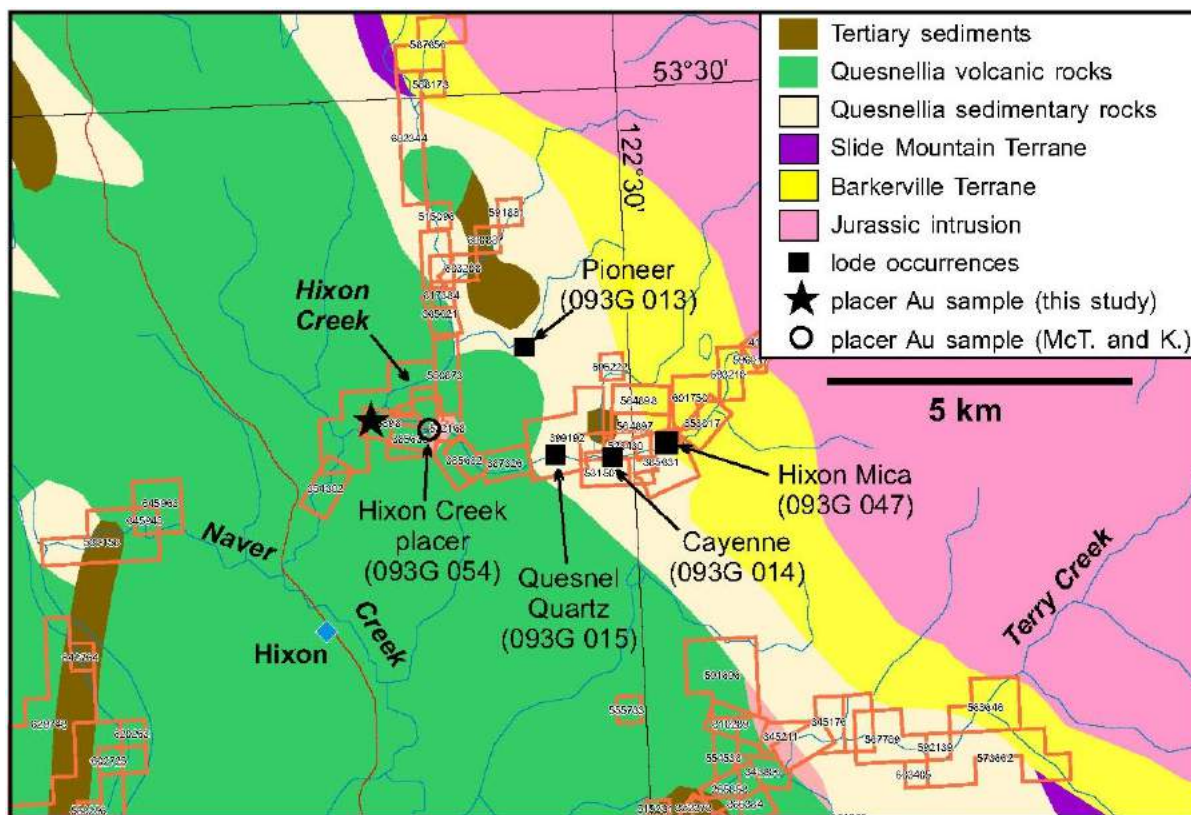


Figure 9. Simplified geology of the Hixon area, east-central British Columbia; currently valid placer leases are shown as red boxes.

Hixon Creek and the range of Ag contents (Figure 10) overall can be suggestive of an epithermal environment (Chapman and Mortensen, 2006). However, the close association of the Hixon Creek placers with Spanish Mountain (or Frasergold)-type gold-bearing veins within phyllite of Quesnellia strongly suggests that mineralization analogous to that at Spanish Mountain or Frasergold is present in the area. The forthcoming examination of the inclusion assemblages present in gold from Hixon Creek may assist in determining the origin of the gold. No inclusions that would be diagnostic of a particular style of mineralization were identified in the sample of fine gold that was collected by McTaggart and Knight (1993). Placer gold is also present on Naver Creek approximately 15 km southeast of Hixon Creek, in an area also underlain by black phyllite of Quesnellia (Figure 9). No lode-gold occurrences are presently known in that area; however, the inference that gold in the Hixon Creek area is likely derived from Spanish Mountain- or Frasergold-type-lode occurrences suggests that exploration for similar mineralization in the Naver Creek area is warranted.

Mineral Microinclusions in Gold

Preliminary results of SEM and EDS examination of the mineral microinclusions present in the placer- and lode-

gold samples from the McTaggart and Knight (1993) sample suite show that, although inclusions are relatively rare in many of the grains (especially the finer placer grains), there is a general correlation between the inclusion suites present in the placer gold and the specific mineralogy of the lode sources from which the gold is thought to have been derived (e.g., argentite, sulpharsenide minerals and pyrite in lodes and placers in the Spanish Mountain area, and a strong bismuth signature—including Bi sulphide, sulpharsenide and carbonate minerals—in lodes and placers in the immediate vicinity of Wells). The results of detailed petrographic work on lode-gold occurrences throughout the CGD, now underway as part of the Rhys et al. (2009) study of orogenic gold in the CGD, will assist in providing a more complete evaluation of the micro-inclusion suite.

Discussion

Preliminary results of this study suggest that distinct signatures can be established for various styles of lode gold in the study area based on gold-alloy composition and, to some extent, on the mineral-microinclusion suite present. Significant compositional variations exist, even within individual mining camps (e.g., the Wells-Barkerville mining camp; Figure 3a), and these differences may make it possible to

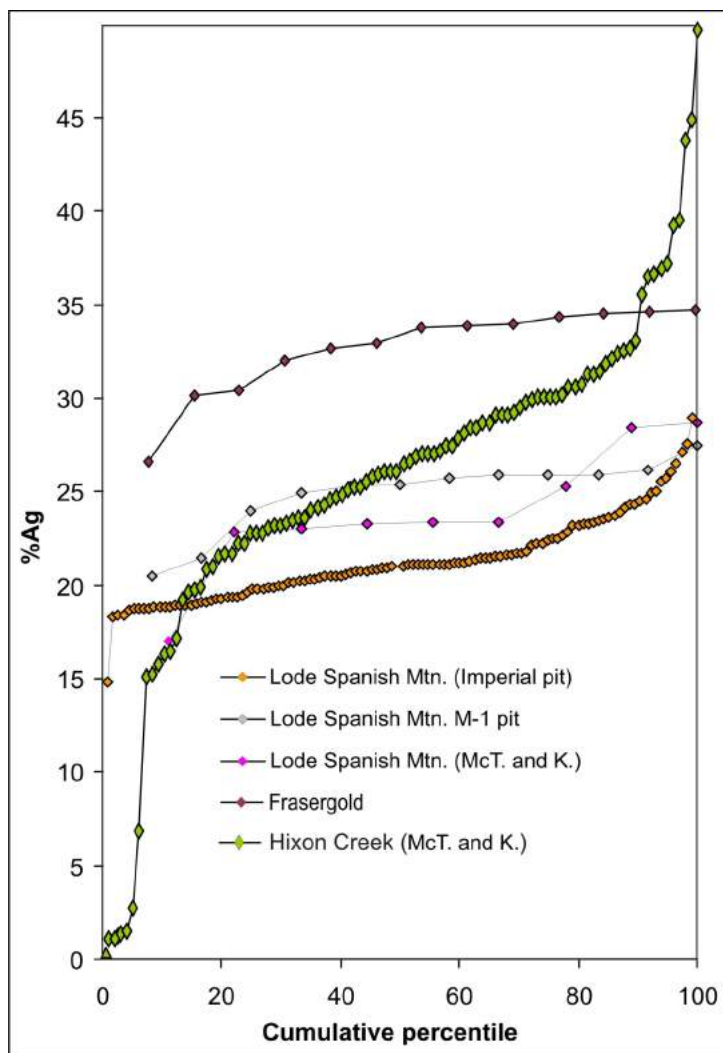


Figure 10. Comparison of compositions of lode gold from the Spanish Mountain and Frasersgold deposits with placer gold from Hixon Creek, east-central British Columbia.

constrain the specific vein occurrences from which individual placer deposits were derived. However, this outcome will require that considerably more detailed sampling be undertaken, especially focusing on placer occurrences in the upper reaches of gold-bearing streams. In addition, gold samples must be obtained from more of the lode occurrences in the region to further develop the compositional ‘fingerprint’ of specific mineral occurrences.

Compositional information for gold from the Mount Polley porphyry Cu-Au deposit or the QR skarn Au deposit (Figure 1) is not yet available. A significant amount of Cu is likely to be present in Au from the Mount Polley deposit and, if so, this may serve to discriminate between Au from porphyry systems and that from orogenic vein systems in the area, which contain no measurable Cu. Work by Stanley (1993) on Cu: Au ratios in many of the alkalic porphyry Cu-Au deposits in the Canadian Cordillera suggested that two

separate mineralizing processes commonly occurred in many of these systems, one characterized by a moderate Cu: Au ratio and one by a low Cu: Au ratio. Gold deposits formed during these processes are also expected to show significant compositional differences. The nature of, and relationships between, these two mineralizing processes is not clear. The relatively Au-rich phase has in many instances been interpreted to have formed after the more Cu-rich phase, possibly related to a late, lower temperature hydrothermal event or to local post-mineral remobilization (e.g., Stanley, 1993; Sillitoe, 1993). In any case, two quite different compositions of gold may be present within the Mount Polley and similar deposits. Gold in the Mount Polley and similar deposits is likely to be very fine grained and may tend not to be concentrated in adjacent placer deposits; instead, gold placers such as are found in the vicinity of Mount Polley may be related to associated but more distal styles of mineralization, which contain coarser grained gold.

The Mount Polley deposit occurs in an area of relatively subdued topography with mainly low-gradient drainages. For this reason, placer deposits that might be related to Mount Polley, if present, are extremely difficult to sample using hand methods, and new placer samples from this area could not be obtained. One sample previously analyzed by McTaggart and Knight (1993) from near the mouth of Morehead Creek (Figure 6) could potentially contain gold derived from the Mount Polley area, although Mount Polley lies approximately 16 km to the southeast of the sample locality. In addition, the placer sample was collected near the mouth of Morehead Creek, and

may simply be gold that was reworked from raised benches along the Quesnel River. Compositional data for the Morehead Creek sample (not shown) closely resembles that of placer gold in the Wells–Barkerville mining camp, suggesting that it was likely derived from lodes in the Barkerville Terrane to the east rather than from occurrences in the Mount Polley area. However, there are current placer leases farther up Morehead Creek that may contain gold from the Mount Polley area. Gold grains that have been identified in suites of polished thin sections from previous studies of Mount Polley mineralization by personnel from the Mineral Deposit Research Unit at the University of British Columbia will be analyzed to establish the compositional signature of this mineralization; in addition, gold will be separated from samples of gold-bearing ore from the QR skarn Au deposit to determine the signature of this style of mineralization.

Planned Outcomes for the Project

The three main products expected from the study are

- a complete characterization of the alloy composition and microinclusion suite for each type of lode gold examined, which will provide a template to identify the source(s) of various placer-gold populations for use in future studies of the region;
- an interpretation of the most probable source of gold in each placer sample, together with documentation of the compositional data itself (in digital form) for archiving; and
- a discussion of the implications of the new data for future lode exploration in the study area and elsewhere in the QUEST Project area.

Acknowledgments

The authors thank K. Hickey for a critical review of an early draft of the paper.

References

- Allan, J.R. (1984): 1983 Summary report: Hixon Creek gold project; BC Ministry of Energy, Mines and Petroleum Resources, Assessment Report 12 129, 35 p.
- Chapman, R.J. (2007): An overview of gold mineralization in the Caledonides of Great Britain and Ireland: insights from placer gold geochemistry (abstract); Proceedings of the 9th Biennial SGAMeeting, C.J. Andrew (ed.), Society for Geology Applied to Mineral Deposits, Dublin, p. 943–946.
- Chapman, R.J. and Mortensen, J.K. (2006): Application of microchemical characterization of placer gold grains to exploration for epithermal gold mineralization in regions of poor exposure; *Journal of Geochemical Exploration*, v. 91, p. 1–26.
- Chapman, R.J., Leake, R.C., Bond, D.P.G., Stedra, V. and Fairgrieve, B. (2009): Chemical and mineralogical signatures of gold formed in oxidizing chloride hydrothermal systems and their significance within populations of placer gold grains collected during reconnaissance; *Economic Geology*, v. 104, no. 4, p. 563–585.
- Crawford, E. (2007): Klondike placer gold—new tools for examining morphology, composition and crystallinity; M.Sc. thesis, University of British Columbia, 100 p.
- Johnston, W.A. and Uglow, W.L. (1926): Placer and vein deposits of Barkerville, Cariboo District, British Columbia; Geological Survey of Canada, Memoir 149, 246 p.
- Knight, J.B., Mortensen, J.K. and Morison, S.R. (1999a): Lode and placer gold composition in the Klondike District, Yukon Territory, Canada: implications for the nature and genesis of Klondike placer and lode gold deposits; *Economic Geology*, v. 94, p. 649–664.
- Knight, J.B., Mortensen, J.K. and Morison, S.R. (1999b): The relationship between placer gold particle shape, rimming and distance of fluvial transport as exemplified by gold from the Klondike, Yukon Territory, Canada; *Economic Geology*, v. 94, p. 635–648.
- Levson, V.M. and Giles, T.R. (1993): Geology of Tertiary and Quaternary gold-bearing placers in the Cariboo region, British Columbia (93A, B, G, H); BC Ministry of Energy, Mines and Petroleum Resources, Bulletin 89, 202 p.
- McTaggart, K.C. and Knight, J. (1993): Geochemistry of lode and placer gold in the Cariboo District, BC; BC Ministry of Energy, Mines and Petroleum Resources, Open File 1993-30, 25 p.
- MINFILE (2009): MINFILE BC mineral deposits database; BC Ministry of Energy, Mines and Petroleum Resources, URL <<http://minfile.ca/>> [November 2009].
- Mortensen, J.K., Chapman, R., LeBarge, W. and Crawford, E. (2006): Compositional studies of placer and lode gold from western Yukon: implications for lode sources; *in* Yukon Exploration and Geology 2005, D.S. Emond, G.D. Bradshaw, L.L. Lewis and L.H. Weston (ed.), Yukon Geological Survey, p. 247–255.
- Rhys, D.A., Mortensen, J.K. and Ross, K. (2009): Investigations of orogenic gold deposits in the Cariboo gold district, east-central British Columbia (parts of NTS 093A, H): progress report; *in* Geoscience BC Summary of Activities 2008, Geoscience BC, Report 2009-1, p. 49–74.
- Sillitoe, R.H. (1993): Gold-rich porphyry copper deposits: geological model and exploration implications; *in* Mineral Deposit Modelling, R.V. Kirkham, W.D. Sinclair, R.I. Thorpe and J.M. Duke (ed.), Geological Association of Canada, Special Paper 40, p. 465–478.
- Stanley, C.R. (1993): A thermodynamic geochemical model for the coprecipitation of gold and chalcopyrite in alkalic copper-gold deposits; Mineral Deposit Research Unit Annual Technical Report, Department of Geological Sciences, University of British Columbia.
- Townley, B.K., Herail, G., Maksiyev, V., Palacios, C., de Parseval, P., Sepulveda, F., Orellana, R., Rivas, P. and Ulloa, C. (2003): Gold grain morphology and composition as an exploration tool: application to gold exploration in covered areas; *Geochemistry: Exploration, Environment, Analysis*, v. 3, p. 29–38.
- Youngson, J.H. and Craw, D. (1995): Evolution of placer gold deposits during regional uplift, central Otago, New Zealand; *Economic Geology*, v. 90, p. 731–745.

Preliminary Study of the Magmatic Evolution, Mineralization and Alteration of the Red Chris Copper-Gold Porphyry Deposit, Northwestern British Columbia (NTS 104H/12W)

J.R. Norris, Mineral Deposit Research Unit, University of British Columbia, Vancouver, BC, jnorris@eos.ubc.ca

C.J.R. Hart, Mineral Deposit Research Unit, University of British Columbia, Vancouver, BC

R.M. Tosdal, Mineral Deposit Research Unit, University of British Columbia, Vancouver, BC

C. Rees, Imperial Metals Corporation, Vancouver, BC

Norris, J.R., Hart, C.J.R., Tosdal, R.M. and Rees, C. (2010): Preliminary study of the magmatic evolution, mineralization and alteration of the Red Chris copper-gold porphyry deposit, northwestern British Columbia (NTS 104H/12W); in Geoscience BC Summary of Activities 2009, Geoscience BC, Report 2010-1, p. 77–86.

Introduction

The Red Chris porphyry copper-gold deposit is a unique deposit in British Columbia because it has geological features that are typical of both alkalic and calcalkalic porphyry deposit types. Quartz-vein stockworks, typically absent in alkalic porphyries, characterize the mineralized zones at Red Chris. Likewise, intense late-stage sericitic alteration, also characteristic of calcalkalic porphyry deposits, is present at Red Chris. Perhaps the most curious feature is the widespread and intense late carbonate alteration (Baker et al., 1999), which is not a common feature of porphyry copper systems (Seedorf et al., 2005). Nonetheless, Red Chris is hosted in monzonitic rocks, has a relatively limited lateral extent of mineralization, is deficient in molybdenum, has characteristic hematite alteration and has the high gold grades typical of BC alkalic porphyry deposits (Newell and Peatfield, 1995; Baker et al., 1999; Holliday and Cooke, 2007).

The property has been explored intermittently by several companies since the mid-1950s, with a hiatus between 1981 and 1994 when more focused drill projects dominated (Newell and Peatfield, 1995). Exploration drilling campaigns continued until 2005 and resulted in a calculated open-pit reserve by bcMetals Corporation of 276 million tonnes grading 0.35% Cu and 0.27 g/t Au (Ferreira, 2009). Following a takeover by Imperial Metals Corporation in February 2007, drilling targeted deeper mineralization in the ‘East zone’. A vertical diamond-drill hole, RC07-335, intersected 1024.1 m of 1.01% Cu, 1.26 g/t Au and 3.92 g/t Ag over the length of the entire hole (Imperial Metals Corporation, 2007), which added new dimensions to the poten-

tial shape, depth, size and grade of the Red Chris deposit. More importantly, the deep drillhole demonstrates great vertical continuity at Red Chris and has significant implications for further exploration and mine planning. On a broader scale, results from the deep drillhole indicate significant potential for elevated gold and copper grades in BC’s alkalic porphyry systems.

In light of this significant development, a research project has been jointly initiated by the Mineral Deposit Research Unit at the University of British Columbia, Imperial Metals Corporation and Geoscience BC. Observations and results presented herein are from investigations at the Red Chris deposit during a seven-week period in July and August of 2009, and provide the foundation for an M.Sc. research project. This project focuses on increasing the understanding of the magmatic evolution, mineralization styles and alteration of the deposit, with particular emphasis on the deeper parts of the system. Whereas significant mineralization is located in both the Main and East zones, this study focuses on the East zone along section line 452700E, where the nature of the intrusive rocks, mineralization, veins and alteration were investigated in four diamond-drill holes, RC94-079, RC94-106, RC95-225 and RC07-335. Previous descriptions of the rock units, mineralization, associated veins and alteration at Red Chris by Schink (1977), Ash et al. (1995), Blanchflower (1995) and Baker et al. (1999) provide additional information on the deposit.

The Red Chris deposit is in northwestern BC (Figure 1), approximately 80 km south of the town of Dease Lake and 12 km east of the Stewart-Cassiar Highway (Highway 37), and is accessed by a 23 km gravel road. Located in NTS area 104H/12W, the deposit is situated at latitude 57°42'N and longitude 129°47'W.

Keywords: *Stikine Terrane, copper, porphyry deposits, alteration*

This publication is also available, free of charge, as colour digital files in Adobe Acrobat® PDF format from the Geoscience BC website: <http://www.geosciencebc.com/s/DataReleases.asp>.

Tectonic Setting

Much of BC is underlain by several tectonic blocks that were accreted to the growing margin of western North America during the Mesozoic. Three of these accreted terranes, the Quesnel (or Quesnellia), the Stikine (or Stikinia) and the Cache Creek, form most of the Intermontane Belt that underlies much of central BC (Monger and Price, 2002). Stikinia and Quesnellia are Late Triassic to Early Jurassic island-arc terranes that host most of BC's porphyry deposits and are separated from each other by the intervening Cache Creek Terrane (McMillan et al., 1995; Figure 1). These dominantly Late Triassic volcanic island-arc terranes, which have surprisingly similar compositions and stratigraphy, formed outboard from the western North American continental margin and were subsequently accreted onto the margin during the Early Jurassic (Monger and Price, 2002). Porphyry copper deposits within Quesnellia and Stikinia formed largely prior to accretion, but some deposits continued to form into the Middle Jurassic (i.e., Mount Milligan; McMillan et al., 1995). The Red Chris porphyry deposit is hosted in the Late Triassic to Early Jurassic arc and arc-marginal sedimentary rocks in the northern portion of Stikinia.

Regional Geology

In the Red Chris area, there are three main geological packages (Figure 2):

The Stuhini Group (**LTrS**) is a package of Late Triassic volcanic and volcanically derived sedimentary rocks that form part of Stikinia. These arc volcanic rocks are dominated by augite-phyric basaltic pillowed flows and flow breccias (Ash et al., 1995). The volcanic rocks are intercalated with fine-grained volcanoclastic siltstone, siliceous siltstone and feldspathic sandstone, on the order of metres to tens of metres.

Plutonic rocks of the Red stock (**LTrRmd**) intruded the Stuhini Group in the Late Triassic. The Red stock is elongated in an east to northeast direction, and is at least 4.5 km long and up to 1.5 km wide (Ash et al., 1995; Ferreira, 2009). The stock consists of medium- to coarse-grained hornblende-plagioclase-porphyrific quartz monzodiorite (Ash et al., 1995). A U-Pb zircon age from a sample taken at ~105 m depth in drillhole RC95-224 gave a crystallization age for the Red stock of 203.8 ± 1.3 Ma (Freidman and Ash, 1997). The South Boundary fault truncates the Red stock at its southern margin and juxtaposes the plutonic rocks against the Bowser Lake Group.

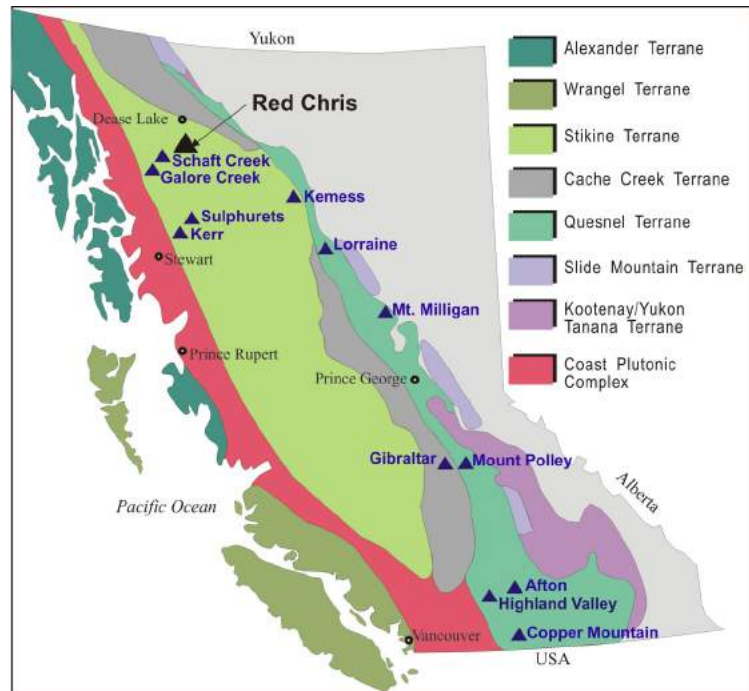


Figure 1. Major tectonic terranes and associated Mesozoic porphyry deposits of the Canadian Cordillera in British Columbia.

Sedimentary rocks of the Middle Jurassic Bowser Lake Group (**MJB**) outcrop south of the South Boundary fault. These marine clastic sedimentary rocks, belonging to the Ashman Formation, were deposited unconformably on top of the Late Triassic volcanic and plutonic rocks. The sedimentary rocks represent the basal unit of the Bowser Lake Group and are composed of siltstone, chert-pebble conglomerate and sandstone (Evenchick and Thorkelson, 1993).

Deformation of the various rock units has complicated the deposit-scale geology. In particular, pre-Middle Jurassic deformation resulted in uplift and erosion of the Red stock and Stuhini volcanic rocks, and eventual depression to form the basement to the Bowser Basin.

Deposit Geology

The Red Chris deposit comprises several mineralized zones, the Main, East, Far West and Gully zones, but only the Main and East zones currently host economic resources (Figure 2). The Main zone has a larger areal extent than the East zone, with their centres ~600 m apart. Both the Main zone and East zone orebodies are vertical to subvertical, apparent pipe-like structures that are elongated along the general east-northeasterly-trending fault structures in the region (Collins et al., 2004).

The ore zones are hosted entirely within the Red stock, a plagioclase-hornblende-porphyrific monzodiorite that may consist of several different intrusive phases. However, the mineralized portion of the stock, particularly the East

zone, is dominated by sericitic and K-silicate alteration, and fresh monzodiorite was not observed in the holes logged in this study. The stock is cut by several late-stage felsic dikes. Several different styles of veins are present in the Red stock. Copper mineralization occurs as disseminated and fracture-controlled chalcopyrite and bornite, whereas gold occurs as microscopic inclusions within these copper-sulphide minerals. Copper and gold occur within banded stockwork veins and sulphide-only veins.

Main Phase

The composite Red stock in the East zone along section line 452700E (Figure 3) consists of two phases (see also Schink, 1977), a main phase and a late phase, both of which are cut by post-mineral dikes.

The main phase of the Red stock is medium grey with phenocrysts of plagioclase and hornblende in a very fine grained groundmass (Figure 4a). The groundmass typically accounts for 40% of the rock and consists of anhedral

microcrystalline alkali feldspar and minor quartz (Schink, 1977). The feldspar phenocrysts are generally buff white, 2–4 mm euhedral to subhedral crystals (Figure 4b–d). Hornblende phenocrysts are altered to secondary biotite and sericite, making the primary texture difficult to ascertain, but are typically euhedral, 2–10 mm crystals with distinct crystal boundaries (Figure 4b–d). The phenocrysts are randomly oriented within the grey aphanitic groundmass (Schink, 1977). Estimated visually, phenocryst abundance typically varies between 15 and 30% but can be as low as 5% and as high as 45% (Figure 4a–d).

Previous studies have demonstrated that the Red stock intrusive suite is monzonite to monzodiorite in composition (Ash et al., 1995). However, it is uncertain if the K-feldspar in the groundmass is primary or of secondary origin due to extensive alteration. Throughout this paper, the Red stock will also be referred to as a monzodiorite.

Variations in phenocryst size and abundance were observed in the drillholes across the section line. These changes may

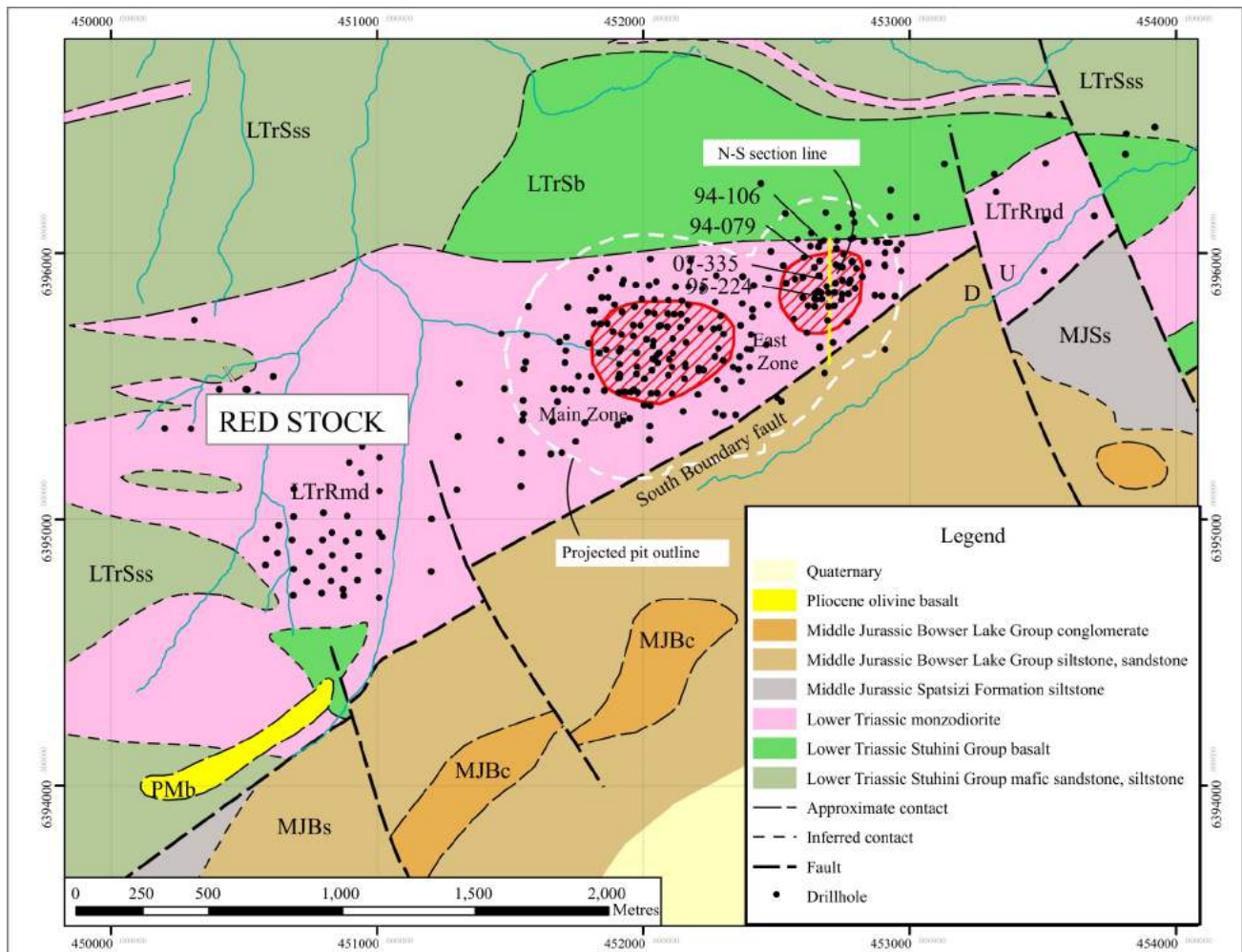


Figure 2. Deposit-scale geology of the Red Chris deposit, northwestern British Columbia, as interpreted by Imperial Metals Corporation. The Main and East zone orebodies are the red striped areas. The planned open-pit outline is indicated by a dashed white line, and the north-south cross-section investigated in this study, with the relevant diamond-drill holes, is a solid yellow line.

indicate that there are different porphyritic phases or intrusions that form the Red stock. Unfortunately, definitive intrusive relationships are uncommon due to late-mineral hydrothermal alteration and post-mineral breccia and faults occupying the contact zones.

Late Phase

A late phase of the Red stock was not observed during this study but is described by Schink (1977) as being very similar in composition to the main phase. It is a grey, medium-grained, plagioclase-hornblende-porphyritic monzonite. The main difference is that the late phase is less altered and barren of copper-Fe sulphides, making it hard to differentiate between a weakly altered main phase and the relatively unaltered late phase. The typical fresh look of the late phase has been used to distinguish it from the main phase. The late phase lacks quartz veins, which is a diagnostic feature in a comparison with the main phase of the intrusion (Blanchflower, 1995).

Post-Mineral Dikes

Two types of 1–5 m wide, diorite to monzodiorite dikes crosscut the Red stock at steep angles. These two types, amygdaloidal monzodiorite and biotite diorite, make up <2% of the stock, do not contain mineralization and are both cut by minor, buff-white carbonate veins. The amygdaloidal monzodiorite dikes are beige to locally light green and very fine grained with carbonate-quartz amygdules 2–10 mm in size. Euhedral hornblende phenocrysts (<3%), up to 4 mm long, are altered to carbonate, ankerite and/or chlorite. The biotite diorite dikes are light to medium green and very fine grained, with up to 10% hornblende and/or biotite phenocrysts, up to 5 mm long, that are locally altered to carbonate, ankerite and/or chlorite.

Alteration

Alteration in the East zone along section line 452700E is dominantly potassic (herein called K-silicate alteration) and is overprinted by sericitic alteration. The main zone of K-silicate alteration is in the deeper parts (>350 m) of the cross-section. The main extent of the K-silicate alteration forms a narrow vertical zone centred near drillhole RC07-335. Potassium-silicate alteration was also noted in a few locations within drillholes RC94-106 and RC94-079, which are within 30 m of drillhole RC07-335. Potassium-silicate alteration in the shallower portion of the section has been overprinted by sericitic alteration, making it difficult to determine the original extent of the K-silicate zone. Primary igneous mafic minerals within the K-silicate-altered zone have been replaced by secondary biotite and have diffuse grain boundaries. These diffuse mafic crystal sites can be used as a general proxy to identify and recognize zones of monzodiorite that experienced K-silicate alteration prior to the sericitic overprint.

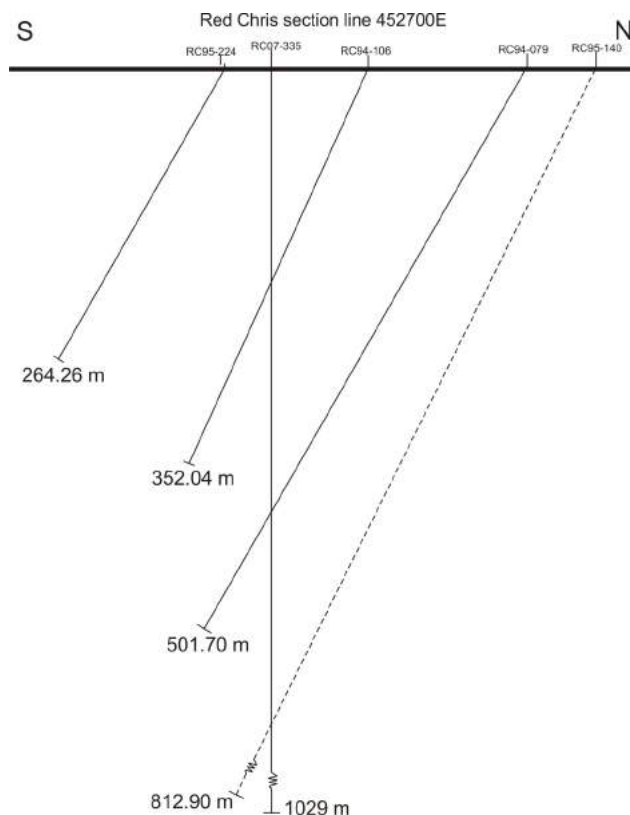


Figure 3.: North-south cross-section along section line 452700E (± 30 m) across the East zone of the Red Chris deposit, northwestern British Columbia. Diamond-drill hole RC95-140 has yet to be investigated in this study.

The K-silicate alteration zone is characterized by secondary biotite and magnetite replacing igneous amphibole, and by texturally destructive K-feldspar that has replaced the groundmass and primary plagioclase feldspar phenocrysts (Figure 5a, b). Baker et al. (1999) noted that the porphyritic igneous texture may be completely destroyed by fine-grained orthoclase and albitic feldspar (Ab_{80-94} ; Schink, 1977). Primary mafic minerals are replaced by secondary biotite and magnetite, and locally by later chlorite (Figure 5c). Hematite, also in the mafic sites, is the dominant oxide above 400 m (vertical depth), whereas magnetite is in much greater abundance below 400 m, an observation also made by Baker et al. (1999). Specular hematite is also observed as 1–2 mm blebs replacing magnetite in secondary biotite within the K-silicate alteration zone. In deeper portions of the zone (below 400 m), magnetite-only veins are directly associated with the K-silicate alteration.

Sericitic alteration is widespread, dominantly in the upper ~300 m of the section (Figure 5d, e) and outboard from the margins of the K-silicate zone. It has a gradational overprint on the K-silicate-altered monzodiorite. Also noted by Baker et al. (1999) are minor lenses of K-silicate-altered monzodiorite with a very weak sericitic overprint, as observed in drillholes RC94-079 and RC94-106. Sericite per-

vasively alters both plagioclase and alkali feldspars and hornblende phenocrysts of the primary monzodiorite to buff white, pale orange and locally pale green colours (Figure 5d, e). Throughout the sericitic zone, pervasive but minor hematite occupies the mafic sites and has both sharp and diffuse crystal boundaries. The hematite is very fine grained and maroon coloured. Pyrite alteration within the sericitic zone tends to increase in the upper portion of the section, occurring as very fine to fine-grained anhedral crystals occurring preferentially within the mafic crystal sites. Pervasive carbonate alteration is spatially associated with the sericitic alteration in the upper portions of the section. Baker et al. (1999) reported a ferroan-dolomite composition for this carbonate alteration (Figure 5e, f).

Veins

Five main vein types are recognized cutting the Red stock. They are described below in order of abundance (by volume).

Quartz Stockwork Veins

Massive quartz stockwork veins cut the Red stock monzodiorite. These veins are banded with repeating zones

of quartz±sulphides±oxides (Figure 6a). The quartz stockwork veins vary significantly in density and can form up to 90% of the rock, as observed in drillcore. A single banded vein is typically 1–5 cm in width but can be up to 10 cm wide in zones of intense veining. Quartz stockwork veins are cut by younger generations of the same vein style but at different orientations. Mineral assemblages within the veins include 1) quartz±magnetite±specular hematite±white carbonate (quartz-oxide-carbonate veins); 2) quartz±bornite±chalcopyrite±pyrite±white carbonate (quartz-sulphide-carbonate veins); or 3) a combination of the two previous types, containing quartz±magnetite±specular hematite±bornite±chalcopyrite±pyrite±white carbonate. The banded quartz veins are locally cut by sulphide-only veins that occur in the vein centres. Quartz veins containing magnetite and hematite occur proximal to the core of the K-silicate-altered zone, whereas quartz veins with hematite as the only oxide decrease in abundance outward from the K-silicate core. Alteration envelopes are not pervasive around the quartz stockwork veins. However, in deep portions of the section, envelopes of K-silicate alteration can occur around thin, wispy chlorite±pyrite±quartz veins (Figure 6b).

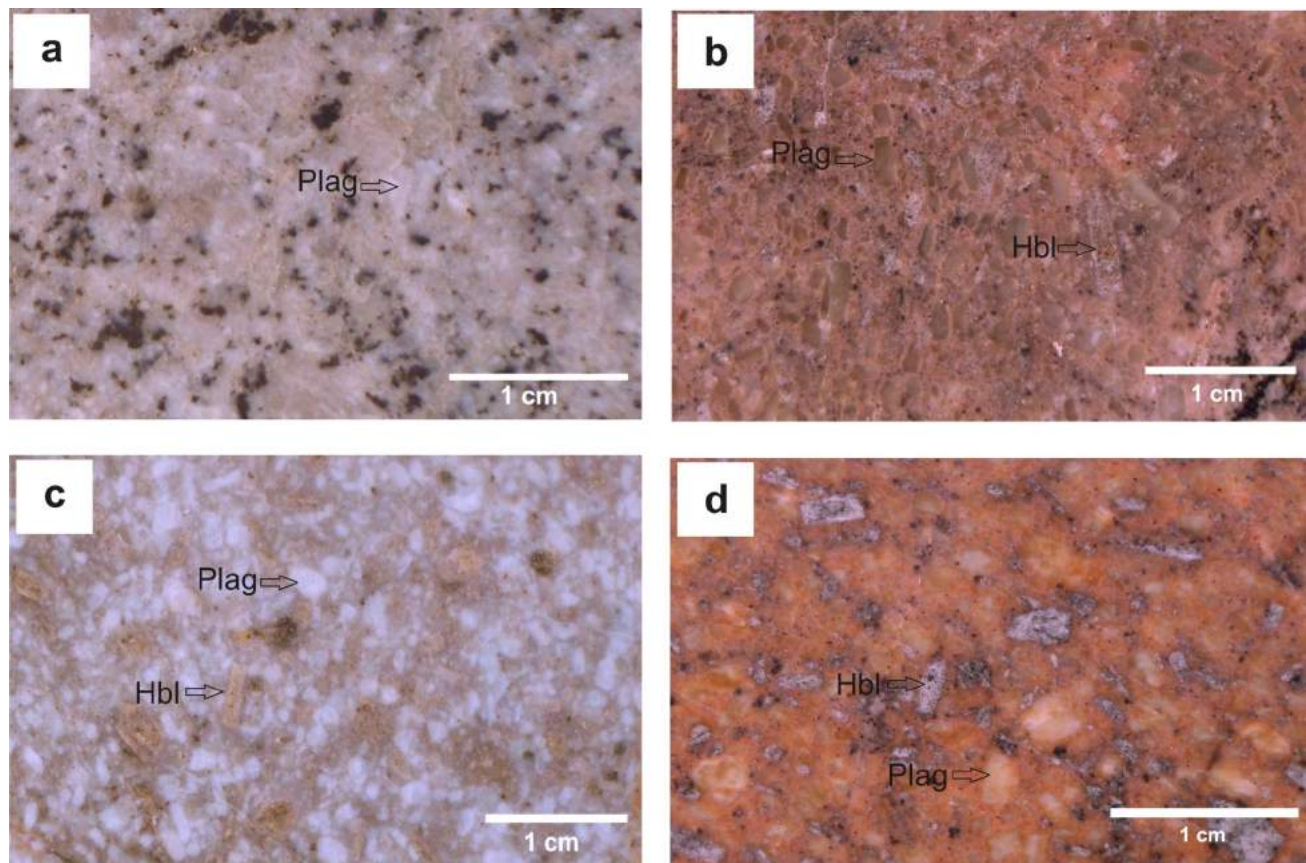


Figure 4. Examples of the Red stock taken from diamond-drill holes on the Red Chris deposit, northwestern British Columbia, illustrating the variability in phenocryst size and abundance. **a)** 10% plagioclase (Plag) up to 2 mm in length, drillhole RC79-003 (51.52 m); **b)** 15% plagioclase up to 4 mm in length and 10% hornblende (Hbl) up to 1 cm in length, drillhole RC106-038 (405.51 m); **c)** 25% plagioclase up to 4 mm in length and 5% hornblende up to 7 mm in length, drillhole RC335-036 (461.90 m). **d)** 10% plagioclase up to 3 mm in length and 15% hornblende up to 5 mm in length, drillhole RC224-006 (124.48 m).

Quartz-Pyrite Veins

Quartz-pyrite veins are common throughout the observed drillholes of the cross-section and are slightly more abundant in the upper sericitic zone. The quartz-pyrite veins are

typically 2–5 mm in width but can be up to 1 cm. These veins are locally banded with three to five bands of quartz containing one or more millimetre-wide, central lines of pyrite. Rare, light green sericitic alteration envelopes are associated with these generally straight-edged quartz-pyrite veins.

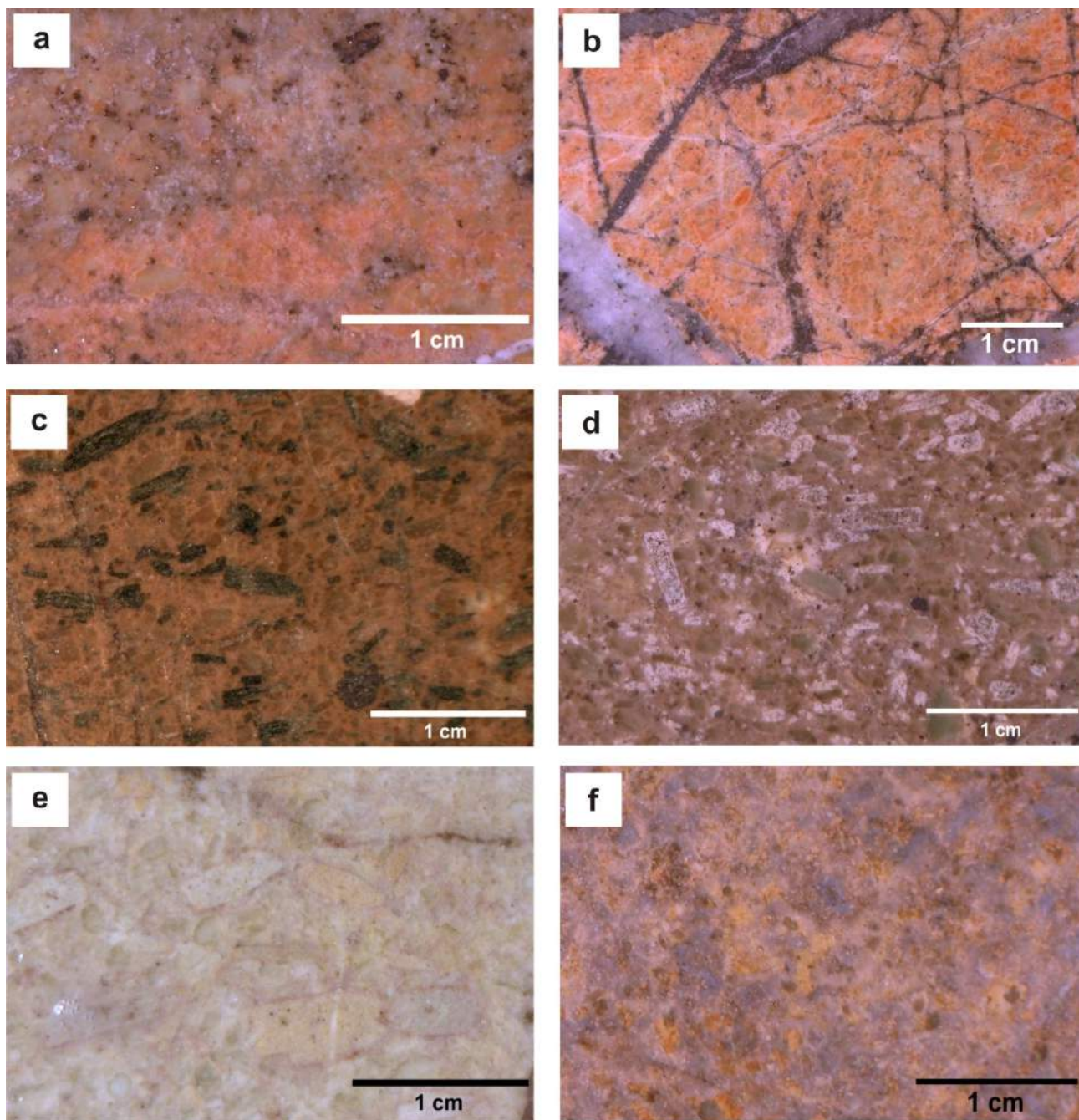


Figure 5. Typical examples of K-silicate and sericitic alteration in the Red stock from drillholes in the East zone of the Red Chris deposit, northwestern British Columbia: **a**) texturally destructive K-silicate alteration of monzodiorite, drillhole RC335-070 (985.37 m); **b**) intense K-silicate alteration of the groundmass, drillhole RC335-060 (863.54 m); **c**) K-silicate alteration of the groundmass with secondary biotite phenocrysts being altered to magnetite and chlorite, drillhole RC335-034 (409.48 m); **d**) illite (light green) alteration of plagioclase phenocrysts and kaolinite (blotchy white) alteration of hornblende phenocrysts (illite and kaolinite logged as sericite), drillhole RC335-041 (532.90 m); **e**) intense kaolinite and illite alteration of the plagioclase and hornblende phenocrysts and of the groundmass (illite and kaolinite logged as sericite), with the groundmass also being pervasively carbonate altered, drillhole RC335-035 (441.17 m); **f**) pervasive carbonate (ankerite?) alteration of plagioclase and hornblende phenocrysts (orange coloured), along with intense carbonate alteration of the groundmass, drillhole RC106-019 (151.31 m).

Barren Quartz Veins

Quartz veins contain minor oxide minerals±sulphide minerals±white carbonate but are barren of significant ore minerals (Figure 6c). These quartz veins can be banded and contain very fine crystals of chalcopyrite, pyrite or hematite. They are generally straight edged, are typically 2–10 mm thick and lack alteration envelopes.

Sulphide-Only Veins

Veins containing only sulphide minerals occur in the deeper K-silicate–altered portions of drillhole RC07-335. These sulphide-only veins are either 1) bornite only, 2) bornite+chalcopyrite, 3) chalcopyrite only, 4) chalcopyrite+pyrite, or 5) pyrite only (Figure 6d, e). Abundant pyrite-only veins occur in the upper portions of the cross-section, where sericitic alteration dominates. They are absent in the lower portion, where K-silicate alteration is dominant. These veins are typically only 1–2 mm in width and are generally straight edged to slightly anastomosing. No obvious alteration envelopes were noted.

Late-Stage Carbonate Veins

Buff-white carbonate veins cut all other types of veins. These veins are typically carbonate only (Figure 6f, g) but locally include pyrite±chalcopyrite (Figure 6h). The pyrite typically forms fine- to medium-grained subhedral crystals and is more abundant than chalcopyrite. Veins are typically 1–30 cm wide. Locally, carbonate veins are associated with breccia zones. Angular clasts of monzodiorite (5–20 mm) and quartz-vein fragments are cemented by carbonate and can form zones up to several metres wide. Carbonate veins are found at all depths of the cross-section.

Mineralization

Copper and gold grades in the East zone at Red Chris are concentrated in both disseminated and vein-hosted bornite and chalcopyrite that are mostly within the banded quartz stockwork veins. Bornite and chalcopyrite are dominantly fine anhedral grains within veins and wallrock. Locally, they form aggregates within quartz veins that host minor to moderate white carbonate. Sulphide-only veins of chalcopyrite and/or bornite, 1–2 mm thick and moderately wavy in character, are particularly common in deeper portions of drillhole RC07-335 where K-silicate alteration dominates. Trace amounts of very fine grained chalcopyrite are present within the K-silicate–altered mafic mineral sites.

Bornite, chalcopyrite and pyrite in quartz veins are observed along the length of drillholes RC94-079, RC94-106, RC95-224 and RC07-335. Sulphide mineral assemblages appear to form a lower chalcopyrite+bornite–only core that is surrounded by a zone of chalcopyrite+pyrite, then surrounded by an outer zone dominated by pyrite. For example, strong to intense pyrite in the uppermost 50 m of

drillhole RC07-335 decreases to trace amounts at the end of the hole, whereas chalcopyrite is variably strong to intense down to depths of 770 m and bornite increases from trace amounts between 240 and 685 m to somewhat more than that by 760 m, with both bornite and chalcopyrite occurring in moderate amounts to the bottom of the hole at 1029 m.

Gold in the East zone at Red Chris has an average ratio of approximately 1:1 with copper (i.e., g/t Au : % Cu) and they are strongly correlated ($r^2 = 0.89$; Baker et al., 1999). No visible gold was observed. The highest gold grades are associated with the highest densities of banded quartz stockwork veins.

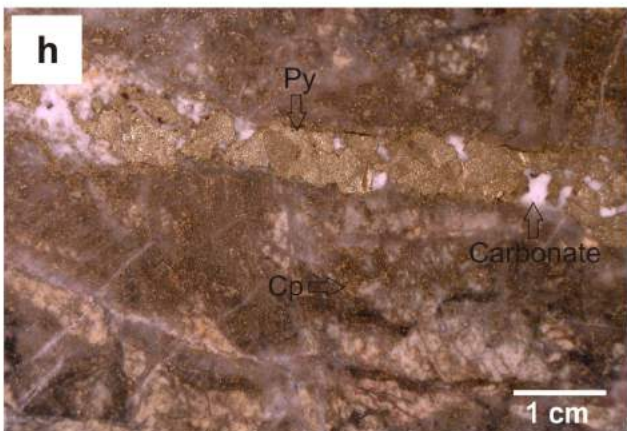
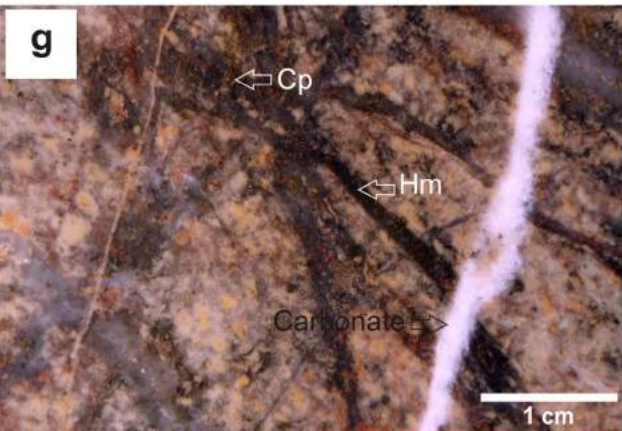
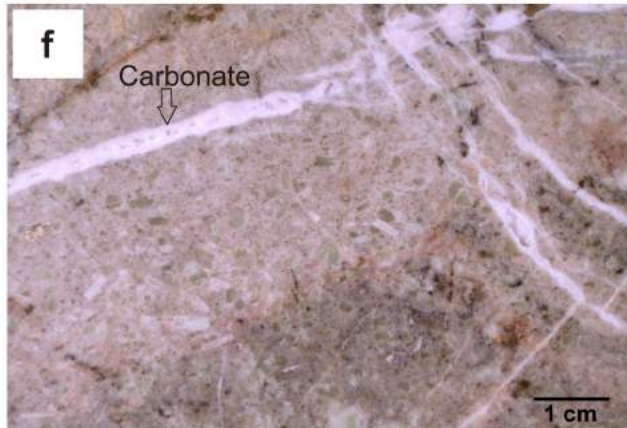
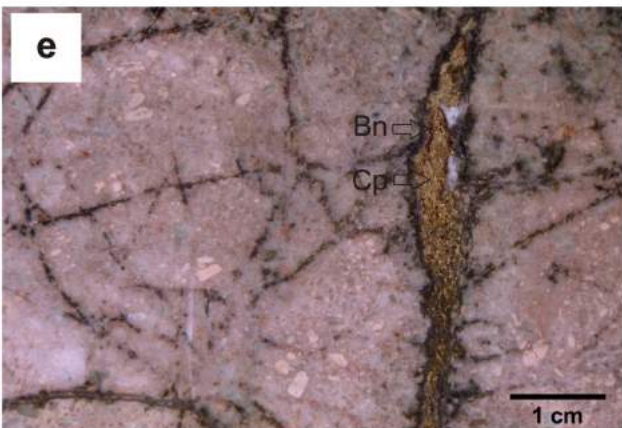
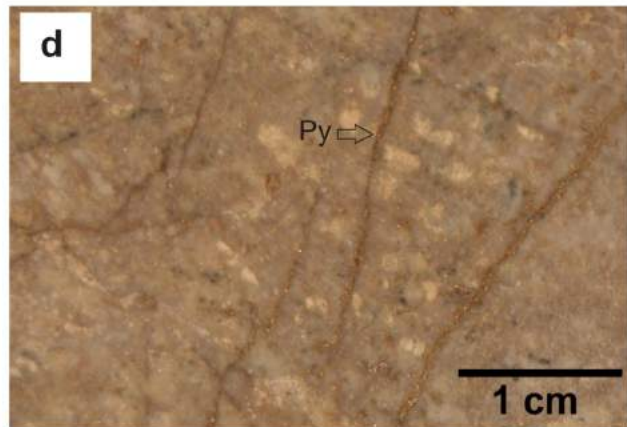
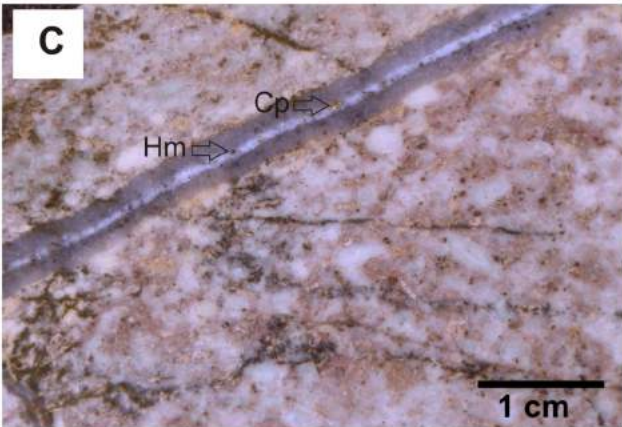
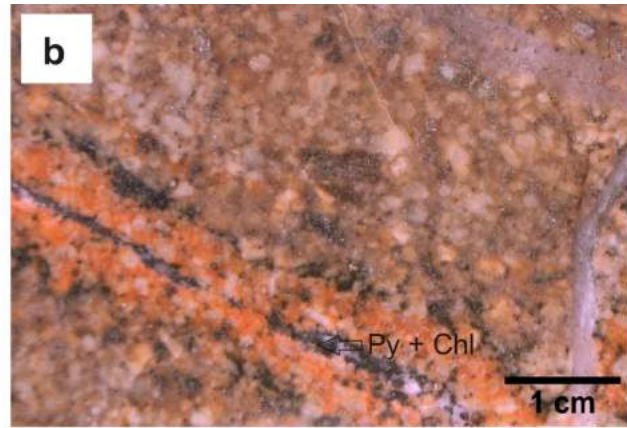
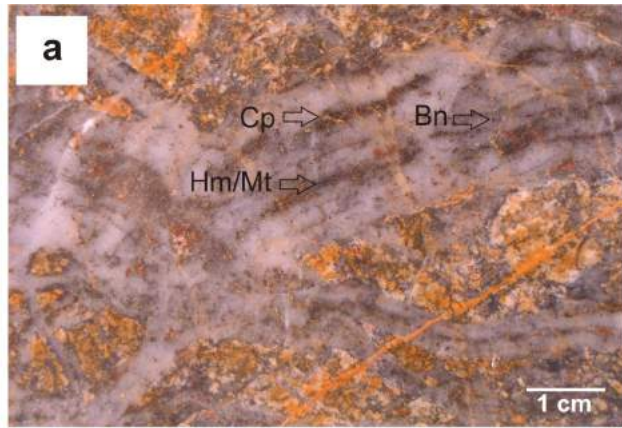
Discussion and Conclusions

Although only one main phase of the Red stock was recognized in this study, observed changes in phenocryst sizes and abundances indicate that several different porphyritic phases may collectively form the Red stock. The contacts between these different phases are typically marked by zones of brecciation, which make crosscutting relationships difficult to determine. It is likely that these brecciated zones represent the original intrusive contacts between different porphyry units that were later exploited by successive structural and fluid events, including deposition of the abundant late carbonate cement that is characteristic of these breccia zones. Some of these porphyry phases have much higher densities of veins and higher copper and gold grades, and are interpreted to be early phases of the intrusion. Simple use of copper and gold grades may therefore help to distinguish between different porphyritic phases in the absence of other paragenetic information.

The typically high-grade mineralization at Red Chris is closely associated with areas that have multiple generations of the banded quartz stockwork veins. In general, the copper and gold grades are much lower in areas where sericitic alteration is intense and dominant. This alteration may have reduced the grade by remobilizing copper sulphide minerals that were deposited in previous mineralizing events.

Controls on the distribution and occurrences of hematite and magnetite remain ambiguous. The presence of hematite and magnetite in veins is directly associated with the K-silicate core. However, the occurrence of hematite and magnetite within mafic sites is patchy and irregular. Magnetite replaces hornblende and secondary biotite locally within the K-silicate–altered zones, whereas hematite occurs in the mafic sites within zones of the widespread sericitic-alteration overprint. The fluids involved in the sericitic alteration of the monzodiorite may have altered the magnetite to hematite.

Numerous crosscutting relationships between the different vein types observed in the East zone make it difficult to confidently determine a relative paragenesis. Fluids associ-



ated with individual porphyritic intrusions fractured earlier intrusions of the Red stock. The evolution of the magmatic compositions and their relationships to the veins, mineralization and alteration, and the characterization of paragenetic vein sequences, are the focus of the next stage of research on the Red Chris deposit.

Acknowledgments

Geoscience BC is acknowledged and thanked for the funding provided for this project. Imperial Metals Corporation is thanked for funding and wide-ranging support for the project; in particular, the support of S. Robertson and P. McAndless is appreciated. J. MacPherson and K. MacKenzie are also thanked for their input and discussion of the hostrocks and mineralization at Red Chris. The entire staff at the Red Chris camp, including J. Bellamy, S. Siegner and M. Seigner, as well as Oregon State University M.Sc. student C. Longton, are thanked for the help they provided in moving endless core boxes around. B. Riedell and M. Thicke are thanked for their stimulating conversations regarding the genesis of the deposit. A. Toma of the Mineral Deposit Research Unit at the University of British Columbia is thanked for logistical support.

References

Ash, C.H., Fraser, T.M., Blanchflower, J.D. and Thurston, B.G. (1995): Tatogga Lake project, northwestern British Columbia (104H/11, 12); *in* Geological Fieldwork 1994, BC Ministry of Energy, Mines and Petroleum Resources, Paper 1995-1, p. 343–358, URL <<http://www.empr.gov.bc.ca/Mining/Geoscience/PublicationsCatalogue/Fieldwork/Pages/GeologicalFieldwork1994.aspx>> [November 2009].

Baker, T., Ash, C.H. and Thompson J.F.H. (1999): Geological setting and characteristics of the Red Chris copper-gold deposit, northwestern British Columbia; *Exploration and Mining Geology*, v. 6, no. 4, p. 297–316.

Blanchflower, J.D. (1995): 1995 exploration report on the Red Chris property; unpublished report for American Bullion Minerals Ltd., 93 p.

Collins, J., Colquhoun, W., Giroux, G.H., Nilsson, J.W. and Tenney, D. (2004): Technical report on the Red Chris copper-gold project, Liard Mining Division; unpublished company report, Red Chris Development Company Ltd.

Evenchick, C. A. and Thorkelson, D. J. (1993): *Geology, Spatsizi River, British Columbia (104H)*; Geological Survey of Canada, Open File 2719, scale 1:250 000.

Ferreira, L. (2009): 2008 diamond drilling report on the Red Chris project located in northwest British Columbia, Liard Mining District; unpublished company report, Red Chris Development Company Ltd.

Friedman, R.M. and Ash, C.H. (1997): U-Pb age on intrusions related to porphyry Cu-Au mineralization in the Tatogga Lake area, northwestern British Columbia (104H/12NW, 104G/9NE); *in* Geological Fieldwork 1996, BC Ministry of Energy, Mines and Petroleum Resources, Paper 1997-1, p.291–298, URL <<http://www.empr.gov.bc.ca/Mining/Geoscience/PublicationsCatalogue/Fieldwork/Pages/GeologicalFieldwork1996.aspx>> [November 2009].

Holliday, J. R. and Cooke, D. R. (2007): Advances in geological models and exploration methods for copper ± gold porphyry deposits; *in* Proceedings of Exploration 07: Fifth Decennial International Conference on Mineral Exploration, B. Milkereit (ed), p. 791–809.

Imperial Metals Corporation (2007): Over one kilometre grading 1.01% copper and 1.26 g/t gold intercepted at Imperial's Red Chris property; Imperial Metals Corporation, press release, October 16, 2007, URL <<http://www.imperialmetals.com/News-2007.asp>> [November 2009].

McMillan, W.J., Thompson, J.F.H., Hart, C.J.R. and Johnston, S.T. (1995): Regional geological and tectonic setting of porphyry deposits in British Columbia and Yukon Territory; *in* Porphyry Deposits of the Northwestern Cordillera of North America, T.G. Schroeter (ed.), Canadian Institute of Mining, Metallurgy and Petroleum, Special Volume 46, p. 40–57.

Monger, J. and Price, R. (2002): The Canadian Cordillera: geology and tectonic evolution; *Canadian Society of Exploration Geophysicists Recorder*, v. 27, no. 2, p. 17–36.

Newell, J.M. and Peatfield, G.R. (1995): The Red-Chris porphyry copper-gold deposit, northwestern British Columbia; *in* Porphyry Deposits of the Northwestern Cordillera of North America, T.G. Schroeter (ed.), Canadian Institute of Mining, Metallurgy and Petroleum, Special Volume 46, p. 674–688.

Schink, E.A. (1977): *Geology of the Red Chris porphyry copper deposit, northwestern British Columbia*; M.Sc. thesis, Queens University, 211 p.

Seedorff, E., Dilles, J.H., Proffett, J.M., Einaudi, M.T., Zurcher, L., Stavast, W.J.A., Barton, M.D. and Johnson, D.A. (2005): Porphyry-related deposits: characteristics and origin of hypogene features; *in* Economic Geology 100th Anniversary Volume, Economic Geology Publishing Company, Littleton, Colorado, p. 251–298.

Figure 6: Typical examples of vein types that cut the Red stock monzodiorite, from drillholes in the Red Chris deposit, northwestern British Columbia: **a)** banded quartz stockwork veins with disseminated and fracture-controlled hematite-magnetite (Hm/Mt), chalcopyrite (Cp) and bornite (Bn), drillhole RC106-032 (316.03 m); **b)** thin quartz-pyrite (Py)±chlorite (Chl) veinlets with K-silicate alteration envelope, drillhole RC335-075 (1020.78 m); **c)** barren quartz vein (banded quartz+carbonate vein with minor disseminated hematite [Hm]+chalcopyrite [Cp]), drillhole RC335-019 (229.88 m); **d)** sulphide-only veins (thin, wispy pyrite veins), drillhole RC106-011 (102.51 m); **e)** sulphide-only vein (chalcopyrite+bornite vein with minor quartz and carbonate and a thin, dark brown-green alteration selvage [secondary biotite? chlorite?]), drillhole RC335-046 (618.13 m); **f)** late-stage carbonate vein (multiple generations of thin carbonate [dolomite?] veins), drillhole RC106-037 (404.07 m); **g)** late-stage, thin white carbonate vein (dolomite?) cutting quartz veins and quartz+hematite±chalcopyrite±bornite veins, the monzodiorite hostrock being weakly K-silicate altered, drillhole RC335-008 (88.27 m); **h)** late-stage carbonate vein with abundant coarse-grained pyrite crosscutting quartz+pyrite+chalcopyrite stockwork veins, drillhole RC335-039 (505.42 m).

Coherent and Clastic Rocks in the Southwest Zone Alkalic Porphyry Copper-Gold System, Galore Creek, Northwestern British Columbia (NTS 104G)

K. Byrne, Mineral Deposit Research Unit, University of British Columbia, Vancouver, BC (current address: Teck Corporation, Vancouver, BC, Kevin.Byrne@teck.com)

R.M. Tosdal, Mineral Deposit Research Unit, University of British Columbia, Vancouver, BC

K.A. Simpson, Mineral Deposit Research Unit, University of British Columbia, Vancouver, BC (current address: Geoscience BC, Vancouver, BC)

Byrne, K., Tosdal, R.M. and Simpson, K.A. (2010): Coherent and clastic rocks in the Southwest Zone alkalic porphyry copper-gold system, Galore Creek, northwestern British Columbia (NTS 104G); in Geoscience BC Summary of Activities 2009, Geoscience BC, Report 2010-1, p. 87–104.

Introduction

Alkalic porphyry deposits are well documented (See-dorff et al., 2005; Holliday and Cooke, 2007). In contrast, alkalic porphyry deposits are less well understood. Lang et al. (1995b, c), Jensen and Barton (2000) and Cooke et al. (2007) highlighted the economic significance of alkalic porphyry Cu-Au deposits and noted the subtle but significant differences from calcalkalic systems, as well as variations within the porphyry class itself. Alkalic porphyry Cu-Au deposits are known in only a few metallogenic terranes, notably the Triassic and Jurassic marine volcanic arcs of British Columbia (Barr et al., 1976; Lang et al., 1995c) and the Ordovician and early Silurian Lachlan Fold Belt in New South Wales, Australia (Cooke et al., 2007).

Galore Creek is an alkalic porphyry Cu-Au district located within the Stikine Terrane at the western margin of the Intermontane Belt in the Canadian Cordillera of northwestern BC (Figure 1). The interplay between breccia formation and mineralization events is integral to ore deposition in several BC alkalic porphyry systems, namely Mount Polley, Galore Creek, Copper Canyon and Crescent (Afton-Ajax area). The Southwest Zone Cu-Au breccia-centred deposit is one of 12 mineralized centres in the Galore Creek alkalic porphyry district and provides an important case study in the role of breccias in alkalic porphyry systems. Hosted in brecciated intrusive rocks that are distinctly younger than Central Zone Cu-Au mineralization (Schwab et al., 2008), the Au-rich Southwest Zone preserves late stages of magmatic-hydrothermal activity in the Galore Creek district (Enns et al., 1995; Schwab et al., 2008). This paper presents detailed coherent and clastic

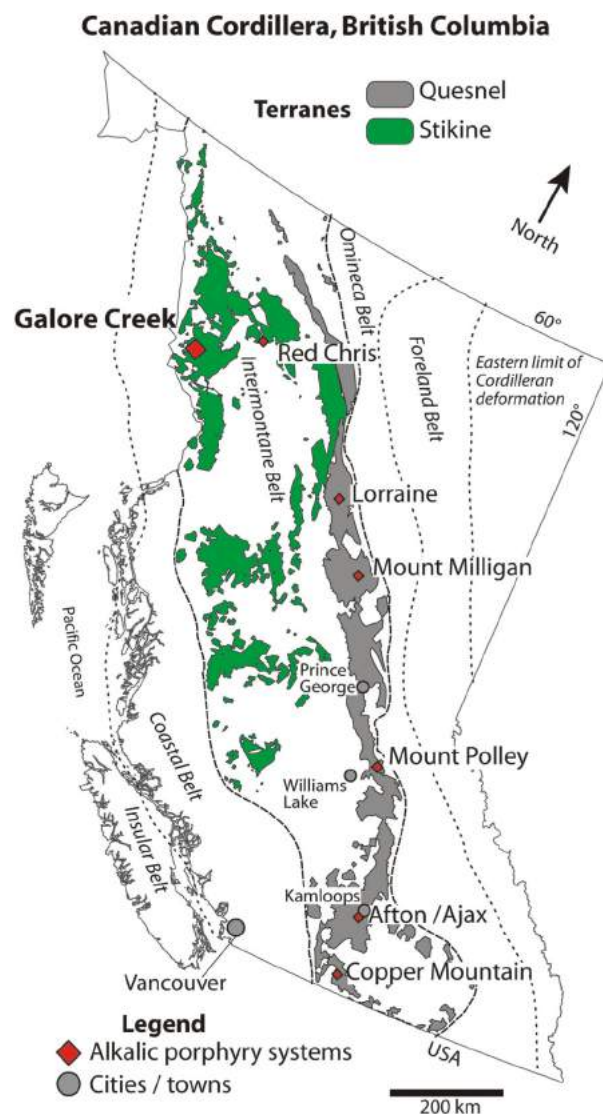


Figure 1. Mapped extent of the accreted Quesnel and Stikine ocean-arc terranes, major alkalic Cu-Au porphyry deposits and morphogeological belts. Galore Creek is located at the western margin of the Intermontane Belt, approximately 70 km east of Wrangell, Alaska. Data sourced from BC MapPlace (BC Geological Survey, 2010).

Keywords: Galore Creek, breccia, intrusive rocks, alkalic porphyry

This publication is also available, free of charge, as colour digital files in Adobe Acrobat® PDF format from the Geoscience BC website: <http://www.geosciencebc.com/s/DataReleases.asp>.

rock descriptions and parageneses in the Southwest Zone. The data presented are based on detailed drillcore logging of boreholes and a compilation of NovaGold Resources Inc. data on two cross-sections.

Regional Geological Setting

A collage of allochthonous oceanic and proximal to distal pericratonic terranes was accreted to the western margin of the North American craton during the Late Paleozoic to Late Mesozoic (Monger and Irving, 1980; Monger et al., 1982; Coney, 1989). McMillan (1991) grouped the Stikine, Cache Creek and Slide Mountain terranes, and parts of the Quesnel and Yukon-Tanana terranes into the Intermontane Superterrane. Quesnel and Stikine arcs host several alkalic intrusive centres and porphyry Cu-Au deposits of similar age (Figure 1), as well as calcalkalic porphyry Cu-(Mo-Au) deposits. Similarities in rock type and geological history between the Stikine and Quesnel terranes, including the presence of the silica-undersaturated alkalic porphyry deposits, have led workers to believe that they are segments of the same Triassic arc (Wernicke and Klepacki, 1988; Nelson and Mihalynuk, 1993; Mihalynuk et al., 1994). The alkalic Cu-Au deposits in both the Stikine and Quesnel ter-

ranes are products of two discrete alkalic magmatic events at the end of the Triassic and in the early Jurassic (Mortensen et al., 1995), and are interpreted to have formed outboard of ancestral North America in island-arc tectonic settings (McMillan, 1991).

District Geology

The Galore Creek alkalic intrusive suite is one of the largest and most silica-undersaturated complexes (Figure 2) to host porphyry Cu-Au deposits (Lang et al., 1995c). Galore Creek alkalic intrusions were emplaced between 210 ± 1 and 200.1 ± 2.2 Ma (Mortensen et al., 1995), and are hosted in supracrustal rocks of the Upper Triassic Stuhini Group (Figure 2B). Syenite, monzonite and monzodiorite stocks are hosted in rocks of shoshonitic affinity consisting of augite-phyric intermediate volcanic rocks, pseudoleucite-bearing phonolite and associated volcanoclastic rocks (Lang et al., 1995b, c). Kennecott Corporation defined a sequence of 12 intrusions for the Galore Creek alkalic intrusive suite (I1–I12; Enns et al., 1995), which is modified herein. The porphyry Cu-Au mineralization in the nearby Copper Canyon area is also hosted in alkalic intrusions (Bottomer and Leary, 1995).

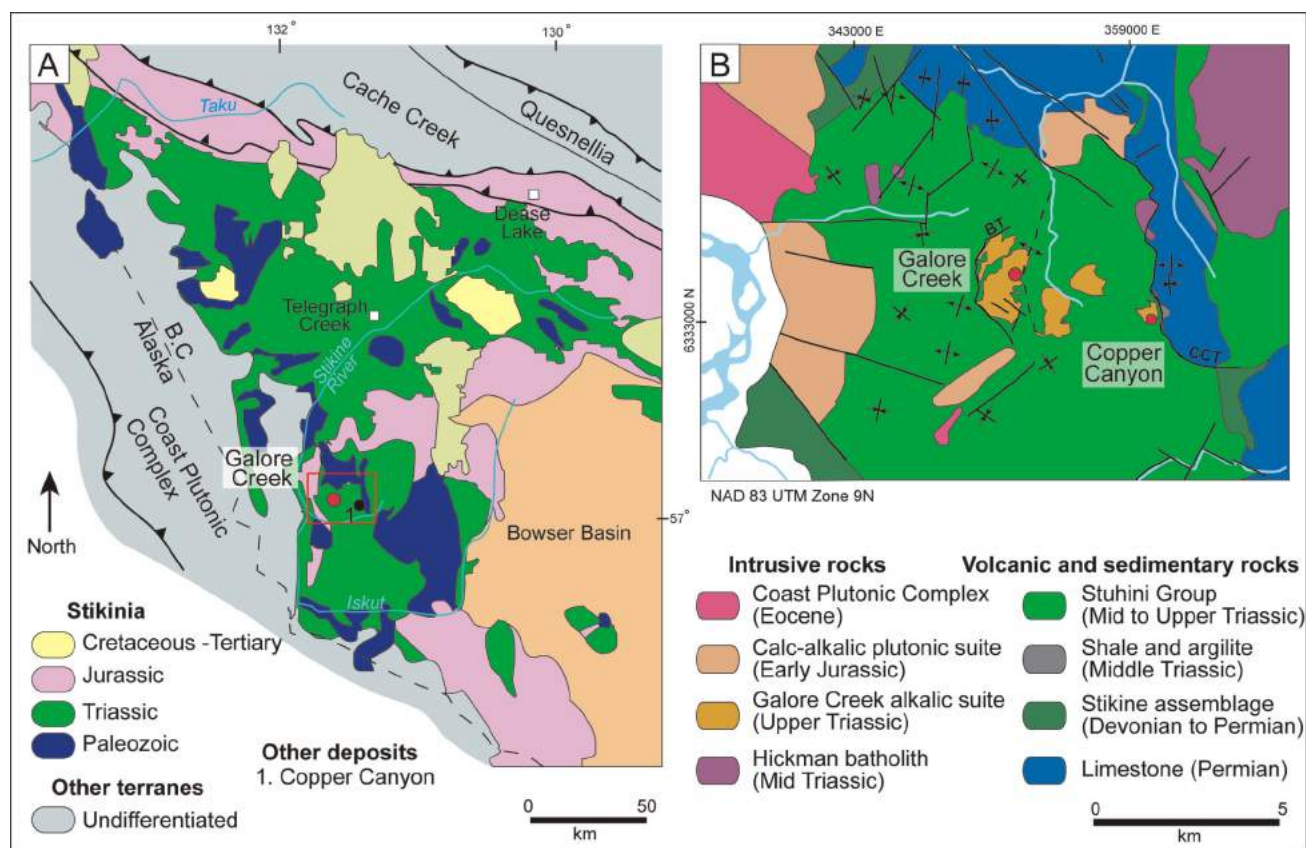


Figure 2. A) Major tectonostratigraphic elements of northwestern British Columbia (modified from Wheeler and McFeely, 1991; Gabrielse et al., 1991; Logan and Koyanagi, 1994) and location of the Galore Creek district (red dot) and Copper Canyon occurrence. The red box shows the location of Figure 2B. **B) Regional-scale geology of Galore Creek district**, showing the location of the Copper Canyon alkalic porphyry Cu-Au occurrence (modified from Logan and Koyanagi, 1994; Enns et al., 1995). Abbreviations: BT, Butte thrust fault; CCT, Copper Canyon thrust fault.

Hydrothermal alteration and mineralization are developed in the multiphase complex of alkalic intrusive and host shoshonitic volcano-sedimentary rocks. Twelve zones of Cu-Au mineralization are known (Figure 3). The largest deposit is the northerly-elongated Central Zone (Lang et al., 1995a; Micko et al., 2007; Schwab et al., 2008). Smaller prospects in the district include the Southwest Zone, Junction and North Junction, Butte, West Rim, Westfork and Saddle (Enns et al., 1995; Schwab et al., 2008). Two periods of hydrothermal activity, punctuated by intrusion of voluminous megacrystic orthoclase-phyric syenite and monzonite dikes, are known in the district (Schwab et al., 2008). Early mineralization occurs in the Central Zone and is hosted mostly in supracrustal rocks with subordinate Cu-Au in intrusions and hydrothermally cemented breccias. Mineralization in the Central Zone is truncated to the west by post-mineral, megacrystic, orthoclase-phyric syenite and monzonite dikes (Enns et al., 1995; Schwab et al., 2008). A second stage of mineralization is hosted in the same megacrystic orthoclase-phyric syenite and monzonite in the Southwest Zone (Figure 3), Middle Creek and Junction prospects (Schwab et al., 2008).

Three phases of deformation are recognized for the oldest Paleozoic rocks and one phase for Upper Triassic strata within the Stikine River–Iskut River region (Panteleyev, 1976; Logan and Koyanagi, 1994; Logan, 2004). The supracrustal rocks at Galore Creek are interpreted to have undergone early and broad-scale post-Triassic north-south compression followed by post-early Jurassic development of northerly-trending folds and thrust faults (Logan and Koyanagi, 1994), manifested by the post-mineral west-dipping Butte thrust fault (Schwab, et al., 2008) and the east-dipping Copper Canyon thrust fault (Bottomer and Leary, 1995). The deformation has tilted the Galore Creek district moderately (Byrne, 2009).

Rocks of the Southwest Zone

The Southwest Zone is situated ~600 m southwest of the South Gold lens in the southern part of the Galore Creek intrusive-volcanic complex (Figure 3), and is buried by glacial cover (Figure 4). The rocks of the Southwest Zone, based on relogging of drillcore, are divided into two groups: coherent and clastic. The coherent facies formed from the cooling and solidification of magma and is characterized by aphanitic or phaneritic textures. The clastic facies includes any fragmental rock; descriptions of these rocks follow McPhie et al. (1993). Characterization of clastic facies on the basis of infill types (matrix and cement) used criteria outlined by Davies et al. (2008b). Matrix, the fine-grained clastic component that occurs between larger clasts, comprises comminuted wallrock (rock flour), specifically lithic and crystal fragments of sand to granule size (<0.5–4 mm). Cement is a crystalline component within the clastic rock that precipitated from an aqueous fluid. Matrix-

bearing breccias are clastic rocks with a component of matrix, with or without any additional cement. In the Southwest Zone, megacrystic orthoclase-phyric syenite and monzonite coherent-facies rocks are crosscut by matrix-bearing breccias, both of which host Cu-Au (Figure 4).

Coherent Rocks

Eight coherent rock types are recognized in the Southwest Zone (Table 1; Figure 5). Numerous dikes of intermediate to mafic composition crosscut all other rocks in the Southwest Zone and are considered unrelated to magmatism of the Galore Creek suite (Enns et al., 1995). The units are grouped as pre- or post-matrix-bearing breccia, based on observed and inferred crosscutting relationships. Of the eight coherent units, six are important to the evolution of the breccia (Figure 6). Three units are pre-breccia and three are post-breccia. The pre-breccia coherent rocks are as follows:

- 1) **Megacrystic orthoclase-phyric syenite** is characterized by tabular orthoclase (1–6 cm) and ~5% lath and equant orthoclase phenocrysts (0.2–1.0 cm) in a crystalline groundmass of K-feldspar, hornblende and biotite (Table 1, unit 2; Figure 6A). The unit occurs as thick (>100 m) composite dikes that intrude feldspar-phyric syenite (Table 1, unit 1).
- 2) **Megacrystic orthoclase- and plagioclase-phyric monzonite** is distinguished from other megacrystic units by plagioclase phenocrysts (Table 1, unit 3; Figure 6B). These megacrystic porphyries (units 2 and 3) host younger, less voluminous intrusions and are the dominant wallrock to clastic rocks (Figure 5).
- 3) **Acicular feldspar-phyric syenite** forms thin (0.5–3 m) dikes intruding the megacrystic porphyries (Table 1, unit 5; Figure 5.). Acicular-feldspar-phyric syenite is also a minor clast type in matrix-bearing breccia and locally displays irregular clast margins.

Post-matrix-bearing breccia coherent units are volumetrically minor and intrude megacrystic orthoclase-phyric syenite and monzonite, and clastic rocks. These include the following:

- 1) **Biotite-phyric monzodiorite** intrudes matrix-bearing breccia and is spatially coincident with much of the high-grade Cu-Au in the Southwest Zone (Table 1, unit 6; Figure 6C).
- 2) **Pyroxene-, hornblende- and biotite-phyric diorite** form dikes less than 2 m wide that cut cemented breccias. This unit locally contains minor Cu at its margins as veins and disseminations (Table 2, unit 7; Figure 6D).
- 3) **Orthoclase- and plagioclase-phyric monzonite** forms 1–5 m wide dikes that crosscut all breccia facies, are distinguished by characteristic glomeroporphyritic feld-

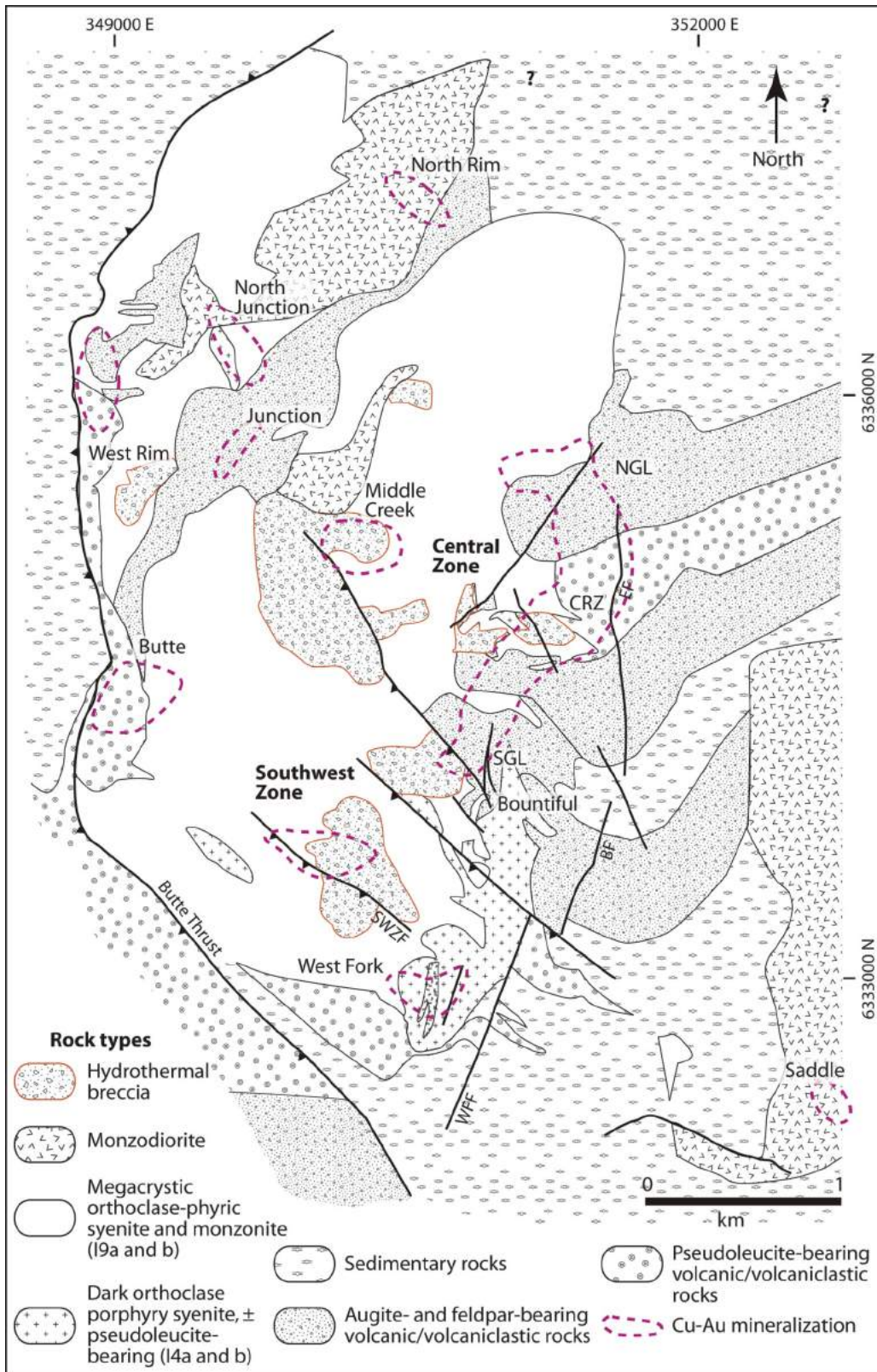


Figure 3. Simplified geology of the Galore Creek district, northwestern British Columbia, showing the location of mineralized centres and major structural features. Base map modified from maps of NovaGold Resources Inc., and rock type and distribution from drillhole and outcrop data. The names I9a, b and I4a, b refer to intrusive rock nomenclature used by Enns et al. (1995) and NovaGold Resources Inc. Abbreviations: NGL, North Gold lens; CRZ, Central Replacement zone; SGL, South Gold lens; SWZF, Southwest Zone fault; WFF, West Fork fault; BF, Bountiful fault; EF, East fault.

spar (Table 1, unit 8; Figure 6E) and postdate the Cu mineralization.

Biotite-phyric monzonite dikes are focused along the contact between the matrix-bearing breccia and porphyry wallrocks. Where it intrudes the matrix-bearing breccia, biotite-phyric monzodiorite forms volumetrically minor interconnected dikelets (Figures 7, 8). Fine-grained margins are observed within the biotite-phyric monzodiorite dikes; in contrast, the peripheral dikelet facies is characterized by irregularly shaped margins with local alignment of biotite phenocrysts (Figure 8). The dikelet facies may reflect peripheral fingering margins where it becomes disaggregated.

Clastic Rocks

There are three principal clastic facies in the Southwest Zone, based on the relative abundances of cement and matrix (Table 2):

- 1) matrix-bearing breccia with negligible cement (M-BX)
- 2) matrix-bearing breccia with 10–40% cement (matrix-dominated, MC-BX) and matrix-bearing breccia with >40% cement (cement-dominated, CM-BX)

3) cement-only breccia (C-BX)

The matrix-bearing breccia body is approximately 400 m wide by 800 m long, extends to at least 600 m below the surface and is discordant to the surrounding pre-fragmentation porphyry dikes. The western matrix-bearing breccia-wallrock contact, in its present geometry, is locally overhanging and trends broadly north and dips 60–70°W (Figures 4, 7). In contrast, the eastern contact is less well defined but appears to have a similar strike and dip. In plan view, the breccia body has an irregular oval shape elongated to the north (Figure 4). Section B–B' (Figure 7) cuts a steeply west-dipping overhanging protrusion of matrix-bearing breccia that results in the observed rollover of the wallrock contact from north to south. The northern and southern matrix-bearing breccia-wallrock contacts are not as well defined, although available drilling suggests the breccia body may continue south. Contacts between M-BX and wallrocks are described in Table 2.

Matrix-bearing breccia with no appreciable cement component (M-BX) is the most abundant breccia facies. Matrix-bearing breccia is predominantly polyolithic, non-

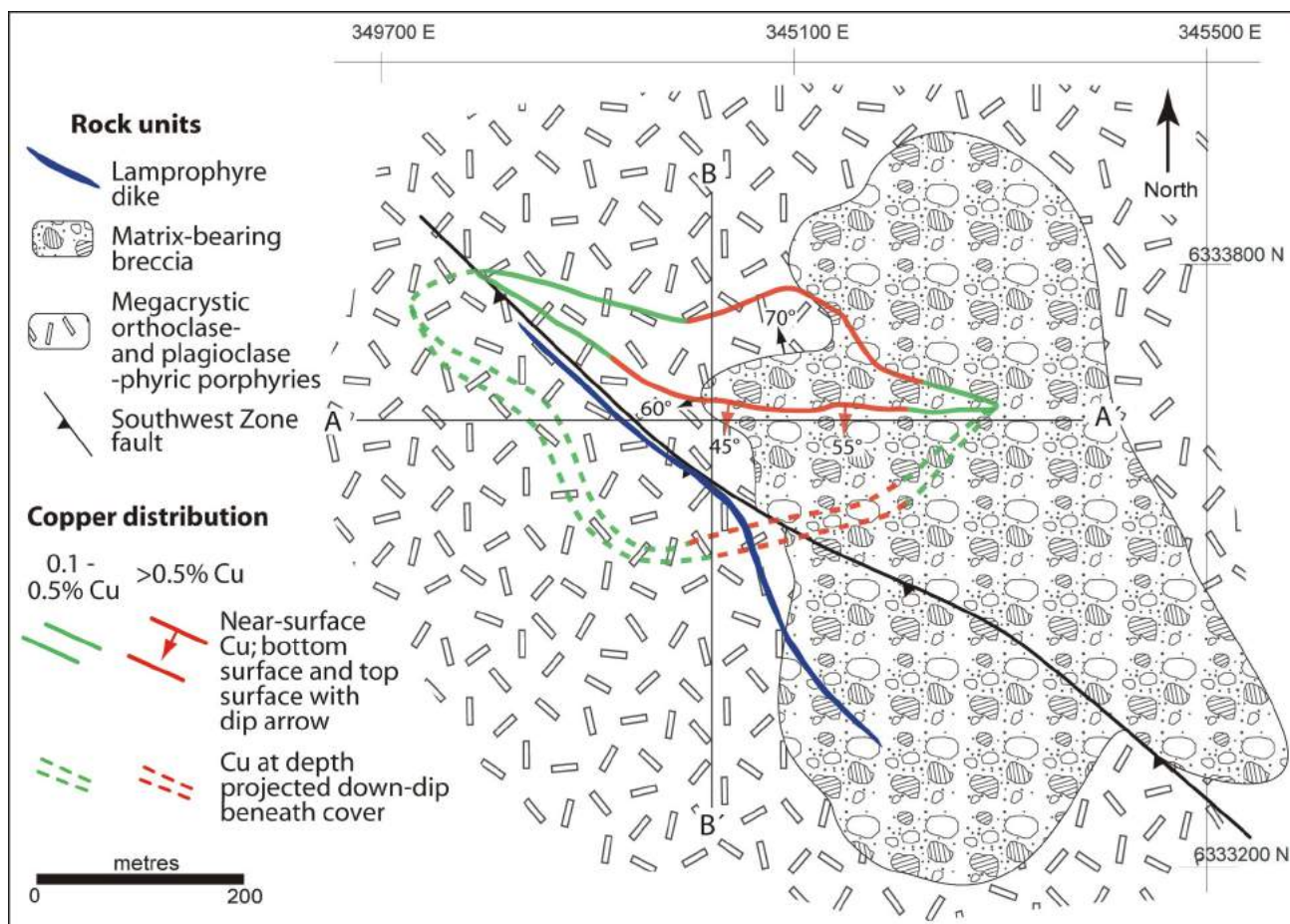


Figure 4. Simplified bedrock geology and Cu-grade distribution in the Southwest Zone, Galore Creek district, northwestern British Columbia, showing the locations of section lines A–A' (6333650N) and B–B' (350030E). Fire-assay data provided by NovaGold Resources Inc.

Table 1. Lithological characteristics of coherent rocks in the Southwest Zone, Galore Creek district, northwestern British Columbia.

Unit ⁽¹⁾	Coherent facies	Name ⁽²⁾	Lithology description	Timing ⁽³⁾
1	Feldspar-phyric syenite	I7	Phenocrysts: 1–2% lath and equant feldspars (0.5–1 cm). Groundmass: medium-grained equigranular. Distinguishing features: forms thick bodies with unclear geometries; appears to have variable phenocryst population containing some megacrysts	Pre
2	Megacrystic orthoclase-phyric syenite	I9A	Phenocrysts: 10–20% tabular orthoclase (1–6 cm) and ~5% lath and equant orthoclase (0.2–1.0 cm). Groundmass: medium-grained salt-and-pepper texture, 7–15% mafic minerals, 60% feldspar	Pre
3	Megacrystic orthoclase- and plagioclase-phyric monzonite	I9B	Phenocrysts: 5–20% tabular orthoclase (1–6 cm), 5–10% lath and equant orthoclase (0.2–1.0 cm), 20–35% lath and subhedral plagioclase (0.2–0.5 cm). Groundmass: medium-grained, 5% mafic minerals, 30–40% feldspar	Pre
4	Megacrystic orthoclase-phyric monzonite	I11	Phenocrysts: 5–15% lath to tabular orthoclase (0.5–2cm). Groundmass: medium-grained equigranular. Distinguishing features: trachytic orthoclase phenocrysts	Pre
5	Acicular-feldspar-phyric syenite	WFP	Phenocrysts: 5–25% acicular feldspar (0.2–1cm). Groundmass: dark, fine-grained. Distinguishing features: sometimes displays irregular clast margins; occurs throughout the matrix-bearing breccia body in minor amounts	Pre–syn?
6	Biotite-phyric monzodiorite	I6, I8B	Phenocrysts: 15–25% biotite (1–2 mm), ~3% hornblende needles (2–3 mm) and 60–70% feldspar. Distinguishing features: centred in the upper cemented breccia domain; typically mineralized by fine-grained chalcopyrite	Post
7	Pyroxene-, hornblende- and biotite-phyric diorite	V1 related dikes?	Phenocrysts: 5–10% hexagonal-shaped pyroxene (~0.2–0.8 cm), 5–10% biotite (booklets; 0.1–0.5 cm), >3% hornblende (0.2–1 cm) and 3–5% equant feldspar (0.2–0.4 cm). Groundmass: dark green, fine-grained. Distinguishing features: host to weak Cu mineralization	Post
8	Orthoclase- and plagioclase-phyric monzonite	I9(C)	Phenocrysts: 5–15% orthoclase (0.5–1.5 cm; rare megacrysts) and 10–25% anhedral plagioclase (0.2–0.6 cm). Groundmass: dark, fine-grained with 5–20% mafic minerals. Distinguishing features: glomeroporphyritic feldspar phenocrysts	Post
9 ⁽⁴⁾	Xenolith-bearing lamprophyre	D1	Phenocrysts: 10–20% biotite (0.1–0.2 cm) and 5–10% hornblende (0.3–0.5 cm). Groundmass: dark green, fine-grained	Post
10 ⁽⁴⁾	Mafic to intermediate dikes	D2-D3	Phenocrysts: 10% lath shaped feldspar (0.2–0.3 cm). Groundmass: fine-grained to aphanitic	Post

⁽¹⁾ Oldest to youngest units listed from top to bottom. Sequence of coherent rocks is based on observed and inferred crosscutting relationships.

⁽²⁾ Name refers to intrusive rock nomenclature used by Enns et al. (1995) and references therein, and NovaGold Resources Inc.

⁽³⁾ Timing is with respect to the formation of matrix-bearing breccia.

⁽⁴⁾ Not part of the Galore Creek alkalic suite.

bedded, poorly sorted to chaotic (massive), matrix rich and matrix supported (Figure 9A, B). Clast to matrix ratio varies from 3:7 to 9:1 and averages approximately 7:3. Matrix is composed mostly of sand- and granule-size wallrock fragments (rock flour) with subordinate igneous biotite (Figure 9C) and feldspar crystals that may be derived from wallrock or possibly juvenile material. Fine-grained phlogopite±chlorite±magnetite is interstitial to granule-size lithic fragments (matrix) and gives the matrix a dark colour (Figure 9C, D). This fine phlogopite±chlorite±magnetite is

observed throughout the matrix-bearing breccia body and may be composed of microcavity fill and alteration of clastic matrix. Clasts in matrix-bearing breccia are typically subrounded pebble to cobble size (Figure 9A, C). Cobble- to boulder-size monomict facies is proximal to the wallrock contact. Breccia margins are generally gradational over short distances but also locally abrupt or marked by dike intrusion. Sorting and stratification are evident over short intervals (5–10 cm) but are uncommon. Clasts in the matrix-bearing breccia are derived exclusively

from surrounding porphyry wallrocks. Acicular feldspar-phyric syenite occurs throughout the matrix-bearing breccia body in minor quantities and locally displays irregular clast margins (Figure 9D).

Numerous breccia clasts record older alteration and mineralization, as evidenced by alteration haloes (Figure 9A) and truncated K-feldspar and fine-grained biotite veins. Some of the pre-fragmentation alteration cannot be directly correlated to surrounding wallrocks, suggesting transportation of fragments from unobserved portions of the system. Pre-fragmentation porphyry dike contacts cannot be traced into the matrix-bearing breccia body, further demonstrating transportation of clasts away from the site of fragmentation.

A phlogopite±K-feldspar±anhydrite±magnetite±diopside±Cu-Fe-sulphide assemblage occurs as both hydrothermal cement and veins that cut the matrix-bearing breccia and host intrusions. Phlogopite and magnetite are the most common cement minerals associated with sulphides. Two spatially distinct cemented-breccia domains, an upper (main) and a composite lower, are present: (Figure 7). The upper cemented-breccia domain has a semi-ellipsoid morphology and is 20–100 m thick, 500 m wide and 400 m in length, tapering towards the tips. Cemented-breccia facies in this upper domain strike ~100°, dip 45–60°S and taper along strike. The lower cemented-breccia domain is characterized by multiple discontinuous cemented facies, 10–30 m thick. These lower cemented breccias are 10–30 m thick and have a geometry similar to those in the upper zone but poor continuity. Hydrothermal cement within the matrix-bearing breccias and older bordering wallrocks varies from negligible to abundant. Cemented-breccia facies are distinguished and mapped by the abundance and type of hydrothermal cement present (Table 2). Cement textures vary throughout MC-BX and CM-BX facies, irregular and straight-walled interconnected fracture fill that cuts both matrix and clasts (Figure 10A) through open-space fill between clast and matrix (Figure 10B–D) to irregularly shaped vugs. The MC-BX facies comprises <40% cement, with matrix making up the greater portion of the infill (Figure 10B, C). The CM-BX facies has >40% cement infill (Figure 10D–F).

Intrusive wallrocks contain in situ cemented breccia (coarse crackle-fracture) that lacks the matrix characteristic of other breccia facies (Figure 11A–C). In situ cemented breccia (C-BX) is both spatially and temporally contiguous with cement-dominated domains within the matrix-bearing breccia (Figure 7). Biotite-phyric monzodiorite dikelets are centred in MC-BX and CM-BX facies and are locally affected by cement, manifested as irregularly shaped vugs. Monolithic cemented breccia (C-BX) is also locally coincident with biotite-phyric monzodiorite dikelets (Figure 11A, B). The C-BX breccia facies is also typically very

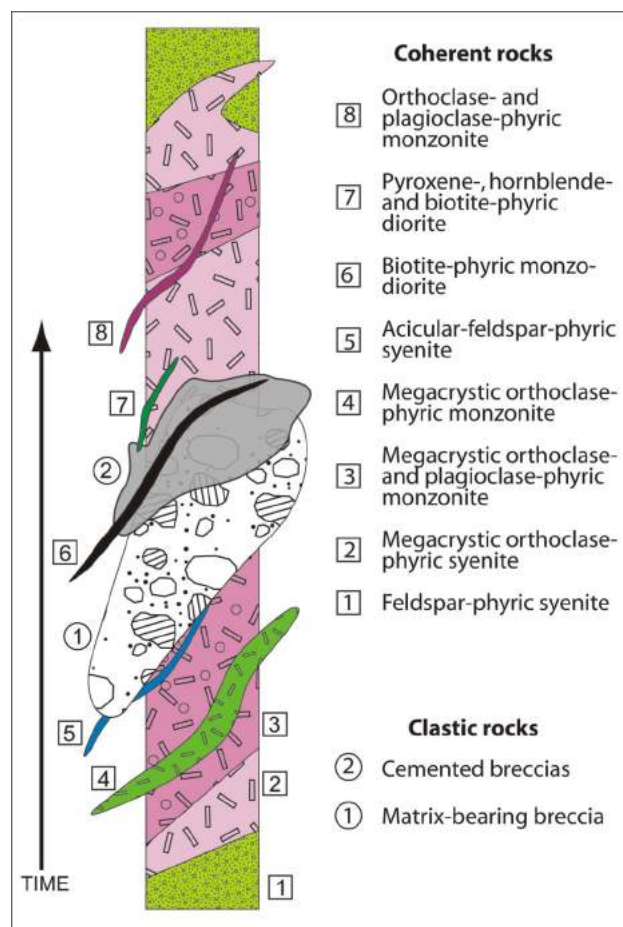


Figure 5. Sequence of coherent and clastic rock emplacement in the Southwest Zone, Galore Creek district, northwestern British Columbia.

coarse and displays a jigsaw-fit clast arrangement (Figure 11B, C). Clast morphology and organization in the polyolithic matrix-bearing breccias suggests rotation and transport. In contrast, superposition of cemented-breccia facies (MC-BX, CM-BX and C-BX) shows little evidence of clast rotation or transport.

Evolution of Coherent and Clastic Rocks

Coherent and clastic rocks in the Southwest Zone are grouped into four paragenetic stages defined by their timing with respect to the fragmentation events associated with the formation of matrix-bearing-breccia and cemented-breccia facies (Table 3).

Feldspar-phyric syenite and megacrystic syenite and monzonite porphyry dikes are cut by matrix-bearing breccia. Acicular feldspar porphyry also occurs as clasts throughout the matrix-bearing breccia. However, some of these clasts display irregular margins, suggesting that the unit was incorporated prior to solidification, thus making it coeval with the matrix-bearing breccia. Therefore, the coherent units crosscut by the matrix-bearing breccia and

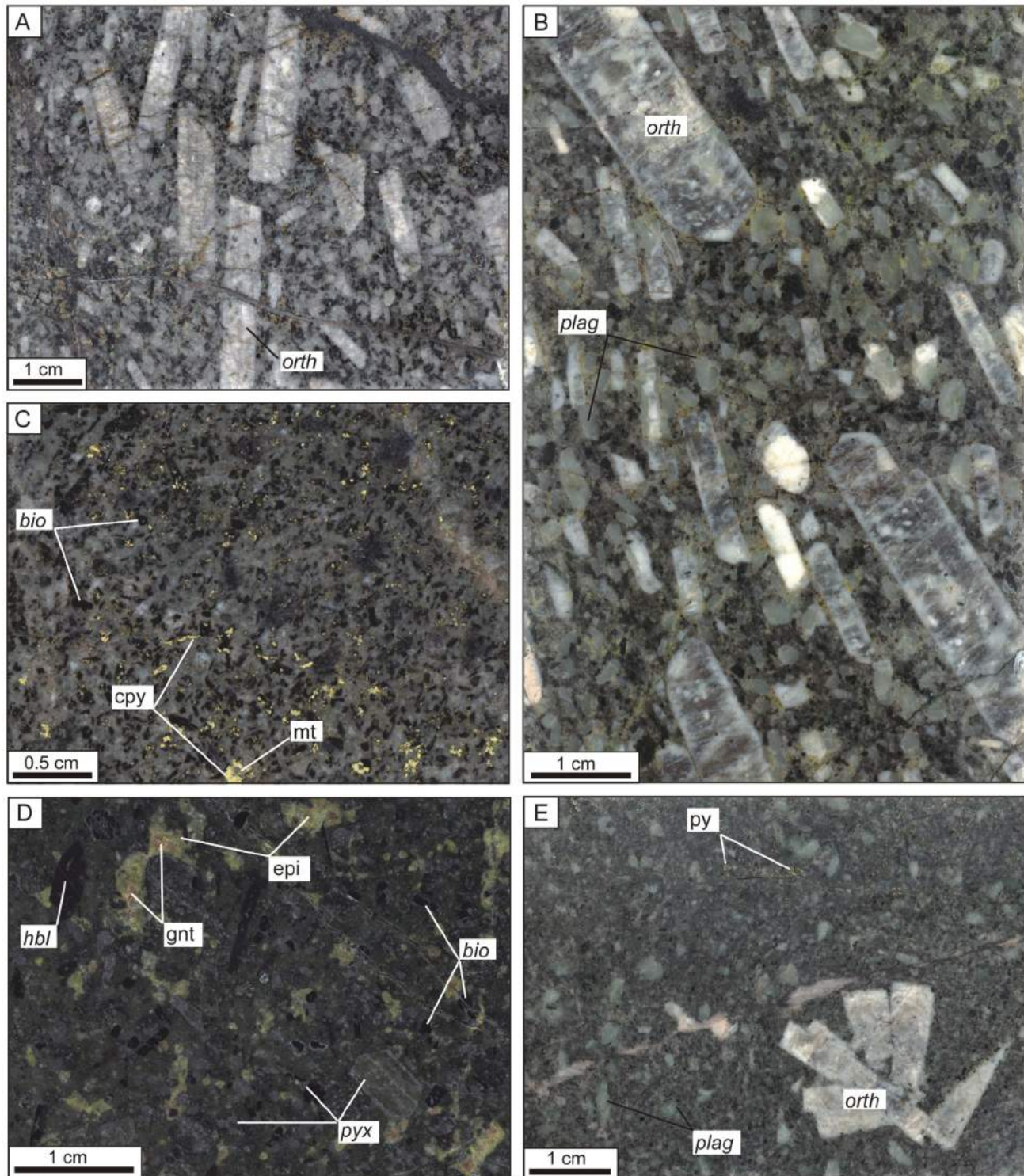


Figure 6. Photographs of coherent rocks in the Southwest Zone, Galore Creek district, northwestern British Columbia: **A)** megacrystic orthoclase-phyric syenite (unit 2); **B)** megacrystic orthoclase- and plagioclase-phyric monzonite dike (unit 3); **C)** biotite-phyric monzodiorite (unit 6); **D)** pyroxene-, hornblende- and biotite-phyric diorite; groundmass is pervasively chlorite altered (unit 7) and epidote-garnet forms clots in the groundmass; **E)** orthoclase- and plagioclase-phyric monzonite dike characterized by glomeroporphyritic orthoclase (unit 8). Abbreviations: bio, biotite; cpy, chalcopyrite; epi, epidote; gnt, garnet; hbl, hornblende; mt, magnetite; orth, orthoclase; plag, plagioclase; py, pyrite; pyx, pyroxene. Mineral abbreviations in italics refer to primary igneous minerals as opposed to alteration minerals.

acicular feldspar porphyry are grouped into stage 1 (Table 3).

Matrix-bearing breccia is superimposed by cemented breccia, locally resulting in the formation of MC-BX and CM-BX breccia facies (Figure 7). Concurrent with cement em-

placement in matrix-bearing breccia, the cemented-breccia facies C-BX formed in adjoining coherent units. Cement emplacement is centred on and transects the older north-trending contact between matrix-bearing breccia and wallrock. Textural features and positions of biotite-phyrlic monzodiorite dikes and dikelets indicate that emplacement

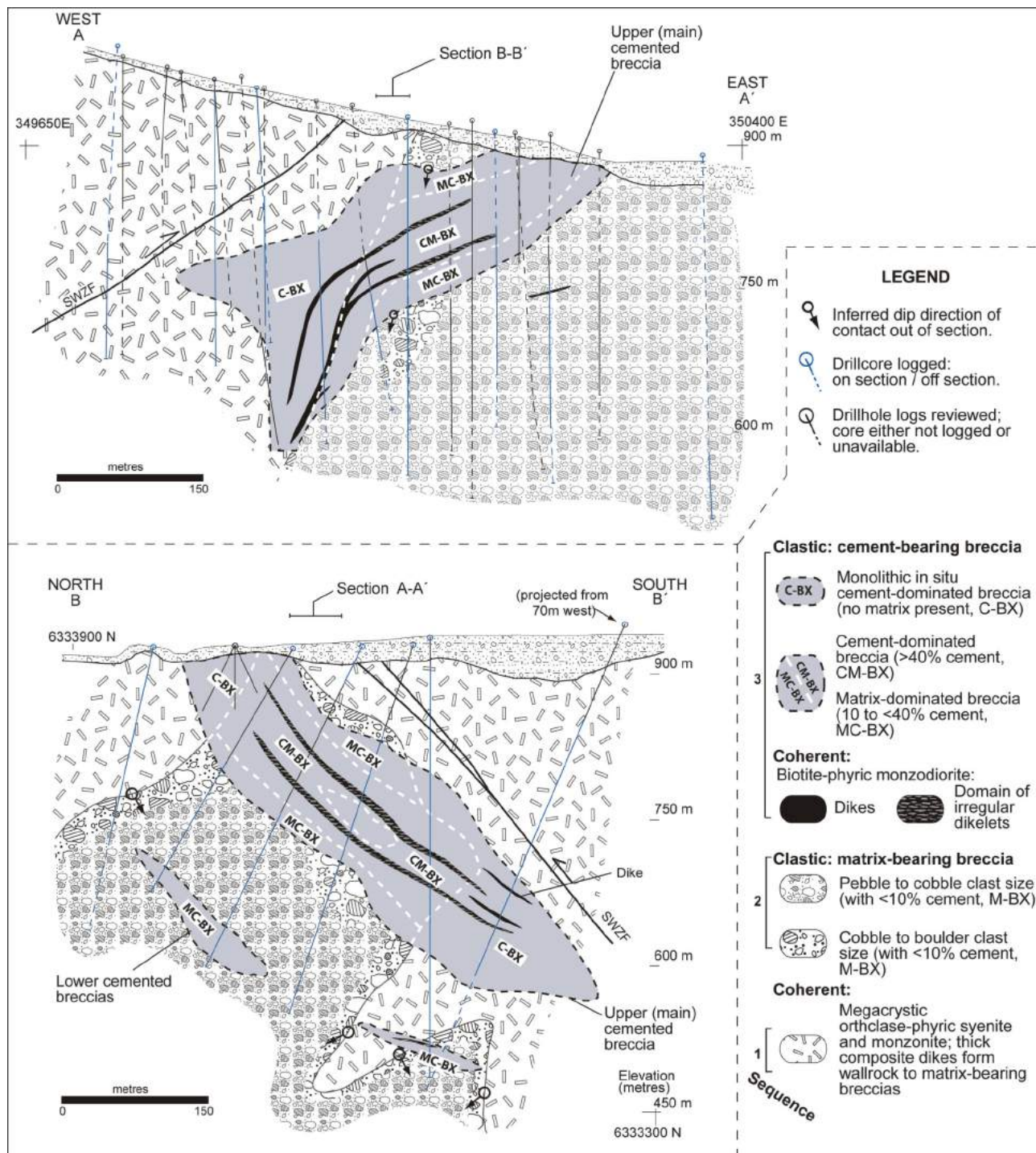


Figure 7. Distribution of clastic facies and simplified coherent facies along cross-sections A-A' (6333650N) and B-B' (350030E), Southwest Zone, Galore Creek district, northwestern British Columbia. See Figure 4 for location of section lines. Coherent-facies units 1, 4, 5, 7, 8, 9 and 10 are excluded from the figure for clarity. Drillhole data within 50 m of section A-A' and 40 m of section B-B' have been projected onto the respective sections. Abbreviation: SWZF, Southwest Zone fault.

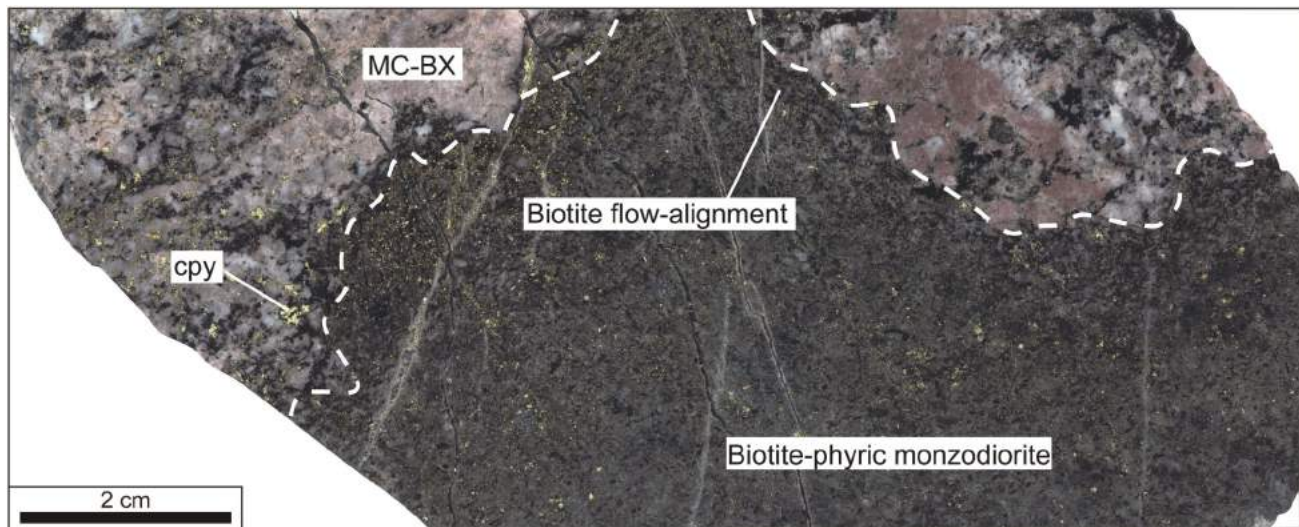


Figure 8. Biotite-phyric monzodiorite dikelet facies intrudes matrix-bearing breccia and exhibits weak flow fabric near the margins (dashed white line), Southwest Zone, Galore Creek district, northwestern British Columbia. Abbreviations: cpy, chalcopyrite; MC-BX, matrix-bearing breccias with 10–40% cement.

Table 2. Lithological characteristics of clastic rocks in the Southwest Zone, Galore Creek district, northwestern British Columbia.

Grouping	Clastic-facies nomenclature ⁽¹⁾	Infill proportion ⁽²⁾	Cement/vein mineralogy ⁽³⁾	Contacts	Lithology description
Matrix-bearing breccia with increasing cement component	M-BX: matrix-bearing breccia	<10% cement, ~90% matrix	phl, K-spar, diop, act, anh, mt, py, cpy	Sharp to gradational contact with wallrock marked by monolithic, very coarse facies	Predominantly polyolithic, unbedded, unsorted to poorly sorted, matrix rich and matrix supported; clasts are subangular to subrounded and pebble to boulder size; clast to matrix
	MC-BX: matrix-dominated breccia	10 to <40% cement, remainder is matrix	phl, K-Spar ± anh, mt, diop, cpy, bn	Gradational from weak stockwork veins and locally sharp	Fractures, irregularly shaped veins and vugs are filled with varying proportions of cement minerals; sub-facies are distinguished by cement type and abundance; clast diameters commonly greater than drillcore width
	CM-BX: cement-dominated breccia	>40% cement, remainder is matrix	phl, K-Spar ± anh, mt, diop, cpy, bn	Over short distances CM-BX is transitional from MC-BX; sharp contact between CM-BX and M-BX also noted; late dikes typically occur proximal to cemented facies contacts	
Cement-only breccia	C-BX: monolithic in situ cement-dominated breccia	greater than ~90% cement, no appreciable matrix component	phl, K-Spar, diop, act, anh, mt, py, cpy, bn	C-BX facies is hosted in intrusive wallrocks and is contiguous with CM-BX and MC-BX; C-BX is transitional to weak stock-work veins	In situ or jig-saw-fit breccias are typically very coarse (large boulders)

⁽¹⁾ Clastic facies nomenclature and sub-facies refer to the scheme applied for sub-facies classification by cement mineralogy.

⁽²⁾ Infill proportions refer to the amount of matrix and cement as proportions of total infill.

⁽³⁾ Abbreviations: act, actinolite; anh, anhydrite; bn, bornite; cpy, chalcopyrite; diop, diopside; K-spar, K-feldspar; mt, magnetite; py, pyrite; phl, phlogopite

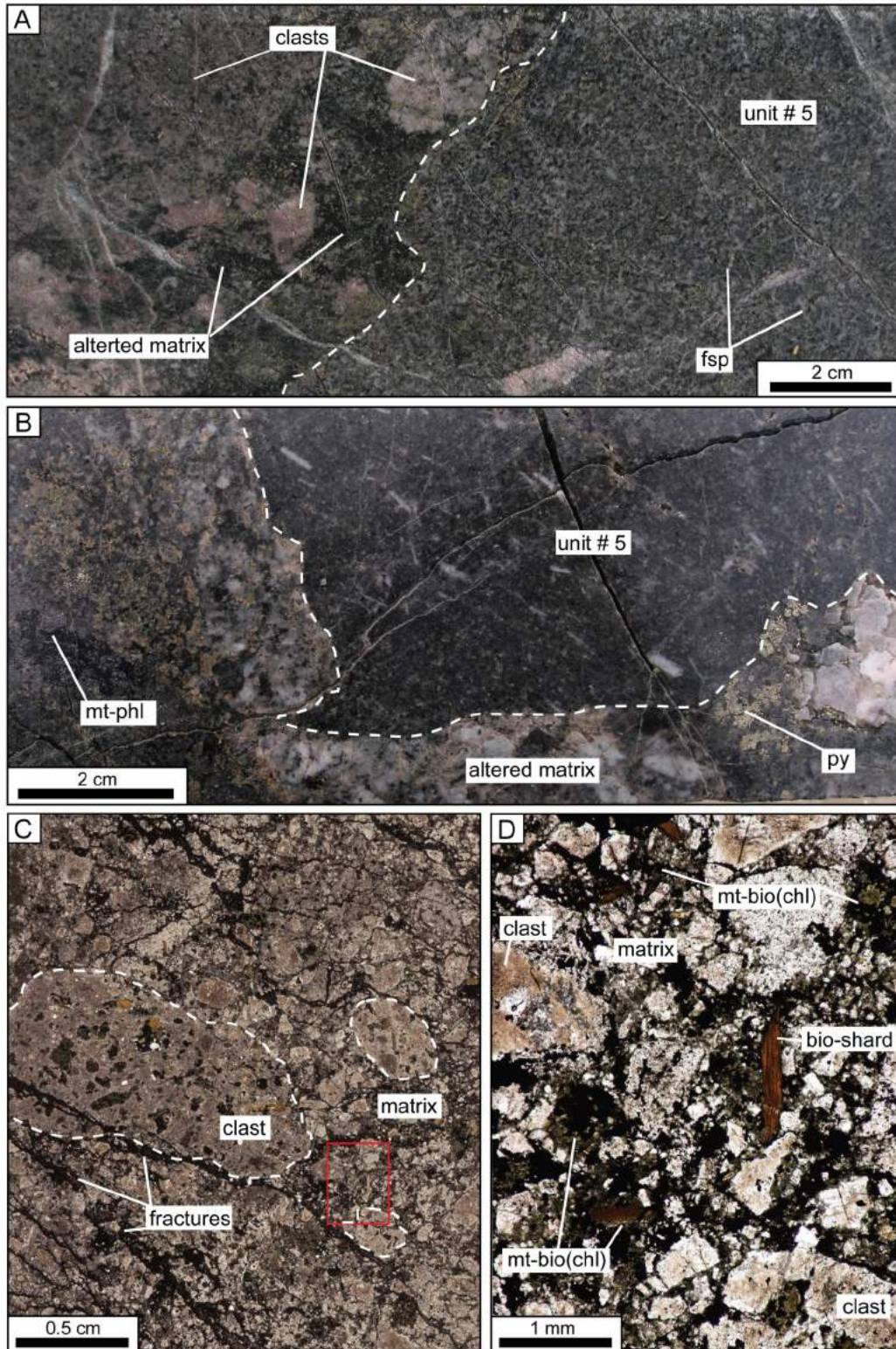


Figure 9. Photographs of diagnostic features in matrix-bearing breccias, Southwest Zone, Galore Creek district, northwestern British Columbia: **A)** polyolithic M-BX with hematite–K-feldspar–altered cobble-size clasts and <10% cement; **B)** M-BX containing oversized clast of acicular feldspar-phyrlic syenite (unit # 5) with an irregular margin; **C)** thin-section scan in which some clasts are highlighted with dashed white lines; red box indicates the area expanded in the next photo; **D)** photomicrograph of matrix composed of sand- and granule-size fragments of wallrock (partially altered to magnetite-biotite and chlorite) and rare biotite crystals; note biotite crystal is not within a larger fragment. Abbreviations: bio, biotite; fsp, feldspar; mt, magnetite; phl, phlogopite; py, pyrite; pyx, pyroxene.

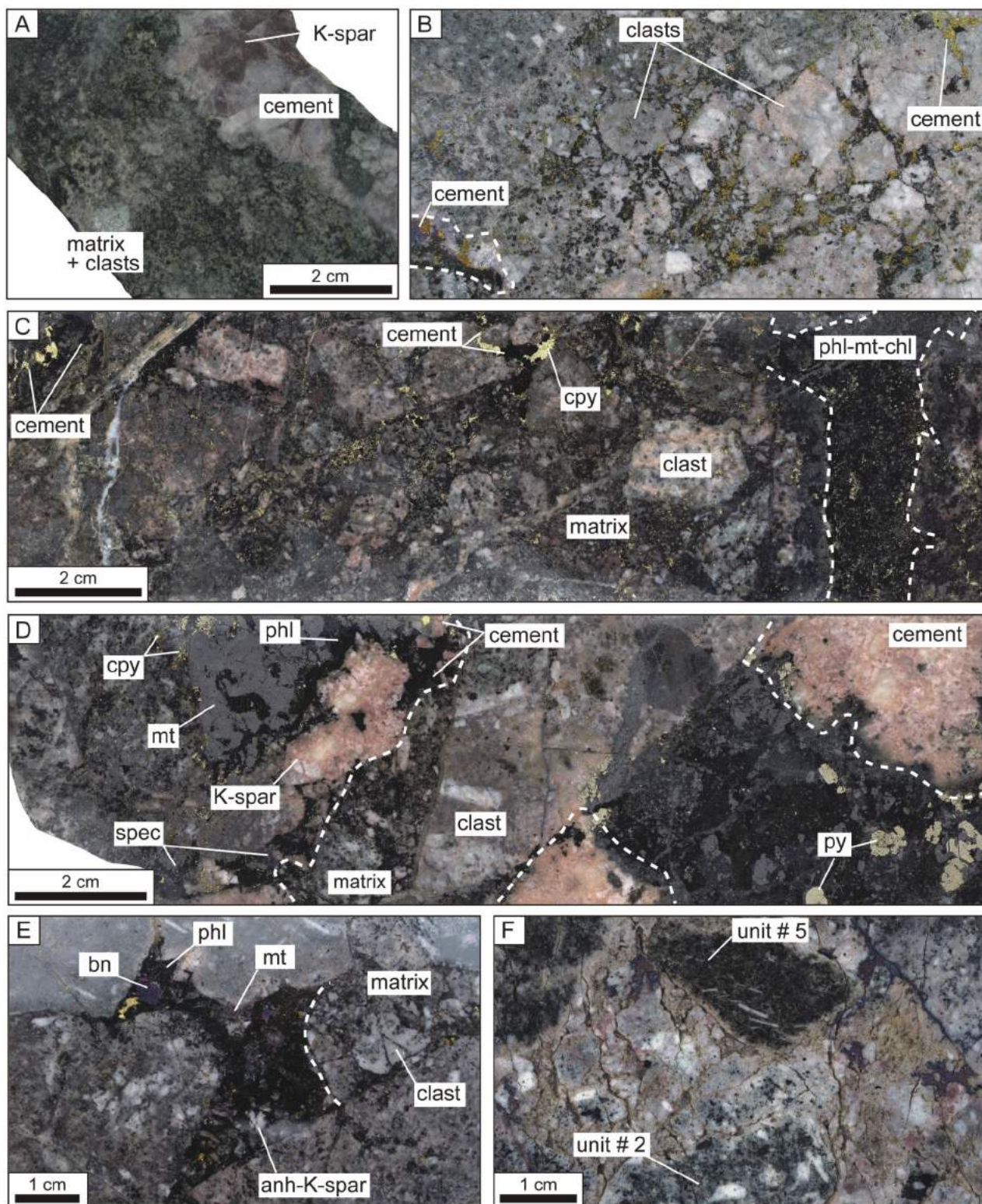


Figure 10. Photographs of cement-bearing breccia facies in the Southwest Zone, Galore Creek district, northwestern British Columbia: **A)** MC-BX, matrix-bearing breccia with <40 % cement; note the coarse K-feldspar cement; matrix is pervasively altered to chlorite-garnet; **B)** MC-BX, phlogopite-chalcopyrite-cemented breccia (highlighted by dashed white line); **C)** MC-BX, phlogopite-chalcopyrite±bornite±magnetite cement cuts matrix infill. **D)** CM-BX, cement-dominated breccia with >40% cement; note pervasive magnetite alteration of matrix (dashed white lines highlight boundaries between cement and matrix); **E)** CM-BX, phlogopite-bornite-chalcopyrite-magnetite-anhydrite-K-feldspar cement with subangular cobble-size clasts; **F)** CM-BX, K-feldspar-rich cement and alteration with bornite. Abbreviations: anh, anhydrite; bn, bornite; chl, chlorite; cpy, chalcopyrite; K-spar, K-feldspar; mt, magnetite; phl, phlogopite; py, pyrite; spec, specularite; unit # 2, megacrystic orthoclase-phyric syenite; unit # 5, acicular feldspar-phyric syenite.

was coeval with cemented-breccia formation. The cemented-breccia facies (MC-BX, CM-BX and C-BX) and biotite-phyric monzodiorite are therefore grouped together in stage 2.

The cemented-breccia facies is crosscut by multiple dikes, composed of pyroxene-, hornblende- and biotite-phyric diorite, and orthoclase- and plagioclase-phyric monzonite, which constitute stage 3 (Figure 12). Xenolith-bearing lam-

prophyre and several dikes of mafic to intermediate composition are not part of the Galore Creek alkalic suite, as defined by Enns et al. (1995), and are grouped as stage 4.

Structural Controls on Rock Distribution

Biotite-phyric monzodiorite dikes occur at the contact between the matrix-bearing breccia and porphyry wallrocks; dikelet facies occur in two discrete planar zones parallel to

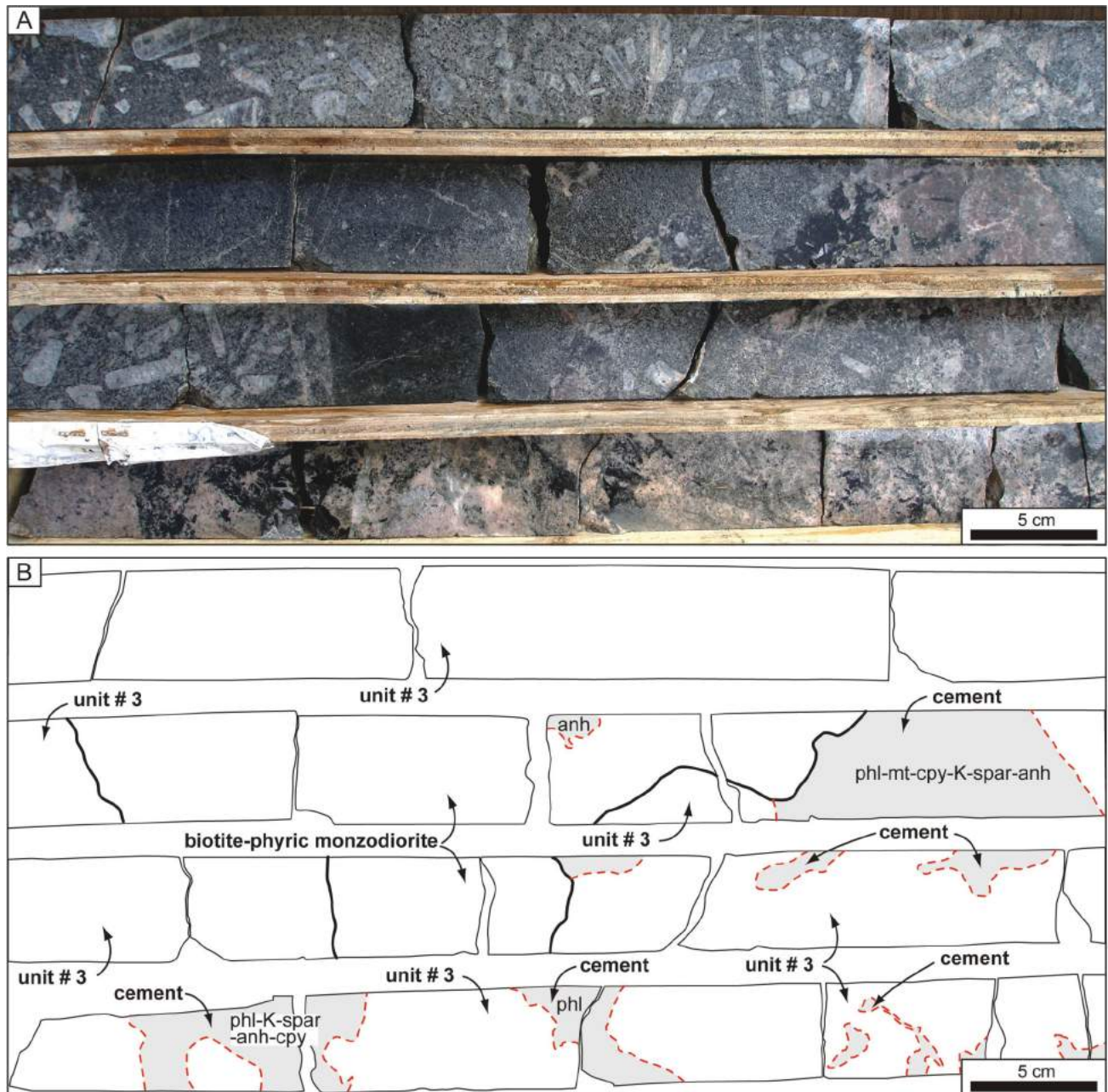


Figure 11. Photographs of monolithic, in situ cement-dominated breccias (C-BX): **A)** monolithic in situ cemented breccia (no matrix present; GC05-677, portions of core between 295.5 and 298.5 m); **B)** line traces illustrating pertinent features of drillcore shown in photo A; cemented domains highlighted with dashed red lines, and biotite-phyric dikelets marked with thick black lines and containing disseminated chalcopyrite and phlogopite alteration. Abbreviations: anh, anhydrite; cpy, chalcopyrite; K-spar, K-feldspar; mt, magnetite; phl, phlogopite; unit # 3, megacrystic orthoclase-phyric monzonite.

Table 3. Paragenetic stages of coherent and clastic rocks in the Southwest Zone, Galore Creek district, northwestern British Columbia.

Paragenetic stages ⁽¹⁾	Stage 1	Stage 2	Stage 3	Stage 4
Clastic rocks ⁽²⁾	Matrix-bearing breccia	Cemented breccia		
Coherent rocks ⁽³⁾	Units 1–5: feldspar-phyric syenite; megacrystic orthoclase-phyric syenite; megacrystic orthoclase- and plagioclase-phyric monzonite; megacrystic orthoclase-phyric monzonite acicular-feldspar-phyric syenite ⁽⁴⁾	Unit 6: biotite-phyric monzodiorite ⁽⁴⁾	Units 7 & 8: pyroxene-, hornblende- and biotite-phyric diorite; orthoclase and plagioclase-phyric monzonite	Units 9 & 10: xenolith-bearing lamprophyre; mafic to intermediate dikes

⁽¹⁾ Paragenetic stages are described in the text.

⁽²⁾ Summary of clastic rock characteristics in Table 2.

⁽³⁾ Summary of coherent rock characteristics in Table 1.

⁽⁴⁾ Syn-breccia timing, paragenesis discussed in the text.

portions of the upper cemented-breccia domain (B–B'; Figure 7). The upper cemented-breccia domain is continuous along strike and down dip, whereas the lower domain is discontinuous, being composed of multiple discontinuous mineralized horizons (Figure 7). The cemented-breccia domains strike ~100°, dip 45–60°S and intersect the north-trending matrix-bearing breccia-wallrock contact. The planar geometry and along-strike and down-dip continuity of

the cemented-breccia domains implies structural control on their formation. Furthermore, the ellipsoid geometry of the upper cemented-breccia domain is analogous to elliptical fault geometries (Peacock, 2002; Walsh et al., 2003). The geometric similarity of the cemented-breccia domains suggests they can be explained by a series of small nucleating faults that propagated into the matrix-bearing breccia and hydrothermal system.

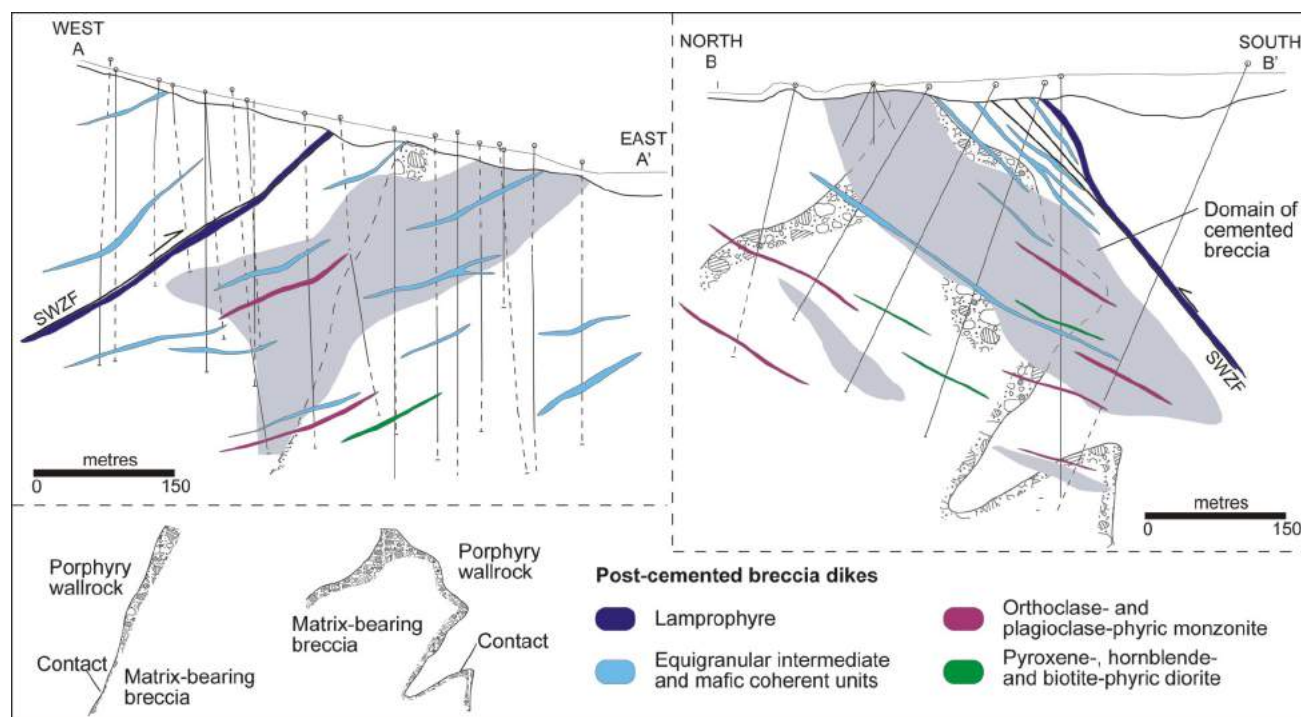


Figure 12. Post-cemented breccia facies coherent units. Abbreviation: SWZF, Southwest Zone fault.

Megacrystic porphyry units and breccias are cut by a post-mineral fault, the Southwest Zone fault (Figure 4). The fault strikes 120–130° and dips ~60°S, similar to reverse faults elsewhere in the district (Figure 3). A lamprophyre dike is locally coincident with this fault (Figure 4). The timing of lamprophyre emplacement, however, is ambiguous. Nonetheless, the extent and direction of displacement of coherent and clastic rocks shows a reverse separation of 200–250 m, although the true displacement is unconstrained. Post-mineral reverse separation along the Southwest Zone fault also locally truncates Cu-Au mineralization and alteration assemblages (Byrne, 2009).

Discussion and Genetic Interpretation

Matrix-Bearing Breccia

Key features of matrix-bearing breccia are as follows: 1) abundant fine-grained phlogopite-magnetite-chlorite alteration and microcavity fill in the matrix; 2) dominantly matrix rich and supported; 3) massive and poorly sorted; 4) polyolithic, rounded to subrounded clasts of exclusively intrusive units; 5) moderately large areal extent (inferred from drillcore); and 6) hosted in porphyry wallrocks. Hydrothermal cement (stage 2) in the matrix-bearing breccia is the result of a younger superimposed event and is not directly linked to brecciation processes.

Matrix in the matrix-bearing breccia is pervaded by phlogopite-magnetite-chlorite as alteration and microcavity fill at most localities. The distribution, mineralogy and textural features of this alteration and microcavity infill suggest that magmatic-derived hydrothermal fluids dominated the environment synchronous with and post fragmentation. Fragment rounding and mixing, matrix (rock flour) generation and differential vertical displacement of fragments are all considered compatible with fluidization as a transport mechanism during the formation of subsurface breccias (McCallum, 1985; Sillitoe 1985). Unbroken phenocrysts in rock-flour–matrix breccias have been interpreted by Seedorff et al. (2005) as juvenile (tuffaceous) material. By analogy with Seedorff et al. (2005), biotite crystals in the matrix (Figure 9D), which do not appear to be part of a clast, are tentatively interpreted as a juvenile component. Moreover, delicate fluidal clasts are not unequivocally present, although acicular feldspar-phyric syenite locally displays irregular clast margins. These irregular margins suggest that the unit was incorporated into the breccia before solidification at some localities. Juvenile fragments and clasts with irregular margins suggest the presence of magma during fragmentation.

Based on their characteristics, matrix-bearing breccias in the Southwest Zone are interpreted to be the product of explosive fragmentation and primarily classified as hydrothermal (Sillitoe, 1985) or hydroclastic subsurface (Davies et al., 2008b) breccias. Explosive fragmentation is inferred

to be the result of rapid expulsion of magmatic-hydrothermal fluids from cooling magma stocks (second boiling), coupled with decompression and liquid-vapour separation of already exsolved aqueous phases (Burnham, 1985; Sillitoe, 1985; Fournier, 1999). Juvenile material in the breccia suggests the presence of magma during fragmentation. In addition, fragmentation caused by steam expansion due to magma-fluid interaction (Sheridan and Woheltz, 1981; Hedenquist and Henley, 1985) is inferred to have produced juvenile material in the matrix. Overall, the evidence suggests that the matrix-bearing breccias were produced by a hybrid of fragmentation processes and can therefore be classified as magmatic-hydrothermal breccias with a subordinate phreatomagmatic component. Top and bottom terminations of the matrix-bearing breccia are not exposed in the present-day geometry and current erosion level. Therefore, it is unknown whether the magmatic-hydrothermal-phreatomagmatic explosions led to the disruption of rocks through to the paleosurface.

Cement-Bearing Breccias

Cement-bearing breccia facies (MC-BX, CM-BX and C-BX), veins and their associated alteration account for much of the Cu-Au budget in the Southwest Zone. Similar open-space filling, hydrothermally cemented breccias are widespread in porphyry systems and can be spatially associated with increased abundance of Cu-Au (Seedorff et al., 2005). Generally, hydrothermally cemented breccias form single or multiple lensoid, ovoid or circular pipe-like bodies with steep to vertical dips (Sillitoe, 1985; Seedorff et al., 2005).

At the Southwest Zone, the most abundant cement forms two subparallel horizons, the upper and lower cemented-breccia domains. Potassic cement minerals indicate moderately high temperature fluids of a dominantly magmatic source (Ulrich et al., 2001; Seedorff et al., 2005). Superimposition of hydrothermally cemented breccia facies on matrix-bearing breccias and porphyry wallrock is not associated with significant clast rotation or transport, implying that fragmentation was nonexplosive. Cement textures indicate emplacement by infill of 1) old and new fractures, 2) original open space between fragments in the matrix-bearing breccias, and by 3) open space generated by possible chemical corrosion or winnowing of matrix fines. Based on cement mineralogy and the environment of formation, cemented breccias are interpreted to be the result of nonexplosive fragmentation caused by the migration of magmatic-hydrothermal fluids. In this scenario, fragmentation of wallrock is the result of mechanical energy released during second boiling, decompression (Philips, 1972; Burnham, 1985) and subsequent hydraulic fracturing (Jébrak, 1997). Based on the inferred fragmentation mechanisms and criteria presented by Sillitoe (1985), Davies (2002) and Davies et al. (2008a), hydrothermally cemented

breccias in the Southwest Zone are interpreted as hybrid magmatic-hydrothermal-hydraulic breccias.

Root zones to the cemented breccias were not directly observed, although some magmatic-hydrothermal breccias are known to root in porphyry intrusions (Zweng and Clark, 1995; Jackson et al., 2007). Infill minerals, alteration and mineralization are centred on, and zoned about, cemented breccias and biotite-phyric monzodiorite facies. Distribution of infill and alteration facies, mineralization and metals are discussed below.

Evolution of the Southwest Zone Breccia Complex

The following model is proposed for the evolution of the Southwest Zone breccia complex, based on the above interpretations. Overpressure at the top of a hydrous magma chamber, due to second boiling, caused a rupture of magmatic-hydrothermal fluids and initiated explosive fragmentation. Fragmentation continued with decompression and was accompanied by subordinate phreatomagmatic explosions caused by the interaction of acicular feldspar-phyric syenite and water. Explosions propagated into megacrystic porphyry wallrocks, causing differential clast displacement, mixing and comminution that resulted in the formation matrix-bearing breccias. Ambient magmatic-hydrothermal fluids cemented microcavities (pore spaces) and altered clastic fines in the matrix-bearing breccias, greatly reducing porosity and permeability in matrix-rich facies.

Permeability regimes established post matrix-bearing breccia focused subsequent magmatic-hydrothermal fluids and strongly influenced the distribution of the cemented-breccia facies. The geometry of the upper and lower cemented-breccia domains suggests that structures played an important role in their genesis. An array of faults or fracture zones is interpreted to have intersected the matrix-bearing breccia-wallrock contact. The faults may have been dilatational features related to paleo-stress fields. Magmatic volatiles are inferred to have accumulated again in a cupola underlying the matrix-bearing breccias and subsequently expelled. The energy released during magmatic-hydrothermal fluid expulsion was sufficient to fracture the roof rocks but was not explosive. Decompression and hydraulic fracturing formed fluid channels that permitted access to the overlying rocks. Metal-bearing potassic fluids were preferentially channelled by the matrix-bearing breccia-wallrock contact and multiple intersecting fracture zones, with additional permeability generated by hydraulic fracturing. Fluid migration through newly formed fracture networks and the pre-existing permeability architecture resulted in formation of the cemented-breccia facies and Cu-Au zones.

Conclusions

Detailed drillcore logging and analyses of samples, on two cross-sections, has characterized the coherent and clastic rocks and their paragenesis in the Southwest Zone in the Galore Creek district of northwestern British Columbia. Matrix-bearing breccias and megacrystic porphyry units host Cu and Au mineralization centred in potassic, hydrothermally cemented breccias. The contact between matrix-bearing breccias and porphyry wallrocks served as the principal conduit and trap for ascending metal-bearing magmatic-hydrothermal fluids and biotite-phyric monzodiorite dikes. An array of faults intersecting this contact strongly influenced fluid-flow and the geometry of cemented breccias.

References

- Barr, D.A., Fox, P.E., Northcote, K.E. and Preto, V.E. (1976): The alkaline suite porphyry deposits: a summary; *in* Porphyry Deposits of Canadian, A. Sutherland Brown (ed.), Canadian Institute of Mining and Metallurgy, Special Volume 15, p. 359–367.
- BC Geological Survey (2010): MapPlace GIS internet mapping system; BC Ministry of Energy, Mines and Petroleum Resources, MapPlace website, URL <<http://www.MapPlace.ca>> [November 2010].
- Bottomer, L.R. and Leary, G.M. (1995): Copper Canyon porphyry copper-gold deposit, Galore Creek area, northwestern British Columbia; *in* Porphyry Copper (\pm Au) Deposits of the Northern Cordillera, T. Schroeter (ed.), Canadian Institute of Mining and Metallurgy Special Volume 46, p. 645–649.
- Burnham, C.W. (1985): Energy release in subvolcanic environments: implications for breccia formation; *Economic Geology*, v. 80, p. 1515–1522.
- Byrne, K. (2009): The Southwest Zone breccia-centered silica-undersaturated alkalic porphyry Cu-Au deposit, Galore Creek, BC: magmatic-hydrothermal evolution and zonation, and a hydrothermal biotite perspective; M.Sc. thesis, Mineral Deposit Research Unit, University of British Columbia, 170 p.
- Cooke, D.R., Wilson, A.J., House, M.J., Wolfe, R.C., Walshe, J.L., Lickfold, V. and Crawford, A.J. (2007): Alkalic porphyry Au-Cu and associated mineral deposits of the Ordovician to Early Silurian Macquarie Arc, New South Wales; *Australian Journal of Earth Sciences*, v. 54, p. 445–463.
- Coney, P.J. (1989): Structural aspects of suspect terranes and accretionary tectonics in western North America; *Journal of Structural Geology*, v. 11, p. 117–125.
- Davies, A.G.S. (2002): Geology and genesis of the Kelian gold deposit, East Kalimantan, Indonesia; Ph.D. thesis, University of Tasmania, 404 p.
- Davies, A.G.S., Cooke, D.R., Gemmill, J.B., Leeuwen, T.V., Cesare, P. and Hartshorne, G. (2008a): Hydrothermal breccias and veins at the Kelian gold mine, Kalimantan, Indonesia: genesis of a large epithermal gold deposit; *Economic Geology*, v. 103, p. 717–757.
- Davies, A.G.S., Cooke, D.R., Gemmill, J.B. and Simpson, K.A. (2008b): Diatreme breccias at the Kelian gold mine, Kalimantan, Indonesia: precursors to epithermal gold mineralisation; *Economic Geology*, v. 103, p. 689–716.

- Enns, S.G., Thompson, J.F.H., Stanley, C.R. and Yarrow, E.W. (1995): The Galore Creek porphyry copper-gold deposits, northwestern British Columbia; *in* Porphyry Copper (\pm Au) Deposits of the Northern Cordillera, T. Schroeter (ed.), Canadian Institute of Mining and Metallurgy Special Volume 46, p. 630–644.
- Fournier R.O. (1999): Hydrothermal processes related to movement of fluid from plastic into brittle rock in the magmatic-epithermal environment; *Economic Geology*, V. 94, p. 1193–1211.
- Gabrielse, H., Monger, J.W.H., Wheeler, J.O. and Yorath, C.J. (1991): Morphogeological belts, tectonic assemblages, and terranes; *in* Geology of the Cordilleran Orogen in Canada, H. Gabrielse and C.J. Yorath (ed.), Geological Survey of Canada, Geology of Canada, no. 4, p. 15–28.
- Hedenquist, J.W. and Henley, R.W. (1985): Hydrothermal eruptions in the Waitapu geothermal system, New Zealand: their origin, associated breccias, and relation to precious metal mineralization; *Economic Geology*, v. 80, p. 1640–1668.
- Holliday, J.R. and Cooke, D.R. (2007): Advances in geological models and exploration methods for copper \pm gold porphyry deposits; *in* Proceedings of Exploration 07, B. Milkereit (ed.), Fifth Decennial International Conference on Mineral Exploration, Toronto, Ontario, p. 791–809.
- Jackson, M., Tosdal, R.M. and Chamberlain, C.A. (2007): Igneous rocks related to brecciation and mineralization in the Mount Polley alkalic Cu-Au porphyry system, British Columbia; Arizona Geological Society, Ores & Orogenesis, Program with Abstracts, p. 166.
- Jébrak, M. (1997): Hydrothermal breccias in vein-type ore deposits: a review of mechanisms, morphology, and size distribution; *Ore Geology Reviews*, v. 12, p. 111–134.
- Jensen, E.P. and Barton, M.D. (2000): Gold deposits related to alkaline magmatism; *Reviews in Economic Geology*, v. 13, p. 279–314.
- Lang, J.R., Lueck, B., Mortensen, J.K., Russell, J.K., Stanley, C.R. and Thompson, J.F.H. (1995a): Triassic–Jurassic silica-undersaturated and silica-saturated alkalic intrusions in the Cordillera of British Columbia: implications for arc magmatism; *Geology*, v. 23, p. 451–454.
- Lang, J.R., Stanley, C.R. and Thompson, J.F.H. (1995b): Porphyry copper deposits related to alkalic igneous rocks in the Triassic–Jurassic arc terranes of British Columbia; *in* Porphyry Copper Deposits of the American Cordillera, F.W. Pierce and J.G. Bolm (ed.), Arizona Geological Society, Digest 20, p. 219–236.
- Lang, J.R., Thompson, J.F.H. and Stanley, C.R. (1995c): Na-K-Ca magmatic hydrothermal alteration associated with alkalic porphyry Cu-Au deposits, British Columbia; *in* Magmas, Fluids and Ore Deposits, J.F.H. Thompson (ed.), Mineralogical Association of Canada, Short Course Series, v. 23, p. 339–366.
- Logan, J.M. (2005): Alkaline magmatism and porphyry Cu-Au deposits at Galore Creek, northwestern British Columbia; *in* Geological Fieldwork 2004, BC Ministry of Energy, Mines and Petroleum Resources, Paper 2005-1, p. 237–248, URL <<http://www.empr.gov.bc.ca/Mining/Geoscience/PublicationsCatalogue/Fieldwork/Pages/GeologicalFieldwork2004.aspx>> [November 2009].
- Logan, J.M. and Koyanagi, V.M. (1994): Geology and mineral deposits of the Galore Creek area, northwestern British Columbia (104G/3 and 4); BC Ministry of Energy, Mines and Petroleum Resources, Bulletin 92, URL <<http://www.empr.gov.bc.ca/Mining/Geoscience/PublicationsCatalogue/BulletinInformation/BulletinsAfter1940/Pages/Bulletin92.aspx>> [November 2009].
- McCallum, M.E. (1985): Experimental evidence for fluidization processes in breccia pipe formation; *Economic Geology*, v. 80, p. 1523–1543.
- McMillan, W.J. (1991): Tectonic evolution and setting of mineral deposits in the Canadian Cordillera; *in* Ore Deposits, Tectonics and Metallogeny in the Canadian Cordillera, BC Ministry of Energy, Mines and Petroleum Resources, Paper 1991-4, p. 1, URL <<http://www.empr.gov.bc.ca/Mining/Geoscience/PublicationsCatalogue/Papers/Pages/1991-4.aspx>> [November 2009].
- McPhie, J., Doyle, M. and Allen, R. (1993): Volcanic textures: a guide to interpretation of textures in volcanic rocks; CODES Key Centre, University of Tasmania, 198 p.
- Micko, J., Tosdal, R.M., Chamberlain, C.M., Simpson, K. and Schwab, D. (2007): Distribution of alteration and sulfide mineralization in the Central Zone of Galore Creek, northwestern British Columbia; Arizona Geological Society, Ores & Orogenesis, Program with Abstracts, p. 175.
- Mihalynuk, M.G., Nelson, J.L. and Diakow, L.J. (1994): Cache Creek terrane: oroclinal paradox within the Canadian Cordillera; *Tectonics*, v. 13, p. 575–595.
- Monger, J.W.H. and Irving, E. (1980): Northward displacement of north-central British Columbia; *Nature*, v. 285, p. 289–294.
- Monger, J.W.H., Price, R.A. and Tempelman-Kluit, D.J. (1982): Tectonic accretion and the origin of two major metamorphic and plutonic belts in the Canadian Cordillera; *Geology*, v. 10, p. 70–75.
- Mortensen, J.K., Ghosh, D.K. and Ferri, F. (1995): U-Pb geochronology of intrusive rocks associated with copper-gold porphyry deposits in the Canadian Cordillera; *in* Porphyry Copper (\pm Au) Deposits of the Northern Cordillera, T.G. Schroeter (ed.), Canadian Institute of Mining and Metallurgy Special Volume 46, p. 142–158.
- Nelson, J.L. and Mihalynuk, M. (1993): Cache Creek ocean: closure or enclosure; *Geology*, v. 21, p. 173–176.
- Panteleyev, A. (1976): Galore Creek map-area; *in* Geological Fieldwork, 1975, BC Ministry of Energy, Mines and Petroleum Resources, Paper 1976-1, p. 79–81, URL <<http://www.empr.gov.bc.ca/Mining/Geoscience/PublicationsCatalogue/Fieldwork/Pages/GeologicalFieldwork1975.aspx>> [November 2009].
- Peacock, D.C.P. (2002): Propagation, interaction and linkage in normal fault systems; *Earth-Science Reviews*, v. 58, p. 121–142.
- Philips, R. (1972): Hydraulic fracturing and mineralization; *Journal of the Geological Society of London*, v. 128, p. 337–359.
- Schwab, D.L., Petsel, S., Otto, B.R., Morris, S.K., Workman, E. and Tosdal, R.M. (2008): Overview of the Late Triassic Galore Creek copper-gold-silver porphyry system; *in* Ores and Orogenesis, Circum-Pacific Tectonics, Geologic Evolution and Ore Deposits, J.E. Spencer and S.R. Titley (ed.), Arizona Geological Society, Digest 22, p. 471–484.
- Seedorff, E., Dilles, J.H., Proffett, J.M., Einaudi, M.T., Zurcher, L., Stavast, W.J.A., Johnson, D.A. and Barton, M.D. (2005): Porphyry deposits: characteristics and origin of hypogene features; *Economic Geology*, 100th Anniversary Volume, p. 251–298.

- Sheridan, M.F. and Wohletz, K.H. (1981): Hydrovolcanic explosions: the systematics of water-pyroclast equilibration; *Science*, v. 212, p. 1387–1389.
- Sillitoe, R.H. (1985): Ore-related breccias in volcanoplutonic arcs; *Economic Geology*, v. 80, p. 1467–1514.
- Ulrich, T., Gunther, D. and Heinrich, C.A. (2001): The evolution of a porphyry Cu-Au deposit, based on LA-ICP-MS analysis of fluid inclusions of fluid inclusions: Bajo de la Alumbrera, Argentina; *Economic Geology*, v. 96, p. 1743–1774.
- Walsh, J.J., Bailey, W.R., Childs, C., Nicol, A. and Bonson, C.G. (2003): Formation of segmented normal faults: a 3-D perspective; *Journal of Structural Geology*, v. 25, p. 1251–1262.
- Wernicke, B. and Klepacki, D.W. (1988): Escape hypothesis for the Stikine block; *Geology*, v. 16, p. 461–464.
- Wheeler, J.O. and McFeely, P. (1991): Tectonic assemblage map of the Canadian Cordillera and adjacent parts of the United States of America; Geological Survey of Canada, Map 1712A, scale 1:2 000 000.
- Zweng, P.L. and Clark, A.H., (1995): Hypogene evolution of the Toquepala porphyry copper-molybdenum deposit, Moquegua, southeastern Peru; *in* *Porphyry Copper Deposits of the American Cordillera*, F.W. Pierce and J.G. Bolm (ed.), *Arizona Geological Society Digest*, v. 20, p. 566–612.

Volcanic Facies, Deformation and Economic Mineralization in Paleozoic Strata of the Terrace–Kitimat Area, British Columbia (NTS 103I)

G.S. Pignotta, Department of Geology, University of Wisconsin, Eau Claire, WI, pignotgs@uwec.edu

J.B. Mahoney, Department of Geology, University of Wisconsin, Eau Claire, WI

B.G. Hardel, Department of Geology, University of Wisconsin, Eau Claire, WI

J.L. Meyers, Department of Geology, University of Wisconsin, Eau Claire, WI

Pignotta, G.S., Mahoney, J.B., Hardel, B.G. and Meyers, J.L. (2010): Volcanic facies, deformation and economic mineralization in Paleozoic strata of the Terrace–Kitimat area, British Columbia (NTS 103I); *in* Geoscience BC Summary of Activities 2009, Geoscience BC, Report 2010-1, p. 105–114.

Introduction

Recent regional mapping by the British Columbia Geological Survey (BCGS) has indicated that a package of Paleozoic volcanogenic strata, the Mount Attree volcanic complex, may host potential volcanic-hosted massive sulphide (VHMS) mineralization (McKeown et al., 2008; Nelson et al., 2008a). These Paleozoic strata are situated along the westernmost margin of Stikinia and intruded by Jurassic–Eocene plutons of the eastern Coast Plutonic Complex (CPC; Figure 1). Along strike to the north, Paleozoic and Mesozoic volcanic rocks similar to the Mount Attree volcanic-complex package host significant VHMS deposits, such as the Tulsequah Chief, Foremore, Eskay Creek, Granduc and Anyox deposits (Figure 1; Höy, 1991; McKeown et al., 2008). The recognition of this economic potential combined with new regional mapping, geophysical data from the recently completed QUEST-West survey and newly released BC regional geochemical survey (RGS) stream-sediment data from the Terrace–Kitimat area provides a solid foundation for additional studies of the area's economic potential.

This work focuses on the structural analysis, geochemical characterization, geochronology, and economic-mineral assessment of six targeted exposures of potential Paleozoic volcanogenic and marine sedimentary strata in the Terrace–Kitimat area. During the summer of 2009, detailed mapping and sample collection was completed in the six target areas outlined on Figure 2. Petrographic, structural, geochemical and geochronological analyses are in progress. These analyses will constrain the nature and timing of economic mineralization and deformation, establish a geochemical framework for volcanic and plutonic rocks in the

area and assess the regional economic potential of these Paleozoic strata.

Geological Setting

Economic mineralization in the Terrace–Kitimat area is concentrated along the intrusive boundary between the eastern margin of the CPC and supracrustal rocks of Stikinia (Figure 1). Devonian–Permian arc-volcanic rocks and platform carbonate rocks form the basement to Stikinia in the Terrace–Kitimat area, and are overlain by Triassic and Lower Jurassic marine sedimentary and volcanic-arc rocks. These supracrustal assemblages are intruded by Jurassic, Late Cretaceous and Eocene plutonic rocks of the CPC (Figure 2; Woodsworth et al., 1985; Gareau et al., 1997a, b).

Stratified units in the Terrace–Kitimat area include

- the newly defined Paleozoic Zymoetz Group consisting of a lower unit of andesitic and lesser rhyolitic flows, tuff and breccia named the Mount Attree volcanic complex (previously mapped as Jurassic Telkwa Formation) overlain by Lower Permian limestone of the Ambition Formation;

- Triassic (?), thinly bedded, radiolarian chert; and volcanic and volcanoclastic rocks of the lower Jurassic Telkwa Formation of the Hazelton Group (Nelson et al., 2006a; Nelson and Kennedy, 2007; Nelson et al., 2008a).

Plutonic rocks in the region are relatively poorly dated, and pluton ages are inferred from relationships with supracrustal rocks and petrological similarities to dated bodies northeast of Terrace (Nelson et al., 2008a). Early Jurassic intrusions, typified by the ca. 200 Ma Kleanza pluton, range from gabbro to granite and are compositionally and texturally heterogeneous and variably foliated (Figure 2; Gareau et al., 1997b; Nelson et al., 2008a). Cretaceous intrusions, which consist of ductilely deformed granodiorite and granite, are less voluminous (Nelson et al.,

Keywords: *geochemistry, geochronology, Mount Attree volcanic complex, Zymoetz Group, Paleozoic, QUEST-West*

This publication is also available, free of charge, as colour digital files in Adobe Acrobat® PDF format from the Geoscience BC website: <http://www.geosciencebc.com/s/DataReleases.asp>.

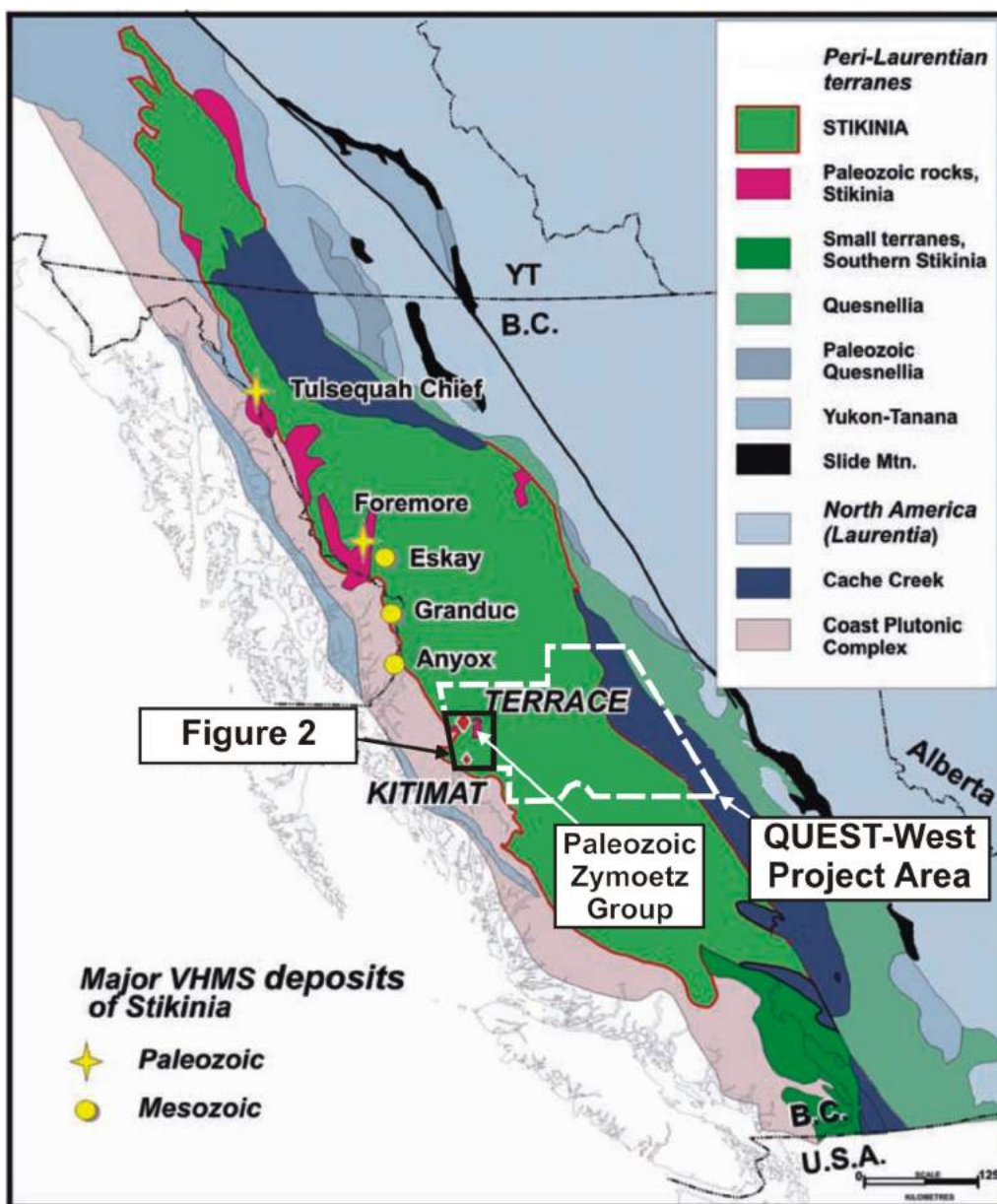


Figure 1. Terrane map of British Columbia, showing location of major volcanic-hosted massive sulphide (VHMS) deposits of Stikinia, location of study area (Figure 2 outline) and overlap of proposed project with QUEST-West Project (area outlined in white; modified from McKeown et al., 2008).

2008a). Eocene intrusions, such as the Carpenter Creek and Williams Creek plutons, consist of large, bulbous, nonfoliated granite and granodiorite units (Figure 2; Gareau et al., 1997b; Nelson et al., 2008a).

Paleozoic strata, such as the Zymoetz Group, are variably deformed but typically have a moderate to strong foliation parallel to bedding, particularly in the Mount Atree volcanic complex (Nelson et al., 2008a). The presence of overlying nonfoliated Jurassic strata indicates that a potentially important Late Paleozoic–Early Mesozoic deformational event involved strata with VHMS potential. Zymoetz Group and Telkwa Formation strata are folded on a regional scale into a northeasterly trending anticline that is oblique

to the main structural grain in the region (Nelson et al., 2008b). The entire region has been affected by Cretaceous–Eocene extensional faulting, and probably occupies the hangingwall of a major low-angle structure associated with unroofing of the Central Gneiss Complex to the west (Heah, 1991; Nelson and Kennedy, 2007; Nelson et al., 2007; Nelson et al., 2008a, b).

Previous Work

Duffell and Souther (1964), Woodsworth et al. (1985) and Gareau et al. (1997a, b) produced regional geological maps and U-Pb geochronology results for the Terrace map area. The lack of regional maps at 1:50 000 scale for NTS 1031

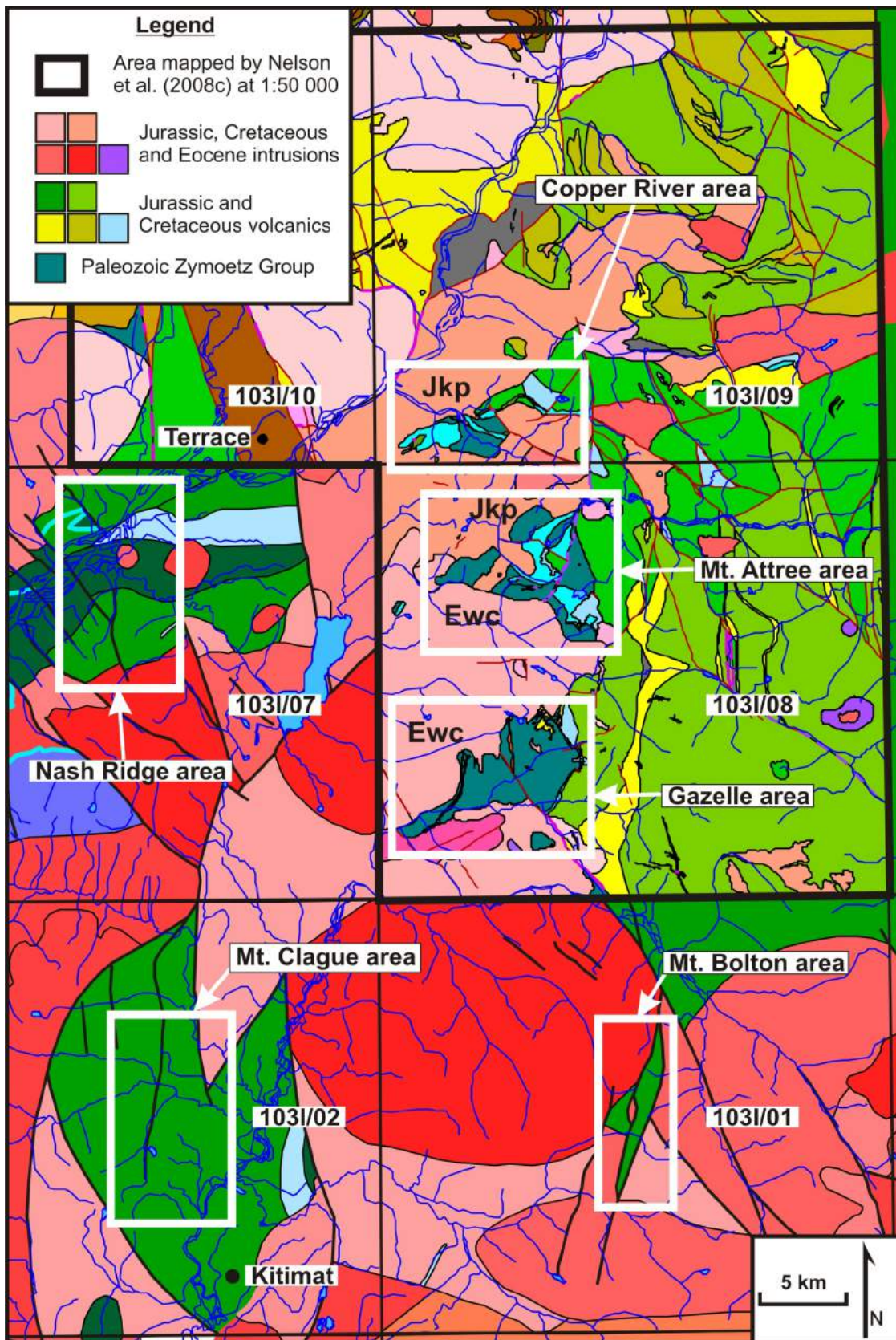


Figure 2. Geology of the Terrace–Kitimat area derived from BC MapPlace (British Columbia Geological Survey, 2008). New geological mapping by Nelson et al. (2008c) falls within the box with the heavy black outline; boxes with white outline highlight targeted exposures of Paleozoic Mount Attree volcanic rocks. Abbreviations: Jkp, Jurassic Kleanza pluton; Ewc, Eocene Williams Creek pluton.

and renewed interest in mineral exploration prompted the BCGS to initiate the Terrace Geological Mapping and Mineral Assessment Project, which was active from 2005–2008 under the direction of J.L. Nelson (Nelson et al., 2006a). This BCGS project has produced a series of reports and maps (Figure 2 outlines new mapping) that provide a modern geological framework for mineral exploration interest in the Terrace–Kitimat area (Nelson et al., 2006a, b; Nelson and Kennedy, 2007; Nelson et al., 2007; McKeown et al., 2008; Nelson et al., 2008a–c; Nelson, 2009).

Newly discovered VHMS-style mineralization in the Paleozoic Mount Attree volcanic complex, discovered during the regional mapping project, is believed to be analogous to that of other VHMS deposits found in Stikinia, such as the Tulsequah Chief deposit (Figure 1; McKeown et al., 2008). This mineralization is characterized by massive sulphide lenses, disseminated sulphide minerals and syngenetic alteration of felsic volcanic rocks to quartz-sericite schist (Höy, 1991; McKeown et al., 2008). Deformed and metamorphosed Mount Attree volcanic-complex rocks and their mineral potential were previously described by Hooper (1984, 1985) when he discovered the Gazelle showing. Mount Attree volcanic-complex rocks in and around the Gazelle showing exhibit intense sericitization and silicification, lenses of chalcopyrite and sphalerite parallel to bedding, disseminated chalcopyrite±galena and massive barite (Figure 2; Hooper, 1984, 1985; McKeown et al., 2008). McKeown et al. (2008) suggested other known and suspected Zymoetz Group exposures may have VHMS potential (shown in boxes on Figure 2).

In addition, mapping identified Mo±Cu±Au–porphyry deposits, polymetallic veins (Ag, Pb, Zn, Au), variably mineralized skarns and shear-zone–hosted polymetallic veins (Ag, Pb, Zn, Au) associated with CPC intrusions, including the Jurassic Kleanza pluton and Eocene Carpenter Creek and Williams Creek plutons (Figure 2; Nelson et al., 2008a). Timing of mineralization with respect to volcanism, magmatism and deformation remains poorly constrained for these deposits (J. Nelson, pers. comm., 2008).

Summary of Targeted Areas

Targeted areas consist primarily of exposures of the Mount Attree volcanic complex and were selected based on previous work that identified or suggested VHMS potential. Analysis of RGS stream sediment data identified an additional target of opportunity near Mount Bolton (Figure 2). Rock types, volcanic facies, alteration, deformation and mineralization vary considerably between the targeted areas, which are described separately. Within each area, samples were collected for geochemical, assay, petrographic and microstructural analyses, and geochronology to help fully characterize the relationships between volcanism, deformation and mineralization. Samples of other representa-

tive units associated with or intruding the targeted Mount Attree volcanic complex were also collected. These samples are being used to assist in timing of deformation and mineralization studies and to provide a basic geochemical framework for future and ongoing study in the Terrace–Kitimat area, including the recent QUEST–West geophysical survey and RGS stream-sediment survey reanalysis (described in Kowalczyk [2009] and Jackaman [2009], respectively). The nature of the rock types, deformation, alteration and mineralization observed in the six targeted areas during summer 2009 fieldwork is summarized below.

Copper River

The Copper (Zymoetz) River area has several large exposures of Mount Attree volcanic rocks (Figure 2). The exposures north of the Copper River are strongly dominated by medium- to coarse-grained nonwelded tuff and upright, generally northwest-striking and moderately north-dipping epiclastic volcanic rocks. There is a general trend of increasing clast size in the volcanoclastic rocks from south to north. Northern exposures consist of coarse-grained fragmental andesitic volcanic rocks and very coarse grained epiclastic units consisting primarily of rounded andesitic volcanic clasts (Figure 3). Northern exposures also contain lesser litharenite to feldspathic litharenite and siltstone interbeds, aphanitic andesite flows and/or sills and conglomerate. In a few localities, channels cut epiclastic volcanic rocks, which consist of fining-upward sequences of polymictic pebble conglomerate to feldspathic litharenite. Samples of these volcanogenic sedimentary sequences were collected for detrital zircon analyses to constrain the age of the Mount Attree volcanic complex. Aphanitic to porphyritic andesite dikes (hornblende) are observed throughout the area.

The Mount Attree volcanic rocks in the Copper River area typically show pervasive chlorite-epidote alteration. Minor quartz veining is observed locally but veins are barren and



Figure 3. Coarse-grained epiclastic volcanogenic rocks from the Copper River area, British Columbia. Clasts are predominantly porphyritic andesite and dacite.

typically undeformed, and do not show a preferred orientation. Intensity and orientation of foliation in this package of volcanic rocks varies spatially. Foliation is often associated with thrust faults, which imbricate the Paleozoic Mount Attree volcanic complex atop a sequence of thin-bedded chert, silt and sand units interpreted to be Triassic (Nelson et al., 2006a, b). Thrusts and subsidiary shear zones in the area strike southwest, dip to the north and give consistent top-to-the-south sense of shear. Slightly folded aphanitic andesite dikes cut the Mount Attree volcanic rocks and Triassic sedimentary units, which suggests that deformation of the sequence is post-Triassic. Economic-mineral potential in the Mount Attree volcanic rocks in this area is limited. Most mineralization noted in the area is associated with the Jurassic Kleanza pluton, which intrudes the volcanic rocks (Figure 2), and is localized around xenoliths of volcanic rocks near the pluton margin, where it consists of disseminated pyrite, chalcopyrite, and rarely disseminated and vein malachite.

Mount Attree

The Mount Attree area is the type locality for the Mount Attree volcanic complex. Volcanic rocks in this area include a western unit that is dominated by aphanitic andesitic flows, sills and small stocks and crosscutting porphyritic andesite dikes. This transitions abruptly to an eastern unit characterized by fine- to medium-grained fragmental volcaniclastic andesite with minor aphanitic andesite flows and sills, and porphyritic andesite dikes. A structural contact between Mount Attree volcanic units and Ambition Formation limestone is exposed in several localities in the Mt. Attree area. Nelson et al. (2006a, b) argued that the Mount Attree volcanic complex and Ambition Formation limestone are conformable, based on interfingering of the volcanic units and limestone. Eastern exposures of volcanic rocks in the Mount Attree area contain lenses of coarse crystalline marble whose protolith is possibly Ambition Formation limestone. Thus, observed structural contacts could be sheared depositional contacts. In other localities in the Terrace–Kitimat area, exposure was poor and it remains unclear whether contact is everywhere a structural contact.

Intruding the package of volcanic rocks in the west is a medium-grained, foliated hornblende-biotite granodiorite, interpreted by Nelson et al. (2008a, b) to be part of the Jurassic Kleanza pluton. Samples of this body were collected for geochemical analysis and comparison to other Kleanza samples. Small stocks of granodiorite and quartz monzonite intrude eastern volcanic and marble units; these smaller intrusions are interpreted to be part of the same Kleanza system and the bodies responsible for metamorphism of the marble observed in the area. Granodiorite dikes that intrude marbles are characterized by slight folding, which likely occurred during the emplacement of the Kleanza pluton and deformation of the marble units.

Foliation in the Mount Attree volcanic package varies spatially in orientation and intensity and often occurs near small shear zones in the package. Where observed, foliation is typically northeast striking and steeply dipping. The Kleanza pluton is variably deformed and exhibits a subsolidus foliation defined by aligned hornblende and elongate plagioclase that strikes generally east- and dips moderately to the north. Alteration of the volcanic package is characterized by a pervasive chlorite-epidote overprint and locally by chlorite-epidote veining. Unlike most exposures of Mount Attree volcanic rocks, chlorite-epidote veining in this area has a consistent, roughly north-striking and steeply dipping orientation. Mineral potential in the type locality is limited. The only mineralization observed consists of a few small (10–50 m) gossans several kilometres east of Mount Attree along the contact between the Kleanza pluton and fine-grained andesitic fragmental units containing disseminated pyrite and minor chalcopyrite. These gossans are interpreted to be related to the intrusion of the Kleanza pluton.

Gazelle

The Gazelle area is a primary target because of previously recognized potential for economic mineralization (e.g., MINFILE 103I 185; MINFILE, 2009) and the interpretation of VHMS-style mineralization in the area (Hooper, 1984, 1985; McKeown et al., 2008). Numerous geochemical, assay and geochronological samples were collected from this area to help assess mineral potential and determine genetic and timing relationships. Most mineralization in the Gazelle area occurs in its central region, where the predominantly felsic volcanic rocks are more intensely deformed and metamorphosed, and contain more gossans than surrounding volcanic rocks in the Gazelle area and all exposures of Mount Attree volcanic rocks east of Terrace (Figure 4a).

Western and southern exposures of Mount Attree volcanic rocks are dominated by andesitic fragmental units that grade into dacitic to rhyolitic tuff to the east. Andesitic units are typically fine- to coarse-grained nonwelded lapilli tuff with minor aphanitic andesite flows and/or sills. These units are metamorphosed to greenschist facies and cut by numerous aphanitic and porphyritic andesite dikes, some of which are folded (Figure 5). Foliation within the andesitic units is consistent, strikes north-northwest and dips moderately to steeply east. The central region of the Gazelle area is characterized by dacitic to rhyolitic tuff protoliths, which have been metamorphosed to upper-greenschist facies or higher and exhibit much more intense deformation (i.e., well-developed foliation everywhere) than observed elsewhere in both the Gazelle and other targeted areas. There is a mix of quartz-sericite schist, biotite schist and fine-grained, quartz-dominated schist found in the central region.



Figure 4. a) Gossan rich in disseminated pyrite, chalcopyrite, arsenopyrite and small undeformed veinlets or stringers of chalcocite from the central region of the Gazelle area, British Columbia. **b)** Magnetite skarn found along contact between Mount Attree volcanic rocks and an Eocene (?) intrusion.

In the western region an undated granodiorite pluton intrudes the western margin of the Mount Attree volcanic rocks. This coarse-grained biotite-granodiorite pluton is texturally identical to the granite found in the Nash Ridge area (described below) and contains 40–45% quartz in large (~1 cm), slightly elongate blebs. The foliation in this Cretaceous (?) granite is parallel to that observed consistently in the rest of the Gazelle area. This pluton is interpreted to constrain the maximum age of the deformation that resulted in the area's foliation, which is likely related to the occurrence of a regional east-west contraction during, and shortly after, crystallization of the granodiorite pluton. The Eocene Williams Creek pluton (or equivalent) to the west shows no evidence of magmatic or subsolidus foliation development.

The Gazelle area is also characterized by numerous large gossans hosted in the central region (Figure 4a). Mineralization observed in the central domain is typically disseminated and undeformed pyrite, arsenopyrite and locally chalcopyrite and chalcocite. In several localities vein pyrite, chalcopyrite, galena and chalcocite stringers are undeformed and crosscut foliation in quartz-sericite schist,



Figure 5. Folded andesite dike cutting nonwelded andesitic fragmental volcanic rocks in the southern part of the Gazelle area, British Columbia.

which suggests that development of at least some of the mineralization in the Gazelle area is a post-foliation event, possibly associated with nearby CPC intrusions. A new discovery of sphalerite±magnetite pods up to 1 m in size was made in a layered Jurassic (?) intrusion west of the main exposure of Mount Attree volcanic rocks. Large xenoliths of dacitic to rhyolitic tuff occur near sphalerite pods. One pod showed evidence for previous prospect activity but this occurrence is not in the MINFILE database. Samples were collected from the sphalerite pod for assay and from the plutonic units for geochemistry. Additional mineralization in the Gazelle area, typically magnetite skarn, was observed along the western contact of volcanic units with the Eocene Williams Creek pluton and other undated (Cretaceous?) plutons (Figure 4b).

Mount Bolton

The Mount Bolton area was not mapped during the most recent BCGS regional mapping campaign in the Terrace–Kitimat area. It was selected as a target because it is along and across strike of other mapped exposures of Mount Attree volcanic rocks and contains proximal RGS Cu, Mo and Au anomalies (Nelson, 2009). This north-trending,

elongate body of volcanic rock was previously mapped as possible Lower Jurassic Telkwa Formation by Woodsworth et al. (1985). The northern half of the target area was mapped and sampled for petrographic, geochemical and geochronological analyses.

The northern tip is an intrusive complex characterized by a 50:50 mix of volcanoclastic units intruded by dikes and stocks. Volcanoclastic rocks consist of dacitic to rhyolitic welded and nonwelded tuffs with round quartz eyes, plagioclase phenocrysts (<1 cm) and minor euhedral biotite. Minor occurrences of volcanogenic siltstone and sandstone, hypabyssal rhyolite sills and crosscutting andesite dikes were also observed. These are intruded by Eocene (?) fine- to medium-grained hornblende-biotite granodiorite, which contains ubiquitous euhedral honey-brown titanite. Often, volcanic units are found as decametre-scale xenoliths and/or rafts within the plutonic rocks near contacts with larger plutons to the north and east. South of the intrusive complex, dacitic to rhyolitic crystal-lithic welded and nonwelded tuffs dominate (Figure 6). Bedding generally strikes west-northwest and dips moderately to the north. Plagioclase and hornblende-phyric andesite dikes, locally folded, cut the package of volcanoclastic rocks.

Overall, the volcanoclastic units observed in the Mount Bolton area appear significantly less metamorphosed and altered than those found in the other target areas. Metamorphic grade appears to be lower-greenschist facies at most, with local exceptions in the intrusive complex. The pervasive chlorite-epidote alteration observed elsewhere in the Mount Attree volcanic complex is absent in this area (Figure 6), except for some local epidote veining and replacement. Epidote replacement appears to be the result of hydrothermal fluid flow in channels or pipes through the volcanic rocks, probably during pluton emplacement. The volcanic units in this area likely belong to the Jurassic Telkwa Formation based on their lower grade of metamorphism and lack of alteration. A sample of quartz-phyric

rhyolitic welded tuff was collected for dating. Mineralization is lacking in this area, with one exception consisting of minor disseminated pyrite and vein pyrite observed in one rhyolite tuff.

Nash Ridge

Distinctly different volcanic lithofacies are observed in the Nash Ridge area (and Mount Clague below), which is located ~10 km due west of type exposures of Mount Attree volcanic rocks (Figure 2). The area consists of a southern region dominated by mixed volcanic units and a northern region (north of the Skeena River) that consists primarily of deformed plutonic rocks. Unique to volcanic units found in the Nash Ridge and Mount Clague areas are spectacular lavender quartz eyes, which distinguish them from all other units to the east (Figure 7).

The southern region consists of rhyolitic to dacitic crystal-lithic tuff, porphyritic dacite flows, aphanitic and porphyritic (plagioclase) andesite flows and/or sills, dacitic to andesitic flows containing rhyolite clasts and medium- to coarse-grained nonwelded andesitic fragmental tuff. Rhyolitic to dacitic units typically contain abundant lavender quartz eyes, but all rock types and most exposures contained some lavender quartz eyes (Figure 7). Intercalated within the volcanic rocks are lenses of coarse-grained, strongly foliated biotite schist. The entire package of volcanic rocks is metamorphosed to upper-greenschist facies. Foliation strikes consistently east-northeast and dips steeply. Aphanitic andesite dikes (variably porphyritic with plagioclase and hornblende phenocrysts) are present throughout the volcanic package and are typically undeformed. A small stock of nonfoliated medium-grained gabbro intrudes the volcanic units. A high-temperature ductile shear zone (<1 m wide), with plastically deformed feldspar and oriented parallel to foliation in the volcanic rocks, cuts the gabbro.

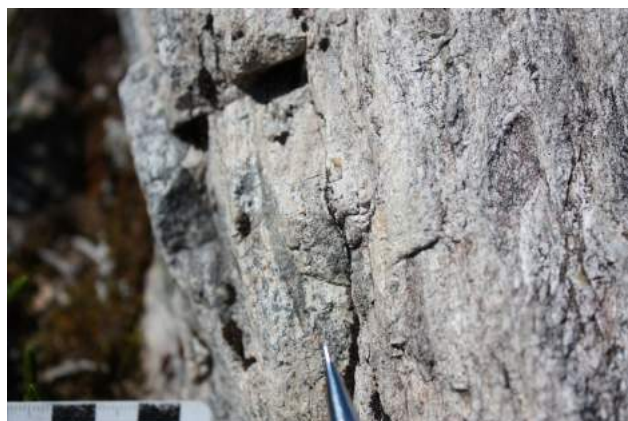


Figure 6. Welded rhyolite tuff with flattened fiamme found in the Mount Bolton area, British Columbia.



Figure 7. Rhyolite tuff with distinctive lavender quartz eyes characteristic of most units found in the Nash Ridge area and some units in the Mount Clague area, British Columbia.

A Cretaceous (?) coarse-grained biotite granodiorite intrudes the volcanic package to the south. It contains 40–45% quartz, which occurs as large, slightly elongate blebs. This pluton is deformed in the solid state and has a consistent foliation defined by the elongate quartz, which is parallel to the foliation found in the volcanic rocks. A sample of the deformed pluton has been collected for dating, which should provide a maximum on the age of deformation in the Nash Ridge area. Late, steep, brittle faults dissect the area and show consistently subhorizontal slickensides indicating strike-slip movement. Undeformed chlorite-epidote veins are noted infrequently in this area and their lack of specific orientation is evidence of late- or post-deformational emplacement. Minor mineral occurrences were found throughout the entire area and typically occur in dacitic to rhyolitic rock types but were also observed in nonwelded andesitic tuff, schist lenses, crosscutting andesite dikes and gabbro. Mineralization consists of pyrite, chalcopyrite, pyrrhotite, arsenopyrite and minor bornite. It is expected that microstructural analyses carried out in the Nash Ridge area will help confirm that mineralization was a syn- or postdeformation event because disseminated pyrite and arsenopyrite crystals are euhedral and appear to overprint foliation.

The northern domain consists primarily of variably foliated and lineated diorite to quartz diorite, minor tonalite and nonwelded andesitic fragmental tuff. Plutonic units here are heterogeneous, containing abundant (50–60%) volcanic, schist, diorite and hornfels xenoliths. In addition, there is strong textural variability in the intrusive units from very fine to coarse-grained, in particular in the roadside outcrops observed along Highway 16, west of Terrace. Fine-grained biotite granodiorite dikes, typically <1 m wide, intrude the diorite package. Andesitic fragmental volcanic rocks, observed locally, show pervasive chlorite-epidote alteration and are interpreted to be xenoliths in the intrusive package. The variable foliation intensity and orientation observed in northern domain intrusions can also be interpreted to be a result of local deformation concentrated around the volcanic xenoliths. Very little mineralization was observed in this northern domain compared to the south, with infrequent occurrences of minor disseminated pyrite hosted by diorite.

Mount Clague

The exposures of Mount Attree volcanic rocks in the Mount Clague area are somewhat similar in character to those found in the Nash Ridge area. Particularly interesting is the presence of lavender quartz eyes in both volcanic and plutonic units found in this area. Volcanic rocks are exposed in the central portion of the outlined target area in Figure 2 and are nearly completely surrounded by a heterogeneous intermediate to mafic intrusive complex. Dominant volcanic rock types include quartz-phyric rhyolitic to

dacitic tuff, where quartz phenocrysts are both of the lavender and clear variety, with the presence of minor occurrences of lithic dacitic tuff and andesitic nonwelded tuff with lavender quartz eyes (xenocrysts?) also noted in the matrix. Most of the Mount Clague area consists of tonalite, diorite and microdiorite intrusions with minor occurrences of granite and gabbro. Felsic plutonic units, in particular granitic intrusions, often contain lavender quartz phenocrysts/xenocrysts (?).

Foliation, typically found in plutonic rocks, is variable in orientation and intensity. A somewhat consistent southwest strike and moderate dip to the north characterize the plutons. Alteration observed in the volcanic units and many of the plutonic units is typically pervasive chlorite-epidote alteration with local chlorite-epidote veining. Veins of radiating actinolite were also observed locally in dacitic tuff; vein orientations are inconsistent throughout the area. The VHMS-style mineralization reported by Nelson (2009) was not observed during summer 2009 fieldwork; however, the presence of disseminated and vein pyrite was noted in rhyolitic volcanic rocks.

Summary

Detailed mapping within the six targeted exposures of Paleozoic Mount Attree volcanic rocks has shown that there are observable volcanogenic lithofacies trends that can help focus exploration studies. One significant trend within the Mount Attree volcanic sequence is the distinct difference between volcanic lithofacies in the areas west of Terrace compared to the eastern areas. In general, western areas are more felsic, contain more intrusive material, are generally higher metamorphic grade and contain ubiquitous lavender quartz eyes, which are completely absent in the eastern Mount Attree volcanic complex exposures, in both volcanic and plutonic rocks. Lithofacies trends have also been noted within the individual targeted exposures and are being examined further through petrographic and geochemical analyses.

The Gazelle area has shown the most economic-mineral potential. Previous work around the Gazelle showing has described the mineralization as VHMS in origin (Hooper, 1984, 1985; McKeown et al., 2008); however, at least some of the mineralization observed in the Gazelle area occurred during or after foliation development, as indicated by crosscutting vein pyrite, chalcopyrite, galena and chalcocite. Furthermore, much of the disseminated mineralization appears to be postdeformational because pyrite is typically euhedral and overprints foliation. This mineralization could be a result of intrusion of CPC plutons or have been remobilized by them. Foliation patterns in Mount Attree volcanic complex exposures in the Gazelle and Nash Ridge areas are parallel to foliations developed in undated

(Cretaceous?) plutons. Geochronological sample preparation is in progress and will help evaluate this possibility.

Ongoing petrographic, geochemical and geochronological work will help constrain the ages of the volcanic packages, their genesis and the timing of mineralization with respect to deposition and deformation. These data, when combined with the results of targeted mapping completed during summer 2009, recent regional mapping, QUEST-West geophysical data and reanalyzed RGS stream data, will provide a more complete geological and mineral potential framework for the Terrace–Kitimat area.

Acknowledgments

Funding was provided primarily by Geoscience BC Grant 2008-027, with additional financial support from the University of Wisconsin-Eau Claire to G. Pignotta and J.B. Mahoney. Thanks also to J.L. Nelson (BCGS) for geological expertise and logistical support and L. McKeown of the Terrace Economic Development Authority. Special thanks to C. Kendall and staff at Canadian Helicopters in Terrace for outstanding helicopter support and salmon dinners.

References

- BC Geological Survey (2008): MapPlace GIS internet mapping system; BC Ministry of Energy, Mines and Petroleum Resources, MapPlace website, URL <<http://www.MapPlace.ca>> [November 2008].
- Duffell, S. and Souther, J.G. (1964): Geology of Terrace map area, British Columbia; Geological Survey of Canada, Memoir 329, 117 p.
- Gareau, S.A., Woodsworth, G.J. and Rickli, M. (1997a): Regional geology of the northeastern quadrant of Terrace map area, west-central British Columbia; *in* Current Research 1997-A/B, Geological Survey of Canada, p. 47–56.
- Gareau, S.A., Friedman, R.M., Woodsworth, G.J. and Childe, F. (1997b): U-Pb ages from the northeastern quadrant of Terrace map area, west-central British Columbia; *in* Current Research 1997-A/B, Geological Survey of Canada, p. 31–40.
- Heah, T.S.T. (1991): Mesozoic ductile shear and Paleogene extension along the eastern margin of the Central Gneiss Complex, Coast Belt, Shames River area, near Terrace, British Columbia; M.Sc. thesis, University of British Columbia, 155 p.
- Hooper, D.G. (1984): Geological report on the Gazelle claim, record number 4229; BC Ministry of Energy, Mines and Petroleum Resources, Assessment Report 12 717, 41 p.
- Hooper, D.G. (1985): Gazelle claim geological report; BC Ministry of Energy, Mines and Petroleum Resources, Assessment Report 14 076, 25 p.
- Höy, T. (1991): Volcanogenic massive sulphide deposits in British Columbia; *in* Ore Deposits, Tectonics and Metallogeny in the Canadian Cordillera, BC Ministry of Energy, Mines and Petroleum Resources, Paper 1991-4, p. 89–124.
- Jackaman, W. (2009): Stream geochemical survey sample reanalysis, Terrace and Prince Rupert map areas, western British Columbia (NTS 103I, part of 103J); *in* Geoscience BC Summary of Activities 2008, Geoscience BC, Report 2009-1, p. 15–18.
- Kowalczyk, P.K. (2009): QUEST-West geophysics in central British Columbia (NTS 093E, F, G, K, L, M,N, 103I): new regional gravity and helicopter time-domain electromagnetic data; *in* Geoscience BC Summary of Activities 2008, Geoscience BC, Report 2009-1, p. 1–6.
- McKeown, M., Nelson, J.L. and Friedman, R. (2008): Newly discovered volcanic-hosted massive sulphide potential within Paleozoic volcanic rocks of the Stikine assemblage, Terrace area, northwestern British Columbia; *in* Geological Fieldwork 2007, BC Ministry of Energy, Mines and Petroleum Resources, Paper 2008-1, p. 103–116.
- MINFILE (2009): MINFILE BC mineral deposits database; BC Ministry of Energy, Mines and Petroleum Resources, URL <<http://minfile.ca>> [November 2009].
- Nelson, J.L. (2009): Terrace Regional Mapping Project Year 4: extension of Paleozoic volcanic belt and indicators of volcanogenic massive sulphide-style mineralization near Kitimat, British Columbia (NTS 103I/02, 07); *in* Geological Fieldwork 2008, BC Ministry of Energy, Mines and Petroleum Resources, Paper 2009-1, p. 7–20.
- Nelson, J.L. and Kennedy, R. (2007): Terrace Regional Mapping Project Year 2: new geological insights and exploration targets (NTS 103I/16S, 10W), west-central British Columbia; *in* Geological Fieldwork 2006, BC Ministry of Energy, Mines and Petroleum Resources, Paper 2007-1 and Geoscience BC, Report 2007-1, p. 149–162.
- Nelson, J.L., Barresi, T., Knight, E. and Boudreau, N. (2006a): Geology and mineral potential of the Usk map area (NTS 103I/09) near Terrace, British Columbia; *in* Geological Fieldwork 2005, BC Ministry of Energy, Mines and Petroleum Resources, Paper 2006-1 and Geoscience BC, Report 2006-1, p. 117–134.
- Nelson, J.L., Barresi, T., Knight, E. and Boudreau, N. (2006b): Geology of the Usk map area (NTS 103I/09); BC Ministry of Energy, Mines and Petroleum Resources, Open File 2006-3, 1:50 000 scale.
- Nelson, J.L., Kennedy, R., Angen, J. and Newman, S. (2007): Geology of the Terrace map area (NTS 103I/09, 10, 15, 16); BC Ministry of Energy, Mines and Petroleum Resources, Open File 2007-4, 1:70 000 scale.
- Nelson, J.L., Kyba, J., McKeown, M. and Angen, J. (2008a): Geology of the Chist Creek map area (NTS 103I/08); BC Ministry of Energy, Mines and Petroleum Resources, 1:50 000 scale.
- Nelson, J.L., Kyba, J., McKeown, M. and Angen, J. (2008b): Terrace Regional Mapping Project Year 3: contributions to stratigraphic, structural and exploration concepts, Zymoetz River to Kitimat River, (NTS 103I/08); *in* Geological Fieldwork 2007, BC Ministry of Energy, Mines and Petroleum Resources, Paper 2008-1, p. 159–174.
- Nelson, J.L., McKeown, M., Cui, Y., Desjardins, P., Nakanishi, T. and Shirvani, F. (2008c): Terrace preliminary geodata release (103I east half); BC Ministry of Energy, Mines and Petroleum Resources, GeoFile 2008-11.
- Woodsworth, G.J., Hill, M.L. and van der Heyden, P. (1985): Preliminary geology map of Terrace (NTS 103I, east half) map area, BC; Geological Survey of Canada, Open File 1136, 1:125 000 scale.

Isotopic Investigation of the Adanac Porphyry Molybdenum Deposit in Northwestern British Columbia (NTS 104N/11): Final Project Report

J.L. Smith, Department of Geology, University of Nevada, Reno, NV, USA; smith264@unr.nevada.edu

G.B. Arehart, Department of Geology, University of Nevada, Reno, NV, USA

Smith, J.L. and Arehart, G.B. (2010): Isotopic investigation of the Adanac porphyry molybdenum deposit in northwestern British Columbia (NTS 104N/11): final project report; *in* Geoscience BC Summary of Activities 2009, Geoscience BC, Report 2010-1, p. 115–126.

Introduction

There are currently numerous poorly understood, relatively underexplored Mo deposits and occurrences in the North American Cordillera that have exploration potential. It would be of great benefit to the exploration community if more data about these Mo deposits in British Columbia are collected and published.

There are geochemical similarities (e.g., redox state of associated plutons; trace- and major-element chemistry of associated plutons; and mineral and elemental assemblages such as high Bi, Te and W, and low and peripheral Cu, Pb and Zn) between porphyry Mo deposits and ‘intrusion-hosted’ Au deposits (e.g., Tombstone belt; Figure 1; Stephens et al., 2004) that suggest a possible genetic link. The Adanac Mo deposit (MINFILE 104N 052; MINFILE, 2009) belongs to an important class of occurrences that lie within the Atlin mining camp. The Adanac deposit contains no Au itself, but placer Au is still being mined on the lower reaches of Ruby Creek below the deposit. Historically, it has always been assumed that the Mo deposit postdates Au mineralization, which occurs in quartz-carbonate-bearing shears in Paleozoic Cache Creek Group volcanic strata and as placer deposits. However, a study by Sack and Mihalynuk (2004) suggests that this may not be the case. Sack and Mihalynuk’s work on Feather Creek suggests that at least some of the placer Au in the Atlin area may have been derived from the Cretaceous Surprise Lake batholith because some of the Au nuggets are associated with thorite and cassiterite. This is consistent with the presence of Au- and W-bearing quartz veins in the Boulder Creek drainage immediately to the south of the Adanac Mo deposit, because wolframite is commonly found peripheral to the molybdenite zone in porphyry Mo deposits (Wallace et al., 1978). Thus, the presence of Au in those wolframite veins raises the question of a potential link between Au-depleted Mo and Au-bearing W ‘intrusion-related’ deposits. Under-

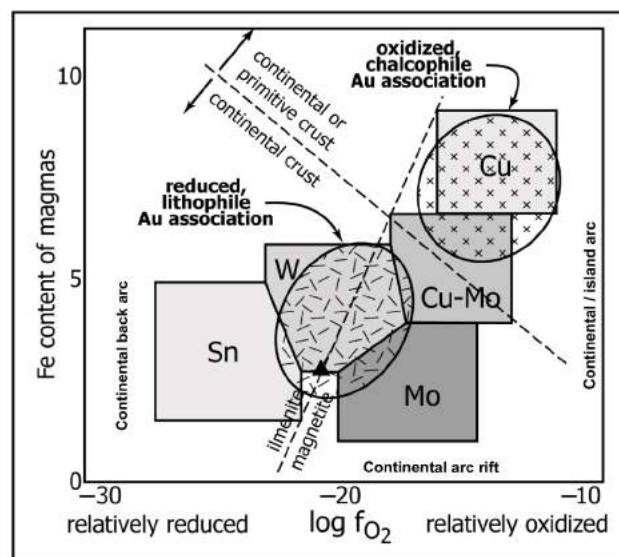


Figure 1. Plot of Fe content versus oxidation state for plutons and associated porphyry mineral deposits. Note that Au is found in both oxidized (porphyry Cu) and reduced (porphyry Sn-W-Mo) environments. The Surprise Lake batholith, British Columbia, plots approximately at the solid triangle. Fields from Thompson et al. (1999).

standing this association (or lack thereof) is an important step toward focusing further exploration in the North American Cordillera for both of these deposit types.

Geological Background

The Adanac Mo deposit is located in the northwestern corner of BC, near the town of Atlin (NTS 104N/11; Figure 2). The geology of the Atlin area was mapped by Aitken (1959) and the regional setting of the deposit was discussed by Christopher and Pinsent (1982). The Atlin area (Figure 3) is underlain by deformed and weakly metamorphosed ophiolitic rocks of the Pennsylvanian and/or Permian-aged Cache Creek Group (Monger, 1975). These rocks, which include serpentinite and basalt as well as limestone, chert and shale, have long been thought to be the source of much of the placer Au found in the Atlin area. The sedimentary and volcanic rocks are cut by two younger batholiths: north of the Adera fault, they are cut by a Jurassic granodiorite to diorite intrusion (Fourth of July batholith), and north and south of Surprise Lake they are cut by a Cre-

Keywords: porphyry Mo, placer Au, Re-Os isotope, U-Pb isotope, Surprise Lake batholith, Atlin

This publication is also available, free of charge, as colour digital files in Adobe Acrobat® PDF format from the Geoscience BC website: <http://www.geosciencebc.com/s/DataReleases.asp>.

taceous granitic to quartz monzonitic intrusion (Surprise Lake batholith). The rocks are locally strongly faulted and the Adanac deposit is located near the intersection of two major syn- to postmineralized fault systems within a satellite stock (Mount Leonard stock) of the Surprise Lake batholith.

The Surprise Lake batholith is a highly differentiated, F-rich (0.27%), U-rich (14.6 ppm), peraluminous granite (Ballantyne and Littlejohn, 1982). The batholith is a known host of quartz-vein stockworks (especially associated with the multiphased Mount Leonard stock) and skarn alteration that hosts base- and precious-metal mineralization including W, Sn, Mo, Cu, Co, Pb, Zn, U, F, Ag and Au that occur as both sulphides and oxides (Ballantyne and Littlejohn, 1982). An important deposit related to the batholith and occurring within 4.8 km (3 mi.) of the Adanac deposit is the Black Diamond W vein (Figure 4). The Black Diamond is a 060°-trending, 60°N-dipping quartz vein containing pyrite, scheelite and wolframite; minor chalcopyrite, arsenopyrite and molybdenite; and anomalous tellurium (Kikauka, 2002). This vein lies mostly within the coarse granite of the Mount Leonard stock, except for the eastern portion, which is in Paleozoic marble. Elevated Au values along with Pb, As and Sb anomalies also occur in this eastern portion. A soil sample survey in this area showed anomalous Cu, Pb, Ag, Sb, Bi and Au (Kikauka, 2002).

The deposit area was described by Sutherland Brown (1970), White et al. (1976), Christopher and Pinsent (1982) and Pinsent and Christopher (1995). The Adanac Mo deposit underlies the valley floor near the head of Ruby Creek, and is largely buried with very little surface expression. The geology underlying the valley floor is derived from drill data (Figure 5). The deposit is partially controlled by the Adera fault system, which trends approximately northeast and defines much of the southern boundary of the pre-ore Fourth of July batholith. This is a normal fault, dipping approximately 80° northwest. Mineralization is hosted within the multiphased Mount Leonard stock and entirely within plutonic rock. It forms at least two blanket-shaped and steeply dipping shells over and around porphyry domes, one in the area of the proposed main pit and another in an area to the west of the proposed pit. Mineralization is in the form of 3–4 cm sized molybdenite rosettes in a stockwork of smoky, ribbon-textured quartz veins. Some late-stage milky-white quartz veins carry smaller and less frequent rosettes, but are typically barren. There is very little fine molybdenite, and some molybdenite exists as paint on fractures and in faults. Other minerals present in the porphyry stockwork include wolframite and rare chalcopyrite, galena and sphalerite.

There were three stages of intrusion at Adanac: an early, generally coarse-grained stage that was deformed prior to the intrusion of several second-stage porphyry domes, and

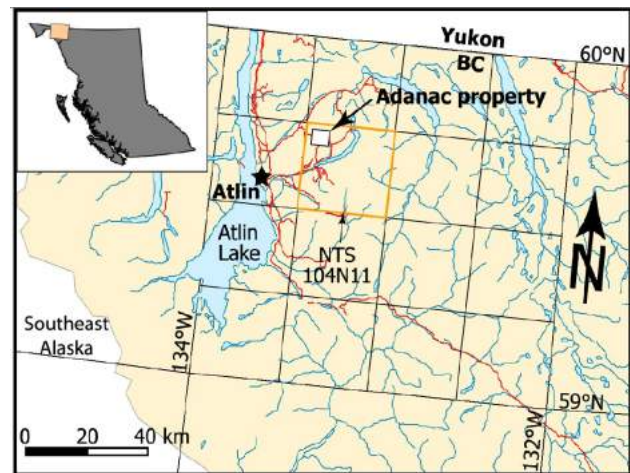


Figure 2. Location of the Adanac Mo deposit, British Columbia (from Pinsent and Christopher, 1995). The white box (Adanac property) is the approximate location of Figure 3 (local geology map). Inset is a location map of BC.

a late fine-grained stage that was injected through the porphyry domes and the early coarse-grained stage. All of the stages of intrusion at Adanac have very little chemical differences and are grouped based on textures and crosscutting relationships. All of the rocks are high-SiO₂, peraluminous alkalic granite formations, and have a Rb/Sr ratio of about 1. Whole-rock geochemistry studies (Smith, 2009) indicate that Adanac hostrocks resemble other hostrocks of Climax-type, high-F porphyry Mo deposits.

Hydrothermal alteration at Adanac is similar to Climax-type porphyry Mo deposits, although it is not as strong or pervasive as described at Climax. Alteration at Adanac consists of a high-SiO₂ ‘core’, or silicification, at the western end of the deposit, and affecting the rest of the deposit area in the form of sill-shaped bodies of silicification trace-

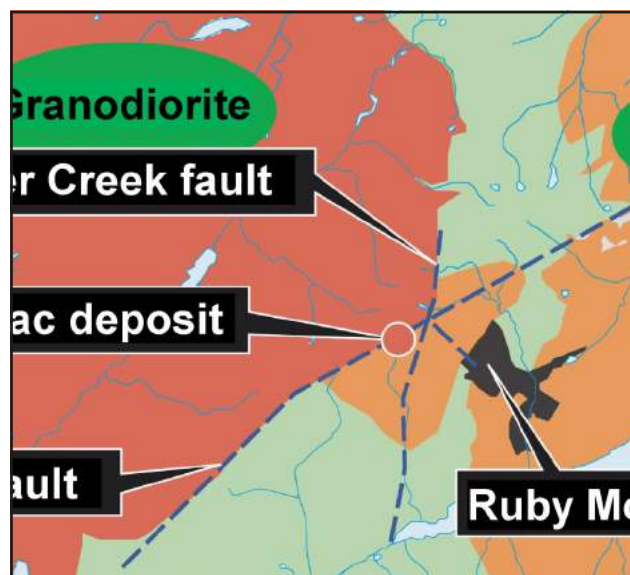


Figure 3. Generalized geology of the Adanac deposit area, British Columbia. Modified from Aitken (1959).

able from one drillhole to the next. Potassic alteration is also strongest at the west end, occurring as zones of pink feldspar flooding in drillcore several metres thick. In the rest of the deposit, potassic alteration is common as pink feldspar envelopes around quartz veins. Hair-line fractures filled with quartz, sericite and pyrite are common, and are cut by other fractures filled with calcite, stilbite and sometimes fluorite. Fresher (unaltered) rocks from the deeper portions of drillcore have illite and kaolinite as clay alteration products, while fault gouge is composed of kaolinite and montmorillonite. There is a weak chlorite overprint on most of the rocks at Adanac, especially those distal to mineralization.

Research Objectives

Rhenium-osmium ages of molybdenite and U-Pb ages of various rock types at Adanac were determined to compare ages of mineralization and magmatism. One goal of this study was to identify the causative or mineralizing intrusion by matching a mineralization age with a

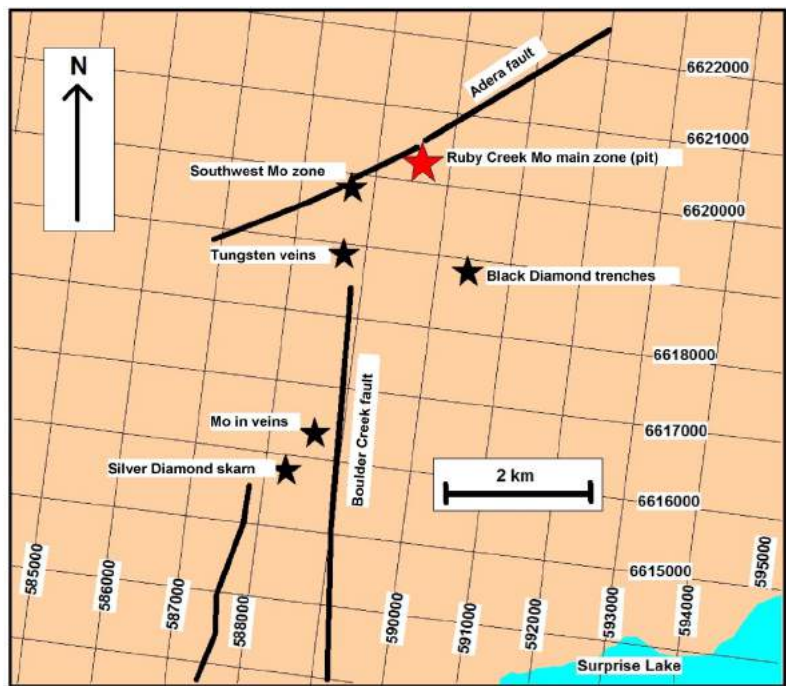


Figure 4. Boulder Creek and Ruby Creek area, showing main mineral occurrences of the Mount Leonard stock and local faults, British Columbia. The Ruby Creek Mo Main zone is the approximate location of Figure 5. Grid shows UTM Zone 9, NAD 83 co-ordinates.

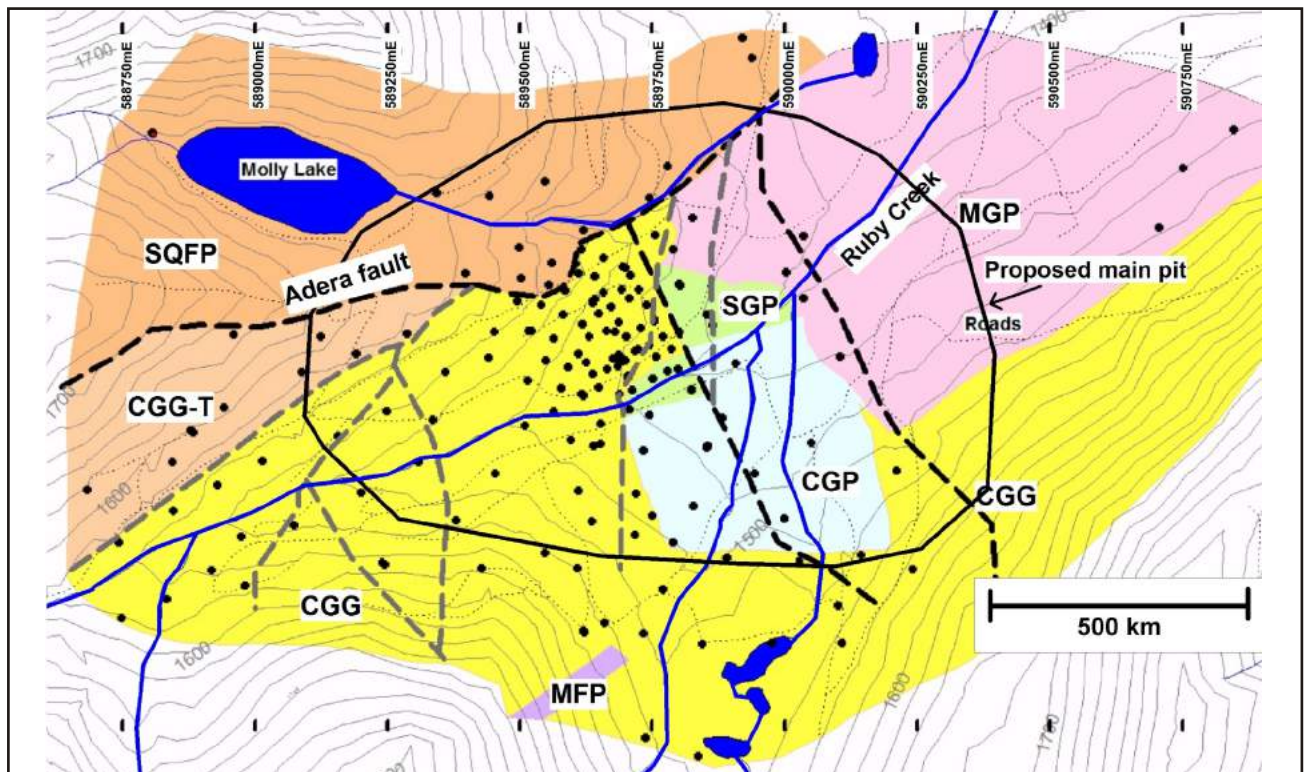


Figure 5. Surface geology of the Adanac Mo deposit (Mo main zone in Figure 4), British Columbia. The black dots are drillholes. The black dashed lines are strong faults that cause displacement, such as the Adera fault. The grey dashed lines are weak faults, or faults that cause no discernible displacement. Rock types CGG (coarse-grained granite), CGG-T (transitional phase), MGP (mafic granite porphyry) and SQFP (sparse quartz feldspar porphyry) are all the first phase of intrusion. The second phase is SGP and CGP (sparse and crowded granite porphyry). The third phase of intrusion, fine-grained aplite dikes, is not represented on the map, but cuts other units at more localized scales. The red lines are cross-sections for alteration- and trace-element zoning discussed in Smith (2009). The grid shows co-ordinates in UTM Zone 8, WGS 84.

Table 1. Molybdenite Re-Os samples. The sample ID refers to the drillhole and the depth from which it was taken.

Sample	Location	Hostrock	Vein Type	Associated Minerals	Probable Paragenesis
375-1054	southwest end	CGG	No vein, feldspar flood	feldspar	1
375-1036	southwest end	CGG	2 cm ductile ribbon textured vein with fine molybdenite	none	2
375-1125	southwest end	CGG	Large, 5 cm milky-white quartz vein with molybdenite rosettes	none	3
364-50	central mineralized blanket	CGG	4 cm milky-white quartz vein	pyrite, chalcopyrite, wolframite, magnetite	4

magmatic age. A second goal was to constrain the lifespan of the hydrothermal system at Adanac. The results of this study can also be used to compare Adanac to other porphyry Mo deposits, because the age of the deposit is an important consideration used in classification. Also, to test the theory of a possible linkage between Adanac and placer Au mineralization downstream of the deposit, the Os signature of Au from Ruby Creek was compared to the Os signature of magnetite from drillcore of the Adanac Mo deposit.

Mineralization Ages

Four samples of molybdenite were analyzed for a Re-Os age to constrain mineralization ages at Adanac. Samples are listed in Table 1, with a description and an inferred relative age based on crosscutting relationships or known characteristics of Climax-type porphyry Mo deposits (i.e., molybdenite associated with other base metals in porphyry deposits are usually later mineralization events). Figure 6 shows a schematic diagram illustrating crosscutting relationships seen in drillcore. All samples were hosted in CGG (coarse-grained granite).

The first three samples in the table are all from drillhole 375, which was drilled in the western end of the deposit where a suspected mineralizing intrusion is located (see Figure 5). They were selected based on differences in vein type (discussed below) or other host (feldspar flood). Their location in one drill-hole within 9 m (30 ft.) of each other adds confidence to the assumption that any differences in ages are not correlated with their distance apart in the deposit but represent temporal changes in vein type. The last sample, 364-50, was chosen from the central part of the deposit, in the

blanket of mineralization located above the SGP (sparse granite porphyry) and the CGP (crowded granite porphyry) intrusions. Below is a list (in expected paragenetic order from oldest to youngest) of the four molybdenite samples and associated description and occurrence.

- 1) 375-1054: This molybdenite was disseminated in a feldspar flood in the potassic-altered core of the deposit.
- 2) 375-1036: This molybdenite was in a ductile, ribbon-textured vein. The quartz in these vein types is usually dark and soot coloured, either from fine molybdenite or because it is smoky quartz. Veins that carry this type of molybdenite and exhibit dark, sooty coloration are usually small (~2 cm) and consistently bear molybdenite. Other quartz veins bearing molybdenite are commonly seen to cut these vein types.

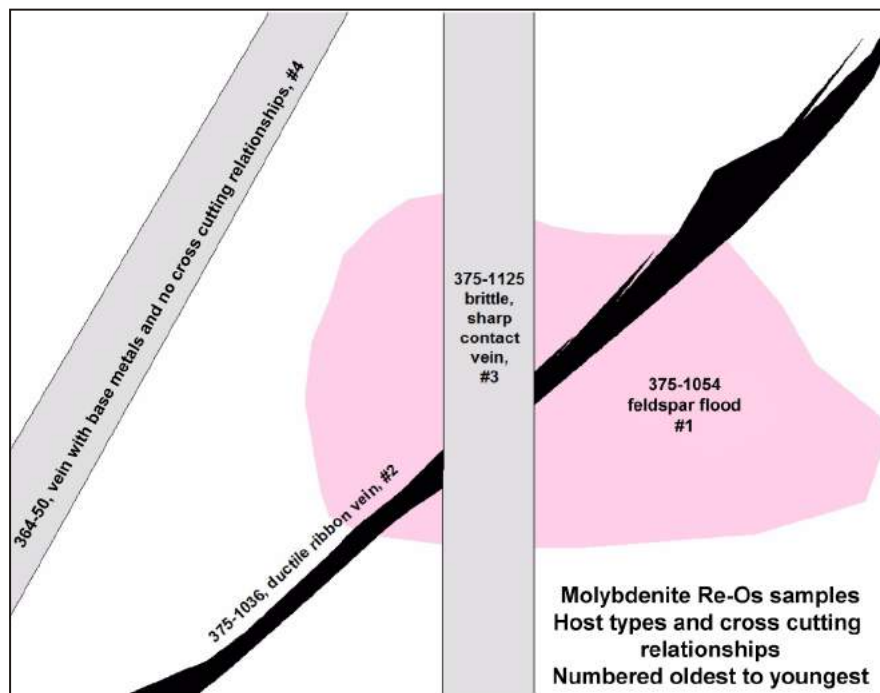


Figure 6. Schematic diagram showing paragenetic relationships (seen in drillcore) of the four Re-Os molybdenite samples. Samples are numbered from oldest to youngest. Sample 364-50 may have no crosscutting relationships with the other samples, but it is presumed to be youngest based on a high base-metal content in the quartz vein. Base metals are usually deposited after main molybdenite mineralization in alkalic porphyry Mo deposits.

Table 2. Summary of data for Re-Os mineralization dates.

Sample ID	Total Re (ppm)	¹⁸⁷ Re (ppm)	¹⁸⁷ Os (ppm)	Age (Ma)	Error 2σ (0.5%)	Sample Host	Relative Age (oldest–youngest)	
							Expected	Measured
375-1054	9.521	5.96	7.036	70.87	0.36	Feldspar flood, in CGG	1	1
375-1036	8.011	5.015	5.828	69.71	0.35	Ductile ribbon vein, in CGG	2	2
364-50	5.572	3.488	4.048	69.61	0.35	With base metals, in CGG	4	2
375-1125	39	24.42	28.38	69.72	0.35	Large, brittle contact vein, in CGG	3	2

- 3) 375-1125: This molybdenite was in a large, 4–6 cm milky-white quartz vein. Molybdenite in these veins usually forms large 2–5 cm rosettes. The contact of the vein with the hostrock, in contrast to the previous sample, is sharp. These veins carry mineralization less frequently and are sometimes barren. This vein type commonly cuts other vein types.
- 4) 364-50: This molybdenite was taken from a vein cutting CGG that had an abundance of other visible opaque minerals, such as pyrite, chalcopyrite, wolframite and magnetite. No distinct temporal relationships with other vein types were observed. However, it is typical in Climax-type porphyry molybdenite deposits to have mineralizing events that have specific temporal relationships that can be partially defined by associated sulphides, such as early events that bear molybdenite only, and later events that bear molybdenite+pyrite (Westra and Keith, 1981). Therefore, this sample was dated to assess the possibility that this vein represents a separate and distinct late mineralizing event.

Samples were prepared by breaking apart the hostrock with a hammer on a clean surface (a sheet of paper) and the molybdenite was handpicked with tweezers. The molybdenite was ground in a steel mortar and pestle and placed in a small dish of water. Because molybdenite is a micaceous mineral, the surface tension of the water held the thin mineral particles at the top of the dish while feldspar, quartz and other impurities sank to the bottom. The water containing the floating molybdenite was decanted and allowed to evaporate. Samples were then examined under a binocular microscope and any other impurities were removed with tweezers. The tweezers, hammer, mortar and pestle, and dish were washed with soap and water between samples. Samples were then sent to the Re-Os geochronology lab at the University of Arizona at Tucson.

At the lab, samples were handpicked and loaded in a Carius tube and dissolved with 8 mL of reverse aqua regia. The

tube was heated to 240°C overnight, and the solution was later treated in a two-stage distillation process for Os separation (Nagler and Frei, 1997). Osmium was further purified using a microdistillation technique similar to that of Birck et al. (1997), and loaded on Pt filaments with Ba(OH)₂ to enhance ionization. After Os separation, the remaining acid solution was dried and later dissolved in 0.1 N HNO₃. Rhenium was extracted and purified through a two-stage column using a AG[®] 1-X8 (100–200 mesh) resin and loaded on Pt filaments with Ba(SO)₄. Samples were analyzed by negative thermal ionization mass spectrometry (NTIMS; Creaser et al., 1991) on a VG 54 mass spectrometer. Osmium was measured using a Daly multiplier collector and rhenium using a Faraday collector. Isochrons and weighted means were calculated using Isoplot (Ludwig, 2001).

Molybdenite ages are calculated using a ¹⁸⁷Re decay constant of 1.666×10^{11} years (Smoliar et al., 1996). Uncertainties for molybdenite analysis include instrumental counting statistics and in the ¹⁸⁷Re decay constant (0.31%). In this work, uncertainties are calculated using error propagation, taking into consideration the uncertainty in the Re decay constant. Results of the analysis are summarized in Table 2.

Sample 375-1054 was molybdenite disseminated in a feldspar flood on the western end of the deposit and, as expected, was the oldest sample at 70.87 ± 0.36 Ma. It was not surprising that this was the oldest sample because this molybdenite was disseminated in a feldspar flood, and potassic alteration is commonly early in the sequence of hydrothermal events. There was no distinction in ages (69.6 Ma) between the other three samples (375-1036, 364-50 and 375-1125) when one considers the error of 0.35 Ma. All three mineralization events occurred in a relatively restricted time of less than 1 Ma. Besides the calculated isotopic age, there are other factors to consider when determining paragenetic sequence. First, crosscutting relationships cannot be ignored. The molybdenite in smoky quartz veins

with a ribbon texture and a ductile contact with the host rock is consistently seen to be cut by thicker milky-white quartz veins that usually bear less molybdenite. Therefore, this vein type (sample 375-1036) is clearly older than veins with milky-white quartz, even if they may be part of the same mineralization event.

Based on Re-Os results, sample 375-1125 should be placed as the last and youngest sample, using the Re concentration as a proxy for fluid evolution. It makes more geological sense for molybdenite samples being deposited to maintain a somewhat consistent Re concentration until there is some change in the environment to force deposition of the element within the molybdenite. In other words, it is unlikely that the hydrothermal system went from depositing molybdenite with 8 ppm Re, then to molybdenite with 39 ppm Re and then back to molybdenite with 5.6 ppm Re. It is more likely that Re concentration jumped at the final stages of mineralization because the element has nowhere else to go, and molybdenite deposition at the final stage of the hydrothermal system must incorporate all the remaining Re, thus increasing the concentration.

It is a possibility that, because no crosscutting relationships were observed between the base metal-carrying vein and other samples, that the vein represents the same paragenetic stage as sample 375-1125, but locally, the Re in the fluid may have been divided between some of the other minerals—magnetite and chalcopyrite—although there is no analysis at Adanac for Re content in minerals other than molybdenite. An addition of Re to other minerals would explain the low Re concentration in sample 364-50. This scenario puts the paragenetic order of the base metal vein in line with what is observed in other porphyry Mo deposits, namely, that base-metal stages usually occur last (Westra and Keith, 1981).

Magmatic Ages

There has been previous work on magmatic ages of the Mount Leonard stock and the Surprise Lake batholith. Mihalynuk et al. (1992) report a U-Pb age of zircons from the Surprise Lake batholith as 83.8 Ma. Christopher and Pinsent (1982) obtained K-Ar ages of biotite from some rock types within the Adanac deposit. The average age was 70.6 Ma and the individual ages of each rock type are shown in Table 3.

For this study, a total of seven samples from Adanac were analyzed for U-Th-Pb ages in zircons to constrain the duration of magmatism of the Mount Leonard stock, to re-test some of the ages reported by Christopher and Pinsent (1982), to determine ages of some new rock types not tested previously and for which relative ages were obscure, and to identify the intrusion responsible for mineralization by comparing the ages of molybdenite to the ages of units.

Table 3. Summary of K-Ar dates from Christopher and Pinsent (1982).

Unit	Age (Ma)
CGG	71.6 ±2.2
MGP	70.3 ±2.4
SGP	71.6 ±2.1
MEG	71.4 ±2.1

Samples were collected on site at Adanac and crushed with a rock crusher before being bagged. In between samples, the crusher was washed with soap and water and vacuumed. Samples were then sent to the Arizona LaserChron Center in Tucson, Arizona. Here, samples were run through a pulverizer to reduce the sample to sand-sized grains. Between samples, the pulverizer was cleaned with soapy water and a wire brush, and then vacuumed. The samples then went through the first of two gravity separation steps and a Wilfley table separation, after which a hand magnet was used to remove magnetic grains. The samples were processed in methylene iodide, and magnetic grains were removed with a Franz magnetic separator. The zircons were stored and carefully labelled. Mounts were made by selecting and arranging zircons and standards on a piece of tape, epoxying the sample, sanding, labelling and finally imaging the sample with enough detail so that individual grains can be seen.

Uranium-lead geochronology of zircons was conducted by laser-ablation multicollector inductively coupled plasma-mass spectrometry (LA-MC-ICP-MS) at the Arizona LaserChron Center under the direction of V. Valencia during June 2008. The ablation of zircons was done with a New Wave/Lambda Physik DUV193 Excimer laser operating at a wavelength of 193 nm, using a spot diameter of 25 μm. Ablated material was carried into a GV Instruments Ltd. isoprobe, where U, Th and Pb isotopes are measured simultaneously in static mode. Each individual zircon analysis began with a 20 s integration on peaks with the laser turned off (for backgrounds) and then twenty 1 s integrations were completed on each zircon with the laser firing. The laser operated at 23 KV with a repetition rate of 8 Hz. The resulting ablation pit was 12 μm across. Interelement fractionation was monitored by analyzing crystals of SL-1, a large concordant zircon crystal from Sri Lanka with a known (by isotope dilution-thermal ionization mass spectrometry) age of 564 ±4 Ma (2 σ; G. Gehrels, unpublished data, 2005). The reported ages for zircons from Adanac are based entirely on ²⁰⁶Pb/²³⁸U ratios. The errors of ²⁰⁷Pb/²³⁵U and ²⁰⁶Pb/²⁰⁷Pb analyses were too large for the ages to be considered reliable because of the low-intensity signal (<0.5 mV) of ²⁰⁷Pb from the young (<1 Ga) zircons. The ²⁰⁶Pb/²³⁸U ratios were corrected for common Pb by using the measured ²⁰⁶Pb/²⁰⁴Pb, the common Pb composition as reported from Stacey and Kramers (1975) and an uncertainty of 1.0 unit on the common ²⁰⁶Pb/²⁰⁴Pb.

Zircon crystals that were analyzed by the laser but showed evidence of lead loss or assumed to be metamictic were ignored. A crystal was determined to have suffered lead loss if, as the laser analyzed successive layers of zircon crystallization deeper into the centre of the crystal, these ages did not plateau or become stable (explained in more detail below). Also, the crystal could be visually determined to be metamictic by displaying a characteristic honey-brown colour, indicating radiation damage to the crystal and thus a mechanism for lead loss.

The reported age of each sample is the weighted mean of 30 individual zircon analyses, excluding crystals that were then statistically assumed to have experienced lead loss or statistically assumed to be inherited. A crystal was statistically identified as being inherited or suffering lead loss if its reported age was outside of a coherent population of ages (at the 95% level). The weighted mean of all the crystals believed to have a reliable age was calculated according to Ludwig (2001). The mean takes into account random errors (i.e., measurement errors). The age of the standard, the calibration correction from the standard, the composition of common Pb and the decay constant uncertainty are contributors to the error in the final age determination. All of these uncertainties are grouped as ‘systematic error.’ Rocks at Adanac displayed a range of 0.9–1.7% in systematic error. The error in the actual age of the sample is determined by quadratically adding the systematic and measurement errors. All age uncertainties are reported at the 2^σ level.

Dated units include CGG, CGG-T (transitional), SQFP (sparse quartz feldspar porphyry), MFP (megacrystic feldspar porphyry), MEG (medium-grained equigranular granite) and two samples of FGG (fine-grained granite). A summary of paragenetic ages of rock types based on crosscutting relationships is shown in Figure 7. The rock types CGG, CGG-T and SQFP are all essentially the same intrusion and are considered the first phase. They are certainly the oldest rocks as all other rock types in the deposit cut these, and they were affected by a deformational event prior to the intrusion of any other rock types in the deposit. The contacts between them are gradational; the coarse-grained unit (CGG) grades upward and outward into both a transitional (CGG-T) and hybrid (CGG-H) variety with increasing groundmass content, or becomes more of a porphyritic unit. Considered separately and slightly older than these three rock types are CQFP (crowded quartz feldspar por-

phyry, not dated) and SQFP, which are basically the porphyritic equivalents of CGG and its transitional and hybrid varieties. They were at one time the upper margin of the intrusion based on geographic location, but the Adera fault has dropped these units to the north. One sample each of CGG, CGG-T and SQFP were submitted for U-Pb zircon dating to obtain an older limit on magmatic ages at Adanac.

Based on crosscutting relationships, MGP (mafic granite porphyry) and then the SGP and CGP intrusions were emplaced. These are considered the second phase of intrusion. Like the CGG and CGG-T and CGG-H units, SGP and CGP are essentially the same intrusion with gradational contacts, and their designation as a separate unit is based on distinct geographic locations and differing phenocryst content. These three units were not dated because both older and younger units were tested, and this constrains the ages of these units to within a relatively small range of geological time.

The relative ages of MEG and MFP are somewhat less certain than other units. Medium-grained equigranular granite (MEG) occurs as an intrusion at depth on the southwestern end of the deposit, cuts both CGG and CGG-T, and is probably part of the second phase of intrusion. The MFP unit is a dike that cuts the CGG, CGG-T, SGP and CGP units. It is not known whether MEG is younger or older than SGP and CGP, nor is the age relationship between MFP and MEG visible. Because the hydrothermal alteration is the most intense in the southwest area above MEG, this unit is thought to have been responsible for mineralization. Mineralizing intrusions in other porphyry deposits are usually directly under the most intense hydrothermal alteration (Westra and

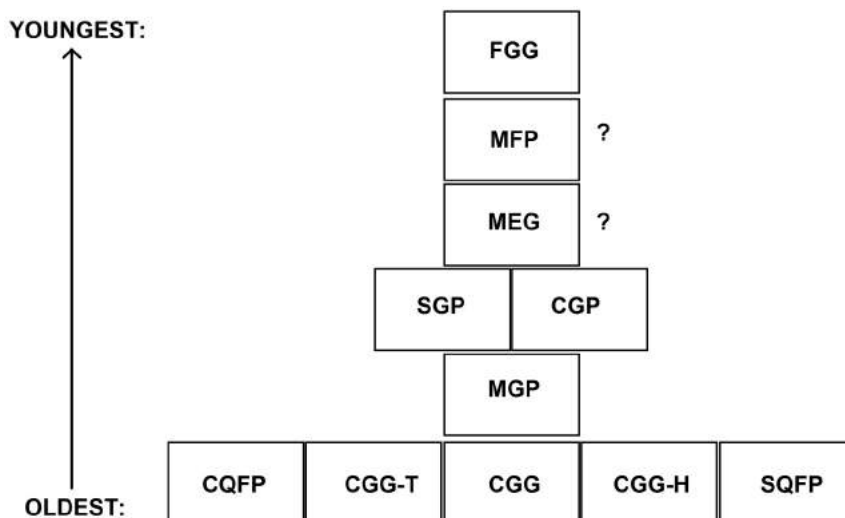


Figure 7. Summary of paragenetic ages for common rock types at Adanac based on crosscutting relationships. Abbreviations: CGG, coarse-grained granite; CGG-H, hybrid phase; CGG-T, transitional phase; CGP, crowded granite porphyry; CQFP, crowded quartz feldspar porphyry; FGG, fine-grained granite; MEG, medium-grained equigranular granite; MFP, megacrystic feldspar porphyry; MGP, mafic granite porphyry; SGP, sparse granite porphyry; and SQFP, sparse quartz feldspar porphyry.

Keith, 1981). Because mineralization cuts the SGP, CGP and MGP, the MEG was, therefore, assumed to be younger than these units as well. Megacrystic feldspar porphyry (MFP), because it is a dike that must have been emplaced after most or all of the previous units, is considered to be one of the younger units. Both MEG and MFP were dated by U-Pb.

Fine-grained granite (FGG) exists in the deposit as dikes that are always seen to cut everything else, and are the third and final phase of intrusion. However, two samples of FGG, one from the pit area and one from the southwest end, were dated to see if there is more than one generation of these dikes. It was recognized that if MEG and FGG have similar ages to the mineralization, it would mean that these units represented, or were at least synchronous with, the mineralizing intrusion.

The summary of the results of isotopic dating are shown in Figure 8. The complete results, including element concentrations, isotopic ratios and Concordia diagrams are included in the M.Sc. thesis associated with this paper (Smith, 2009).

The ages for rock types at Adanac span 77.5–81.6 Ma, giving the Mount Leonard stock a minimum lifespan of 1 Ma when factoring in errors. Most of the ages of the units are indistinguishable from one another due to uncertainties in the reported age. However, several relationships are apparent from these ages. On the basis of the geochronology, FGG from the pit area is older than CGG. This cannot be the case, as FGG cuts CGG. Also, FGG from the pit area returns an age that is older than FGG from the southwest area, and these rock types represent two different FGG intrusions or injections. This relationship is uncertain, however, due to the fact that FGG (pit area) has a suspect age. The U-Pb ages in Figure 8 also indicate that there is no intrusion that matches the age range for the mineralization. The temporal gap between the oldest possible mineralization (71.23 Ma) and youngest possible magmatism (74.5 Ma) is 3.3 Ma. From the earliest possible start of magmatism to the latest (or youngest) close of mineralization would be 13.4 Ma.

There are three possibilities that could explain the difference in ages and the relationship between mineralization and magmatism. One possibility is that all of the reported magmatism ages are correct and the mineralizing intrusion has not yet been dated. This seems unlikely because the FGG (pit area) age is incorrect relative to CGG. Also, in porphyry Mo deposits, the mineralizing intrusion is usually directly under min-

eralization itself. The bulk of molybdenite mineralization at Adanac forms blankets directly above both MEG and SGP/CGP, and is therefore likely genetically related to either or both of them.

The second possibility is that the ages are correct, but that the intrusion stayed hot for long enough to account for the temporal gap between the mineralization and magmatism. This possibility still seems unlikely because the FGG (pit area) age cannot be correct.

The third possibility is that several aspects of the statistically calculated ages are not relevant or meaningful in this study. First, there is probably a high incidence of inherited zircons in each rock type that shift the mean age to what is older than reasonably expected. In any given 305 m (1000 ft.) drillhole at Adanac, there may be up to five igneous intrusive phases that would be passed through in close spatial relationship to each other. It is unlikely that each of these rock types did not inherit a significant number of zircons from rock types older than it, including from the Surprise Lake batholith. Second, zircons that probably did not experience lead loss were discarded as such, further skewing the ages to what is older than reasonably expected.

There are two ways that a zircon could have been considered to have undergone lead loss. If a zircon age fell statistically below 95% of the population, it was discarded as anomalous and was therefore likely experiencing lead loss (for example, see Figures A-23–A-35 in Smith, 2009). The other way to determine lead loss was more dependent on measurements taken directly from the zircon crystal. When each zircon from a rock is analyzed for an age, the laser fires many times and creates an ablation pit in the zircon. Each firing of the laser reports an age and analyzes successively deeper layers of the zircon crystal. The outer layers are expected to show some lead loss, and the ages get progressively older as the laser analyzes closer to the core. If

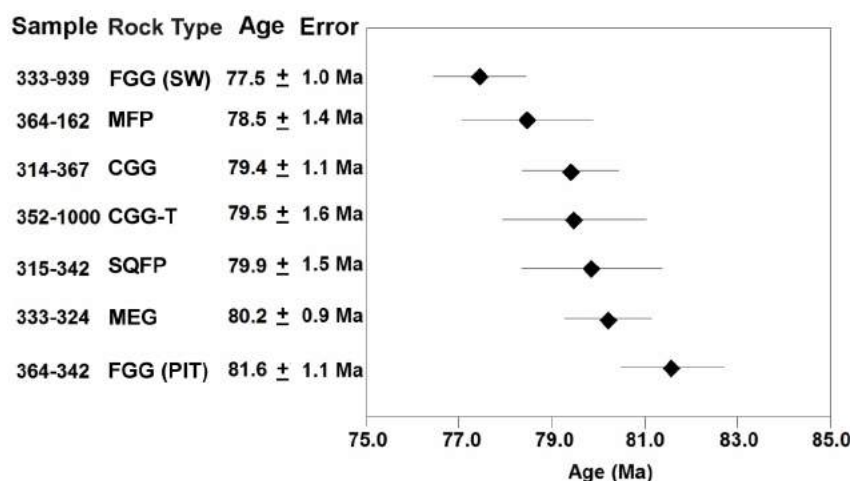


Figure 8. Results of U-Pb zircon ages for each rock type tested. The sample IDs are the drillhole, the footage depth and the rock tested. Uncertainties are reported at 2

the ages plateau, then the core is considered to represent a real crystallization age. If there is no plateau of ages, then the entire zircon is considered to have experienced lead loss, and that particular zircon is not included in the 30 tallied zircon crystals for the weighted mean. Analyses continue until there are a total of 30 crystals that show reliable core ages. Zircon crystals that did show a diagnostically reliable core age were discarded from the weighted mean because they were outside of 95% of the population. However, 95% of the population is not representative of an age for the rock because there are too many inherited zircons. Table 4 shows the lowest reported age for a zircon from each rock type. All of the zircons in the table had reliable plateau core ages.

Most of the ages in Table 4 are slightly older than the mineralization but not a single zircon gave an age that is lower or younger than one would expect considering the mineralization ages. If these zircons had experienced lead loss it would be reasonable to expect that at least some of them would be younger than the mineralization. This probably means that the ages seen here are real crystallization ages. The two samples of the FGG dikes did not contain any zircons that are younger than the other rock types. This is not surprising because the FGG dikes are low-volume rock types (not much of the rock exists at Adanac relative to the volume of other rock types in the deposit) and this makes it less likely that a zircon that crystallized completely within the dike would be sampled. Because the FGG dikes cut across all other rocks, they probably had a much higher incidence of inheritance relative to other rock types in the deposit.

Based on the fact that every unit dated has some zircons that show no lead loss and that closely resemble the age of mineralization, it is likely that all of the units at Adanac were experiencing some crystallization right before mineralization occurred. Therefore, using U-Pb zircon dating does not reliably identify a single intrusion that caused mineralization. What this does mean is that magmatism probably began by 82.7 Ma during the waning stages of crystallization of the Surprise Lake batholith and continued until at least 69 Ma. This represents a time span of about 13.7 Ma. There were a number of inherited zircons from the Surprise Lake batholith spanning from 85 Ma to about 90 Ma. There were no inherited zircons from the Fourth of July batholith, which is Jurassic in age. The crystallization ages of biotite using the K-Ar method from 1982 are likely recording the last hydrothermal event they were affected by, since the closing temperature of biotite using this method is 300°C.

Relationship between Adanac and Nearby Placer Gold Deposits

There are many similarities between porphyry Mo deposits and intrusion-hosted Au deposits such as Pogo and Fort

Table 4. Lowest reported age for a zircon from each rock type. Because they were the lowest reported, the ages were excluded from the statistical mean. Each zircon had a plateau core age.

Sample	Unit	Youngest Age (Ma)
333-939	FGG (SW)	72.1 ±1.0
333-324	MEG	71.1 ±1.0
364-342	FGG (PIT)	74.6 ±2.3
314-367	CGG	69.0 ±1.2
352-1000	CGG-T	71.4 ±2.2
315-342	SQFP	72.5 ±1.3
364-162	MFP	73.1 ±1.1

Knox in Alaska. These similarities include redox states and trace- and major-element chemistry of the hostrocks, and mineral and elemental assemblages of the deposits themselves. Porphyry Mo deposits and intrusion-hosted Au deposits both are hosted in relatively reduced and alkalic or felsic magmas, and hostrocks typically belong to the S-type magma series (Thompson et al., 1999). The trace elements and mineral assemblages present in intrusion-hosted Au deposits are characterized by Bi, W, As, Sn, Mo, Te and Sb. While the Adanac deposit itself contains no minerals or trace elements in significant quantities other than Mo and W, within 4.8 km (3 mi.) of the deposit and clearly related to the Mount Leonard stock are several deposits and veins (Figure 4) that have the same trace elements as intrusion-hosted Au deposits (e.g., Donlin Creek or Fort Knox). These include elevated Te, As and Bi, along with wolframite, Au (unknown whether it is native Au or electrum), cassiterite, molybdenite and stibnite in quartz veins hosted in the same igneous rocks that host Adanac. Gold in intrusion-hosted deposits like Fort Knox can be concentrated in locations distal (1–3 km) to an intrusion, are correlated with Bi and Te, and typically occur in sheeted veins (Stephens et al., 2004). Molybdenum and tungsten can occur more closely to the intrusion. Therefore, the mineral assemblage at and within the vicinity of Adanac is consistent with that of intrusion-hosted Au deposits. Intrusion-hosted Au deposits are also associated with Phanerozoic arc settings and W-Sn provinces (such as Fort Knox; Thompson et al., 1999). This is consistent with the setting for the Adanac Mo deposit, which is very close to Logtung (MINFILE 104O 016; a porphyry W deposit) and other Sn deposits such as the Germaine porphyry Sn deposit (MINFILE 116 004) and the JC Sn skarn (MINFILE 105B 040).

Sack and Mihalynuk (2004) showed that Au from the Atlin mining camp may be at least in part derived from an intrusive source, because cassiterite, thorite and granitoid clasts were found to be intimately associated with some Au nuggets in the camp. The Surprise Lake batholith is enriched in Sn and is known to contain thorite. Because the Adanac deposit occurs at the head of two creeks (the Ruby and Boulder creeks) that have placer Au deposits on their lower drainages, Adanac presents a good opportunity to test for a

possible genetic link between porphyry Mo deposits and intrusion-hosted Au deposits.

To test this theory, the Os ratios of Au from Ruby Creek were compared with Os ratios of magnetite from drillcore of the Adanac Mo deposit. Both the Au and magnetite samples were dissolved and homogenized using the same Carius tube technique as described for the molybdenite ages and analyzed by thermal ionization mass spectrometry (TIMS). This was done at the Re-Os geochronology lab at the University of Arizona, Tucson, and the results are summarized in Table 5.

The Au analyzed had little Re and a very small resulting Re/Os ratio. No age regression was possible for Au. For magnetite, there was not enough material submitted for multiple analyses, even though the largest known single magnetite crystal from Adanac was selected for the analysis. Therefore, no isochron could be made for magnetite because multiple analyses are needed for an isochron. Regardless of these problems, the question of whether Au is related to the hydrothermal system that generated the Adanac deposit can still be answered with reasonable certainty. The Au has a $^{187}\text{Os}/^{188}\text{Os}$ that is very primitive, even lower than the current mantle value of 0.129, and so is likely from the mantle, not from a porphyry deposit (see Figure 9). Also, the Os content of the Au sample is very high and variable, suggesting the presence of osmiridium grains, which would likely be in a source associated with chromite or peridotite, not a porphyry deposit. It is interesting that the Os and Re concentrations of the Au are very high in relation to other porphyry Au deposits, and are actually quite similar to the mantle-derived Witwatersrand in South Africa (Figure 9).

Although the results of this study suggest the Au on Ruby Creek is unrelated to the hydrothermal system at Adanac, this does not mean that none of the Au in the Atlin mining camp is related to Adanac. It likely would have been better to sample Au from placer deposits on Boulder Creek rather than Ruby Creek. Also, it may have been better to get multiple samples as well, because if some of the Au is derived from the Surprise Lake batholith (and the Mount Leonard stock), this means that Au in the Atlin mining camp is from mixed sources. Multiple samples would have in-

Table 5. Results of the Au (Ruby Creek-1 and -1*; -1* is a duplicate of the same Au sample) and magnetite (Mt, Adanac 351-957) Re and Os analyses.

Sample	Phase	$^{187}\text{Os}/^{188}\text{Os}$	Error	$^{187}\text{Re}/^{188}\text{Os}$	Os (ppb)	Re (ppb)
Ruby Creek-1	Au	0.125	0.0005	0.016	345	1.16
Ruby Creek-1*	Au	0.125	0.0005	0.001	4538	0.82
Adanac 351-957	Mt	1.237	0.0110	872.250	0.015	2.42

creased the likelihood of identifying at least one sample that is igneous derived.

Conclusions

Rhenium-osmium analysis of molybdenite confirmed at least two generations of mineralization at 70.87 ± 0.36 Ma and about 69.66 ± 0.35 Ma, with the youngest mineralization occurring at the southwest end of the deposit above the MEG intrusion and disseminated in a feldspar flood. Uranium-lead ages of zircons from Adanac hostrocks place magmatism at 81.6 ± 1.1 Ma to 69 ± 1.2 Ma, giving the Mount Leonard stock a probable lifespan of almost 14 Ma. When using the weighted mean of 30 zircon analyses for each rock type, no appropriate age match was found for an intrusion and mineralization episode, and the FG (pit) age is certainly incorrect. There are too many inherited zircon grains for a mean age to be reliable, and statistical methods for determining lead loss discredit ages that are most likely

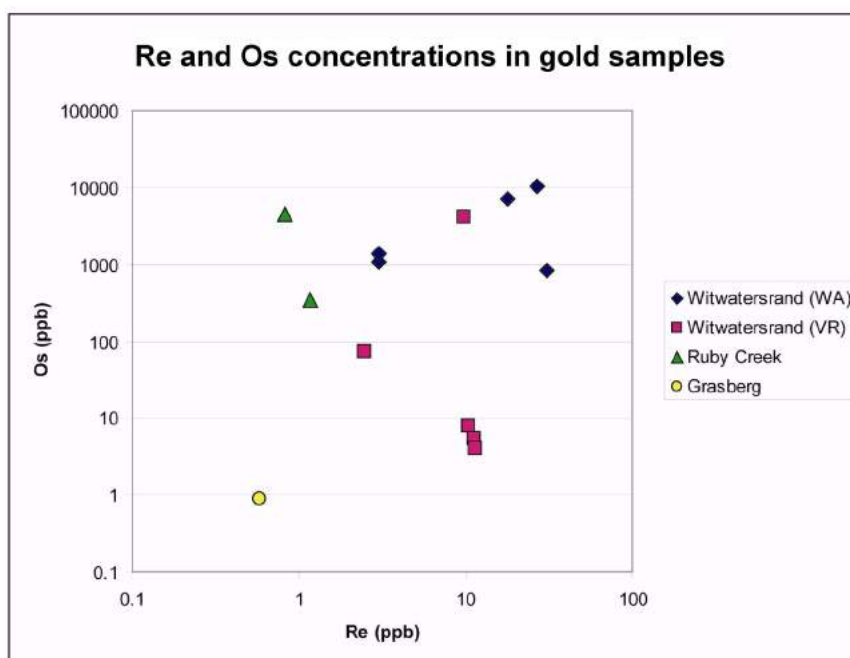


Figure 9. Osmium and rhenium concentrations of Au deposits compared with Au from Ruby Creek. The Witwatersrand deposit is historically the largest Au deposit in the world, accounting for about 40% of total world production (Frimmel and Minter, 2002) and is mantle-derived (Kirk et al., 2002). The two Witwatersrand samples are from different formations: WA (Western Area) and VR (Vaal Reef). The Grasberg is a porphyry Cu-Au deposit in Indonesia. Modified from Kirk et al. (2002).

valid. It is probably true that most, if not all, of the rock types that were dated at Adanac were still undergoing some crystallization just before (1 Ma) or during mineralization.

The Au from Ruby Creek analyzed in comparison with magnetite from Adanac is derived from rocks more like peridotite than porphyry-deposit hostrocks. The question of whether some of the Au in the Atlin mining camp is igneous derived remains unanswered. The next step in answering this question would be to try to get multiple samples of magnetite from the Mount Leonard stock or the Surprise Lake batholith to compare with multiple Au samples from the Boulder Creek placer deposits or Au from sheeted quartz veins to the southwest of Adanac.

References

- Aitken, J.D. (1959): Atlin map area, British Columbia; Geological Survey of Canada, Memoir 307, p. 1–89.
- Ballantyne, S.B. and Littlejohn, A.L. (1982): Uranium mineralization and litho-geochemistry of the Surprise Lake batholith, British Columbia; *in* Uranium in Granites, Y.T. Maurice (ed.), Geological Survey of Canada, Paper 81-23, p. 145–155.
- Birck, J.L., RoyBarman, M. and Capmas, F. (1997): Re-Os measurements at the femtomole level in natural samples; *Geostand Newsletter*, v. 20, p. 19–27.
- Christopher, P.A. and Pinsent, R.H. (1982): Geology of the Ruby Creek–Boulder Creek area (Adanac Molybdenum Deposit); BC Ministry of Energy, Mines and Petroleum Resources, Preliminary Map 52, scale 1:12 000.
- Creaser, R.A., Papanastassiou, D.A. and Wasserburg, G.J. (1991): Negative thermal ion mass spectrometer of Os, Re and Ir; *Geochimica et Cosmochimica Acta*, v. 55, p. 397–401.
- Frimmel, H.E. and Minter, V.E.L. (2002): Recent developments concerning the geological history and genesis of the Witwatersrand gold deposits, South Africa; *Society of Economic Geologists, Special Publication 9*, p. 17–45.
- Kikauka, A. (2002): Geological, geophysical, and geochemical report on the Adanac claim group, Surprise Lake, Boulder Creek, Atlin; submitted by Stirrup Creek Gold Ltd., BC Ministry of Energy, Mines and Petroleum Resources, Assessment Report 26 895, 58 p.
- Kirk, J., Ruiz, J., Chesley, J., Walshe, J. and England, G. (2002): A major Archean, gold and crust forming event in the Kaapvaal craton, South Africa; *Science*, v. 297, no. 5588, p. 1856–1858.
- Ludwig, K.R. (2001): Isoplot/Excel version 2.49, a geochronological toolkit for Microsoft Excel; Berkeley Geochronological Center, Special Publication 1a.
- Mihalynuk, M.G., Smith, M.T., Gabites, J.E. and Runkle, D. (1992): Age of emplacement and basement character of the Cache Creek terrane as constrained by new isotopic and geochemical data; *Canadian Journal of Earth Sciences*, v. 29, p. 2463–2477.
- MINFILE (2009): MINFILE BC mineral deposits database; BC Ministry of Energy, Mines and Petroleum Resources, URL <<http://minfile.ca>> [November 2009].
- Monger, J.W.H. (1975): Upper Paleozoic rocks of the Atlin Terrane; BC Ministry of Energy, Mines and Petroleum Resources, Paper 74-47, 63 pages.
- Nagler T.F. and Frei, R. (1997): Plug in plug osmium distillation; *Schweizerische Mineralogische und Petrographische Mitteilungen*, v. 77, p. 123–127.
- Pinsent, R.H. and Christopher, P.A. (1995): Adanac (Ruby Creek) molybdenum deposit, northwestern British Columbia; *Canadian Institute of Mining and Metallurgy, Special Volume 46*, p. 712–717.
- Sack, P.J. and Mihalynuk, M.G. (2004): Proximal gold-cassiterite nuggets and composition of the Feather Creek placer gravels: clues to a lode source near Atlin; *in* Geological Fieldwork 2003, BC Ministry of Energy, Mines and Petroleum Resources, Paper 2004-1, p. 147–161.
- Smith, J.L. (2009): Geology of the Adanac porphyry molybdenum deposit with a comparison to other porphyry molybdenum deposits throughout the North American Cordillera; University of Nevada, Reno, MSc thesis, 205 p.
- Smoliar, M.I., Walker, R.J. and Morgan, J.W. (1996): Re-Os ages of group IIA, IIIA, IVA and IVB iron meteorites; *Science*, v. 271, p. 1099–1102.
- Stacey, J. and J. Kramers (1975): Approximation of terrestrial lead isotope evolution by a two-stage model; *Earth and Planetary Science Letters*, v. 26, p. 207–221.
- Stephens, J.R., Mair, J.L., Oliver, N.H.S., Hart, C.J.R. and Baker, T. (2004): Structural and mechanical controls on intrusion-related deposits of the Tombstone Gold belt, Yukon, Canada, with comparisons to other vein-hosted ore-deposit types; *Journal of Structural Geology*, v. 26, p. 1025–1041.
- Sutherland Brown, A., (1970): Adera; *in* Geology, Exploration, and Mining in British Columbia 1969, BC Ministry of Energy, Mines and Petroleum Resources, p. 29–35.
- Thompson, J.F.H., Sillitoe, R.H., Baker, T., Lang, J.R. and Mortensen, J.K. (1999): Intrusion related gold deposits associated with tungsten-tin provinces; *Mineralium Deposita*, v. 34, p. 323–334.
- Wallace, S.R., MacKenzie, W.B., Blair, R.G. and Muncaster, N.K. (1978): Geology of the Urad and Henderson molybdenite deposits, Clear Creek County, Colorado, with a section on a comparison of these deposits with those at Climax, Colorado; *Economic Geology*, v. 73, p. 325–368.
- Westra, G. and Keith, S.B. (1981): Classification and genesis of stockwork molybdenum deposits; *Economic Geology*, v. 76, p. 844–873.
- White, W.H., Stewart, D.R. and Ganster, M.W. (1976): Adanac (Ruby Creek), porphyry molybdenum deposits of the calc-alkalic suite; *Canadian Institute of Mining and Metallurgy, Special Volume 15*, p. 476–483.

Geology of the Deer Park Map Area, Southeastern British Columbia (NTS 082E/08)

T. Höy, Consultant, Sooke, BC, V9Z 0X6

Höy, T. (2010): Geology of the Deer Park map area, southeastern British Columbia (NTS 082E/08); *in* Geoscience BC Summary of Activities 2009, Geoscience BC, Report 2010-1, p. 127–140.

Introduction

The Deer Park map area NTS 082E/08 (1:50 000 sheet) is located in the southern Monashee Mountains of southeastern British Columbia (Figure 1); it extends from Lower Arrow Lake in the eastern part of the sheet to west of the Granby River, covering an area of more than 1000 km². Nearly a third of the area, the south-central part, is taken up by Gladstone Park, a largely inaccessible wilderness area, which straddles the highlands of the Christina Range north of Christina Lake. Access to the western part of the area is mainly via numerous logging access roads that branch off a well-maintained paved, then gravel-covered road, which extends north from Grand Forks following the Granby River and Burrell Creek. Access to the southeastern part is along logging roads, which extend north from Highway 3 between the towns of Castlegar and Christina Lake, while access to the northeastern corner, on the eastern side of Lower Arrow Lake, is via the Deer Park road, which essentially follows the shoreline of the lake, north from Castlegar.

The area is relatively mountainous and heavily forested, though a considerable part has been logged. The nearest towns are Grand Forks, Christina Lake and Castlegar, all located south of the map area; there are no towns or communities within the study area.

The geology of the area, which was last mapped as part of a government survey at a scale of approximately 1:250 000 in the mid 1950s (Little, 1957) and also included in the regional compilation of the Penticton map sheet (NTS 082E) by Tempelman-Kluit (1989), is not well-known or understood. Although the area is located between the Rossland mining camp to the southeast, the Greenwood camp to the southwest and the Franklin camp in the sheet immediately to the north, exploration has been limited, possibly due to past inaccessibility to the area, lack of modern geological

surveys and under appreciation of the contribution of Tertiary structures and magmatic controls to mineralization.

The 2009 Geoscience BC project involved geological mapping of a large part of the 1:50 000 sheet, with publication in 2010 of a regional geological map (NTS 082E/08) and several 1:20 000 sheets. Accompanying papers will discuss mineral deposits and exploration models for the area, with particular reference to Tertiary mineralization.

Geological and Exploration History

The Deer Park area falls within the Kettle Valley sheet (NTS 082, east half) mapped at a scale of 1:253 440 (one inch to four miles) by Little (1957). Templeman-Kluit (1989) relied on this regional map for his compilation of the Penticton sheet (NTS 082E), with only minor modifications in the Deer Park area, mainly involving structures related to Eocene extension. The geology of the Grand Forks map sheet (NTS 082E/01), located immediately to the south, was recently published by Höy and Jackaman (2005), who remapped and compiled studies by other authors (Acton et al., 2002; Laberge and Pattison, 2007) and, more notably, a Ph.D. thesis by V. Preto (1970) on the Grand Forks complex. The Greenwood mining camp, located immediately west of the Grand Forks sheet, has been studied in considerable detail, initially by Little (1979) and more recently by Church (1986) and Fyles (1990). Mapping east of the Deer Park area includes the regional study of the Lardeau (west half) area by Little (1960) and farther southeast, more detailed geological mapping of the Rossland (Höy and Dunne, 2001) and Nelson (Höy and Dunne, 2004) areas.

Mineral exploration, focused largely in the south, dates back to the mid- to late 1800s, with discovery and development of rich gold and copper deposits in the Greenwood and Rossland mining camps, as well as the building of smelters in Greenwood, Grand Forks and Trail to process the Rossland deposits. Mineralization was discovered in the early 1900s in the Franklin mining camp (Drysdale, 1915), located immediately north of the Deer Park map area; this camp produced intermittently until 1989 (MINFILE, 2009).

There have been few precious or base-metal producers in the Deer Park map area. Considerable past exploration has focused on a molybdenite deposit, formerly called ‘Midas’,

Keywords: *Grand Forks complex, Granby fault, Kettle River fault, Jurassic Nelson intrusions, Coryell intrusions, Midas molybdenite property, JJ Main occurrence, Deer Park property, Tertiary mineralization*

This publication is also available, free of charge, as colour digital files in Adobe Acrobat® PDF format from the Geoscience BC website: <http://www.geosciencebc.com/s/DataReleases.asp>.

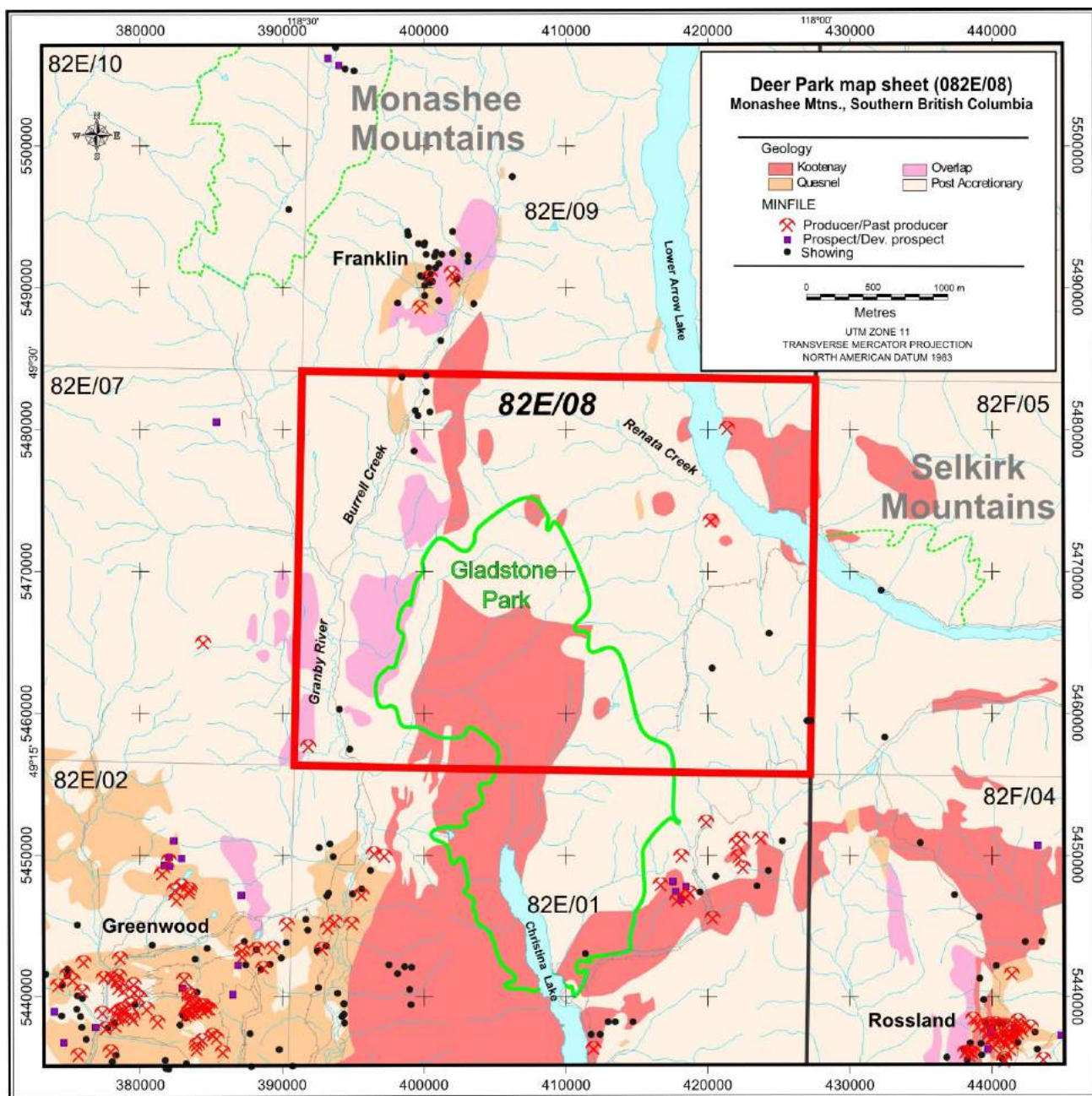


Figure 1. Location and regional geology of the Deer Park map area (1:50 000 sheet), southeastern British Columbia.

near the southeastern part of the map area, and recent work by Kootenay Gold Inc. is looking at both molybdenite and base-metal potential in that immediate area. Several mineral occurrences have been studied in the northwestern part of the area, immediately south of the Franklin mining camp. Recent work by prospectors T. and C. Kennedy focusing on precious-metal mineralization possibly related to Tertiary tectonics has led to the discovery of several new showings and mineralized areas, most notably in the area of the JJ showing in the southeastern part of the study area and in the Deer Park area on the eastern side of Lower Arrow Lake.

The geology of these areas is described below (see 'Mineralization').

This study involved 42 days of field mapping, concentrated mainly in areas accessible by four-wheel drive truck. Where possible, it concentrated on areas of known mineralization, with field mapping done at a scale of 1:20 000 for publication at this scale and as a compilation of the entire map sheet at a scale of 1:50 000. No work was done in Gladstone Park, which covers nearly a third of the south-central part of the Deer Park map area (1:50 000 sheet).

Regional Geology

The Deer Park area is located immediately north of the Grand Forks complex (Preto, 1970), one of a number of metamorphic-core complexes in the southern Omineca Belt, which appear to be related to Eocene faulting, extension and denudation (Brown and Journeay, 1987; Parrish et al., 1988). The complex is bounded on the west by the west-dipping Granby fault and on the east by the Kettle River fault. Normal movements on these faults are determined to be Early Tertiary, constrained by ages of intrusive rocks (Carr et al., 1987, Parrish et al., 1988). Numerous paleomagnetic tilt measurements support Eocene extensional normal movement on these and several other north-trending faults and further define relative timing (Marquis and Irving, 1990; Wingate and Irving, 1994). More recent studies have focused on structure and metamorphism related to both the Granby fault (Laberge and Pattison, 2007) and the Kettle River fault (Cubley and Pattison, 2009).

Geology of Deer Park Map Area (NTS 082E/08)

The Deer Park map area is underlain by mainly Middle Jurassic (Nelson suite), Cretaceous and Early Eocene (Coryell suite) intrusive rocks (Figure 2). These intrude Late Paleozoic metasedimentary and metavolcanic rocks, exposed east of Lower Arrow Lake in the eastern part of the area, and west of the Granby fault in the western part. Structures in the area are dominated by steeply dipping, generally north-northwest-trending faults, many of which are related to the northern extensions of the bounding faults of the Grand Forks complex. These faults appear to control the distribution of most base- and precious-metal deposits or occurrences in the area.

Late Paleozoic Succession (Lower Arrow Lake Area)

A succession of mainly metasedimentary rocks is exposed in the northeastern part of the map area, east of Lower Arrow Lake. Regional mapping by Little (1957) also showed small exposures on the western side of the lake and although their presence was not confirmed during 2009 mapping, their locations are included on both the regional (1:50 000 sheet; Figure 2) and the Terrain Resource Information Management (TRIM 1:20 000 sheet; Figure 3) maps. The succession includes interlayered quartzite, siltstone, argillaceous siltstone, some dark limestone and mafic volcanic rocks. The geology of the area, including this succession, is described in more detail in a Kootenay Gold Inc. assessment report (Höy, 2008).

A schematic representation of the succession's stratigraphy is shown in Figure 4. The structurally (and probably lowest) unit is a thick (several hundred metres) sequence of mixed amphibolite, hornblende gneiss and granodiorite. It

is overlain, possibly unconformably, by interlayered siltstone, minor argillite, calcisilicate schist and dark impure marble, and two sequences of mafic volcanic rocks. The top of the succession comprises mainly dark argillite and argillaceous siltstone.

The age of this succession is not known with certainty. Tempelman-Kluit (1989) correlated it with Ordovician–Devonian rocks, implying that they are part of the Kootenay Terrane. However, they could be part of the lithologically similar Carboniferous–Permian Mount Roberts Formation, which underlies Triassic and Jurassic arc volcanic rocks in the Quesnel Terrane.

Late Paleozoic Succession (Granby River Area)

Metasedimentary and metavolcanic rocks are exposed west of the Granby fault in the Granby River and Burrell Creek drainages. These rock units were not mapped in detail during this study, although some exposures in the northwestern part of the map area (Figure 2) were briefly examined.

Unit CPa, correlated with the Anarchist Group (Tempelman-Kluit, 1989), comprises dark grey weathering amphibolite and greenstone, as well as quartz-chlorite and quartz-biotite schists. Minor serpentinitized peridotite and chert breccia occur locally. Small exposures mapped in the northwestern portion of TRIM map 082E049 (Figure 5), included mafic volcanic rocks, dark schist and argillite, and minor dark argillaceous limestone.

Intrusive Rocks

Intrusive rocks underlie a large part of the map area and their differentiation, and relationship to mineralization, formed a large part of the present study. As these intrusions have not been chemically analyzed, dated nor studied petrographically, the following reports are based entirely on field observations and descriptions. Previous workers (Little, 1957; Tempelman-Kluit, 1989; and several assessment reports, described below under 'Mineralization') have recognized three main suites: the Middle Jurassic Nelson plutonic suite, Jurassic–Cretaceous (?) granites and Coryell intrusions.

Middle Jurassic Nelson Plutonic Suite

Rocks that have been assigned to the Nelson plutonic suite underlie a considerable part of the central and southern part of the Deer Park map area (Figure 2). They have not been previously differentiated and have been described as generally massive to foliated granodiorite, quartz diorite and granite. As noted by Tempelman-Kluit (1989), these rocks may include younger granitic rocks. As the exposures of Nelson plutonic rocks typically represent discrete bodies, separated by younger intrusive rocks, they are described separately below.

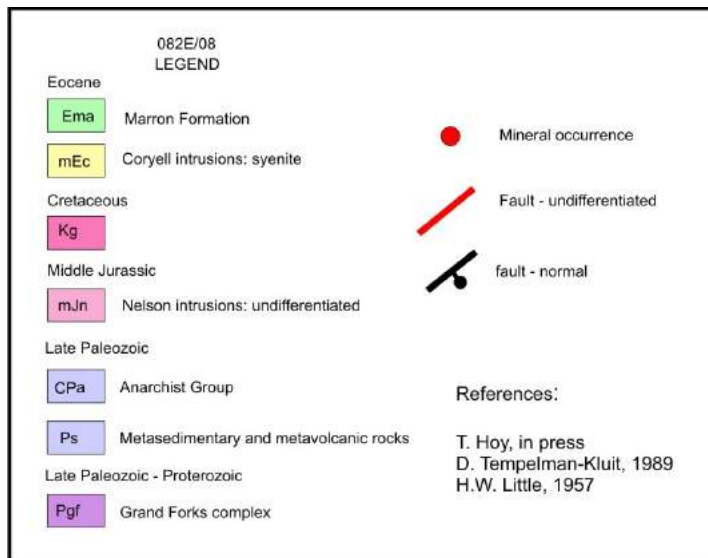
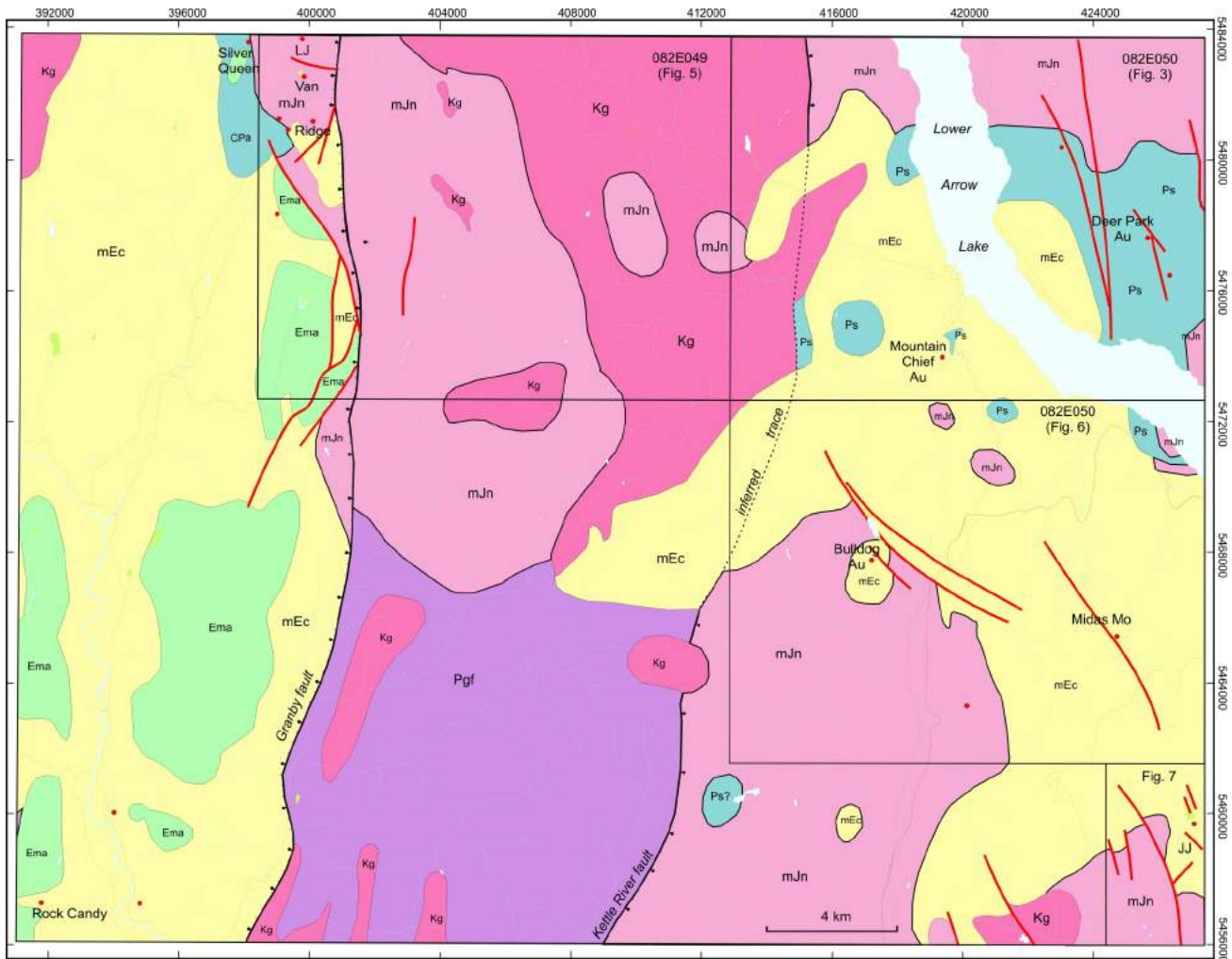


Figure 2. Geology of map area NTS 082E/08 (1:50 000 sheet), southeastern British Columbia.

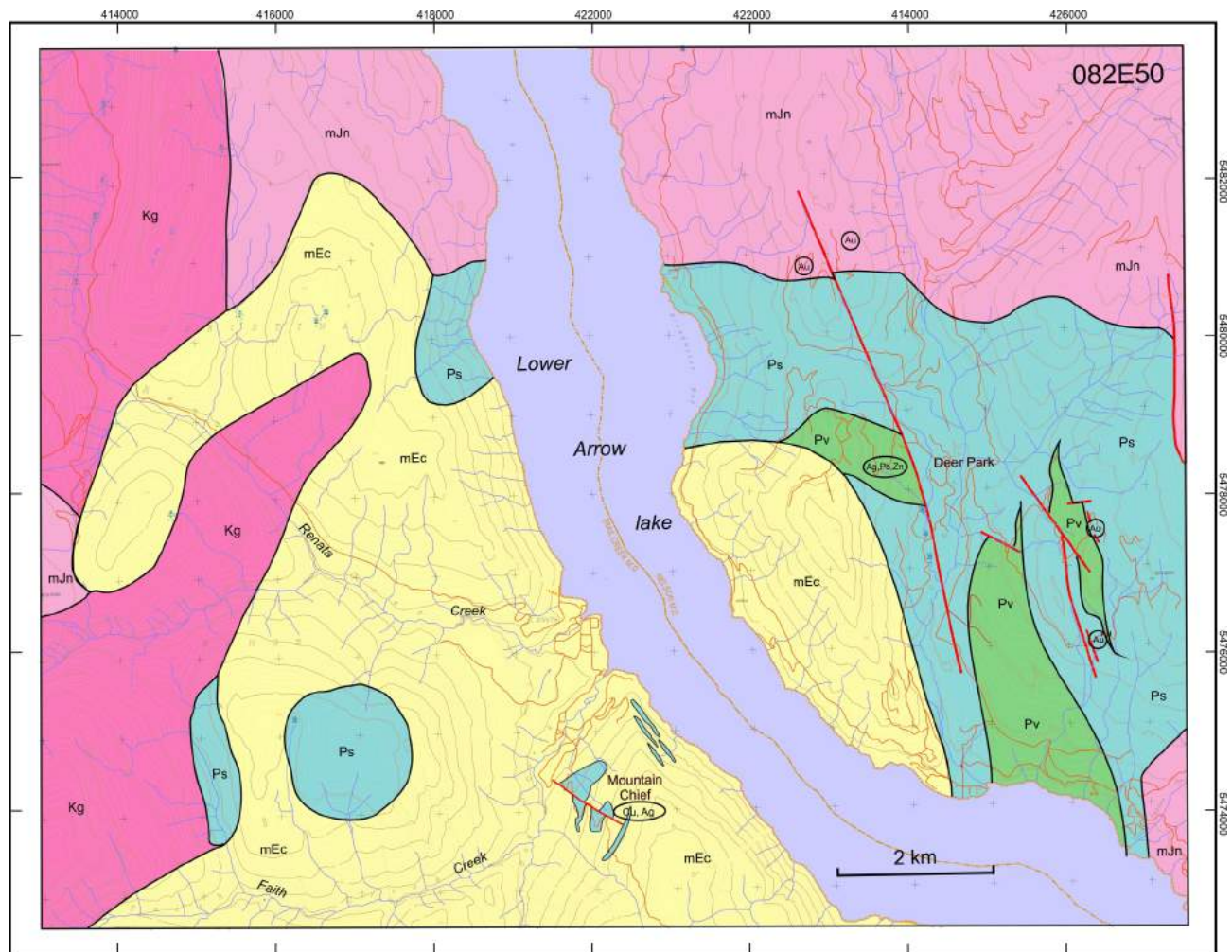
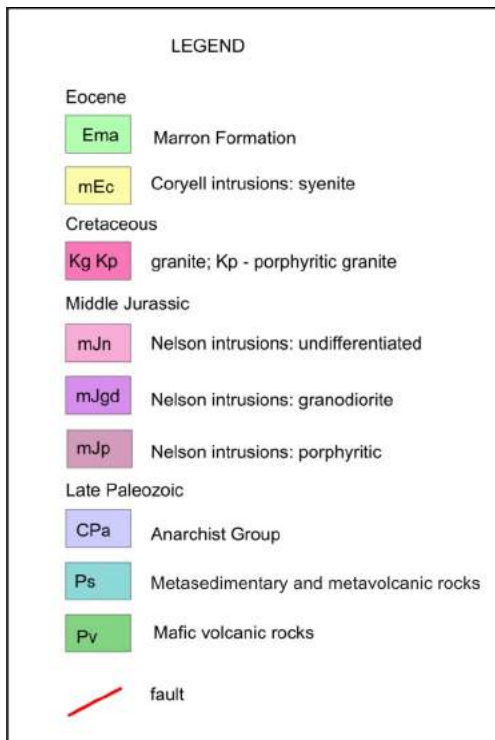


Figure 3. Geology of TRIM map 082E/050 (1:20 000 sheet), southeastern British Columbia.



TRIM Map Sheet 082E/050: unit mJn

The dominant phase on the eastern side of Lower Arrow Lake (northern portion of sheet 082E/050; Figure 3) is a relatively fresh biotite-hornblende granodiorite to granite. It is typically medium- to coarse-grained, with local minor propylitic alteration, rusted fractures and common inclusions of country rock. Numerous north-trending Eocene (?) dikes cut the intrusion.

TRIM Map Sheet 082E/040: units mJn, mJp

Exposures farther south, in TRIM map sheet 082E/040 (Figure 6), have been subdivided into two main units, a coarse-grained 'K-feldspar' megacrystic 'granite' (unit mJp) and a more massive, equigranular granite to granodiorite phase (unit mJn). The megacrystic granite includes large (typically several centimetres) subhedral to euhedral pink to beige feldspar phenocrysts in a medium- to coarse-grained granite or granodiorite matrix. Megacryst content ranges from widely scattered crystals to more than 50% of the rock. With decreasing megacryst content, this

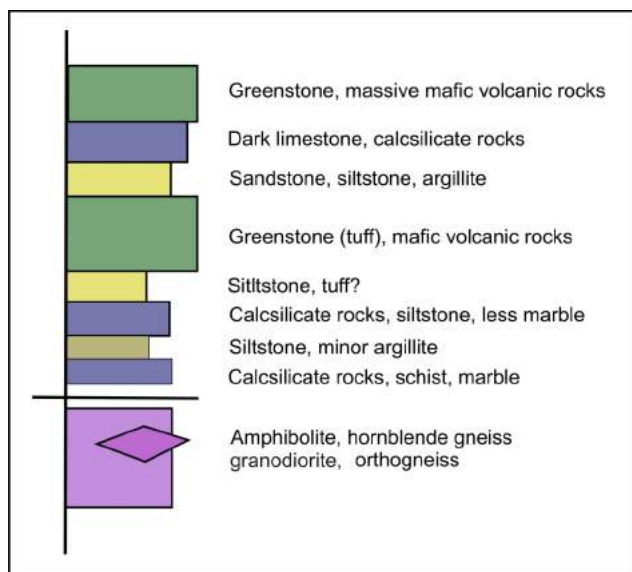


Figure 4. Paleozoic succession in the northeastern part of the Deer Park property, southeastern British Columbia.

phase grades into the more massive, equigranular granite or granodiorite. Propylitic alteration of the matrix is fairly common, particularly in the more eastern exposures, and possibly jarosite coated fractures, minor disseminated pyrite, quartz-pyrite veins and pervasive silicification occur locally.

The massive ‘granite’ typically surroundings the porphyritic granite is medium- to coarse-grained, with only minor (usually <10%) mafic rocks and biotite+hornblende+magnetite. It locally shows evidence of either propylitic or potassic alteration, particularly in more eastern exposures. Potassic alteration includes both pink K-feldspar and pale sericitic alteration, both accompanied by silicification—thin quartz veins with minor sulphides including pyrite, chalcopyrite and, locally, galena.

These intrusive phases are included in the Nelson plutonic suite, though they appear to be less deformed, more felsic and more homogeneous than Nelson intrusive rocks elsewhere. It is possible that they are part of the more leucocratic Jurassic–Cretaceous granitic suite, but are included in the Nelson suite until conclusive radiometric analyses can determine their age.

TRIM Map Sheet 082E/049: units mJn-mJp

A large exposure of Nelson granitic rocks occurs in the footwall of the Granby fault in the western part of the area. On TRIM map 082E/049 (Figure 5), it extends from the northern part of sheet southward into Gladstone Park on sheet 082E/039. As on sheet 082E/040, it comprises both massive to porphyritic granodiorite and, nearer the Granby fault, intensely foliated or gneissic granodiorite, which was included in unit Pg_f (undifferentiated Grand Forks gneiss) by Tempelman-Kluit (1989).

The porphyritic granite-granodiorite (unit mJp) is the most common phase, underlying a large part of the map area, and undoubtedly extending beyond its mapped limits as shown in Figure 5. It is a distinctive phase containing large (commonly up to 10 cm), subhedral, pink to beige to occasionally white feldspar crystals in a medium- to coarse-grained, typical granodiorite matrix, which contrasts with the previously described, more typical, pink granitic matrix in exposures on sheet 082E/040. The porphyritic phase is variably altered, ranging from relatively fresh to propylitic; potassic alteration was not noted, except very locally in contact exposures with Coryell syenite. The unit varies from massive to foliated to gneissic, particularly in western exposures near the Granby fault.

The massive undifferentiated Nelson intrusion (unit mJn) is typically a medium- to coarse-grained granodiorite, with variable though generally higher hornblende content than the porphyritic phase. Near the faulted (?) contact with the Coryell suite on the western portion of the sheet, this unit is termed ‘granite’, probably due to potassic alteration. Banded hornblende and granodiorite gneisses in the western part of the area are included in the undifferentiated mJn unit. Banded to foliated granodiorite (unit mJgd) also occurs along the eastern side of the intrusion, along the contact with Coryell syenite.

TRIM Map Sheet 082E/030

Nelson plutonic rocks in the southeastern part of the area have been mapped by Dunne (2004) and included in an assessment report on the JJ property (Höy, 2006). Dunne (2004) separated the Nelson granitic rocks into four phases:

- unit mJg: a fine- to medium-grained, equigranular granite–granodiorite with 10–15% biotite+hornblende and host to the JJ Main showing
- unit mJlg: a distinctive fine- to medium-grained leucocratic granite with up to 5% mafic minerals, which commonly occur as irregular ‘box-shaped’ segregations with quartz
- unit mJd: a fine-grained diorite to quartz diorite with up to 50% mafic minerals
- unit mJgd: a medium- to coarse-grained porphyritic ‘granite’ characterized by white feldspar and distinctive prismatic hornblende phenocrysts

These Nelson plutonic rocks contrast with those farther north in the variety of their phases, typically finer grain size and the number of associated dikes.

Cretaceous (?) Granite

A large exposure of mainly granitic rock occurs in the north-central part of the map area. Its age is not known, although it is similar to granitic rocks farther east referred to by Little (1960) as the ‘Valhalla plutonic rocks’, which were interpreted to be Late Cretaceous by Parrish et al.

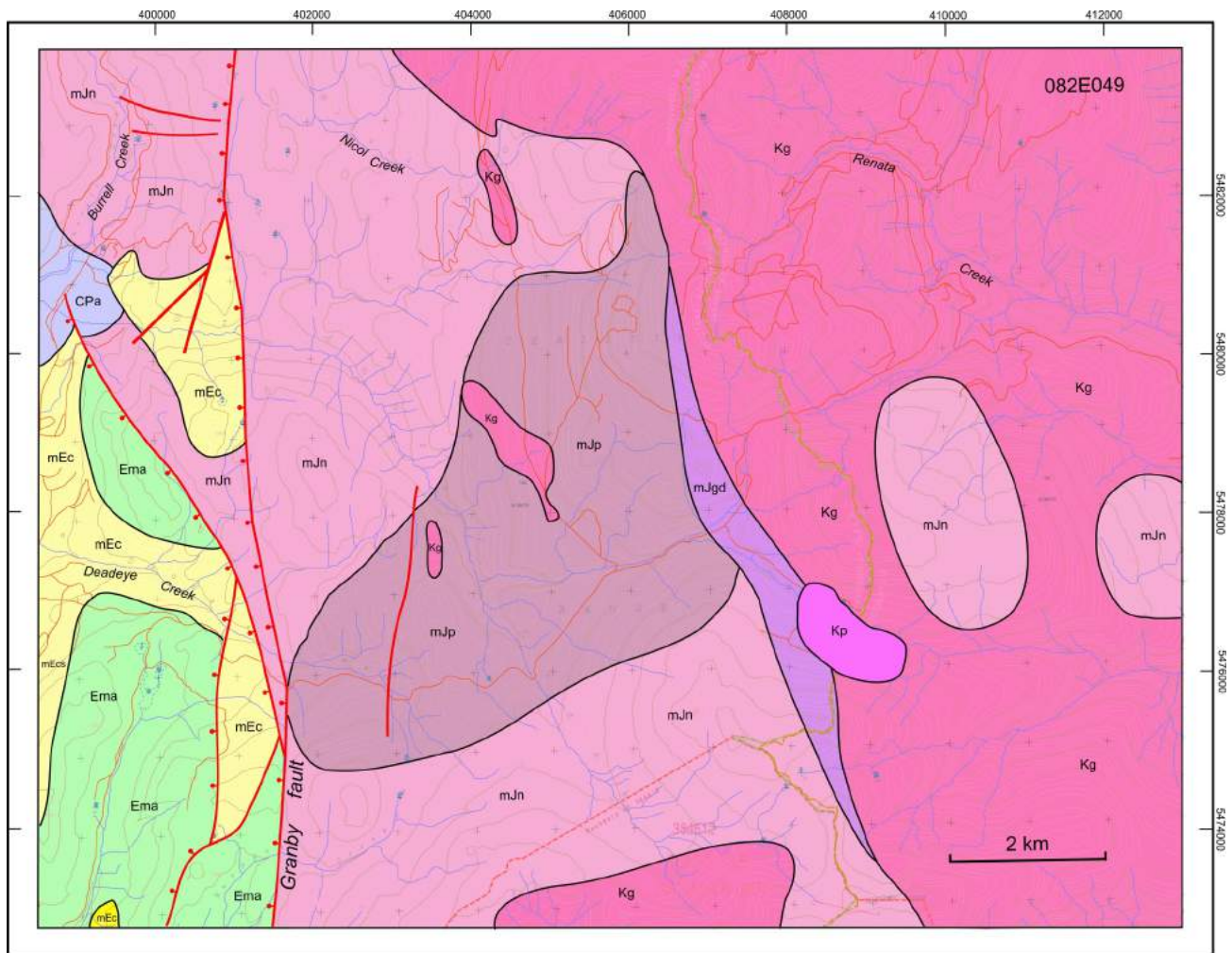
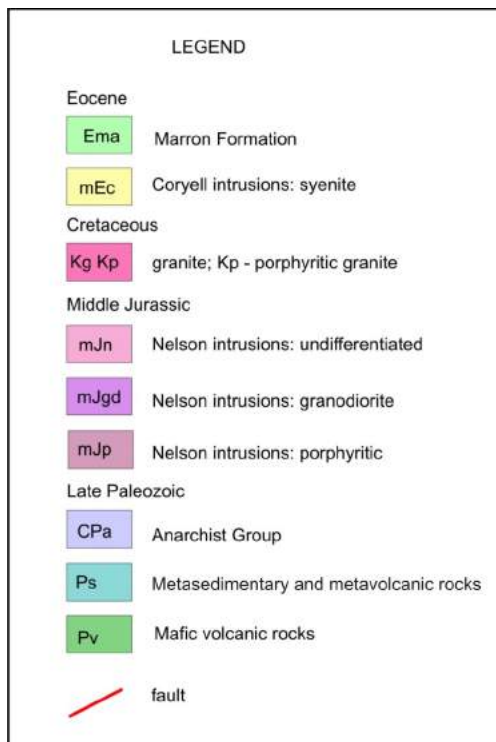


Figure 5. Geology of TRIM map 082E/049 (1:20 000 sheet) in the Deer Lake area, southeastern British Columbia.



(1988). It is also similar to ‘Okanagan batholith’ rocks exposed mainly west of the Deer Park area, which Templeman-Kluit (1989) indicated were ‘Cretaceous and/or Jurassic’ and Parrish et al. (1988), ‘Early Eocene’. If Cretaceous in age, the granites may be part of the mid-Cretaceous Bayonne suite, which Logan (2000) described and related to a variety of gold and other deposit types.

The granite is exposed mainly in the northern part of the Deer Park map area, on TRIM map sheets 082E/049 and 082E/050. Only the western part of it has been mapped, which can be divided into a massive medium- to coarse-grained phase and a porphyritic phase. The massive unit (Kg) is a leucocratic, medium- to coarse-grained, white to pink granite with only minor (generally <10%) mafic content. It is locally foliated and occasionally banded, due to variable grain size or mafic content. Pegmatite phases are locally observed. The massive granite grades into a porphyritic phase (unit Kg) characterized by pink K-feldspar phenocrysts, typically several centimetres across, in a granitic matrix. The porphyritic granite is similar to the previ-

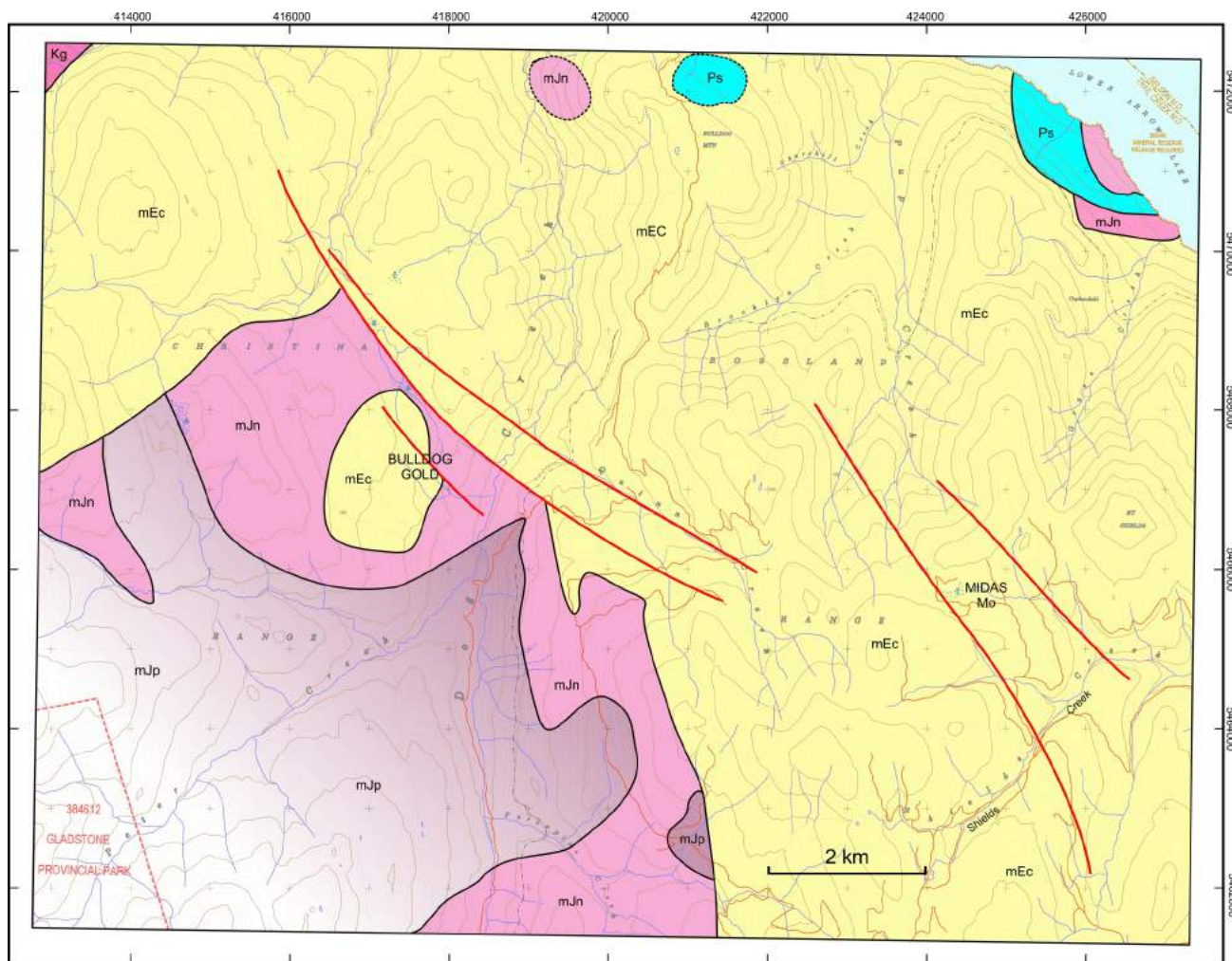


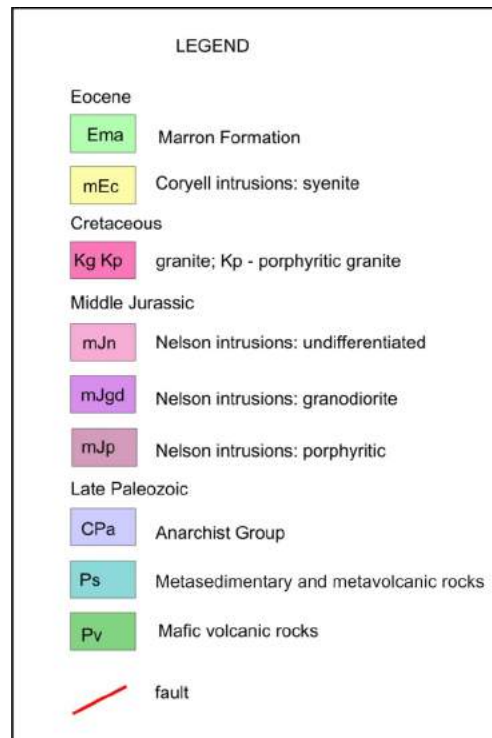
Figure 6. Geology on TRIM map 082E/040 (1:20 000 sheet) in the Deer Lake area, southeastern British Columbia.

ously described porphyritic K-feldspar megacrystic phase of the Nelson suite, but more detailed work (e.g., petrographic and radiometric analyses) is required to establish this distinction with certainty.

A number of small isolated granitic stocks and bodies included in the Cretaceous (?) suite intrude Nelson plutonic rocks west of the main granitic body on TRIM map sheet 082E/049. The larger body, near the centre of the map sheet (Figure 5), contains some pegmatite, brecciation with silicification, druse quartz, minor pyrite and pervasive jarosite alteration.

Coryell Plutonic Suite

Coryell intrusions are a Middle Eocene, alkalic to calcalkalic plutonic suite. In the Deer Park map area (Figure 2), Coryell intrusive rocks are exposed as two large bodies separated by the extensive central uplifted block that marks the northern extension of the Grand Forks complex. The western Coryell body, which has been dated at ca.



51 Ma (U-Pb zircon: Carr and Parkinson, 1989), is largely restricted to an area west of the Granby fault and, in many cases, is truncated by the fault. The eastern Coryell body appears to occur mainly east of the northern projection of the Kettle River fault, though a western lobe in the central part of the map area was shown by Little (1957) to lie west of the fault extension.

The eastern Coryell body is mainly coarse-grained pink syenite with variable (generally <10%) biotite+ hornblende; it commonly grades to a white feldspar-biotite rock with similar texture, but locally higher mafic mineral content. In the field, and on the accompanying maps, phases with mixed pink and white feldspar are termed 'monzonites' and those with mainly white feldspar are termed 'leucocratic diorite'. These phases appear to have gradational rather than intrusive contacts, with an apparent random distribution. The eastern Coryell body is finer grained near its margins, and numerous fine-grained feldspar-porphyry dikes cut the marginal phases and the immediate country rock. In addition, finer grained syenite phases, commonly with intrusive contacts, are frequently observed in the southern part of the eastern Coryell body, in the area within the central and southern portions of TRIM map sheet 082E/040 and on sheet 082E/030.

Only a small part of the western Coryell body was mapped, in the northern and central part of the Deer Park map area. Exposures were similar to those in the east, consisting dominantly of pink syenite with some 'monzonite' phases. Feldspar-porphyry dikes were also common, particularly close to contacts with the Nelson intrusions.

Structural Geology

Structure in the Deer Park map area is dominated by generally north-trending faults that are related to the northern extension of the Grand Forks complex, which is bounded on the west by the west-dipping Granby fault and on the east by the east-dipping Kettle River fault. Detailed structural and metamorphic studies of both the hangingwall and footwall rocks suggest that depth contrasts reach approximately 5 km across both the Granby (Laberge and Pattison, 2007) and Kettle River faults (Cubley and Pattison, 2009).

The Granby fault can be traced the length of the Grand Forks (Höy and Jackaman, 2005) and Deer Park map areas (Figure 2). Immediate hangingwall rocks comprise mainly Coryell intrusive rocks structurally (?) overlain by Eocene Marron Formation volcanic rocks; footwall rocks comprise Middle Jurassic Nelson intrusive rocks and a younger (Cretaceous?) granitic suite. The fault, which is defined as the most eastern splay separating the Coryell and Nelson suites, is constrained to a few metres along the Deadeye Creek road on TRIM map sheet 082E/049 (Figure 5). It is marked there by steeply dipping, closely spaced fractures, brecciation, silicification, potassic (K-feldspar) alteration

and pyrite mineralization. Several fault splays with mainly west-side-down–inferred movement are also mapped in the hangingwall (Figure 5), and thin zones of steep west-dipping mylonite continue for up to 1 km into Nelson rocks in the footwall. Similar splay faults and more complex geometry were also noted in the Granby fault zone farther south where they were mapped in detail by Laberge and Pattison (2007).

The Kettle River fault, on the eastern side of the Grand Forks complex, is extended into the central part of the Deer Park map area (Figure 2) and was inferred by Tempelman-Kluit (1989) to be truncated by the eastern Coryell intrusion (Figure 2); his compilation was based on regional mapping by Little (1957) and the exact distribution of units is not known here. Hence, both the Coryell and older (Tertiary?) intrusion could either cut, or be offset by, the Granby fault. More detailed mapping (Figure 6) indicates that east of the fault the western extension of the Coryell intrusion lies farther north, thereby making an offset of the Coryell by the fault permissive.

Numerous other faults have been recognized in the map area, and the larger of these are shown on the regional (Figure 2) and more detailed TRIM maps (Figures 3, 5, 6). Most have been recognized by offsets or truncations of units, including the youngest intrusions (the Coryell), and many are marked by topographic features. These faults are generally north-trending, parallel to the north-trending Kettle River and Granby faults, or north-northwest-trending, particularly in the eastern part of the map area. They are also generally brittle and marked by minor brecciation, commonly silicification and rare shear fabrics. Quartz veining, with or without minor sulphide minerals, occurs locally along many of these faults and many of the mineralized (gold or precious metal) occurrences are intimately associated with these large structures.

A number of mineral occurrences are known in the map area, but few have had any past production. This report focuses only on the base- and precious-metal occurrences, not on industrial minerals, which are shown on Figure 2 using descriptions from BC MINFILE.

Most occurrences are in the north-trending Granby fault structural zone, or along north- to northwest-trending faults in the eastern block, east of the Kettle River fault. Few, if any, occurrences are noted in the central block, which is underlain by mainly deeper level Middle Jurassic Nelson granites and the younger Cretaceous (?) granitic suite.

Mineralization

The following sections describe briefly some of these mineral occurrences, with specific reference to their structural controls. These descriptions include several occurrences discovered in recent years and not included in BC

MINFILE, and some that have been recently explored; descriptions of other occurrences are given in BC MINFILE.

Deer Park

The Deer Park property, located on the eastern side of Lower Arrow Lake, includes a variety of mineral occurrences discovered by T. Kennedy and optioned to Kootenay Gold Inc. There are no BC MINFILE occurrences here, although there is evidence of past exploration, including a number of trenches and pits. Numerous small copper veins occur within mafic volcanic rocks, a massive north-trending pyrrhotite vein contains anomalous copper and gold, and several areas with silicification and gold-quartz veining occur along prominent north-trending faults and Coryell dikes. These latter occurrences have been the focus of recent exploration by Kootenay Gold Inc. and are described in more detail by Kennedy (2007) and Höy (2008).

The gold-quartz veins appear to be related to late, mainly north-trending faults and shears. These structures are the loci for a suite of steeply dipping dikes of the Coryell suite. The dikes are particularly common in the western part of the Deer Park area where they form a swarm (approximately 700 m wide) extending south over a distance of >3 km toward a large Coryell intrusive body. Several similar and parallel dikes occur approximately 4–5 km to the southeast and also occur parallel to or within steeply dipping faults.

Gold mineralization occurs in both these areas, typically as thin quartz veinlets and extension veins within the shears. Assays of hand samples, collected by T. Kennedy, returned values of 6.3 g/t and 9.5 g/t Au in the northwestern area, and up to 23 g/t Au in the southeastern area.

The north-trending structures are interpreted to be Eocene; they are steeply dipping, trending parallel to regional Eocene structural trends and clearly associated with Coryell dikes. Mineralization, mainly gold with minor sulphide minerals and quartz, commonly occurs in these structures as small extensional veins, which are oblique to the main northerly structural grain.

Bulldog

Bulldog is a recent gold discovery, located near the centre on TRIM map sheet 082E/040 (Figure 6). A series of prominent northwest-trending shears associated with intense propylitic alteration cut an isolated body of Coryell syenite and monzonite within Nelson intrusive rocks. Several parallel faults located to the northeast extend toward the Midas molybdenite property, 12 km to the southeast; they are steeply dipping and at least one of them has minor serpentinized peridotite (?) along it. Mineralization at Bulldog occurs as thin quartz veins and silicification, com-

monly with pyrite and jarosite alteration, and anomalous gold values.

JJ

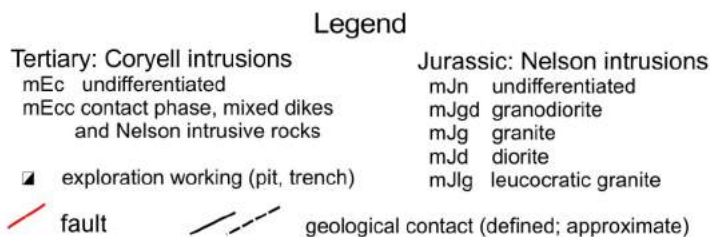
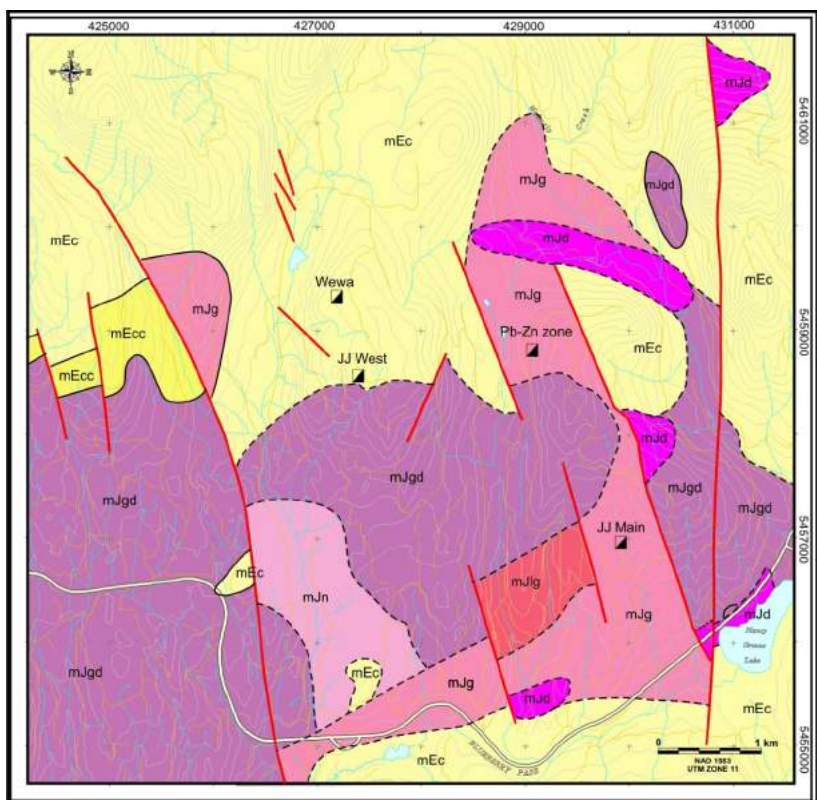
The northern part of the JJ property, optioned by Kootenay Gold Inc. to Astral Mining Corporation, extends into the southeastern part of the Deer Park map area. The property includes a large area that encompasses the past-producing Granville Mountain gold mining camp and several new gold discoveries. These new discoveries, termed ‘JJ West’ and ‘JJ Main’, were the focus of an extensive drilling program by Astral in 2007–2008 and are described below.

The JJ showings occur just north of Blueberry Pass and Nancy Green Lake along Highway 3 (Figure 7) between Castlegar and Christina Lake. They occur mainly in the contact zone between the Middle Eocene Coryell intrusions and host Middle Jurassic Nelson intrusions (Figure 7). The area is structurally complex, with a variety of Nelson intrusive phases and numerous mostly north- to northwest-trending dikes which follow prominent fault and shear zones and extend from the Nelson rocks into the Coryell suite.

The JJ property comprises the two main gold showings, JJ Main and JJ West, as well as the former Wewa occurrence. The Wewa is reported to be a vein, breccia and stockwork showing containing fluorite, chalcopyrite, pyrite and magnetite, and associated with a fault-breccia and molybdenite-bearing quartz vein (MINFILE 082ESE167). The JJ West showing occurs as a number of north-trending shear zones of silicified rock and quartz veining, up to several metres wide, cutting Coryell intrusions. Gold values are locally high, but mostly range up to 1 g/t. The JJ Main showing occurs as a number of roughly northeast-trending shear zones with mineralized quartz veins in fine- to medium-grained ‘granite’ of the Nelson intrusions (Dunne, 2004; Höy, 2006).

The showings occur as quartz stockworks, vein-breccias, ladder veining and a series of parallel-sheeted veins within the shear zones. Larger quartz veins (up to 30 cm thick) consist of quartz with trace pyrite, arsenopyrite and galena. Maximum assay values of 19 g/t Au were obtained from some surface exposures of the veins, although values of up to 2 g/t Au are more common. Höy (2006) established that mineralization at JJ Main appears spatially associated with Coryell ‘syenite’ and mafic dikes, and inferred that mineralization was Eocene.

Astral Mining Corporation completed a 5070 m drilling program on the JJ property in late 2008 and reported that the JJ Main zone has been extended to a strike length of 900 m and to a vertical depth of 240 m. Together with their joint venture partner, Kootenay Gold Inc., they reported “results up to 4 m at 21.04 g/t gold from infill drilling at the



References: Dunne (2004); Hoy (2008); Hoy (this report)

Figure 7. Geology of the JJ property in the Deer Park map area, southeastern British Columbia.

discovery zone” (Astral Mining Corporation and Kootenay Gold Inc., 2008), supporting previous work (Brittcliffe, 2008).

These JJ showings are exciting new gold showings related to Eocene structures and located within several kilometres of the past-producing Granville Mountain gold mining camp.

Midas

Midas is a molybdenite property in Coryell intrusive rocks near the centre on TRIM map sheet 082E/040 (Figure 6). It has seen considerable past exploration, including diamond drilling (Sellmer and DePaoli, 1974), and has recently been acquired by Kootenay Gold Inc.

A variety of Coryell intrusive rocks underlie the Midas property, including coarse-grained syenite, porphyritic quartz syenite and aphanitic feldspar porphyry. These are intruded by dominantly northwest-trending, steeply dipping syenite-porphyry, andesite and lamprophyre dikes. A breccia zone “of nearly the same age as the dyke swarm trends east-west across the intrusive grain” and “a variable, locally intense quartz vein and/or quartz/magnetite vein stockwork cuts all rock types” (Sellmer and DePaoli, 1974), but is most intense next to the breccia zone.

Molybdenite mineralization is found in a variety of environments on the property, including the breccia zone and its margins, quartz veining in highly fractured medium-grained quartz monzonite and with chlorite-magnetite alteration in shear zones cutting the subporphyritic coarse-grained syenite. Sellmer and DePaoli (1974) noted that a mineralized zone intersected in a drillhole at the edge of the breccia contained 0.3% MoS₂ across approximately 16 m.

Mineralization-related structures on the Midas property trend north to northwest, cutting all units. This structural trend is prominent in the eastern part of the Deer Park map area; as these structures cut Coryell rocks, they are syn- to post-Middle Eocene and likely developed late in the extensional history of the area. Furthermore, based on regional mapping, the variety of Coryell rock types and the abundance of dikes suggest emplacement of late porphyritic intrusions at relatively high levels within the main Coryell body.

Summary and Discussion

The Deer Park map area straddles the northern extension of the Grand Fork complex, an uplifted, exhumed-core complex bounded on the west and east by north-trending Eocene extensional faults. Eocene intrusions, the Coryell suite, dominate in the hangingwall of these faults and extend locally from the east into the central uplifted block. Middle Jurassic and Cretaceous (?) intrusions dominate in the central part of the area, north of para- and orthogneisses that define the complex in much of the Gladstone Park area.

The Granby fault defines the western limit of the complex, and extends north the entire length of the Deer Park map area. It cuts and truncates Coryell intrusive rocks and the (structurally?) overlying Eocene age Marron volcanic rocks. The Kettle River fault defines the eastern boundary. It has been traced or extrapolated northward into the Deer Park sheet and, based on early regional mapping (Little, 1957) is inferred to be cut by the Coryell intrusions (Templeman-Kluit, 1989), constraining its age to pre-ca. 51 Ma. This relationship is not well established and requires more detailed mapping before it can be verified.

The area has been traditionally underexplored, despite the importance of the Greenwood, Rosslund and Franklin mining camps located to the south and north. This may be due, in part, to lack of recent government or university surveys, inaccessibility, and perceived nonprospective environment (i.e., lack of structures and area dominated by mainly large Middle Jurassic or Middle Eocene intrusions). However, recent exploration has led to the discovery of several significant new gold occurrences and prospects, most notably mineralized vein systems on the Deer Park property east of Lower Arrow Lake and on the JJ property in the southeastern part of the map area. Furthermore, the exploration and mapping done during this study have shown that the relatively complex internal structure of the Coryell suite in some areas shows a variety of late, high-level intrusive phases and dike swarms, as well as numerous Eocene or younger north- and northwest-trending faults. These faults are commonly the loci for Eocene intrusive activity and, locally, brecciation, as well as for a variety of mineral deposits or occurrences. The faults and associated mineralization appear to be developed at various structural levels, ranging from high-level breccias with epithermal-style mineralization to shear and mylonitic fabrics developed at intermediate structural levels, all of which is evidence that relatively rapid uplift and exhumation of the Grand Forks complex occurred during the Tertiary.

Acknowledgments

Geoscience BC is thanked for its financial support for this study. Several mining companies, most notably Kootenay Gold Inc. and Astral Mining Corporation allowed access to their data, some of which have been incorporated into this study. Numerous discussions with T. Kennedy and C. Kennedy helped in the understanding of both regional and more detailed geology, and field visits with these prospectors as well as J. MacDonald introduced the author to many of the recently discovered mineral occurrences. W. Jackaman is thanked for help in preparing base maps used in the study and G. DeFields for her assistance in the field.

References

Acton, S.L., Simony, P.S. and Heaman, L.M. (2002): Nature of the basement to Quesnel Terrane near Christina Lake, south-

eastern British Columbia; *Canadian Journal of Earth Sciences*, v. 69, p. 65–78.

Astral Mining Corporation and Kootenay Gold Inc. (2008): Astral and Kootenay intersect new stockwork zone and extend main discovery zone to 900 m at Jumping Josephine; Astral Mining Corporation and Kootenay Gold Inc., Marketwire joint press release, 18 November 2008, URL <<http://www.stockhouse.com/BULLBOARDS/MessageDetailThread.aspx?p=0&m=23868417&l=0&r=0&s=AST&t=LIST>> [November 2009].

Brittcliffe, D.A. (2008): Assessment report on diamond drilling at the Jumping Josephine property, Trail and Greenwood mining divisions, southeastern British Columbia; BC Ministry of Energy, Mines and Petroleum Resources, Assessment Report 27 747, 58 p.

Brown, R.L. and Journeay, M. (1987): Tectonic denudation of the Shuswap metamorphic terrane of southeastern British Columbia; *Geology*, v. 15, p. 142–146.

Carr, S.D. and Parkinson, D.L. (1989): Eocene stratigraphy, age of the Coryell batholith, and extensional faults in the Granby valley, southern British Columbia; *Geological Survey of Canada, Paper 89-1E*, p. 79–87.

Carr, S.D., Parrish, R.R. and Brown, R.L. (1987): Eocene structural development of the Valhalla complex, southeastern British Columbia; *Tectonics*, v. 6, p. 175–196.

Church, B.N. (1986): Geological setting and mineralization in the Mount Attwood-Phoenix area of the Greenwood camp; BC Ministry of Energy, Mines and Petroleum Resources, Paper 1986-2.

Cubley, J. and Pattison, D. (2009): Metamorphic contrast across the Kettle River fault, southeastern British Columbia, with implications for magnitude of fault displacement; *Geological Survey of Canada, Current Research 2009-9*.

Drysdale, C.W. (1915): *Geology of the Franklin mining camp*; Geological Survey of Canada, Memoir 15, 246 p.

Dunne, K.P.E. (2004): Geological field mapping report, JJ property, southeastern British Columbia; Kootenay Gold Inc., unpublished internal company report.

Fyles, J.T. (1990): *Geology of the Greenwood-Grand Forks area*, British Columbia; BC Ministry of Energy, Mines and Petroleum Resources, Open File 19.

Höy, T. (2006): *Geology and rock geochemistry, JJ property*, southeastern British Columbia; BC Ministry of Energy, Mines and Petroleum Resources, Assessment Report 28 301.

Höy, T. (2008): *Geology and mineralization, Deer Park property*, southern British Columbia; BC Ministry of Energy, Mines and Petroleum Resources, Assessment Report 29 356.

Höy, T. (in press): *Geology of the Deer Park map area*, southeastern British Columbia (NTS 082E/08); Geoscience BC, 1:50 000 scale.

Höy, T. and Dunne, K.P.E. (2001): *Metallogeny and mineral deposits of the Nelson-Rosslund area*; BC Ministry of Energy, Mines and Petroleum Resources, Bulletin 109.

Höy, T. and Dunne, K.P.E. (2004): *Geology of the Nelson map sheet*; BC Ministry of Energy, Mines and Petroleum Resources, Geoscience Map 2004-2, scale 1:50 000.

Höy, T. and Jackaman, W. (2005): *Geology of the Grand Forks map sheet*; BC Ministry of Energy, Mines and Petroleum Resources, Geoscience Map 2005-2, scale 1:50 000.

- Kennedy, T. (2007): Assessment report on prospecting Deer 2 property, Deer Creek area; BC Ministry of Energy, Mines and Petroleum Resources, Assessment Report 29 003, 9 p.
- Laberge, J.R. and Pattison, D.R.M. (2007): Geology of the western margin of the Grand Forks Complex: high grade Cretaceous metamorphism followed by early Tertiary extension on the Granby fault; *Canadian Journal of Earth Sciences*, v. 44, p. 199–208.
- Little, H.W. (1957): Kettle River, British Columbia; Geological Survey of Canada, Map 6-1957.
- Little, H.W. (1960): Nelson map-area, west half, British Columbia; Geological Survey of Canada, Memoir 308.
- Little, H.W. (1979): Geology of the Greenwood map area, British Columbia; Geological Survey of Canada, Paper 79-29.
- Logan, J. (2000): Plutonic related gold-quartz veins in southern British Columbia; *in* Geological Fieldwork 1999, BC Ministry of Energy, Mines and Petroleum Resources, Paper 2000-1, p. 193–206.
- Marquis, G. and Irving, E. (1990): Observing tilts in midcrustal rocks by paleomagnetism: examples from southeastern BC; *Tectonics*, v. 9, no. 5, p. 925–934.
- MINFILE (2009): MINFILE BC mineral deposits database; BC Ministry of Energy, Mines and Petroleum Resources, URL<<http://minfile.ca>> [November 2009].
- Parrish, R.R., Carr, S.D. and Parkinson, D.L. (1988): Eocene extensional tectonics and geochronology of the southern Omineca belt, British Columbia and Washington; *Tectonics*, v. 72, p. 181–212.
- Preto, V.A. (1970): Structure and petrology of the Grand Forks Group, BC; Geological Survey of Canada, Paper 69-22.
- Sellmer, H.W. and DePaoli, G.M. (1974): 1973 geological, geochemical and geophysical assessment report; BC Ministry of Energy, Mines and Petroleum Resources, Assessment Report 5197.
- Tempelman-Kluit, D.J. (1989): Geology, Penticton, British Columbia; Geological Survey of Canada, Map 1736A.
- Wingate, M. and Irving, E. (1994): Extension in high grade terranes of the southern Omineca Belt, British Columbia: evidence from paleomagnetism; *Tectonics*, v. 13, no. 2, p. 686–711.

Ultramafic Intrusions, Detailed Geology and Geobarometry of the Jurassic Bonanza Arc in the Port Renfrew Region, Southern Vancouver Island (NTS 092C)

D. Canil, School of Earth and Ocean Sciences, University of Victoria, Victoria, BC; dcanil@uvic.ca

D. Canil (2010): Ultramafic intrusions, detailed geology and geobarometry of the Jurassic Bonanza Arc in the Port Renfrew region, southern Vancouver Island; in Geoscience BC Summary of Activities 2009, Geoscience BC, Report 2010-1, p. 141–148.

Introduction

Several isolated bodies of ultramafic rock were discovered in the Port Renfrew area of southern Vancouver Island over the past nine years by G. Pearson. A field mapping study jointly funded by Geoscience BC and Emeralds Fields Resources was conducted to ascertain the areal extent of the ultramafic bodies and to determine their relationship with other rocks of southern Vancouver Island. The objective was to use this and other petrological information from the surrounding area to assess the economic significance of the ultramafic bodies as a potential target for Ni-Cu or platinum-group element (PGE) deposits, and the overall structural thickness and setting of the Jurassic Bonanza Arc. This report summarizes results of the geological fieldwork, including detailed mapping, sampling, geobarometry and geochemical assays of the ultramafic rocks.

Field Area and Access

The field area on southern Vancouver Island (NTS 092B, C, F, G) is bordered by the San Juan River to the south, Cowichan Lake to the north, Nitinat Lake to the west and the Fleet River to the east (Figure 1). The area of interest is in and surrounding the NTS 092C map area. The physiography of the area is one of generally steep forested slopes, divided by streams cutting through bedrock and alluvium to create considerable relief. Open valleys are present along the San Juan River and to a lesser degree along the Gordon River.

The area is accessed by a network of logging roads in various states of preservation. Overall, bedrock exposures are best along active logging roads and in elevated areas that have been recently logged. Most areas were accessed by four-wheel drive truck, but a few remote mountaintops with overgrown logging roads could be accessed only by helicopter.

Keywords: ultramafic, arc, Jurassic, nickel, Bonanza, geobarometry

This publication is also available, free of charge, as colour digital files in Adobe Acrobat® PDF format from the Geoscience BC website: <http://www.geosciencebc.com/s/DataReleases.asp>.

Survey Methods

Bedrock geology was mapped at 1:25 000 scale on Terrain Resource Inventory Mapping (TRIM) map sheets and compiled to 1:50 000 scale (Figure 1). Samples for thin-section petrography, geochemistry, fire assay and geochronology were taken (Figure 2). Detailed examinations of select ultramafic bodies could not be compiled onto the 1:50 000 scale geology maps but are described in detail in related papers (Larocque and Canil, 2007, 2009).

Regional Geology Overview

Previous geological maps in the area were mapped at 1:100 000 scale and compiled to 1:250 000 scale (Muller, 1983). Most of the area is underlain by rocks of Wrangellia. The Devonian Sicker Group forms the basement to Wrangellia on Vancouver Island, and consists of mafic and felsic volcanic and volcanoclastic rocks, overlain by epiclastic and carbonate sedimentary rocks of the Permian Buttle Lake Group. Unconformably overlying the Buttle Lake Group are the Triassic Karmutsen basalts, in turn overlain by the Quatsino Formation, a thin (<75 m) sequence of micritic limestone. The Parsons Bay Formation, a 35 m thick sequence of thinly bedded argillaceous mudstone, limestone, siltstone and sandstone, conformably overlies the Quatsino Formation (Nixon and Orr, 2007).

The Port Renfrew region is underlain mostly by rocks of the Jurassic Bonanza Arc, which intrudes, as well as unconformably overlies, the older units of Wrangellia. Clastic sedimentary rocks of the Oligocene Carmanah Group unconformably overlie all older units along the western coast of the island. Quaternary glacial till and alluvium covers stream valleys.

Jurassic Bonanza Arc

In the field area, rocks of the Bonanza Arc are separated from the Jurassic-Cretaceous Pacific Rim Terrane to the south by the San Juan fault and from the Sicker Group to the north by the Cowichan fault. The Jurassic-aged rocks of the Bonanza Arc in Wrangellia include, from base to top, the Westcoast Crystalline Complex (WCC), the Island Plutonic suite and the Bonanza Group volcanics. These rocks have undergone zeolite- to locally greenschist-facies

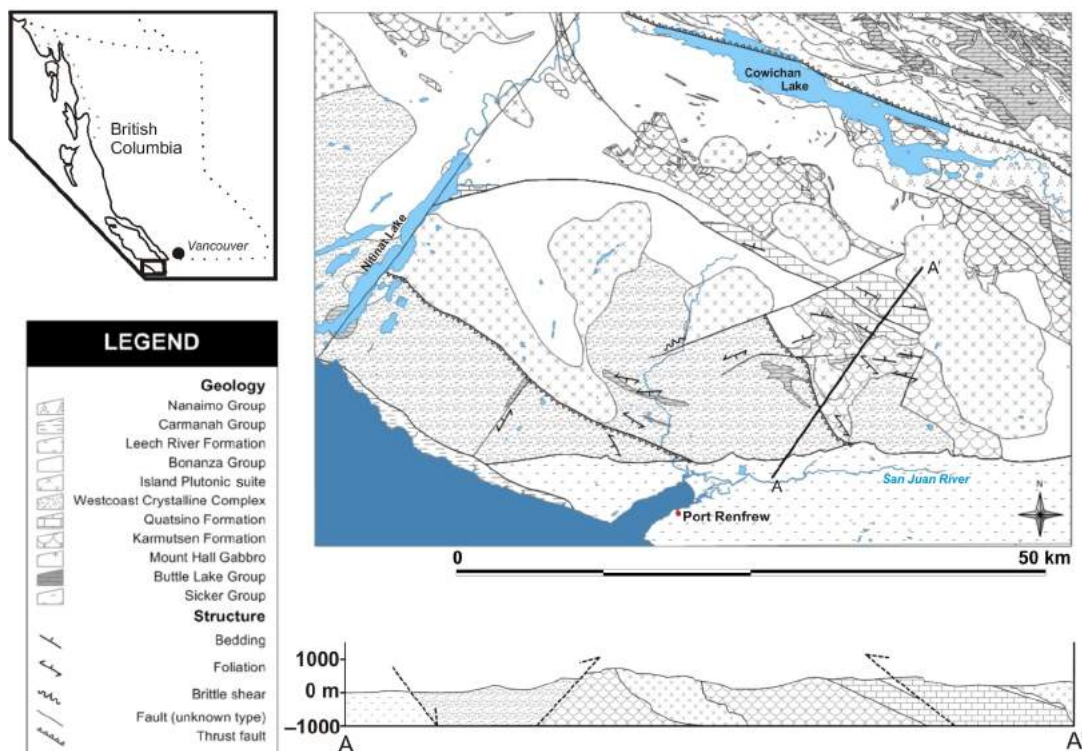


Figure 1. Geology of the field area and location of the field area (inset map), southern Vancouver Island, British Columbia. The cross-section (lower left) is along the line of A-A'. The region was mapped at a scale of 1:20 000 and compiled to 1:50 000 scale. Also shown for reference are the town of Port Renfrew, Nitinat Lake, Cowichan Lake and the trace of the major structures (San Juan fault and Cowichan uplift).

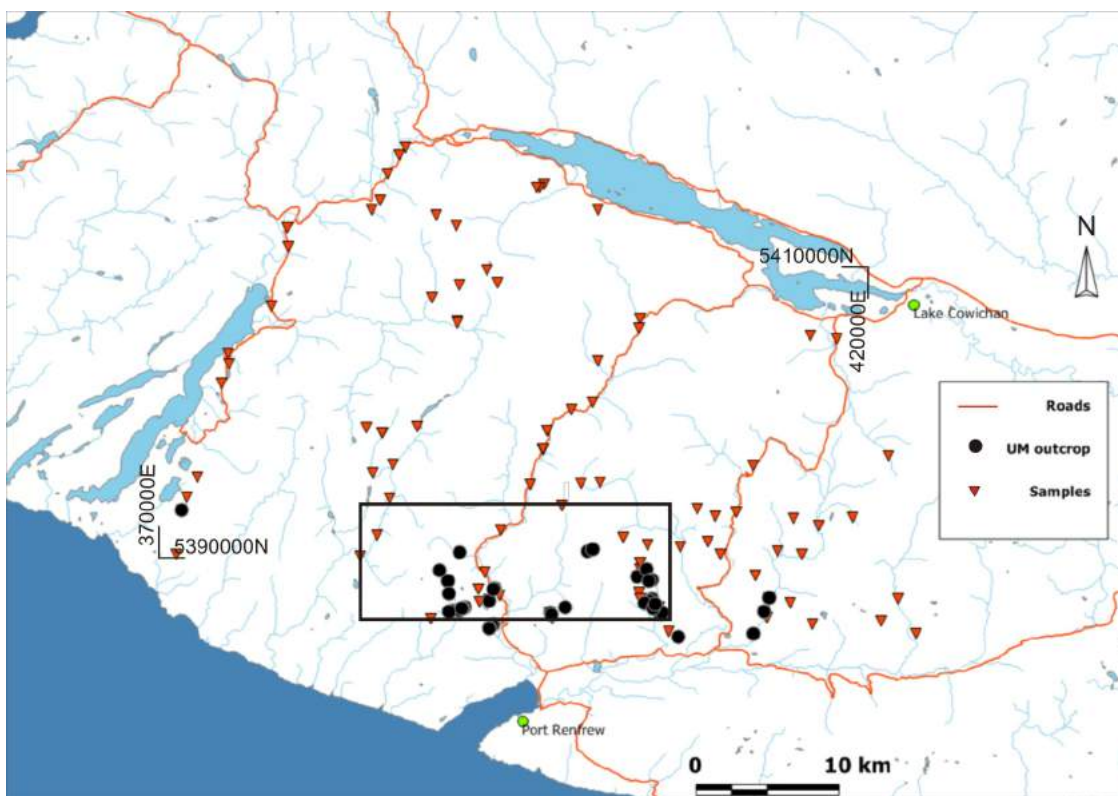


Figure 2. Areas traversed with all sample locations (red inverted triangles), the mainline forestry roads (red lines) and ultramafic outcrop locations (black circles), southern Vancouver Island, British Columbia. The box in the centre shows the location of the Pearson claim block.

metamorphism, but original igneous lithological names are used in their description.

Westcoast Crystalline Complex

The Westcoast Crystalline Complex (WCC) represents the deepest preserved structural level of the Bonanza Arc and is dominantly quartz diorite and gabbro with varying amounts of hornblende, biotite, orthopyroxene and clinopyroxene with accessory magnetite, ilmenite, pyrite and pyrrhotite. Weakly concordant diabase bodies are found locally in the WCC in the field area southwest of the Gordon River. Grain sizes vary from fine grained to pegmatoid and are heterogeneous over a scale of metres.

Distinct units of light grey impure marble 3–10 m thick occur in the diorite. Some marble units can be traced for a few kilometres along an orientation parallel to regional strike. Marble outcrops found in the eastern part of the field area are more irregular in outcrop pattern. Minor magnetite-rich skarn bodies, with variably developed diopside-garnet and magnetite-chalcopyrite-pyrite assemblages, are found at the contact of diorite or diabase with the marble. Due to the

metamorphosed nature of these carbonate rocks, they are here suggested to represent fragments and/or faulted slices of carbonate rocks belonging to the Permian Buttle Lake Formation or the older Sicker Group, which are now screens or septa in the intrusive rocks of the WCC.

Ultramafic Rocks

The largest concentrations of ultramafic rocks are present along the Granite Creek mainline and at the top of Fairy mountain (Figure 2). Other bodies are recognized west of the Griesen mainline in the Twin Lakes area. Details of their geochemistry, petrology and origin can be found elsewhere (Larocque, 2008; Larocque and Canil, 2009)

Ultramafic rocks occur as discrete bodies within the WCC diorite, ranging in size from a metre to several tens of metres. Although their borders are often obscured by overburden, there is some lateral continuity or concentration of the ultramafic bodies over distances of up to 1 km. Contact relationships between the ultramafic bodies and the WCC diorite are quite variable. Smaller bodies, which tend to be more olivine rich, have either abrupt, undeformed contacts

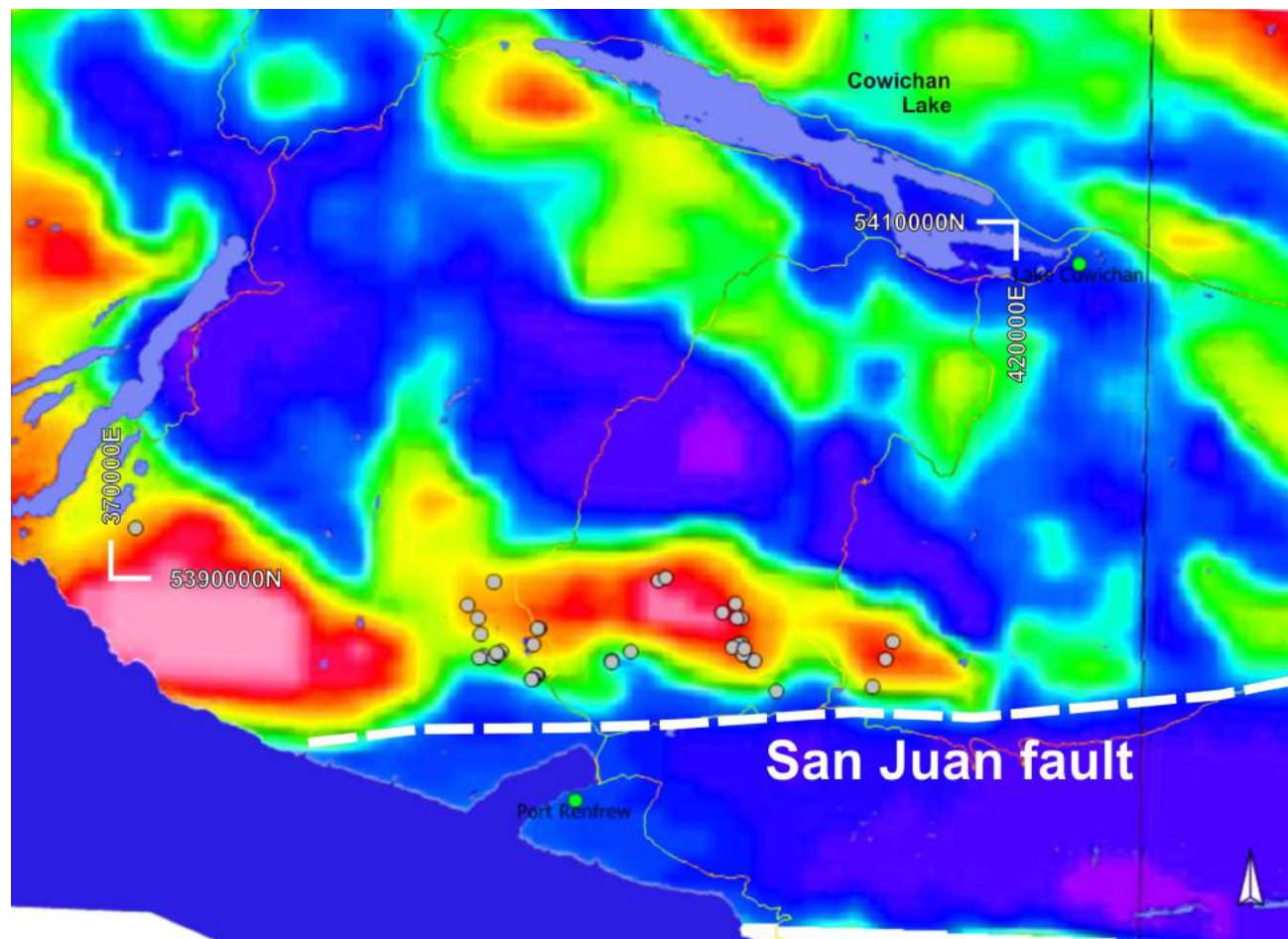


Figure 3. Regional aeromagnetic map (from BC Geological Survey, 2009) superimposed on locations of ultramafic rocks (grey circles) in the map area, southern Vancouver Island, British Columbia.

with their host or are present as sheared pods. Larger bodies, which are mostly olivine gabbro, grade into the diorite of the WCC. In several locations, the association of olivine pyroxenite with pegmatitic hornblende diorite has been noted.

In thin section, peridotite and olivine pyroxenite consist of variably serpentinized cumulus olivine with inclusions of euhedral spinel, poikilolitically enclosed by either orthopyroxene, amphibole, or more rarely, clinopyroxene. Orthopyroxene and clinopyroxene coexist in several samples. Weakly to strongly altered plagioclase is present as an intercumulus phase in some samples. In these samples, olivine is never directly in contact with plagioclase, and is always mantled by a corona of pyroxene. Where present, amphibole appears as the result of reaction with pyroxene, along grain boundaries or along exsolution lamellae. Igneous phlogopite is also present as a minor phase in some samples.

Gabbro and gabbro-norite display cumulus plagioclase, plus or minus orthopyroxene, clinopyroxene and, in one case, olivine. Much of the postcumulus clinopyroxene has been replaced by amphibole. Plagioclase in these samples is invariably less altered than in the peridotite and olivine pyroxenite samples. Chromite is the dominant opaque phase in the ultramafic samples. Magnetite with minor ilmenite exsolution is both a euhedral and intercumulus phase in the gabbroic rocks. Minor amounts of chalcopyrite are noted in most samples. Rare inclusions of round, white, high-reflectivity grains in olivine (possibly identified as pentlandite) are also noted.

Regional-scale aeromagnetic data available for southern Vancouver Island shows a prominent magnetic high, running parallel to, and extending north from, the San Juan fault. At this resolution, the magnetic anomaly appears to roughly correspond to areas underlain by the WCC (and ultramafic) rocks (Figure 3).

Island Plutonic Suite

The Island Plutonic suite occurs as a roughly southeast aligned series of medium-grained plutons ranging in composition from quartz diorite to alkali feldspar granite. The Island Plutonic suite most commonly intrudes the Triassic Karmutsen basalts, and is distinguished from plutons of similar composition of the WCC by lacking any foliation. The contact between the Island Plutonic suite and the WCC is not well defined. In the field area, rocks of the Island Plutonic suite occur mainly in the northern and eastern parts of the field area, separated from the WCC to the southwest by intervals of Karmutsen basalt and Quatsino limestone, which are in fault contact (to the southwest) with rocks of the WCC.

Bonanza Volcanics

The Bonanza volcanics are only very weakly metamorphosed, displaying assemblages indicative of the zeolite facies and varying from aphanitic basalt through plagioclase-, pyroxene- and/or hornblende-phyric andesite to minor dacite and lesser pyroclastic deposits. The lateral extent and continuity of these deposits is obscured by vegetation and overburden. No contacts between Bonanza volcanics and plutonic rocks were observed.

Geochronology

Geochronological investigations were undertaken to constrain the age of rocks that host the ultramafic bodies. Four samples were obtained in different parts of the map area and were submitted for age dating by the U-Pb zircon method at the Pacific Centre for Isotopic and Geochemical Research (PCIGR) at The University of British Columbia. The ages obtained as of this writing are still preliminary but the range in U-Pb ages of zircons is between 194 and 174 Ma (Table 1). In the WCC near Lens Creek in the southeastern part of the map area, melanodiorite is crosscut by a dike of leucodiorite. Both the leuco- and melanodiorite returned ages of 174 Ma. In the southwest, mylonitized diorite near Twin Lakes has an age of 194 Ma. Further west, an undeformed granodiorite pluton near Glad Lake also returned an age of 192 Ma. Thus, magmatism spans an age of at least 20 Ma. All the ages obtained in this study fall within those of the Bonanza Arc elsewhere along strike in the Port Alberni and Bamfield areas (DeBari et al., 1999). Because the diorite hosting ultramafic rocks along both the Granite Creek mainline and on top of Browns mountain is identical to that for which ages were obtained, the ultramafic rocks in the Port Renfrew area are almost certainly Jurassic in age and are related to the Bonanza Arc. A Jurassic age rules out that the ultramafic rocks are cumulate blocks from the older Triassic Karmutsen lavas.

Structural Geology

Foliations within the WCC rocks are defined by a planar fabric of hornblende or biotite, or by a gneissosity of mafic and felsic layers, and generally strike northwest and dip 60–75° to the southwest. Poles to foliations in the WCC between Gordon River and Harris Creek (Figure 1) define a great circle with a pole plunging approximately 50° to the south-southeast (Figure 4). Well-developed minor folds in

Table 1. Uranium-lead zircon ages for samples from the Bonanza Arc in the Port Renfrew region, southern Vancouver Island, British Columbia.

Location	Sample Number	Rock type	U-Pb age (Ma)
Lens Creek	JL110B	leucodiorite	174.1 ± 0.4
Lens Creek	JL110	melanodiorite	174.8 ± 0.5
Twin Lakes	DC0507	diorite mylonite	193.7 ± 0.5
Glad Mainline	DC0637	granodiorite	192.6 ± 0.4

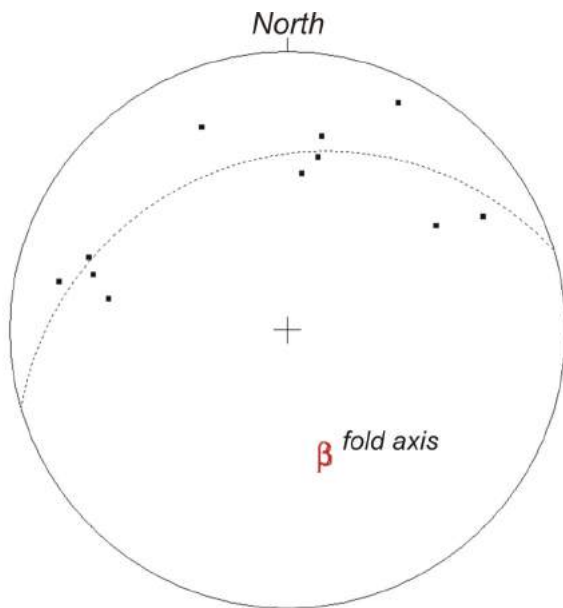


Figure 4. Stereonet projection of poles to foliations for WCC diorite in the area between Gordon River and Harris Creek. Poles to foliations define a girdle having a pole () that defines the regional fold axis (plunging 50° to the south-southeast). Minor folds in diorite on Fairy mountain and near Twin Lakes have nearly identical orientations.

the WCC are evident on Browns mountain and near the Twin Lakes region, and have axes plunging with nearly identical orientations as the major fold axis in Figure 5.

The map pattern of the same rocks northwest of the Gordon River mainline, however, is more consistent with closed folds but plunges northwest rather than southeast. One possible explanation is that the Jurassic units (at least the WCC) are folded along doubly plunging axes (both northwest and southeast) that converge to form a dome structure somewhere between Twin Lakes and Browns mountain. The location where the fold axis changes plunge from northwest to southeast contains the highest concentration of ultramafic rocks. Thus, the WCC, the Island Plutonic suite and the Bonanza Group in the field area are all part of a larger fold structure plunging with fold axes in the northwest and southeast directions, exposing varying structural depth.

Near Harris Creek, a large area of Karmutsen basalt is juxtaposed with the WCC diorite along a 10 m thick shear zone with the same attitude as the pervasive foliation in the diorite. The shear zone is well exposed along the Harris Creek and southern Hemmingsen mainlines. Less obvious shear zones are defined by centimetre- to metre-thick mylonite horizons in the more western parts of the field area, within the WCC diorite near Camper Creek and Twin Lakes. These faults are expressed on topographic and aeromagnetic maps in the southwest portion of the map area.

The common orientation and sense of shear (tops to north-east) in both the mylonite near Twin Lakes and the Harris Creek–Hemmingsen shear zone suggest that the WCC occurs as a series of east-verging thrust-faulted panels. At least two major thrust-faulted panels are recognized: the westernmost panel thrusts the WCC over itself, and the easternmost panel places the WCC onto the Karmutsen basalts and the Quatsino limestone (Figure 1). In this way, it is possible that the WCC is an imbrication of several thrust-faulted panels, but some of the faults are not recognized due to cover.

Downplunge projections of the rock units (along a fold axis plunging 50° to the south-southeast) suggest that at least 15 km of structural depth is exposed in the Jurassic units throughout the entire field area. This is generally consistent with pressures of crystallization obtained by aluminum-in-hornblende geobarometry on granodiorite and diorite plutons in the map area along a line normal to regional strike from Twin Lakes in the west to Cowichan Lake in the east.

Geobarometry

The overall thickness of the entire Bonanza Arc section on Vancouver Island is not known due to a lack of constraints on its structural thickness. This portion of the study addressed this problem by estimating the relative depth of exposure and structural thickness in the Bonanza Arc using aluminum-in-hornblende barometry of its felsic plutons. Coupled with geological data, the structure of exposed arc crust comprising Vancouver Island is assessed.

Felsic rocks were sampled from different parts of the WCC (quartz diorite and granodiorite) and medium- and coarse-grained granodiorite to monzonite were sampled from the Island Plutonic suite. Major and minor elements were determined for amphibole and plagioclase using a CAMECA SX50 electron microprobe at The University of British Columbia. Operating conditions were 15 kV acceleration voltage at a beam current of 20.1 nA and counting times of 20 s on peaks. Standards included natural olivine, diopside, anorthite, albite, orthoclase, kaersutite, rutile and fayalite. In each sample, from four to ten grains each of amphibole and plagioclase were measured, with analyses of both cores and rims on each grain.

The aluminum-in-hornblende barometer (P_{Hbl}) was applied to rocks containing quartz to buffer silica activity and with hornblendes having $Mg/Mg+Fe > 0.35$ (Anderson and Smith, 1995). Where plagioclase was fresh, the hornblende–plagioclase geothermometer (Holland and Blundy, 1994) was applied to estimate temperature. For the samples, a aluminum-in-hornblende barometer formulation is applied that accounts for the effects of temperature T_{HB} on the Al content of hornblende using T_{HB} (Anderson and Smith, 1995).

This study, which was extended for Jurassic plutons across much of Vancouver Island (Canil et al., in press), consistently shows the highest crystallization depths in WCC plutons (10–18 km; Figure 6), supporting the notion that this unit represents the deepest levels of the Bonanza Arc (DeBari et al., 1999). The WCC is well exposed in southernmost Vancouver Island in the Victoria area (Figure 6) and in the Port Renfrew area extending along the west coast of Vancouver Island. If the San Juan fault is considered a strike-slip fault, the restoration of ~80 km of sinistral movement along this fault brings the depths recorded in the WCC in the Victoria area in line with those in Port Renfrew (13 km) and Gold River (12 km), suggesting these plutons were once continuous along strike. If so, the San Juan fault must be younger than the Bonanza Arc (170 Ma) and older than the maximum age of the Nanaimo Group (93 Ma; Mustard, 1994), because sedimentary rocks of the latter are not offset by this fault. Considering any dip-slip component in this fault will reduce the estimate of strike-slip movement.

On southern Vancouver Island, five samples of the Island Plutonic suite all crystallized at depths of approximately 4–5 km but are too sparsely distributed to reveal any regional structural information along a transect normal to regional strike from Port Renfrew in the west to Ladysmith in the east. The depths of exposure from this study for plutons on southern Vancouver Island suggest this suite must exist as numerous thin, tabular bodies to fit within the stratigraphically measured thicknesses of pre-Jurassic supracrustal rocks on Wrangellia (Figure 6). When comparing P_{Hbl} with stratigraphic sections for Wrangellia, the results are not supportive of previous interpretations (Yorath et al., 1985) that Paleozoic and Mesozoic strata of Wrangellia are ‘roof pendants’ perched on an underlying Jurassic plutonic complex. To fit the depths from hornblende barometry and map patterns, the Jurassic arc intrusions must be tabular and intrude within the stratigraphy of the older units of Wrangellia, which can be mapped as septa within the intrusions.

There are fewer constraints on the Wrangellia stratigraphy into which the lesser sampled and more mafic WCC intruded. The few depth constraints for crystallization suggest that unlike the more evolved granitic Island Plutonic suite, this mafic-ultramafic unit intruded depths greater than any measured stratigraphic thicknesses of Devonian

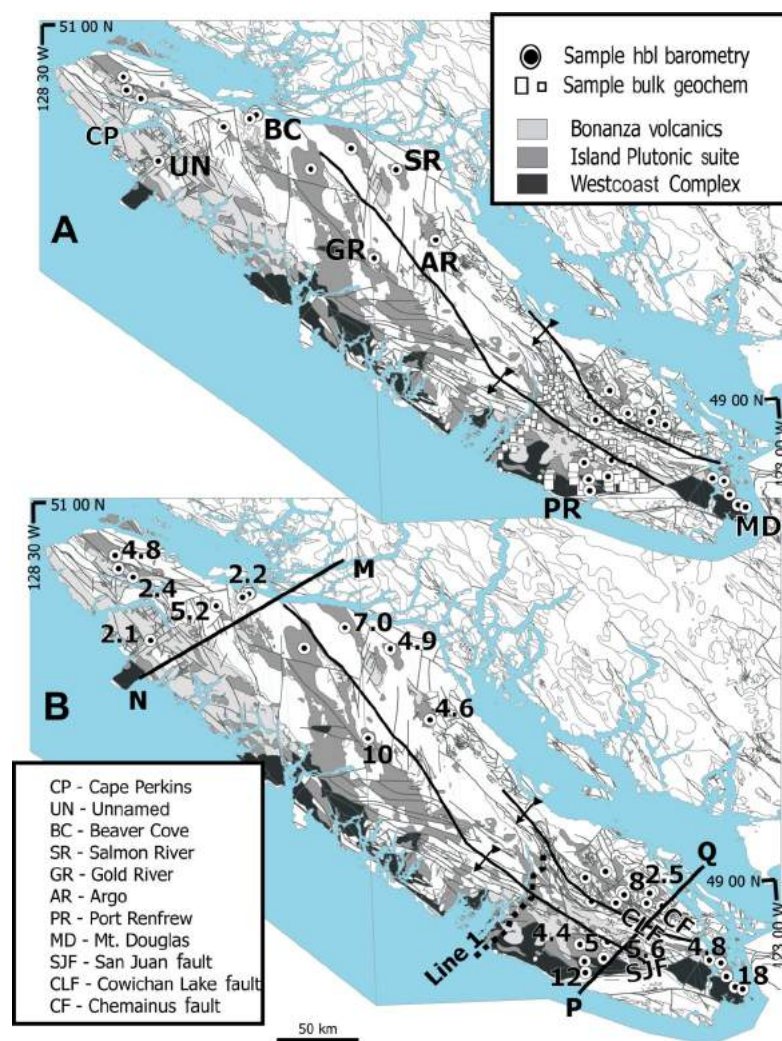


Figure 5. Vancouver Island, British Columbia, showing only the major regional structures and geology of the Jurassic Bonanza Arc, subdivided into Bonanza volcanic rocks, Island Plutonic suite and Westcoast Crystalline Complex: a) Sample locations for hornblende barometry (this study); b) As above but showing depth of crystallization of plutons from aluminum-in-hornblende barometry (assuming 100 MPa = 3 km depth). Not all barometric results are shown for clarity.

and Triassic supracrustal rocks, likely in the middle and lower crust below them (Figure 6).

Economic Geology

Assays of the ultramafic rocks returned generally low values of Au, Pt and Pd (1–7 ppb). This is not surprising given the low amounts of sulphide in the samples. Ultramafic rocks occur in several geological settings. The ultramafic cumulates in the WCC around the Port Renfrew area are inconsistent with an ophiolite association or ‘Alaskan-type’ intrusion (Larocque and Canil, 2007)

Peridotite and pyroxenite bodies with identical petrographic and geological relationships are noted to occur towards the middle and base of crust in exhumed island arc terranes. Such an interpretation for these rocks in the Port

Renfrew area is commensurate with their thermobarometry (Canil et al., in press; Larocque and Canil, 2009). The Bonanza Arc and its setting on Vancouver Island are very similar to the Talkeetna Arc in south-central Alaska, and it has been proposed that the two are of similar age and can be correlated along strike (DeBari et al., 1999).

Future Work

The majority of the ultramafic bodies in the Port Renfrew area are discontinuous and tend to be distributed in patches throughout the WCC. Areas of significant concentration are on Fairy mountain and along the Granite Creek mainline. Areas of the WCC that host ultramafic rocks appear to correspond with magnetic highs in both the regional and detailed aeromagnetic surveys. The aeromagnetic highs may also correspond with laterally discontinuous magnetite skarn, which are strongly magnetic in outcrop. Because neither of the latter rock types is specifically associated with ultramafic rocks, further detailed magnetic surveys in the field area will not be exclusive to the detection of ultramafic rocks.

If the regional magnetic signal is controlled by the presence of ultramafic rocks, there may be a significant amount of these rocks hidden at depth within the WCC. Geophysical investigations (detailed gravity survey) or drilling may re-

veal the continuity between these or other surface ultramafic bodies at depth beneath the area.

No significant concentrations of chromite, sulphides or platinum-group minerals were noted in the ultramafic rocks in outcrop, hand sample or thin section. Only minor amounts (<2%) of Cu- and Ni-sulphides (chalcopyrite, pentlandite, pyrrhotite) or chromite are seen in thin section. For this reason, and in view of the discontinuous exposure of the ultramafic rocks, heavy-mineral stream sampling is not likely to be an effective method for uncovering further occurrences of these rocks.

Magnetite skarn bodies, if of significant economic interest, may be detected near the surface by magnetic surveys, looking for a contrast of units with weak magnetism (marble) adjacent to strong magnetism (magnetite). Because the marble bodies appear to have some structural continuity (Figures 4, 5), areas for detailed survey are best accomplished along strike of existing magnetite bodies. The Jurassic rock units are folded, however, and it is possible that the magnetite skarn bodies plunge with depth along the regional fold axes, explaining why they are not observed continuously along strike in outcrop at the surface. Further delineation at depth of the existing magnetite bodies might be located by drilling orthogonal to the plunge of regional folds.

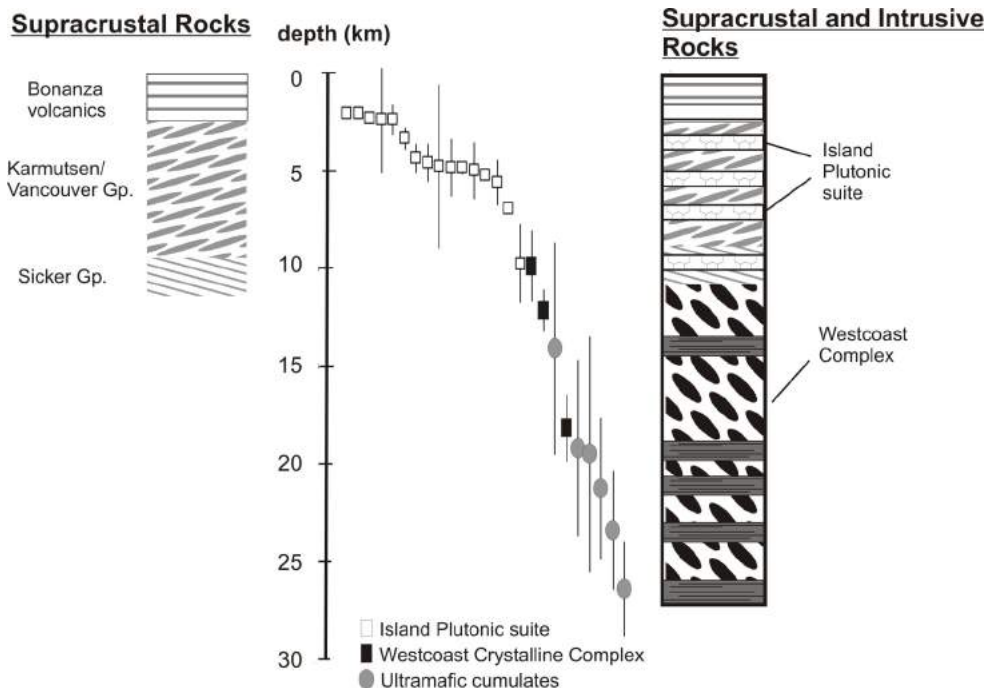


Figure 6. Sections for Wrangellia on Vancouver Island, British Columbia, drawn to accommodate the measured stratigraphic thicknesses for Bonanza volcanic rocks and pre-Jurassic supracrustal rocks of the Vancouver and Sicker groups (left-hand panel) with the depths of crystallization from hornblende barometry of plutons from the Island Plutonic suite and the Westcoast Crystalline Complex (Canil et al., in press) and ultramafic cumulates (Larocque, 2008). The right-hand panel shows how the range of hornblende pressures can be accommodated in the section by having the Island Plutonic suite intrude as several thinner tabular bodies throughout the pre-Jurassic stratigraphy, and with plutons of the Westcoast Crystalline Complex emplaced below both of the latter.

Acknowledgments

First and foremost, the author thanks P. Heatherington and G. Pearson in Port Renfrew for their support, assistance and generosity in this project. J. Larocque carried out the majority of this project for his M.Sc. thesis. Assistance for various aspects of the project was provided by R. Friedman, H. Steenkamp, E. Bonnet, J. Kyba, J. Styan and O. Canil. The author thanks N. Massey, G. Nixon, L. Coogan, A. Hynes, S. DeBari, S. Johnston and P. Luffi for their criticism, comments, reviews or input at various stages.

References

- Anderson, J.L. and Smith, D.R. (1995): The effects of temperature and fO_2 on the Al-in-hornblende barometer; *American Mineralogist*, v. 80, p. 549–559.
- BC Geological Survey (2009): MapPlace GIS internet mapping system; BC Ministry of Energy, Mines and Petroleum Resources, MapPlace website, URL <<http://www.MapPlace.ca>> [November 2009].
- Canil, D., Styan, J., Larocque, J., Bonnet, E. and Kyba, J. (in press): Thickness and composition of the Bonanza Arc crustal section, Vancouver Island, Canada; *Geological Society of America Bulletin*.
- DeBari, S., Anderson, R.G. and Mortensen, J.K. (1999): Correlation among lower to upper crustal components in an island arc: the Jurassic Bonanza Arc, Vancouver Island, Canada; *Canadian Journal of Earth Sciences*, v. 36, p. 1371–1413.
- Holland, T. and Blundy, J. (1994): Non-ideal interactions in calcic amphiboles and their bearing on amphibole-plagioclase thermometry; *Contributions to Mineralogy and Petrology*, v. 116, p. 433–447.
- Larocque, J. (2008): The role of amphibole in the evolution of arc magmas and crust: the case from the Jurassic Bonanza Arc section, Vancouver Island, Canada; M.Sc. Thesis, University of Victoria, 160 p.
- Larocque, J. and Canil, D. (2007): Ultramafic rock occurrences in the Jurassic Bonanza Arc near Port Renfrew (NTS 092C/09, 10, 15, 16), southern Vancouver Island; *in Geological Fieldwork 2006*, BC Ministry of Energy, Mines and Petroleum Resources, Paper 2007-1 and Geoscience BC, Report 2007-1, p. 319–324.
- Larocque, J. and Canil, D. (2009): The role of amphibole in the evolution of arc magmas and crust: the case from the Jurassic Bonanza Arc section, Vancouver Island, Canada; *Contributions to Mineralogy and Petrology*, doi:10.1007/s00410-009-0436-z.
- Muller, J.E. (1983): *Geology of Victoria*; Geological Survey of Canada, Map 1553A, scale 1:100 000.
- Mustard, P.J. (1994): The Upper Cretaceous Nanaimo Group, Georgia Basin, *in* Monger, J.H. (ed.), *Geological Hazards of the Vancouver Region*, south-western British Columbia, Geological Survey of Canada, p. 97–170.
- Nixon, G.H. and Orr, A.J. (2007): Recent revisions to the early Mesozoic stratigraphy of Vancouver Island and metallogenic implications, British Columbia; *in Geological Fieldwork 2006*, BC Ministry of Energy, Mines and Petroleum Resources, Paper 2007-1, p. 163–177.
- Yorath, C.J., Green, A.G., Clowes, R.M., Sutherland Brown, A., Brandon, M.T., Kanasewich, E.R., Hyndman, R.D. and Spencer, C. (1985): Lithoprobe, southern Vancouver Island: seismic reflection sees through Wrangellia to the Juan de Fuca Plate; *Geology*, v. 13, p. 759–762.

New Results of Geological Mapping and Micropaleontological and Lead Isotopic Studies of Volcanogenic Massive Sulphide–Hosting Stratigraphy of the Middle and Late Paleozoic Sicker and Buttle Lake Groups on Vancouver Island, British Columbia (NTS 092B/13, 092C/16, 092E/09, /16, 092F/02, /05, /07)

T. Ruks, Mineral Deposit Research Unit, Department of Earth and Ocean Sciences, University of British Columbia, Vancouver BC; tyler_ruks@hotmail.com

J.K. Mortensen, Mineral Deposit Research Unit, Department of Earth and Ocean Sciences, University of British Columbia, Vancouver BC

F. Cordey, CNRS UMR 5125, Université Claude Bernard Lyon 1, 69622, Villeurbanne Cedex, France

Ruks, T., Mortensen, J.K. and Cordey, F. (2010): New results of geological mapping, micropaleontological and lead isotopic studies of volcanogenic massive sulphide–hosting stratigraphy of the middle and late Paleozoic Sicker and Buttle Lake groups on Vancouver Island, British Columbia (NTS 092B/13, 092C/16, 092E/09, /16, 092F/02, /05, /07); in Geoscience BC Summary of Activities 2009, Geoscience BC, Report 2010-1, p. 149–170.

Introduction

Volcanogenic strata of the mid-Paleozoic Sicker Group on Vancouver Island (Figure 1) occur in several distinct basement highs (referred to herein as ‘uplifts’). These rocks host the world-class Myra Falls volcanogenic massive sulphide (VMS) deposit (combined production and proven and probable reserves in excess of 40 million tonnes of Zn-Cu-Au-Ag sulphides), as well as numerous other VMS deposits and occurrences, including those in the Big Sicker Mountain area in the southeastern part of the Cowichan Lake uplift (Figure 1). Three of these deposits in the Cowichan Lake uplift, the Lenora, Tye and Richard III (MINFILE occurrences 092B 001, 092B 002, 092B 003; MINFILE, 2010), have seen limited historical production. The Lara deposit (MINFILE occurrence 092B 129), farther to the northwest, also contains a significant drill-indicated resource of 1 146 700 tonnes grading 3.01% Zn, 1.05% Cu, 0.58% Pb, 32.97 g/t Ag and 1.97 g/t Au (Kelso et al., 2007).

Geological mapping (Massey and Friday, 1987; Ruks and Mortensen, 2007) indicates that the Big Sicker Mountain area consists mainly of deformed mafic to felsic volcanic and volcanoclastic rocks of the Nitinat and McLaughlin Ridge formations, and high-level intrusions of the Saltspring intrusive suite, as well as abundant gabbroic dikes and sills of the Triassic Mount Hall gabbro (Figure 2). Recent geological mapping in the Cowichan Lake uplift

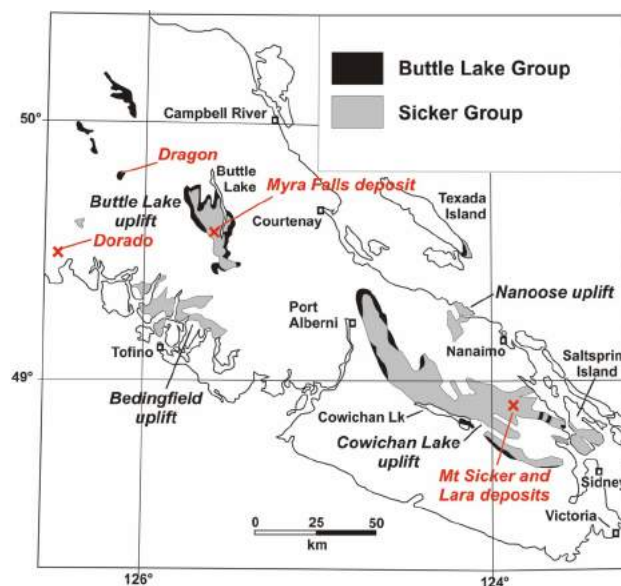


Figure 1. Distribution of Paleozoic strata of the Sicker and Buttle Lake groups on Vancouver Island and the Gulf Islands.

(Ruks et al., 2009a; this study) has been a continuation of the authors’ efforts to develop a stratigraphic framework for the Sicker Group and contained VMS mineralization. Work conducted on mineral tenure owned by project sponsors Treasury Metals Inc. and Westridge Resources Inc. in the Cowichan Lake uplift concentrated on resolving the geological setting and age of the Lara VMS deposit and other VMS occurrences in the area, as well as examining new exposures created by recent logging activity. In 2008, reconnaissance fieldwork on new bedrock exposure owned by Westridge Resources Inc. culminated in the discovery of a new VMS occurrence (Ruks et al., 2009a). Mapping in 2008 in the Mount Brenton area on mineral tenures owned by Treasury Metals Inc. identified a prospective zone

Keywords: Vancouver Island, Paleozoic, Sicker Group, Buttle Lake Group, Cowichan Lake uplift, volcanogenic massive sulphide, stratigraphy, U-Pb zircon geochronology, litho geochemistry

This publication is also available, free of charge, as colour digital files in Adobe Acrobat® PDF format from the Geoscience BC website: <http://www.geosciencebc.com/s/DataReleases.asp>.

where intensely sericite-altered and pyrite-mineralized felsic ash tuff is overlain by silicified argillite and a chlorite-altered ash tuff of intermediate composition (Ruks et al., 2009a). A similar geological setting is recognized in the vicinity of VMS mineralization at the Lenora deposit north of the Chemainus River (Ruks and Mortensen, 2007). Geological mapping and sampling were also focused in the vicinity of the Lady A, Lady C and Lady D iron formations (MINFILE occurrences 092B 029, 092B 033 and 092B 076, respectively; Ruks et al., 2009a). These iron formations are similar to other iron formations occurring in rocks that are interpreted to lie stratigraphically above VMS mineralization at the Lenora, Tyee and Richard III occurrences, and are believed to represent oxide-facies iron mineralization related to hydrothermal mineralizing systems similar to those that formed the underlying VMS deposits. Resolving the timing of iron formation mineralization in the Sicker Group is critical for establishing the duration of VMS-related hydrothermal activity.

Geological mapping in the Cowichan Lake uplift of the Port Alberni area (Massey and Friday, 1989) indicates that this area is largely underlain by basalt to basaltic andesite of the Duck Lake and Nitinat formations, respectively, in addition to felsic tuffaceous volcanoclastic rocks belonging to the McLaughlin Ridge Formation. McLaughlin Ridge Formation rocks in the Port Alberni area are interpreted to represent deposition distal from a volcanic centre, which is thought to be represented in the Saltspring Island–Cowichan Lake area by felsic intrusive rocks of the Saltspring intrusive suite (Massey and Friday, 1989). However, geological mapping and geochronology of new exposures in the Port Alberni area (Ruks et al., 2009a; this study) indicate that significant quantities of felsic volcanic rocks of McLaughlin Ridge Formation age or younger are present in this area. In addition, mafic volcanic rocks in the Lacy Lake area that were previously assigned to the pre–Late Devonian Duck Lake Formation have been demonstrated to be Permian in age, based on microfossil dating (Ruks et al., 2009a). These stratigraphic revisions necessitate a reinterpretation of the nature of the Sicker Group and its VMS potential in the Port Alberni area.

Sedimentary, mafic volcanic and carbonate rocks of the Nanoose uplift have been tentatively correlated with both the Sicker and Buttle Lake groups (Yorath et al., 1999). However, no geochronological or biostratigraphic constraints are currently available from this area; hence, correlation with the Sicker Group is unproven. Reconnaissance fieldwork in the Nanoose uplift in 2009 focused on sampling prospective rock types for geochronology and biostratigraphy in order to resolve the relationship between volcanic and sedimentary rock units in the Nanoose uplift and the Sicker and younger strata elsewhere on Vancouver Island.

Muller, 1977 (Vancouver Island)		Juras, 1987 (Buttle Lake Uplift)		Yorath et al., 1999 (Alberni area)	
Sicker Gp	Buttle Lk Fm	Buttle Lake Gp	Henshaw Fm	Buttle Lake Gp	St. Mary Lk Fm
	Sediment Sill Unit		Mt Mark Fm		Mt Mark Fm
	Myra Fm	Flower Ridge Fm	Sicker Gp		McLaughlin Ridge Fm
	Nitinat Fm	Thelwood Fm		Nitinat Fm	
			Myra Fm		Duck Lk Fm
			Price Fm		

Figure 2. Stratigraphic nomenclature for the Sicker and Buttle Lake groups on Vancouver Island (modified from Yorath et al., 1999).

A large expanse of volcanic and sedimentary rocks and associated VMS mineralization, inferred to be of Paleozoic age, has been mapped by previous workers in the Beddingfield uplift, near the entrance to Bedwell Sound, north of Tofino (e.g., Muller, 1977; Gatchalian, 1985; Figure 1). These units have been tentatively correlated with the Sicker Group; however, no isotopic or fossil ages are presently available for this area. Fieldwork in this area in 2009 concentrated on resolving the age of VMS mineralization and its host stratigraphy.

Mapping in the Hesquiat and Gold River areas, on the Dorado and Dragon properties, respectively (Paget Resources Corporation; Figure 1), has identified several new VMS occurrences hosted in rocks that have been tentatively correlated with the Sicker Group (Ruks et al., 2009a). Geological mapping and sampling on the Dragon property by previous workers identified several polymetallic massive sulphide lenses with grades up to 7.33% Zn, 1.34% Pb, 173 ppm Cu, 680 ppb Au and 19.2 g/t Ag over thicknesses of up to 2 m (Jones, 1997). Geological mapping of the Dragon property indicates that mafic and felsic volcanic rocks and contained VMS mineralization are overlain by volcano-sedimentary and carbonate rocks, including calcareous tuffaceous sedimentary rocks and fossiliferous limestone, respectively (Jones, 1997; Ruks et al., 2009a; this study). Nowhere else in the Sicker Group are carbonate rocks observed to directly, and apparently conformably, overlie felsic volcanic rocks and VMS mineralization. This relationship indicates that radical stratigraphic differences exist between rocks of the Dragon property and better studied exposures of the Sicker Group in the Cowichan Lake and Myra Falls areas. These stratigraphic differences may be explained by regional changes in volcanic and sedimentological facies or, alternatively, the presence of an unrecognized cycle of Paleozoic arc magmatism and VMS mineralization on Vancouver Island.

Fieldwork in the Sicker Group in 2009 commenced in late July and finished in mid-October. Both reconnaissance and detailed geological mapping, together with sampling for lithogeochemistry, U-Pb zircon dating, and Nd, Hf and Pb isotopic studies, were conducted in the Cowichan Lake, Port Alberni, Nanoose, Bedingfield, Gold River and Hesquiat areas during this period. This paper presents a summary of this fieldwork, with emphasis on key stratigraphic relationships and areas of economic importance.

Regional Geology of the Sicker Group

The mid-Paleozoic Sicker Group on southern and central Vancouver Island represents the oldest rocks in Wrangellia. Equivalents of the Sicker Group are not present in Wrangellia in northwestern British Columbia, southwestern Yukon and southern Alaska, where the oldest rock units are the Skolai Group, which is no older than Pennsylvanian (e.g., Katvala, 2006). This, and other differences between the Wrangellian stratigraphy on Vancouver Island and that in more northerly exposures, emphasize the lack of understanding regarding much of Wrangellia (e.g., Katvala, 2006) and the need for further studies. The Cowichan Lake uplift on Vancouver Island and adjacent portions of the Gulf Islands is the largest of four uplifts that expose the Sicker Group and the overlying late Paleozoic Buttle Lake Group (Figure 1).

Previous detailed studies of the Sicker Group have focused mainly on the stratigraphic setting of VMS mineralization at the Myra Falls deposits in the Buttle Lake uplift (Figure 1; e.g., Juras, 1987; Barrett and Sherlock, 1996). Regional mapping of the Cowichan Lake uplift by Massey and Friday (1987, 1989) and Yorath et al. (1999) led to a stratigraphic framework that may be applicable to the entire Sicker Group (Figure 2). This framework, however, is based on mapping in only one of the four main uplifts of Sicker Group rocks, and is supported by a limited amount of biostratigraphic and isotopic age data (e.g., Brandon et al., 1986). Major along- and across-strike facies changes and geochemical variations are to be expected in submarine volcanic sequences such as the one that forms the Sicker Group; hence, the regional applicability of the stratigraphic framework of Yorath et al. (1999) must be tested with detailed mapping and subsequent lithogeochemical and U-Pb dating studies. This is critical for regional exploration for VMS deposits within the Sicker Group. For example, the questions of whether VMS deposits and occurrences in the Cowichan Lake uplift are all of the same age, and whether their hostrocks are directly correlative with those that host the Myra Falls deposit, are of obvious importance.

The most recent regional mapping and stratigraphic work within Sicker Group rocks of the Cowichan Lake uplift has been conducted by Massey (1995) and Yorath et al. (1999). The following information regarding Sicker Group geol-

ogy and stratigraphy in the Cowichan Lake uplift is derived from these accounts. The Sicker Group within the Cowichan Lake uplift is presently interpreted to represent three distinct volcanic and volcanoclastic assemblages that together are thought to record the evolution of an oceanic magmatic arc (Massey, 1995; Yorath et al., 1999). The lowermost Duck Lake Formation yields mainly normal mid-ocean-ridge basalt (N-MORB) geochemical signatures (Massey, 1995) and is interpreted to represent the oceanic-crust basement on which the Sicker arc was built. The upper portions of the Duck Lake Formation yield tholeiitic to calcalkaline compositions and may represent primitive arc rocks. The Duck Lake Formation is overlain by the Nitinat Formation, which comprises mafic, submarine volcanic and volcanoclastic rocks with dominantly calcalkaline compositions and trace-element signatures typical of volcanic arc settings. These rocks are interpreted as an early stage of arc development. The andesitic to mainly dacitic and rhyolitic McLaughlin Ridge Formation overlies the Nitinat and is believed to be correlative with the Myra Formation, the hostrocks for the Myra Falls deposits (Figure 2). Rocks of the McLaughlin Ridge and Myra Formations reflect a more evolved stage of arc activity. Eruption of Nitinat volcanic and volcanoclastic rocks appears to have occurred from several widely scattered centres, whereas the McLaughlin Ridge Formation within the Cowichan Lake uplift is thought to represent eruption from one or more major volcanic edifices. The abundance of proximal felsic volcanoclastic rocks and the presence of voluminous comagmatic felsic intrusions in the Saltspring Island and Duncan areas (Figure 1) indicate that one of these major volcanic centres was located in this area. Plant fossils indicate that at least a minor amount of the McLaughlin Ridge volcanism occurred in a subaerial setting. In the Port Alberni area, the McLaughlin Ridge Formation has previously been interpreted to comprise felsic, fine-grained tuffaceous volcanoclastic and epiclastic rocks, suggesting deposition distal from a volcanic centre (Yorath et al., 1999). The identification of significant quantities of proximal felsic volcanic rocks in the Alberni area in 2009 suggests that an additional felsic volcanic centre may be in the Port Alberni area. Deposition of sedimentary and volcanosedimentary rocks of the overlying Fourth Lake Formation of the Buttle Lake Group followed the cessation of Sicker arc magmatism, and scarce mafic volcanic rocks contained within the Fourth Lake Formation yield enriched tholeiitic rather than the calcalkaline compositions that characterize the McLaughlin Ridge. Massey (1995) speculated that the Buttle Lake Group may represent a marginal-basin assemblage that developed on top of the Sicker arc.

Studies of the Sicker and Buttle Lake groups on southern Saltspring Island by Sluggett (2003) and Sluggett and Mortensen (2003) provided new U-Pb zircon age constraints on both felsic volcanic rocks of the McLaughlin

Ridge Formation and several bodies of Saltspring intrusions. This work demonstrated that two distinct episodes of felsic magmatism occurred in this portion of the Cowichan Lake uplift. One sample of felsic volcanic rocks from the McLaughlin Ridge Formation and three samples of Saltspring intrusions yielded U-Pb ages in the range 356.5–359.1 Ma. A somewhat older U-Pb age of 369.7 Ma was obtained from a separate body of the Saltspring intrusions at Burgoyne Bay on the southwest side of Saltspring Island, indicating that magmatism represented by the McLaughlin Ridge Formation and associated Saltspring intrusions occurred over a time span of at least 15 m.y. There is insufficient age control available at this point to determine whether the magmatism was continuous or episodic during this time period.

Rocks in the Nanoose uplift (Figure 1) have been tentatively correlated with both the Sicker Group and the Buttle Lake Group, and comprise fine clastic rocks, chert, diabasic to andesitic volcanic rocks and limestone (Yorath et al., 1999). A fossil sample from crinoidal limestone in the Nanoose uplift provided brachiopods that yielded a Permian age and fusulinids that yielded a Middle Pennsylvanian age (Muller, 1980). However, diabasic and andesitic pillow lavas in the area have unknown stratigraphic affinities. On the Ballenas Islands, however, these pillow lavas are associated with green and grey chert, and are interbedded with a red tuff breccia that contains both scoriaceous mafic volcanic clasts and crinoidal limestone clasts. The association between mafic flows, chert and a conspicuous breccia unit containing crinoidal limestone clasts is strikingly similar to geological relationships observed in the Lacy Lake–Horne Lake region (Ruks and Mortensen, 2008), suggesting a potential correlation between the two areas.

Rocks and VMS mineralization in the Bedingfield uplift (Figure 1), proximal to the entrance to Bedwell Sound, have historically been correlated with those of the Sicker Group, although no geochronological or biostratigraphic data exist to support this claim. Felsic volcanic rocks, comprising water-laid rhyolite flows and tuffs, represent the oldest rocks in the area. These have been correlated by previous workers with the McLaughlin Ridge Formation. Limestone assigned to the Buttle Lake Group is interpreted to unconformably overlie felsic volcanic rocks throughout the field area (Blackwell and Lajoie, 1986), but no description of the nature of this unconformity is provided. Polymetallic VMS mineralization occurs in several showings throughout the field area, most notably at the Bay Creek, Rant Point and Claim Post MINFILE occurrences (MINFILE 092F 343, 092F 494 and 092F 290, respectively). Volcanogenic massive sulphide mineralization in the area is hosted by variably silica-sericite-altered felsic volcanic rocks, with the most notable grades reported from the Bay Creek showing, where a 4 m thick lens of massive sulphide mineralization is reported to grade 228.00 g/t Ag,

0.41 g/t Au, 0.62% Pb, 0.061% Cu and 0.017% Zn (Gatchalian, 1985).

The age and stratigraphy of rocks underlying the Dragon and Dorado properties, in the vicinity of Gold River and Hesquiat, respectively, is poorly constrained. The Dragon property is located approximately 80 km west of Campbell River, 20 km northwest of Gold River and 65 km northwest of the Myra Falls mine of Breakwater Resources Ltd. (Figure 1). Regional mapping of the Dragon property area by Muller (1977) led to an interpretation of the rocks underlying the property as amphibolite-grade metamorphic rocks belonging to the Westcoast Crystalline Complex. Muller described the Westcoast Crystalline Complex as amphibolite-facies metamorphic rocks belonging to the middle Paleozoic Sicker Group, the late Paleozoic Buttle Lake Group and the Triassic Karmutsen Formation. After the discovery of massive sulphides in float on the Dragon property by prospector E. Specogna, work by Noranda Exploration Co. Ltd. culminated in the discovery of the Falls and North VMS occurrences (Kemp and Gill, 1993). Further geological mapping and diamond-drilling by Noranda and Westmin Resources Ltd. indicated that these showings, with grades up to 7.33% Zn, 1.34% Pb, 173 ppm Cu, 680 ppb Au, and 19.2 g/t Ag over a 2 m thickness, are associated with the contact zone between underlying bimodal volcanic rocks and overlying sedimentary rocks and limestone (Jones, 1997). Volcanic rocks of the Dragon property that underlie massive sulphide mineralization consist of massive, flow-banded rhyolite, andesite and tuffaceous felsic and intermediate volcanic rocks. Sedimentary and carbonate rocks overlying and interlayered with massive sulphide mineralization on the Dragon property consist of chert, mudstone, calcareous mudstone, fossiliferous felsic tuff, fossiliferous wackestone and marble.

The Dorado property is located approximately 17 km north of the village of Hesquiat, on the west coast of Vancouver Island. Like the Dragon property, rocks underlying the Dorado property were originally interpreted by Muller (1977) as amphibolite-facies metamorphic rocks assigned to the Westcoast Crystalline Complex. However, geological mapping of the area by Marshall et al. (2006) has shown the region to be underlain by abundant mafic volcanic rocks of potential Sicker Group affinity, and by sedimentary and carbonate rocks of potential Buttle Lake Group affinity. Following up on reports by Marshall et al. (2006) of polymetallic VMS-style stockwork mineralization in the area, Paget Resources Corporation staked the Dorado property and soon after discovered several polymetallic massive sulphide occurrences (Ruks et al., 2009a). Massive sulphide mineralization on the Dorado property is associated with the contact between massive, variably silica-altered, clinopyroxene- and feldspar-phyric basalt and calcareous sedimentary rocks.

Results of New Fieldwork in the Cowichan Lake Area

Mapping for 2009 fieldwork was conducted using ESRI's ArcPad™ 7 on a Hewlett-Packard IPaq HX4700 Pocket PC wirelessly connected to a GlobalSat® BT-359W Bluetooth GPS receiver. The BC Geological Survey's regional geology compilation for UTM Zones 9 and 10, southwestern BC, as well as numerous geological maps (Massey et al., 2005) derived from mineral exploration assessment reports, were used for reference.

Westridge Resources Inc.

Fieldwork on mineral tenure owned by Westridge Resources Inc. focused on new exposures of prospective bedrock on the north side of Big Sicker Mountain and in the Breen lake¹ area (Figure 3). In the Breen lake area, the most significant VMS showing is the Jane occurrence (MINFILE 092B 084), which consists of two adits reported to intersect several massive sulphide lenses (pyrrhotite-sphalerite-chalcopyrite) up to 0.46 m wide and 1.52 m long, from which a 0.91 m sample assayed 16.1% Zn (Fyles, 1950; Pattison and Money, 1988). In 2008, a new VMS occurrence was discovered by the authors in the Breen lake area, located approximately 1 km east of the Jane showing. This new showing comprises massive pyrite±chalcopyrite and is hosted by a dark green, silica+chlorite-altered, stockwork pyrite-mineralized, sandy intermediate (?) tuff (Figure 4A, B). Massive sulphide mineralization is concordant with the predominant fabric in the host lithology (bedding or foliation?), which dips steeply to the northeast. Due to overburden cover, the true dimensions of this VMS mineralization could not be established. Exposed VMS mineralization can be traced for approximately 3 m along strike, with a thickness of at least 1 m. Reconnaissance-scale mapping in the Breen lake area indicates that VMS showings are hosted predominantly in felsic volcanic rocks. Reworked, intermediate tuffaceous rocks become predominant to the north, presumably upsection.

Several new showings that are thought to be syngenetic in nature were discovered in the Big Sicker Mountain area. Approximately 700 m northwest of the Northeast Copper zone (MINFILE 092B 099; Figure 3), intensely silica-sericite-altered felsic crystal tuff contains up to several percent disseminated sulphides (pyrite±chalcopyrite) with abundant malachite staining in places. This mineralized tuffaceous horizon is interbedded with graphitic argillite and intermediate sandy to silty tuff. As in the Breen lake area, reworked intermediate tuffaceous rocks predominate upsection of felsic volcanic rocks (to the north). Approximately 1 km east of the Northeast Copper zone on new exposure created by recent logging road construction, a new

discovery of massive magnetite mineralization was located within a variably silica-sericite-chlorite-altered quartz-feldspar porphyry. Here, veins and pods of massive magnetite up to 1 m thick cut variably altered quartz-feldspar porphyry (Figure 4C). Magnetite veins commonly have cores of semimassive pyrite. Flanking the area of massive magnetite mineralization to the west, strongly sericitized quartz-feldspar porphyry is cut by abundant stringers of pyrite and chalcopyrite. Strong chlorite alteration is localized along the margins of these stringers. Farther to the west, quartz-feldspar porphyry becomes intensely silicified and contains up to 30% disseminated pyrite±trace chalcopyrite mineralization. Stringers of pyrite and chalcopyrite also occur in this zone, with sulphide vein margins often flanked by zones of chlorite alteration.

Treasury Metals Inc.

Fieldwork on mineral tenure owned by Treasury Metals Corp. north of the Chemainus River continued to focus on establishing the timing and geological setting of VMS occurrences on the property, as well as constraining the longevity of VMS mineralizing systems in the area through establishing the age of exhalative iron formation mineralization. The Lara property is host to many VMS occurrences, the most notable of which is the Lara VMS deposit or 'Coronation Trend' (Figure 3), which consists of two main zones, the Coronation and Coronation Extension. The indicated resource for the Coronation and Coronation Extension zones (at a 1% Zn cut-off) is 1 146 700 tonnes at 3.01% Zn, 1.05% Cu, 0.58% Pb, 32.97 g/t Ag and 1.97 g/t Au (Kelso et al., 2007). Sulphide mineralization of the Coronation and Coronation Extension zones is hosted by strongly silicified, coarse-grained rhyolite crystal tuff and ash tuff (Kelso et al., 2007; Ruks et al., 2009a).

The Randy North showing (MINFILE 092B 128), located approximately 2 km north of the Coronation zone (Figure 3), consists of several zones of anomalous polymetallic mineralization hosted in strongly sericite-altered felsic volcanoclastic rocks (Kelso et al., 2007). Recent mapping (2008 fieldwork) of the Randy North zone shows that intense pyrite stockwork mineralization is hosted by moderately to strongly sericite-altered and highly foliated felsic crystal tuff, with 1–3% quartz crystals up to 5 mm in size (Ruks et al., 2009a). The Anita zone (MINFILE 092B 037), located approximately 4.7 km northwest of the Coronation zone (Figure 3), consists of polymetallic sulphide mineralization situated close to the contact between mafic tuffaceous rocks and felsic volcanoclastic rocks. The best drill intersection of the Anita horizon to date is diamond-drill hole 87-37, which intersected 2.5 m of 2.37% Cu, 0.73% Pb, 2.73% Zn, 46 g/t Ag and 0.72 g/t Au hosted in a pyritic felsic tuff. Another hole, 88-49, included a 4.9 m interval of 2.3% Cu, 0.49% Pb, 3.66% Zn, 73.9 g/t Ag and 1.9 g/t Au.

¹ unofficial place name

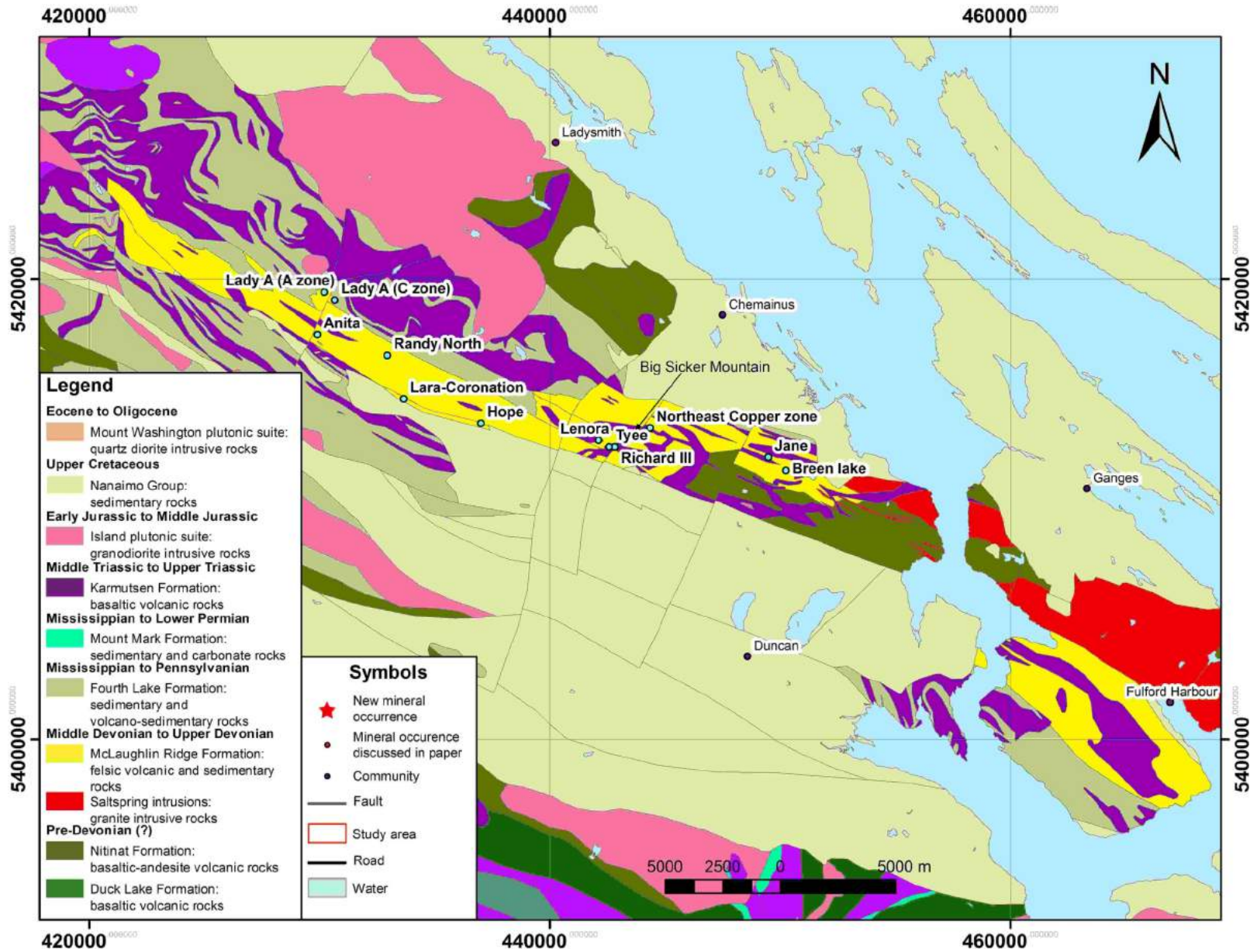


Figure 3. Regional geology, selected mineral occurrences and areas of study for 2009 fieldwork in the Cowichan Lake area, southern Vancouver Island (modified from Massey et al., 2005).

Rehabilitation of existing logging roads in the vicinity of the Lara and Randy North areas (MINFILE occurrences 092B 129 and 092B 128, respectively) since 2008 fieldwork created abundant new bedrock exposure. Mixed reconnaissance and 1:2000 scale geological mapping of this area, combined with data collected during 2008 fieldwork (Ruks et al., 2009a), indicate that stratigraphy hosting the Lara and Randy North VMS occurrences comprises largely felsic volcanic rocks, including crystal tuff, ash tuff and flows. A pervasive foliation coupled with variable quartz-sericite alteration makes protolith identification difficult in places. Although felsic volcanic units dominate the area, they are punctuated by thin zones of argillite and fine-grained intermediate tuff, indicating periods of quiescence between felsic volcanic events, and prospective stratigraphy for VMS mineralization. Exposures near the Anita shaft consist of quartz-sericite-altered felsic volcanoclastic rock with variable concentrations of sulphide mineralization. In the immediate vicinity of the Anita shaft, intensely quartz-sericite-altered felsic volcanic rock with less than 1% quartz phenocrysts contains up to 1% chalcopyrite veinlets, often associated with zones of strong silicification (Figure 5A). Similar to the Breen lake and Big Sicker Mountain areas, fine-grained, variably hematite-altered intermediate tuffaceous rocks and argillite predominate upsection of the Coronation, Randy North and Anita VMS occurrences (to the north; Figure 5B).

Exhalative magnetite iron formation of the Lady A (A zone) and Lady A (C zone) occurrences (MINFILE 092B 029 and 092B 033, respectively; Figure 3), located approximately 5 km northwest of the Lara VMS deposit, is associated with this unit. The contact between fine-grained, reworked, intermediate tuffaceous rocks, argillite and underlying variably altered and sulphide-mineralized felsic volcanic stratigraphy represents a regionally and economically significant feature coincident with the cessation of Sicker Group volcanism. Significant VMS mineralization is associated with similar contacts at large VMS deposits worldwide, including Noranda (Franklin et al., 2005) and Anyox (Macdonald et al., 1996). At the giant Bathurst camp, VMS mineralization is overlain by a district-wide exhalative chert-magnetite iron formation, similar to that of the Lady A occurrences (Galley et al., 2007).

Results of New Fieldwork in the Port Alberni Area: Bitterroot Resources Ltd.

Mapping of Sicker Group bedrock geology and sampling for litho geochemistry, U-Pb zircon geochronology, and Pb, Nd and Hf isotope tracer studies was conducted in the Port

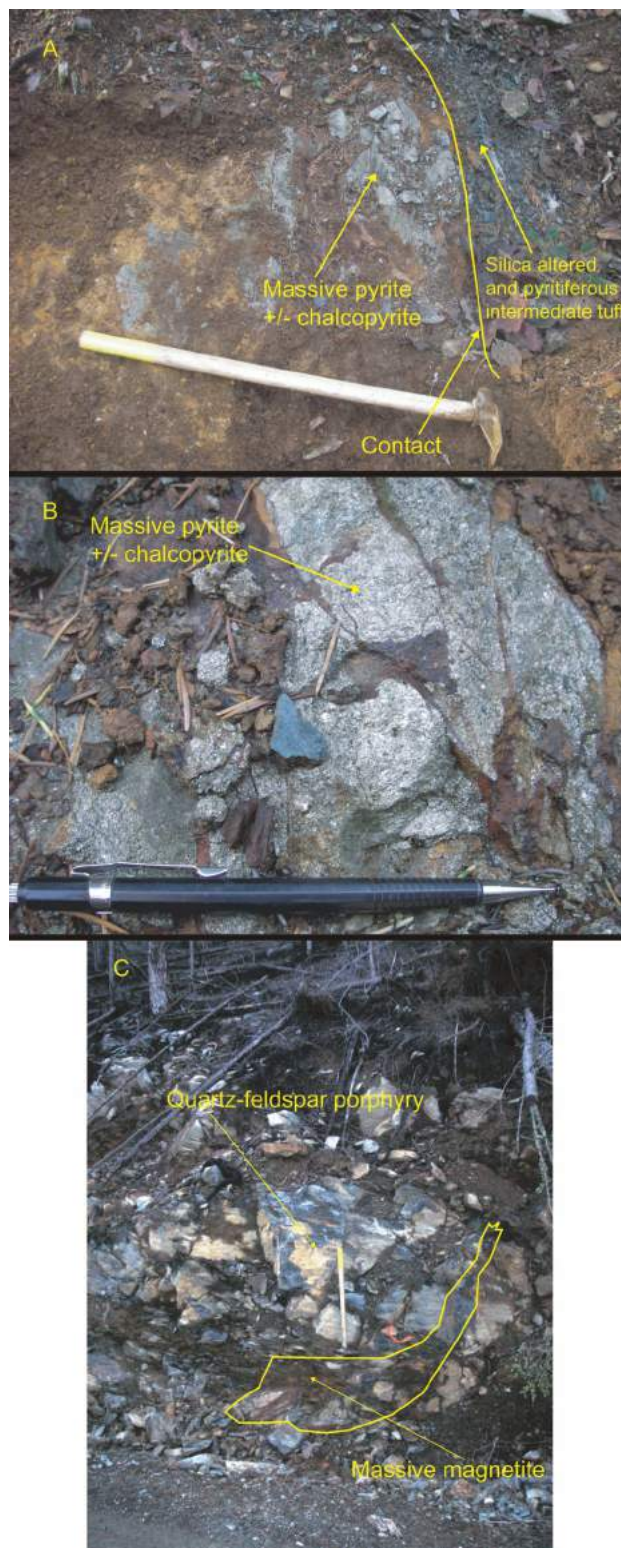


Figure 4. Mineralization in the Cowichan Lake area, southern Vancouver Island: **A)** massive pyrite+chalcopyrite mineralization, discovered during 2008 fieldwork (Ruks et al., 2009a), hosted in a silica-altered intermediate tuff and located approximately 1 km east of the Jane showing (MINFILE 092B 084) on Westridge Resources Inc. mineral tenure (UTM Zone 10, 449958E, 5412112N, NAD83); **B)** close-up of massive pyrite and chalcopyrite VMS mineralization discovered on Westridge Resources Inc. mineral tenure during 2008 fieldwork (Ruks et al., 2009a); **C)** new discovery of massive magnetite mineralization within a variably silica-sericite-chlorite-altered quartz-feldspar porphyry, approximately 1 km east of the Northeast Copper zone (MINFILE 092 099) on Westridge Resources Inc. mineral tenure (UTM Zone 10, 445393E, 5413282N).

Alberni area, much of which is covered by mineral tenure owned by project sponsor Bitterroot Resources Ltd. (Figure 1). This work was concentrated in 1) the vicinity of recent logging activity west of Horne Lake (Figure 6, study area A); 2) the vicinity of recent logging in the Duck Lake and China Creek areas (Figure 6, study areas B and C, respectively); and 3) the Rift Creek area, east of Mount Spencer (Figure 6, study area D). Bedrock exposure in all areas is moderate, with the best exposures occurring in logging-road cuts. Off-road exposures are typically covered with thick layers of moss and organic detritus, commonly in forested, low-light conditions that greatly hamper geological mapping.

Recent logging activity west of Horne Lake (Figure 6, study area A) has created significant new bedrock exposure. Examination of these new exposures has revealed the presence of a stratigraphic section with important implications for late Paleozoic magmatism in southern Wrangellia. At the base of this section, close to the shore of Horne Lake, clinopyroxene-phyric basaltic-andesite volcanic and volcanoclastic rocks of probable Late Devonian age dominate. This unit is assumed to be correlative with similar clinopyroxene-phyric mafic volcanic rocks in the vicinity of a microwave tower, approximately 6 km to the southeast (Figure 6). At the microwave tower, mafic volcanic rocks are interbedded with felsic ash tuff, which has yielded a Late Devonian U-Pb zircon age.

Overlying the mafic volcanic rocks on the west side of Horne Lake is a package of sedimentary rocks, including, in upwards stratigraphic order, medium-grained sandstone (arkosic?), chert, interbedded felsic crystal tuff and chert, and a package of felsic volcanoclastic rocks. Felsic volcanoclastic rocks in this area are similar in nature and stratigraphic position to those observed to the south of Horne Lake (Ruks et al., 2009a), and comprise rhyolitic to rhyodacitic crystal tuff, lapilli tuff and tuff breccia (Figure 7A).

Felsic volcanic rocks are overlain by a thin unit of fine-grained, intermediate tuffaceous rock and argillite, which are in turn overlain by ribbon chert and crinoidal limestone. This ribbon chert and limestone are interpreted to be correlative with a similar package in the Lacy Lake area, which has yielded radiolarian biostratigraphic ages ranging from Early to Middle Permian (Ruks et al., 2009b). Ribbon chert exposures west of Horne Lake are, in places, riddled with thick stringers and pods of fine-grained pyrite, up to 5 cm in thickness, and is overlain by a chert pebble-boulder conglomerate. This conglomerate is in turn overlain by massive pillow basalts that are probably correlative with the Middle Triassic Karmutsen Formation. The presence of probable Permian chert and limestone proximally underlain by a package of felsic volcanic rock suggests a late Paleozoic age for felsic volcanic rocks in the Horne Lake area.



Figure 5. Mineralization on Treasury Metals Inc. mineral tenure, Cowichan Lake area, southern Vancouver Island: **A**) in the immediate vicinity of the Anita shaft (MINFILE 092B 037), intensely quartz-sericite-altered felsic volcanic rock with less than 1% quartz phenocrysts contains up to 1% chalcopyrite veinlets, often associated with zones of strong silicification (UTM Zone 10, 429869E, 5417127N); **B**) similar to the Breen lake and Big Sicker Mountain areas, fine-grained, variably hematite-altered intermediate tuffaceous rocks and argillite predominate upsection of the Coronation, Randy North, and Anita VMS occurrences (to the north).

This age is in stark contrast to historic interpretations for the bedrock geology of the area, which assigned this complete stratigraphic package to the pre-Late Devonian Nitinat Formation and the Late Devonian McLaughlin Ridge Formation.

Rocks of the China Creek–Duck Lake area (Figure 6, study area B) were the focus of continued efforts to resolve the age of Duck Lake Formation mafic volcanic rocks and associated VMS mineralization. Much of the bedrock underlying the Bitterroot Resources mineral tenure in the China Creek–Duck Lake area is interpreted to comprise rocks of the Duck Lake and Nitinat formations (Massey and Friday, 1989). The Duck Lake Formation consists of pillow basalt, pillow breccia and interflow mafic tuffaceous sedimentary rocks, and is believed to represent the oceanic crust upon

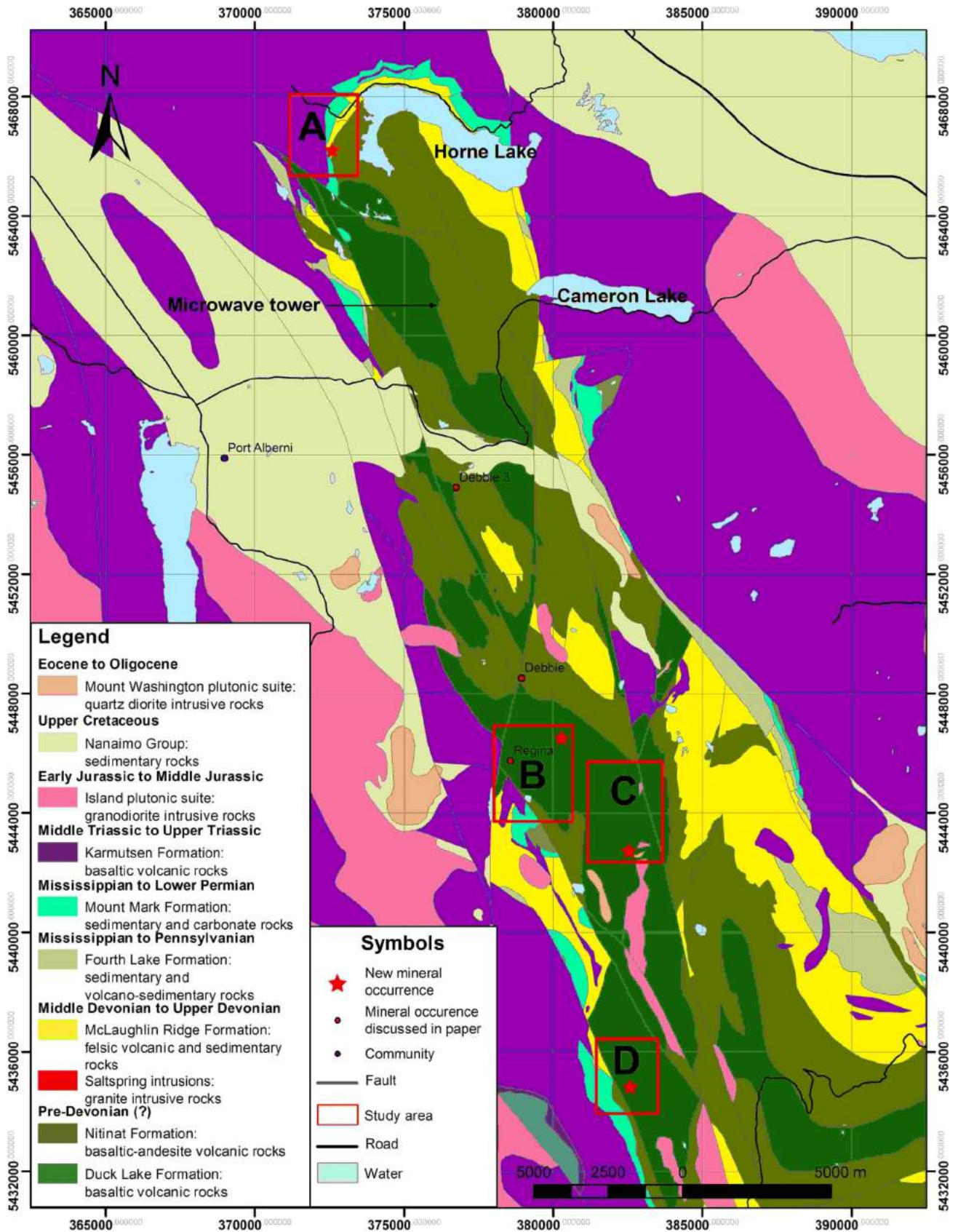


Figure 6. Regional geology (modified from Massey, 2005), selected mineral occurrences and areas of study for 2008 fieldwork in the Port Alberni area, southern Vancouver Island.

which the Sicker arc was built (Massey and Friday, 1989). As such, Duck Lake Formation rocks are interpreted as the oldest in the Sicker Group and, by default, the oldest in Wrangellia (Massey and Friday, 1989). The VMS mineralization of the Debbie 3 occurrence (MINFILE 092F 445), owned by Bitterroot Resources, consists of four stratiform lenses of banded massive sphalerite with minor chalcopyrite and galena, each band ranging between 5 and 20 cm in thickness. The best grade obtained from sampling of this mineralization by previous workers was 14.1% Zn, 0.87% Pb and 0.12% Cu over a 20 cm thickness. The mineralization is hosted in fine-grained chloritic schist with variable carbonate, sericite and silica alteration (Ruks and Mortensen, 2008). The chloritic schist hosting Debbie 3 mineralization is spatially associated with clinopyroxene-phyric andesitic volcanic rocks assigned to the Nitinat Formation. The Debbie 3 VMS occurrence is therefore believed to represent the oldest VMS mineralization in the Sicker Group. Since most exploration for VMS mineralization in the Sicker Group has focused on bimodal volcanic rocks belonging to the McLaughlin Ridge and Myra formations, the relatively unexplored Duck Lake and Nitinat formations represent attractive targets for this style of mineralization.

Fieldwork in 2008 in the China Creek–Duck Lake area discovered additional massive sulphide mineralization near the base of the Duck Lake type section (Yorath et al., 1999; Ruks et al., 2009a). Here, a bed of fine-grained massive sulphide (dominantly pyrite) was discovered in a new exposure along China Creek mainline (Figure 6, study area B), approximately 1.8 km northeast of the Regina occurrence (MINFILE 092F 078), where polymetallic VMS-style mineralization has also been reported. The bed is approximately 20 cm wide and interbedded with siliceous argillite. Mafic sandy tuff and scoriaceous mafic volcanic rocks are also found in the immediate vicinity of the mineralization. Siliceous interbeds within the massive sulphide mineralization were sampled for radiolarian biostratigraphy in 2008. Poorly preserved radiolarians were recovered from siliceous interbeds within the massive sulphide mineralization, and additional sampling of these horizons in 2009 was carried out to provide a biostratigraphic age.

Reconnaissance geological mapping of new exposure created by recent logging road construction approximately 3.4 km east of Duck Lake (Figure 6, study area C) reveals a thick section of pillow basalt and associated basaltic volcanoclastic rocks (Duck Lake Formation) overlain by a sedimentary succession comprising interbedded chert, argillite, siltstone and sandstone (McLaughlin Ridge Formation?). A new mineral occurrence was discovered in graphitic argillite of this sedimentary package, consisting of en échelon quartz-pyrite veins with strong silica-pyrite alteration haloes (Figure 7B). This sedimentary succession is similar in nature to that identified in the Peak and Kammat



Figure 7. Rocks and mineralization in the Port Alberni area, southern Vancouver Island: **A)** potential late Paleozoic rhyolite lapilli tuff, west of Horne Lake; **B)** newly discovered en échelon quartz-pyrite veins with strong silica-pyrite alteration haloes hosted in graphitic argillite, located approximately 3.4 km east of Duck Lake (UTM Zone 10, 382588E, 5442746N); **C)** newly discovered, 10–15 cm wide stratiform band of massive fine-grained pyrite with trace chalcopyrite, interbedded with grey-green ribbon chert, located in the Rift Creek area, east of Mount Spencer (UTM Zone 10, 382597E, 5434781N).

lakes area during 2008 fieldwork, from which Late Devonian radiolarians were recovered (Ruks et al., 2009a, b), and is potentially correlative. Sampling of least-deformed pillow basalt rims from this section for U-Pb geochronology on microbial titanite (e.g., Banerjee et al., 2007) was carried out in an attempt to constrain the age of Duck Lake Formation mafic volcanic rocks in the area.

In the Rift Creek area east of Mount Spencer (Figure 6, study area D), reconnaissance geological mapping resulted in the discovery of a new massive sulphide occurrence. This occurrence, presumably hosted in rocks of the Duck Lake Formation, consists of a 10–15 cm wide stratiform band of massive, fine-grained pyrite with trace chalcopyrite, interbedded with grey-green ribbon chert (Figure 7C). The chert unit that hosts the massive sulphide mineralization sits on top of a package of mafic tuffaceous turbidites, which are spatially associated with basalt flow breccia. The mineralogy and geological setting of this new VMS occurrence is similar to VMS mineralization discovered in the China Creek area during 2008 fieldwork (Ruks et al., 2009a).

Results of New Fieldwork in the Nanoose Area

Fieldwork in the Nanoose uplift (Figure 1) concentrated on resolving the age and geological setting of abundant Paleozoic mafic volcanic rocks in the area, which have uncertain stratigraphic relationships to the Sicker Group (Yorath et al., 1999). A large body of granodiorite of the Early to Middle Jurassic Island intrusions on Nanoose Peninsula has caused strong contact metamorphism of the mafic volcanic and interlayered clastic, chert and limestone in large parts of the Nanoose uplift. As a result, radiolarians are recrystallized and no age determinations are possible. In order to find better preserved microfossils for biostratigraphic purposes and facilitate dating of this enigmatic package of rocks, fieldwork in the Nanoose uplift in 2009 was concentrated on northern Ballenas Island, where younger intrusions are absent (Yorath et al., 1999). Here, abundant basaltic volcanic rocks are interbedded with and overlie a sedimentary package comprising interbedded crinoidal limestone, argillite, chert and siltstone. Basaltic volcanic rocks contain abundant pillow flows (Figure 8A), with associated zones of basaltic pillow breccia, tuff breccia and finer grained tuffaceous rocks. Pillow basalt flows are variably plagioclase phyric, with phenocrysts often reaching sizes of 5 mm or greater and concentrations of up to 40–50%. Crinoidal limestone locally forms the matrix to brecciated mafic volcanic rocks, indicating deposition in a carbonate-rich environment (Figure 8B). Intraflow basaltic volcanoclastic rocks are often interbedded with multiple layers of stratiform, hematite-rich sedimentary rocks resembling exhalative iron formations, with individual beds reaching thicknesses of 30 cm or more (Figure 8C). Sam-



Figure 8. Rocks in the Nanoose area, southern Vancouver Island: **A)** pillow basalt on northern Ballenas Island; **B)** basalt tuff breccia with crinoidal limestone matrix (white zones), indicating volcanism in a carbonate-rich environment; **C)** stratiform, hematite-rich sedimentary rocks resembling exhalative iron formations occurring in volcano-sedimentary rocks between basalt flows.

ples of chert and carbonate were collected for both radiolarian and conodont biostratigraphy. Samples of mafic volcanic rocks were collected for U-Pb geochronology and litho geochemistry on pillow basalt microbial titanite.

Results of New Fieldwork in the Bedingfield Uplift

Fieldwork in the Bedingfield uplift (Figure 1) concentrated on resolving the age and geological setting of proposed Sicker Group stratigraphy and VMS occurrences in the area. Reconnaissance fieldwork in the Bedingfield area was conducted over the course of four days in September. All-terrain vehicles and a 4 m (14 ft.) aluminum boat were barged to a landing at Cypress Bay, with accommodation located at the Tranquil Timber Ltd. floating barge camp near Whitepine Cove.

Volcanogenic massive sulphide mineralization of the Bay Creek, Claim Post and Rant Point occurrences (MINFILE 092F 343, 092F 290 and 092F 494, respectively; Figure 9) are located on shoreline near the entrance to Bedwell Sound, and are accessed by boat. Stockwork-style VMS mineralization of the Bay Creek showing (Figure 9) consists of 1–2% pyrite, chalcopyrite and sphalerite stringers and blebs hosted in gossanous aphyric to quartz-phyric rhyolite flows (Figure 10A). Chlorite veins and blebs are abundant. Host felsic volcanic rocks are foliated, with quartz phenocrysts often exhibiting subgrain development and stretching parallel to a southwest-dipping foliation. Mineralization in the vicinity of the Claim Post (MINFILE 092F 290) showing (Figure 10B) consists of bands of malachite-stained, semimassive pyrite and chalcopyrite up to 5 cm in thickness, hosted by strongly quartz-sericite-altered, gossanous felsic ash and crystal tuff. Deformed quartz-feldspar-phyric rhyolite porphyry plugs, which are texturally similar to the Saltspring intrusions (Figure 10C), are present in the vicinity of the showing. Mineralization in the area of the Rant Point showing (MINFILE 092F 494) consists of a shoreline gossan comprising massive, foliated rhyolite crystal tuff with up to 15–20% disseminated pyrite and trace chalcopyrite.

Work in the Herbert Inlet and Cypre River areas (Figure 9, study areas A and B, respectively) focused on examining the nature of the contact between proposed carbonate rocks assigned to the Buttle Lake Group (Mount Mark Formation) and underlying rocks assigned to the Sicker Group, as well as on locating new areas prospective for VMS mineralization. Although no continuous stratigraphic section was observed, massive recrystallized limestone with varying proportions of interbedded chert and argillite was observed juxtaposed with abundant rhyolite flows and tuffs in several locations. Previous workers in the Bedingfield area have suggested that Buttle Lake Group rocks are observed to sit unconformably on felsic volcanic rocks (e.g.,

Blackwell and Lajoie, 1986), but they have not documented the nature of this unconformity. The juxtaposition of carbonate rocks and underlying felsic volcanic rocks in the Bedingfield area is strikingly similar to stratigraphic relationships observed at the Dragon property, north of Gold River, where carbonate rocks are observed to conformably overlie felsic volcanic rocks, with VMS mineralization between them (e.g., Ruks et al., 2009a). In the Cypre River area, a localized gossanous zone, consisting of 5–10% pyrrhotite+pyrite+chalcopyrite stringers and blebs, is observed proximal to the contact between a volcano-sedimentary unit (comprising siltstone, mudstone and felsic lapilli tuff) and gabbro.

Results of Geological Mapping on the Dorado and Dragon Properties (Paget Resources Corporation), Hesquiat–Gold River Area

Dorado Property

Fieldwork on the Dorado property and Hesquiat Peninsula was conducted over six days in October 2009 (Figure 1). This fieldwork was designed to resolve the age and geological setting of the Dorado VMS occurrences and potential Paleozoic host stratigraphy in the area (e.g., Marshall et al., 2006; Ruks et al., 2009a). A truck and ATV were barged from Gold River into Mooyah Bay, where accommodation was located in a floating barge camp operated by Port Neville Logging Co. Ltd. Polymetallic VMS-like stockwork mineralization was first discovered on the Hesquiat Peninsula by Marshall et al. (2006). Follow-up reconnaissance geological mapping in the vicinity of Marshall's showing by Paget Resources Corporation led to the discovery of polymetallic massive sulphide mineralization and additional polymetallic, VMS-style, stockwork sulphide occurrences (Ruks et al., 2009a). Massive sulphide mineralization has so far been discovered in two locations on the Dorado property, associated with the contact between mafic volcanic rocks and calcareous sedimentary rocks (Figure 11). The first massive sulphide mineralization discovered on the Dorado property is located in a shot-rock blast pit near the contact between a variably silica-altered, chlorite amygdule-bearing, feldspar-phyric basaltic flow and intermediate tuffaceous sandstone. Here, a massive sulphide pod, measuring 1.5 m by 3 m and consisting of fine-grained pyrrhotite with trace chalcopyrite, is hosted within the basalt (Figure 12A). Sulphide stringers up to 1 cm wide are abundant near the massive sulphide mineralization. Numerous massive sulphide boulders of similar composition are found close to the showing; some of them have been used as substrate for a bridge crossing a creek that drains immediately east of the pit. The most silicified zones within the host basalt are associated with abundant quartz and epidote veinlets. Some zones of autobreccia are present in the basalt host. These zones contain abundant

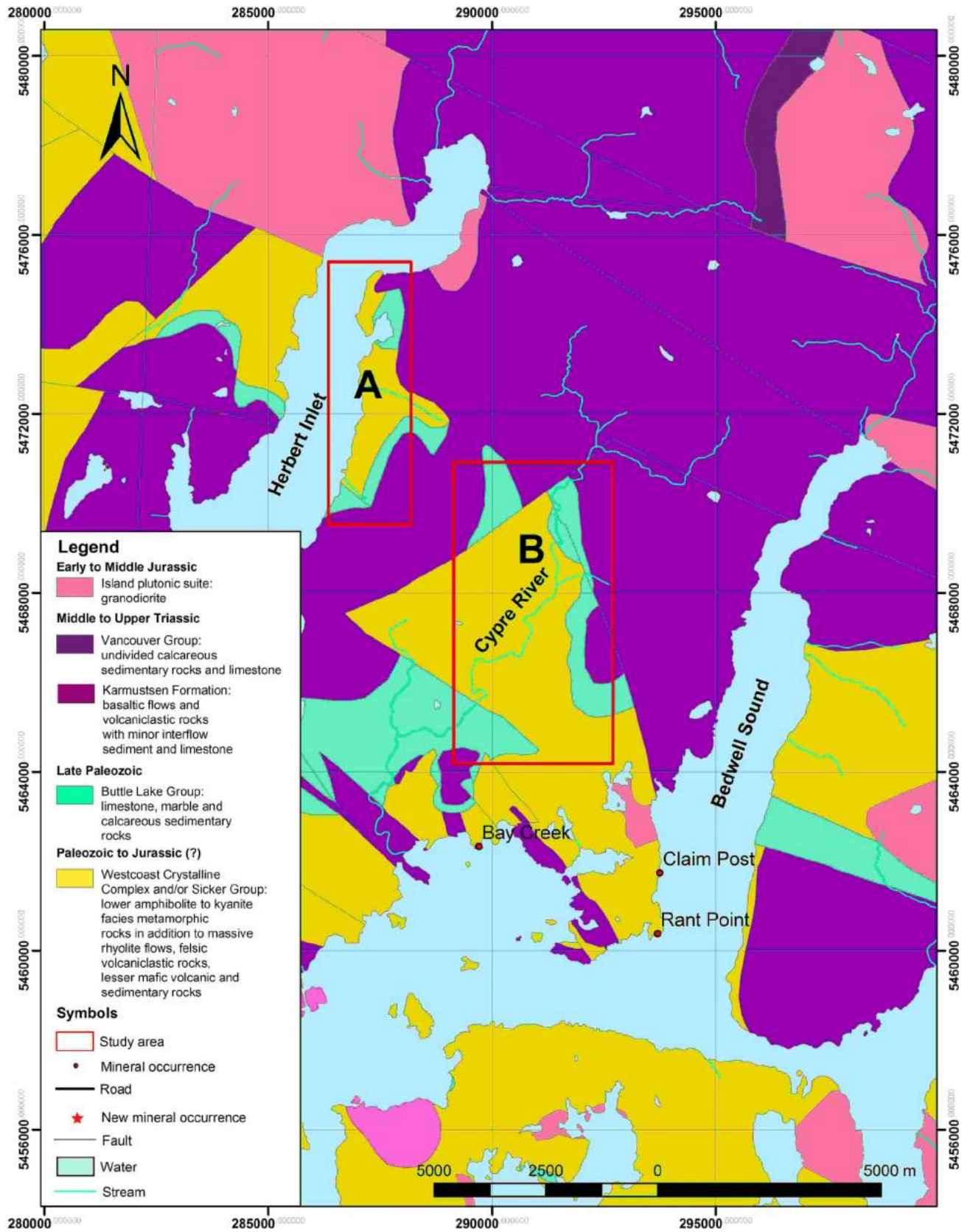


Figure 9. Geology of the Bedingfield area (after Massey et al., 2005), central Vancouver Island, showing locations of 2009 fieldwork.

grey, glassy, angular silicified clasts up to 2 cm in size. Approximately 430 m southwest of this zone is a second zone of massive sulphide mineralization. Here, boulders of fine- to medium-grained massive pyrrhotite+chalcopyrite, up to 50 cm in size, occur as float beneath a large gossanous outcrop of highly silica-altered, feldspar-clinopyroxene-phyric basalt porphyry. Pyrrhotite mineralization is abundant, as both stringers and disseminations. This altered and mineralized porphyry was traced in the map area for approximately 350 m to the southwest along an overgrown logging skidder road. Variably altered, variably sulphide-mineralized examples of feldspar- and clinopyroxene-phyric basalt are abundant to the north of the massive sulphide occurrences and are most likely representative of massive intermediate flows. These mafic volcanic rocks are massive, and less porphyritic to nearly aphyric in nature. They often contain abundant epidote alteration in the form of ovoid patches up to 10 cm in width. Fine-grained sulphide minerals are often found in the cores of these patches. In places, pyrrhotite and chalcopyrite stringers are present, typically with strong silica alteration along their margins.

Sedimentary rocks spatially related to the Dorado blast-pit sulphide occurrence first appear approximately 100 m to the south. These comprise a moderately east-dipping outcrop of recrystallized, interbedded marble and cherty carbonate. Approximately 50 m farther south, variably altered clinopyroxene- and feldspar-phyric basalt, similar to Dorado VMS hostrock, intrudes a sedimentary package (Mooyah Formation?) comprising recrystallized carbonate, chert, siltstone and fine sandstone (Figure 12B). Similar to Dorado VMS hostrocks, alteration is intense, with much of the basalt being reduced to assemblages of epidote and quartz, especially in areas proximal to contacts with sedimentary rocks.

Reconnaissance geology throughout the northern portion of the Hesquiat Peninsula concentrated on sampling exposures of potential Paleozoic stratigraphy (Mooyah Formation; Marshall et al., 2006) for geochronology and biostratigraphy, as no Paleozoic ages exist for the area. However, due to the presence of significant expanses of granitic intrusive rocks of probable Jurassic age (e.g., Marshall et al., 2006), exposures of potential Paleozoic stratigraphy are very sparse. Where observed in this study, the Mooyah Formation typically comprises a mixture of graphitic argillite, recrystallized carbonate and chert, and lesser amounts of siltstone and sandstone (Figure 12C). Carbonate hostrocks to the Silverado skarn occurrence (MINFILE 092E 017), located only 6 km east of the Mooyah Formation type section in Mooyah Bay, yield Triassic preliminary conodont ages (Marshall et al., 2006). This suggests that a potential Triassic age for the Mooyah Formation should also be considered.

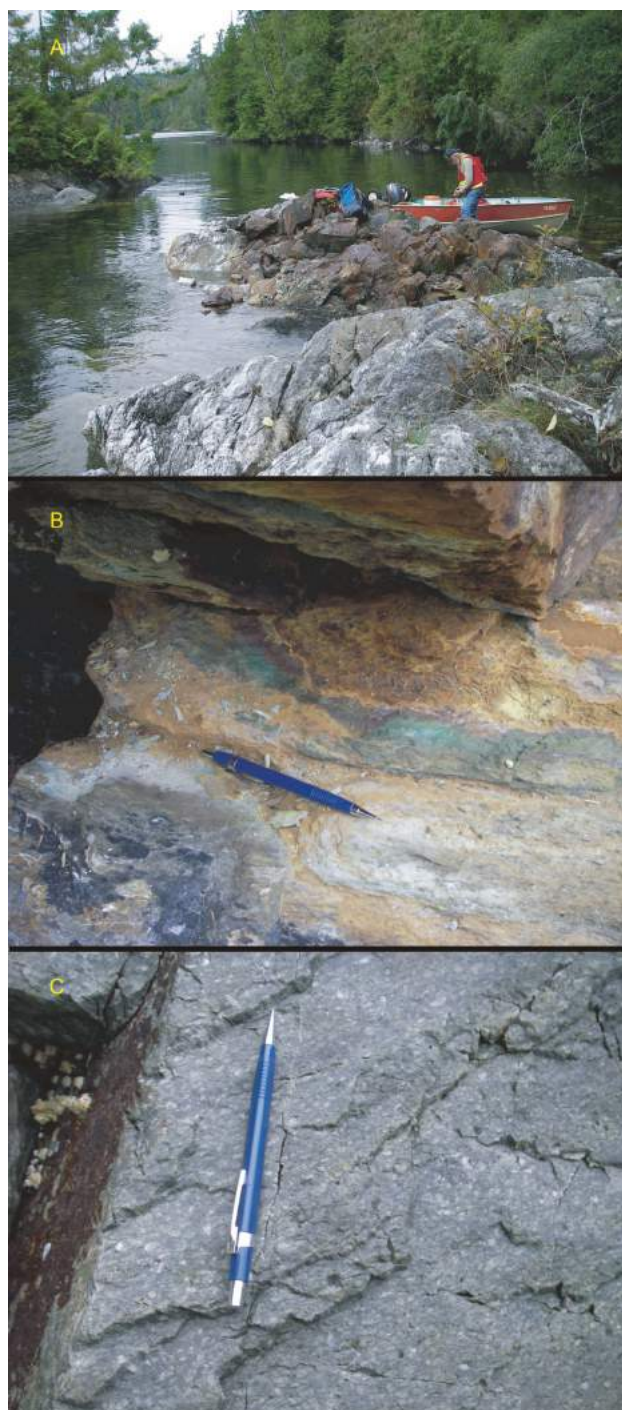


Figure 10. Rocks and mineralization in the Bedingfield uplift area, central Vancouver Island: **A)** stockwork-style VMS mineralization of the Bay Creek showing (MINFILE 092F 343), consisting of 1–2% pyrite, chalcopyrite and sphalerite stringers and blebs hosted in gossanous aphyric to quartz-phyric rhyolite flows; **B)** Claim Post showing (MINFILE 092F 290), consisting of bands of malachite-stained, semimassive pyrite and chalcopyrite up to 5 cm in thickness, hosted in strongly quartz-sericite-altered, gossanous felsic ash and crystal tuff; **C)** deformed quartz-feldspar rhyolite porphyry near the Claim Post showing, reminiscent of the Saltspring intrusions.

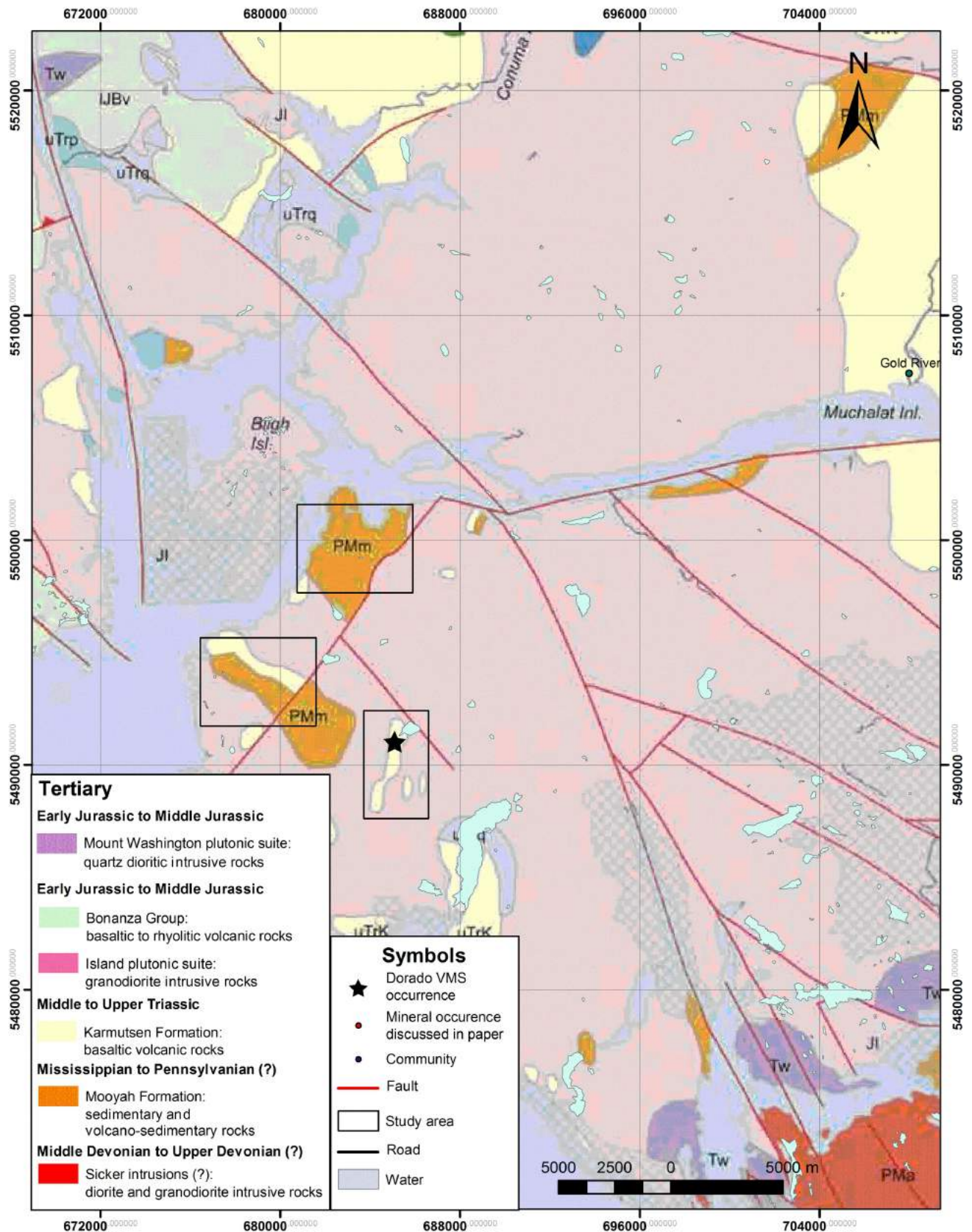


Figure 11. Geology of the Hesquiat Peninsula area (modified from Marshall et al., 2006), central Vancouver Island, showing locations of 2009 fieldwork and VMS mineral occurrences of note.

Dragon Property

The Dragon property is located approximately 80 km west of Campbell River, 20 km northwest of Gold River and 65 km northwest of the Myra Falls mine of Breakwater Resources Ltd. (Figure 1). Fieldwork in 2009 continued efforts to establish the geological setting for known mineral occurrences on the property, and for understanding the stratigraphy of the property geology in general. The work was successful in identifying several new prospective zones of mineralization.

Massive sulphide mineralization on the Dragon property typically consists of varying proportions of fine- to medium-grained massive pyrrhotite, chalcopyrite and sphalerite at the contact between felsic volcanic rocks and overlying volcano-sedimentary and carbonate rocks. Fieldwork in 2009 has been successful in tracing this prospective horizon over a strike length of 8 km, where it shows signs of VMS-style alteration and mineralization throughout (Figure 13).

The original massive sulphide discoveries on the Dragon property include the Falls and North showings, which comprise three massive sulphide lenses with grades up to 7.33% Zn, 1.34% Pb, 173 ppm Cu, 680 ppb Au and 19.2 g/t Ag over 2 m (Jones, 1997; Figure 13; Figure 14A). This massive sulphide mineralization is interlayered with laminated chert, mudstone and calcareous mudstone that strike southwesterly and dip steeply to the northwest. Bivalve (?) fossils have been observed in cherty tuff overlying the Falls and North showings. Several new VMS showings were discovered on the Dragon property during the course of 2008 fieldwork. Massive sulphide mineralization was discovered approximately 1 km south of the Falls and North showings, and abundant VMS stockwork sulphide mineralization was discovered approximately 1 km north of these two showings (Ruks et al., 2009a). In both new discoveries, VMS mineralization is associated with the contact between variably altered and sulphide-mineralized felsic volcanic rocks (often rhyolite flows) and overlying calcareous sedimentary rocks.

Fieldwork was carried out in the eastern portion of the property to identify potential deeper and older Paleozoic stratigraphy (Figure 13, study area A). However, only more felsic volcanic rocks were encountered, comprising rhyolite flows and associated volcaniclastic and tuffaceous rocks. In places, felsic volcanic rocks are intruded by gabbroic sills of probable Middle Triassic Karmutsen Formation (Mount Hall gabbro) affinity. The presence of felsic volcanic rocks towards the eastern edge of the Dragon property is attributed to a progressive flattening of dip angles as one moves eastward on the property. Work in the southern and southeastern portions of the property (Figure 13) has revealed additional locations where variably

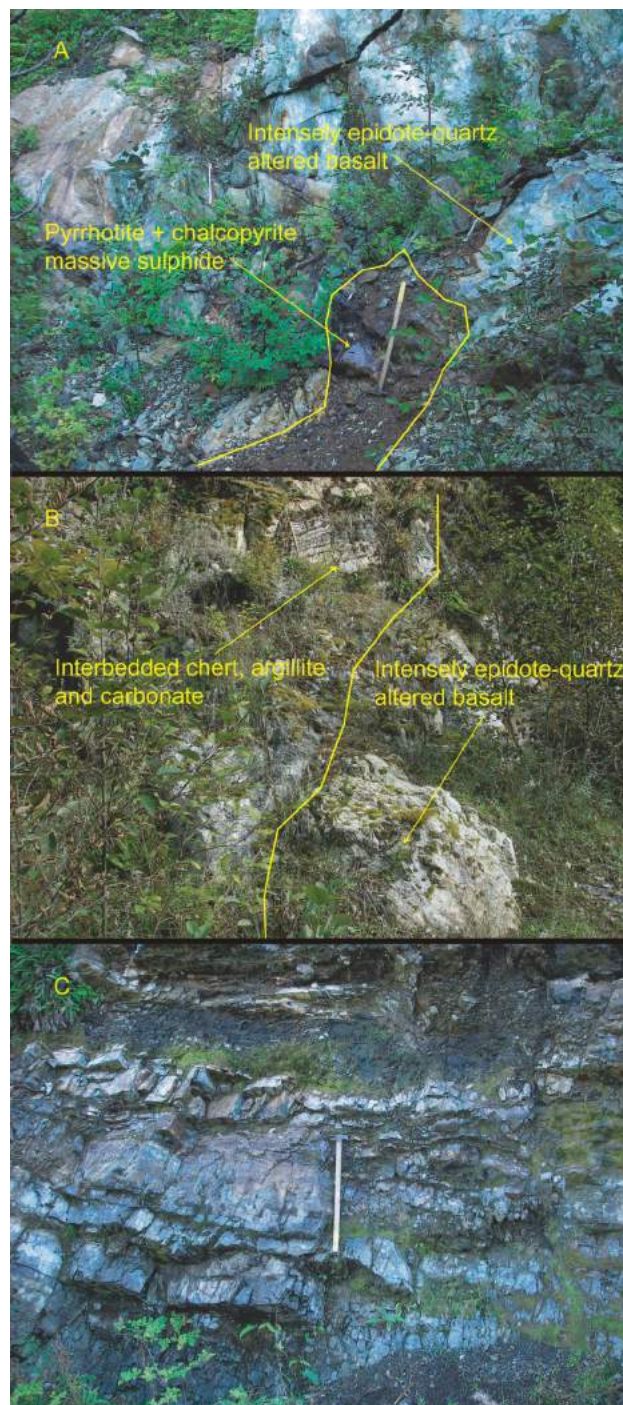


Figure 12. Rocks and mineralization of the Hesquiat Peninsula area, central Vancouver Island: **A)** pyrrhotite+chalcopyrite massive sulphide mineralization, measuring 1.5 m by 3 m, is hosted within strongly epidote-quartz–altered basalt (UTM Zone 9, 685043E, 5490975N); **B)** variably altered clinopyroxene- and feldspar-phyric basalt, similar to the Dorado VMS hostrock, intrudes a sedimentary package (Mooyah Formation?) comprising recrystallized carbonate, chert, siltstone and fine sandstone; **C)** interbedded graphitic argillite and chert of the Mooyah Formation.

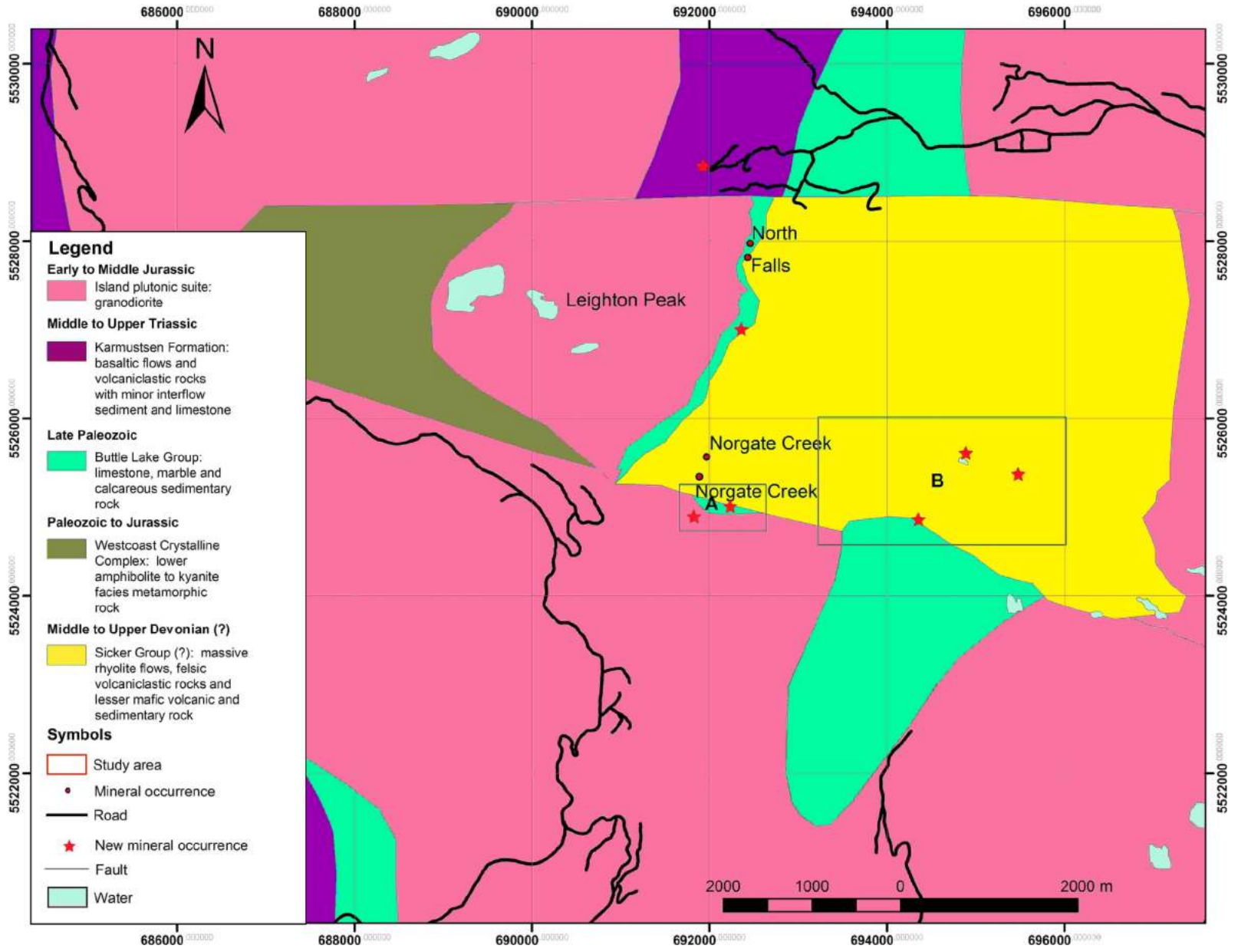


Figure 13. Regional geology of the Dragon property of Paget Resources Corporation (modified from Massey, 2005; Jones, 1997), central Vancouver Island, showing selected mineral occurrences and areas of study for 2009 fieldwork.

silica-sericite-altered and sulphide-mineralized felsic volcanic rocks (dominantly rhyolite flows) are overlain by a mixture of graphitic argillite, chert and massive carbonate. Similar to eastern portions of the property, a significant flattening of bedding exists. Several new mineral occurrences were discovered throughout the field area during the course of 2009 work. In study area A (Figure 13), gabbroic sills of probable Karmutsen Formation affinity were found on several occasions to contain chalcopyrite veins up to 1 cm width and pods of massive chalcopyrite up to 5–7 cm in width (Figure 14B). East of this occurrence, a dacitic unit was found to contain gossanous zones with stockwork-style chalcopyrite mineralization (Figure 14C). Several zones of stockwork-style VMS mineralization were encountered in study area B (Figure 13), comprising largely localized zones of pyritic stockwork-style mineralization associated with silicified felsic volcanic rocks.

Summary

Fieldwork in 2009 has continued to focus on resolving the stratigraphy and tectonic history of the Sicker Group and its contained mineral occurrences in the Cowichan Lake, Port Alberni, Nanoose, Bedingfield, Gold River and Hesquiat areas. This is being accomplished using a combination of bedrock mapping and sampling for geochronology (U-Pb, Ar/Ar), biostratigraphy (macrofossils, radiolarians and conodonts), geochemistry (major and trace elements) and isotopic analyses (Nd and Pb; whole rock and sulphides, respectively). Work in the Cowichan area was directed toward establishing the stratigraphic position and geological setting of VMS occurrences on mineral tenure owned by project sponsors Treasury Metals Inc. and Westridge Resources Inc. In addition, fieldwork and sampling were also concentrated on various exhalative iron formations to constrain the longevity of the VMS mineralizing hydrothermal system(s) in the Cowichan Lake area. Fieldwork in the Port Alberni area, sponsored by Bitterroot Resources Ltd., focused on resolving the age and geological setting of mafic volcanic rocks and associated VMS occurrences within the Nitinat and Duck Lake formations. Resolving the ages of these units is critical for understanding the temporal and metallogenic evolution of the Sicker arc, and the earliest history of Wrangellia.

Fieldwork in the Horne Lake area, in rocks previously assigned to the Nitinat and McLaughlin Ridge formations, has identified a stratigraphic section containing abundant, potential late Paleozoic volcanic rocks. This new section, coupled with recent dating studies done as part of this project, indicates that rocks in this area are probably no older than Late Devonian. Abundant mafic and newly identified felsic volcanic rocks at the top of the section are spatially associated with recently dated Early to Late Permian chert, suggesting the presence of a significant cycle of late Paleozoic magmatism in the area (Ruks et al., 2009b). New min-

eralization was discovered at the top of this stratigraphic section, where abundant stockwork pyrite mineralization is hosted by ribbon chert of probable Permian age.



Figure 14. Mineralization on the Dragon property of Paget Resources Corporation, central Vancouver Island: **A**) massive sulphide mineralization of the Falls showing, interlayered with laminated chert, mudstone and calcareous mudstone (UTM Zone 9, 692434E, 5527815N); **B**) massive chalcopyrite mineralization associated with Karmutsen Formation gabbro (691798E, 5524865N); **C**) stockwork-style chalcopyrite stringer mineralization in altered dacite (692265E, 5525028N).

Approximately 30 km south of the Horne Lake area, reconnaissance fieldwork east of Mount Spencer (Figure 6, study area D) resulted in the discovery of a new VMS occurrence hosted in stratigraphy of the Duck Lake Formation. This mineralization consists of a 10–15 cm wide stratiform band of massive, fine-grained pyrite with trace chalcopyrite, interbedded with grey-green ribbon chert, which sits upon a package of mafic volcanic and associated volcanoclastic rocks.

Fieldwork in the Nanoose area concentrated on resolving the stratigraphic position and geological setting of mafic volcanic rocks in the area. Pillow basalts and associated basalt volcanoclastic rocks of northern Ballenas Island overlie and are interbedded with crinoidal limestone and chert. The spatial relationship of basalt, chert and crinoidal limestone in the Nanoose area is similar to that observed in the Lacy Lake area (e.g., Ruks et al., 2009a), where recent radiolarian biostratigraphy by F. Cordey has confirmed an Early to Late Permian age. Sampling of chert and carbonate units in the Nanoose area for conodont and radiolarian biostratigraphy was carried out to resolve the age of this stratigraphy.

Fieldwork on the Dorado property (Paget Resources Corporation) in the Hesquiat Peninsula area has confirmed that the oldest rocks in the area are probably sedimentary rocks assigned to the Mooyah Formation (Marshall et al., 2006), which is undated and has unknown stratigraphic affinities. Mooyah Formation rocks comprise varying proportions of graphitic argillite, siltstone, sandstone, recrystallized carbonate and chert. In the vicinity of the Dorado VMS occurrences, they are intruded by strongly silica-epidote-altered clinopyroxene and feldspar-phyric basalt subvolcanic rocks, which host VMS mineralization. Variably altered basalt flows overlie basalt subvolcanic rocks and, in places, contain stockwork-style VMS mineralization (Marshall et al., 2006; Ruks et al., 2009a), suggesting the potential for multiple stratigraphic lenses of VMS mineralization on the Dorado property. Volcanogenic massive sulphide-style alteration and mineralization in the contact areas between basalt subvolcanic rocks and host sedimentary rocks suggest that both rock types are of similar age. Significant sampling for geochronology and biostratigraphy was carried out on Mooyah Formation rocks in the Hesquiat area to ascertain potential stratigraphic affinities with Paleozoic rocks of Wrangellia.

Fieldwork on the Dragon property, north of Gold River (Paget Resources Corporation) has identified additional localities where variably altered and sulphide-mineralized felsic volcanic rocks are overlain by a package of graphitic argillite, chert and carbonate. This economically significant contact hosts VMS mineralization at the Falls and North occurrences (Ruks et al., 2009a), and has now been traced for a length of 8 km, exhibiting significant potential

for VMS mineralization throughout. Fieldwork in the eastern part of the property was conducted to evaluate the potential for deeper stratigraphy and associated VMS mineralization. Here, additional stockwork-style VMS mineralization was documented, and sampling of felsic volcanic hostrocks for geochronology was carried out to ascertain the age and geological setting of mineralization.

Fieldwork in proposed Sicker Group rocks and VMS mineralization of the Bedingfield area has shown that numerous VMS occurrences, including the Bay Creek, Claim Post and Rant Point occurrences (MINFILE 092F 343, 092F 290 and 092F 494) are hosted in water-laid felsic volcanic rocks, comprising rhyolite flows and associated felsic volcanoclastic and tuffaceous rocks. Fieldwork in the Cypre River and Herbert Inlet areas indicates that felsic volcanic rocks are spatially associated with carbonate rocks, suggesting a potential stratigraphic scenario similar to that observed at the Dragon property north of Gold River, where carbonate rocks are observed to conformably overlie VMS mineralization and felsic volcanic rocks. If carbonate rocks of the Bedingfield and Dragon areas are Permian in age, this places them in a similar age range to widespread carbonate rocks of the Mount Mark Formation. This would suggest the presence on Vancouver Island of a widespread cycle of previously undocumented late Paleozoic bimodal magmatism and VMS mineralization possibly correlative with Paleozoic rocks of the Queen Charlotte Islands (Hesthammer et al., 1991) and southwestern Yukon Territory–southeastern Alaska (Israel and Cobbett, 2008). Such a correlation would suggest that Wrangellia is a long-lived, metallogenically well-endowed terrane of large geographic extent.

Future Work

Fieldwork in 2009 constitutes the final fieldwork for this project. Uranium-lead zircon dating, together with litho-geochemical and Nd and Pb isotopic studies of samples collected during the past field season, are now in progress and will be completed during the next six months. Results of this work will constrain the age and magmatic evolution of Paleozoic Wrangellia and help develop a framework through which VMS occurrences hosted by this stratigraphy can be distinguished from younger, epigenetic sulphide occurrences.

Acknowledgments

This project is jointly funded by a Geoscience BC grant, Bitterroot Resources Ltd., Paget Resources Corporation, Treasury Metals Inc., Westridge Resources Inc., a Natural Sciences and Engineering Research Council of Canada (NSERC) Discovery Grant to JKM, and an NSERC post-graduate scholarship to TR. The authors thank N. Massey for discussions and insights into the geology of the Sicker

Group and S. McKinley of Cambria Geosciences Inc. for having provided a critical review of this manuscript. The authors thank W. Ruks and B. Smyth for capable assistance in the field, and Island Timberlands and the District of North Cowichan for land access assistance in the Cowichan area. For logistical support and accommodations while working in the Beddingfield and Hesquiat areas, the authors thank D. Drake and B. Taylor of Isaak Forest Resources Ltd., Coulson Forest Products Ltd., D. Lorney of Tranquil Timber Ltd. and D. Scott of Port Neville Logging Co. Ltd. For excellent transportation services in the Clayoquot Sound and Nootka Sound areas, the authors thank G. Boddey and Nootka Sound Service Ltd. Thanks also go to several prospectors, consultants and explorationists working on Vancouver Island, especially M. Becherer of Mineral Creek Ventures Inc., M. Carr of Bitterroot Resources Ltd., J. Bradford of Paget Resources Corporation, E. Specogna of Specogna Minerals Corp., T. Sadlier-Brown of Westridge Resources Inc., S. McKinley of Cambria Geosciences, J. Miller-Tait and P. Gray of Selkirk Metals Corp., J. Houle, H. McMaster, the late S. Tresierra and the late A. Francis, for sharing their time and knowledge of Sicker Group geology and mineralization.

References

- Banerjee, N.R., Simonetti, A., Furnes, H., Muehlenbachs, K., Staudigel, H., Heaman, L. and Van Kranendonk, M.J. (2007): Direct dating of Archean microbial ichnofossils; *Geology*, v. 35, no. 6, p. 487–490.
- Barrett, T.J. and Sherlock, R.L. (1996): Volcanic stratigraphy, litho-geochemistry and seafloor setting of the H-W massive sulfide deposit, Myra Falls, Vancouver Island, British Columbia; *Exploration and Mining Geology*, v. 5, p. 421–458.
- Blackwell, J.D. and Lajoie, J.J. (1986): Geology and geophysics of the Beddingfield 1–15, Cypre 1 mineral claims, Alberni Mining Division, Tofino area, British Columbia; BC Ministry of Energy, Mines and Petroleum Resources, Assessment Report 15152, 111 p., URL <http://aris.empr.gov.bc.ca/search.asp?mode=repsum&rep_no=15152> [November 2009].
- Brandon, M.T., Orchard, M.J., Parrish, R.R., Sutherland Brown, A. and Yorath, C.J. (1986): Fossil ages and isotopic dates from the Paleozoic Sicker Group and associated intrusive rocks, Vancouver Island, British Columbia; *in* Current Research, Part A, Geological Survey of Canada, Paper 86-1A, p. 683–696.
- Franklin, J.M., Gibson, H.L., Jonasson, I.R. and Galley, A.G. (2005): Volcanogenic massive sulfide deposits; *Economic Geology 100th Anniversary Volume*, p. 523–560.
- Fyles, J.T. (1950): Jane, Sally and Sally No. 2; *in* Minister of Mines Annual Report, 1949, BC Ministry of Energy, Mines and Petroleum Resources, p. A224–A225.
- Galley, A.G., Hannington, M.D. and Jonasson, I.R. (2007): Volcanogenic massive sulphide deposits; *in* Mineral Deposits of Canada: A Synthesis of Major Deposit-Types, District Metallogeny, the Evolution of Geological Provinces, and Exploration Methods, W.D. Goodfellow (ed.), Geological Association of Canada, Mineral Deposits Division, Special Publication 5, p. 141–161.
- Gatchalian, F. (1985): Geochemical and prospecting report on the Cypress claim groups, Alberni Mining Division (NTS 92F/5); BC Ministry of Energy, Mines and Petroleum Resources, Assessment Report 14003, 31 p., URL <http://aris.empr.gov.bc.ca/search.asp?mode=repsum&rep_no=14003> [November 2009].
- Hesthammer, J., Indredlid, J., Lewis, P.D. and Orchard, M.J. (1991): Permian strata on the Queen Charlotte Islands, British Columbia; *in* Current Research, Part A, Geological Survey of Canada, Paper 91-1A, p. 321–329.
- Israel, S. and Cobbett, R. (2008). Kluane Ranges bedrock geology, White River area (parts of NTS 115F/9, 15 and 16; 115G/12 and 115K/1, 2); *in* Yukon Exploration and Geology 2007, D.S. Emond, L.R. Blackburn, R.P. Hill and L.H. Weston (ed.), Yukon Geological Survey, p. 153–167.
- Jones, M.I. (1997): 1996 assessment report, Dragon property, diamond drilling, Alberni and Nanaimo Mining Divisions, NTS map areas 92E/16E, 92L/1E, latitude 49 55 00 N, longitude 126 20 00 W; BC Ministry of Energy, Mines and Petroleum Resources, Assessment Report 24895, 189 p., URL <http://aris.empr.gov.bc.ca/search.asp?mode=repsum&rep_no=24895> [November 2009].
- Juras, S.J. (1987): Geology of the polymetallic volcanogenic Buttle Lake camp, with emphasis on the Price hillside, central Vancouver Island, British Columbia, Canada; Ph.D. thesis, University of British Columbia, 279 p.
- Katvala, E.C. (2006): Re-examining the stratigraphic and paleontologic definition of Wrangellia; *Geological Society of America, Abstracts with Program*, v. 38, p. 24.
- Kelso, I., Wetherup, S. and Takats, P. (2007): Independent technical report and mineral resource estimation, Lara polymetallic property, British Columbia, Canada; unpublished company report prepared by Caracle Creek International Consulting for Laramide Resources Ltd.
- Kemp, R. and Gill, G. (1993): Geological, geochemical and diamond drilling report on the Specogna-Muchalat property, NTS 92E/16, Alberni Mining Division; BC Ministry of Energy, Mines and Petroleum Resources, Assessment Report 23125, 48 p., URL <http://aris.empr.gov.bc.ca/search.asp?mode=repsum&rep_no=23125> [November 2009].
- Macdonald, R.W.J., Barrett, T.J., and Sherlock, R.L. (1996): Geology and litho-geochemistry at the Hidden Creek massive sulphide deposit, Anyox, west-central British Columbia; *Exploration and Mining Geology*, v. 5, p. 369–398.
- Marshall, D., Lesiczka, M., Xue, G., Close, S. and Fecova, K. (2006): Update on the mineral deposit potential of the Nootka Sound region (NTS 092E), west coast of Vancouver Island, British Columbia; *in* Geological Fieldwork 2005, BC Ministry of Energy, Mines and Petroleum Resources, Paper 2006-1 and Geoscience BC, Report 2006-1, p. 323–330, URL <<http://www.em.gov.bc.ca/mining/GeolSurv/Publications/Fieldwork/2005/toc.htm#GeoscienceBC>> [November 2009].
- Massey, N.W.D. (1995): Geology and mineral resources of the Duncan sheet, Vancouver Island, 92B/13; BC Ministry of Energy, Mines and Petroleum Resources, Paper 1992-4, URL <<http://www.empr.gov.bc.ca/Mining/Geoscience/PublicationsCatalogue/Papers/Pages/1992-4.aspx>> [November 2009].
- Massey, N.W.D. and Friday, S.J. (1988): Geology of the Chemainus River–Duncan area, Vancouver Island (92C/16, 92B/13); *in* Geological Fieldwork 1987, BC Ministry of En-

- ergy, Mines and Petroleum Resources, Paper 1988-1, p. 81–91, URL <<http://www.empr.gov.bc.ca/Mining/Geoscience/PublicationsCatalogue/Fieldwork/Pages/GeologicalFieldwork1987.aspx>> [November 2009].
- Massey, N.W.D. and Friday, S.J. (1989): Geology of the Alberni–Nanaimo Lakes area, Vancouver Island (92F/1W, 92F/2E and part of 92F/7); BC Ministry of Energy, Mines and Petroleum Resources, Open File 1987-2, URL <<http://www.empr.gov.bc.ca/Mining/Geoscience/PublicationsCatalogue/OpenFiles/1987/Pages/1987-2.aspx>> [November 2009].
- Massey, N.W.D., MacIntyre, D.G., Desjardins, P.J. and Cooney, R.T. (2005): Digital map of British Columbia: Tile NM10 Southwest BC; BC Ministry of Energy, Mines and Petroleum Resources, GeoFile 2005-3, URL <<http://www.empr.gov.bc.ca/Mining/Geoscience/PublicationsCatalogue/GeoFiles/Pages/2005-3.aspx>> [November 2009].
- MINFILE (2010): MINFILE BC mineral deposits database; BC Ministry of Energy, Mines and Petroleum Resources, URL <<http://www.minfile.ca>> [November 2010].
- Muller, J.E. (1977): Geology of Vancouver Island; Geological Survey of Canada, Open File 463, 1:250 000 scale.
- Muller, J.E. (1980): The Paleozoic Sicker Group of Vancouver Island, British Columbia; Geological Survey of Canada, Paper 79-30, 23 p.
- Pattison, J.M. and Money, D.P. (1988): 1987 drilling report on the West claims, project # 094/107, situated 1 km west of Crofton, BC in the Victoria Mining Division; BC Ministry of Energy, Mines and Petroleum Resources, Assessment Report 17007, 252 p., URL <http://aris.empr.gov.bc.ca/search.asp?mode=repsum&rep_no=17007> [November 2009].
- Ruks, T.R. and Mortensen, J.K. (2007): Geological setting of volcanogenic massive sulphide occurrences in the Middle Paleozoic Sicker Group of the southeastern Cowichan Lake uplift (NTS 092B/13), southern Vancouver Island; *in* Geological Fieldwork 2006, BC Ministry of Energy, Mines and Petroleum Resources, Paper 2007-1 and Geoscience BC, Report 2007-1, p. 381–394, URL <<http://www.empr.gov.bc.ca/mining/Geosurv/Publications/Fieldwork/2006/toc.htm#GeoscienceBC>> [November 2009].
- Ruks, T. and Mortensen, J.K. (2008): Geological setting of volcanogenic massive sulphide occurrences in the Middle Paleozoic Sicker Group of the Cowichan Lake uplift, Port Alberni area, southern Vancouver Island, British Columbia; *in* Geoscience BC Summary of Activities 2007, Geoscience BC, Report 2008-1, p. 77–92, URL <<http://www.geosciencebc.com/s/SummaryofActivities.asp?ReportID=358405>> [November 2009].
- Ruks, T., Mortensen, J.K. and Cordey, F. (2009a): Preliminary results of geological mapping, uranium-lead zircon dating, and micropaleontological and lead isotopic studies of volcanogenic massive sulphide-hosting stratigraphy of the Middle and Late Paleozoic Sicker and Lower Buttle Lake groups on Vancouver Island, British Columbia (NTS 092B/13, 092C/16, 092E/09, /16, 092F/02, /07); *in* Geoscience BC Summary of Activities 2008, Geoscience BC, Report 2009-1, p. 103–122, URL <<http://www.geosciencebc.com/s/SummaryofActivities.asp?ReportID=358404>> [November 2009].
- Ruks, T., Mortensen, J.K. and Cordey, F. (2009b): Stratigraphic and paleotectonic studies of the Middle Paleozoic Sicker Group and contained volcanogenic massive sulphide (VMS) occurrences, Vancouver Island, British Columbia (abstract); Geological Society of America Annual Meeting, Cordilleran Section, May 7–9, 2009, GSA Abstracts with Programs, Paper 7-3.
- Sluggett, C.L. (2003): Uranium-lead age and geochemical constraints on Paleozoic and Early Mesozoic magmatism in Wrangellia Terrane, Saltspring Island, British Columbia; B.Sc. thesis, University of British Columbia, 56 p.
- Sluggett, C.L. and Mortensen, J.K. (2003): U-Pb age and geochemical constraints on the paleotectonic evolution of the Paleozoic Sicker Group on Saltspring Island, southwestern British Columbia (abstract); Geological Association of Canada–Mineralogical Association of Canada, Joint Annual Meeting, Program with Abstracts, v. 28.
- Yorath, C.J., Sutherland Brown, A. and Massey, N.W.D. (1999): LITHOPROBE, southern Vancouver Island, British Columbia: geology; Geological Survey of Canada, Bulletin 498, 145 p.

Development of a Google Earth Query Tool for Wider Dissemination of British Columbia Geochemical Data to the Geoscience Community

W.M. Cadell, Timberline Natural Resource Group, Prince George, BC, will.cadell@timberline.ca

G. Mulligan, Golder Associates, Calgary, AB

Cadell, W.M. and Mulligan, G. (2010): Development of a Google Earth query tool for wider dissemination of British Columbia geochemical data to the geoscience community; *in* Geoscience BC Summary of Activities 2009, Geoscience BC, Report 2010-1, p. 171–174.

Introduction

Timberline Natural Resource Group and Golder Associates have developed a Google Earth™-based query tool. This tool is for the exploration of the QUEST Project geochemical data recently released by Geoscience BC and is available through Geoscience BC's website (<http://www.geosciencebc.com/s/DataReleases.asp>).

Being able to query the regional geochemical data provides the user an extra dimension of visualization. Instead of seeing every sample location point and having to discern which are of interest, the user is able to input specific criteria (element concentrations) into a web form and the result will be the selected points, which match the criteria, delivered directly into Google Earth. This way each user is empowered with a tool that allows for the exploration of the Geoscience BC geochemical data, interacting with it rather than simply looking at it.

The data explorer currently includes three QUEST Project geochemical datasets released by Geoscience BC in 2008 (Figure 1; Jackaman, 2008a–c). All QUEST Project datasets and reports can be downloaded from Geoscience BC's website (<http://www.geosciencebc.com/s/DataReleases.asp>). The geochemical datasets used in the data explorer are

Geoscience BC Report 2008-3: QUEST Project sample reanalysis (Jackaman, 2008a),

Geoscience BC Report 2008-5: Regional lake sediment and water geochemical data, northern Fraser Basin, central British Columbia (parts of NTS 093G, H, J, K, N & O; Jackaman, 2008b), and

Geoscience BC Report 2008-7: Regional stream sediment and water geochemical data, Pine Pass (NTS 093O), British Columbia (Jackaman, 2008c).

In addition, the collection and analyses of the QUEST Project geochemical samples are described in Jackaman and Balfour (2008).

Project Background and Motivation

Geoscience BC has invested considerable time, effort and money in providing a wealth of new public geoscience data for the central interior of BC. With highly technical products like data, it is crucial that it is both accessible and interpretable by all users, both in the mineral exploration industry and the general public. Often data in its rawest form can be very difficult to work with.

For the technically proficient user, there are freely available resources on the web to help interpret the available data. However, choosing something the user is already familiar with will increase the ease of use and successful interpretation of the data. For this reason, Google Earth was chosen as the platform for the Geoscience BC data, as many in the mineral exploration field already use Google Earth on a regular basis for planning, research or recreational purposes. In addition, the user does not need to rely on a number of different applications to make their decisions. Logistical planning can be undertaken from the same interface as the actual geological research and the user's own data can be easily added and viewed in context with Geoscience BC's data.

Data Explorer

The data explorer (Cadell and Mulligan, 2009) is based on Google Earth with the integration of bespoke web and database technologies. It interrogates an optimized spatial database of geochemical samples at the behest of the user, providing the answer as a Google Earth visualization (a KML file). The questions the user can ask are based on the chemical breakdown of each sample. For example, the data explorer can be queried to identify all reanalyzed stream-sediment samples with Au >100 ppb and Cu >500 ppm. A KML file identifying all samples with these characteristics will be returned to the user. This file is delivered to the computer of the user so they can store the results of any queries they run. Each sample is identified by a placemark, which when selected displays the geographic co-ordinates of the

Keywords: *geochemistry, Google Earth™, GIS, web, data sharing*
This publication is also available, free of charge, as colour digital files in Adobe Acrobat® PDF format from the Geoscience BC website: <http://www.geosciencebc.com/s/DataReleases.asp>.

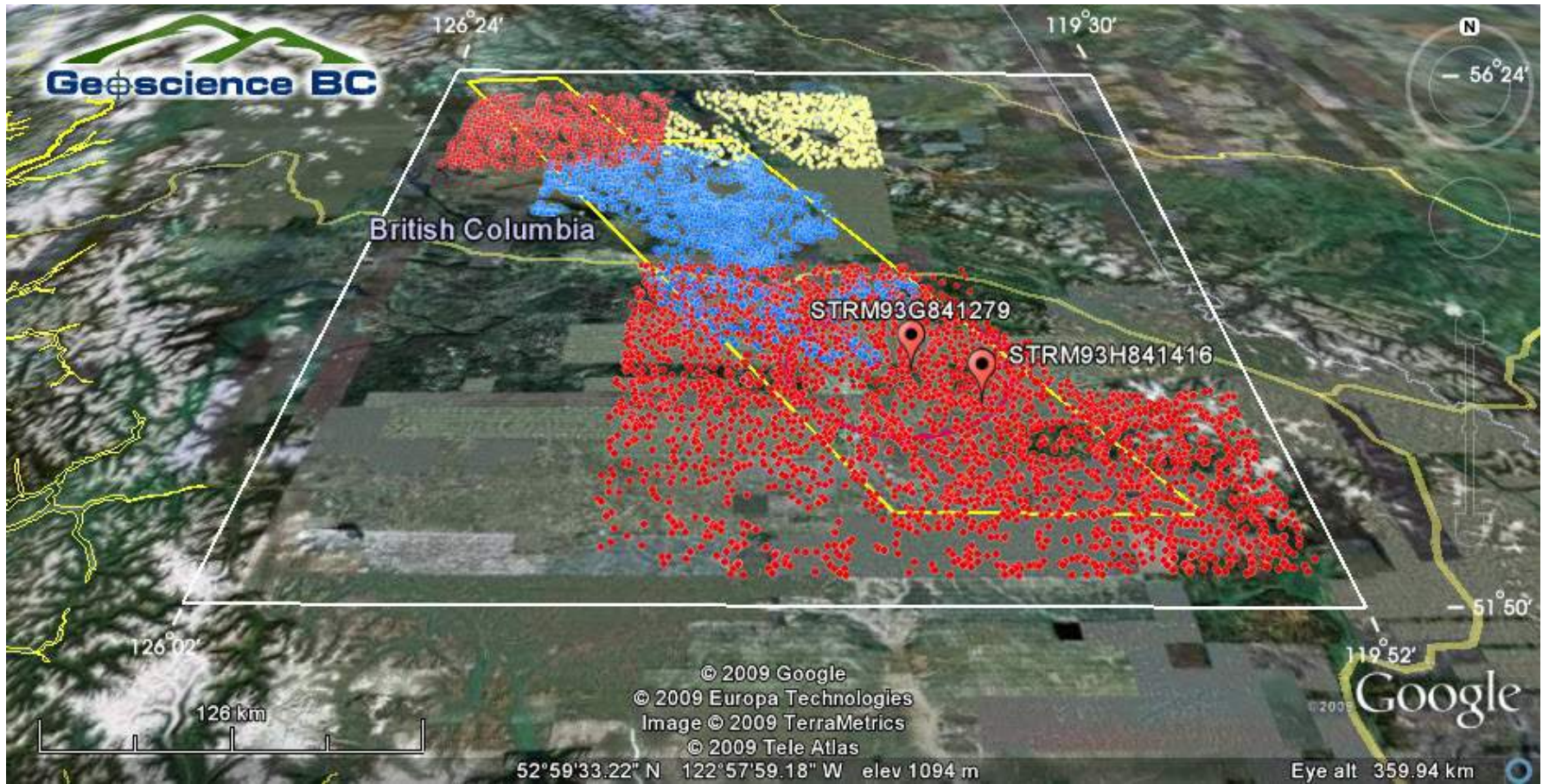


Figure 1. Sample locations included in Geoscience BC's three geochemical datasets, which the data explorer currently interrogates, shown with a query result (two placemarks), British Columbia. The QUEST Project area is outlined in white and the QUEST-South Project geophysical survey area is outlined in yellow.

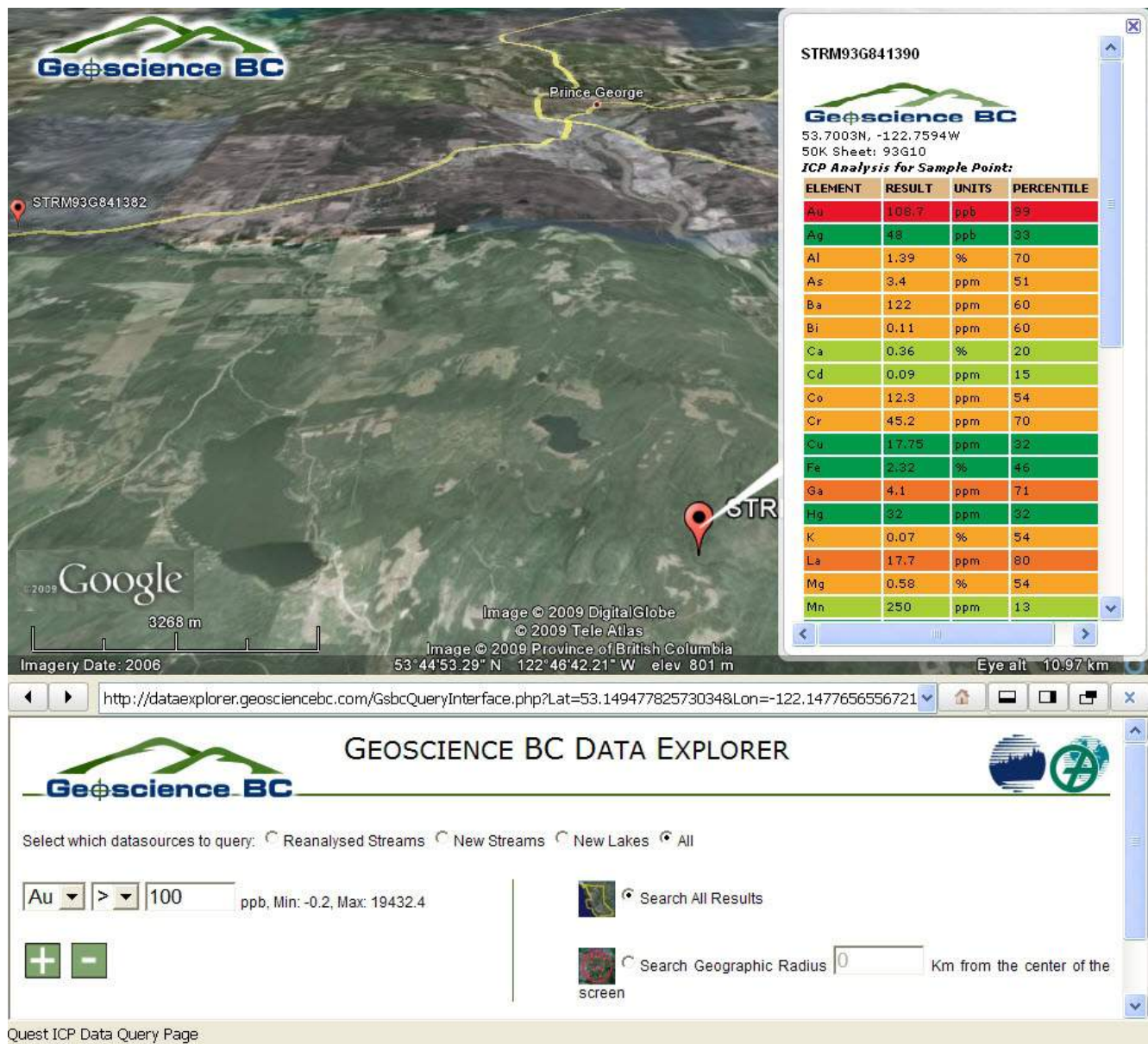


Figure 2. A screen shot of the data explorer interface, after a query is run (south of Prince George, British Columbia).

sample, the 1:50 000 map sheet the sample is from, and the entire geochemical dataset for that sample (colour-classed by percentile) in a balloon (Figure 2). Alternately, the user can choose to run a geographic query where the analysis is only undertaken within a specific radius of the centre point of the screen (e.g., find all samples with Cu >400 ppm within 30 km of a given location).

Background data available to the user includes a) polygons outlining the QUEST study area; b) polygons outlining the area covered by the QUEST Project geophysical surveys (Barnett and Kowalczyk, 2008); and c) a layer of all the geochemical sample points from the three projects. The latter allows the user to compare their queried findings with the point locations of all three entire datasets. Additionally, all the standard background data associated with Google Earth is available and the user can add any of their own datasets, as they would with Google Earth normally.

Conclusion

This project sought to increase the accessibility to the Geoscience BC QUEST Project geochemical data. The data explorer does this by providing the data in a nonproprietary format, which is readily accessible by a free and hugely popular platform. Since its release, the data explorer has witnessed 1000 page views from 21 different countries.

The data explorer can be accessed through Geoscience BC's website ([http://www.geosciencebc.com/s/2009-](http://www.geosciencebc.com/s/2009-08.asp)

[08.asp](http://www.geosciencebc.com/s/2009-08.asp); Geoscience BC Report 2009-8) or directly at <http://dataexplorer.geosciencebc.com:8080/>.

References

- Barnett, C.T. and Kowalczyk, P.L. (2008): Airborne electromagnetics and airborne gravity in the QUEST Project area, Williams Lake to Mackenzie, British Columbia (parts of NTS 093A, B, G, H, J, K, N, O; 094C, D); *in* Geoscience BC Summary of Activities 2007, Geoscience BC, Report 2008-1, p. 1-6.
- Cadell, W. and Mulligan, G. (2009): Geoscience BC data explorer; Geoscience BC, Geoscience BC Report 2009-8, URL <<http://dataexplorer.geosciencebc.com:8080/>> [November 2009].
- Jackaman, W. (2008a): QUEST Project sample reanalysis; Geoscience BC, Report 2008-3, 4 p.
- Jackaman, W. (2008b): Regional lake sediment and water geochemical data, northern Fraser Basin, central British Columbia (parts of NTS 093G, H, J, K, N & O); Geoscience BC, Report 2008-5, 446 p.
- Jackaman, W. (2008c): Regional stream sediment and water geochemical data, Pine Pass (NTS 093O), British Columbia; Geoscience BC, Report 2008-7, 262 p.
- Jackaman, W. and Balfour, J.S. (2008): QUEST Project geochemistry: field surveys and data reanalysis, central British Columbia (parts of NTS 093A, B, G, H, J, K, N, O); *in* Geoscience BC Summary of Activities 2007, Geoscience BC, Report 2008-1, p. 7-10.

QUEST and QUEST-West Property File: Analysis and Integration of Property File's Industry File Documents with British Columbia's MINFILE (NTS 093; 094A, B, C, D; 103I)

N.D. Barlow, Purple Rock Editing, Victoria, BC, nicole@purplerockediting.com

K.E. Flower, Purple Rock Editing, Victoria, BC

S.B. Sweeney, Purple Rock Editing, Victoria, BC

G.L. Robinson, Purple Rock Editing, Victoria, BC

J.R. Barlow, Purple Rock Editing, Victoria, BC

Barlow, N.D., Flower, K.E., Sweeney, S.B., Robinson, G.L. and Barlow, J.R. (2010): QUEST and QUEST-West Property File: analysis and integration of Property File's Industry File documents with British Columbia's MINFILE (NTS 093; 094A, B, C, D; 103I); in Geoscience BC Summary of Activities 2009, Geoscience BC, Report 2010-1, p. 175–188.

Introduction and Background

This paper outlines contributions to the British Columbia Geological Survey's Property File digital database, implemented by Purple Rock Editing and funded by Geoscience BC as part of their QUEST initiative (Figure 1). It describes a number of previously discovered but not publicly reported mineral occurrences. Highlighted herein are a potential Zn target in the Kimball Creek–Black Stuart Mountain area, a potential stockwork Mo deposit near Burns Lake and a potential epithermal Au system near Clisbako. These and other locations examined in the past and documented in Property File may have since become of economic significance.

Property File is an eclectic archive of about 100 000 geoscientific documents that have accumulated during the last 150 years of BC's mining history. Many of these documents contain the only known copies of original research and exploration reports. Prior to 2007, Property File had never been indexed, microfiched or scanned, so none of the information it contains was readily accessible to the public. About 35 000 of these documents (including those processed through this project) have been scanned and indexed, with just over 9 000 of these documents currently accessible to the public. Property File can be accessed online at <http://propertyfile.gov.bc.ca/>. Property File documents can also be found frequently referenced in the BC Geological Survey's mineral inventory database, MINFILE.

A substantial portion of Property File's documents was donated by companies, including Falconbridge, Cyprus-An-

vil, Rimfire, Chevron and Placer Dome, as well as individuals, scientists, prospectors and small companies. In this project, these Industry File documents (specifically those from Cyprus-Anvil, Rimfire, Chevron and Placer Dome) from the QUEST areas were scanned, indexed, added to the online database and used to update any related MINFILE occurrences.

During the course of this project, numerous mineral occurrences were found documented in Property File but not present in MINFILE. This report highlights these discoveries, along with notable updates to existing MINFILE occurrences.

Project Summary

In this project, 2619 documents were scanned, processed, added to the Property File database and integrated with the appropriate MINFILE geological description and bibliographies. Another 241 previously scanned Property File documents were similarly integrated with MINFILE. In total, 483 MINFILE occurrences were updated and 17 new MINFILE occurrences were identified.

Table 1 shows a breakdown of the Property File documents processed by collection.

Results

General Files

Some Property File documents from the QUEST area contain widespread projects that fall into the 'general file' cate-

Table 1. Documents processed, by Industry File collection.

Collection	Number of documents processed
Cyprus Anvil	494
Rimfire	1339
Chevron	304
Placer Dome	482
Total	2619

Keywords: QUEST, QUEST-West, Property File, mineral exploration, MINFILE

This publication is also available, free of charge, as colour digital files in Adobe Acrobat® PDF format from the Geoscience BC website: <http://www.geosciencebc.com/s/DataReleases.asp>.

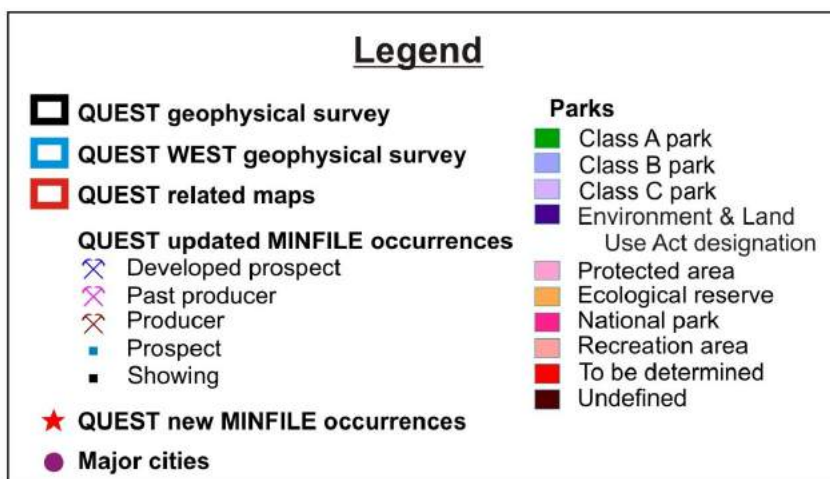
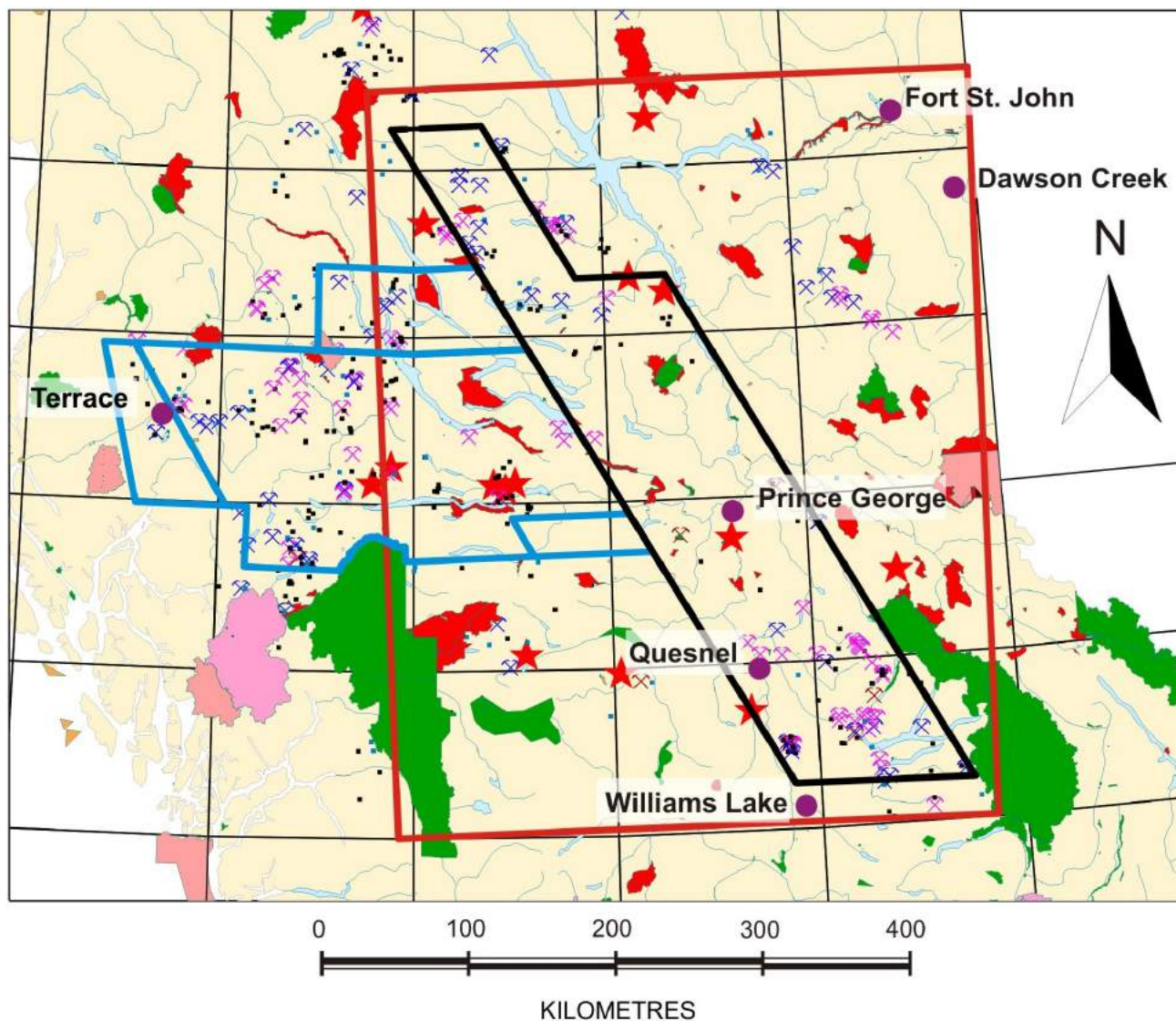


Figure 1. Location of the QUEST and QUEST-West areas in central British Columbia and relevant MINFILE occurrences (modified from MapPlace, 2009).

gory and are not associated with a known MINFILE occurrence. These are referenced by a system similar to MINFILE numbers; for example, the general file for a 1:250 000 map sheet can be 093 GEN. This section contains a review some of the more interesting document findings in the general file category.

Cordilleran Sediments Project: Quesnel Lake Area

The Chevron collection contains a set of documents that describes the Cordilleran Sediments Project in 093A GEN (Dillon, 1980a). These documents include maps, analyses and sample sheets from two stream geochemical surveys conducted in the Quesnel Lake–Barkerville area. The ‘Cordilleran Sediments geochemical stream sediment program, Quesnel Lake–Barkerville area’ report (Dillon, 1980a) covers two geochemical studies. The first is a reconnaissance-level study, which covered a 6000 km² area and comprised 384 samples. The researchers concluded that two areas, both in NTS 093A/14, were promising and warranted more detailed exploration.

The follow-up study in the same report included 230 samples collected over a 462 km² area, 75% of which was accessible only by helicopter. The first anomalous area, Cunningham Creek–Roundtop Mountain, was dismissed by the researchers because the anomalously high Pb values were due to past placer operations in the area. The samples in the Kimball Creek–Black Stuart Mountain area, however, proved more interesting. The highest Zn values (2620 and 2605 ppm) occurred within the Midas Formation (black shale and phyllite) or downstream from its contact with the Yank’s Peak quartzite. This led the author of the above-mentioned report to recommend that the most likely point of Zn mineralization is “near the upper contact of the Midas Formation with the Yank’s Peak quartzite” (Dillon, 1980a). There is no record of any follow-up work.

Cordilleran Sediments Project: Chetwynd Area

The Cordilleran Sediments Project also included exploration in the Chetwynd area. The program report (Dillon, 1980b) described a reconnaissance stream silt geochemical program that was conducted in NTS 093O/7 and /10 from August 15 to 20, 1980. Forty-two samples taken over 842 km² returned primarily weakly anomalous Zn values—except for one sample, which returned 860 ppm Zn, 240 ppm Pb, 150 ppm Cu and 5.4 ppm Ag (Figure 2).

Eutsuk Project

Two Property File reports from the Cyprus-Anvil collection support the Eutsuk Project. Woodcock (1971) is a report on Mo in the Pond claim group (MINFILE 093E 058; MINFILE, 2009), a region with Cu and/or Ag occurrences but no other known reports of molybdenite. In this study of a large pyritic gossan zone 130 km southwest of Burns Lake, Woodcock claimed that the region has a tectonic and

geological setting suitable for a stockwork molybdenite deposit.

The gossan zone in question measures 3.2 km by 1.2 km and has an hourglass shape. Some of the results of stream, silt and rock geochemistry performed on the property (e.g., the low values of Mo in silt) are similar to those from the nearby Red Bird molybdenite deposit (MINFILE 093E 026). Other results, including up to 35 000 ppm F in the rock samples from the central gossan, led Woodcock to believe that fluorspar or topaz was present in the area. Also, Mo is extremely low in the water samples (up to only 7 ppb), which had pH values as low as 3.7. According to Woodcock, the depletion of Mo is considerable in BC because of the abundant rain that increases the pH of nearby water. Molybdenum is soluble in more basic waters. This unique setting lends credence to Woodcock’s theory and he recommended drilling two holes of 305 m (1000 ft.) into the gossan to test it.

Sawyer and Mark (1972) briefly corresponded regarding Woodcock’s report. Although they believed “the molybdenum prospect does look to be a long shot”, Sawyer said that he “would recommend serious consideration largely on the basis of Woodcock’s ability and experience” (Sawyer and Mark, 1972). It seems, however, that this project was never pursued.

Hogem Batholith

The Hogem batholith is discussed in two Property File reports: ‘Hogem Batholith (South)’ (Reynolds, 1970), covering the southern portion of the batholith; and ‘Hogem Batholith Reconnaissance Project’ (Johnson, 1971a), covering portions of NTS 093N, 094C and 094D.

Reynolds’s report records the results of a reconnaissance stream sediment geochemistry survey on a portion of Omineca intrusive rocks in a 4100 km² portion of the Hogem batholith, completely within NTS 093N. The survey, which was in search of porphyry-Cu-type deposits, collected soil and water samples every 19 km (12 mi.) of total drainage and at major stream intersections throughout the drainage area. Copper values did not exceed 200 ppm, but the survey did identify four anomalous areas and recommended staking and further exploration of the GIL 1–120 claims in NTS 093N/07.

Johnson provided further details in an assessment report (Johnson, 1971b). Although his report recommended no further work, he recorded up to 600 ppm Cu in the 1500 soil and silt samples collected and claimed that “the largest and strongest anomalous zones appear to be along the contact of the intrusive (?) syenite-monzonite. Although no Cu mineralization was seen in these areas, it is highly probable that above background, low grade hydrothermal solutions would accompany the intrusive which would create these

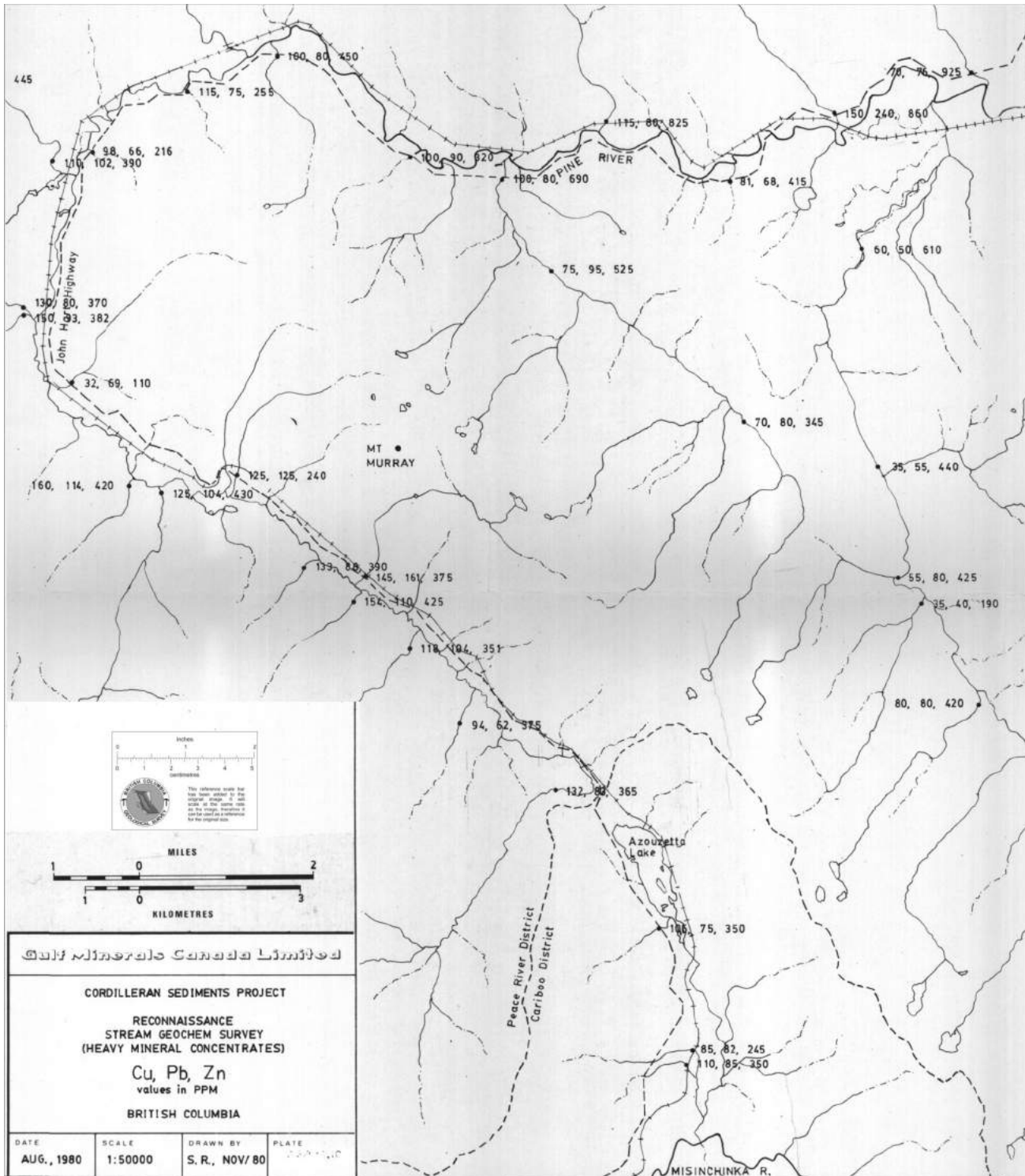


Figure 2. Portion of a stream geochemical survey map of Cu, Pb and Zn in heavy mineral concentrates, Chetwynd area, central British Columbia (Dillon, 1980b).

anomalous non-economic concentrations” (Johnson, 1971b).

Johnson’s report (1971a) in Property File is a 140-page document that includes the reconnaissance survey of both Hogem North and Hogem South, the follow-up soil and silt surveys on the areas of interest, the geochemical results for the samples taken, and the sample results and locations plotted on both large- and small-scale maps of the region. The most interesting prospect in the Hogem Batholith project is Duckling Creek, which shows soil anomalies of up to 391 ppm Cu. Another anomalous sample in the reconnaissance project returned greater than 1000 ppm Zn. Since only one sample was taken at that particular river, it is not possible to tell whether this sample indicates a significant anomaly.

New MINFILE Occurrences

In addition to documents about general or widespread parts of the QUEST area, this project identified new MINFILE occurrences through portions of larger documents or reports documenting exploration work done on specific, previously unidentified mineral occurrences. This section provides a summary of several notable new MINFILE occurrences that were identified as a result of this project. The entire list of new MINFILE occurrences is provided in Table 2.

Tub 1–3 (093B 065)

After successfully panning for Au on his property, H. Tuura asked A. Burton to conduct a more complete exploration of the Tub 1–3 and Tuura Ten 1–4 claims (Burton, 1991). The claims are located on an unnamed creek flowing into

Narcosli Creek near Webster Lake, 31.5 km southwest of Quesnel.

Fieldwork was completed from August to October 1991 and included collecting samples from the creek. Five and a half kilometres of the creek contained anomalous Au values. Five samples returned more than 1000 ppb Au, including one that yielded 6820 ppb Au. See Figure 3 for the locations of 11 samples.

Given the location of the occurrence, just east of the well-explored Clisbako region, and the favourable geology of underlying intrusive and volcanic masses paired with a network of normal, thrust and transcurrent faults, Burton (1991) concluded that “...the anomalies extend over a large enough cohesive area to be compatible with two moderate or one large epithermal lode gold system.”

Although this property is called “worthy of further exploration” and is given a “high odds of success” (Burton, 1991), no assessment reports have been written on the area except for the nearby 30817, which reports on a small project and is currently under review. All nearby MINFILE occurrences record diatomite or clay.

QFP (093B 066)

The document supporting the QFP MINFILE occurrence (Heberlein, 1992a) is a five-page report on the limited work done on the property, including preliminary mapping and a rock and soil sampling program. Approximately half of the 19 rock samples collected yielded Au values of up to 145 ppb, with one sample of chalcedonic quartz returning 3100 ppb Au (Heberlein, 1992a). Unfortunately, the soil samples were not as promising. The geological setting of

Table 2. New MINFILE occurrences from the QUEST Property File project.

MINFILE No.	Names	Status	Commodities	NTS area	Latitude, longitude (NAD 83)
093B 065	Tub 1-3, Tuura Ten 1-4	Showing	Au	093B10E	52°43'48" N, 122°39'00"W
093B 066	QFP, Fishpot	Showing	Au, Cu	093B13W	52°58'48"N, 123°55'48"W
093F 034	Tat	Showing	Cu	093F09E	53°30'21"N, 124°52'12"W
093F 069	Ram 1-2, Mstsacha	Showing	Au, Cu, Zn, Pb	093F02W	53°06'00"N, 124°52'12"W
093G 031	Wed, Minou	Showing	Cu, Au, Mo	093G15W	53°46'12"N, 122°46'12"W
093H 046	Cochran, L'Orsa	Showing	Cu	093H11E	53°31'48"N, 121°07'12"W
093K 105	Bonus	Anomaly	Mo	093K03E	54°05'24"N, 125°03'03"W
093K 107	Chess	Anomaly	Mo	093K03E	54°07'12"N, 125°10'48"W
093L 330	Orion	Showing	Ag, Zn	093L01W	54°07'48"N, 126°25'12"W
093L 331	Benamy, Lucky Ben 2, Foxy Creek	Showing	Ag	093L01E	54°13'48"N, 126°13'48"W
093M 196	David, Joy, Spark	Showing	Mo, Cu	093M08W	55°15'36"N, 126°21'36"W
093N 226	Diver Lake Group, DAG	Showing	Cu	093N12W	55°41'24"N, 125°53'24"W
093O 051	K Group, Nat, Horribilis	Showing	Au	093O05E	55°21'00"N, 123°43'48"W
094B 034	Len, Oak	Showing	Pb, Zn, Ag	094B11W	56°32'24"N, 123°28'48"W
094B 035	Brin, Nebasche, Bertha	Showing	Pb, Zn, Ag	094B05E	56°18'00"N, 123°30'36"W
094D 190	May	Showing	Cu, Ag, Zn, Mo	094D15E	56°58'48"N, 126°33'36"W
094G 037	Cusker, Bertha	Showing	Zn, Ag, Pb, Cu	094G04W	57°00'36"N, 123°47'24"W

the QFP MINFILE occurrence is significant because the QFP claims are underlain by a quartz-eye rhyolite porphyry body that shows alteration, and the adjacent Fishpot claims are underlain by similar porphyritic dikes. Altered epiclastic sedimentary rocks, including chert-pebble conglomerate, shale and tuffaceous sandstone, host these intrusions. Breccia veins with episodic banding cut the sediments. This geological setting suggests a potential significant epithermal system nearby, masked by the overburden that almost completely blankets the area (Heberlein, 1992a).

The report concluded with a recommendation not to proceed with further exploration and development of the property. The recommendation was apparently ignored because Assessment Reports 20277, 21594, 22400 and 23045 were subsequently written on the QFP property, and Assessment Reports 20022, 20874, 23695 and 24177 were subsequently written on the Fishpot claims. The occurrence remains in the exploration stage.

Ram 1-2 (093F 069)

The Ram 1-2 occurrence is located on Tsacha Mountain, with one of the closest established MINFILE occurrences

being the Capoose deposit (MINFILE 093F 040), 27 km to the southeast.

Several documents from the Placer Dome collection called the claim group 'Mtsacha' during the 1980s, and one document from the Rimfire collection called it 'Ram' during the 1990s.

The Placer Dome documents include a hand-drawn soil, rock and silt sample location map (JMT Group, 1982b); a soil geochemical survey map showing As sample values and As contours (Figure 4; Placer Development Limited, 1982); a soil, rock and silt sample location map showing Cu and Zn values (Anonymous, 1982a); and two geochemical maps delineating Cu values greater than 500 ppm (Anonymous, 1982b) and Zn values greater than 200 ppm (Anonymous, 1982c).

Also in the Placer Dome collection is a 23-page report (Kimura, 1982b) on a property evaluation commissioned by the JMT Group. The question was whether this property may have a similar geological setting and potential to the nearby Capoose deposit (MINFILE 093F 040). The document reported the results of geochemical mapping and soil sampling of 80% of the claim area during the field season of

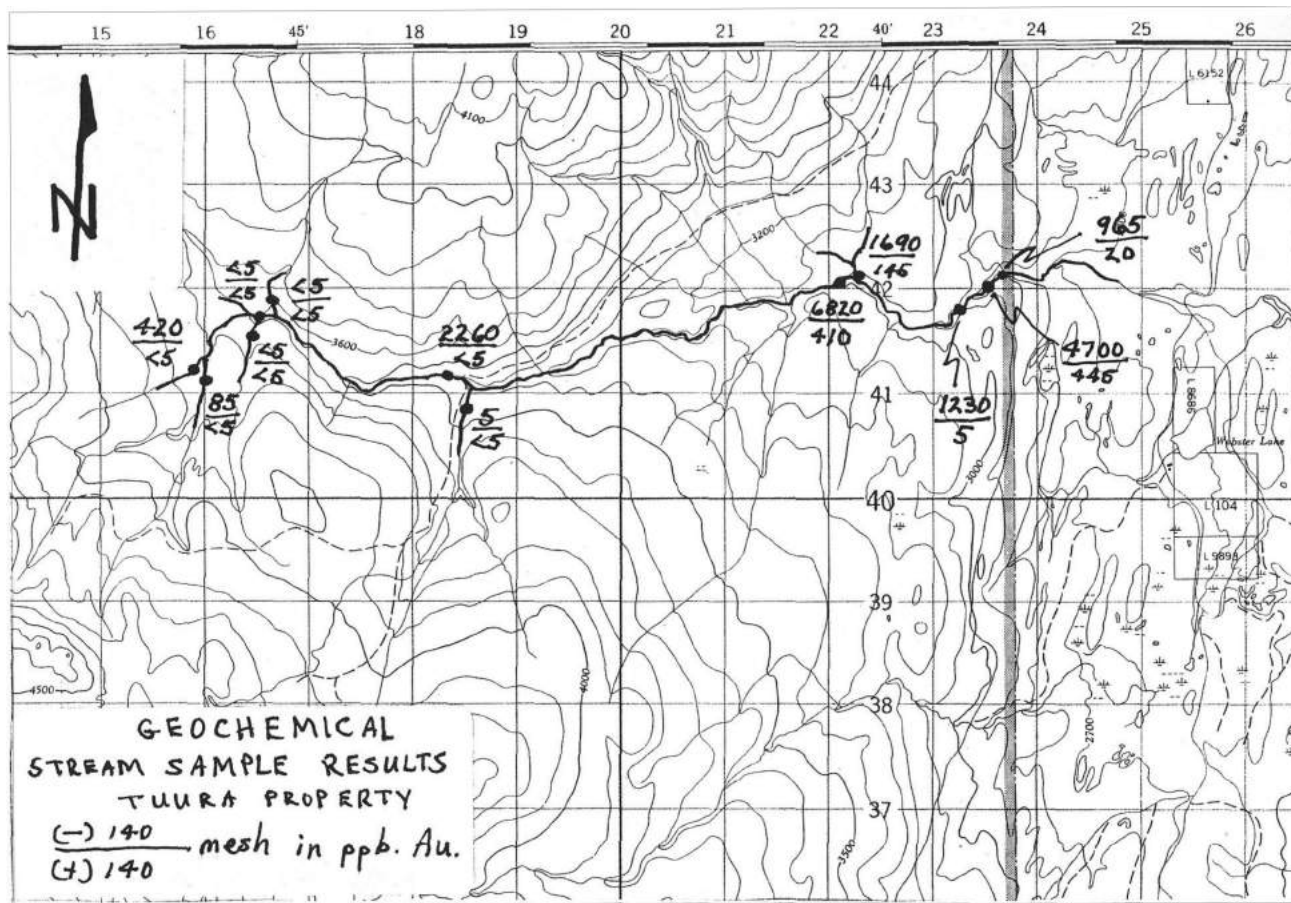


Figure 3. Sketch map of geochemical stream sample results, Tub occurrence, central British Columbia (MINFILE 093B 065; Burton, 1991).

1982. Although only minor pyrite and rare chalcopyrite mineralization was detected, the soil samples returned As values in the range 500–900 ppm, consistent with Cu and Zn rather than Au mineralization. The report also noted a persistent Zn anomaly. In a separate but contemporary report, Kimura's geochemical analysis sheets from Mtsacha (Kimura, 1982a) show values in various samples as high as 2000 ppm Zn, 260 ppm Cu, 390 ppm Pb, 500 ppm As, 2.1 ppm Ag and 1.29 ppm Au. Kimura (1982b), however, did not recommend pursuing this property further.

The Property File document that supports the creation of the Ram MINFILE occurrence is a two-page report (Kasper, 1993) that outlines and describes the Ram 1–2 claims. Although the report recommended declining the property, it noted three areas of mineralization: the first contained rock samples showing Zn values ranging from 1460 ppm to 3.3% Zn; the second contained mineralization of potassium feldspar, chlorite, epidote, garnet alteration and veins of skarn material containing pyrite and magnetite; and the third contained “a 400 by 600 m wide band of low-order Cu-Zn-Pb-As soil anomalies.”

At the time of the document's publication, access to the property was limited to helicopter or ATV. Now the Digital Road Atlas layer on the BC Geological Survey's MapPlace shows roads leading directly to the site.

In addition to the documents from Property File, Assessment Reports 22539 and 23520 support this new MINFILE occurrence.

Brin (094B 035)

The Brin MINFILE occurrence occurs on a tributary of the Nabesche River in NTS area 094B/05. Reconnaissance exploration began in this area as a result of the discovery of the Barrier–Robb Lake Pb-Zn occurrence (the developed prospect, MINFILE 094B 005). In discussing the Pine Point deposit and deposits in southeastern Missouri, Campbell (1972) explained that the analogous Robb Lake occurrence would also contain mineralized reefal dolomite of the Middle Devonian. This unit is well exposed on Brinex claim block 5. Tavela (1972) recorded Zn values of 300 and 700 ppm on the Nabesche claims (part of the Brin claim group). In total, three Zn, one Cd, two Pb and nine Ag anomalies were also found on the Brin claim group (Campbell, 1972).

During the 1970s, assessment work was done on many claims in the area surrounding the Brin group. Of particular interest is Pearson (1974), which is an assessment report covering the same Nabesche claims that are found in the Property File Cyprus-Anvil document (Dickie, 1972) and discussed in Campbell (1972) and Tavela (1972). Little exploration has been recorded in the area since these reports.

Cusker (094G 037)

The documents supporting the Cusker MINFILE occurrence summarize reconnaissance exploration that began after the discovery of the Barrier–Robb Lake occurrence. The Cusker occurrence lies 12 km north-northwest of Robb Lake on Sidenius Creek and was explored as a result of the same regional studies that led to discovery of the Brin occurrence. Rich float was reported on the southwestern Bertha claims, with sphalerite, copper and galena found on the property (Campbell, 1972; Tavela, 1972). Two significant geochemical anomalies exceeded 1000 ppm Zn (Campbell, 1972). Tavela's (1972) paper also reported the existence of Zn-Cd-Pb anomalies that occur mostly south of Sidenius Creek, likely a continuation of the mineralized field from the Robb Lake occurrence. Detailed geochemical maps support Tavela's recommendations.

Campbell (1972) agreed with many of Tavela's statements regarding the area, although he took a different approach: Tavela's (1972) report was a 'geochemical exploration', whereas Campbell's report was an 'office study', focusing on analogous deposits at Pine Point and in southeast Missouri. Along with the Cusker and Bertha claims, Campbell mentioned the 'Dodson submittal', which included a discovery of significant mineralization. We believe that this 'submittal' is possibly the same occurrence as Assessment Report 4149 (Leighton and Dodson, 1972).

Westoll and Sullivan (1973) and Adamson and Saunders (1973) did further work on the area and are the most recent studies known to date.

Updated MINFILE Occurrences

In addition to adding new MINFILE occurrences to the database, information uncovered during this project was used to enhance 483 existing occurrences by adding references to relevant documents in the MINFILE bibliographies, hyperlinking them and adding information to the geological descriptions. The examples described in this section either originally had very small MINFILE geological descriptions, which increased significantly following addition of the Property File information, or key information on occurrences was missing and the Property File documents enabled that information to be added to the descriptions.

Bob (093B 054)

The Bob occurrence originally had a geological description that included the regional geology and the geology of the claim locations. Using ten documents from the Property File Rimfire collection, the geological description now includes the initial staking by Lac Minerals; the drilling history of the Bob group; the drilling and geochemical surveys of the Naz group; line-cutting and a geochemical survey on the McKay claims; and a geochemical survey, IP surveys

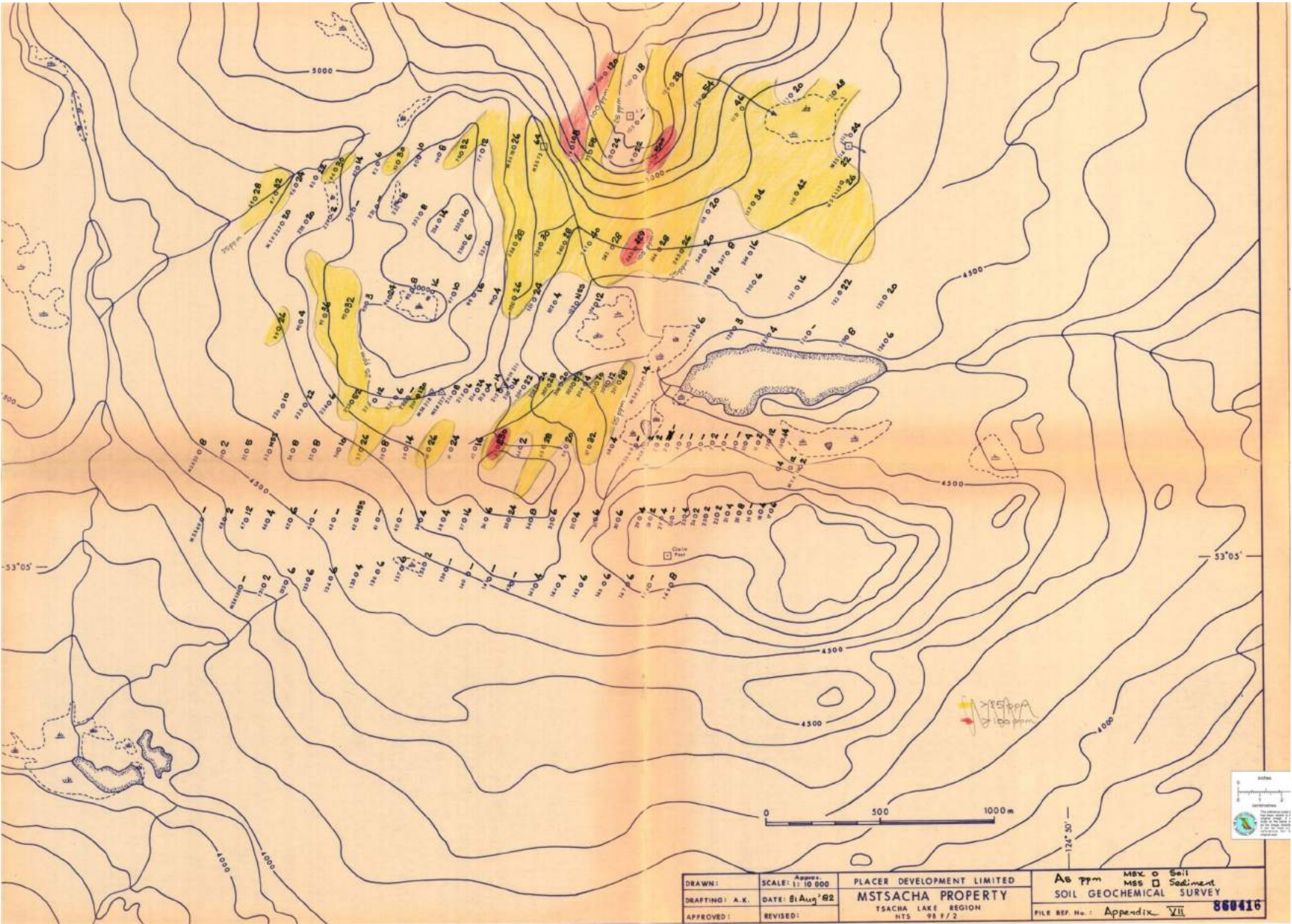


Figure 4. Soil and sediment geochemical survey map showing As sample values and contours, Ram occurrence, central British Columbia (Placer Development Limited, 1982).

and drilling on the Esker claims. Exploration of the multi-element soil geochemical anomaly occurred between 1983 and 1988, and returned 0.10% Cu over 2 m (Eldor Resources Ltd., 1987), 300 ppb Au over a thickness of 3.05 m (Anonymous, 1987) and a mineral inventory of 384 200 t grading 0.75 g/t Au (Eighty Eight Resources Ltd., 1990). The distribution of the latter Au values can be seen in Figure 5.

Tetrahedrite (093E 059)

Prior to this report, the Tetrahedrite occurrence contained only a small geological description. This project expanded the description so that it now also contains the exploration history. The most significant work on the site was by the Meteor Mining Co. Ltd. One of the two Property File documents (Meteor Mining Co. Ltd., 1966) includes a geochemical survey map and a self-potential survey, which indicates anomalous values of both Ag and Cu. The other document (Pavelic and Chisholm, 1967) includes various sample assays taken in 1922 and 1924, an excerpt from the Report of the Minister of Mines in 1923, seven 'ore' sample assays from the Cascade mineral claims conducted in 1926 and excerpts from a report by W.H. Plumb in 1956. These documents demonstrate continued exploration interest in the property over numerous decades.

Wolf (093F 045)

The Property File Rimfire collection contains 306 documents on the Wolf occurrence, including geological sketches and maps, drilling sections, drill logs and maps, reports, photographs of samples, airphoto overlays, geochemical analyses, IP survey maps, biogeochemical survey results, surface trenching maps and VLF-EM maps and profiles. Also, the Rimfire collection includes an M.Sc. thesis (Andrews, 1988) that focuses on the development and mineralization of the property, and a report on the Nechako project (including the Wolf occurrence; Nelson, 1985). These documents span 15 years of exploration (1979–1994), during which Lucero Resources Ltd. conducted exploration on the Ridge and Pond zones and Minnova conducted biogeochemistry, airborne magnetic and electromagnetic surveys, and diamond-drilling after optioning the property from Lucero Resources.

Of particular interest is the report by Heberlein (1992b), which provides results from the property thus far, including trenches containing mineralized hydrothermal breccias that returned values of up to 2.64 g/t Au. In the same report, Heberlein wrote that new targets will be explored based on high resistivity values and northeast-trending structures. Heberlein (1994) included some interesting values, such as 21.65 g/t Au over 3 m and 6.12 g/t Au over 3 m on a shallowly west-dipping breccia in the trenches on the Ridge zone.

Despite being classified as only a prospect in the MINFILE database, the Wolf property is an epithermal Au-Ag occurrence that has been well documented over the years. Little exploration has occurred since the mid-1990s.

G-South (093G 007)

The Property File Cyprus-Anvil collection contains 26 documents on the G-South occurrence and the Rimfire collection contains another two. Combined, these documents provide information on the history of the work done on the property by Alrae Engineering Ltd., Cariboo Minelands Ltd. and Gabriel Resources Ltd.

The oldest Rimfire document is correspondence regarding the Ahbau Creek area that describes a moderate interest in the property (Sirola, 1964). Alrae Engineering Ltd. wrote a report detailing a mineral examination, geochemical soil sampling program and a ground magnetometer survey (Jury, 1968). That report recommended further exploration that was, in turn, documented in a diamond-drill record (Cariboo Minelands Ltd., 1969) and a summary report (Simpson, 1969), which records eight drillholes totalling almost 914 m (3000 ft.). Diamond-drill hole 1 assayed 3.54 g/t (0.16 oz./ton) Au, 3.89 g/t (1.16 oz./ton) Ag, 0.17% Cu and 0.53% Pb over 1.83 m (6 ft.) of core, and hole 6 assayed 5.67 g/t (0.20 oz./ton) Au, 72.01 g/t (2.54 oz./ton) Ag, 1.86% Cu, 0.2% Pb and 0.57% Zn; however, the company indicated "only subsidiary interest" in the property (Simpson, 1969).

Another document from the Rimfire collection combined a series of news releases from the late 1980s from Gabriel Resources Ltd., who optioned the property in 1981 (Hughes, 1988). These include results from geochemical, airborne magnetometer, electromagnetic, VLF-EM and IP surveys, as well as 43 diamond-drill holes and trenching.

Eleven assessment reports have been written on the area, and the G-South occurrence has been upgraded to a 'developed prospect' in the MINFILE database.

Cob (093M 088)

The Cob Mo-Cu showing originally had a mere two-sentence MINFILE geological description, specifying only its location and regional geology. Ten documents from the Cyprus-Anvil collection enhanced this information significantly, including three reports published in consecutive years and seven supporting maps of related work. Leigh and Kahlert (1967) reported multidirectional fracturing and quartz veining that contained visible molybdenite flakes. The most favourable trench result averaged 0.09% MoS₂ over 12 m (40 ft.). The North zone rock samples averaged 0.07% MoS₂ and the South zone rock samples averaged 0.03% MoS₂. The report includes duplicate sample assays from two laboratories. In light of the results, Leigh and

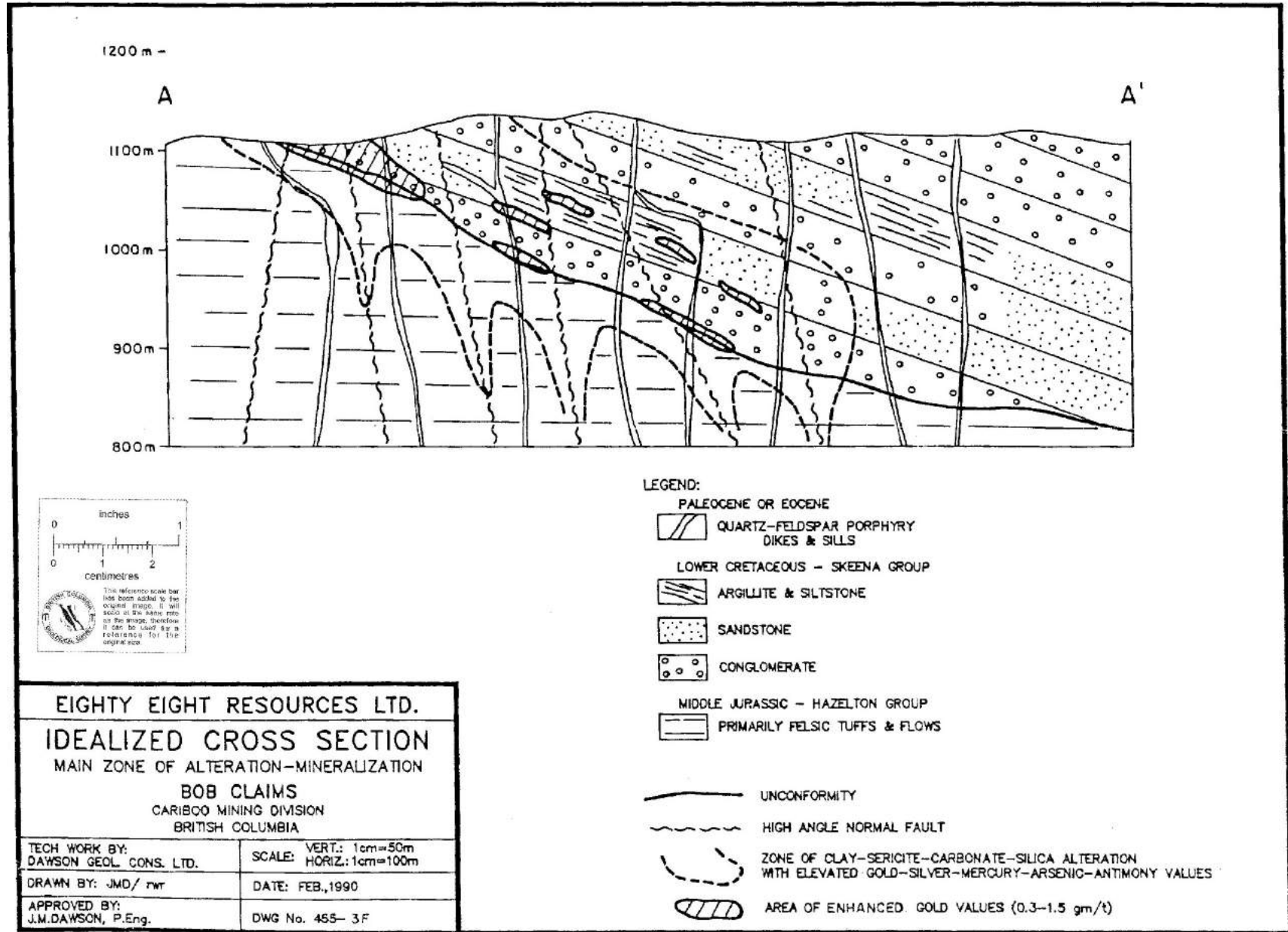


Figure 5. Idealized cross-section of the main zone of alteration-mineralization on the Bob claims, central British Columbia (MINFILE 093B 054; Eighty Eight Resources Ltd., 1990).

Kahlert recommended that Canadian Superior Exploration Ltd. perform a drilling program.

Kahlert (1968) documented the results of that drilling and further geochemical rock sampling, and determined that “the most encouraging untested zone” was on the eastern slope of Graham Peak with Mo values exceeding 400 ppm (Kahlert, 1968).

Kahlert (1969) followed up with 610 m (2000 ft.) of drilling in two holes on the eastern slope of Graham peak.¹ Hole A-5-69 averaged 0.02% Mo over 307 m (1007 ft.) and hole A-6-69 averaged 0.15% Mo over 294 m (963 ft.). Kahlert determined through this drilling that, contrary to expectations, molybdenite decreases with depth, thus making it unlikely that mineralization occurs in the area.

Within 30 km, however, ten MINFILE occurrences exist, nine of which are occurrences of Mo and one of which has an associated Property File document. Only one assessment report has been written in the same area (Miller, 1978).

Vega (094C 021)

Only one document appears in Property File on the Vega occurrence, but the 14-page report (Weishaupt, 1989) from the Placer Dome collection provides significant information on the long exploration history of this location. The original MINFILE geological description included several sentences summarizing previous work done in the 1930s and 1970s. This Placer Dome report provides further details, beginning with the original exploration and staking in 1935 and concluding with a 1989 field season report. In addition, one of the assay plan maps from exploration in 1938 on the property is included in a Property File collection not covered by this project and is available for download (Consolidated Mining and Smelting Company Limited, 1938).

According to Weishaupt (1989), the exploration history of the Vega occurrence includes diamond-drilling, trenching, prospecting, a thin-section study, airborne and ground geophysics surveys, and other work. Most recently, a soil geochemical survey returned values up to 2380 ppb Au, 2876 ppm Cu, 1652 ppm As and 521 ppm Zn (Weishaupt, 1989). Limited sampling of existing underground workings was also performed. It seems, however, that exploration at Vega concluded around 1990.

Conclusions

This project identified 17 new MINFILE occurrences and updated 483 existing MINFILE occurrences. It is likely

¹ unofficial feature at latitude 55.958 N, longitude 127.402 W

that even more new MINFILE occurrences are hidden within the ~2900 recently processed files.

The findings from this project described in this paper have synthesized information from various sources and noted interesting possibilities. Many of the occurrences noted here were not pursued, and the reasons for these decisions are not always clear. Oftentimes, the occurrences were inaccessible, of a lower grade than was economic at the time, or the concerned companies had more promising projects elsewhere. It is entirely possible that some of these forgotten possibilities may have since become viable; however, it should be noted that the authors of this paper have not carried out any ground-truthing in preparing this report. All of the information contained herein is no more accurate than the original reports; however, since this information is available in a digital, organized and downloadable format, it is a cost-effective way to conduct a preliminary exploration of prospects within the QUEST areas.

The Property File documents described here comprise only a small fraction of documents processed during the course of this project. By synthesizing information found in the Property File database with the information from the ARIS and MINFILE databases and the MapPlace, valuable interpretations can be made that will guide exploration in the future.

Acknowledgments

The authors thank Geoscience BC for funding this project and the BC Geological Survey for access to the Property File archives and online database, and their continued support for the project. Specifically, we are grateful to L. Jones, K. Hancock and S. Meredith-Jones for MINFILE support, and to P. Desjardins for creating a KML file of the new and updated MINFILE occurrences. This project could not have been completed without the impeccable document scanning done by L. and S. Groseth of Camirage Imaging and the database support provided by Spot Solutions. This manuscript greatly benefited from a review by K. Hancock.

References

- Adamson, R.S. and Saunders, C.R. (1973): Geochemical report on the Dave-Doug property; BC Ministry of Energy, Mines and Petroleum Resources, Assessment Report 4148, 24 p.
- Andrews, K.E. (1988): Geology and genesis of the Wolf precious metal epithermal prospect and the Capoose base and precious metal porphyry style prospects; M.Sc. thesis, University of British Columbia, unpublished report donated to BC Ministry of Energy, Mines and Petroleum Resources, Property File document 821614, 173 p.
- Anonymous (1982a): Soil, rock and silt sample location map, 50 m interval – Mtsacha; unpublished report donated to BC Ministry of Energy, Mines and Petroleum Resources, Property File document 860419, unknown scale, 1 p.
- Anonymous (1982b): Geochemical map of Mtsacha showing Cu >500 ppm; unpublished report donated to BC Ministry of

- Energy, Mines and Petroleum Resources, Property File document 860421, unknown scale, 1 p.
- Anonymous (1982c): Geochemical map of Mtsacha showing Zn + 200 ppm; unpublished report donated to BC Ministry of Energy, Mines and Petroleum Resources, Property File document 860422, unknown scale, 1 p.
- Anonymous (1987): Report – Bob; unpublished report donated to BC Ministry of Energy, Mines and Petroleum Resources, Property File document 821865, 8 p.
- Burton, A. (1991): Report on the Tub 1–3 Tuura Ten 1–4 mineral claims, Cariboo Mining Division, Narcosli Creek, B.C.; unpublished report donated by Burton Consulting Inc. to BC Ministry of Energy, Mines and Petroleum Resources, Property File document 821847, 15 p.
- Campbell, N. (1972): Office study, Robb Lake project, Halfway River area, northeastern British Columbia; unpublished report donated by British Newfoundland Exploration Limited to BC Ministry of Energy, Mines and Petroleum Resources, Property File document 810808, 38 p.
- Cariboo Minelands Ltd. (1969): Cariboo Minelands Ltd. diamond drill record; unpublished report donated by Cariboo Minelands Ltd. to BC Ministry of Energy, Mines and Petroleum Resources, Property File document 810867, 30 p.
- Consolidated Mining and Smelting Company Limited (1938): Vega M.C. assay plan; unpublished report donated by Consolidated Mining and Smelting Company Limited to BC Ministry of Energy, Mines and Petroleum Resources, Property File document 16621, scale 1 inch to 20 feet, 1 p.
- Dickie, G.J. (1972): Geology of the Nabesche area, north east B.C.; unpublished report donated to BC Ministry of Energy, Mines and Petroleum Resources, Property File document 810789, scale 1:50 000, 1 p.
- Dillon, E.P. (1980a): Cordilleran sediments geochemical stream sediment program, Quesnel Lake–Barkerville area, British Columbia, May 26 to July 2 and August 26 to September 27, 1980; unpublished report donated by Gulf Minerals Canada Ltd. to BC Ministry of Energy, Mines and Petroleum Resources, Property File document 840311, 55 p.
- Dillon, E.P. (1980b): Cordilleran sediments geochemical stream sediment program, Chetwynd area, British Columbia, August 15 to 20, 1980; unpublished report donated by Gulf Minerals Canada Ltd. to BC Ministry of Energy, Mines and Petroleum Resources, Property File document 840304, 18 p.
- Eighty Eight Resources Ltd. (1990): Report – Bob property; unpublished report donated by Eighty Eight Resources Ltd. to BC Ministry of Energy, Mines and Petroleum Resources, Property File document 821866, 6 p.
- Eldor Resources Ltd. (1987): Property summaries – NAZ; unpublished report donated by Eldor Resources Ltd. to BC Ministry of Energy, Mines and Petroleum Resources, Property File document 821838, 32 p.
- Heberlein, D. (1992a): QFP epithermal Au property; unpublished report donated by Minnova Inc. to BC Ministry of Energy, Mines and Petroleum Resources, Property File document 821834, 5 p.
- Heberlein, D. (1992b): Wolf property, progress report and 1992 exploration plans; unpublished report donated by Minnova Inc. to BC Ministry of Energy, Mines and Petroleum Resources, Property File document 821398, 5 p.
- Heberlein, D. (1994): Wolf project summary and drill proposal; unpublished report donated by Metall Mining Corporation to BC Ministry of Energy, Mines and Petroleum Resources, Property File document 821696, 4 p.
- Hughes, R.W. (1988): Gabriel Resources Inc. Ahbau Creek property summary; unpublished report donated by Gabriel Resources to BC Ministry of Energy, Mines and Petroleum Resources, Property File document 821951, 8 p.
- JMT Group (1982a): Claim map with overlay – Mtsacha property; unpublished report donated to BC Ministry of Energy, Mines and Petroleum Resources, Property File document 860414, unknown scale, 1 p.
- JMT Group (1982b): Soil, rock and silt sample location map – Mtsacha; unpublished report donated to BC Ministry of Energy, Mines and Petroleum Resources, Property File document 860415, scale 1:10 000, 1 p.
- Johnson, D.G.S. (1971a): Hogen Batholith reconnaissance project; unpublished report donated by Development Company of Canada Ltd. to BC Ministry of Energy, Mines and Petroleum Resources, Property File document 840359, 140 p.
- Johnson, D.G.S. (1971b): Geological and geochemical report on the Gil 1 to 120 mineral claims; BC Ministry of Energy, Mines and Petroleum Resources, Assessment Report 3408, 142 p.
- Jury, R.G. (1968): Cariboo Minelands Ltd., Thunder Creek property; unpublished report donated by Alrae Engineering Ltd. to BC Ministry of Energy, Mines and Petroleum Resources, Property File document 810868, 10 p.
- Kahlert, B.H. (1968): Report of exploration programme carried out by Canadian Superior Exploration Limited on Sicintine Mines Limited property; unpublished report donated by Canadian Superior Exploration Ltd. to BC Ministry of Energy, Mines and Petroleum Resources, Property File document 812847, 31 p.
- Kahlert, B.H. (1969): Canadian Superior Exploration Limited, Atna project, 1969; unpublished report donated by Canadian Superior Exploration Ltd. to BC Ministry of Energy, Mines and Petroleum Resources, Property File document 812850, 11 p.
- Kasper, B. (1993): Ram 1–2 claims; unpublished report donated to BC Ministry of Energy, Mines and Petroleum Resources, Property File document 821734, 2 p.
- Kimura, E. (1982a): Geochemical analysis sheets – Mtsacha; unpublished report donated by Placer Development Ltd. to BC Ministry of Energy, Mines and Petroleum Resources, Property File document 860418, 7 p.
- Kimura, E. (1982b): Geological and geochemical evaluation of Mtsacha property, Tsacha Mountain; unpublished report donated by Placer Development Ltd. to BC Ministry of Energy, Mines and Petroleum Resources, Property File document 860424, 23 p.
- Leigh, O.E. and Kahlert, B.H. (1967): Report on geological, geochemical, trenching & assaying programme on the Atna agreement area; unpublished report donated by Canadian Superior Exploration Ltd. to BC Ministry of Energy, Mines and Petroleum Resources, Property File document 812846, 25 p.
- Leighton, D.G. and Dodson, E.D. (1972): Geological report, Tye claims near Robb Lake, B.C.; BC Ministry of Energy, Mines and Petroleum Resources, Assessment Report 4149, 16 p.
- MapPlace (2009): British Columbia Geological Survey MapPlace website; BC Ministry of Energy, Mines and Petroleum Resources, URL <<http://mapplace.ca/>> [August 2009].

- Meteor Mining Co. Ltd. (1966): Prospectus; unpublished report donated by Meteor Mining Co. Ltd. to BC Ministry of Energy, Mines and Petroleum Resources, Property File document 812671, 29 p.
- Miller, D. (1978): Geological, geochemical and prospecting report on the Fog and Peak claims; BC Ministry of Energy, Mines and Petroleum Resources, Assessment Report 7116, 17 p.
- MINFILE (2010): MINFILE BC mineral deposits database; BC Ministry of Energy, Mines and Petroleum Resources, URL <<http://www.minfile.ca/>> [November 2010].
- Nelson, J. (1985): Final report – Nechako project – B.C. gold reconnaissance project; unpublished report donated by Kerr Addison Mines Ltd. to BC Ministry of Energy, Mines and Petroleum Resources, Property File document 822315, 12 p.
- Pavelic, N. and Chisholm, E.O. (1967): Property submission: Port Hardy and Tesla Mountain; unpublished report donated to BC Ministry of Energy, Mines and Petroleum Resources, Property File document 812672, 6 p.
- Pearson, B.D. (1974): Geological and geochemical report, Nabesche No. 1, 2, 3 and 4 groups of mineral claims; BC Ministry of Energy, Mines and Petroleum Resources, Assessment Report 4874, 29 p.
- Placer Development Ltd. (1982): Soil geochemical survey map: As ppm – Mtsacha property; unpublished report donated by Placer Development Ltd. to BC Ministry of Energy, Mines and Petroleum Resources, Property File document 860416, scale 1:10 000, 1 p.
- Reynolds, N. (1970): Hogem Batholith (South), British Columbia; unpublished report donated by Great Plains Development Co. of Canada Ltd. to BC Ministry of Energy, Mines and Petroleum Resources, Property File document 840043, 37 p.
- Sawyer, J.B.P. and Mark, C.A. (1972): J.R. Woodcock – Eutsuk Project and related proposal; unpublished report donated by Cyprus Exploration Corporation Ltd. to BC Ministry of Energy, Mines and Petroleum Resources, Property File document 812669, 7 p.
- Simpson, J.G. (1969): Cariboo Minelands, Quesnel property, summary of data to December 18, 1969; unpublished report donated to BC Ministry of Energy, Mines and Petroleum Resources, Property File document 810887, 6 p.
- Sirola, W.M. (1964): J.J. Group of claims – Ahbau Creek area; unpublished report donated by Kerr-Addison Gold Mines Ltd. to BC Ministry of Energy, Mines and Petroleum Resources, Property File document 821918, 10 p.
- Tavela, M. (1972): Geochemical exploration report, Lady Laurier Lake area, northeastern B.C., summer 1972; unpublished report donated to BC Ministry of Energy, Mines and Petroleum Resources, Property File document 810785, 57 p.
- Weishaupt, P.J. (1989): Vega property summary report; unpublished report donated by Canasil Resources Inc. to BC Ministry of Energy, Mines and Petroleum Resources, Property File document 860364, 14 p.
- Westoll, N. and Sullivan, J. (1973): Geological and geochemical report, Mt. Bertha area claims; BC Ministry of Energy, Mines and Petroleum Resources, Assessment Report 4203, 61 p.
- Woodcock, J.R. (1971): Eutsuk project – Omineca Mining Division; unpublished report donated by Taurus Resources Syndicate to BC Ministry of Energy, Mines and Petroleum Resources, Property File document 812668, 46 p.

MINFILE Update of the QUEST Project Area, Central British Columbia (Parts of NTS 093A, B, G, H, J, K, N, O, 094C, D)

G. Owsiacski, Consultant, Total Earth Science Services, Victoria, BC; george.o@shaw.ca

G. Payie, Consultant, Total Earth Science Services, Victoria, BC

Owsiacski, G. and Payie, G. (2010): MINFILE update of the QUEST project area, central British Columbia (parts of NTS 093A, B, G, H, J, K, N, O, 094C, D); in Geoscience BC Summary of Activities 2009, Geoscience BC, Report 2010-1, p. 189–202.

Introduction

The online provincial mineral inventory database, MINFILE, is recognized as an important mineral exploration tool (BC Geological Survey, 2009a). MINFILE updates (MINFILE, 2009) were carried out in the QUEST project area (parts of NTS 093A, B, G, H, J, K, N, O; 094C, D), in an area of approximately 47 560 km² in central British Columbia (Figure 1). The QUEST project involved a regional airborne electromagnetic and gravity survey that covered an area extending roughly from Williams Lake to Germansen Landing and geochemical sampling over parts of eight NTS map areas. As a result of these new datasets, there has been significant new exploration activity in the QUEST project area.

Most MINFILE occurrence descriptions in the project area are up to 20 years out of date—the last updates range from 1989 to 1996. Subsequent and recent staking activity has resulted in submission of new assessment reports that have enhanced geological data for some mineral occurrences and added new mineral occurrences.

The objectives of this project were to update or create new MINFILE occurrences based on a review of assessment reports, Property File documents (BC Geological Survey, 2009b), news releases, formal publications and recent exploration data. This update of MINFILE provides the mineral exploration community with a more current, high-

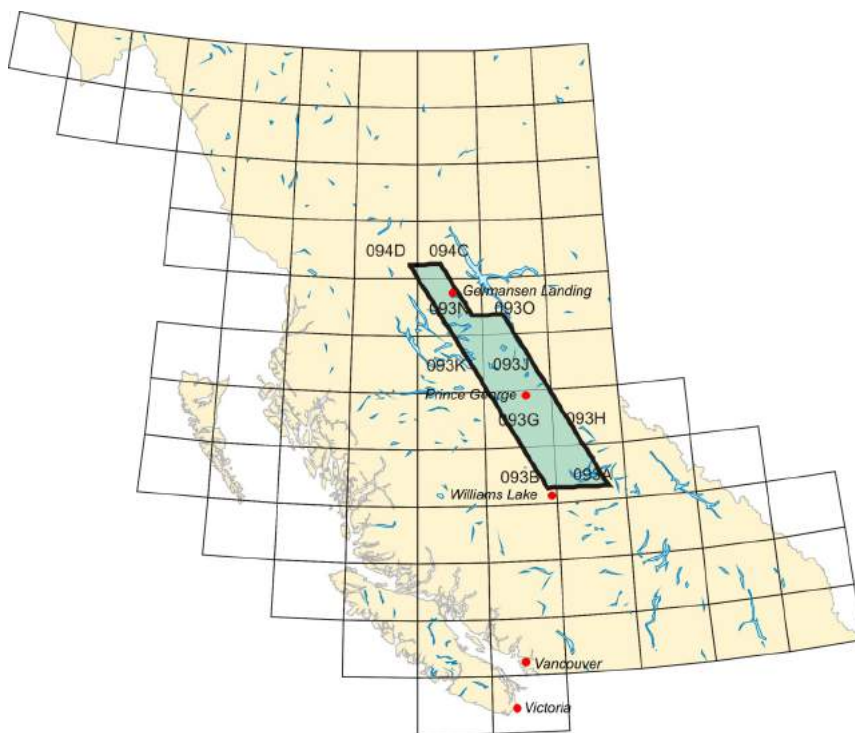


Figure 1. Location of MINFILE updates (green shaded area) relative to the QUEST project geophysical survey area (black outline) in central British Columbia.

quality, online geological dataset that will help guide exploration efforts in the QUEST project area. It is hoped that the data generated as part of this project will contribute toward longer-term benefits evidenced by increased mineral exploration activity in an area focusing on the Quesnel Terrane between Williams Lake in the south and Germansen Landing in the north.

Approximately 1400 assessment reports were reviewed by the authors, culminating in the revision and updating of 486 occurrences, of which 139 are newly created showings (Table 1). In 2008, exploration spending in the QUEST project area totalled about \$70 million (DeGrace, 2008).

Data were entered into the online MINFILE data-entry system and reviewed by the BC Geological Survey for compliance with MINFILE coding standards. Updated data

Keywords: QUEST project area, mineral exploration, assessment reports, MINFILE updates, new showings

This publication is also available, free of charge, as colour digital files in Adobe Acrobat® PDF format from the Geoscience BC website: <http://www.geosciencebc.com/s/DataReleases.asp>.

Table 1. Updated MINFILE occurrences by NTS map sheet, QUEST project area, central British Columbia. Grey shaded entries are new showings.

(NAD 83)							
MINFILE Number	Names	Status	Commodities	NTS Maps	Latitude	Longitude	Deposit Types
093A 189	Park	Showing	Silver	093A01W	52 ° 12' 14" N	120° 24' 24" W	Au-quartz veins
093A 188	Cariboo Rand	Showing	Copper, gold, silver	093A03W, 093A06W	52 ° 14' 44" N	121° 18' 03" W	Au-quartz veins
093A 017	Antoine Creek	Past producer	Gold	093A05E	52 ° 24' 53" N	121° 34' 15" W	Surficial placer deposits; buried-channel placer deposits
093A 115	Ant	Showing	Copper	093A05E	52 ° 24' 18" N	121° 32' 35" W	Alkalic porphyry Cu-Au
093A 208	Boulder	Showing	Copper, lead, silver, zinc	093A05E	52 ° 20' 00" N	121° 30' 40" W	I104: Epithermal Au-Ag-Cu: high sulphidation
093A 242	Beaver Lake Creek	Past producer	Gold	093A05E	52 ° 21' 38" N	121° 30' 20" W	Surficial placer deposits; buried-channel placer deposits
093A 016	Black Creek	Past producer	Gold	093A06E	52 ° 18' 45" N	121° 05' 34" W	Surficial placer deposits; buried-channel placer deposits
093A 048	Lo	Showing	Gold, copper	093A06E	52 ° 28' 50" N	121° 02' 13" W	Au-quartz veins; polymetallic veins Ag-Pb-Zn±Au
093A 079	Bren	Showing	Copper, gold, molybdenum	093A06E	52 ° 18' 44" N	121° 02' 18" W	Polymetallic veins Ag-Pb-Zn±Au; porphyry Cu ± Mo ± Au
093A 114	Corey	Showing	Copper	093A06E	52 ° 21' 38" N	121° 05' 34" W	Alkalic porphyry Cu-Au
093A 002	Pine	Showing	Copper, gold	093A06W	52 ° 20' 58" N	121° 14' 51" W	Alkalic porphyry Cu-Au
093A 042	Hobson's Horsefly	Past producer	Gold	093A06W	52 ° 23' 36" N	121° 24' 54" W	Surficial placer deposits; buried-channel placer deposits
093A 058	Redgold	Prospect	Copper, gold, zinc	093A06W	52 ° 27' 50" N	121° 29' 03" W	Alkalic porphyry Cu-Au
093A 064	Red	Showing	Copper	093A06W	52 ° 17' 48" N	121° 27' 11" W	Volcanic redbed Cu
093A 075	Moffat	Showing	Copper	093A06W	52 ° 17' 24" N	121° 26' 05" W	Volcanic redbed Cu
093A 077	Kwun Lake	Showing	Gold, copper	093A06W	52 ° 23' 53" N	121° 21' 13" W	Alkalic porphyry Cu-Au
093A 112	Hook	Showing	Copper	093A06W	52 ° 25' 58" N	121° 22' 19" W	Alkalic porphyry Cu-Au
093A 116	BM	Showing	Copper	093A06W	52 ° 25' 14" N	121° 22' 19" W	Alkalic porphyry Cu-Au
093A 134	Horsefly	Developed prospect	Silica, volcanic, ash	093A06W	52 ° 17' 24" N	121° 19' 32" W	Volcanic ash – pumice
093A 155	Beekeeper	Showing	Copper, gold, mercury	093A06W	52 ° 23' 40" N	121° 20' 24" W	Alkalic porphyry Cu-Au
093A 150	Frasergold	Developed prospect	Gold, silver, copper, zinc, lead	093A07E	52 ° 18' 20" N	120° 34' 43" W	Au-quartz veins; porphyry Cu ± Mo ± Au
093A 012	Zed	Showing	Copper	093A07W	52 ° 27' 32" N	120° 53' 06" W	Polymetallic veins Ag-Pb-Zn±Au
093A 092	Tcp 1	Showing	Gold	093A07W	52 ° 27' 18" N	120° 46' 11" W	Au-quartz veins
093A 096	McKee	Showing	Gold, copper	093A07W	52 ° 15' 01" N	120° 47' 37" W	Polymetallic veins Ag-Pb-Zn±Au
093A 117	Dor	Showing	Copper, gold	093A07W	52 ° 18' 14" N	120° 56' 15" W	Porphyry Cu ± Mo ± Au; polymetallic veins Ag-Pb-Zn±Au
093A 149	Doreen	Showing	Gold, copper, silver	093A07W	52 ° 17' 53" N	120° 55' 18" W	Polymetallic veins Ag-Pb-Zn±Au
093A 190	Offset Lake	Showing	Gold	093A07W	52 ° 17' 17" N	120° 49' 55" W	Au-quartz veins
093A 191	North Doreen	Showing	Copper, gold	093A07W	52 ° 18' 01" N	120° 55' 32" W	Polymetallic veins Ag-Pb-Zn±Au
093A 046	Eaglet	Developed prospect	Fluorite, molybdenum, strontium, silver, zinc, lead	093A10W	52 ° 34' 05" N	120° 58' 56" W	Barite-fluorite veins; L08: porphyry Mo (climax-type)
093A 193	Plate	Showing	Silver	093A11E	52 ° 33' 09" N	121° 07' 57" W	Polymetallic veins Ag-Pb-Zn±Au
093A 003	Providence	Past producer	Silver, lead, zinc, gold	093A11W	52 ° 38' 35" N	121° 25' 17" W	Au-quartz veins; polymetallic veins Ag-Pb-Zn±Au
093A 043	Spanish Mountain	Developed prospect	Gold, silver, lead, copper, zinc	093A11W	52 ° 35' 19" N	121° 27' 18" W	Au-quartz veins
093A 074	Hobson	Showing	Silver, copper, lead, gold	093A11W	52 ° 36' 18" N	121° 16' 52" W	Au-quartz veins; polymetallic veins Ag-Pb-Zn±Au

093A 143	Big Gulp	Showing	Zinc, copper, lead, silver	093A11W	52 ° 43' 40" N	121° 23' 24" W	Besshi massive sulphide Cu-Zn
093A 154	Trump	Showing	Silver, lead	093A11W	52 ° 38' 47" N	121° 26' 59" W	Polymetallic veins Ag-Pb-Zn±Au
093A 192	Spanish Mountain Placer	Showing	Gold	093A11W	52 ° 35' 15" N	121° 27' 18" W	Surficial placer deposits; buried channel placer deposits
093A 194	Duck	Showing	Copper, zinc, lead	093A11W	52 ° 43' 50" N	121° 28' 01" W	Polymetallic veins Ag-Pb-Zn±Au
093A 195	Hepburn Lake	Showing	Gold	093A11W	52 ° 36' 22" N	121° 29' 09" W	Au-quartz veins
093A 197	Dog	Showing	Gold	093A11W	52 ° 35' 35" N	121° 28' 44" W	Au-quartz veins
093A 217	Cedar Dam	Showing	Copper, zinc, gold	093A11W	52 ° 33' 59" N	121° 29' 03" W	Noranda/Kuroko massive sulphide Cu-Pb-Zn; polymetallic veins Ag-Pb-Zn±Au
093A 232	Rollie Creek	Past producer	Gold	093A11W	52 ° 43' 45" N	121° 27' 58" W	Surficial placer deposits
093A 152	Frank Creek	Prospect	Copper, lead, zinc, silver, gold	093A11W, 093A14W	52 ° 44' 52" N	121° 21' 41" W	Besshi massive sulphide Cu-Zn
093A 066	B	Showing	Copper	093A12E	52 ° 32' 41" N	121° 44' 08" W	Volcanic redbed Cu
093A 072	Joy	Showing	Copper, lead, gold, silver, zinc	093A12E	52 ° 34' 33" N	121° 31' 10" W	Polymetallic veins Ag-Pb-Zn±Au
093A 080	Murder Gulch Placer	Past producer	Gold	093A12E	52 ° 39' 41" N	121° 32' 15" W	Surficial placer deposits; buried channel placer deposits
093A 136	Shaw	Showing	Lead, zinc	093A12E	52 ° 40' 13" N	121° 39' 40" W	Polymetallic veins Ag-Pb-Zn±Au
093A 141	Cedar Creek	Past producer	Gold	093A12E	52 ° 34' 07" N	121° 30' 15" W	Surficial placer deposits; buried channel placer deposits
093A 160	Lloyd-Nordik	Developed prospect	Copper, gold	093A12E	52 ° 34' 17" N	121° 38' 41" W	Alkalic porphyry Cu-Au
093A 198	Westenhiser Creek	Showing	Gold	093A12E	52 ° 40' 30" N	121° 37' 45" W	Au-quartz veins
093A 202	Road Zone	Prospect	Copper, gold	093A12E	52 ° 34' 05" N	121° 38' 13" W	Alkalic porphyry Cu-Au
093A 207	ML	Prospect	Copper, molybdenum	093A12E	52 ° 41' 23" N	121° 42' 03" W	Porphyry Cu ± Mo ± Au
093A 213	Mac	Showing	Copper, gold	093A12E	52 ° 37' 54" N	121° 38' 28" W	Alkalic porphyry Cu-Au
093A 214	October East	Showing	Copper	093A12E	52 ° 38' 17" N	121° 39' 44" W	Alkalic porphyry Cu-Au
093A 215	Ora	Showing	Lead, silver, gold	093A12E	52 ° 41' 30" N	121° 34' 07" W	Polymetallic veins Ag-Pb-Zn±Au
093A 216	Hampton's Pit	Showing	Gold, zinc	093A12E	52 ° 35' 07" N	121° 31' 32" W	Alkalic porphyry Cu-Au
093A 218	Hazel	Showing	Copper	093A12E	52 ° 31' 52" N	121° 32' 10" W	Alkalic porphyry Cu-Au
093A 234	Poquette Creek	Past producer	Gold	093A12E	52 ° 36' 44" N	121° 32' 25" W	Surficial placer deposits
093A 235	Kangaroo Creek	Past producer	Gold	093A12E	52 ° 40' 33" N	121° 38' 41" W	Surficial placer deposits
093A 236	Lawless (Half Mile) Creek	Past producer	Gold	093A12E	52 ° 39' 17" N	121° 39' 33" W	Surficial placer deposits; buried channel placer deposits
093A 237	Rose Gulch	Past producer	Gold	093A12E	52 ° 38' 31" N	121° 38' 54" W	Surficial placer deposits; buried channel placer deposits
093A 238	Quesnel River	Past producer	Gold	093A12E	52 ° 37' 28" N	121° 37' 10" W	Surficial placer deposits; buried channel placer deposits
093A 069	Morehead Creek	Past Producer	Gold	093A12W	52 ° 38' 12" N	121° 47' 30" W	Surficial placer deposits; buried channel placer deposits
093A 118	ML	Showing	Copper	093A12W	52 ° 35' 42" N	121° 46' 47" W	Sediment-hosted Cu; alkalic porphyry Cu-Au
093A 119	Maud	Showing	Copper, gold	093A12W	52 ° 43' 31" N	121° 54' 48" W	Alkalic porphyry Cu-Au
093A 196	Little Lake	Showing	Gold	093A12W	52 ° 37' 24" N	121° 47' 26" W	Alkalic porphyry Cu-Au
093A 199	Kellin	Showing	Copper, silver	093A12W	52 ° 44' 50" N	121° 50' 43" W	Alkalic porphyry Cu-Au
093A 243	Birrell Creek	Past producer	Gold	093A12W	52 ° 40' 30" N	121° 56' 11" W	Surficial placer deposits; buried channel placer deposits

093A 153	Galleon	Showing	Silver, lead, copper, gold	093A13E	52 ° 58' 00" N	121° 42' 35" W	Polymetallic veins Ag-Pb-Zn±Au
093A 219	North Minerals Star	Showing	Jade/nephrite, asbestos	093A13E	52 ° 48' 27" N	121° 37' 30" W	Jade
093A 220	CAC 3	Showing	Copper	093A13E	52 ° 49' 26" N	121° 31' 16" W	Polymetallic veins Ag-Pb-Zn±Au
093A 244	Fontaine Creek	Past producer	Gold	093A13E	52 ° 58' 07" N	121° 44' 52" W	Surficial placer deposits
093A 245	Little Swift River	Past producer	Gold	093A13E	52 ° 56' 26" N	121° 40' 07" W	Surficial placer deposits
093A 246	Swift River	Past producer	Gold	093A13E	52 ° 53' 24" N	121° 42' 59" W	Surficial placer deposits
093A 140	Cariboo	Showing	Silica	093A13E, 093A14W, 093H04E	52 ° 58' 15" N	121° 29' 35" W	Silica veins
093A 013	Sovereign Creek	Developed prospect	Talc, nickel, silver, zinc, gold	093A13W	52 ° 59' 30" N	121° 53' 35" W	Ultramafic-hosted talc-magnesite; tholeiitic intrusion-hosted Ni-Cu
093A 130	Sovereign	Showing	Nickel, talc	093A13W	52 ° 59' 15" N	121° 51' 51" W	Ultramafic-hosted talc-magnesite; tholeiitic intrusion-hosted Ni-Cu
093A 221	Isasa	Showing	Nickel, chromium	093A13W	52 ° 59' 19" N	121° 57' 14" W	Tholeiitic intrusion-hosted Ni-Cu
093A 187	Lost Swede	Showing	Gold	093A13W, 093B16E	52 ° 55' 02" N	121° 58' 33" W	Buried-channel placer deposits
093A 068	MB	Showing	Lead, silver, gold	093A14E	52 ° 56' 53" N	121° 02' 05" W	Polymetallic veins Ag-Pb-Zn±Au
093A 087	Mae	Showing	Lead, zinc, copper	093A14E	52 ° 47' 05" N	121° 01' 37" W	Besshi massive sulphide Cu-Zn
093A 110	Maybe	Developed prospect	Zinc, lead, silver	093A14E	52 ° 50' 43" N	121° 11' 44" W	Irish-type carbonate-hosted Zn-Pb
093A 142	Ace	Prospect	Copper, gold, lead, zinc, silver	093A14E	52 ° 48' 24" N	121° 08' 57" W	Besshi massive sulphide Cu-Zn; Au-quartz veins
093A 148	Comin Throu Bear	Showing	Lead, zinc, silver, barite	093A14E	52 ° 53' 10" N	121° 04' 05" W	Mississippi Valley-type Pb-Zn; polymetallic veins Ag-Pb-Zn±Au
093A 081	Maeford Lake	Past producer	Marble, dimension stone, building stone	093A14E, 093A15W	52 ° 47' 49" N	120° 59' 23" W	Dimension stone – marble; limestone
093A 145	Mt. Kimball	Showing	Limestone	093A14E, 093A15W, 093H03E	52 ° 57' 48" N	121° 03' 44" W	Limestone
093A 004	Keithley Creek	Producer	Gold	093A14W	52 ° 46' 33" N	121° 26' 23" W	Surficial placer deposits; buried-channel placer deposits
093A 005	Little Snowshoe Creek	Past producer	Gold	093A14W	52 ° 50' 50" N	121° 27' 58" W	Surficial placer deposits
093A 006	Cariboo Quartzite	Showing	Silica	093A14W	52 ° 54' 40" N	121° 17' 55" W	Silica sandstone
093A 021	Corban	Prospect	Gold, silver	093A14W	52 ° 50' 27" N	121° 26' 13" W	Au-quartz veins
093A 022	Homestake	Showing	Gold	093A14W	52 ° 50' 14" N	121° 24' 35" W	Au-quartz veins
093A 023	Sockett	Showing	Gold, lead, zinc	093A14W	52 ° 49' 49" N	121° 25' 51" W	Au-quartz veins
093A 024	French Snowshoe Creek	Past producer	Gold	093A14W	52 ° 50' 23" N	121° 24' 48" W	Surficial placer deposits; buried-channel placer deposits
093A 026	Luce Creek	Past producer	Gold	093A14W	52 ° 51' 24" N	121° 26' 21" W	Surficial placer deposits; buried-channel placer deposits
093A 027	Jane (L. 11338)	Prospect	Gold, silver, lead	093A14W	52 ° 51' 28" N	121° 25' 39" W	Au-quartz veins; polymetallic veins Ag-Pb-Zn±Au
093A 028	Talbot Veins	Showing	Gold	093A14W	52 ° 50' 44" N	121° 26' 33" W	Au-quartz veins
093A 029	Amparo	Showing	Tungsten, lead	093A14W	52 ° 50' 33" N	121° 24' 45" W	Au-quartz veins
093A 030	Old Timer (L. 11337)	Prospect	Gold, silver, lead	093A14W	52 ° 51' 28" N	121° 25' 39" W	Au-quartz veins; polymetallic veins Ag-Pb-Zn±Au
093A 031	Bertha (L. 11332)	Prospect	Gold	093A14W	52 ° 51' 42" N	121° 25' 42" W	Au-quartz veins
093A 032	Betty (L. 11335)	Showing	Gold, silver	093A14W	52 ° 51' 19" N	121° 26' 08" W	Au-quartz veins

093A 033	Saddle (L. 4668)	Prospect	Gold, lead, zinc, copper	093A14W	52 ° 50' 45" N	121° 25' 25" W	Au-quartz veins; polymetallic veins Ag-Pb-Zn±Au
093A 034	Lipsey Vein	Showing	Gold, lead, zinc	093A14W	52 ° 50' 52" N	121° 25' 05" W	Au-quartz veins; polymetallic veins Ag-Pb-Zn±Au
093A 035	Midas (L. 4670)	Past producer	Gold, silver, lead, zinc	093A14W	52 ° 50' 52" N	121° 25' 05" W	Au-quartz veins; polymetallic veins Ag-Pb-Zn±Au
093A 036	Boulder Ledge	Showing	Gold, lead	093A14W	52 ° 51' 48" N	121° 26' 05" W	Au-quartz veins; polymetallic veins Ag-Pb-Zn±Au
093A 037	Jim	Prospect	Gold, silver, lead, zinc	093A14W	52 ° 50' 42" N	121° 24' 51" W	Au-quartz veins; polymetallic veins Ag-Pb-Zn±Au
093A 038	Holmes Ledge	Prospect	Silver, gold, lead, tungsten, zinc, copper	093A14W	52 ° 53' 07" N	121° 27' 10" W	Au-quartz veins; intrusion-related Au pyrrhotite veins
093A 039	Monte Christo	Showing	Lead, zinc	093A14W	52 ° 50' 06" N	121° 24' 53" W	Au-quartz veins; polymetallic veins Ag-Pb-Zn±Au
093A 051	Hibernian	Prospect	Gold, silver, lead	093A14W	52 ° 54' 58" N	121° 21' 09" W	Au-quartz veins; polymetallic veins Ag-Pb-Zn±Au
093A 052	Gisco	Showing	Gold, lead	093A14W	52 ° 58' 07" N	121° 25' 11" W	Au-quartz veins; polymetallic veins Ag-Pb-Zn±Au
093A 053	Pitt I	Showing	Copper, silver, gold	093A14W	52 ° 58' 12" N	121° 25' 11" W	Au-quartz veins; polymetallic veins Ag-Pb-Zn±Au
093A 054	Spitfire	Showing	Gold	093A14W	52 ° 59' 42" N	121° 25' 05" W	Au-quartz veins
093A 055	Zone	Showing	Gold	093A14W	52 ° 57' 56" N	121° 25' 53" W	Au-quartz veins
093A 056	Cariboo Canyon	Showing	Gold	093A14W	52 ° 58' 09" N	121° 25' 05" W	Au-quartz veins
093A 057	Pittman	Showing	Zinc, lead, silver	093A14W	52 ° 57' 47" N	121° 25' 15" W	Au-quartz veins; polymetallic veins Ag-Pb-Zn±Au
093A 060	Park	Showing	Lead, zinc, silver, gold	093A14W	52 ° 55' 04" N	121° 22' 07" W	Au-quartz veins; polymetallic veins Ag-Pb-Zn±Au
093A 070	Vic	Showing	Lead, zinc, silver	093A14W	52 ° 57' 08" N	121° 21' 30" W	Sedimentary exhalative Zn-Pb-Ag
093A 071	Cariboo Hudson	Past producer	Gold, silver, lead, zinc, tungsten	093A14W	52 ° 53' 19" N	121° 19' 42" W	Au-quartz veins; intrusion-related Au pyrrhotite veins; polymetallic veins Ag-Pb-Zn±Au
093A 090	Skarn	Past producer	Silver, gold, copper, lead, zinc, tungsten, antimony	093A14W	52 ° 54' 26" N	121° 19' 50" W	Polymetallic veins Ag-Pb-Zn±Au
093A 091	Cariboo Thompson	Past producer	Gold, silver, lead, zinc, tungsten	093A14W	52 ° 54' 26" N	121° 20' 42" W	Au-quartz veins; intrusion-related Au pyrrhotite veins
093A 093	Peter Gulch	Showing	Tungsten, lead, zinc	093A14W	52 ° 53' 40" N	121° 20' 22" W	Au-quartz veins; Pb-Zn skarn
093A 094	Crazy Creek	Past producer	Gold	093A14W	52 ° 54' 47" N	121° 21' 01" W	Surficial placer deposits
093A 095	International	Showing	Gold, lead, zinc	093A14W	52 ° 52' 10" N	121° 18' 34" W	Polymetallic veins Ag-Pb-Zn±Au
093A 098	Sylvain	Showing	Gold	093A14W	52 ° 48' 36" N	121° 20' 05" W	Au-quartz veins
093A 099	Plateau D'Or	Prospect	Silver, gold, lead, zinc	093A14W	52 ° 52' 03" N	121° 24' 21" W	Au-quartz veins; polymetallic veins Ag-Pb-Zn±Au
093A 100	Cornish Ledges	Prospect	Lead, silver	093A14W	52 ° 52' 34" N	121° 25' 01" W	Au-quartz veins; polymetallic veins Ag-Pb-Zn±Au
093A 101	Hebson Vein	Prospect	Gold, lead, zinc	093A14W	52 ° 52' 20" N	121° 26' 39" W	Au-quartz veins; polymetallic veins Ag-Pb-Zn±Au
093A 102	Taylor Tungsten	Prospect	Tungsten, lead, zinc	093A14W	52 ° 52' 24" N	121° 26' 47" W	Au-quartz veins; W veins
093A 103	Bralco	Showing	Gold, lead, zinc, copper	093A14W	52 ° 53' 42" N	121° 19' 24" W	Au-quartz veins; polymetallic veins Ag-Pb-Zn±Au; sedimentary exhalative Zn-Pb-Ag
093A 105	Slide	Showing	Gold, silver, zinc, lead	093A14W	52 ° 57' 05" N	121° 21' 35" W	Sedimentary exhalative Zn-Pb-Ag; Au-quartz veins
093A 106	Canadian	Showing	Gold, silver, lead, zinc	093A14W	52 ° 55' 20" N	121° 21' 40" W	Au-quartz veins; sedimentary exhalative Zn-Pb-Ag
093A 107	Sterling	Showing	Gold	093A14W	52 ° 52' 50" N	121° 20' 34" W	Au-quartz veins
093A 108	Cariboo - Nordine	Showing	Gold, lead	093A14W	52 ° 53' 36" N	121° 22' 45" W	Au-quartz veins; polymetallic veins Ag-Pb-Zn±Au
093A 109	Imperial	Prospect	Gold	093A14W	52 ° 52' 28" N	121° 25' 59" W	Au-quartz veins
093A 111	Sylvain/Langis	Showing	Gold	093A14W	52 ° 50' 15" N	121° 17' 28" W	Sedimentary exhalative Zn-Pb-Ag

093A 125	F.M. Wells	Showing	Gold	093A14W	52 ° 54' 11" N	121° 23' 36" W	Au-quartz veins
093A 126	Crystal	Prospect	Gold, silver, lead, zinc	093A14W	52 ° 52' 03" N	121° 24' 51" W	Au-quartz veins; polymetallic veins Ag-Pb-Zn±Au
093A 128	Gold Recoveries Ltd.	Showing	Lead	093A14W	52 ° 47' 03" N	121° 20' 19" W	Polymetallic veins Ag-Pb-Zn±Au
093A 129	Mount Burdett	Showing	Gold	093A14W	52 ° 58' 30" N	121° 29' 36" W	Au-quartz veins
093A 144	Roundtop Mountain Limestone	Showing	Limestone	093A14W	52 ° 55' 39" N	121° 16' 57" W	Limestone
093A 158	Cunningham Creek Barite	Prospect	Barite	093A14W	52 ° 55' 30" N	121° 20' 02" W	Sediment-hosted barite
093A 159	Vic Barite	Prospect	Barite	093A14W	52 ° 57' 05" N	121° 21' 34" W	Sediment-hosted barite
093A 161	Antler Creek	Past producer	Gold	093A14W	52 ° 58' 18" N	121° 25' 45" W	Buried-channel placer deposits
093A 165	Aster Ast-3-91	Showing	Gold, silver, lead	093A14W	52 ° 54' 05" N	121° 26' 13" W	Au-quartz veins; polymetallic veins Ag-Pb-Zn±Au
093A 166	Aster A-Y-5	Showing	Lead, silver	093A14W	52 ° 54' 26" N	121° 25' 48" W	Au-quartz veins; polymetallic veins Ag-Pb-Zn±Au
093A 167	Aster K0451	Showing	Lead, silver	093A14W	52 ° 54' 03" N	121° 25' 39" W	Au-quartz veins; polymetallic veins Ag-Pb-Zn±Au
093A 168	Aster K0452	Showing	Gold, silver, lead, zinc	093A14W	52 ° 53' 45" N	121° 25' 57" W	Au-quartz veins; polymetallic veins Ag-Pb-Zn±Au
093A 169	Aster TR22	Showing	Gold, silver, lead	093A14W	52 ° 53' 33" N	121° 25' 45" W	Au-quartz veins; polymetallic veins Ag-Pb-Zn±Au
093A 170	Ben	Showing	Lead, silver, copper, zinc	093A14W	52 ° 56' 00" N	121° 21' 15" W	Sedimentary exhalative Zn-Pb-Ag; polymetallic veins Ag-Pb-Zn±Au
093A 171	China Creek	Showing	Lead	093A14W	52 ° 59' 53" N	121° 24' 29" W	Polymetallic veins Ag-Pb-Zn±Au
093A 172	Copper Creek	Showing	Gold, silver, tungsten, lead	093A14W	52 ° 54' 19" N	121° 20' 26" W	Au-quartz veins; polymetallic veins Ag-Pb-Zn±Au
093A 173	DS 327	Showing	Gold, silver, lead	093A14W	52 ° 52' 03" N	121° 24' 59" W	Au-quartz veins; polymetallic veins Ag-Pb-Zn±Au
093A 174	DS 335	Showing	Lead, silver	093A14W	52 ° 52' 38" N	121° 25' 19" W	Au-quartz veins; polymetallic veins Ag-Pb-Zn±Au
093A 175	DS 336	Showing	Lead, silver	093A14W	52 ° 52' 25" N	121° 25' 15" W	Au-quartz veins; polymetallic veins Ag-Pb-Zn±Au
093A 176	Evening	Showing	Zinc, lead, silver	093A14W	52 ° 56' 43" N	121° 21' 38" W	Sedimentary exhalative Zn-Pb-Ag
093A 177	Fat Vein	Showing	Gold, silver, lead	093A14W	52 ° 53' 51" N	121° 26' 11" W	Au-quartz veins; polymetallic veins Ag-Pb-Zn±Au
093A 178	Moneta	Showing	Lead, zinc	093A14W	52 ° 53' 31" N	121° 20' 19" W	Polymetallic veins Ag-Pb-Zn±Au; Au-quartz veins
093A 179	North Simlock	Showing	Gold, silver, lead	093A14W	52 ° 52' 45" N	121° 19' 10" W	Polymetallic veins Ag-Pb-Zn±Au
093A 180	Nugget	Showing	Lead	093A14W	52 ° 58' 25" N	121° 24' 47" W	Polymetallic veins Ag-Pb-Zn±Au
093A 181	Pine	Showing	Lead, zinc	093A14W	52 ° 47' 55" N	121° 19' 57" W	Polymetallic veins Ag-Pb-Zn±Au
093A 182	Simlock Creek	Showing	Gold, silver, lead, copper	093A14W	52 ° 51' 23" N	121° 18' 30" W	Polymetallic veins Ag-Pb-Zn±Au
093A 183	Switchback	Showing	Gold, silver, lead	093A14W	52 ° 55' 21" N	121° 21' 30" W	Au-quartz veins; polymetallic veins Ag-Pb-Zn±Au
093A 184	Toby	Showing	Lead	093A14W	52 ° 59' 53" N	121° 23' 46" W	Polymetallic veins Ag-Pb-Zn±Au
093A 185	X-14	Showing	Lead, zinc	093A14W	52 ° 55' 16" N	121° 20' 01" W	Sedimentary exhalative Zn-Pb-Ag
093A 186	1500 and 1650 Trenches	Showing	Gold, lead	093A14W	52 ° 55' 30" N	121° 21' 37" W	Au-quartz veins; polymetallic veins Ag-Pb-Zn±Au
093A 222	Cunning	Showing	Lead, zinc	093A14W	52 ° 58' 54" N	121° 18' 32" W	Sedimentary exhalative Zn-Pb-Ag
093A 223	Harveys Creek	Past producer	Gold	093A14W	52 ° 50' 27" N	121° 16' 04" W	Buried-channel placer deposits
093A 224	NMG 26	Showing	Nickel, chromium	093A14W	52 ° 48' 59" N	121° 27' 57" W	Tholeiitic intrusion-hosted Ni-Cu

093A 225	J1	Showing	Gold	093A14W	52 ° 48' 17" N	121° 27' 42" W	Au-quartz veins
093A 226	Gold	Showing	Gold	093A14W	52 ° 51' 46" N	121° 22' 54" W	Au-quartz veins
093A 227	McMartin Creek	Past producer	Gold	093A14W	52 ° 52' 24" N	121° 28' 27" W	Surficial placer deposits
093A 228	Barr Creek	Past producer	Gold	093A14W	52 ° 51' 40" N	121° 28' 46" W	Surficial placer deposits
093A 229	Weaver Creek	Past producer	Gold	093A14W	52 ° 47' 39" N	121° 27' 55" W	Surficial placer deposits
093A 230	Four Mile Creek	Past producer	Gold	093A14W	52 ° 46' 43" N	121° 26' 27" W	Surficial placer deposits
093A 231	Frank Creek	Past producer	Gold	093A14W	52 ° 45' 33" N	121° 22' 14" W	Surficial placer deposits
093A 233	Nigger (Pine) Creek	Past producer	Gold	093A14W	52 ° 47' 34" N	121° 19' 25" W	Surficial placer deposits
093A 239	Cunningham Creek	Past producer	Gold	093A14W	52 ° 58' 07" N	121° 21' 49" W	Surficial placer deposits
093A 240	Nugget Gulch	Past producer	Gold	093A14W	52 ° 57' 56" N	121° 24' 50" W	Surficial placer deposits
093A 241	Wolf Creek	Past producer	Gold	093A14W	52 ° 59' 46" N	121° 24' 34" W	Surficial placer deposits
093A 247	Wolf	Showing	Lead, silver	093A14W	52 ° 59' 47" N	121° 24' 35" W	Polymetallic veins Ag-Pb-Zn±Au
093A 248	Wolf 17	Showing	Lead, zinc	093A14W	52 ° 55' 57" N	121° 21' 53" W	Sedimentary exhalative Zn-Pb-Ag
093A 104	Antler Mountain	Showing	Gold, lead, zinc	093A14W, 093H03W	52 ° 59' 55" N	121° 26' 58" W	Au-quartz veins
093A 050	Lam	Showing	Lead, zinc	093A15W	52 ° 49' 43" N	120° 57' 15" W	Polymetallic veins Ag-Pb-Zn±Au
093A 065	Grizzly Lake	Prospect	Lead, zinc	093A15W	52 ° 48' 45" N	120° 54' 10" W	Mississippi Valley-type Pb-Zn
093B 051	Sawmill	Developed prospect	Copper, molybdenum	093B08W	52 ° 28' 05" N	122° 16' 24" W	Porphyry Cu ± Mo ± Au
093B 058	Bud 7	Showing	Copper, molybdenum	093B08W	52 ° 29' 30" N	122° 15' 35" W	Porphyry Cu ± Mo ± Au; Cu skarn
093B 067	Susic Q	Showing	Gold	093B08W	52 ° 26' 05" N	122° 24' 05" W	Buried-channel placer deposits; surficial placer deposits
093B 052	Granite Mountain	Showing	Copper, molybdenum	093B09E	52 ° 32' 00" N	122° 13' 05" W	Porphyry Cu ± Mo ± Au
093B 063	Chris	Showing	Copper	093B09E	52 ° 33' 25" N	122° 12' 53" W	Porphyry Cu ± Mo ± Au
093B 068	Catalan Copper	Showing	Copper, molybdenum	093B09E	52 ° 30' 31" N	122° 10' 44" W	Porphyry Cu ± Mo ± Au
093B 061	Bysouth	Showing	Copper	093B09W	52 ° 37' 00" N	122° 18' 10" W	Porphyry Cu ± Mo ± Au
093B 062	Rick	Showing	Copper, zinc, molybdenum, gold	093B09W	52 ° 32' 21" N	122° 19' 01" W	Porphyry Cu ± Mo ± Au
093B 023	Lot 906	Past producer	Diatomite	093B15E	52 ° 57' 37" N	122° 32' 19" W	Lacustrine diatomite
093B 064	Cantin Creek	Prospect	Gold	093B16E	52 ° 55' 21" N	122° 10' 21" W	Au-quartz veins
093B 069	Buckshot 2	Showing	Gold	093B16E	52 ° 58' 44" N	122° 02' 07" W	Buried-channel placer deposits
093B 070	Sovereign Creek	Past producer	Gold	093B16E	52 ° 58' 58" N	122° 01' 42" W	Surficial placer deposits
093B 018	Quesnel Canyon	Developed prospect	Gold	093B16W	52 ° 59' 37" N	122° 21' 16" W	Surficial placer deposits
093H 066	Iltzul Ridge	Showing	Limestone, dolomite	093H03E	53 ° 07' 38" N	121° 12' 59" W	Limestone
093H 071	Babcock Lake	Showing	Zinc, silver, copper	093H03E	53 ° 00' 46" N	121° 13' 42" W	Sedimentary exhalative Zn-Pb-Ag; polymetallic veins Ag-Pb-Zn±Au
093H 138	Bill	Showing	Silver, lead, zinc	093H03E	53 ° 03' 31" N	121° 31' 21" W	Au-quartz veins; polymetallic veins Ag-Pb-Zn±Au
093H 008	Grouse Creek	Past producer	Gold	093H03W	53 ° 02' 13" N	121° 26' 56" W	Surficial placer deposits; buried-channel placer deposits
093H 009	Canadian Creek	Past producer	Gold	093H03W	53 ° 03' 38" N	121° 27' 39" W	Surficial placer deposits; buried-channel placer deposits

093H 021	Prosperine	Prospect	Gold, silver, lead, zinc	093H03W	53 ° 02' 28" N	121° 29' 49" W	Au-quartz veins; polymetallic veins Ag-Pb-Zn±Au
093H 029	Dowsett	Showing	Tungsten	093H03W	53 ° 00' 08" N	121° 24' 54" W	Au-quartz veins; polymetallic veins Ag-Pb-Zn±Au
093H 048	Warspite	Prospect	Gold, silver, lead, zinc	093H03W	53 ° 01' 57" N	121° 29' 10" W	Au-quartz veins; polymetallic veins Ag-Pb-Zn±Au
093H 049	Tipperary	Showing	Silver, gold, lead	093H03W	53 ° 01' 42" N	121° 29' 15" W	Au-quartz veins; polymetallic veins Ag-Pb-Zn±Au
093H 050	Kitchener	Prospect	Gold, silver, lead, zinc	093H03W	53 ° 01' 37" N	121° 28' 54" W	Au-quartz veins; polymetallic veins Ag-Pb-Zn±Au
093H 051	Independence	Prospect	Gold, silver, lead	093H03W	53 ° 01' 28" N	121° 28' 36" W	Au-quartz veins; polymetallic veins Ag-Pb-Zn±Au
093H 052	Hard Cash	Prospect	Gold, lead	093H03W	53 ° 01' 15" N	121° 28' 05" W	Au-quartz veins; polymetallic veins Ag-Pb-Zn±Au
093H 063	Summit Creek	Past producer	Gold	093H03W	53 ° 11' 50" N	121° 27' 30" W	Surficial placer deposits; buried-channel placer deposits
093H 125	Little Valley Creek	Past producer	Gold	093H03W	53 ° 05' 49" N	121° 29' 05" W	Surficial placer deposits; buried-channel placer deposits
093H 126	French Creek	Past producer	Gold	093H03W	53 ° 04' 03" N	121° 28' 32" W	Surficial placer deposits; buried-channel placer deposits
093II 127	Guyet Placer	Past producer	Gold	093II03W	53 ° 02' 15" N	121° 24' 57" W	Surficial placer deposits; buried-channel placer deposits
093H 128	Stevens Gulch	Past producer	Gold	093H03W	53 ° 00' 37" N	121° 24' 25" W	Surficial placer deposits
093H 129	California Gulch	Past producer	Gold	093H03W	53 ° 00' 19" N	121° 24' 23" W	Surficial placer deposits
093H 142	Dufferin	Prospect	Gold, silver, lead	093H03W	53 ° 01' 00" N	121° 28' 11" W	Au-quartz veins; polymetallic veins Ag-Pb-Zn±Au
093H 148	Placer Pit South	Showing	Gold, silver, lead	093H03W	53 ° 01' 34" N	121° 28' 00" W	Au-quartz veins; polymetallic veins Ag-Pb-Zn±Au
093H 151	St. Lawrence Creek	Showing	Gold	093H03W	53 ° 02' 07" N	121° 26' 19" W	Surficial placer deposits; buried-channel placer deposits
093II 152	Grouse Creek	Showing	Gold	093II03W	53 ° 01' 60" N	121° 27' 57" W	Au-quartz veins
093II 067	Cunningham Pass	Showing	Limestone, dolomite	093II03W, 093H04E	53 ° 04' 40" N	121° 26' 16" W	Limestone
093H 147	Pin Money	Showing	Silver, lead	093H04E	53 ° 02' 49" N	121° 29' 52" W	Polymetallic veins Ag-Pb-Zn±Au
093H 025	Myrtle	Prospect	Gold	093H04E	53 ° 04' 36" N	121° 32' 45" W	Au-quartz veins
093H 027	Black Jack	Past producer	Gold, lead	093H04E	53 ° 03' 45" N	121° 31' 15" W	Au-quartz veins; polymetallic veins Ag-Pb-Zn±Au
093H 034	Morning Star	Showing	Gold, lead	093H04E	53 ° 04' 02" N	121° 31' 43" W	Au-quartz veins; polymetallic veins Ag-Pb-Zn±Au
093H 058	Canusa	Prospect	Gold, lead, zinc, bismuth	093H04E	53 ° 04' 13" N	121° 32' 52" W	Au-quartz veins; polymetallic veins Ag-Pb-Zn±Au
093H 078	Black Bull	Prospect	Gold	093H04E	53 ° 04' 25" N	121° 33' 15" W	Au-quartz veins
093H 079	Steadman	Showing	Gold, copper, lead, zinc	093H04E	53 ° 03' 12" N	121° 31' 13" W	Au-quartz veins; polymetallic veins Ag-Pb-Zn±Au
093H 080	Pani	Showing	Silver, lead, zinc	093H04E	53 ° 02' 20" N	121° 30' 46" W	
093H 117	McArthur Gulch	Past producer	Gold	093H04E	53 ° 05' 43" N	121° 32' 00" W	Surficial placer deposits; buried-channel placer deposits
093H 118	Lowhee Creek	Past producer	Gold	093H04E	53 ° 04' 34" N	121° 33' 26" W	Buried-channel placer deposits; surficial placer deposits
093H 119	Williams Creek	Past producer	Gold	093H04E	53 ° 03' 44" N	121° 31' 21" W	Buried-channel placer deposits; surficial placer deposits
093H 120	Stouts Gulch	Past producer	Gold	093H04E	53 ° 04' 02" N	121° 32' 25" W	Surficial placer deposits; buried-channel placer deposits

093H 121	Emory Gulch	Past producer	Gold	093H04E	53 ° 03' 56" N	121° 32' 40" W	Surficial placer deposits; buried-channel placer deposits
093II 122	Conklin Gulch	Past producer	Gold	093II04E	53 ° 03' 49" N	121° 30' 44" W	Buried-channel placer deposits
093II 123	Walker Gulch	Past producer	Gold	093II04E	53 ° 03' 06" N	121° 31' 25" W	Surficial placer deposits; buried-channel placer deposits
093H 124	Mink Gulch	Past producer	Gold	093H04E	53 ° 02' 37" N	121° 31' 09" W	Surficial placer deposits
093H 137	Bald	Showing	Silver, lead	093H04E	53 ° 00' 26" N	121° 30' 39" W	Au-quartz veins; polymetallic veins Ag-Pb-Zn±Au
093H 139	B.C. Vein	Past producer	Gold, lead, zinc, copper, bismuth	093H04E	53 ° 04' 29" N	121° 33' 02" W	Au-quartz veins; polymetallic veins Ag-Pb-Zn±Au
093H 140	Bonanza Ledge	Developed prospect	Gold, lead, zinc, copper	093H04E	53 ° 04' 18" N	121° 32' 48" W	Au-quartz veins; polymetallic veins Ag-Pb-Zn±Au
093H 141	Cariboo	Showing	Gold, silver, lead	093H04E	53 ° 04' 25" N	121° 32' 20" W	Au-quartz veins; polymetallic veins Ag-Pb-Zn±Au
093H 144	Home Rule	Showing	Silver, gold, zinc, lead	093H04E	53 ° 04' 20" N	121° 31' 26" W	Polymetallic veins Ag-Pb-Zn±Au
093H 146	King Fraction	Showing	Gold, silver, lead	093H04E	53 ° 02' 50" N	121° 30' 57" W	Au-quartz veins; polymetallic veins Ag-Pb-Zn±Au
093H 149	Sergeant Lindsay	Showing	Silver	093H04E	53 ° 02' 23" N	121° 32' 22" W	Au-quartz veins
093H 150	Victory	Showing	Gold, silver, lead	093H04E	53 ° 02' 51" N	121° 30' 17" W	Au-quartz veins; polymetallic veins Ag-Pb-Zn±Au
093H 061	R.T.	Showing	Nickel, chromium	093H04W	53 ° 00' 48" N	121° 54' 09" W	Tholeiitic intrusion-hosted Ni-Cu
093J 025	Giscome	Producer	Limestone	093J01W	54 ° 03' 40" N	122° 17' 39" W	Limestone
093J 024	Windy	Showing	Copper, gold, palladium	093J13W	54 ° 56' 27" N	123° 50' 06" W	Alkalic porphyry Cu-Au
093J 023	Ruby	Showing	Gold, silver, lead	093J14W	54 ° 56' 54" N	123° 17' 58" W	Epithermal Au-Ag: low sulphidation
093K 048	Calex	Showing	Mercury	093K08E	54 ° 29' 28" N	124° 08' 20" W	Almaden Hg; silica-Hg carbonate
093K 012	Murray Ridge	Showing	Chromium	093K09E	54 ° 31' 53" N	124° 11' 30" W	Podiform chromite
093K 020	Max	Showing	Copper, gold	093K16E	54 ° 55' 30" N	124° 03' 29" W	Alkalic porphyry Cu-Au
093N 207	KBE	Showing	Copper, gold	093K16E, 093N01E	55 ° 00' 27" N	124° 24' 09" W	Alkalic porphyry Cu-Au
093K 004	HA-1	Showing	Copper	093K16W	54 ° 51' 21" N	124° 18' 25" W	Unknown
093K 077	Dem	Showing	Arsenic, gold, silver	093K16W	54 ° 45' 06" N	124° 26' 48" W	Au skarn
093K 080	Tas	Prospect	Gold, copper	093K16W	54 ° 54' 17" N	124° 18' 38" W	Alkalic porphyry Cu-Au
093K 083	Lynx	Showing	Copper	093K16W	54 ° 51' 13" N	124° 04' 13" W	Cu Skarn
093K 086	K-2	Showing	Copper, silver	093K16W	54 ° 55' 18" N	124° 06' 00" W	Cu±Ag quartz veins
093K 091	Frec Gold Zone	Showing	Gold, copper	093K16W	54 ° 53' 32" N	124° 19' 30" W	Alkalic porphyry Cu-Au
093N 194	Mount Milligan	Developed prospect	Gold, copper, silver, lead, zinc, molybdenum	093N01E	55 ° 07' 26" N	124° 01' 39" W	Alkalic porphyry Cu-Au
093N 096	Taylor	Showing	Copper, gold	093N01W	55 ° 07' 01" N	124° 25' 20" W	Cu skarn; Au skarn
093N 131	Webb	Showing	Copper	093N01W	55 ° 06' 48" N	124° 20' 03" W	Porphyry Cu ± Mo ± Au; alkalic porphyry Cu-Au
093N 141	Wit	Developed prospect	Zinc, lead, silver, gold	093N01W	55 ° 12' 52" N	124° 26' 57" W	Epithermal Au-Ag: low sulphidation
093N 218	Cas	Showing	Copper	093N01W	55 ° 04' 17" N	124° 27' 49" W	Alkalic porphyry Cu-Au
093N 104	SRM	Prospect	Copper, gold	093N01W, 093N02E	55 ° 14' 01" N	124° 31' 21" W	Alkalic porphyry Cu-Au
093N 208	Rig Breccia	Showing	Zinc, copper, silver, gold, lead	093N01W, 093N02E	55 ° 12' 21" N	124° 30' 22" W	Epithermal Au-Ag: low sulphidation
093N 209	GG	Showing	Copper, lead, zinc	093N01W, 093N02E	55 ° 13' 06" N	124° 30' 28" W	Polymetallic veins Ag-Pb-Zn±Au
093N 219	WN	Showing	Copper	093N01W, 093N02E	55 ° 08' 22" N	124° 29' 31" W	Alkalic porphyry Cu-Au
093N 083	Creek	Showing	Copper, gold	093N02E	55 ° 12' 39" N	124° 32' 08" W	Alkalic porphyry Cu-Au
093N 084	Moss	Showing	Copper, gold, lead	093N02E	55 ° 08' 19" N	124° 32' 03" W	Alkalic porphyry Cu-Au; Cu skarn

093N 140	Skook	Prospect	Gold, silver, copper, zinc, lead	093N02E	55 ° 12' 00" N	124° 31' 42" W	Alkalic porphyry Cu-Au
093N 164	Witch	Showing	Copper	093N02E	55 ° 08' 58" N	124° 31' 28" W	Alkalic porphyry Cu-Au
093N 101	Col	Developed prospect	Copper, gold	093N02E, 093N02W, 093N07E, 093N07W	55 ° 14' 57" N	124° 45' 33" W	Alkalic porphyry Cu-Au
093N 079	Jean	Developed prospect	Copper, molybdenum, silver, gold	093N02W	55 ° 06' 18" N	124° 57' 22" W	Porphyry Cu ± Mo ± Au
093N 091	Nighthawk	Prospect	Copper, gold, silver	093N02W	55 ° 11' 03" N	124° 51' 46" W	Alkalic porphyry Cu-Au
093N 092	Vector	Prospect	Copper, gold, silver	093N02W	55 ° 12' 06" N	124° 53' 19" W	Alkalic porphyry Cu-Au
093N 139	Mid	Showing	Copper, gold, silver	093N02W	55 ° 11' 41" N	124° 52' 50" W	Alkalic porphyry Cu-Au
093N 185	Gibson	Prospect	Gold, silver, lead, zinc, copper	093N02W	55 ° 10' 13" N	124° 53' 42" W	Polymetallic veins Ag-Pb-Zn±Au; epithermal Au-Ag-Cu; high sulphidation
093N 068	Falcon	Prospect	Copper, molybdenum, lead	093N03E	55 ° 12' 16" N	125° 05' 41" W	Alkalic porphyry Cu-Au
093N 069	Fal	Showing	Copper, zinc, lead, silver, arsenic	093N03E	55 ° 12' 30" N	125° 04' 11" W	Alkalic porphyry Cu-Au
093N 071	Heath #3	Showing	Copper, silver, gold	093N03E, 093N06E	55 ° 16' 01" N	125° 08' 54" W	Alkalic porphyry Cu-Au
093N 072	Heath #1	Prospect	Copper, silver, gold, lead, zinc	093N03E, 093N06E	55 ° 16' 15" N	125° 09' 46" W	Alkalic porphyry Cu-Au
093N 112	Rotracker Creek	Showing	Copper, gold, silver	093N06E	55 ° 24' 10" N	125° 11' 41" W	Alkalic porphyry Cu-Au
093N 160	Hal 4	Showing	Copper, silver	093N06E	55 ° 24' 24" N	125° 10' 47" W	Alkalic porphyry Cu-Au
093N 019	Kwanika	Showing	Mercury, arsenic	093N06W	55 ° 29' 01" N	125° 19' 18" W	Almaden IIg; silica-IIg carbonate
093N 159	Chuchi Lake	Developed prospect	Copper, gold	093N07E	55 ° 15' 47" N	124° 32' 43" W	Alkalic porphyry Cu-Au
093N 210	Gertie	Showing	Copper, silver	093N07E	55 ° 18' 26" N	124° 44' 12" W	Volcanic redbed Cu
093N 032	Klawli	Prospect	Copper, gold, silver	093N07W	55 ° 17' 29" N	124° 46' 56" W	Cu±Ag quartz veins; alkalic porphyry Cu-Au
093N 053	Valleau Creek	Showing	Gold	093N07W	55 ° 28' 42" N	124° 55' 15" W	Surficial placer deposits
093N 085	Aplite Creek	Prospect	Copper, gold	093N07W	55 ° 19' 25" N	124° 52' 46" W	Alkalic porphyry Cu-Au
093N 111	Valley Girl	Showing	Gold, copper	093N07W	55 ° 28' 18" N	124° 57' 00" W	Au-quartz veins
093N 169	Sooner	Showing	Molybdenum	093N07W	55 ° 19' 12" N	124° 54' 18" W	Alkalic porphyry Cu-Au
093N 215	Wudtisi	Showing	Copper	093N07W	55 ° 27' 55" N	124° 53' 55" W	Porphyry Cu ± Mo ± Au
093N 006	KC	Showing	Copper	093N11E	55 ° 31' 08" N	125° 08' 36" W	Alkalic porphyry Cu-Au
093N 067	Tak	Prospect	Copper, gold, silver	093N11E, 093N11W	55 ° 42' 13" N	125° 14' 46" W	Alkalic porphyry Cu-Au
093N 009	Lustdust	Developed prospect	Silver, zinc, lead, gold, antimony, copper	093N11W	55 ° 33' 57" N	125° 24' 52" W	J01:Polymetallic manto Ag-Pb-Zn; polymetallic veins Ag-Pb-Zn±Au
093N 015	Snell	Showing	Mercury, antimony	093N11W	55 ° 40' 33" N	125° 26' 57" W	Almaden IIg; silica-IIg carbonate
093N 073	Swan	Developed prospect	Copper, gold, molybdenum	093N11W	55 ° 30' 27" N	125° 20' 00" W	Porphyry Cu ± Mo ± Au
093N 082	Takla-Rainbow	Developed prospect	Gold, silver, copper, lead, zinc	093N11W	55 ° 39' 44" N	125° 18' 18" W	Porphyry Cu ± Mo ± Au
093N 001	Misty	Developed prospect	Copper	093N13E	55 ° 54' 57" N	125° 30' 49" W	Alkalic porphyry Cu-Au
093N 065	Mariposite	Showing	Mercury	093N13E	55 ° 52' 37" N	125° 42' 47" W	Almaden Hg; silica-Hg carbonate
093N 171	Haw	Showing	Copper	093N13E	55 ° 58' 54" N	125° 42' 01" W	Alkalic porphyry Cu-Au
093N 093	Tam	Developed prospect	Copper, silver	093N13E, 093N14W	55 ° 58' 19" N	125° 30' 14" W	Alkalic porphyry Cu-Au
093N 002	Lorraine	Developed prospect	Copper, gold, silver	093N14W	55 ° 55' 40" N	125° 26' 27" W	Alkalic porphyry Cu-Au
093N 005	Rhonda	Developed prospect	Copper	093N14W	55 ° 54' 48" N	125° 17' 30" W	Alkalic porphyry Cu-Au
093N 007	Dorothy	Prospect	Copper, molybdenum, zinc, lead, gold	093N14W	55 ° 53' 07" N	125° 20' 15" W	Alkalic porphyry Cu-Au
093N 066	Bishop	Prospect	Copper, gold	093N14W	55 ° 55' 12" N	125° 25' 21" W	Alkalic porphyry Cu-Au

093N 074	Elizabeth	Showing	Copper	093N14W	55 ° 52' 33" N	125° 19' 41" W	Alkalic porphyry Cu-Au
093N 097	Steelhead	Showing	Copper	093N14W	55 ° 58' 34" N	125° 24' 05" W	Alkalic porphyry Cu-Au
093N 105	Fox	Showing	Copper	093N14W	55 ° 55' 25" N	125° 19' 47" W	Alkalic porphyry Cu-Au
093N 223	Mackenzie	Prospect	Copper, gold, silver	093N14W	55 ° 49' 52" N	125° 19' 57" W	Alkalic porphyry Cu-Au
093N 225	All Alone Dome	Prospect	Copper	093N14W	55 ° 56' 13" N	125° 27' 60" W	Alkalic porphyry Cu-Au
093O 044	Royer Lake	Showing	Iron, magnetite	093O03E	55 ° 03' 30" N	123° 12' 16" W	Magmatic Fe-Ti±V oxide deposits
093O 048	LS1	Developed prospect	Limestone	093O03E	55 ° 10' 12" N	123° 13' 00" W	Limestone
093O 047	Sparky	Developed prospect	Limestone	093O04W	55 ° 03' 04" N	123° 46' 43" W	Limestone
093O 051	Nat	Showing	Gold, platinum	093O05E	55 ° 20' 17" N	123° 42' 53" W	M05:Alaskan-type Pt+Os+Rh+Ir
094C 019	Pluto	Showing	Copper, gold	094C03W	56 ° 08' 24" N	125° 24' 11" W	Polymetallic veins Ag-Pb-Zn±Au
094C 020	Thane	Showing	Copper, gold	094C03W	56 ° 07' 18" N	125° 23' 23" W	Polymetallic veins Ag-Pb-Zn±Au
094C 044	Thane Creek	Showing	Mercury	094C03W	56 ° 06' 58" N	125° 21' 46" W	Silica-Hg carbonate
094C 069	Cat	Prospect	Gold, copper, silver	094C03W	56 ° 03' 44" N	125° 22' 14" W	Alkalic porphyry Cu-Au
094C 071	Oy	Showing	Copper	094C03W	56 ° 12' 51" N	125° 25' 57" W	Alkalic porphyry Cu-Au
094C 100	Kiwi	Showing	Copper	094C03W	56 ° 04' 22" N	125° 21' 31" W	Alkalic porphyry Cu-Au
094C 018	Matetlo	Showing	Copper	094C04E	56 ° 12' 26" N	125° 36' 48" W	Cu±Ag quartz veins; alkalic porphyry Cu-Au
094C 112	DM	Showing	Copper	094C04E	56 ° 12' 06" N	125° 32' 17" W	Alkalic porphyry Cu-Au
094C 113	Yak	Showing	Copper	094C04E	56 ° 12' 35" N	125° 36' 00" W	Alkalic porphyry Cu-Au; Cu±Ag quartz veins
094C 114	Koala	Showing	Copper	094C04E	56 ° 12' 42" N	125° 36' 20" W	Alkalic porphyry Cu-Au; Cu±Ag quartz veins
094C 115	Intrepid	Showing	Copper	094C04E	56 ° 12' 36" N	125° 39' 10" W	Alkalic porphyry Cu-Au; Cu±Ag quartz veins
094C 116	Bill	Showing	Copper, gold	094C04E	56 ° 12' 59" N	125° 39' 28" W	Alkalic porphyry Cu-Au; Cu±Ag quartz veins
094C 117	Yeti	Showing	Copper	094C04E	56 ° 14' 00" N	125° 39' 28" W	Porphyry-related Au
094C 118	Dragon	Showing	Copper	094C04E	56 ° 13' 07" N	125° 35' 39" W	Alkalic porphyry Cu-Au
094C 138	Hawk (Ad)	Prospect	Gold, copper, lead, zinc	094C04E	56 ° 02' 07" N	125° 40' 26" W	Polymetallic veins Ag-Pb-Zn±Au; Au-quartz veins
094C 139	Hawk (Radio)	Prospect	Gold, copper	094C04E	56 ° 01' 22" N	125° 40' 06" W	Cu±Ag quartz veins
094C 140	Hawk (HSW)	Showing	Gold, copper	094C04E	56 ° 01' 40" N	125° 42' 17" W	Au-quartz veins; polymetallic veins Ag-Pb-Zn±Au
094C 136	Tut 6	Showing	Copper, gold, silver	094C05E	56 ° 15' 32" N	125° 43' 27" W	Alkalic porphyry Cu-Au
094C 137	Tut 3	Showing	Gold, silver, copper, molybdenum	094C05E	56 ° 16' 50" N	125° 40' 09" W	Alkalic porphyry Cu-Au
094C 146	Choice	Showing	Copper	094C05E	56 ° 16' 09" N	125° 39' 11" W	Alkalic porphyry Cu-Au
094C 147	Ache	Showing	Copper	094C05E	56 ° 15' 24" N	125° 41' 34" W	Alkalic porphyry Cu-Au
094C 120	CR	Showing	Copper	094C06W	56 ° 15' 15" N	125° 24' 03" W	Volcanic redbed Cu
094C 121	Nuthatch	Showing	Copper	094C06W	56 ° 15' 33" N	125° 25' 15" W	Volcanic redbed Cu

include comprehensive geological descriptions, mineralogy, deposit type, bibliography, work histories, resource and/or reserve statistics and analytical results and are available through MINFILE.

Study Area

The MINFILE update area covers the QUEST project area within the Interior Plateau of central British Columbia, which includes parts of NTS 093A, B, G, H, J, K, N, O and 094C, D (Figure 1). The southern half of the project area covers mainly the Quesnel Highland and Cariboo plateau physiographic regions, whereas the northern half covers the Nechako Basin and part of the Omineca Mountains. The project area extends from Williams Lake in the southeast to

Germanen Landing in the northwest and is about 520 km long and 80 km wide. Prince George is located at the approximate project centre and Highway 97 transects the area in a north-south orientation, with Highway 16 providing east-west corridor access (Figures 2, 3).

The central portion of the project area covers predominantly Quesnel Terrane rocks. The Quesnel Terrane is generally bound to the east by the Kootenay, Slide Mountain and Cariboo terranes. To the west are Cache Creek and Overlap Assemblage terranes. To date, the principal exploration focus has been on porphyry copper and copper-gold prospects in the Quesnel and eastern Stikine terranes. In addition to porphyry copper-gold deposits (Kwanika, Lorraine-Jajay, Mount Milligan), other important targets

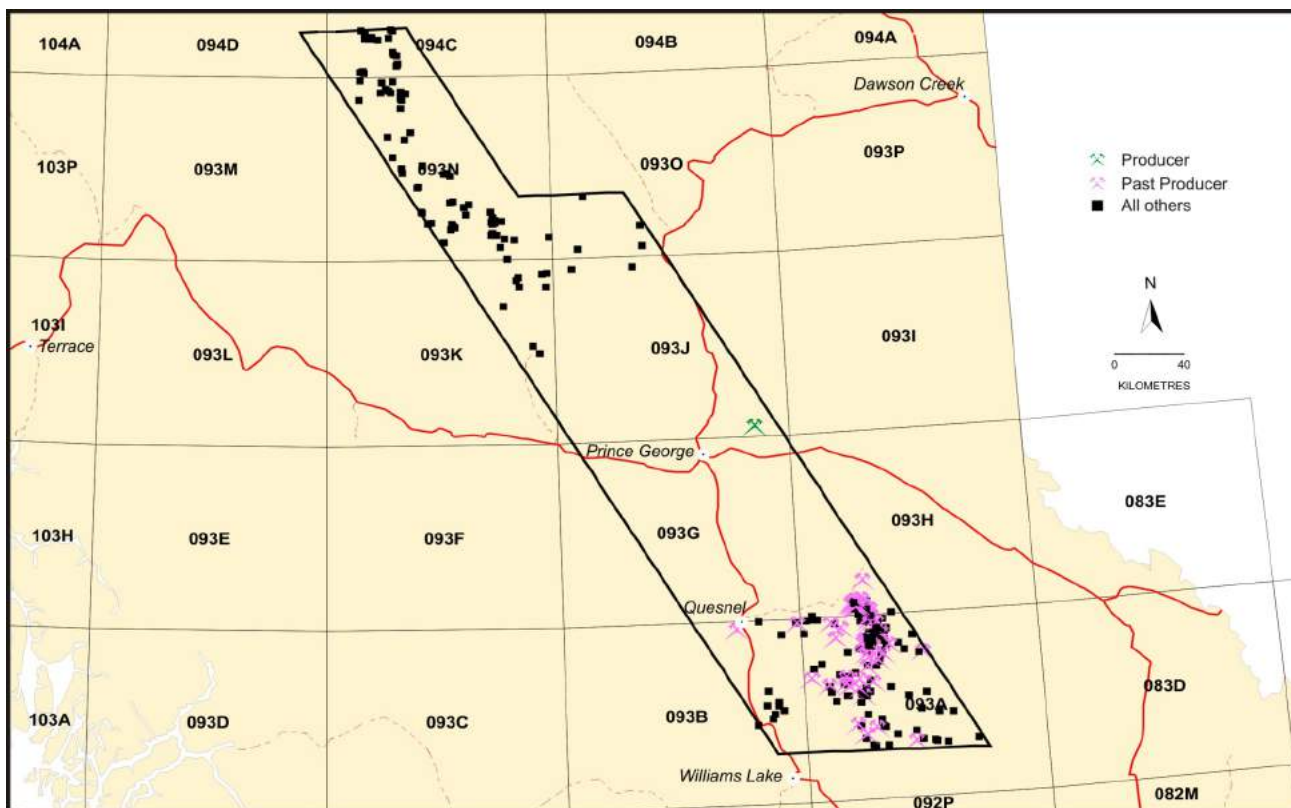


Figure 2. MINFILE occurrences updated in the QUEST geophysical survey area, British Columbia.

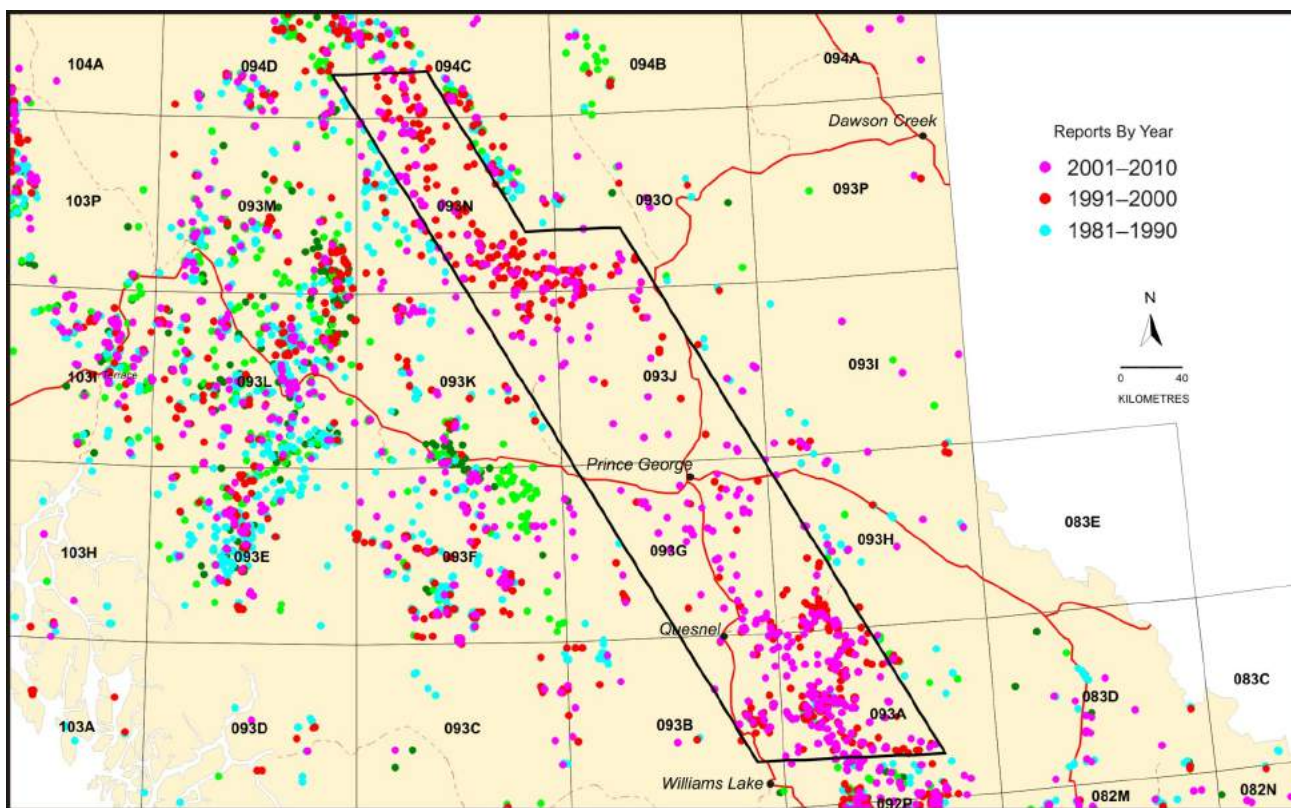


Figure 3. Assessment reports reviewed from the QUEST geophysical survey area, British Columbia.

are porphyry copper-molybdenum (Jean), sediment-hosted gold (Spanish Mountain), volcanogenic massive sulphide (Frank Creek), skarn (QR, Lustdust), polymetallic massive sulphide veins (G-South) and mesothermal gold-quartz vein deposits (Bonanza Ledge, Frasergold). Placer gold exploration and mining is also a significant traditional activity within this region (DeGrace, 2008). Production continues at two open-pit metal mines in the project area—Gibraltar (porphyry-copper-molybdenum) producing copper and molybdenum, and Mount Polley (alkalic porphyry copper-gold) producing copper, gold and silver. Both mines have experienced many years of successful operation. The QR mine began underground production from its gold skarn deposit near Likely, phasing out its previous open pit (International Wayside Gold Mines Ltd., 2009). However, operations at the mine have resulted in lower-than-expected ore production and grade, and the mine is currently closed.

Other mining activity includes a small limestone quarry about 5 km southeast of Giscome that appears to have been inactive in 2008, but made shipments from stockpiled material. Within the community of Giscome itself, the Canadian National Railway Company continued production from its basalt quarry to supply road ballast requirements for maintenance of its main and spur lines (DeGrace, 2008).

Following eight years of steady increases in exploration expenditures in the QUEST project area, the total amount in 2008 (\$70 million) was down slightly from that in 2007 (\$81 million) but still well above 2006 levels (\$41 million). Likewise, drilling activity in 2008 (186 280 m) was down from 2007 (216 380 m) but still high compared to other recent years (Lane, 2006; DeGrace, 2007, 2008).

Exploration highlights in the project area include grass-roots, early-stage exploration and advanced-stage exploration/deposit appraisal categories. Some highlights include, from north to south, Tam, Misty, Lorraine-Jajay, Lustdust, Kwanika, Falcon, Jean, Mount Milligan, G-South, Mouse Mountain, Bonanza Ledge, Frank Creek, Spanish Mountain and Frasergold (see Table 1). The Mount Milligan copper-gold mine project is in an advanced stage of development and has received an environmental assessment (EA) certificate (Environmental Assessment Office, 2009).

Methodology

The MINFILE update process consists of gathering information necessary for the complete coding of a new occurrence or revision, modification or even deletion of a pre-existing occurrence. These occurrences, which may include mineral, coal or industrial mineral categories, are updated by accessing, researching, compiling, interpreting and inputting geoscientific data into the BC Geological Survey's mineral and coal inventory file (MINFILE). Each updated occurrence has a textual description of mineral and geological information and work history, and a complete bibliog-

raphy; all critical searchable data fields are populated with the appropriate information. The MapPlace (BC Geological Survey, 2009c; <http://www.MapPlace.ca>) in conjunction with the Ministry's MINFILE and ARIS (BC Geological Survey, 2009d; <http://aris.empr.gov.bc.ca/>) databases and other appropriate information and online databases are important repositories that facilitate the quality and timeliness of the update process. The accuracy and quality of the coding and editing are done in accordance to the standards described in MINFILE documentation (BC Geological Survey, 2007) and the British Columbia Geological Survey Branch Style Guide (Grant and Newell, 1992). Information sources include assessment reports, current fieldwork, open files and reports, geoscience maps, *Geological Fieldwork* and *Exploration in British Columbia* publications, bulletins, papers, press material, Minister of Mines Annual Reports, Property File, maps, miscellaneous reports and theses, in addition to communicating with BC Geological Survey staff with expertise in the map areas. References are made to Geological Survey of Canada maps, reports, papers and other appropriate material and publications, which are available in the BC Geological Survey records housed in the Jack Davis Building library, Victoria, BC.

The completed work is submitted through the MINFILE online coding form accessed with permission of the BC Geological Survey. The deliverable is updated data integrated into the MINFILE database system, which is available for immediate public and industry use.

Summary

The MINFILE data that resulted from the 2008 QUEST project initiative will stimulate mineral exploration by presenting updated geological information for an area of the province that is considered to have a high potential for future discoveries of copper and copper-gold deposits, such as those at the Gibraltar and Mount Polley mines, and the Mount Milligan deposit. It is expected that significant new exploration activity will be generated with focus on sediment-hosted gold, mesothermal gold-quartz veins, skarns and volcanogenic massive sulphide deposits.

The results of this project are 486 updated MINFILE occurrences, including 139 newly documented showings. The results are available for viewing through the BC Geological Survey's MINFILE database (<http://minfile.gov.bc.ca>).

Acknowledgments

Geoscience BC is gratefully acknowledged for funding this MINFILE project. B. Ryan is thanked for his review of this manuscript and S. Meredith-Jones is thanked for administering the MINFILE data delivery.

References

- BC Geological Survey (2007): MINFILE Coding Manual Version 5.0; BC Ministry of Energy, Mines and Petroleum Resources, Information Circular 2007-4, URL <<http://www.empr.gov.bc.ca/Mining/Geoscience/MINFILE/ProductsDownloads/MINFILEDocumentation/CodingManual/Pages/default.aspx>> [October 2009].
- BC Geological Survey (2009a): Development of MINFILE – Uses of MINFILE; BC Ministry of Energy, Mines and Petroleum Resources; URL <<http://www.empr.gov.bc.ca/Mining/Geoscience/MINFILE/Pages/history.aspx#uses of min file>> [November 2009].
- BC Geological Survey (2009b): Property File digital document database; BC Ministry of Energy, Mines and Petroleum Resources, URL <<http://propertyfile.gov.bc.ca>> [October 2009].
- BC Geological Survey (2009c): MapPlace GIS internet mapping system; BC Ministry of Energy, Mines and Petroleum Resources, MapPlace website, URL <<http://www.MapPlace.ca>> [October 2009].
- BC Geological Survey (2009d): ARIS assessment report indexing system; BC Ministry of Energy, Mines and Petroleum Resources, URL <<http://aris.empr.gov.bc.ca>> [October 2009].
- DeGrace, J.R. (2007): North-central region review; *in* Exploration and Mining in British Columbia 2007, BC Ministry of Energy, Mines and Petroleum Resources, pages 37–50, URL <<http://www.empr.gov.bc.ca/Mining/Geoscience/PublicationsCatalogue/ExplorationinBC/Pages/2007.aspx>> [October 2009].
- DeGrace, J.R. (2008): North-central region review; *in* Exploration and Mining in British Columbia 2008, BC Ministry of Energy, Mines and Petroleum Resources, pages 43–57, URL <<http://www.empr.gov.bc.ca/Mining/Geoscience/PublicationsCatalogue/ExplorationinBC/Pages/2008.aspx>> [October 2009].
- Environmental Assessment Office (2009): Home page; BC Ministry of Environment, URL <<http://www.eao.gov.bc.ca/>> [November 2009].
- Grant, B. and Newell, J.M. (1992): British Columbia Geological Survey Branch Style Guide; BC Ministry of Energy, Mines and Petroleum Resources, Information Circular 1992-7, URL <<http://www.empr.gov.bc.ca/Mining/Geoscience/PublicationsCatalogue/InformationCirculars/Pages/IC1992-07.aspx>> [October 2009].
- International Wayside Gold Mines Ltd. (2009): Home page; International Wayside Gold Mines Ltd., URL <<http://www.wayside-gold.com/s/Home.asp>> [November 2009].
- Lane, B. (2006): Central region review; *in* Exploration and Mining in British Columbia 2006, BC Ministry of Energy, Mines and Petroleum Resources, pages 57–71, URL <<http://www.empr.gov.bc.ca/Mining/Geoscience/PublicationsCatalogue/ExplorationinBC/Pages/2006.aspx>> [October 2009].
- MINFILE (2009): MINFILE BC mineral deposits database; BC Ministry of Energy, Mines and Petroleum Resources, URL <<http://minfile.gov.bc.ca>> [October 2009].

Near-Surface Volcanic Rocks in the Southeastern Nechako Basin, South-Central British Columbia (Parts of NTS 092N, O, 093B, C): Interpretation of the Canadian Hunter Seismic Reflection Surveys and First-Arrival Tomographic Inversion

N. Hayward, Department of Earth Sciences, Simon Fraser University, Burnaby, BC, nhayward@nrcan.gc.ca

A.J. Calvert, Department of Earth Sciences, Simon Fraser University, Burnaby, BC

Hayward, N. and Calvert, A.J. (2010): Near-surface volcanic rocks in the southeastern Nechako Basin, south-central British Columbia (parts of NTS 092N, O, 093B, C): interpretation of the Canadian Hunter seismic reflection surveys and first-arrival tomographic inversion; in Geoscience BC Summary of Activities 2009, Geoscience BC, Report 2010-1, p. 203–226.

Introduction

Renewed interest in the Nechako Basin has been a result of development of the region's mineral resources following the impacts of pine beetle infestation on the region's forestry industry. Although forestry road access into the region is good, there are a number of impediments to interpretation of the basin's stratigraphy and structure, and to the evaluation of its hydrocarbon and mineral potential. These include the extensive vegetation and surficial deposits, the limited outcrop of Jura-Cretaceous rocks, and the sparsity and variable quality of seismic reflection data. In this paper, the geology and structure of near-surface rocks are investigated using first-arrival tomographic-inversion velocity models.

The Nechako Basin is primarily a Jurassic to Oligocene successor basin located in the interior plateau of south-central British Columbia (Figure 1), between the Rocky Mountains and Coast Mountains (Hickson, 1990). The basin is bounded by the Coast Mountains and the Yalakom fault to the west, the Fraser fault to the east, the Cretaceous Skeena Arch to the north and the Jura-Cretaceous Tyaughton Basin to the south.

The basin formed in part from and following accretion of the terranes of the western Canadian Cordillera, where the oceanic Cache Creek Terrane separates surface exposures

Keywords: Nechako Basin, tomography, potential field, physical properties

This publication is also available, free of charge, as colour digital files in Adobe Acrobat® PDF format from the Geoscience BC website: <http://www.geosciencebc.com/s/DataReleases.asp>.

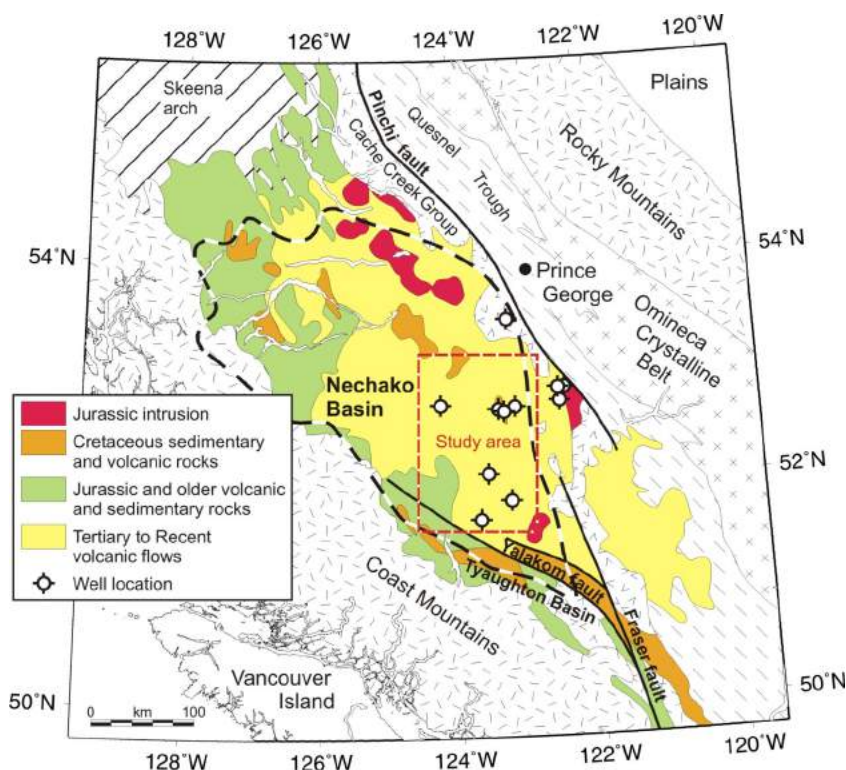


Figure 1. Location of the Nechako Basin and simplified geology of its western Canadian Cordillera setting (modified from Hayward and Calvert; 2009b). Black and white dashed box shows the study area (Figure 2).

of the Stikine and Quesnel volcanic arc terranes (Struik and MacIntyre, 2001). Westward-directed thrusting occurred during basin initiation prior to 165 Ma (Schiarizza and MacIntyre, 1999) at the boundary between the Stikine and Cache Creek terranes, and transpressional tectonic processes were dominant until the Eocene. The primary Yalakom and Fraser faults are associated with this Eocene shift to a dextral transtensional regime (Price, 1994), which was accompanied by regional volcanism. These Eocene volcanic rocks, which blanket the Jura-Cretaceous sedimentary basin, were later overlain by a varying thickness of Neogene volcanic rocks and Quaternary glacial and drift deposits.

Summary of Basin Stratigraphy and Structure

Seismic reflection profiles acquired by Canadian Hunter Exploration Limited (Canadian Hunter) in the 1980s were recovered and reprocessed in 2006 by Arcis Corporation.¹ These data formed the basis for the re-examination of the subsurface structure and stratigraphy of the southeastern Nechako Basin by Hayward and Calvert (2008b). Regional interpretation of the seismic reflection data was divided

into four blocks based on seismic data location and variations in geological structure and stratigraphy (Figure 2):

- 1) Block A (southern Redstone area), in the southern part of the study area, is centred on the Canadian Hunter Redstone wells d-94-G and b-82-C, and seismic lines 160-01 to -19.
- 2) Block B (western Redstone area), centrally located, includes the single seismic line 160-17, which intersects Hudson's Bay well c-75-A. The single crooked seismic line in this block could not be modelled by the two-dimensional (2-D) tomographic methods used here.
- 3) Block C (Chilcotin area), in the northwestern part of the study area, contains the Canadian Hunter Chilcotin well b-22-K and seismic lines 161-01 to -09.

¹ These seismic data are currently confidential, but can be obtained for noncommercial purposes through Geoscience BC with a specific research agreement.

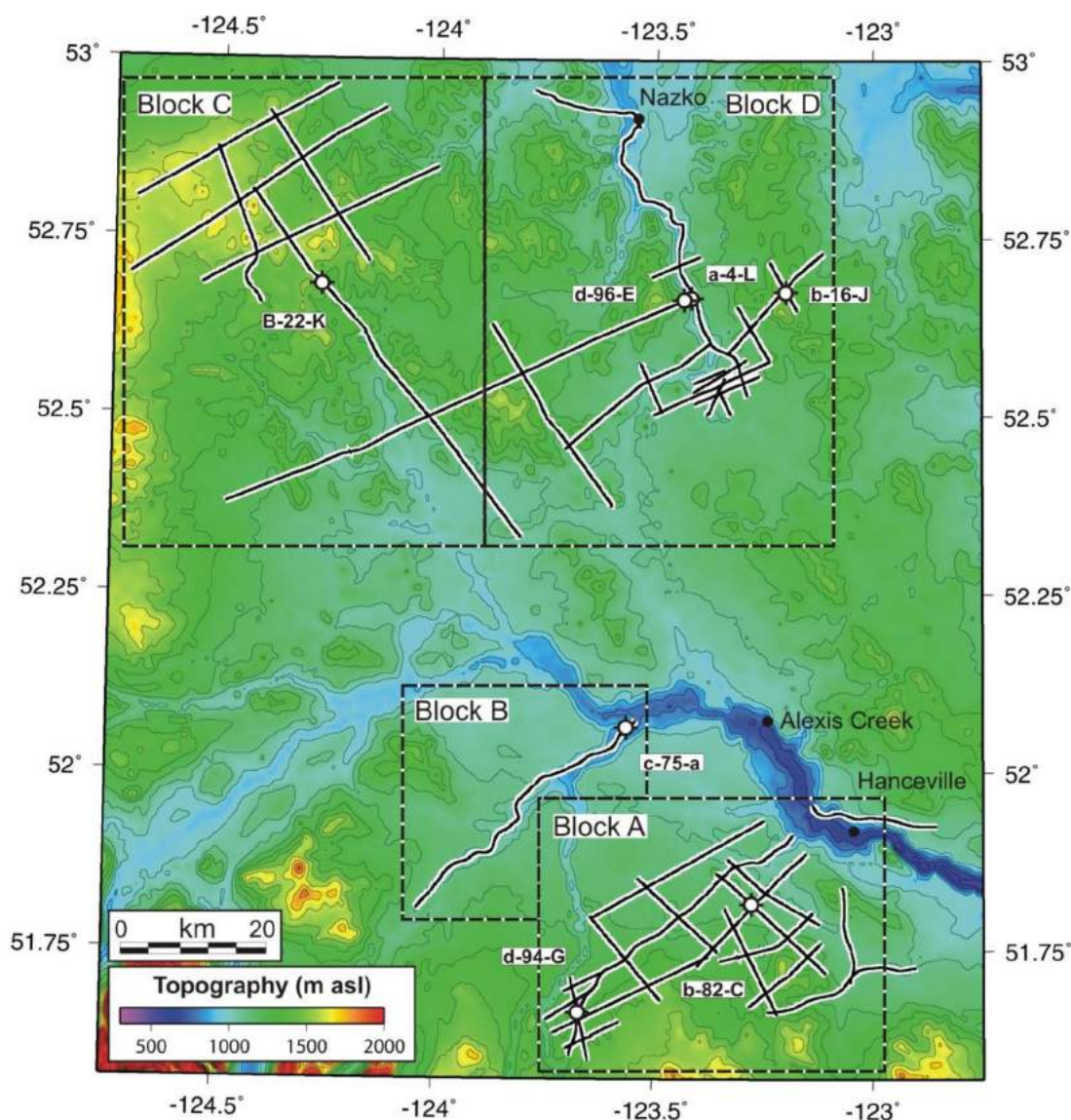


Figure 2. Location of Canadian Hunter seismic reflection lines (white bordered black lines) and topography of the study region, southeastern Nechako Basin, south-central British Columbia. Contour interval 100 m. Large dashed boxes show the original study blocks (A, B, C and D). Black circles show well locations.

- 4) Block D (Nazko area), in the northeastern part of the study area, includes wells Honolulu Nazko a-4-L, Canadian Hunter Nazko d-96-E and Canadian Hunter–Esso Nazko b-16-J, and seismic lines 159-01 to -15 and 162-02.

The southeastern Nechako Basin consists of remnants of Cretaceous fold-and-thrust belts that have been segmented during roughly north-northwest-trending Eocene dextral transtension associated with the Fraser and Yalakom faults (Figure 3). Jura-Cretaceous rocks that remain in the basin are interspersed with volcanic and intrusive basement highs and Eocene pull-apart basins that host volcanoclastic deposits. Seismic interpretation of the Cretaceous thrust faults suggests roughly east-west convergence, which is generally in agreement (Rusmore et al., 2000) with the mid-Cretaceous contractional event that was responsible for the formation of the northeast-verging Waddington thrust belt (Rusmore and Woodsworth, 1991).

In block A (Figure 3), Cretaceous compressional structures were reactivated under Eocene dextral transtension. A sub-basin in the vicinity of well d-94-G contains Cretaceous rocks of the Taylor Creek Group, which overlie volcanic rocks of the Cretaceous Spences Bridge Group. Rocks of the sub-basin form a northwest-plunging faulted anticline, which shows evidence of northwest-southeast Eocene strike-slip deformation. A low-angle, southwest-dipping detachment divides these rocks from shallow basement to the northeast. Another sub-basin, adjacent to well b-82-C, is more poorly deformed. Faulting is concentrated at the northwest (thrusting) and southeast (strike-slip) margins, which are marked by basement and Bouguer gravity highs (Figure 3b).

The block C region is dominated by a north-northeast-trending extensional basin that contains more than 4 km of Eocene volcanoclastic and sedimentary rocks (Riddell et al., 2007). Faults bounding and within the basin have strikes that echo the two dominant trends (northwest and north-northeast) observed in the potential field anomalies (Figure 3b). The basin was likely formed during Eocene dextral transtension, with internal basin folding and faulting occurring late in its history.

In the block D region, sedimentary rocks of the Taylor Creek Group, thrust eastwards during the Cretaceous, were subsequently deformed and truncated by strike-slip faults during Eocene dextral transtension. Strike-slip faults in southwestern block D (trend similar to the Yalakom fault system) and eastern block D (trend similar to the Fraser fault system) may form an extensional right-stepping system along an east-west discontinuity that divides the Eocene strike-slip faults in southwestern block D from Cretaceous thrust faults in northwestern block D.

Near-Surface Rocks in the Southeastern Nechako Basin

Geological mapping in the southeastern Nechako Basin (e.g., Riddell, 2006) has broadly constrained the areal extent of the volcanic units that overlie the Jura-Cretaceous rocks (Figure 4a); however, detailed interpretation is limited by lack of observable relationships. The low density of surface exposures precludes a full understanding of the extent, thickness and variations in lithology of the volcanic rocks below the widespread overburden (be it Quaternary deposits or volcanic rocks younger than the age of the rocks of interest). Interpretations of near-surface stratigraphy derived from oil exploration wells (Figure 5) do not always match surface geological maps. Regionally incomplete mineralogical descriptions and limited geochronology may also lead to incorrect identification (Haskin et al., 1998) of the volcanic rocks of the Neogene Chilcotin Group (28–1 Ma; Anderson et al., 2001), and the Eocene Endako Group (ca. 51–45 Ma) and Ootsa Lake Group (ca. 53–48 Ma) in the field.

Seismic reflection data gave very poor images of the near surface, irrespective of lithology. Therefore, seismic velocity estimated from the tomographic inversion of first arrivals from these seismic reflection data can provide a valuable additional constraint on the distribution and thickness of the near-surface Eocene and Neogene volcanic rocks (Hayward and Calvert, 2009a). All relevant geological and geophysical information, including wells (drilled by Canadian Hunter Exploration Limited, Esso, Honolulu Oil Corporation Limited and Hudson's Bay Oil and Gas Company Limited) and geological maps (e.g., Riddell, 2006) guided the interpretation. Primary stratigraphic control is provided by well data (Riddell et al., 2007), and surface geological maps (e.g., Riddell, 2006) aided in the classification of the near-surface stratigraphy.

The Chilcotin Group has been locally interpreted to include a diverse range of lithofacies, including the Chasm (Mathews, 1989; Farrell et al., 2007), Bull Canyon (Gordee et al., 2007) and Dog Creek (Farrell et al., 2007). The Chilcotin Group consists primarily of flat to shallow-dipping basaltic flows, which are columnar jointed or massive with some hyaloclastite, tephra and pillow basalt, and weathered paleosols (Riddell, 2006; Andrews and Russell, 2007).

Volcanic rocks of the Eocene Endako and Ootsa Lake groups have undergone limited local study. Geological mapping (Riddell, 2006) showed that the Endako Group consists of vesicular and amygdaloidal basaltic to andesitic flows with tuff, breccia, and minor sedimentary rocks. The Ootsa Lake Group is characterized by intermediate to felsic flows, accompanied by tuff, breccia and sedimentary rocks. In the vicinity of Fort Fraser and Burns Lake (54°N, 125°W), to the north of the current study area, the Endako

and Ootsa Lake groups have been dated at ca. 51–45 Ma and ca. 53–48 Ma, respectively (Grainger et al., 2001).

Cretaceous sedimentary rocks, which include sandstone, conglomerate and minor volcanoclastic rocks, outcrop (Figure 4b) in central block D (Taylor Creek Group) and southwestern block A (Taseko River strata; Riddell, 2006). The Cretaceous Spences Bridge Group outcrops in southwestern block A (Figure 4b), around well d-94-G, and comprises volcanic flows, breccia and tuff, with volcanic siltstone to conglomerate (Riddell, 2006). Jurassic or Cretaceous granodioritic intrusions are found in contact with the Spences Bridge Group in block A and in southwestern block C.

First-Arrival Tomographic Inversion (2-D)

Seismic waves propagate laterally through the near surface and are recorded by geophones deployed along the seismic line. The arrival times of these waves at different source-receiver offsets provide an indication of the speed of propagation through the subsurface (i.e., seismic velocity). First-arrival traveltimes are usually the most accurately determined because there are no interfering secondary arrivals. First arrivals form the basis for a class of seismic tomographic methods that derive the vertical and lateral variation in seismic P-wave velocity (e.g., Aldridge and Oldenburg, 1993; Zelt and Barton, 1998). The depth of investigation is limited by the maximum source-receiver offset and the vertical velocity gradient; seismic waves propa-

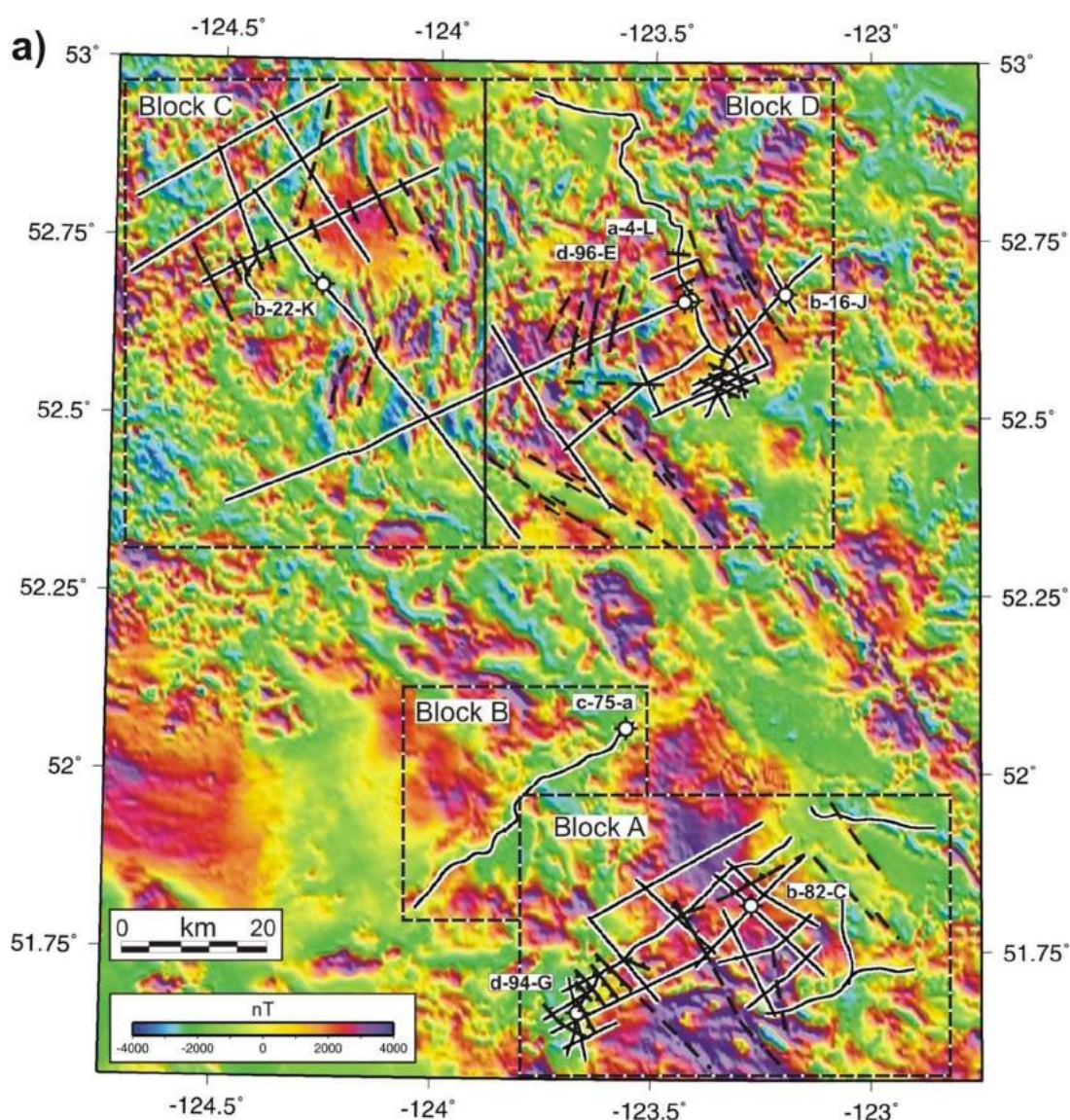


Figure 3: Summary of the structure of the southeastern Nechako Basin, south-central British Columbia: **a)** magnetic anomalies, **b)** [facing page] Bouguer (2.30 g/cm^3) gravity anomalies. Canadian Hunter seismic reflection lines shown by white bordered black lines. Large dashed boxes show the modified study blocks (A, C and D). Black circles show well locations.

gate preferentially through the upper part of low-gradient layers.

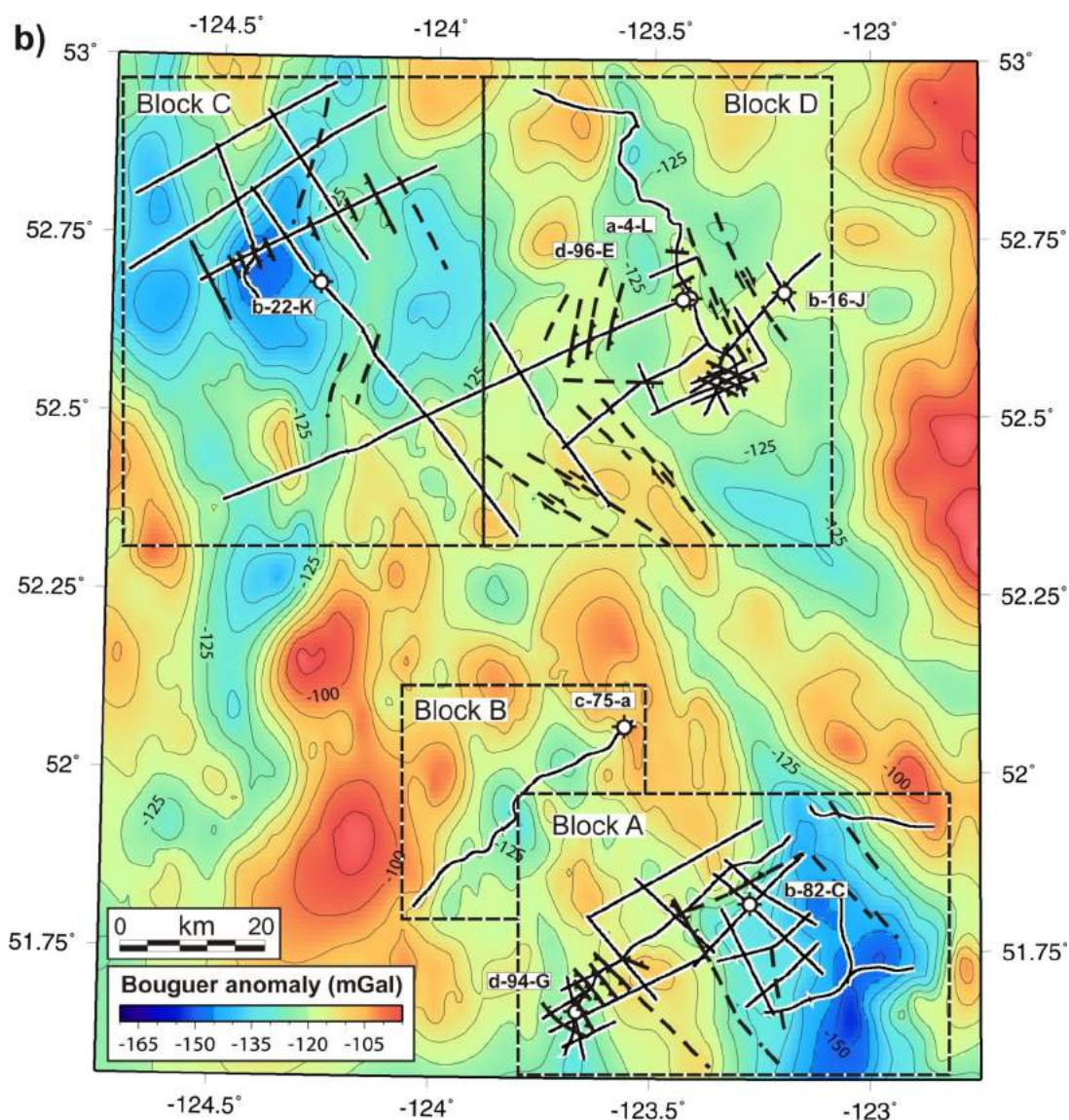
First-arrival tomographic inversion methods have been used effectively to investigate the geological structure and near-surface velocity. For example, tomographic models have revealed along-strike variation in the structure of the Devil's Mountain fault (Hayward et al., 2006) and the Seattle fault zone (Calvert et al., 2003) in Washington. Hayward and Calvert (2007) used similar methodology to constrain the seismo-stratigraphy of the Tofino Basin, offshore Western Canada. Schmid et al. (2001) used similar techniques to show the velocity structure across the Tan-Lu fault in the easternmost Dabie Shan, China.

In the southeastern Nechako Basin (Hayward and Calvert, 2008a), preliminary results showed that these velocity models can reveal both vertical and lateral near-surface stratigraphic variation in rocks that are otherwise poorly

imaged by seismic reflection profiles. Seismic reflection images are often poor in areas where Chilcotin and/or Endako and Ootsa Lake Group rocks outcrop, especially to the northwest (block C, Figure 4b). However, the lack of a clear relationship between surface lithology and seismic image quality (Figure 6) suggests significant variations in the thickness, physical properties and structure of the surface volcanic rocks.

Canadian Hunter Seismic Reflection Data

The seismic reflection data used in this study were acquired along cutlines by Canadian Hunter Exploration Limited in the early 1980s. A vibroseis source (five 16,000 lb. Failing vibes over 100 m) gave a 15 s sweep over a frequency of 10–70 Hz (linear). The shot interval was 100 m except for lines CH159-02, -02A, -11, -12, -13, -14 and -15, which had an interval of 50 m (Figure 4b). A split-spread array with 96 or 48 (lines CH159-02 and -02A) channels, with in-



dividual receiver groups 100 m long, consisted of L-15 geophones (frequency of 8 Hz) centred every 50 m. The maximum source-receiver offset was 2550 m, except for lines CH159-02 and -02A, where it was 1350 m. Four seconds of data were recorded at a sample interval of 4 ms.

Tomographic Inversion Method (2-D)

First arrivals (the direct wave and subsurface refractions) are clearly identified on most shot gathers to the farthest offset. The first-arrival traveltimes picked during seismic reflection reprocessing by Arcis in 2006 were manually ed-

ited (Figure 7) in ProMAX™ software (Landmark Graphics Corporation) to eliminate pick errors and improve pick accuracy (± 25 ms). Pronto software (Aldridge and Oldenburg, 1993) was used to invert these traveltimes for seismic P-wave velocity for all (total of ~ 790 km) straight seismic profiles (Figure 4b). A finite-difference solution to the eikonal equation was used to derive first-arrival times to all locations in a subsurface velocity grid (25 m grid spacing). Ray paths from source to receiver were created through the traveltimes grid, along the steepest descent direction.

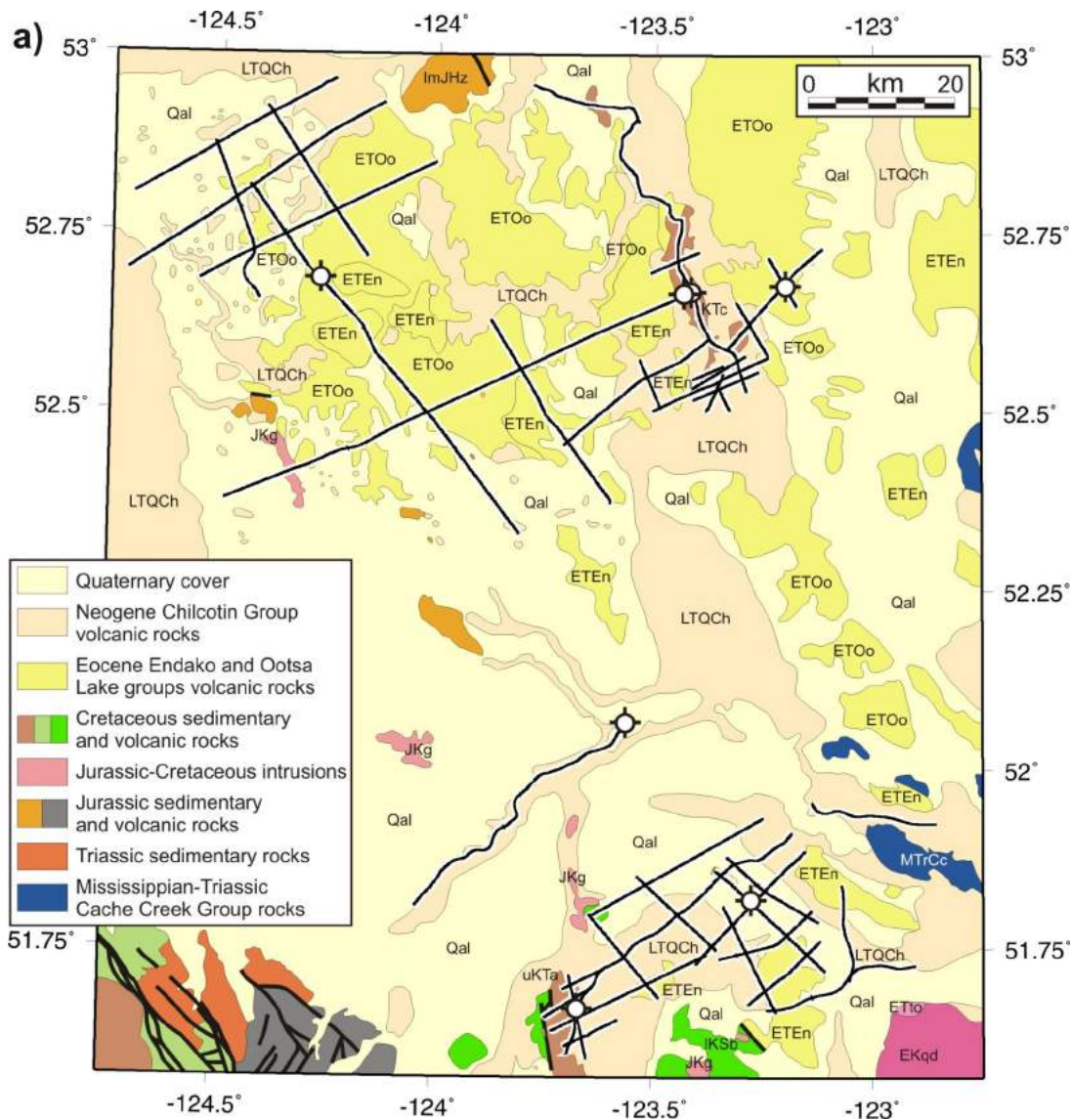


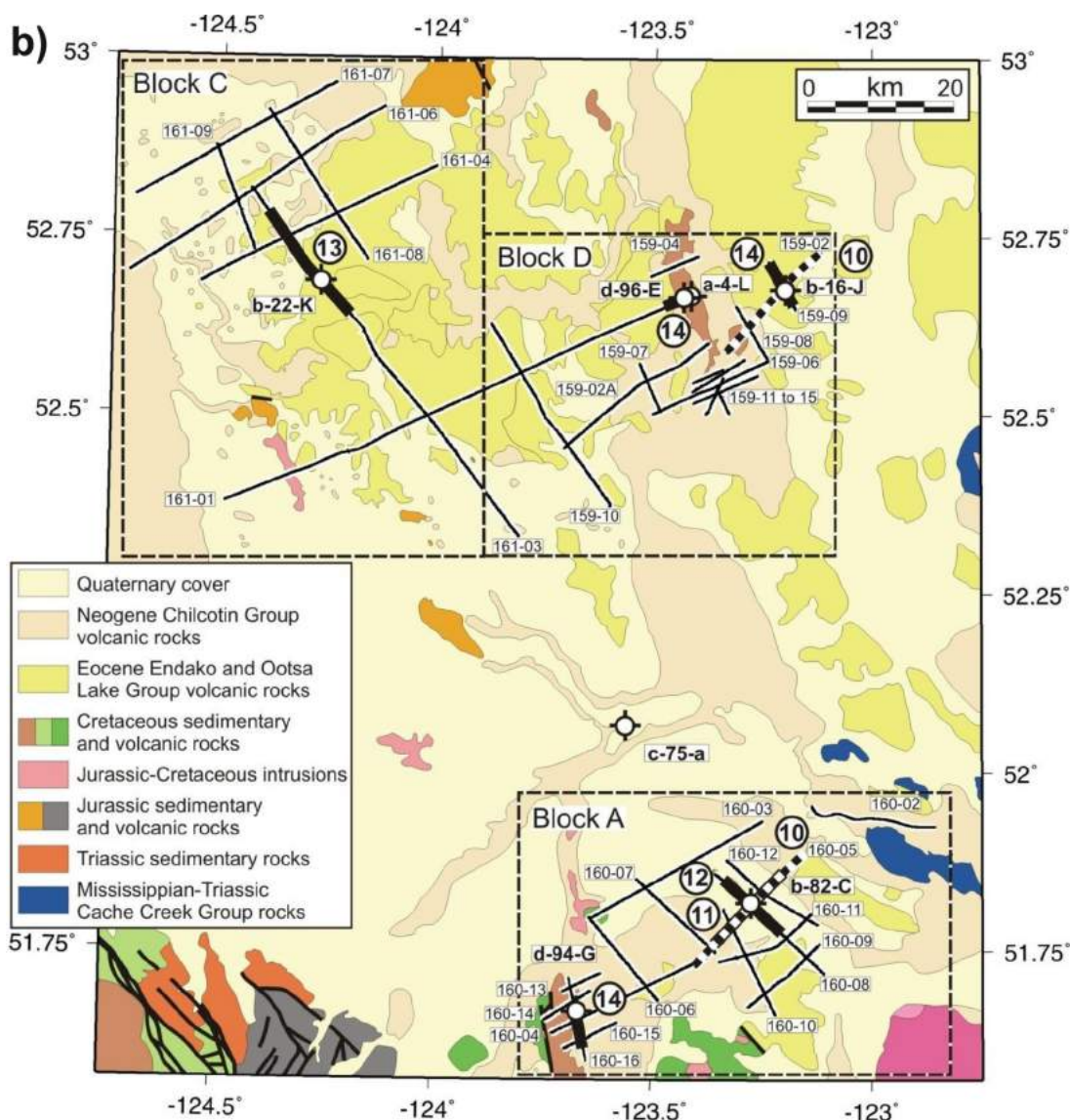
Figure 4: Geology of the study area (modified from Riddell, 2006), southeastern Nechako Basin, south-central British Columbia, showing: **a)** location of seismic reflection profiles (white bordered black lines); and **b)** [facing page] location of presented first-arrival tomographic models (heavy black lines), with heavy dotted lines showing presented corugation models, large dashed boxes showing the modified study blocks (A, C and D) and boxed text showing seismic line numbers and wells. Abbreviations: ETEEn, Eocene Endako Group; ETOo, Eocene Ootsa Lake Group; ETto, Eocene tonalite; LTQCh, Neogene Chilcotin Group; KTc, Cretaceous Taylor Creek Group; EKqd, Cretaceous quartz diorite; uKTa, Taseko River strata; IKSb, Cretaceous Spences Bridge Group; Qal, Quaternary deposits; ImJHz, Jurassic Hazleton Group; JKg, Jura-Cretaceous granodiorite.

In order to obtain a realistic final model, a starting model is required that closely matches the true P-wave velocity. Available sonic logs from six wells (Figure 5) guided the selection of starting-model parameters. However, near-surface sonic data are often absent and well logs are only representative of point locations in a region where velocity is highly variable. The chosen 1-D starting model was estimated from a few trial inversions with a magnitude and gradient that is overall similar to the well sonic logs (Figure 5). Increasing the magnitude of the velocity in the starting model results in unrealistic near-surface velocity gradients. For example, an increase in surface velocity of the starting model for line CH160-05 to 4000 m/s (with a gradient of 1.5 s^{-1}) results in a negative velocity gradient of $\sim 25 \text{ s}^{-1}$ and a decrease of $\sim 400 \text{ m/s}$ in the upper $\sim 30 \text{ m}$ of the model, rather than a smooth increase in velocity with depth. Therefore, following evaluation of the results of a range of starting-model parameters, the surface velocity of the starting

model (Figure 5) for all lines was set to 3500 m/s (gradient of 1.5 s^{-1}), for model consistency and smoothness.

A perturbation in the velocity model was calculated from the difference between the calculated and observed first-arrival traveltimes for each of 15 iterations to give each final velocity model. The models show a combined reduction in traveltimes misfit (e.g., Figures 8a, b) from a mean RMS error of 70.6 ms to 20.6 ms. The velocity and ray data were smoothed for display using a continuous-curvature gridding algorithm (Smith and Wessel, 1990) at a grid spacing of 5 m.

Maximum ray penetration is controlled primarily by the maximum source-receiver offset (2550 or 1350 m) and subsurface geology. The highest density of rays typically gave a well-constrained estimate of the P-wave velocity for depths of up to $\sim 450 \text{ m}$, although ray penetration some-



times locally reached ~700 m. The lower maximum offset of 1350 m for two seismic lines (CH-159-02 and -02A) resulted in a significantly reduced depth of maximum ray penetration. Here, estimates of P-wave velocity are best constrained for depths of up to ~100 m, but locally up to ~500 m.

Reliability of the Velocity Model Estimates

The reliability of the velocity models was assessed by comparing the mean velocity in the upper 175 m between the final (starting model surface velocity 3500 m/s with a 1.5 s⁻¹ gradient) and alternative models, using starting models with a lower surface velocity (2500 and 3000 m/s). For seismic reflection line CH160-05, the model derived from a starting model with a surface velocity of 3000 m/s (1.5 s⁻¹

gradient) gave velocities 20 m/s higher to 70 m/s lower (mean 14.02, standard deviation 17.18) than the final model. The model derived using a starting model with a surface velocity of 2500 m/s (1.5 s⁻¹ gradient) gave a model with velocities 30 m/s higher to 140 m/s lower (mean 29.01, standard deviation 34.83) than the final model. Despite the 500–1000 m/s reduction in the starting-model velocity, the result is robust, with a mean velocity that varies only by a maximum of 4% of the final model in the upper 175 m.

Velocity Model Resolution

Corrugation tests were used to assess the ability of the tomographic velocity models in the Nechako Basin to accurately reflect lateral variations in velocity and structure across the modelled depth range. Corrugation tests for lines

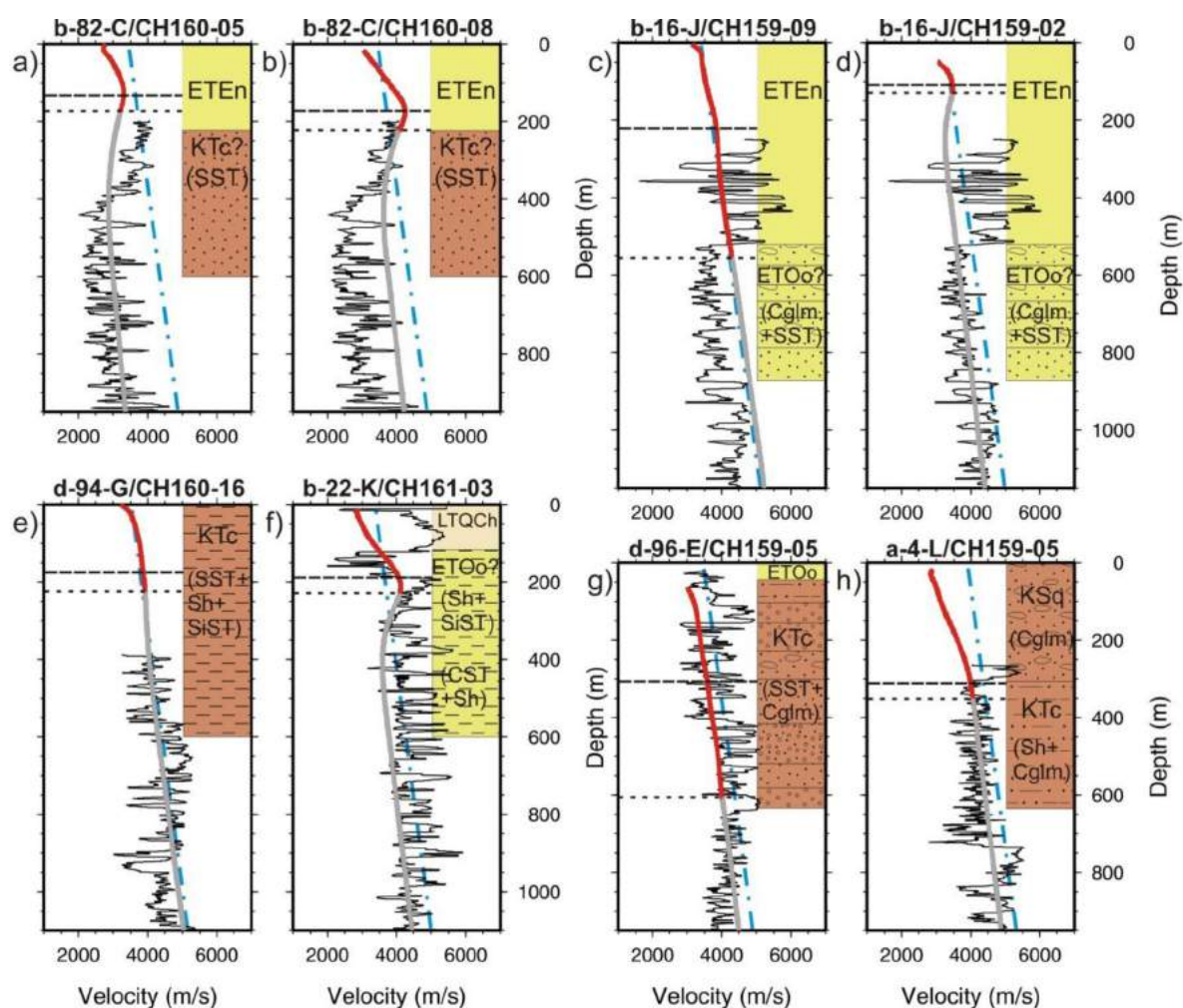


Figure 5: Comparison of tomographic velocity models (heavy red/grey lines) with well sonic logs (thin solid black lines) and stratigraphy (Ferri and Riddell, 2006), southeastern Nechako Basin, south-central British Columbia. Abbreviations: ETEn, Endako Group; ETOo, Ootsa Lake Group; LTQCh, Chilcotin Group; KTc, Taylor Creek Group; KSq, Silverquick Group. Rock types: CgIm, conglomerate; Sst, sandstone; SiSt, siltstone; CST, claystone; Sh, shale. Heavy red lines show constrained model and heavy grey lines show unconstrained model. Thin solid black lines show the well sonic log (manually de-spiked, and filtered with a four-point (~60 cm) median filter). Pale blue dot-dashed line shows the starting velocity model. Horizontal dashed line shows the depth of maximum ray density at the well. Horizontal dotted line shows the base of the velocity model (base of ray coverage) at the well. Depth is relative to the topography at the well. Non-coincidence of the top of the velocity model and the well top is due to topography and projection of the well onto the model profile.

CH160-05 and CH159-02, with maximum offsets of 2550 and 1350 m respectively, are shown in Figures 9a and b. For each test, vertical corrugations with constant widths (0.25, 0.5 and 1.0 km), depths from the ground surface to the base of the model, and a variation in the slowness of $\pm 10\%$ velocity variation were added to the final velocity model to create three independent tests for each line. The predicted traveltimes calculated through the perturbed models were used to create a corrugation velocity model with the final velocity model as the starting model. When the final velocity model is subtracted from the corrugation velocity model, the regenerated corrugations shown in Figure 9 remain.

The corrugation tests show that the ability to resolve velocity anomalies at depth increases with anomaly width. Anomalies with a width of 1.0 km are well resolved above a depth of ~ 300 m, or the maximum depth of ray penetration if shallower. Anomalies of 0.5 km width are resolved above a depth of ~ 250 m and those of 0.25 km width are only resolved in the near surface. Lines with a maximum offset of 1350 m (CH-159-02 and -02A) show no reduction in resolution, despite the reduced depth of maximum ray penetration.

Near-Surface Velocity Character of the Southeastern Nechako Basin

Comparison of Velocity Models with Well Sonic Logs and Lithology

Subsurface lithological information where the surface geology is often obscured by vegetation or Quaternary deposits is provided by six wells (Figure 5) that intersect the modelled seismic reflection lines. Most of the wells penetrated the volcanic rocks, which dominate the surface geology, the thicknesses of which are shown in Table 1. Well lithology may be referenced to the velocity models and available well sonic logs for the analysis of the region's velocity character.

In well b-82-C (Figures 5a, b), ~ 221 m of the Endako Group volcanic rocks overlie Cretaceous sandstone (Ferri and Riddell, 2006). Velocity models CH160-05 (Figure 10b) and CH160-08 (Figure 11b) have a high density of rays (Figures 10a, 11a) that focus just above the base of the Endako Group (at ~ 170 m and ~ 220 m, respectively). The interval of the Endako Group estimated by the tomographic model has a velocity of ~ 2600 – 4250 m/s at well b-82-C.

At the top of well b-22-K (Figure 5f), ~ 116 m of Chilcotin Group basaltic rocks are interpreted (Ferri and Riddell, 2006) to overlie 477 m of shale, siltstone and minor volcanic rocks, possibly of the Ootsa Lake Group (Riddell et al., 2007). Adjacent to the well (Figure 4b), however, geologi-

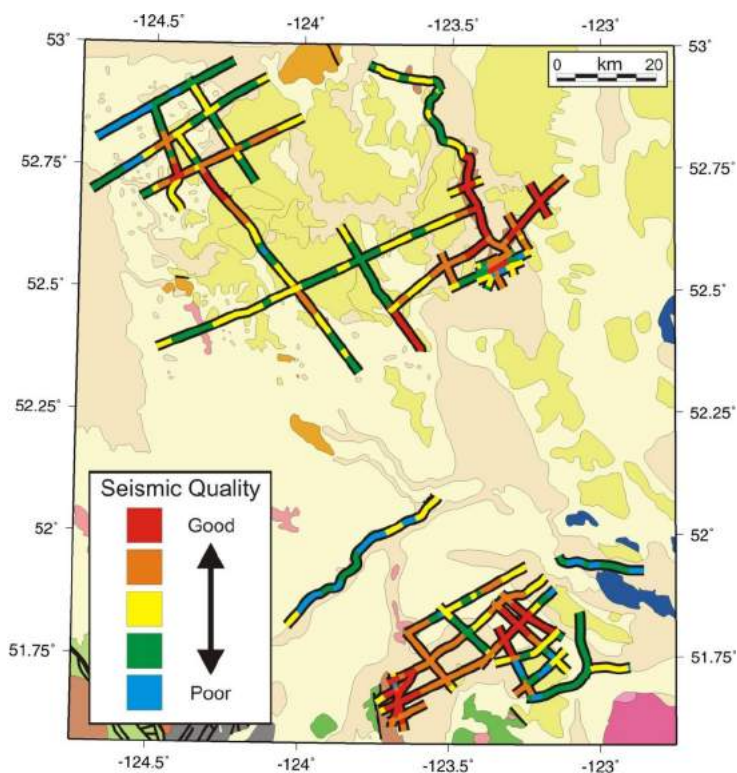


Figure 6: Seismic reflection data quality overlain on surface geology (Riddell, 2006) of the southeastern Nechako Basin, south-central British Columbia. Legend: blue, no coherent reflections; green, reflections that are slightly coherent over short distances; yellow, some coherent reflections, laterally continuous over short distances; orange, coherent reflections to a two-way traveltme (TWTT) of ~ 1 s, laterally continuous over short to medium distances; red, coherent reflections to a TWTT of > 1 s, laterally continuous over short to medium distances.

cal maps show volcanic rocks of the Ootsa Lake Group. Velocity models (Figures 5f, 12b) show a good correspondence with the sonic log velocity of the upper part of the sedimentary section, but underestimate that of the Chilcotin Group. A sharp increase (~ 1500 m/s) in the sonic velocity at a depth of ~ 180 m is coincident with the peak of ray density (Figures 12a and 5f).

Approximately 517 m of Eocene Endako volcanic rocks, which overlie sedimentary rocks of Paleocene to possibly Eocene age (Ferri and Riddell 2006), were intersected by well b-16-J (Figure 5c). The highest density of rays (Figure 13a) for velocity model CH159-09 is in the upper ~ 220 m, where sonic log data are absent. Model velocities are smooth, in the range of ~ 3400 – 4250 m/s, and of similar gradient to the starting model (Figure 5c). The model velocity below ~ 220 m is coincident with the lower range of the highly variable sonic log (Figure 5c). The neutron porosity log shows a decrease from $\sim 50\%$ to $\sim 15\%$ at a depth of ~ 250 m, suggesting a change in the character of the volcanic rocks.

Well d-96-E (Figure 5g) intersected ~ 44 m of volcanic rocks of the Ootsa Lake Group, which overlie Cretaceous

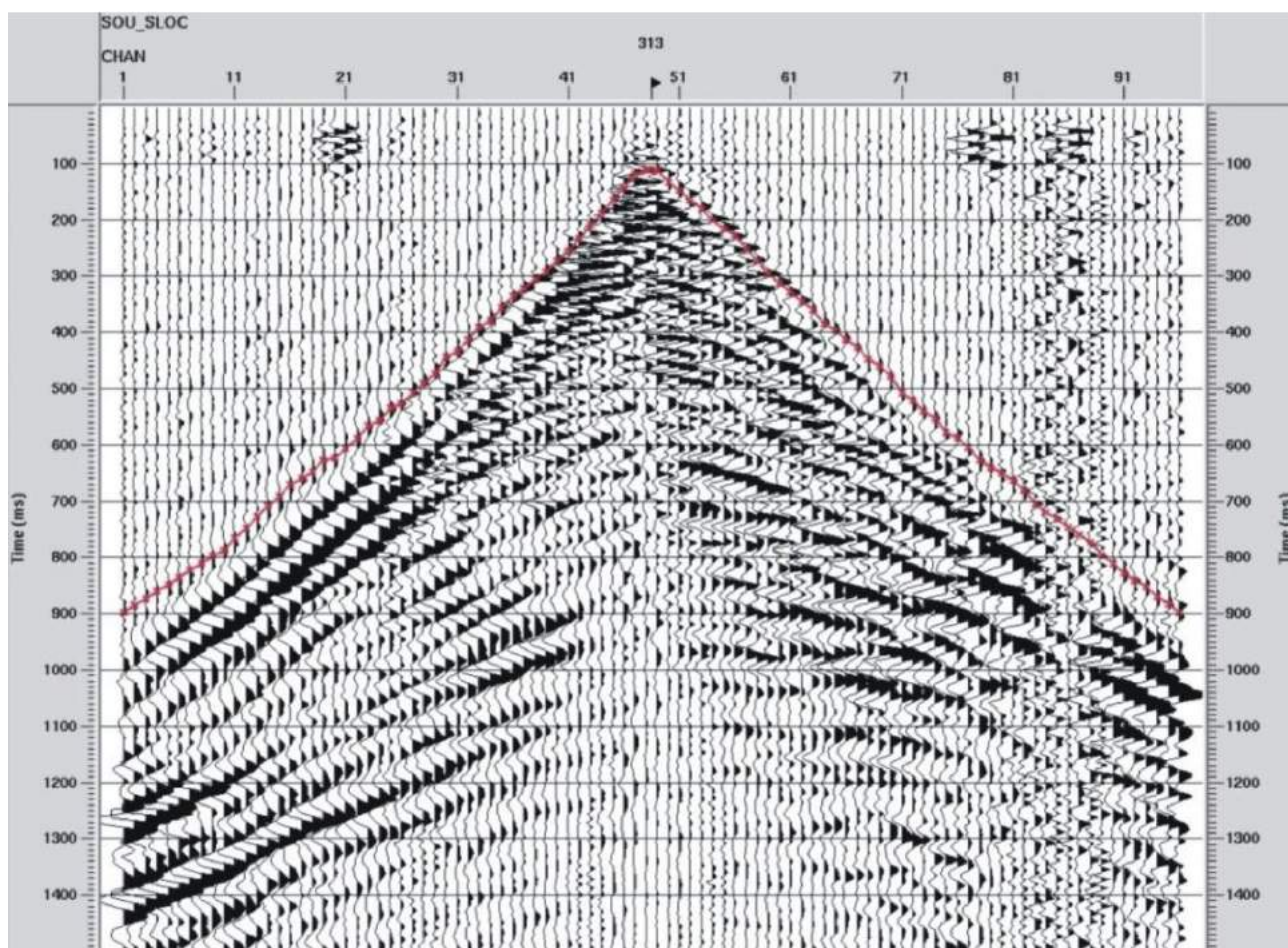


Figure 7: Example of first-arrival traveltimes picks of a shot gather from the Canadian Hunter seismic reflection data, southeastern Nechako Basin, south-central British Columbia.

sandstone and conglomerate. Velocity model CH161-03 (Figure 13d) underestimates the velocity above a depth of 150 m. However, immediately to the southwest of the well, constrained by a zone of high ray density (Figure 13c), the model velocity (~3750 m/s) more tightly matches the sonic log (Figure 5g). Maximum ray density occurs at a depth of ~300 m (Figure 5g), where there is a transition from conglomerate above to sandstone below. Below 300 m, the model velocity estimates (~3750–4000 m/s) are within the range of the sonic log.

A Cretaceous conglomerate overlies conglomerate and shale at well a-4-L (Figure 5h) and near-surface volcanic rocks are absent. Rays converge just below the base of the Cretaceous conglomerate at a depth of ~310 m (Figures 5h and 13d). Here, the model velocity (~4000 m/s) shows close agreement with the sonic log. Near-surface sonic data are absent for the overlying sedimentary rocks, but velocities in the adjacent well d-96-E (Figure 5g) are generally below 4000 m/s.

Near-surface volcanic rocks are also absent in well d-94-G (Figure 5e), which intersected a fairly homogeneous se-

quence of interbedded sandstone, shale and conglomerate of Cretaceous age (Ferri and Riddell, 2006; Riddell et al., 2007). Model velocity (Figure 13f) ranges from ~3500 to ~4000 m/s and, although shallow sonic data are not able to confirm the result, the velocity model echoes the overall trend of the deeper sonic data. The top ~80 m of the well intersected sandstone similar to nearby surface exposures, but the rocks below are generally more fine grained (Ferri and Riddell, 2006). This lithological variation and near-surface weathering may account for the change in gradient of the model velocity in the upper section of the well.

Seismic Velocity Constraint from Well Sonic Logs and Samples

Interpretation of the tomographic velocity models is aided by laboratory samples and borehole sonic logs. The P-wave velocity was measured (G. Andrews, pers. comm., 2009) for approximately 50 samples from the Chilcotin Group, collected primarily within and to the east of the block A area (Figure 4b). Basaltic lava-flow samples from the Chilcotin Group gave a wide velocity range (~4500–6000 m/s), with the majority of values at ~5000–5700 m/s. Anomalously

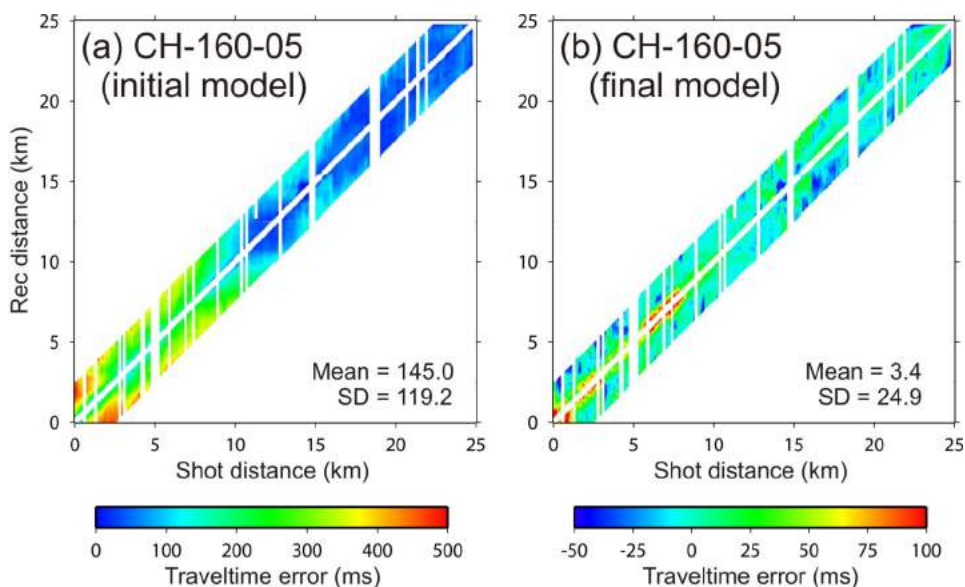


Figure 8. Stacking chart of traveltimes errors for line CH160-05, southeastern Nechako Basin, south-central British Columbia: **a)** initial model, **b)** final model. Distances are in kilometres from the north-eastern end of the line.

low velocities of ~4250–4760 m/s were obtained from a sample of volcanic breccia from the Bull Canyon lithofacies, just south of block C. Similarly, three samples from the Chasm lithofacies, to the east of block A, also gave low velocities of ~4070–4710 m/s. One sample of grano-

diorite from the Jurassic Thuya batholith, to the east of block A, gave high velocities of ~5520–5930 m/s.

A comparison of velocity from models, laboratory samples and well sonic logs is presented in Figure 14. Laboratory samples and sonic logs suggest typical velocities greater

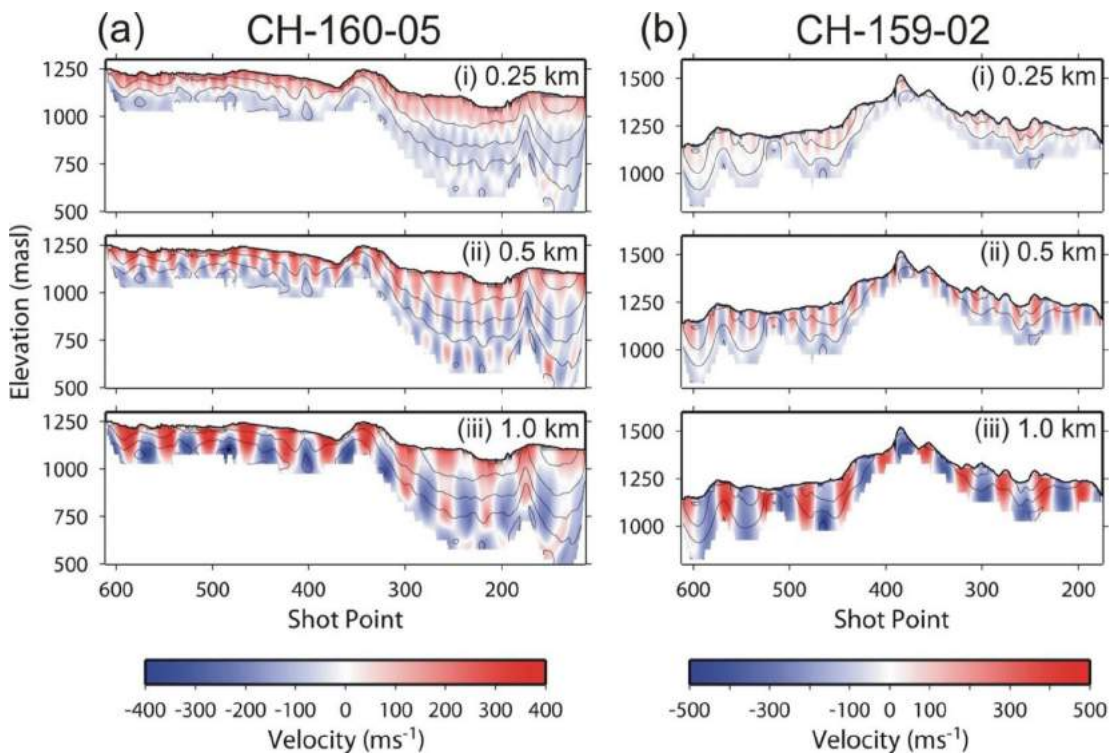


Figure 9. Corrugation models for lines CH-160-05 **(a)** and CH-159-02 **(b)**, southeastern Nechako Basin, south-central British Columbia. Vertical perturbations of slowness of $\pm 10\%$ velocity variation with widths of **i)** 0.25 km, **ii)** 0.5 km, and **iii)** 1 km. Black lines show tomographic velocity contours at an interval of 400 m/s.

Table 1: Thickness of volcanic rocks of the Neogene Chilcotin and Eocene Endako and Ootsa Lake groups intersected by wells in the Nechako Basin, south-central British Columbia (Ferri and Riddell, 2006; Riddell et al., 2007).

Well	Thickness of Volcanic Rocks (m)	Assigned Facies at Surface
Redstone b-82-C	221	Endako Group
Nazko b-16-J	517	Endako Group
Nazko d-96-E	44	Endako Group
Chilcotin b-22-K	116	Chilcotin Group
	477	Ootsa Lake Group?
Redstone d-94-G	0	n/a
Nazko a-4-L	0	n/a

than 4500 m/s for the Chilcotin Group volcanic rocks. Rocks of the Eocene Endako and Ootsa Lake groups exhibit a wide range of sonic log velocities, but most are ~3500–5000 m/s, commonly lower than the Chilcotin Group. Volcaniclastic and sedimentary rocks of Eocene age often show a lower velocity; for example, the shale, siltstone and minor volcanic rocks below the Chilcotin Group in well b-22-K (>120 m) have velocities of ~2900–3500 m/s. This lithological variation within the Eocene Endako and Ootsa Lake groups, with interbeds of lavas that are sometimes vesicular (high porosity), volcaniclastic and sedimentary rocks, and near-surface weathering may explain the wide range of sonic velocities. In seismic reflection surveys of volcanic flows on the Columbia Plateau

(Jarchow et al., 1994), interbedding is associated with large contrasts in impedance, which significantly degraded seismic imaging. Similar interbedding of the varied rock types within the Endako and Ootsa Lake groups may also be a reason for the poor seismic imaging associated with some of these rocks.

Model Velocity of the Near- Surface

In order to investigate regional variation in near-surface velocity (in relation to lithology), the mean velocity was calculated from 0 to 175 m (below ground surface) for each velocity model profile. When plotted in map view (Figure 15) along seismic profiles, lateral changes in the mean velocity can be correlated with near-surface geology (Riddell, 2006). The choice of a greater depth range results in data gaps due to locally shallow ray penetration (especially for lines CH159-02 and -02A) and does not alter the overall interpretation. Model velocities for the mapped near-surface rock types are compared with sonic logs and available laboratory samples in Figure 14.

Jura-Cretaceous granodiorite shows the highest velocity for rock types sampled by the models (~3600–4800 m/s), but this is lower than for laboratory samples of the Jurassic Thuya batholith (~5520–5930 m/s). The Cretaceous Spences Bridge Group volcanic rocks similarly have fairly

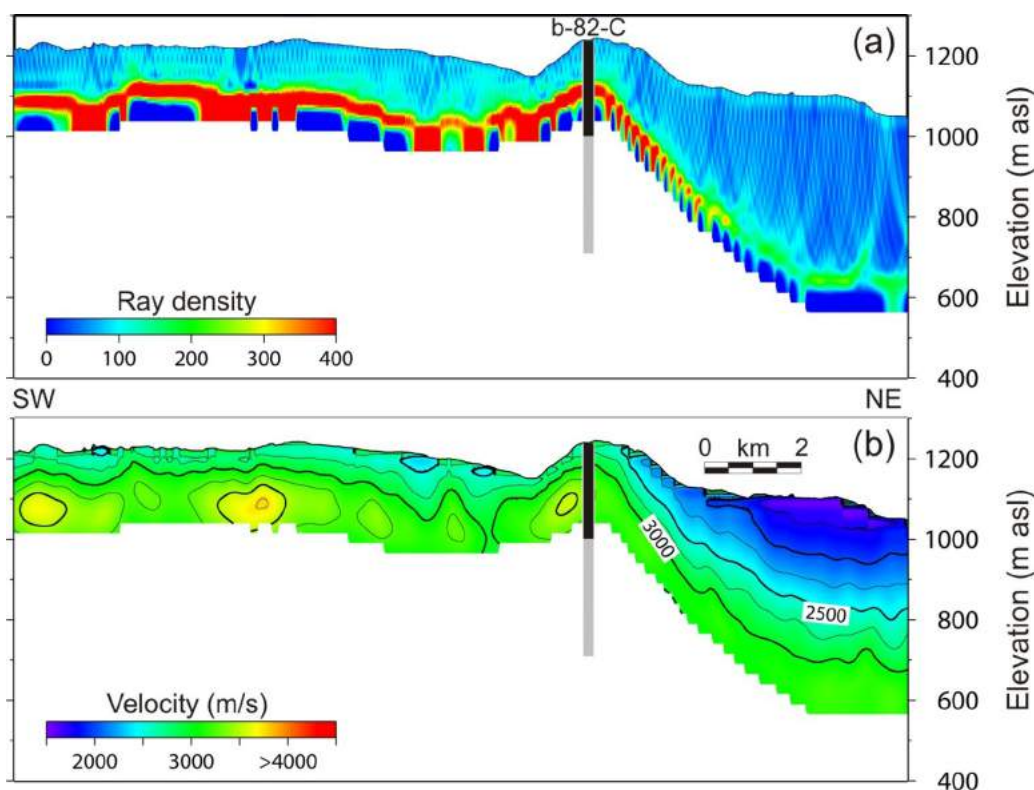


Figure 10: First-arrival tomographic inversion model for Canadian Hunter line CH160-05 (see Figure 4b for location), southeastern Nechako Basin, south-central British Columbia, showing **a)** ray density, and **b)** velocity. Heavy black line shows the thickness of Eocene Endako Group volcanic rocks in well b-82-C (see Figure 5a).

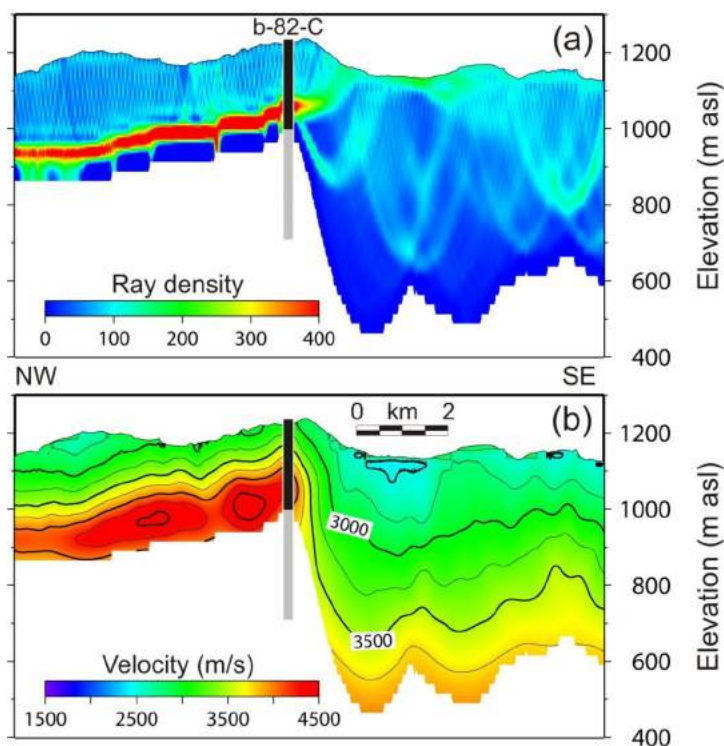


Figure 11: First-arrival tomographic inversion model for Canadian Hunter line CH160-08 (see Figure 4b for location), southeastern Nechako Basin, south-central British Columbia, showing **a)** ray density, and **b)** velocity. Heavy black line shows the thickness of Eocene Endako Group volcanic rocks in well b-82-C (see Figure 5b).

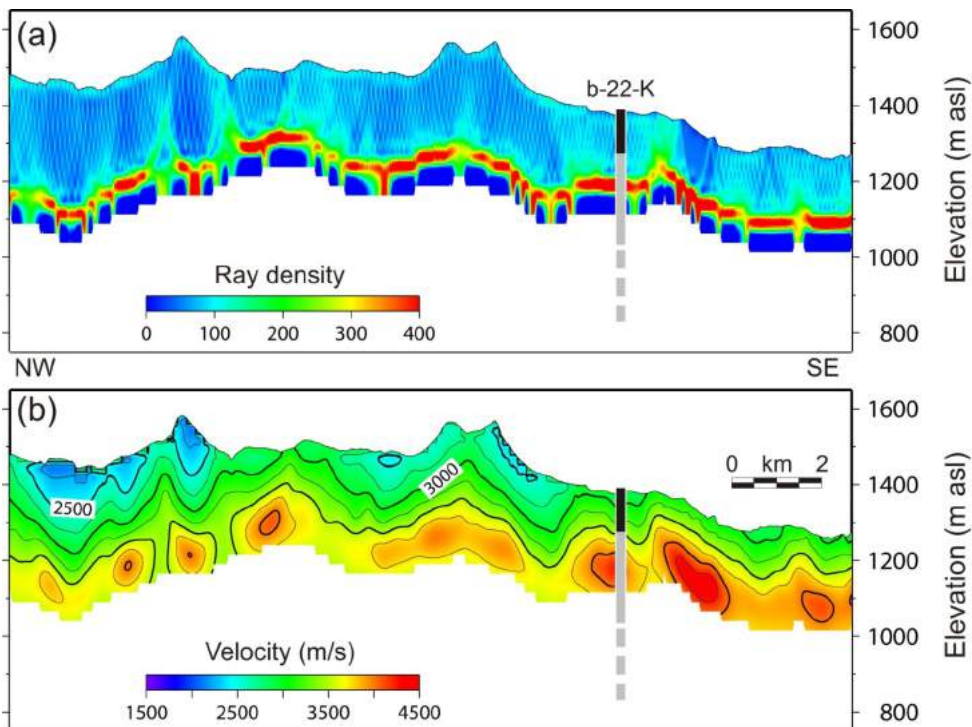


Figure 12: First-arrival tomographic inversion model for a section of Canadian Hunter line CH161-03 (see Figure 4b for location), southeastern Nechako Basin, south-central British Columbia, showing **a)** ray density, and **b)** velocity. Heavy black line shows the thickness of Neogene Chilcotin Group volcanic rocks in well b-22-K (see Figure 5f).

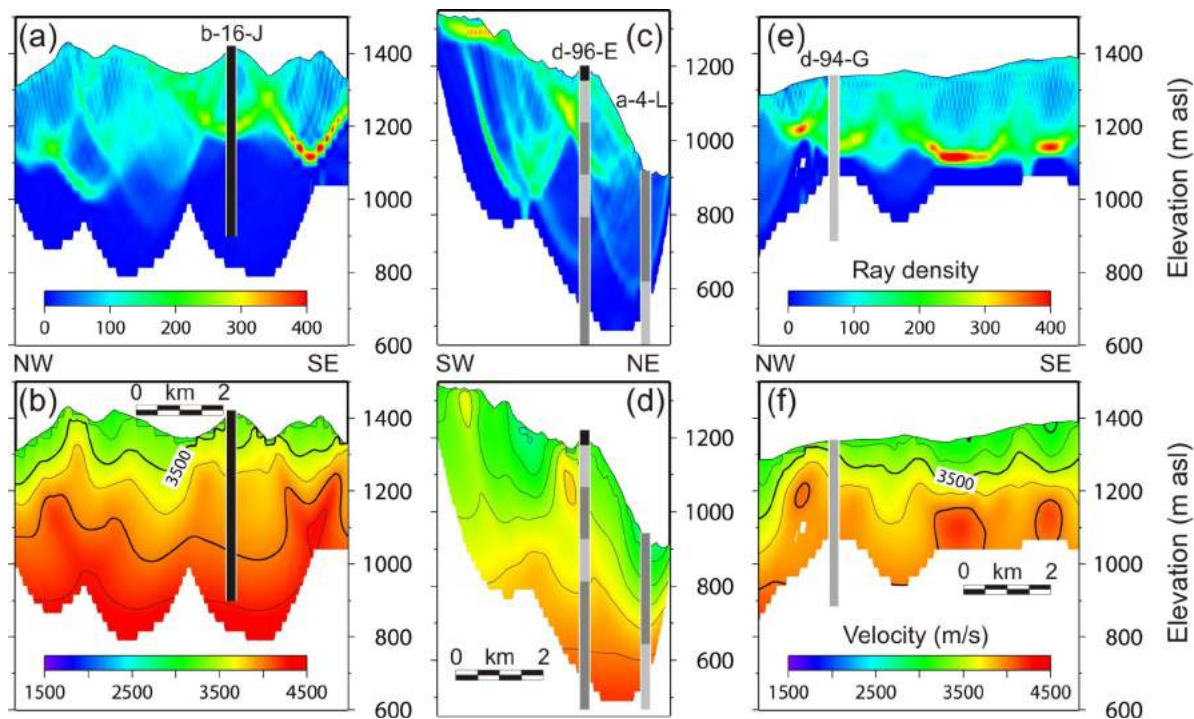


Figure 13: First-arrival tomographic inversion models (see Figure 4b for locations), showing ray density and velocity for sections of seismic reflection lines, southeastern Nechako Basin, south-central British Columbia: **a)** and **b)** line CH-159-09; heavy black line shows the Eocene Endako Group rocks in well b-16-J (see Figure 5c); **c)** and **d)** line CH-159-05; heavy black line shows the Eocene Ootsa Lake Group rocks at the top of well d-96-E and heavy grey lines show changes in the Cretaceous sedimentary rocks of wells d-96-E and a-4-L from finer grained (i.e., shale and siltstone, indicated by darker grey) to coarser grained (i.e., sandstone and conglomerate, indicated by lighter grey; see Figures 5g, h); **e)** and **f)** line CH-160-16; heavy grey line shows well d-94-G (see Figure 5e).

high model velocities (~3400–4200 m/s). The Cretaceous sedimentary rocks have a model velocity range of ~2600–4600 m/s, similar to the sonic logs. The Eocene Endako and Ootsa Lake groups have a model velocity range of ~2600–4600 m/s, which is also in agreement with sonic logs. Although the Endako and Ootsa Lake groups in blocks C and D have a smaller velocity range (3200–4000 m/s) than the Endako Group rocks in block A (3000–4200 m/s), the two groups are not distinguishable on the basis of velocity. Chilcotin Group rocks have much lower model velocities (~1600–3200 m/s; Figure 14) than those from laboratory samples (4500–6000 m/s) and well sonic logs (4200–5300 m/s). These model velocities for the Chilcotin Group are also lower than laboratory samples of volcanic breccia of the Bull Canyon facies (~4250–4760 m/s). The Chilcotin Group model velocity is most similar to that of the Quaternary deposits (2000–2800 m/s).

Block A

Mean tomographic velocities in block A (Figure 15) show typical values of ~3400 m/s, with slightly lower velocities usually associated with the outcrop of Chilcotin Group rocks and Quaternary deposits. The lowest mean velocities in the southeastern Nechako Basin are to the northeast of well b-82-C, where they are commonly ~1900–2400 m/s

but can be as low as ~1700 m/s in some locations. These lows correspond to the outcrop of Chilcotin Group volcanic rocks and Quaternary deposits. The changes in ray character in models that cross this zone, specifically lines CH160-05 (Figure 10a), CH160-03 and -02 (Figure 4b), suggest a change in subsurface physical properties. Rays vary from focused convergence at a shallow depth (~200 m) at the margins to a deeper (~450 m) and lower ray density within. Another anomalous low in mean velocity (~2100–2500 m/s) is observed directly to the south of well b-82-C at latitude 51.75°N, longitude 123.25°W (Figure 15).

The outcrop of Spences Bridge Group volcanic rocks and Jurassic or Cretaceous granodiorite north of well d-94-G (Figure 15) is associated with a mean velocity high of ~4200 m/s. High mean velocities (~4300 m/s) towards the centre of line CH-160-04, east of well d-94-G (Figure 15), may be related to the local outcrop of Endako Group volcanic rocks. High values are not, however, observed in association with Endako Group rocks to the south of well b-82-C. The outcrop of Cretaceous sedimentary rocks to the west of well d-94-G also shows mean velocities (~3400–3900 m/s) that are slightly higher than normal.

Ray density and depth predicted by the velocity models are related to the P-wave velocity of the subsurface and the

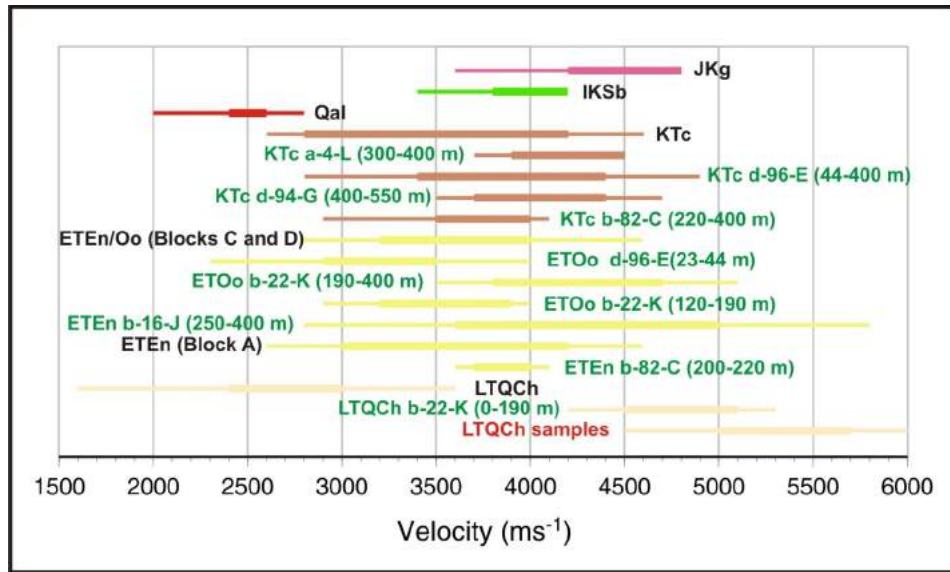


Figure 14: Comparison of seismic velocity from tomographic inversion models (black labels), well sonic logs (green labels) and laboratory samples (red labels) for key rock types in the southeastern Nechako Basin, south-central British Columbia. Thick lines indicate the range of the majority of values. Line colours: pink, Jura-Cretaceous granodiorite; green, Cretaceous Spences Bridge Group volcanic rocks; red, Quaternary deposits; brown, Cretaceous Taylor Creek Group sedimentary rocks; yellow, volcanic rocks of the Eocene Endako and Ootsa Lake groups; beige, Neogene Chilcotin Group rocks.

maximum offset of the seismic reflection profile. The maximum offset used in the Canadian Hunter seismic reflection survey is quite small (2550 m), which places limits on the depth of ray convergence. As a result, for example, rays across most of block A converge at a depth of ~200 m. A high density of rays of this character is observed on models CH160-05 (Figure 10a) and CH160-08 (Figure 11a), at and to the west of well b-82-C, where ~221 m of Endako Group volcanic rocks were intercepted. Rays of similar character can be mapped across the central region of block A to define two areas (orange dashed lines in Figure 15). Outside these areas, rays are less focused and show deeper but variable penetration depths; examples include the southeastern end of CH160-08 (Figure 11a), northeastern end of CH160-05 (Figure 10a) and near well d-94-G (e.g., CH160-16, Figure 13e). This variation in ray character suggests that a change in lithology accompanies a change in subsurface seismic velocity.

Block C

Mean velocities in block C have background values of ~3400 m/s. High mean velocities (up to ~4200 m/s) are generally coincident with the outcrop of Eocene volcanic rocks (Figure 15). The outcrop of Chilcotin Group volcanic rocks and Quaternary deposits, which are observed mainly towards the northwest, are related to lower velocities (down to ~2300 m/s). The predicted bedrock geology (Figure 16), derived from stream sediment geochemistry (Barnett and Williams, 2009), suggests that the Quaternary overburden in this area is underlain by rocks of the Chilcotin Group. The generally poor correlation of mean velocity with the

predicted bedrock geology suggests that the near-surface structure and the thickness of the overlying Quaternary deposits have a large influence on the mean velocity. Lithological variation is also suspected to have a large influence. For example, the predicted bedrock geology (Figure 16) reveals that rocks mapped (Riddell, 2006) as the Eocene Ootsa Lake Group have two different geochemical signatures in central block C and northeast of block D, the latter being locally more similar to the Endako Group.

An outcrop of Quaternary deposits in the southeastern corner of block C is also associated with a notably lower velocity (~2300 m/s). A Jura-Cretaceous granodiorite in southern block C (Figure 15) is associated with an anomalously high mean velocity. The width of the velocity anomaly (~4 km) suggests that the intrusion may only be slightly wider in the near surface than its mapped extent beneath the surrounding Quaternary deposits.

A highly variable ray character is observed in block C. Rays exhibit clear focusing along line CH161-03 (Figure 12a), in a region where well b-22-K showed Chilcotin Group basalt overlying shale and siltstone. Within the Jura-Cretaceous granodiorite and also in association with Endako Group rocks to the southeast of well b-22-K, rays exhibit very shallow focusing (~75–175 m and ~75–200 m, respectively). Elsewhere a consistent connection between surface lithology and ray character is not clear, which suggests wide lithological variation. The great thickness of Eocene volcanoclastic deposits, breccia and lava flows (possibly Ootsa Lake Group; Riddell et al., 2007) intersected by well b-22-K suggests that Eocene rocks here have a different

and likely more variable character than the Endako Group rocks in block A.

Block D

Mean velocities in block D (Figure 15) are generally higher, due primarily to the high velocity of volcanic rocks of the Eocene Endako Group (~3700–4000 m/s) and slightly lower velocity rocks of the Ootsa Lake Group (~3100–3900 m/s). The Chilcotin Group in the area around line CH-159-02A (Figures 4b and 15) has velocities higher (~3500–3900 m/s) than typically observed elsewhere in

models of the southeastern Nechako Basin. These higher velocities suggest that a thin Chilcotin Group is underlain by the Eocene volcanic rocks.

The Cretaceous sedimentary rocks show two mean velocity signatures. From northern to central block D (lat. 52.6°–52.7°N), the mean velocities (~3400–3600 m/s) are slightly lower than those near well d-94-G (block A). The southernmost outcrops of Cretaceous rocks in block D (lat. 52.55°N, long. 123.4°W) show anomalous lows (~2700 m/s). Surface Cretaceous rocks here were observed to be highly de-

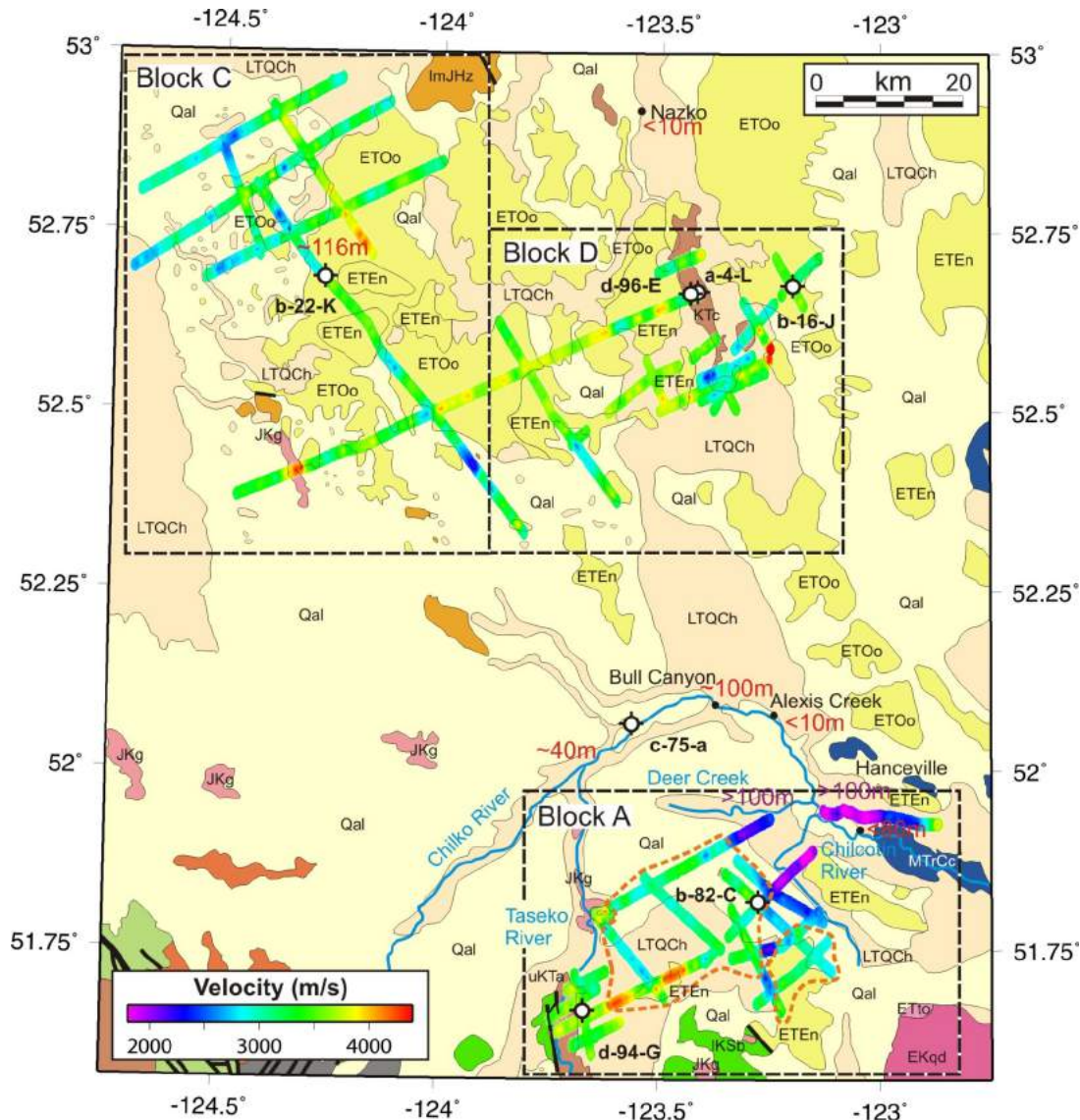


Figure 15: Mean velocity from the ground surface to a depth of 175 m from first-arrival tomographic models, southeastern Nechako Basin, south-central British Columbia. Geological map simplified from Riddell (2006). Red numbers show Chilcotin Group thickness from field and well observations (Andrews and Russell, 2007, 2008; Gordee et al., 2007; Riddell et al., 2007). Purple numbers show the thickness of the Chilcotin Group (Mihalynuk, 2007) modelled from digital elevation models. Orange dashed line shows the probable extent of Eocene volcanic rocks. Blue lines show selected rivers. Heavy dashed black boxes show the study blocks. Abbreviations: ETEEn, Eocene Endako Group; ETOo, Eocene Ootsa Lake Group; ETto, Eocene tonalite; LTQCh, Neogene Chilcotin Group; KTc, Cretaceous Taylor Creek Group; EKqd, Cretaceous quartz diorite; uKTa, Taseko River strata; IKSb, Cretaceous Spences Bridge Group; Qal, Quaternary deposits; ImJHz, Jurassic Hazleton Group; JKg, Jura-Cretaceous granodiorite.

formed with near-vertical dips (J. Riddell, pers. comm., 2007). This deformation is related to steep faulting observed on seismic reflection images, and fracture porosity associated with this faulting may account for the lower mean velocity.

In the southwestern corner of block D (CH159-10, Figure 4b), another velocity low (~2800 m/s) is associated with Quaternary deposits (Figure 15) directly to the east of another velocity low in southeastern block C (CH161-03, Figure 4b). Where associated with the Eocene volcanic rocks, rays along line CH159-10 are focused and continuous, similar to those near well b-22-K (Figure 12a). The rays become less dense and penetrate to a greater depth in relation to the outcrop of Quaternary deposits before becoming focused again at the southeast end, where Eocene rocks are again encountered.

Bouguer Gravity of the Southeastern Nechako Basin

Composite Bouguer Gravity Map

New high-resolution airborne helicopter gravity data (corrected with Bouguer densities of 2.30 and 2.67 g/cm³), acquired by the Geological Survey of Canada in 2008 (Dumont, 2008), provides coverage for the northeastern part of the study region (Figure 17a). Land-based gravity data acquired by Canadian Hunter were used to provide gravity coverage to the southwest. The Canadian Hunter data were manually de-spiked and simple Bouguer corrections applied to the original Bouguer gravity (2.35 g/cm³). The Canadian Hunter data were low-pass filtered (2625 m-0% to 5250 m-100%), similar to that previously applied to the airborne data.

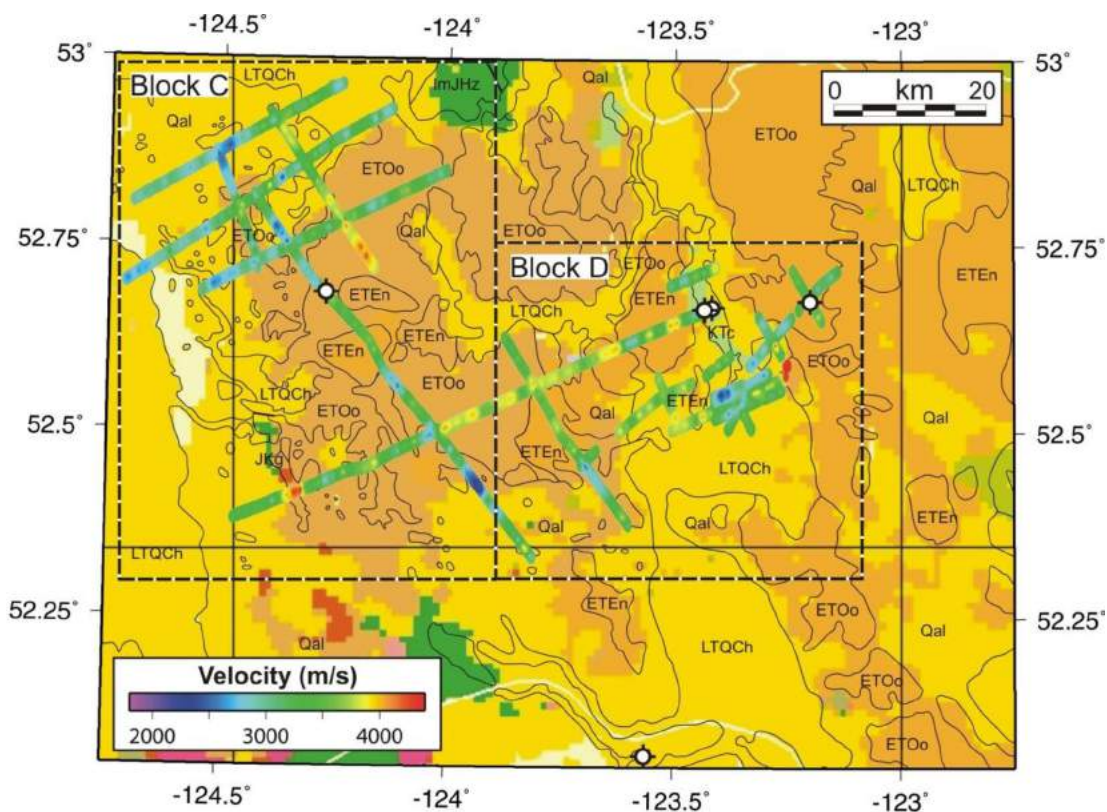


Figure 16: Mean seismic velocity (0–175 m) overlain on the geology predicted from the analysis of stream sediment geochemistry (Barnett and Williams, 2009), southeastern Nechako Basin, south-central British Columbia. Thin black lines and black labels show the geology from the corresponding bedrock geology map (Riddell, 2006). Abbreviations: ETEn, Eocene Endako Group; ETOo, Eocene Ootsa Lake Group; LTQCh, Neogene Chilcotin Group; KTC, Cretaceous Taylor Creek Group; Qal, Quaternary deposits; ImJHz, Jurassic Hazelton Group; JKg, Jura-Cretaceous granodiorite.

The offset of the corrected Canadian Hunter survey from the airborne data is 785.31 mGal (standard deviation 1.52) for a Bouguer density of 2.30 g/cm³ and 785.82 mGal (standard deviation 1.49) for a Bouguer density of 2.67 g/cm³. The Canadian Hunter data were levelled accordingly to create the maps shown in Figures 17b and c.

Addition of the sparsely sampled regional land-based gravity data, acquired by the Geological Survey of Canada, resulted in artifacts. These artifacts were point-location gravity highs and lows resulting from a mismatch with the other two surveys. The regional gravity data were therefore omitted in the construction of the final gravity maps.

Preliminary Interpretation of Bouguer Gravity and Velocity Models

First-order comparison of velocity models and Bouguer gravity reveals that there are few relationships between the observed gravity and velocity anomalies. This suggests that the majority of the gravity anomalies are the result of lithological/density variations at depths greater than the penetration of the velocity models. Thus, the mismatch between the mean velocity and gravity anomalies may be indicative of regions where the near-surface geology does not represent the geology at depth.

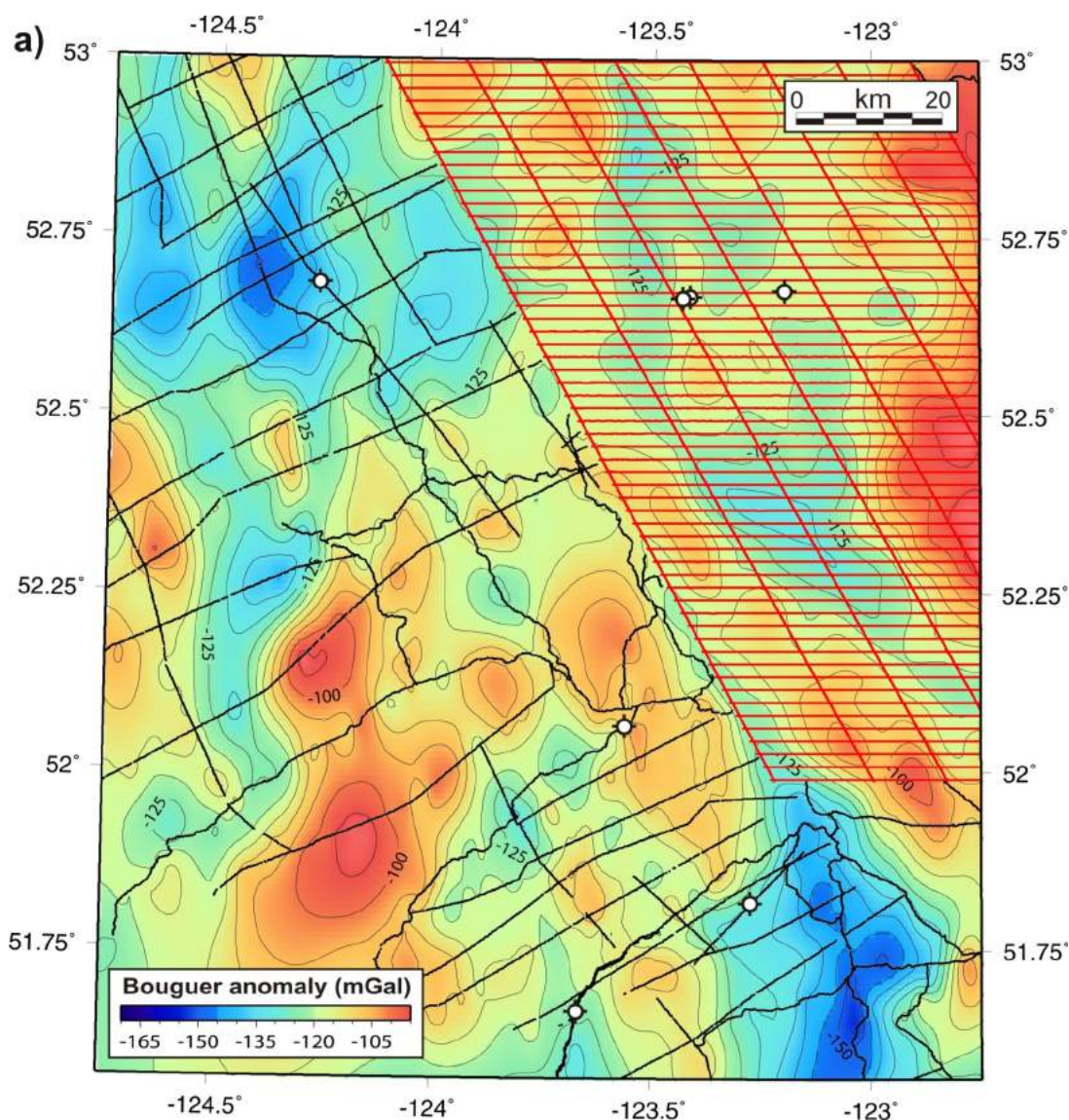


Figure 17. Composite (Canadian Hunter land and Geological Survey of Canada [GSC] airborne data) Bouguer gravity of the southeastern Nechako Basin, south-central British Columbia: **a)** data location; red lines, GSC airborne data; black lines, Canadian Hunter land data; **b)** [facing page] mean velocity (0–175 m) superimposed on the composite Bouguer gravity map corrected to 2.30 g/cm³; contour interval 5 mGal; **c)** [page 222] mean velocity (0–175 m) superimposed on the composite Bouguer gravity map corrected to 2.67 g/cm³; contour interval 5 mGal.

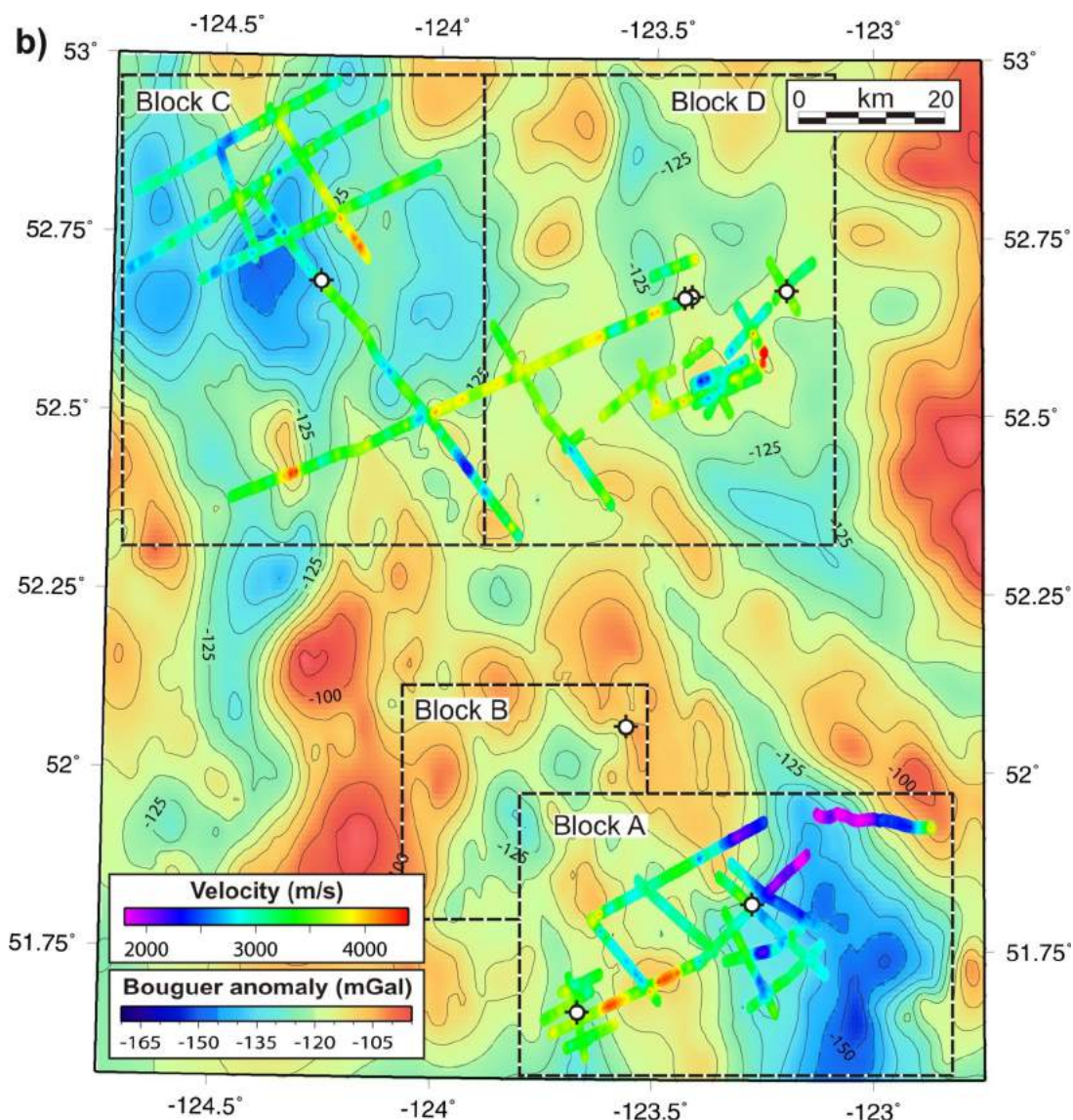
However, a number of near-surface velocity anomalies are associated with short-wavelength gravity anomalies. High-velocity anomalies related to Jura-Cretaceous granodiorite and Spences Bridge Group volcanic rocks in northwestern block A (Figure 17) correspond to a small gravity high that likely delineates the extent of these intrusive and/or volcanic rocks. An outcrop of Jura-Cretaceous granodiorite in southern block C exhibits a clear correlation between the high velocity and gravity anomalies, confirming that this intrusion is confined to a small area despite the masking effect of the recent deposits.

Preliminary 3-D Tomographic Velocity Modelling

First arrivals follow the shortest traveltimes path from source to receiver, which may not be coincident with the surface trace of the crooked seismic lines. Therefore, a 3-D

modelling approach must be applied to estimate near-surface velocity. Crooked seismic lines, which were not modelled by the 2-D methods presented above, include Canadian Hunter lines CH159-01, -01A, 160-01, -18, -19, 161-09 and 162-02, and new Geoscience BC lines 5, 6, 10, 11, 12, 13, and 15 (Figure 18). See Calvert et al. (2009) for detailed information on the acquisition of the Geoscience BC data. The Geoscience BC lines have a greater maximum offset (14 390 m), which will allow the estimation of velocity to a depth greater than for the relatively short offset (2550 m) Canadian Hunter lines.

In order to assess the application of 3-D modelling to crooked lines from the Canadian Hunter survey, and in preparation for analysis of the new data from Geoscience BC, a model was created for (straight) seismic reflection line CH160-05 using the FAST software package (Zelt and Barton, 1998). Model parameters similar to those used for



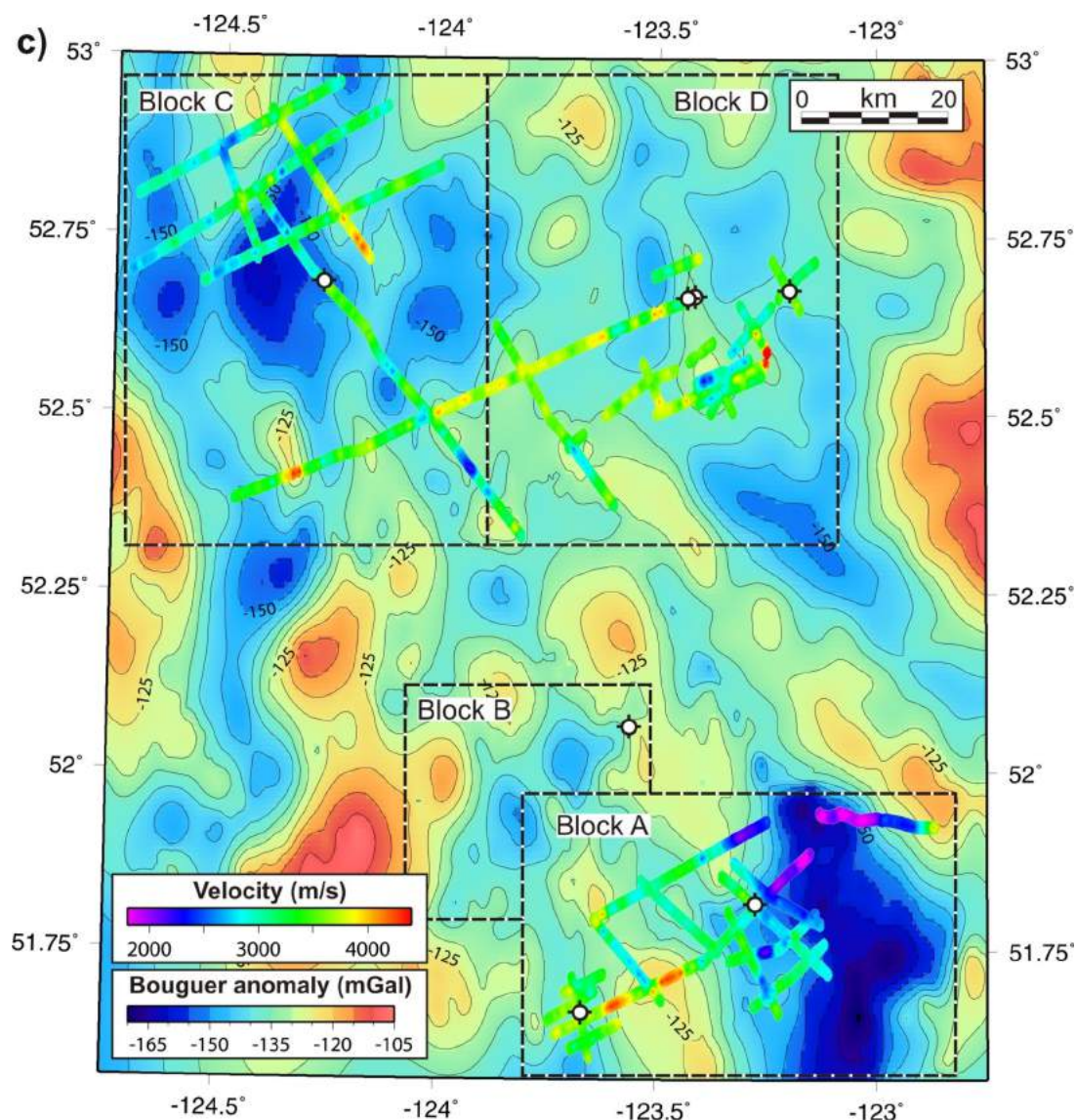
2-D modelling were employed, with a cell size of 25 m and a starting model with a surface velocity of 3500 m/s (gradient of 1.5 s^{-1}). The greatly increased number of cells in a 3-D model can be prohibitive due to a lack of computer memory or extended run time. The northeast-trending seismic line was therefore rotated into an easterly direction to minimize model size.

A perturbation in the velocity model was calculated from the difference between the calculated and observed first-arrival traveltimes for each of nine iterations to give a final velocity model (Figure 19). The models show a reduction in traveltimes misfit from an RMS residual of 185.17 ms to 108.11 ms. The velocity and ray data were smoothed for display using a continuous-curvature gridding algorithm (Smith and Wessel, 1990) at a grid spacing of 5 m.

Initial testing of line CH160-05 produces features similar to those of the 2-D model (Figure 19), such as low velocities to the northeast. Following this successful test, the first-arrival traveltimes for Canadian Hunter lines CH159-01, -01A, CH160-01, -18, -19 and CH162-02 were manually edited in preparation for 3-D modelling.

Discussion

Where seismic imaging is poor and outcrop is often obscured by Quaternary deposits and vegetation, tomographic velocity models provide an additional tool in the investigation of the near-surface character of the rocks in the southeastern Nechako Basin. Velocity estimates for most of the primary rock types are in agreement with the velocities obtained from well sonic logs and laboratory samples. However, model velocities from the Chilcotin Group are



lower than those obtained from laboratory samples and sonic logs, which suggests that the Chilcotin Group is typically of higher velocity than the Eocene Endako and Ootsa Lake groups (Figure 14). The overall model velocity of the Chilcotin Group is similar to that of the Quaternary deposits (2000–2800 m/s).

The Chilcotin Group comprises a number of facies (Andrews and Russell, 2007). The Bull Canyon facies comprises hyaloclastite and breccia, with pillow lavas at the top. These rocks were observed along the Chilcotin River on Highway 20, west of Williams Lake, where it is more breccia dominant (Andrews and Russell, 2007) than at Bull

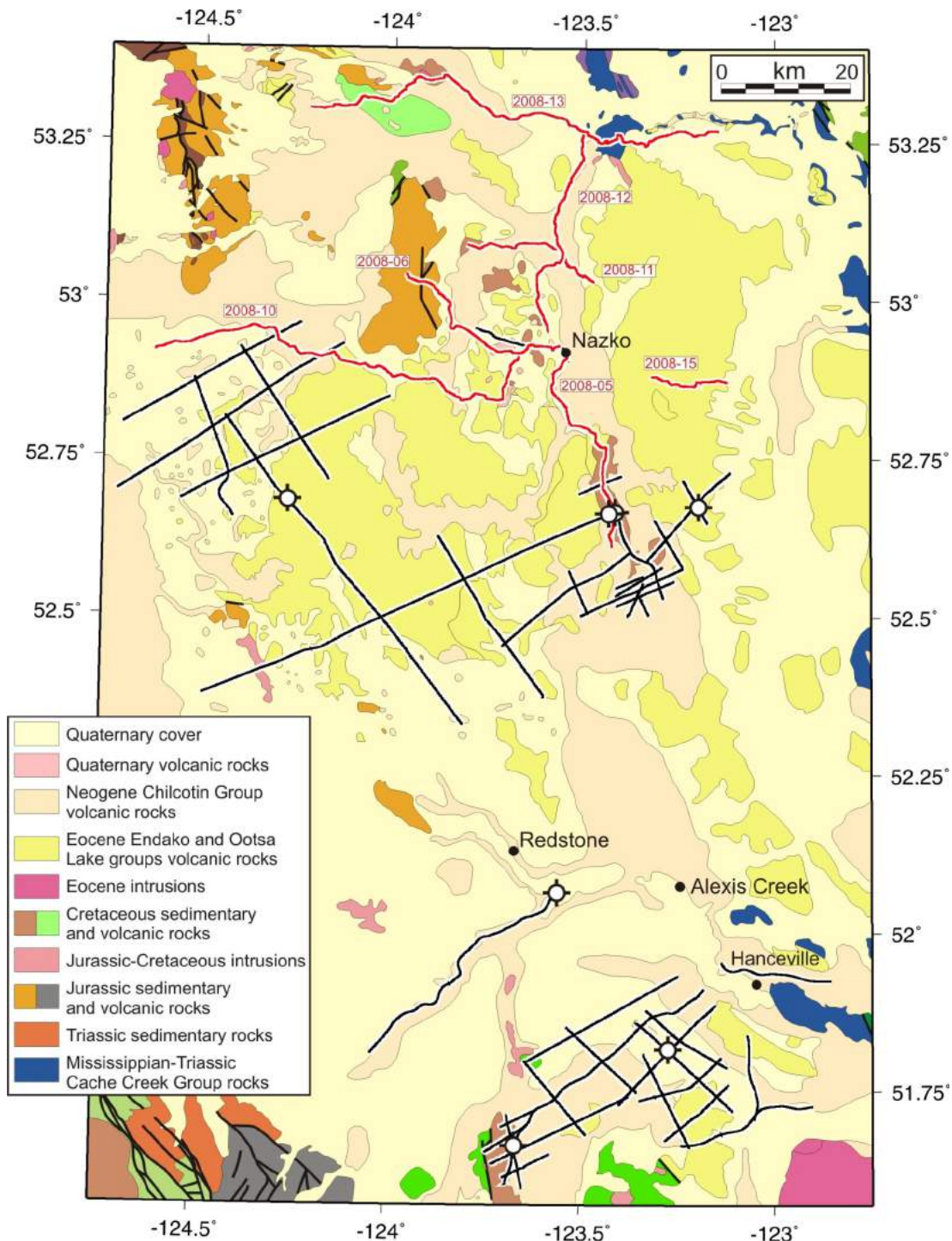


Figure 18: Location of new Geoscience BC vibroseis seismic reflection lines (see Calvert et al., 2009), southeastern Nechako Basin, south-central British Columbia. Red lines show the Geoscience BC data; black lines show the Canadian Hunter data. Bedrock geology modified from Riddell (2006).

Canyon Provincial Park (Figure 15) to the northwest. The Chasm facies consists of thick lavas and hyaloclastite breccia (Andrews and Russell, 2007), which is observed along the Chilko and Taseko rivers (Figure 15). The Dog Creek facies is generally more lava dominant and was described along the Fraser River.

Field investigations (Andrews and Russell, 2008), including the analysis of water-well data, have shown that the Chilcotin Group is regionally thin (<50 m, probably <25 m) and that considerable areas are overlain by Quaternary deposits (typically ~10–50 m; Andrews and Russell, 2008) with variable proportions of basalt contained within (G. Andrews, pers. comm., 2009). Water wells near Alexis Creek (Figure 15) show ~10–50 m of Quaternary drift (Andrews and Russell, 2008). Locally, thicker accumulations of the Chilcotin Group are related to paleo-drainage channels (Andrews and Russell, 2008). In the Chilko River canyon, the Chilcotin Group is ~40 m thick (Andrews and Russell, 2007). Based on water-well samples near Nazko and Alexis Creek (Figure 15), the thickness of the group is estimated to be less than 10 m (Andrews and Russell, 2008). At Bull Canyon Provincial Park (Figure 15), the group is interpreted locally to be ~100 m thick (Gordee et al., 2007). To the southeast, along the Chilcotin River near Hanceville (Figure 15), it has a thickness of <80 m (Andrews and Rus-

sell, 2007). To the north, in well b-22-K, it may be as thick as ~116 m (Riddell et al., 2007).

The results of first-order thickness modelling (Mihalynuk, 2007), based on a digital elevation model (DEM) and mapped basal contacts, echo the interpretation of a regionally thin Chilcotin Group with locally thicker accumulations related to paleo drainage. The model predicts a thickness of ~100–150 m near Hanceville on the Chilcotin River, and a similar thickness to the south of Deer Creek (Figure 15).

In the Chilcotin River area (Figure 15), thick accumulations of Chilcotin Group rocks of the breccia-rich Bull Canyon facies, within a paleo valley, are related to the overall lowest model velocities. These breccias exhibit high porosity and poor consolidation, and often lack a matrix (G. Andrews, pers. comm., 2008), characteristics that would result in the lower seismic velocity relative to consolidated lavas. The elevation of fractured and brecciated Chilcotin Group rocks above the water table at this location would also lower the seismic velocity and may, in part, explain the discrepancy with velocities obtained from fluid-saturated laboratory tests.

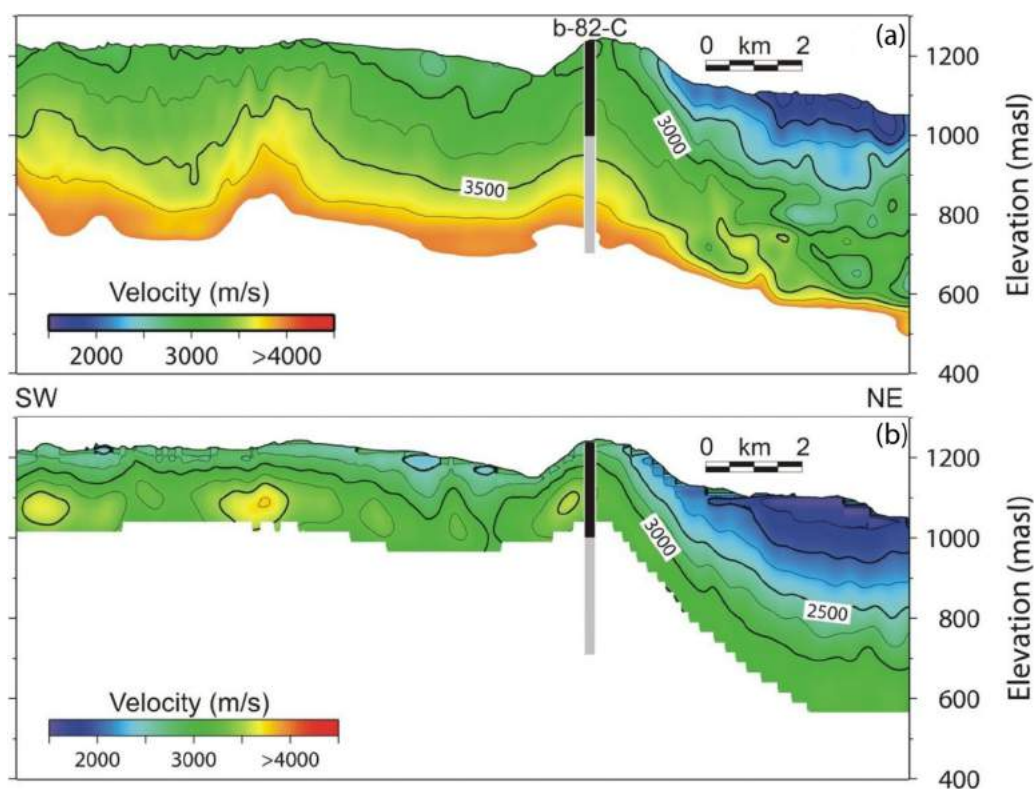


Figure 19: First-arrival tomographic inversion model for Canadian Hunter line CH160-05 (see Figure 4b for location), southeastern Nechako Basin, south-central British Columbia, showing **a)** velocity from 3-D (FAST) model, and **b)** velocity from 2-D (Pronto) model. Heavy black line shows the extent of Eocene Endako Group volcanic rocks in well b-82-C (see Figure 5a).

Anomalously low velocities associated with the Chilcotin Group, such as in northwestern block C and central block A (Figure 15), suggest a mixture of poorly consolidated Quaternary deposits and Chilcotin Group rocks. Elsewhere, the regionally limited thickness of the Chilcotin Group results in the mean velocity being close to that of the underlying rocks.

Ray character (density, focus and penetration depth) and velocity variations were used to define two areas (orange dashed lines, Figure 15) in block A. The tie with well b-82-C (~221 m of Eocene Endako Group) and surface geology allow prediction of the subsurface extent of the Eocene Endako Group in this area. A mean-velocity low to the south of well b-82-C, which divides the two areas, is related to a zone of approximately north-trending strike-slip faulting. Fracturing of rocks in the fault zone, a greater thickness of Quaternary deposits or high-porosity volcanic breccia may account for this velocity low.

Conclusions

Velocity models from the southeastern Nechako Basin agree closely with well sonic logs and laboratory samples. However, mapped occurrences of the Chilcotin Group typically exhibit anomalously low mean velocities, similar to the Quaternary deposits that blanket the region. These low mean velocities likely result from the broad sampling of high porosity, undersaturated, brecciated and fractured rocks, compared to laboratory measurements on water-saturated, consolidated lavas.

In northeastern block A, the lowest mean velocities are related to anomalously thick deposits of the breccia-rich, high-porosity Bull Canyon facies of Chilcotin Group. The distribution of these low mean velocities is consistent with the interpretation of thicker Chilcotin Group rocks in paleo-river valleys.

Where a higher mean velocity is associated with outcrop of the Chilcotin Group, these rocks are locally thin and/or of a velocity similar to underlying rocks. Such Chilcotin Group rocks may be of a more lava-dominant facies, which would have a higher velocity.

The subsurface extent of two areas of Eocene Endako Group, adjacent to well b-82-C, is constrained by variations in the mean velocity and the character (density, focus and penetration depth) of rays, and ties with well and surface geology. These areas are separated by a velocity low related to north-trending strike-slip faulting and possibly a related increased thickness of Quaternary deposits or high-porosity volcanic rocks.

Acknowledgments

The authors thank J. Riddell and F. Ferri for their observations and suggestions regarding the stratigraphic and structural interpretation; and B. Struik for his advice regarding

regional tectonics. Funding for this work was provided by Geoscience BC and the Natural Sciences and Engineering Research Council of Canada (NSERC).

References

- Aldridge, D.F. and Oldenburg, D.W. (1993): Two dimensional tomographic inversion with finite difference travel times; *Journal of Seismic Exploration*, v. 2, p. 257–274.
- Anderson, R.G., Resnick, J., Russell, J.K., Woodsworth, G.J., Villeneuve, M.E. and Grainger, N.C. (2001): The Cheslatta Lake suite: Miocene mafic, alkaline magmatism in central British Columbia; *Canadian Journal of Earth Sciences*, v. 38, p. 697–717.
- Andrews, G.D.M. and Russell, J.K. (2007): Mineral exploration potential beneath the Chilcotin Group, south-central BC: preliminary insights from volcanic facies analysis; *in Geological Fieldwork 2006*, BC Ministry of Energy, Mines and Petroleum Resources, Paper 2007-1 and Geoscience BC, Report 2007-1, p. 229–238, URL <<http://www.em.gov.bc.ca/mining/Geosurv/Publications/Fieldwork/2006/toc.htm#GeoscienceBC>> [November 2009].
- Andrews, G.D.M. and Russell, J.K. (2008): Cover thickness across the southern Interior Plateau, British Columbia (NTS 0920, P; 093A, B, C, F): constraints from water-well records; *in Geoscience BC Summary of Activities 2007*, Geoscience BC, Report 2008-1, p. 11–20, URL <<http://www.geosciencebc.com/s/SummaryofActivities.asp?ReportID=358405>> [November 2009].
- Barnett, C.T. and Williams, P.M. (2009): Using geochemistry and neural networks to map geology under glacial cover; *Geoscience BC, Report 2009-3*, 26 p., URL <<http://www.geosciencebc.com/s/2009-03.asp>> [November 2009].
- Calvert, A.J., Fisher, M.A., Johnson, S.Y. and SHIPS Working Group (2003): Along-strike variations in the shallow seismic velocity structure of the Seattle fault zone: evidence for fault segmentation beneath Puget Sound; *Journal of Geophysical Research*, v. 108, doi:10.1029/2001JB001703.
- Calvert, A.J., Hayward, N., Smithyman, B.R. and Takam Takougang, E.M. (2009): Vibroseis survey acquisition in the central Nechako Basin, south-central British Columbia (parts of 093B, C, F, G); *in Geoscience BC Summary of Activities 2008*, Geoscience BC, Report 2009-1, p. 145–150, URL <<http://www.geosciencebc.com/s/SummaryofActivities.asp?ReportID=358404>> [November 2009].
- Dumont, R. (2008): Bouguer anomaly, Nechako Basin airborne gravity survey, Quesnel / Anahim Lake (NTS 93B and part of 93C), British Columbia; Geological Survey of Canada, Open File 5884, 1 map at 1:250 000 scale, URL <http://apps1.gdr.nrcan.gc.ca/mirage/mirage_list_e.php?id=225541> [November 2009].
- Farrell, R.E., Andrews, G.D.M., Russell, J.K. and Anderson, R.G. (2007): Chasm and Dog Creek lithofacies, Chilcotin Group basalt, Bonaparte Lake map area, British Columbia; Geological Survey of Canada, Current Research 2007-A5, 11 p., URL <http://geopub.nrcan.gc.ca/moreinfo_e.php?id=223728&_h=Current%20Research%202007-A5> [November 2009].
- Ferri, F. and Riddell, J. (2006): The Nechako Basin project: new insights from the southern Nechako Basin; *in Summary of Activities 2006*, BC Ministry of Energy and Mines and Petroleum Resources, p. 89–124, URL <<http://www.em>>

- pr.gov.bc.ca/OG/oilandgas/publications/TechnicalDataandReports/Pages/Summary2006.aspx [November 2009].
- Gordec, S.M., Andrews, G.D.M., Simpson, K. and Russell, J.K. (2007): Sub-confined volcanism within the Chilcotin Group, Bull Canyon Provincial Park (NTS 093B/03), south-central British Columbia; *in* Geological Fieldwork 2006, BC Ministry of Energy, Mines and Petroleum Resources, Paper 2007-1 and Geoscience BC, Report 2007-1, p. 285–290, URL <<http://www.em.gov.bc.ca/mining/Geosurv/Publications/Fieldwork/2006/toc.htm#GeoscienceBC>> [November 2009].
- Grainger, N.C., Villeneuve, M.E., Heaman, L.M. and Anderson, R.G. (2001): New U-Pb and Ar/Ar isotopic age constraints on the timing of Eocene magmatism, Fort Fraser and Nechako River map areas, central British Columbia; *Canadian Journal of Earth Sciences*, v. 38, p. 679–696.
- Hayward, N., and Calvert, A.J. (2007): Seismic reflection and tomographic velocity model constraints on the evolution of the Tofino forearc basin, British Columbia; *Geophysical Journal International*, v. 168, p. 634–646.
- Hayward, N., and Calvert, A.J. (2008a): Structure of the southeastern Nechako Basin, south-central British Columbia (NTS 092N, O; 093B, C): preliminary results of seismic interpretation and first-arrival tomographic modelling; *in* Geoscience BC Summary of Activities 2007, Geoscience BC, Report 2008-1, p. 129–134, URL <<http://www.geosciencebc.com/s/SummaryofActivities.asp?ReportID=358405>> [November 2009].
- Hayward, N. and Calvert, A.J. (2008b): Structure of the southeastern Nechako Basin, British Columbia: interpretation of the Canadian Hunter seismic reflection surveys and preliminary first-arrival tomographic inversion; Geoscience BC, unpublished report.
- Hayward, N. and Calvert, A.J. (2009a): Eocene and Neogene volcanic rocks in the southeastern Nechako Basin, British Columbia: interpretation of the Canadian Hunter seismic reflection surveys using first-arrival tomography; *Canadian Journal of Earth Sciences*, v. 46, p. 707–720.
- Hayward, N. and Calvert, A.J. (2009b): Preliminary first-arrival modelling constraints on the character, thickness and distribution of Neogene and Eocene volcanic rocks in the southeastern Nechako Basin, south-central British Columbia (NTS 092N, O, 093B, C); *in* Geoscience BC Summary of Activities 2008, Geoscience BC, Report 2009-1, p. 151–156, URL <<http://www.geosciencebc.com/s/SummaryofActivities.asp?ReportID=358404>> [November 2009].
- Hayward, N., Nedimovic, M., Cleary, M. and Calvert, A.J. (2006): Structural variation along the Devils Mountain fault zone, northwestern Washington; *Canadian Journal of Earth Sciences*, v. 43, p. 433–446.
- Haskin, M.L., Snyder, L.D. and Anderson, R.G. (1998): Tertiary Endako Group volcanic and sedimentary rocks at four sites in the Nechako River and Fort Fraser map areas, central British Columbia; *in* Current Research 1998-A, Geological Survey of Canada, p. 155–164.
- Hickson, C.J. (1990): A new frontier geoscience project: Chilcotin-Nechako region, central British Columbia; *in* Current Research, Part F, Geological Survey of Canada, Paper 90-1F, p. 115–120.
- Jarchow, C.M., Catching, R.D. and Lutter, W.J. (1994): Large-exposure source, wide recording aperture, seismic profiling on the Columbia Plateau, Washington; *Geophysics*, v. 59, no. 2, p. 259–271.
- Mathews, W.H. (1989): Neogene Chilcotin basalts in south-central British Columbia: geology, ages, and geomorphic history; *Canadian Journal of Earth Sciences*, v. 26, p. 969–982.
- Mihalynuk, M.G. (2007): Neogene and Quaternary Chilcotin Group cover rocks in the Interior Plateau, south-central British Columbia: a preliminary 3-D thickness model; *in* Geological Fieldwork 2006, BC Ministry of Energy, Mines and Petroleum Resources, Paper 2007-1 and Geoscience BC, Report 2007-1, p. 143–147, URL <<http://www.em.pr.gov.bc.ca/Mining/Geoscience/PublicationsCatalogue/Fieldwork/Pages/GeologicalFieldwork2006.aspx>> [November 2009].
- Price, R.A. (1994): Cordilleran tectonics in the evolution of the Western Canada Sedimentary Basin; Chapter 2. *in* Geological Atlas of the Western Canada Sedimentary Basin, G.D. Mossop, and I. Shetsen (comp.), Canadian Society of Petroleum Geologists and Alberta Research Council, Special Report 4, 510 p., URL <http://www.ags.gov.ab.ca/publications/wcsb_atlas/atlas.html> [November 2009].
- Riddell, J.M., compiler (2006): Geology of the southern Nechako Basin, NTS 92N, 92O, 93B, 93C, 93F, 93G; BC Ministry of Energy and Mines and Petroleum Resources, Petroleum Geology Map 2006-1, 3 sheets, 1:400 000 scale.
- Riddell, J., Ferri, F., Sweet, A. and O’Sullivan, P. (2007): New geoscience data from the Nechako Basin project; *in* Nechako Initiative Geoscience Update 2007, BC Ministry of Energy and Mines and Petroleum Resources, Petroleum Geology Open File 2007-1, p. 59–98.
- Rusmore, M.E. and Woodsworth, G.L. (1991): Coast Plutonic Complex: a mid-Cretaceous contractional orogen; *Geology*, v. 19, p. 941–944.
- Rusmore, M.E., Woodsworth, G.L. and Gehrels, G.E. (2000): Late Cretaceous evolution of the eastern Coast Mountains, Bella Coola, British Columbia; *in* Tectonics of the Coast Mountains, Southeastern Alaska and British Columbia, H.H. Stowell and W.C. McClelland (ed.), Geological Society of America, Special Paper 343, p. 89–105.
- Schiarizza, P. and MacIntyre, D.G. (1999): Geology of Babine Lake–Takla Lake area, central British Columbia (93K/11, /12, /13, /14; 93N/3, /4, /5, /6); *in* Geological Fieldwork 1998, BC Ministry of Energy, Mines and Petroleum Resources, Paper 1999-1, p. 33–68.
- Schmid, R., Ryberg, T., Ratschbacher, L., Schulze, A., Franz, L., Oberhänsli, R. and Doug, S. (2001): Crustal structure of the eastern Dabie Shan interpreted from deep reflection and shallow tomographic data; *Tectonophysics*, v. 333, p. 347–359.
- Smith, W.H.F. and Wessel, P. (1990): Gridding with continuous curvature splines in tension; *Geophysics*, v. 55, no. 3, p. 293–305.
- Struik, L.C. and MacIntyre, D.G. (2001): Introduction to the special issue of *Canadian Journal of Earth Sciences*: the Nechako NATMAP Project of the central Canadian Cordillera; *Canadian Journal of Earth Sciences*, v. 38, p. 485–494.
- Zelt, C.A. and Barton, P.J. (1998): 3D seismic refraction tomography: a comparison of two methods applied to data from the Faeroe Basin; *Journal of Geophysical Research*, v. 103, p. 7187–7210.

Improved Near-Surface Velocity Models from the Nechako Basin Seismic Survey, South-Central British Columbia (Parts of NTS 093B, C, F, G), Part 1: Traveltime Inversions

B.R. Smithyman, Department of Earth and Ocean Sciences, University of British Columbia, Vancouver, BC, bsmithyman@eos.ubc.ca

R.M. Clowes, Department of Earth and Ocean Sciences, University of British Columbia, Vancouver, BC

Smithyman, B.R. and Clowes, R.M. (2010): Improved near-surface velocity models from the Nechako Basin seismic survey, south-central British Columbia (parts of NTS 093B, C, F, G), part 1: traveltime inversions; *in* Geoscience BC Summary of Activities 2009, Geoscience BC, Report 2010-1, p. 227–234.

Introduction

Multichannel vibroseis reflection data were collected in the Nechako Basin during the summer of 2008 to identify possible features of interest to the petroleum industry (Calvert et al., 2009). The data were processed by CGGVeritas primarily to identify targets at depth. Knowledge of the near-surface seismic structure can improve resolution of these deeper targets and provide valuable information for geological interpretation. Since the downgoing signal energy used in seismic reflection must travel twice through the shallow subsurface, an improved model of near-surface velocity can substantially improve the resolution of deeper reflections. As well, good velocity models can help identify rock types and thus aid geological interpretations. This paper describes results from processing vibroseis data of the 2008 Nechako Basin seismic survey to generate velocity models for the upper 3000 m using tomography techniques. The initial results come from the processing of hand-picked first arrivals using traveltime-tomography methods. The paper also discusses the benefits and challenges of processing the long-offset early-arriving waveforms using full-waveform-inversion methods, which is part of our continuing research.

Refraction processing of surface vibroseis data is typically limited to near-offset refraction statics using traveltime-based procedures. The ultimate goal of this project is to produce detailed models of near-surface velocity using full-waveform-inversion methods on a wide range of offsets. Waveform tomography combines inversion of first-arrival traveltime data with full-waveform inversion of densely sampled refracted waveforms (Pratt and Worthington, 1990; Pratt, 1999). Since inversion of the waveform ampli-

tude and phase is not limited by the ray-theory approximation, identification of low-velocity zones and small scattering targets is possible. In order to proceed with the full-waveform inversion of refraction data, it is important to have a suitably accurate starting velocity model. This is typically a synthesis of velocity models from refraction-statics processing and/or traveltime inversion (i.e., ray tracing) along with a priori geological information (Pratt and Gouly, 1991).

Geological Background

The Nechako Basin is a sedimentary basin in the Intermontane Belt of the western Canadian Cordillera (Figure 1). This area has been characterized as prospective for hydrocarbon development. Hayes et al. (2003) identified the southeastern portion of the basin as having the highest prospectivity. The initial study area for this project, line 10, traces the northern border of this subsection of the basin (shown in detail in Figure 2).

The Stikine Terrane, of which the Hazelton Group is a part, underlies much of the area covered by the Nechako Basin seismic survey. It comprises a succession of volcanic and sedimentary rocks more than 1000 m in thickness and ranging in age from Carboniferous to Middle Jurassic (Schiarizza and MacIntyre, 1999; MacIntyre et al., 2001). This succession is not of interest in hydrocarbon exploration (Hannigan et al., 1994). The Stikine succession is overlain by Jurassic–Tertiary clastic sedimentary rocks of the Skeena Group. These are Early to mid-Cretaceous nonmarine sandstone and conglomerate, with some regional interbedded shale that may limit migration of fluids. These rocks represent the most prospective unit in the assemblage (Hannigan et al., 1994). Within the basin proper, approximately 2500 m (Hannigan et al., 1994) of mid- to Late Cretaceous, transitional marine and terrestrial clastic sedimentary rocks overlie the Skeena Group rocks. However, line 10 is located on the northern border of the southeastern portion of the basin, and these overlying sediments do not outcrop locally. At the basin edge, Eocene volcanic

Keywords: *Nechako Basin, seismic surveys, seismic tomography, seismic inversion, first-arrival interpretation, waveform tomography, velocity models*

This publication is also available, free of charge, as colour digital files in Adobe Acrobat® PDF format from the Geoscience BC website: <http://www.geosciencebc.com/s/DataReleases.asp>.

rocks may directly overlie Skeena Group sedimentary rocks. Tertiary rhyolite and mixed volcanic rocks, correlated with the Ootsa Lake and Endako groups and therefore presumed to be Eocene based on similar assemblages throughout British Columbia, underlie much of the area of investigation (Figure 2). According to Schiarizza and MacIntyre (1999), these are vesicular and amygdaloidal flows interbedded with volcanoclastic conglomerate where exposed.

The data for this initial study come from seismic line 10 of the Nechako Basin seismic survey (Figure 2). The geology underlying line 10 is dominated by basalt and rhyolite, divided between younger volcanic sedimentary rocks of Neogene–Paleogene age and deeper Stikine Terrane sedimentary and volcanic successions. Quaternary deposits of varying thickness overlie these rocks.

Traveltime Inversions

Velocity models of the shallow subsurface are typically developed as part of the reflection-seismology workflow to facilitate common depth point (CDP) stacking and migration; however, these models are often coarse and of limited use for interpretation. When applying waveform tomography, it is important to produce detailed velocity models at the traveltime-inversion stage; this, in turn, requires precise traveltime picks. Without a sufficiently accurate starting model, waveform-inversion methods cannot succeed. This paper presents results from two independent inversions of these traveltime data.

Figure 1 shows the plan-view extent of the study area on a map of the relevant geological terranes. Data were selected from the central, nearly straight portion of seismic line 10, with the reduced dataset comprising 699 shots, each with 960 active geophone channels (Figure 2). These data were reorganized for processing purposes to occupy 699 shot gathers, each containing 2362 receiver stations. In any given shot gather, nominally 960 of these stations are active and the remaining stations contain no data. To use two-dimensional (2-D) processing software, the locations of the shot and receiver stations were projected to a 2-D plane oriented at 106° (red and blue lines on Figure 2). The orientation of this line was determined by a least-squares fit to receiver positions. The portions of the 2-D geometry covered by the shot and receiver arrays are indicated.

As input to traveltime interpretation, the authors made 671 000 first-arrival picks (i.e., one for each active source-receiver pair), distributed between 0 and 14 km offset. Incorporating a wide range of offsets is critical for a more complete characterization of the near-surface. These picks were processed using several methods, including

Generalized Linear Inversion (GLI3D) by Hampson-Russell Software Services (Hampson and Russell, 1984) in layer-velocity mode;

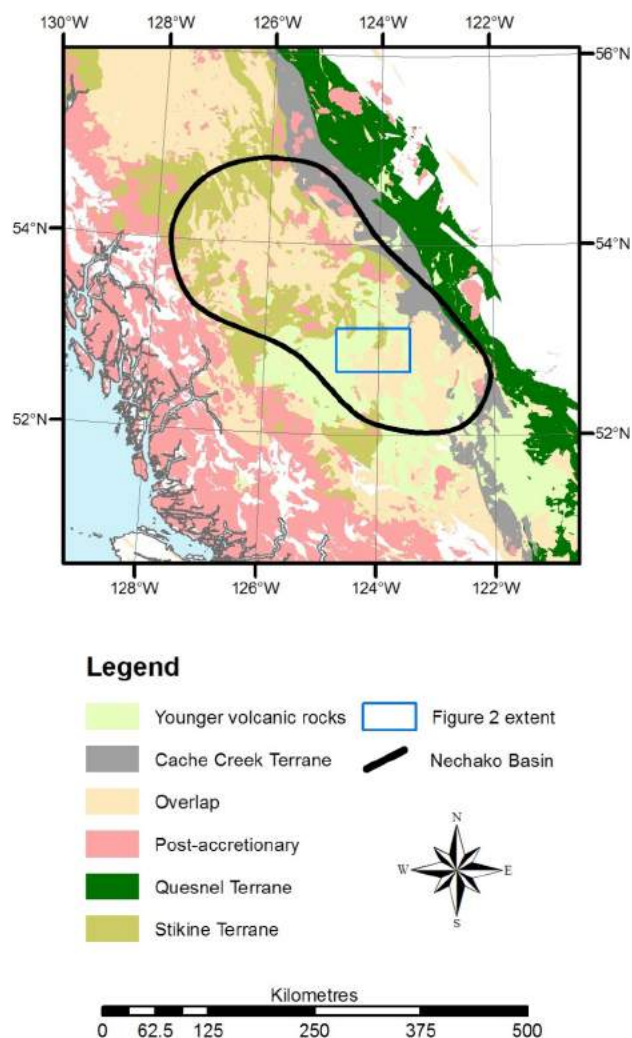


Figure 1. Relevant terranes of south-central British Columbia, showing the location of the study area, including seismic line 10. The Nechako Basin is subdivided into two main regions; the line 10 study follows the northern edge of the southeastern region, roughly at the boundary between rocks of the Stikine Terrane and those of the basin proper (Massey et al., 2005).

GLI3D in ray-tracing mode, which follows a tomographic approach; and

First Arrival Seismic Tomography (FAST), which is an academic development (Zelt and Barton, 1998).

Figure 3 shows the velocity model (and corresponding layer-velocity variation) from GLI3D layer-velocity inversion. In comparison, Figure 4 presents the gridded velocity models produced in ray-tracing tomography from both GLI3D (top) and FAST (bottom). The GLI3D tomography model was developed from tomographic inversion of the traveltime data using the GLI3D layer-velocity result as an initial model. The initial tomography model for FAST used a 1-D monotonically increasing gradient in velocity from surface to mid-depth, and a constant velocity of 6000 m/s in the lower portion. This was updated iteratively to an RMS misfit of 20 ms on the traveltime picks. Three methods were

used to identify robust features common to different interpretations of the seismic data. Additionally, this allowed assessment of possible consequences of the 2-D approximation used in FAST model inversion.

Figure 5 presents a comparison between real data of a central shot gather and the corresponding synthetic data generated from the FAST velocity model (Figure 4). The synthetic data were computed using frequency-domain finite-difference forward modelling, a component of the waveform-tomography algorithm, with additional constraints that include

- a fixed attenuation model with seismic quality factor (Q) of 200 (at 35 Hz); seismic Q is proportional to the inverse of attenuation at a fixed frequency; and
- a source-signature inverted from the true data, closely matching the frequency content and phase of the original vibroseis source.

In order that the entire dynamic range of these data could be shown, an automatic gain control (AGC) filter with a 2 s window was applied in each panel.

Discussion

Figure 3 presents results from Generalized Linear Inversion (GLI3D) inversion for layers and velocities. The starting model for this inversion was derived from traveltime-distance (t-x) interpretation (layer assignment) of the picks at 41 points along seismic line 10. The GLI3D inversion allows the layer depths to vary below each shot point, and the velocity to vary within each layer. Considerable variation

in both layer thicknesses and velocities is indicated, but the well-defined layers probably do not accurately represent the geology of the study area.

The GLI3D and First Arrival Seismic Tomography (FAST) models resulted from ray-tracing-based traveltime inversion of the first-arrival picks, but the methods differ as outlined in Table 1. Significantly, these two results were determined in parallel, from the same data but without any common processing steps.

The two tomography models share many characteristics. Both models identify high-velocity anomalies 1 km or less in size within 500 m of the surface (Figure 4, feature A). These appear to be a semicontinuous layer on the GLI3D model, extending more than 20 km through the western end of the model cross-section. This layer is identified on the western portion of seismic line 10, where Chilcotin basalt overlies the Ootsa Lake rhyolite, and may indicate that these units are distinguishable by seismic velocity. The identified high-velocity anomalies are immediately underlain by a 1–2 km thick region of moderate velocities, on the order of 4000 m/s (Figure 4, feature B) and approximately what would be expected for the Ootsa Lake rhyolite. The solid line on Figure 4 indicates the bottom of this low-velocity region. A higher velocity zone (Figure 4, feature C) appears as a shallowing of this interface. It corresponds to the position where Hazelton Group volcanic rocks of the Stikine Terrane outcrop adjacent to the line (Figure 2). The volcanic rocks appear to exhibit a comparatively high seismic velocity of ~6000 m/s. These results are consistent with an expectation that the basin thickens towards the south.

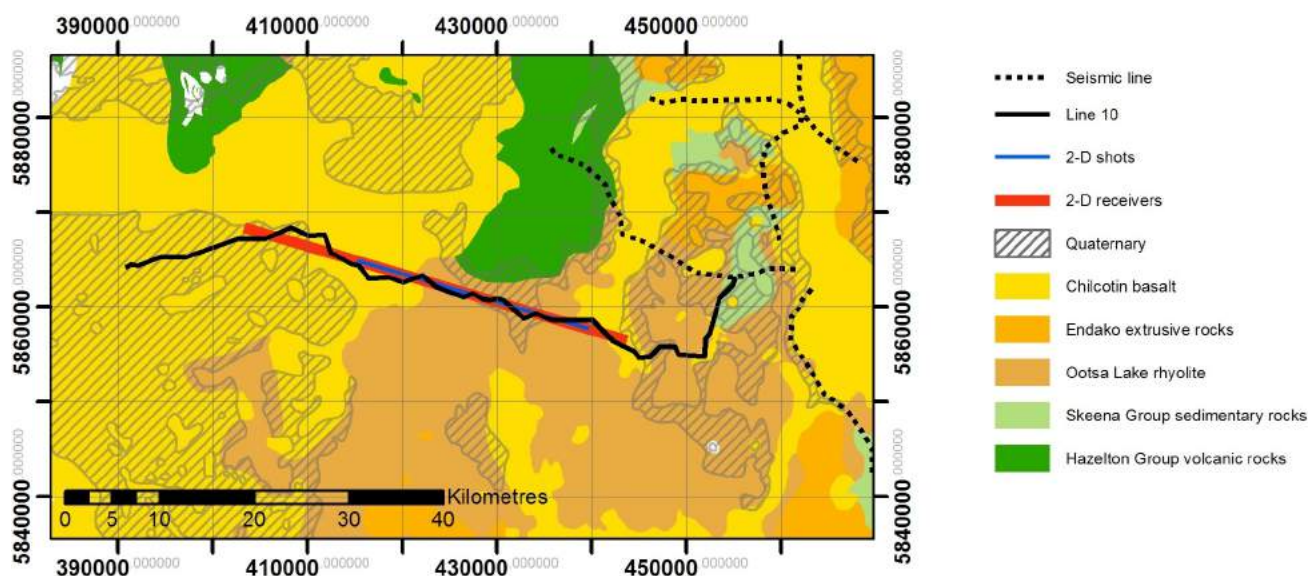


Figure 2. Geometry of seismic line 10 in relation to lithology and several other seismic lines from the 2008 Nechako Basin seismic survey, south-central British Columbia. The 2-D approximate geometry used in first-arrival seismic tomography (FAST) inversion is highlighted (with corresponding extents of the active source [blue line] and receiver [red line] arrays). The surface of the central portion of line 10 is dominated by the Ootsa Lake rhyolite, whereas both flanks are overprinted by the Chilcotin basalt. To the north, the Hazelton Group volcanic rocks of the Stikine Terrane appear to plunge beneath line 10 towards the south (Massey et al., 2005). Abbreviation: MSL, mean sea level.

The Hazelton Group rocks appear to plunge below the surface volcanic rocks and Quaternary cover at a depth of a few hundred metres where they are crossed by line 10. In both models, the rocks of the Stikine Terrane appear to be indistinguishable from the overlying Skeena Group and Cretaceous sedimentary units, which are presumed to underlie the Ootsa Lake rhyolite and Chilcotin basalt in the western portion of the cross-section. There is evidence of a high-velocity (~7000 m/s) layer at the western end of both models (Figure 4, feature D). The interface between this and the overlying Ootsa Lake rhyolite (Figure 4, feature B) appears to be at a depth of 2–2.5 km. However, data from sources west of the 12 000 m point have not been included

on Figure 4, and confidence in the model in this area is therefore reduced.

In order to estimate the extent to which these velocity models may represent the subsurface, waveform forward-modelling was carried out using a frequency-domain finite-difference acoustic code, part of the waveform-tomography algorithm (Pratt, 1999), to generate synthetic shot gathers. Figure 5 shows a synthetic shot gather computed using the FAST velocity model (Figure 4), compared with real data for the same area. The frequency content of the source was inverted from the real data. First-arrival picks (the data for this study) are overlain on both images. Refracted arrivals

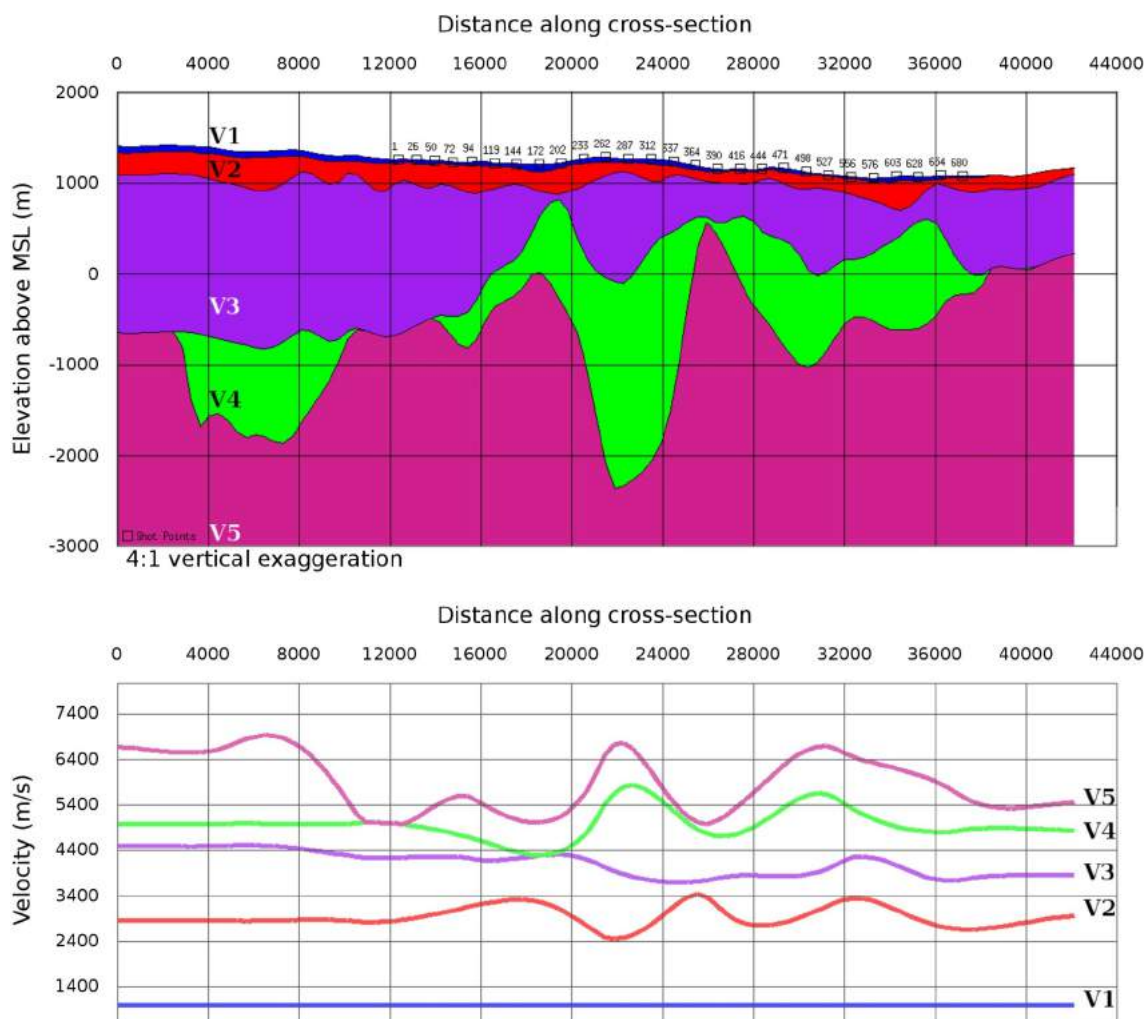


Figure 3. Layer model (upper) and varying velocities within layers (lower) from Generalized Linear Inversion (GLI3D); the model follows the true 3-D geometry of seismic line 10, Nechako Basin seismic survey, south-central British Columbia. However, because of the approximations in this model, it most likely does not represent the true geology. The authors believe that V1 and V2 are controlled mainly by near-surface heterogeneity. Surficial geology (Figure 2) indicates the presence of Chilcotin basalt overlying the Ootsa Lake rhyolite on the western portion of line 10. The small-scale variations in the depth of the second interface (V2 to V3) at the western side of the model may be due to its inability to represent accurately this overlap. It appears that V3, which may correlate with the Ootsa Lake rhyolite, thickens towards the western end of the study area. Layers V4 and V5 may represent collectively an interface between overlying volcanic rocks and the rocks of the Skeena and Hazelton groups below, but precise interpretation is difficult. Because of the locally flat assumptions made in the seismic inversion, the utility of this model is limited.

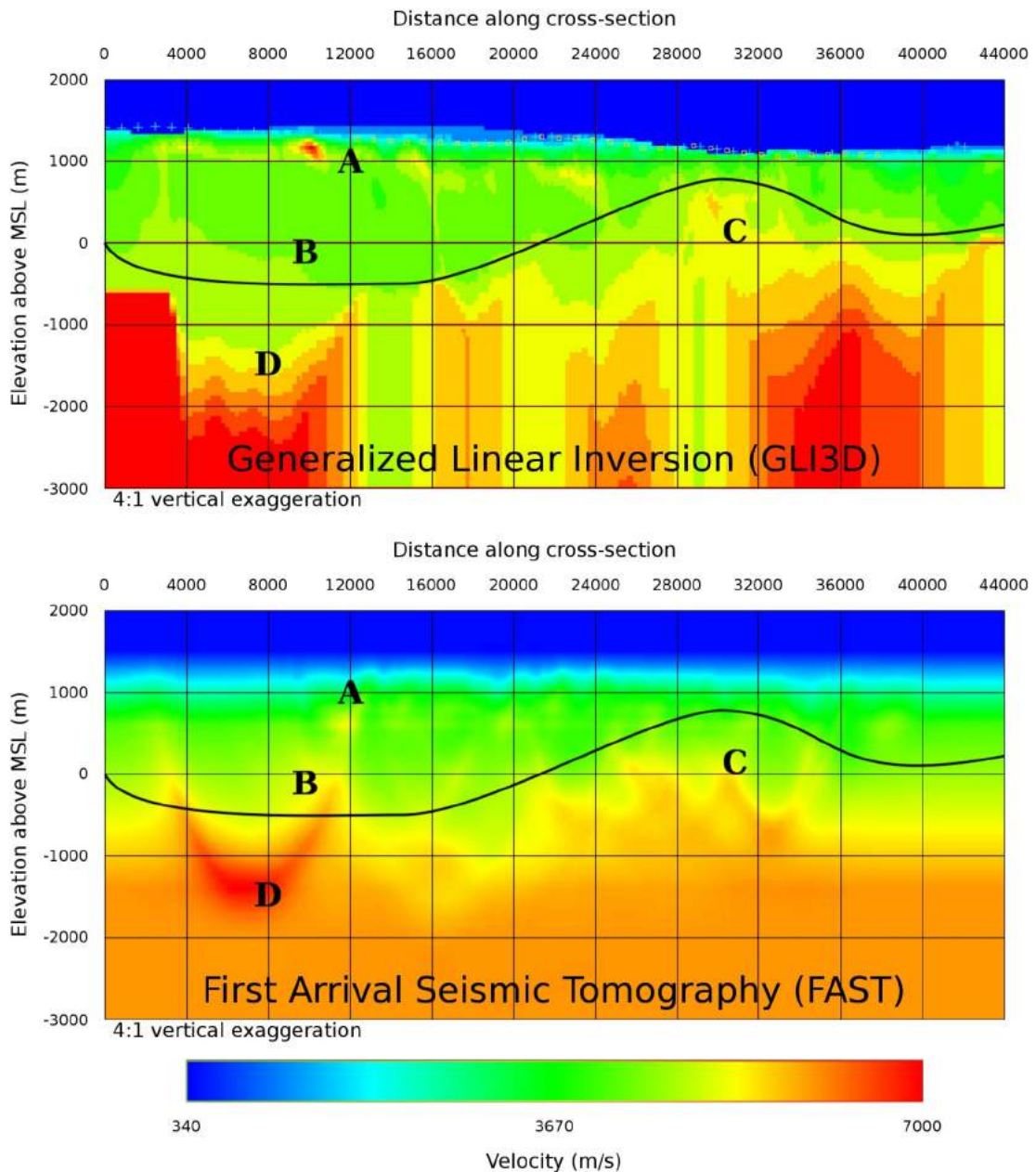


Figure 4. Tomography velocity models from Generalized Linear Inversion (GLI3D, upper) and First Arrival Seismic Tomography (FAST, lower), Nechako Basin seismic survey, south-central British Columbia. The GLI3D tomography model follows the true 3-D geometry of seismic line 10, whereas the FAST model is a cross-section through the projected 2-D geometry shown in Figure 2. Also shown are several areas of interest that are discussed in detail in the text. Feature A represents semicontiguous high-velocity anomalies near the surface, which may be related to the presence of the Chilcotin basalt (see Figure 2). Feature B shows a relatively thick (2–2.5 km) layer of comparatively moderate seismic velocity, which appears to correlate with the presence of the Ootsa Lake rhyolite. The volcanic layers appear to thicken towards the western end of the models, with an interpreted interface between volcanic and sedimentary rocks of the Skeena Group indicated by the solid black line. Feature C appears to correlate with the presence of the Hazelton Group volcanic rocks to the north; this is interpreted to indicate that the Hazelton rocks plunge southward below the seismic line (see Figure 2). The high seismic velocities at feature D are present on both velocity models, and indicate a sharp boundary between overlying volcanic rocks and the sedimentary basement. However, the western end of the modelled region is not well constrained by the subset shot array, so these features have a lower confidence associated with their interpretation than those in the central portions of the model.

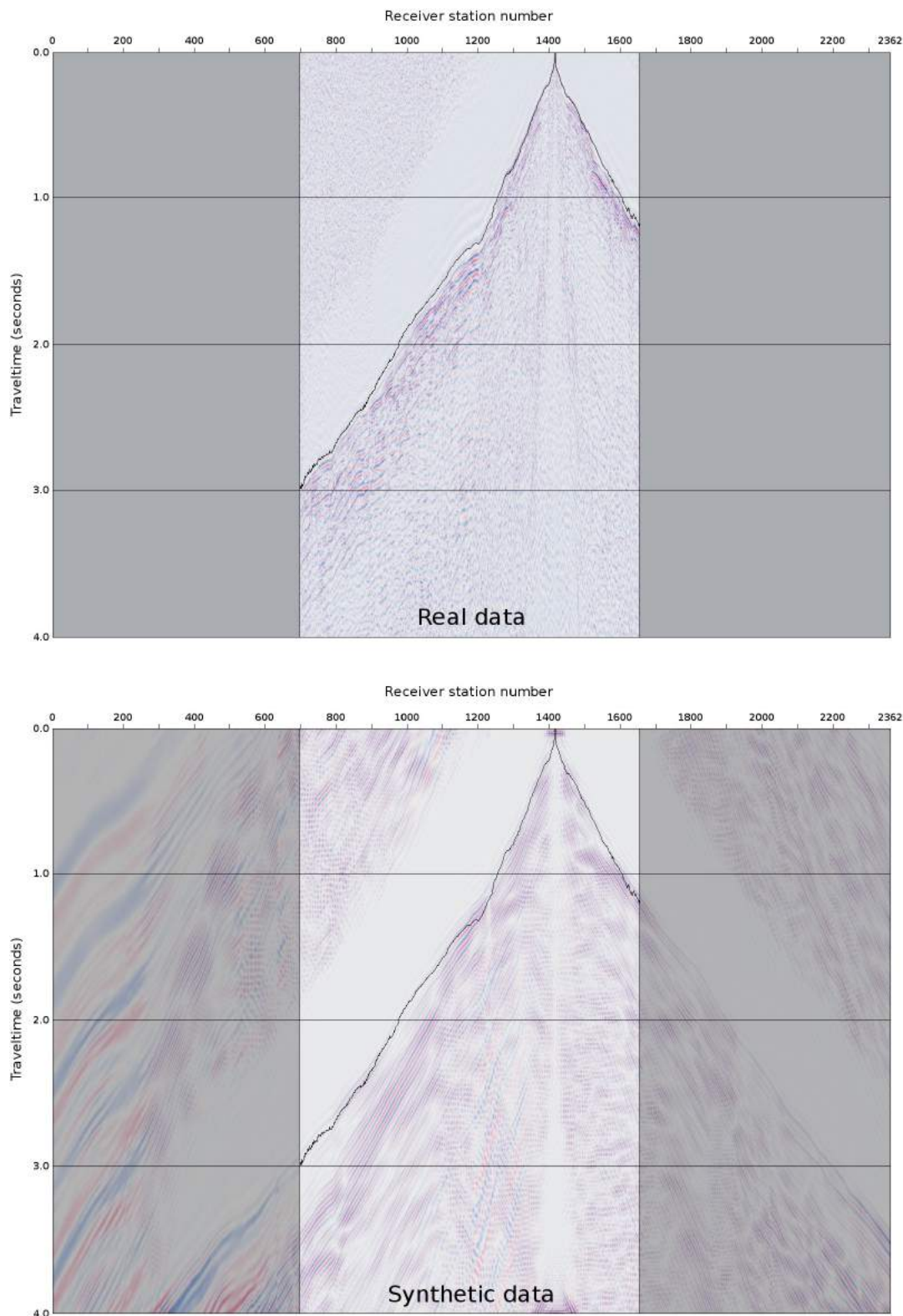


Figure 5. Real and synthetic data from a shot gather midway along seismic line 10, Nechako Basin seismic survey, south-central British Columbia. A black line indicates the first-arrival picks on each shot gather; these represent the data of interest for traveltimes inversions. The waveform data will act as input to the full-waveform–inversion portion of this project. Synthetic data were produced by forward propagation of the data waveforms using a frequency-domain acoustic-wave-equation method (Pratt, 1999) and the First Arrival Seismic Tomography (FAST) velocity model (Figure 4). The synthetic data incorporate source amplitude and phase information that was inverted from the real data. The model was additionally constrained by incorporating a constant attenuation, parameterized by a seismic Q of 200 (at 35 Hz).

Table 1. Significant differences between Generalized Linear Inversion (GLI3D) and First Arrival Seismic Tomography (FAST).

	Generalized Linear Inversion (GLI3D)	First Arrival Seismic Tomography (FAST)
Starting model	GLI3D layered velocity/depth model (Figure 3)	1-D velocity gradient; did not include topography
Regularization	Smoothing prior to each iteration	Pursuit of a specific RMS traveltime misfit; model weights on smoothness and size
Geometry	True 3-D line geometry; topography included in terms of source and receiver elevations	Projected to a 2D plane striking at 106° Source and receiver positions are specified in 2D

in the synthetic data are visibly similar to those in the real data. The most substantial misfits (below station 1200 and stations 700 to 900) appear to be due to the approximate 2-D line geometry implicit in the FAST model (Figure 2). Direct-wave arrivals are visibly similar to those in the observed data, even 200–300 ms beyond the first-arrival picks. The amplitudes of the first-arriving waveforms at long offset in the synthetic gather are lower than those in the real data, indicating that a more complex attenuation model may be necessary to explain fully the waveform arrivals.

Planned Future Work

The ultimate goal of this project is to develop improved velocity models from full-waveform inversion. This report presented velocity models from several traveltime-inversion methods, aimed both at interpretation and at developing a starting model well suited to full-waveform inversion. Using waveform tomography, the authors plan to build useful, detailed, near-surface velocity models for both the reflection workflow and direct interpretation.

The results in Figures 4 and 5 represent preliminary models from conventional refraction processing of traveltime data. It is expected that full-waveform inversion of these data will improve resolution; the waveform-tomography method incorporates amplitude information and thus can delineate low-velocity zones that are not sampled by the first-arrival data.

Several subtleties exist in first-arrival analysis and waveform inversion of vibroseis data. Some of these have been identified and accounted for, whereas developing techniques to deal with others remains a research component of this project. Because of the use of a nonlinear frequency-domain approach to the solution of this inverse problem, low data frequencies are important in comparison with conventional reflection processing. Tight band-limiting due to vibroseis correlation makes initial model fidelity extremely important. This motivates the care taken in the development of traveltime-tomography initial models. The mixed-phase vibroseis source signature exhibits variations in phase with offset that are difficult to quantify without detailed a priori knowledge of the near-surface. This causes difficulties with picking and initial model building, which are critical for nonlinear waveform inversion. These diffi-

culties are resolved, in part, by careful manual review of first-arrival picks; the full-waveform-inversion stage can account for attenuation by modelling the inverse of seismic Q (attenuation).

Elastic propagation modes and mode-converted arrivals must be considered as systematic noise because the 2-D acoustic approximation to the wave equation that is used in waveform tomography does not account for such arrivals. Appropriate preprocessing steps are required to reduce their effects. Windowing and removal of ground roll from the observed shot gathers are also carried out to allow implementation of the 2-D waveform-inversion procedure. The use of a 2-D approximation to the true 3-D geometry introduces amplitude variation with offset (AVO) errors that must be accounted for in order for attenuation inversion to be possible. To accomplish this, heuristic methods are used to match the large-scale AVO characteristics of the real data to the synthetic data at each stage of processing.

Careful analysis of the early-arriving waveforms is necessary to deal with approximations due to the waveform-inversion implementation, which are not easily separable from the approximations implicit in vibroseis acquisition. However, the potential benefits in near-surface velocity characterization and their wide applicability make the results of this research important for seismic processing and near-surface geological interpretation.

References

- Calvert, A.J., Hayward, N., Smithyman, B.R. and Takam Takougang, E.M. (2009): Vibroseis survey acquisition in the central Nechako Basin, south-central British Columbia (parts of NTS 093B, C, F, G); *in* Geoscience BC Summary of Activities 2008, Geoscience BC, Report 2009-1, p. 145–150, URL <<http://www.geosciencebc.com/s/SummaryofActivities.asp?ReportID=358404>> [November 2009].
- Hampson, D. and Russell, B. (1984): First-break interpretation using generalized linear inversion; *Journal of the Canadian Society of Exploration Geophysicists*, v. 20, no. 1, p. 40–54.
- Hannigan, P., Lee, P., Osadetz, K., Dietrich, J. and Olsen-Heise, K. (1994): Oil and gas resource potential of the Nechako-Chilcotin area of British Columbia; BC Ministry of Energy, Mines and Petroleum Resources, GeoFile 2001-6, 167 p. and 5 maps at 1:1 000 000 scale, URL <<http://www.empr.gov.bc.ca/OG/oilandgas/petroleumgeology/Convention>>

- [alOilAndGas/InteriorBasins/Pages/default.aspx](#)> [November 2009].
- Hayes, B.J., Fattahi, S. and Hayes, M. (2003): The Nechako Basin—frontier potential close to home (abstract); unpublished paper presented at Canadian Society of Petroleum Geologists, 2003 Annual Convention, URL <<http://www.cspg.org/conventions/abstracts/2002abstracts/051S0118.pdf>> [November 2009].
- MacIntyre, D., Villeneuve, M. and Schiarizza, P. (2001): Timing and tectonic setting of Stikine Terrane magmatism, Babine-Takla lakes area, central British Columbia; *Canadian Journal of Earth Sciences*, v. 38, p. 579–602.
- Massey, N.W.D., MacIntyre, D.G., Desjardins, P.J. and Cooney, R.T. (2005): Digital map of British Columbia: whole province; BC Ministry of Energy, Mines and Petroleum Resources, GeoFile 2005-1, URL <<http://www.empr.gov.bc.ca/Mining/Geoscience/PublicationsCatalogue/GeoFiles/Pages/2005-1.aspx>> [November 2009].
- Pratt, R.G. (1999): Seismic waveform inversion in the frequency domain, part 1: theory and verification in a physical scale model; *Geophysics*, v. 64, p. 888–901.
- Pratt, R.G. and Gouly, N.R. (1991): Combining wave equation imaging with travelttime tomography to form high resolution images from cross-hole data; *Geophysics*, v. 56, p. 208–224.
- Pratt, R.G. and Worthington, M.H. (1990): Inverse theory applied to multi-source cross-hole tomography, part 1: acoustic wave-equation method; *Geophysical Prospecting*, v. 38, p. 287–310.
- Schiarizza, P. and MacIntyre, D. (1999): Geology of the Babine Lake–Takla Lake area, central British Columbia (93 K/11, 12, 13, 14; 93 N/3, 4, 5, 6); *in* Geological Fieldwork 1998, BC Ministry of Energy, Mines and Petroleum Resources, Paper 1999-1, p. 33–68, URL <<http://www.empr.gov.bc.ca/Mining/Geoscience/PublicationsCatalogue/Fieldwork/Pages/GeologicalFieldwork1998.aspx>> [November 2009].
- Zelt, C.A. and Barton, P.J. (1998): 3D seismic refraction tomography: a comparison of two methods applied to data from the Faeroe Basin; *Journal of Geophysical Research*, v. 103, p. 7187–7210.

Passive Source Seismic Studies of the Sediments, Crust and Mantle Beneath the Nechako Basin, South-Central British Columbia (NTS 092O, 093B, C, F, G)

J.F. Cassidy, Geological Survey of Canada, Victoria, BC, jcassidy@nrcan.gc.ca

H. Kim, University of Victoria, Victoria, BC

O. Idowu, University of Alberta, Edmonton, AB

H. Kao, Geological Survey of Canada, Victoria, BC

S. Dosso, University of Victoria, Victoria, BC

A. Frederiksen, University of Manitoba, Winnipeg, MB

J-P. Mercier, University of British Columbia, Vancouver, BC

M. Bostock, University of British Columbia, Vancouver, BC

A. Frassetto, University of Arizona, Tucson, AZ

G. Zandt, University of Arizona, Tucson, AZ

Cassidy, J.F., Kim, H., Idowu, O., Kao, H., Dosso, S., Frederiksen, Mercier, J-P., Bostock, M., Frassetto, A. and Zandt, G.A. (2010): Passive source seismic studies of the sediments, crust and mantle beneath the Nechako Basin, south-central British Columbia (NTS92O, 093B, C, F, G); in *Geoscience BC Summary of Activities 2009*, Geoscience BC, Report 2010-1, p. 235–244.

Introduction

During the summer of 2006, an array of seven three-component broadband POLARIS seismic stations was deployed across the Nechako Basin (Figures 1a, b; Table 1). The goal of this deployment was to record large distant earthquakes, which could be used to image the Earth's structure beneath central British Columbia. Two additional seismic stations were deployed in the autumn of 2007 to study an unusual swarm of local earthquakes near the Nazko cone (unofficial place name). The passive-source seismic datasets are being used for a wide range of studies, including

- mapping the near-surface structure (e.g., sediment and volcanic cover thickness);
- mapping the overall basin geometry;
- estimating crustal thickness;
- mapping upper-mantle structure; and
- inferring flow patterns in the upper mantle based on SKS-splitting observations.

Key parameters useful for resource assessment (oil, gas and mineral potential) that are obtained from these passive-source seismic datasets include S-wave velocity (sensitive to fluids and fractures), Poisson's ratio (sensitive to lithology, porosity and fracture density), thickness of sediments

and volcanic cover, and overall basin geometry (key for oil and gas potential). This report provides an update on the field operations and data collection, and briefly summarizes some of the applications of this passive-source seismic dataset to both resource assessment and improved estimates of volcanic and seismic hazards in the region.

Data Collection

Field Operations

Deployment of the first POLARIS-Nechako seismograph stations began on August 24, 2006. Each station utilized either AC power (if available) or DC power from solar panels and provided real-time data via satellite to Geological Survey of Canada (GSC) offices in Sidney, BC and Ottawa, ON. Five stations were decommissioned in 2008 and the last POLARIS station was decommissioned on August 27, 2009 (see Table 1 for details).

Data Availability

Waveform data are archived with data from the Canadian National Seismograph Network (CNSN) and are available in a number of ways. The easiest way to access these data is via the website: http://earthquakescanada.nrcan.gc.ca/stndon/AutoDRM/autodrm_req-eng.php. An alternative method is to use the 'AutoDRM' service. For information on this, see <http://earthquakescanada.nrcan.gc.ca/stndon/AutoDRM/index-eng.php>.

Keywords: seismic, regional geophysical survey, Nechako Basin
This publication is also available, free of charge, as colour digital files in Adobe Acrobat® PDF format from the Geoscience BC website: <http://www.geosciencebc.com/s/DataReleases.asp>.

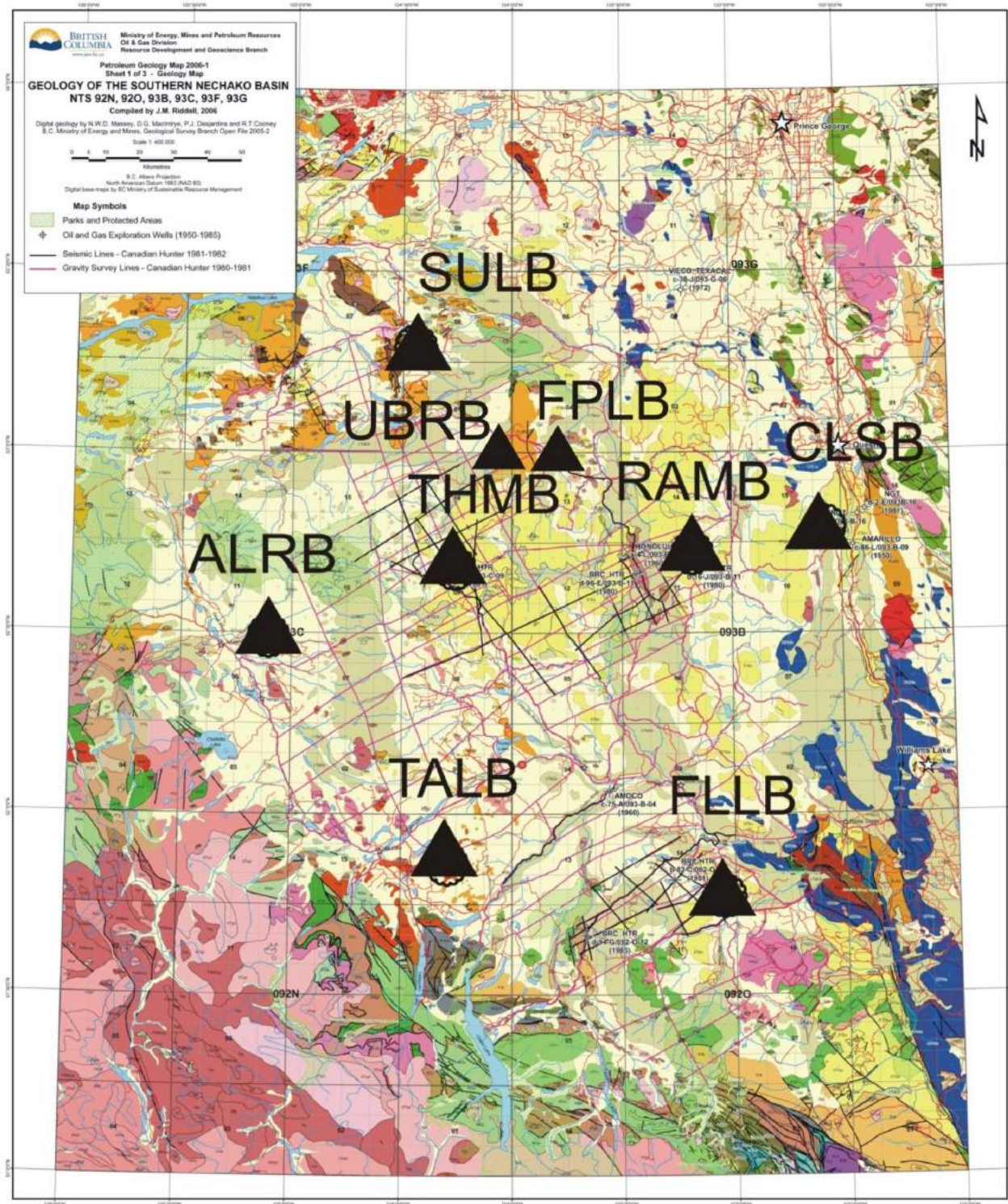


Figure 1a. Map (Riddell, 2006) of station locations (triangles), south-central British Columbia.

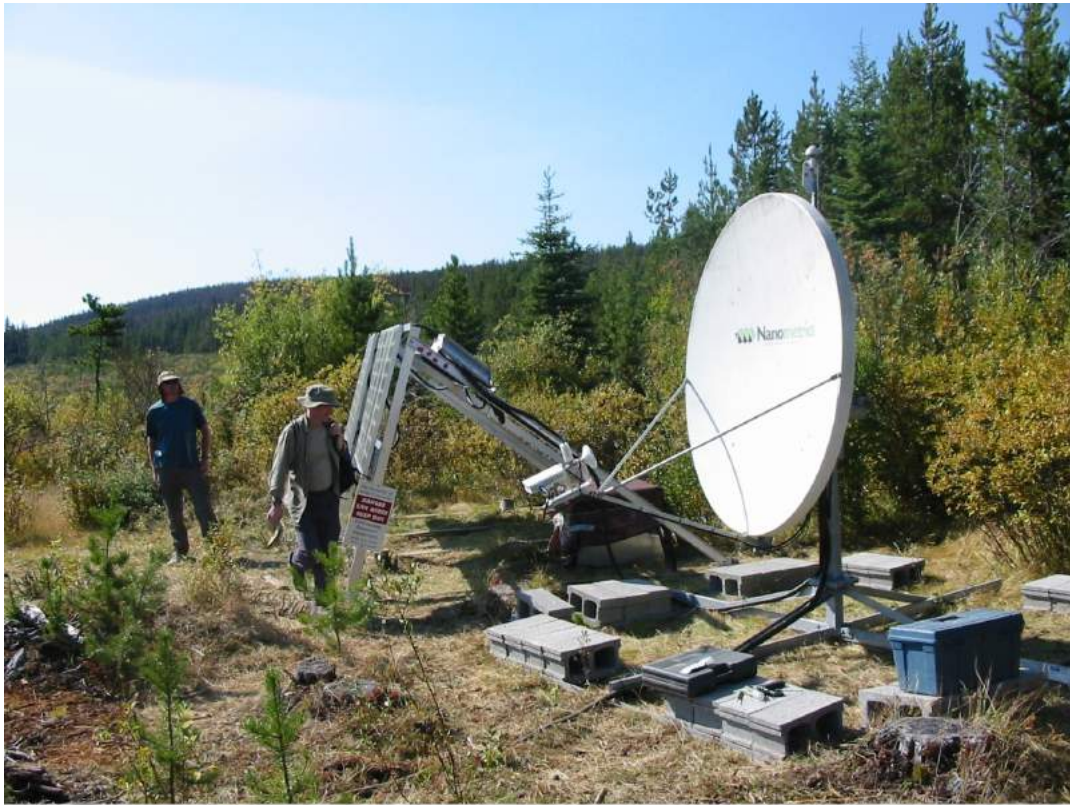


Figure 1b. A typical seismograph site (top) and topography (bottom) in south-central British Columbia. Photographs provided by I. Al-Khoubbi.

Table 1. Location, station codes and dates of operation of the broadband seismic stations in the Nechako Basin, south-central British Columbia. Stations UBRB and FPLB were deployed as a part of the Canadian National Seismograph Network in late 2007 to help monitor a swarm of earthquakes in the Anahim volcanic belt.

Seismic station location	Code	Latitude	Longitude	Elevation		
				(km)	Start date	End date
Anahim Lake	ALRB	52.51	-125.084	1.237	30-Aug-06	27-Aug-09
Cack lake ¹	CLSB	52.759	-122.555	0.792	09-Jan-06	26-Aug-09
Fletcher Lake	FLLB	51.739	-123.106	1.189	24-Aug-06	06-Oct-08
Southwest Quesnel	RAMB	52.632	-123.123	1.259	09-Mar-06	06-Dec-08
South of Vanderhoof	SULB	53.279	-124.358	1.171	09-May-06	25-Aug-09
Tatla Lake	TALB	52.015	-124.254	1.127	28-Aug-06	06-Nov-08
Thunder Mountain	THMB	52.549	-124.132	1.126	27-Aug-06	06-Oct-08
Upper Baezaeko River	UBRB	52.89	-124.083	1.243	20-Oct-07	
Fishpot Lake	FPLB	52.954	-123.779	1.005	22-Nov-07	06-Nov-08

¹ Unofficial place name

Data Analysis and Methodologies

Data Analysis

This is a unique, high-quality dataset, which provides new opportunities to examine the structure and tectonics of the area. A variety of data analysis methods have been utilized by researchers at several institutions to examine the Earth's structure beneath the Nechako Basin. These methods are briefly described below, primarily to highlight the advantages and applications of each and to provide references for additional information.

Receiver-Function Analysis

Receiver-function studies are being applied at each of the Nechako Basin sites to examine the S-wave velocity structure. Receiver-function studies (for details on the methodology, see Langston, 1977; Ammon, 1991; Ammon et al., 1991; Cassidy, 1992, 1995) provide site-specific information such as S-wave-velocity structure directly beneath the recording site and constraints on interface geometry (dip angle and direction of velocity discontinuities). This method is based on the conversion of P-wave to S-wave energy occurring at velocity contrasts beneath a recording site (Figure 2). The amplitude of the Ps-converted phase is related to the velocity contrast, and the arrival time of the Ps phase is related to the depth and average velocity. Receiver-function studies have proven very useful in mapping sedimentary basins in other areas of the world, including the Bohai Bay Basin of China (Zheng et al., 2005), the Rocas Verdes Basin of Patagonia, Chile (Lawrence and Wiens, 2004), and the Mississippi embayment (Julia et al., 2004). The in-

version method of Sambridge (1999) is used to quickly test thousands of Earth models to determine the model that generates synthetic waveforms which best match the observed waveforms.

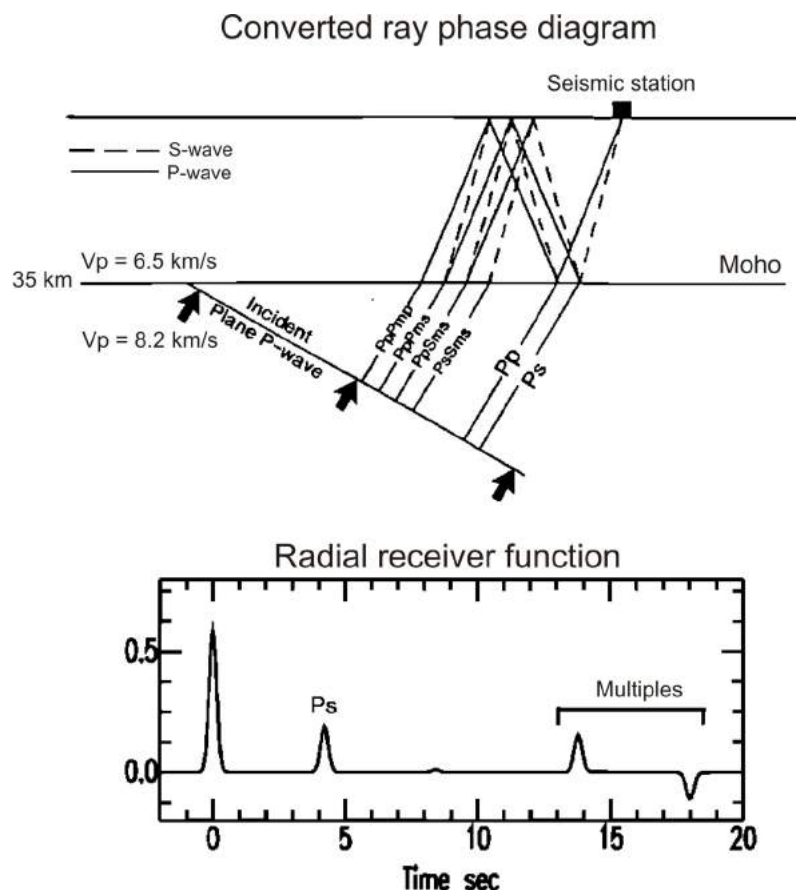


Figure 2. Schematic diagram of the receiver-function method: an incoming planar P-wave generates P-to-S conversions and free-surface multiples at velocity discontinuities beneath a recording site; through deconvolution of the vertical component from the horizontal components of shaking, receiver functions that highlight the locally generated phases can be isolated. The amplitude of the receiver function represents the ratio of the radial component of the P-wave to the vertical component of the P-wave.

Ambient Noise Tomography

Ambient ‘seismic noise’ recorded at the Nechako Basin seismic stations has been used to map the group-velocity structure and layer thickness across the basin. This technique utilizes seismic noise recorded at stations 20–100 km apart. The recordings are typically dominated by Rayleigh waves for the vertical components of the data and all possible station combinations are utilized to compute dispersion curves. Inversion techniques are applied to the dispersion curves to constrain the average group-velocity structure between stations. This complements the site-specific models derived from receiver functions. By combining all possible ‘station-pairs’ a 3-D image of the basin structure can be obtained. Details of this methodology and applications to other sedimentary basins are described in Sabra et al. (2005), Shapiro et al. (2005) and Bensen et al. (2007).

Regional P-Wave Tomography

The arrival times of P- and S-waves from distant earthquakes made at permanent and temporary seismic stations deployed in western Canada can be used to map the velocity structure of the crust and mantle to depths of 500–700 km. With the deployment of temporary networks such as the Nechako array, the Batholiths array and the Canoe array (see Mercier et al., 2009), high-resolution models can be developed across large portions of western Canada. Details on the methodology are provided in VanDecar (1991) and Mercier et al. (2009), and the results of this study are described below.

SKS-Splitting Studies

Seismic anisotropy of the upper mantle has been documented in a wide range of tectonic settings worldwide. Mantle anisotropy is generally attributed to shear deformation and the alignment of olivine crystals, which is often associated with mantle flow patterns. Shear-wave splitting measurements using SKS phases recorded at stations in the Nechako Basin are being used to map mantle anisotropy in this region. For details of this analysis method and data processing, see Silver and Chan (1991) and Currie et al. (2004).

Results

Ambient Noise Tomography

Ambient noise data recorded by 12 POLARIS and CNSN seismic stations between September 2006 and November 2007 were utilized to map the thickness of sediments, volcanic cover and crustal thickness (e.g., Figure 3) across central BC (Idowu, 2009). As a two-station method was used, the results represent an average thickness between each pair of stations considered. The ambient noise and resulting Green’s functions are dominated by Rayleigh waves. Dispersion curves for the Rayleigh waves were computed and an inversion method was applied to produce

2-D group-velocity maps between 0.03 and 0.55 Hz and 1-D S-velocity models for the Nechako Basin and surrounding region. The average 1-D model within the basin was indicative of a six-layered medium: surface/near surface sediment (~1.8 km), volcanic rock (~0.6 km), the sedimentary basin (~2.0 km), the Precambrian basement (~9.1 km), the lower crust (~17.0 km) and the upper mantle. The average 1-D model outside the basin is similar to the model within the basin, except that the volcanic and sedimentary layers are absent. Zones of low group-velocity structures within the area suggest that the region consists of a major deep and laterally extensive sedimentary package at the basin centre, and a shallow sedimentary package at the southern edge of the Nechako Basin. Detailed results are presented in Idowu (2009) and Idowu et al. (work in progress, 2010).

Receiver Functions

Teleseismic receiver functions have been computed for all stations in the Nechako Basin. These data cover a wide azimuthal and distance range and allow for resolution of dipping structure and interface geometry. For example, the obvious differences in receiver functions between stations (Figure 4) require significant variations in sediment thickness and crustal structure across the basin.

Site-specific models are currently being developed for each site. An example is provided for the station SULB (Figure 5). The observed receiver functions from a range of directions (BAZ) and distances (DIST) are compared with predicted receiver functions (Figure 5, left) using the ‘best-fitting’ model developed (Figure 5, right). These receiver functions are the simplest of all the Nechako Basin sites. The key features required by the data are a continental Moho near 35 km depth, a low-velocity surface layer about 1 km thick and a low-velocity zone in the lower crust. Each of these features was required, regardless of the combination of receiver-function data that were inverted, or the variety of inversions attempted. At this station there is no clear evidence for the volcanic layer, or sediments beneath the volcanic rocks. These layers may not be present at this station, or they may be too thin to resolve (<0.5–1 km) using this dataset.

Regional P-Wave Tomography

A regional-scale study utilizing recordings of distant earthquakes made at all CNSN stations, the Nechako seismic stations and other temporary deployments was recently completed by Mercier et al. (2009). Recordings of 1609 earthquakes made at 234 seismic stations (Figure 1 of Mercier et al., 2009) were used to map the P- and S-wave velocity structure across all of western Canada. One of the most prominent and interesting features is a low-velocity zone imaged beneath the Anahim volcanic belt (the east-west line shown in Figure 6). This low-velocity zone extends from the Nazko cone (the most recent of the volcanic cones in this belt) seaward, and is imaged into the mantle to

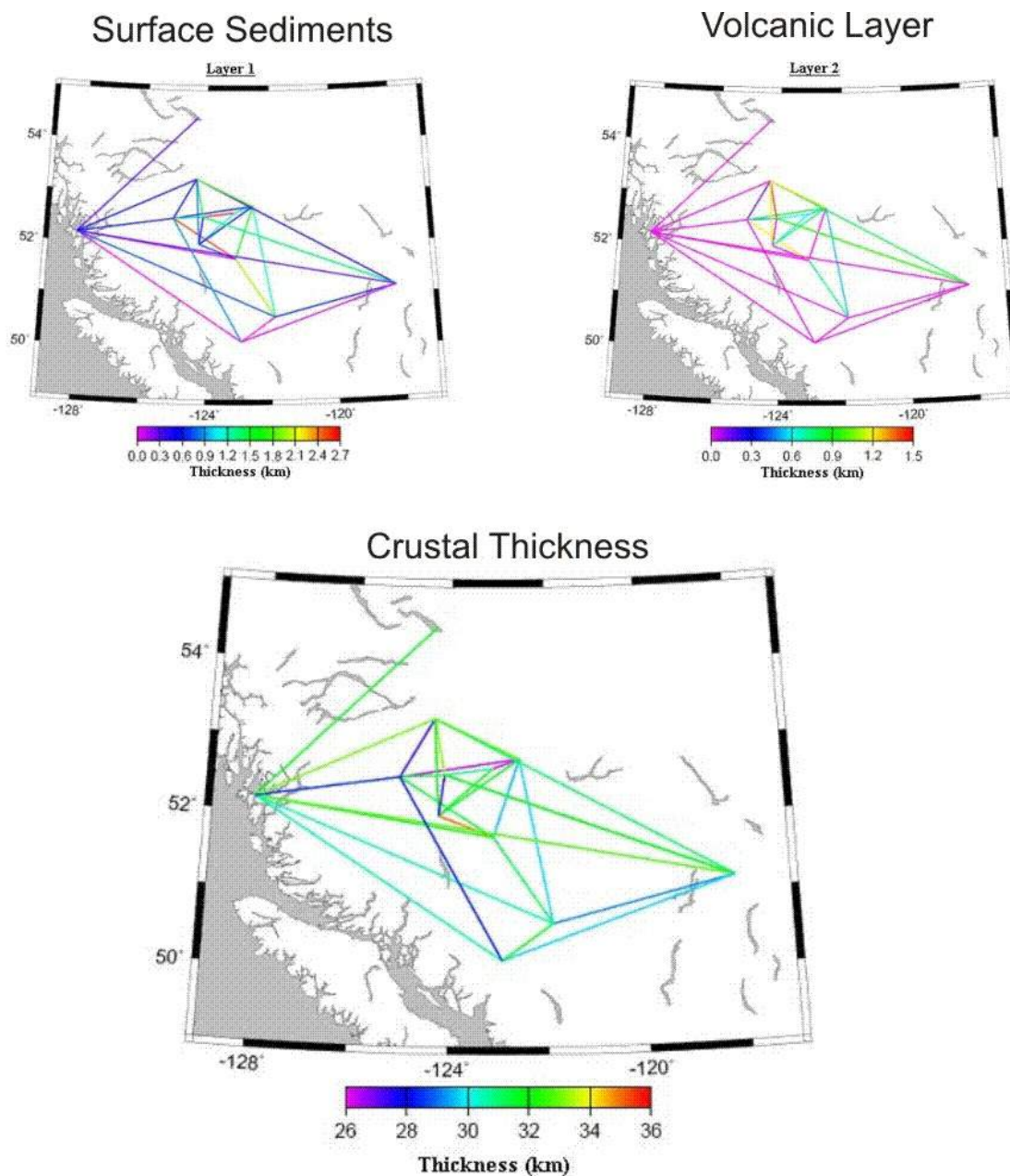


Figure 3. Average thickness of sediments, volcanic layer and crust beneath the Nechako Basin, south-central British Columbia, based on ambient noise data.

depths of about 400 km (Figure 6). This is consistent with a deep magma source and mantle-scale processes in the region of the Anahim volcanic belt.

SKS-Splitting Studies

Seismic data recorded at two temporary arrays—‘Batholiths’ extending from the coast near Bella Bella to Anahim Lake in the Nechako Basin and the POLARIS stations in the Nechako Basin—were examined for teleseismic (SKS) shear-wave splitting. Energy-minimization methods in the SplitLab software package were used to analyze the

SKS phases (Zandt et al., 2009). There is a very clear pattern of east-west-oriented splitting from the west coast through the Nechako Basin (Figure 7). This pattern does not fit the northwest-oriented structural fabric, but is consistent with upwelling and asthenospheric flow around the northern edge of the subducting Explorer plate (see Audet et al., 2008). Detailed analysis of this pattern is presented in Zandt et al. (2009) and other studies are currently underway (A. Frassetto, work in progress, 2010; A. Frassetto et al., work in progress, 2010).

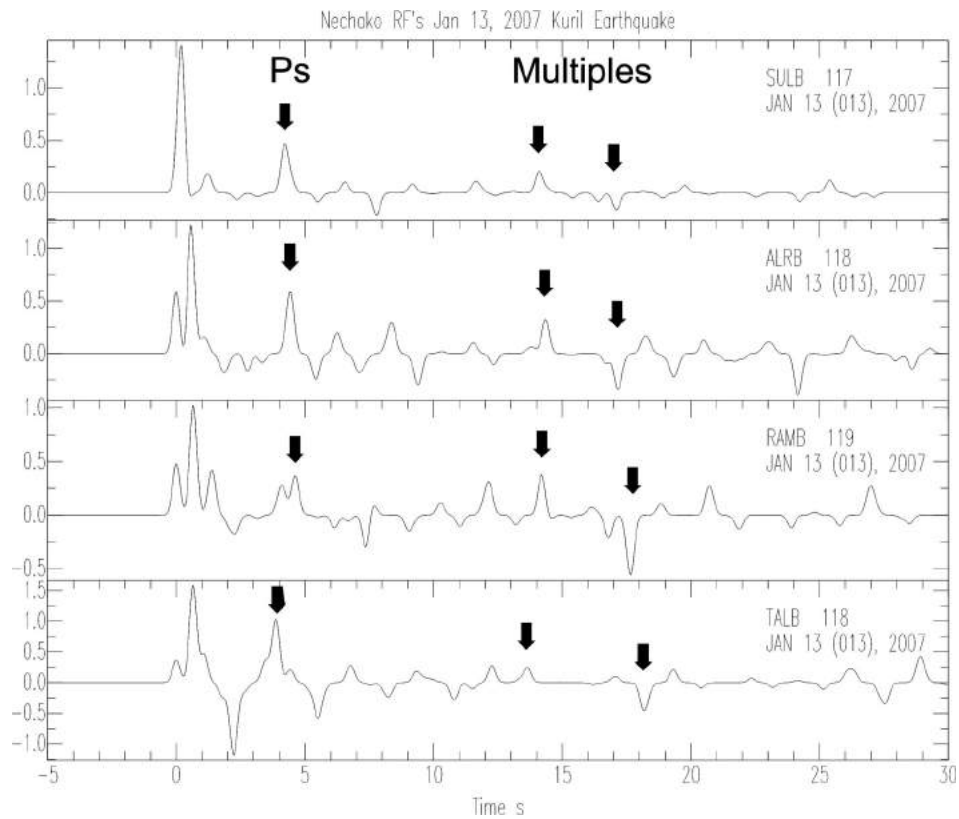


Figure 4. Sample receiver functions across the Nechako Basin, south-central British Columbia. Note the significant differences in the character of the waveforms, especially in the first 1–3 seconds ($T = 0\text{--}3$ s). Arrows highlight the interpreted Ps conversion associated with the continental Moho (near $T = 4$ s) and free-surface multiples ($T = 13\text{--}18$ s). The amplitude of the receiver function represents the ratio of the radial component of the P-wave to the vertical component of the P-wave.

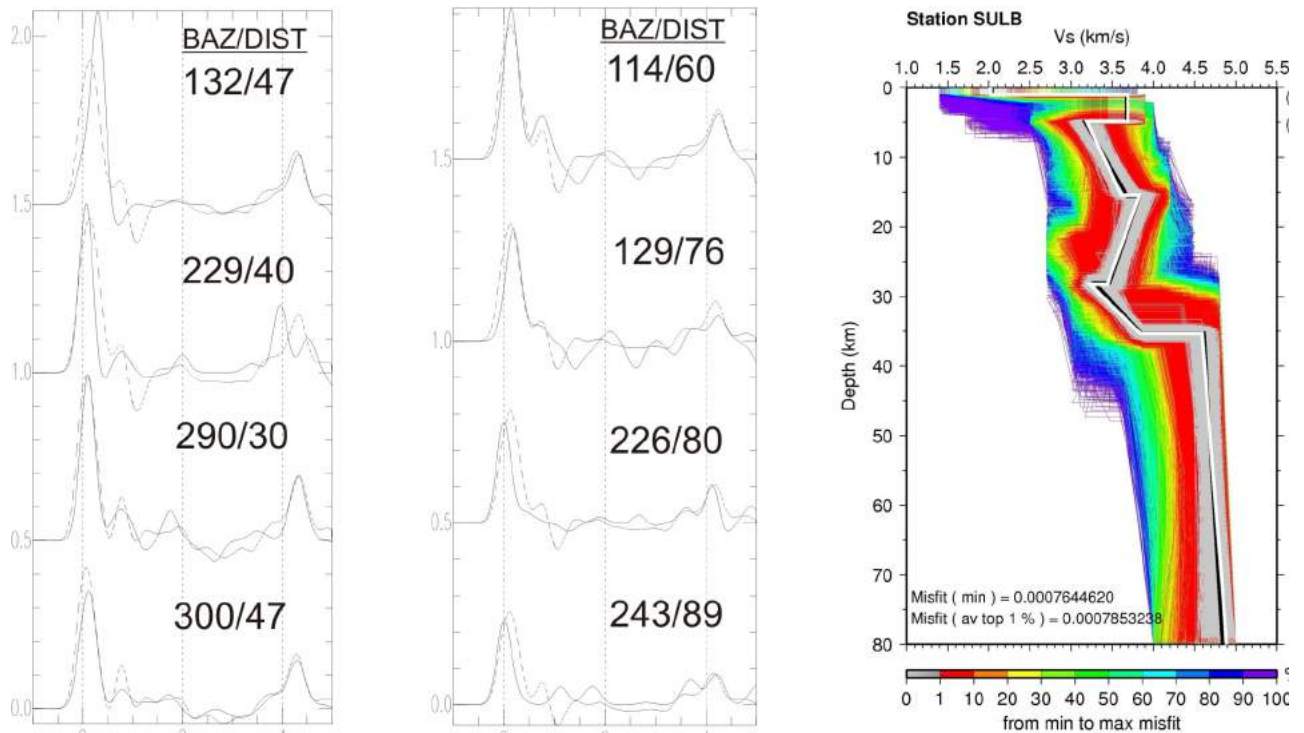


Figure 5. Receiver-function modelling at SULB: solid lines are observed receiver functions, dashed lines are synthetic receiver functions generated using the 'best-fit' model. The 3000 Earth models that were explored in this inversion modelling process are shown to the right. The minimum misfit (best) model is the white line. The amplitude of the receiver function represents the ratio of the radial component of the P-wave to the vertical component of the P-wave.

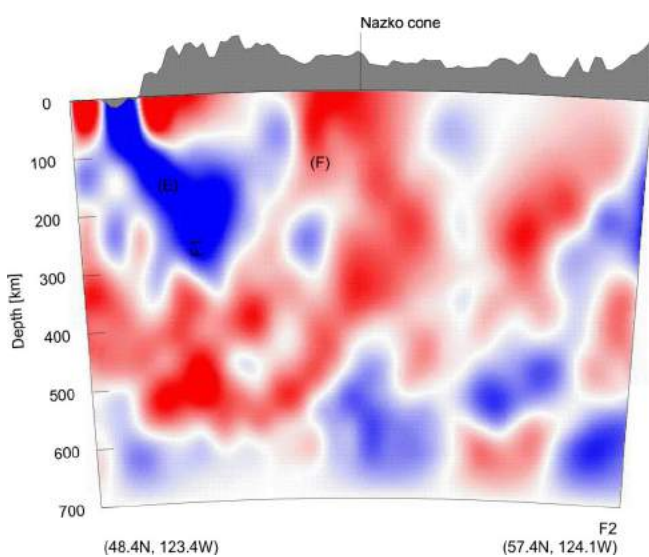
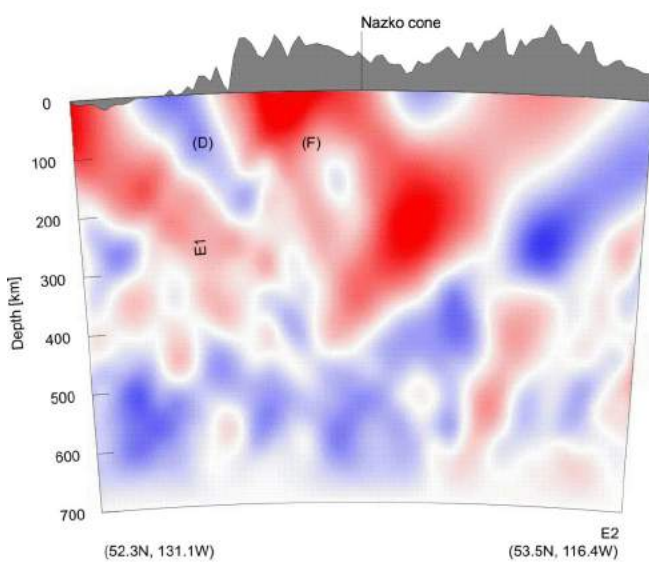
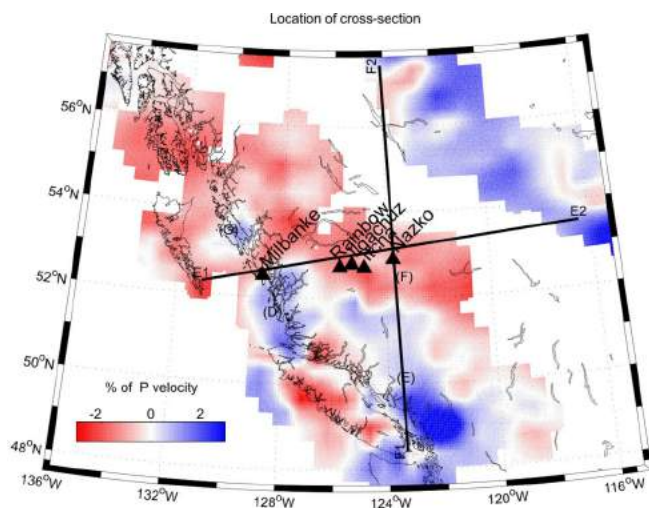


Figure 6. Tomographic P-velocity model across British Columbia, showing the low-velocity zone (red) in the upper mantle beneath central BC (east-west line), including the Nechako Basin and the Nazko cone.

Current and Future Work and Applications to Resource Assessment

A number of research activities utilizing Nechako Basin POLARIS data are ongoing. By early 2010, the receiver-function study will be completed. This will provide site-specific S-wave velocity models for each of the POLARIS stations. These models will be compared with the tomographic results from the ambient noise study (Idowu, 2009), and with gravity, magnetotelluric and seismic reflection datasets to help map the structure and geometry of the Nechako Basin. Specific results that will benefit the exploration community include estimates of sediment thickness, basin geometry, P-wave and S-wave velocities for various units, and Poisson's ratio (useful for constraining lithology, fractures and porosity). In addition, a detailed SKS study (Zandt et al., 2009) and a tomographic study (Mercier et al., 2009) of the upper mantle help to better understand mantle flow patterns, especially in relationship to volcanism in the area. Seismic data from this project have also been used for assessing the Nechako Basin earthquake swarm and volcanic hazards (Cassidy et al., work in progress, 2010).

Acknowledgments

The authors gratefully acknowledge the financial support of the BC Ministry of Energy, Mines, and Petroleum Resources, the Geological Survey of Canada and Geoscience BC in deploying and operating this seismic network. I. Al-Khoubbi is thanked for his key role in deploying and maintaining this seismic network, J. McCutcheon of the University of Manitoba and S. Williams of the Geological Survey of Canada for their assistance in deploying instruments, I. Asudeh and the POLARIS team for helping to maintain this network, and staff of the Canadian Hazards Information Service for archiving these data.

Natural Resources Canada, Earth Sciences Sector contribution 20090239.

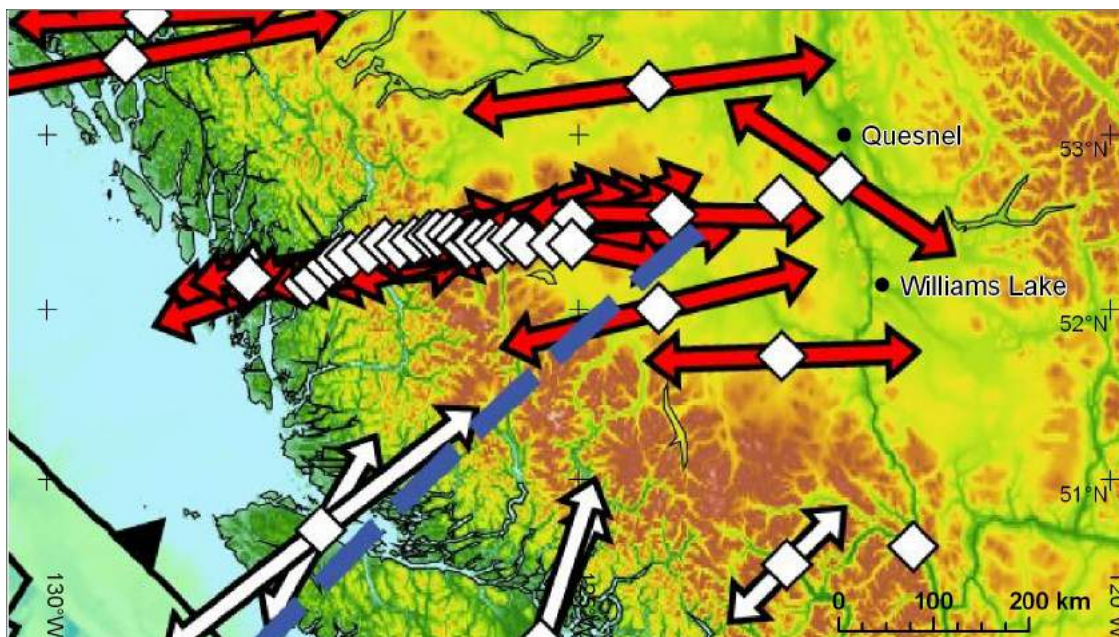


Figure 7. SKS results across the batholiths corridor and Nechako Basin (modified from Zandt et al., 2009), south-central British Columbia. White diamonds indicate seismic station locations, red arrows indicate the fast direction for SKS derived by Zandt et al. (2009) and blue dashes indicate the northern end of the subduction zone.

References

- Ammon, C.J. (1991): The isolation of receiver effects from teleseismic P waveforms; *Bulletin of the Seismological Society of America*, v. 81, p. 2504–2510.
- Ammon, C.J., Randall, G.E. and Zandt, G. (1991): On the non-uniqueness of receiver function inversions; *Journal of Geophysical Research*, v. 95, p. 15 303–15 318.
- Audet, P., Bostock, M.G., Mercier, J-P. and Cassidy, J.F. (2008): Morphology of the Explorer/Juan de Fuca slab edge in Northern Cascadia: imaging plate capture at a ridge-trench-transform triple junction; *Geology*, v. 36, p. 895–898, doi:10.1130/G25356A.1.
- Bensen, G.D., Ritzwoller, M.H., Barmin, M.P., Levshin, A.L., Lin, F., Moschetti, M.P., Shapiro, N.M. and Yang, Y. (2007): Processing seismic ambient noise data to obtain reliable broadband surface wave dispersion measurements; *Geophysical Journal International*, v. 169, p. 1239–1260.
- Cassidy, J.F. (1992): Numerical experiments in broadband receiver function analysis; *Bulletin of the Seismological Society of America*, v. 82, p. 1453–1474.
- Cassidy, J.F. (1995): A comparison of the receiver structure beneath stations of the Canadian National Seismograph Network; *Canadian Journal of Earth Sciences*, v. 32, p. 938–951.
- Currie, C.A., Cassidy, J.F., Hyndman, R.D. and Bostock, M.G. (2004): Shear wave anisotropy beneath the Cascadia Subduction Zone and western North American craton; *Geophysical Journal International*, v. 157, p. 341–353, doi: 10.1111/j.1365-246X.2004.02175.x.
- Idowu, O. (2009): Surface wave tomography of the Nechako Basin, British Columbia, using ambient seismic noise; M.Sc. thesis, University of Manitoba, 221 p.
- Julia, J., Herrmann, R.B., Ammon, C.J. and Akinci, A. (2004): Evaluation of deep sediment velocity structure in the New Madrid seismic zone; *Bulletin of the Seismological Society of America*, v. 94, p. 334–340.
- Langston, C. (1977): The effect of planar dipping structure on source and receiver responses for constant ray parameter; *Bulletin of the Seismological Society of America*, v. 67, p. 1029–1050.
- Lawrence, J.F. and Wiens, D.A. (2004): Combined receiver-function and surface wave phase-velocity inversion using a niching genetic algorithm: application to Patagonia; *Bulletin of the Seismological Society of America*, v. 94, p. 977–987.
- Mercier, J-P., Bostock, M.G., Cassidy, J.F., Dueker, K., Gaherty, J.B., Garnero, E.J., Revenaugh, J. and Zandt, G. (2009): Body-wave tomography of western Canada; *Tectonophysics*, v. 475, no. 3–4, p. 480–492, doi: 10.1016/j.tecto.2009.05.030.
- Riddell, J.M. (2006): Geology of the southern Nechako Basin NTS 92N, 92O, 93B, 93C, 93F, 93G; BC Ministry of Energy, Mines and Petroleum Resources, Petroleum Geology Map 2006-1, 3 sheets at 1:400 000 scale.
- Sabra, K.G., Gerstoft, P., Roux, P., Kuperman, W.A. and Fehler, M.C. (2005): Surface wave tomography from microseisms in southern California; *Geophysical Research Letters*, v. 32, L14311, doi: 10.1029/2005GL023155.
- Sambridge, M. (1999): Geophysical inversion with a neighbourhood algorithm—I. Searching a parameter space; *Geophysical Journal International*, v. 138, no. 2, p. 479–494.
- Shapiro, M.C., Campillo, M., Stehly, L. and Ritzwoller, M.H. (2005): High-resolution surface wave tomography from ambient seismic noise; *Science*, v. 307, no. 5715, p. 1615–1618, doi: 10.1126/science.1108339.
- Silver, P.G. and Chan, W.W. (1991): Shear wave splitting and sub continental mantle deformation; *Journal of Geophysical Research*, v. 96, p. 16 429–16 454.

VanDecar, J. (1991): Upper-mantle structure of the Cascadia subduction zone from nonlinear teleseismic travel-time inversion; Ph.D. thesis, University of Washington.

Zandt, G., Frassetto, A.M., Cassidy, J.F. and Bostock, M.G. (2009): Regional variations of mantle anisotropy across the Cana-

dian Cordillera from teleseismic shear-wave splitting (abstract); EOS, Transactions, American Geophysical Union.

Zheng, T., Zhao, L. and Chen, L. (2005): A detailed receiver function image of the sedimentary structure of the Bohai Bay Basin; Physics of the Earth and Planetary Interiors, v. 152, p. 129–143.

Horn River Basin Aquifer Characterization Project, Northeastern British Columbia (NTS 094I, J, O, P): Progress Report

B.J.R. Hayes, Petrel Robertson Consulting Ltd., Calgary, AB, bhayes@petrelrob.com

Hayes, B.J.R. (2010): Horn River Basin aquifer characterization project, northeastern British Columbia (NTS 094I, J, O, P): progress report; in Geoscience BC Summary of Activities 2009, Geoscience BC, Report 2010-1, p. 245–248.

Introduction

Devonian shale units of the Horn River Basin (HRB) in northeastern British Columbia are the focus of one of the leading shale gas plays in North America. Economic gas production from these shale units requires drilling of up to 16 multileg horizontal wells from a single drilling pad, and conducting up to 16 staged hydraulic fracture stimulation (frac) jobs in each horizontal leg. Each frac injects up to 4000 m³ of water into the reservoir, along with chemicals and proppants (generally high-grade silica sands) to ensure that the rock is effectively fractured, and that fractures remain open. Upon completion, the well flows back some of this water, contaminated by the injected chemicals.

Thousands of wells will be drilled to fully develop the HRB shale gas play. Enormous volumes of water will be required for reservoir stimulation (fracing) and safe disposal must be ensured for equally huge volumes of produced water. Deep subsurface aquifers, carrying nonpotable water and lying far below the water table and domestic water wells, represent ideal sources and sinks for the water volumes required. Shallower aquifers, such as buried valley fills associated with Quaternary glaciation and drainage, are less desirable targets, as there is less separation from surface and well waters. Surface water may serve as isolated, short-term water sources, but surface disposal of frac fluids will not be contemplated.

The petroleum industry is in its infancy in the HRB, and so suffers from lack of well control and other information to support characterization of subsurface aquifers. While numerous wells have been drilled on the basin margins for conventional gas reservoirs, there are relatively few wells in the basin proper, and large areas remain virtually undrilled. New wells target the Devonian gas shale units, and most new geological studies have focused on their reservoir characteristics. Within the past year, however, many

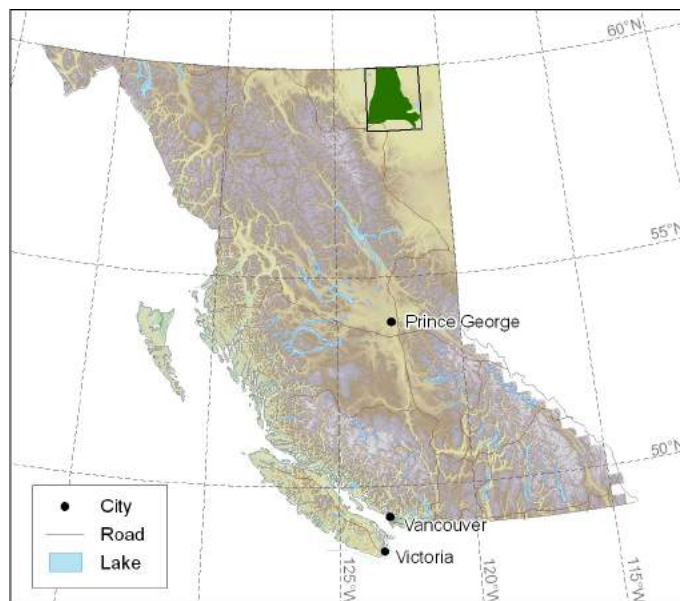


Figure 1. Location map showing the Horn River Basin (in green) and study area (outlined in black), northeastern British Columbia.

industry operators have begun to drill water-source and disposal wells on their properties, and are working toward understanding subsurface aquifers as potential water sources and sinks.

To determine whether subsurface aquifers have sufficient water volumes and flow capacity to support long-term development in the HRB, comprehensive regional mapping and reservoir characterization is required. The Horn River Basin Producers Group (HRBPG), a consortium of industry operators, recognized this issue in 2008, and asked Geoscience BC to undertake such a study. Geoscience BC commissioned Petrel Robertson Consulting Ltd. (PRCL) to develop a project workplan, manage the collection of test data from new HRBPG wells, undertake the required technical work, and to produce a report summarizing the findings.

Regional Setting

The HRB lies in northeastern BC, and is bounded to the east and south by Devonian carbonate platforms (Figure 1). The

Keywords: Horn River Basin, shale gas, Muskwa Member, Debolt Formation, Rundle Group, Mattson Formation, Gething Formation, Bluesky Formation, aquifer, hydrostratigraphic unit

This publication is also available, free of charge, as colour digital files in Adobe Acrobat® PDF format from the Geoscience BC website: <http://www.geosciencebc.com/s/DataReleases.asp>.

Bovie fault zone (BFZ), a major structural feature, separates the HRB from the Liard Basin to the west. The HRB continues northward into the Northwest Territories, but land, infrastructure and regulatory issues confine oil and gas activity to the BC portion (Moore, 1993).

Shale gas targets of the HRB occur in the siliceous, organic-rich Evie and Muskwa shale members of the Middle to Upper Devonian Horn River Formation. Westward and northward of the Devonian carbonate platform margins, the Horn River Formation forms the basal part of a thick Devonian–Mississippian shale section (Figure 2; Moore, 1993). Stacked carbonate ramps and/or platforms of the Mississippian Rundle Group and Debolt Formation prograde across the Horn River Basin, passing basinward into the Prophet and Besa River formations to the west and north (Richards et al., 1993). Cretaceous Buckinghorse Formation shale units lie unconformably on the Mississippian carbonate rocks, except on the southern and eastern margins of the basin, where basal Cretaceous sandstone units are assigned to the Bluesky and Gething formations, respectively. Quaternary glacial deposits up to 100–150 m in thickness cap the Buckinghorse Formation shale units and Upper Cretaceous Dunvegan Formation sandstone and conglomerate units, which are preserved locally (Figure 2; Stott, 1982).

Westward across the BFZ, the top of the Mississippian carbonate ramp drops approximately 1000 m, and the overlying section thickens correspondingly (Figure 2; Monahan,

1999). The uppermost Mississippian Mattson Formation, a sand-dominated deltaic succession, lies on the carbonate platform above transgressive Golata Formation shale units, and thickens rapidly westward from the BFZ to a maximum thickness of several hundred metres. Chert and sandstone units of the Permian Fantasque Formation cap an unconformity overlying the Mattson Formation. The Triassic Toad and Grayling formations are primarily siltstone and shale equivalents to the Montney Formation of the Peace River area (Monahan, 1999). Overlying the pre-Cretaceous unconformity is the basal Chinkeh Formation sandstone, succeeded by Cretaceous shale units, themselves punctuated by widespread, generally low-quality sandstone units of the Scatter and Sikanni formations (Leckie et al., 1991; Leckie and Potocki, 1998).

Methodology

Stratigraphic mapping and reservoir characterization were supported by interpretation of well logs, cores, sample cuttings and well test data. The HRB well database comprises all available wells penetrating the pre-Cretaceous unconformity in the study area, 556 wells in total.

To establish a stratigraphic framework, 16 regional cross-sections were constructed (Figure 3), establishing correlations from the literature and previous studies, and calibrating them with observations from cores and sample cuttings. Logs from each well were tied to the cross-section grid to interpret stratigraphic tops. All cores that appeared to provide significant reservoir or stratigraphic information were

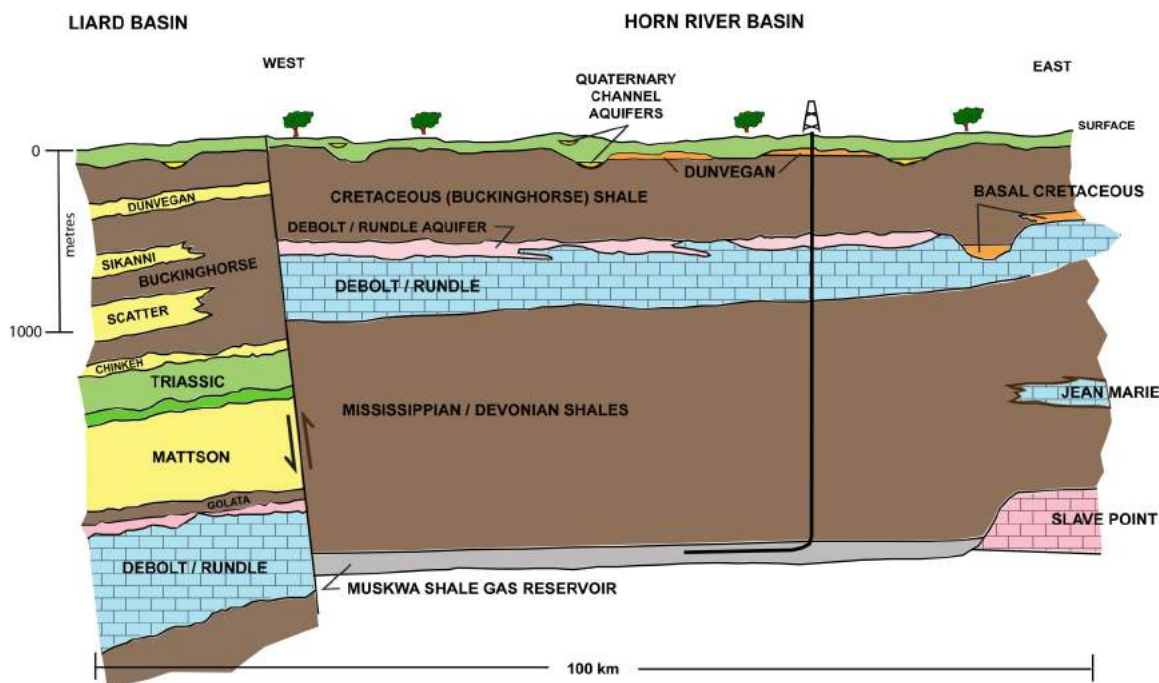


Figure 2. Schematic stratigraphic cross-section, Horn River Basin and adjacent Liard Basin, northeastern British Columbia.

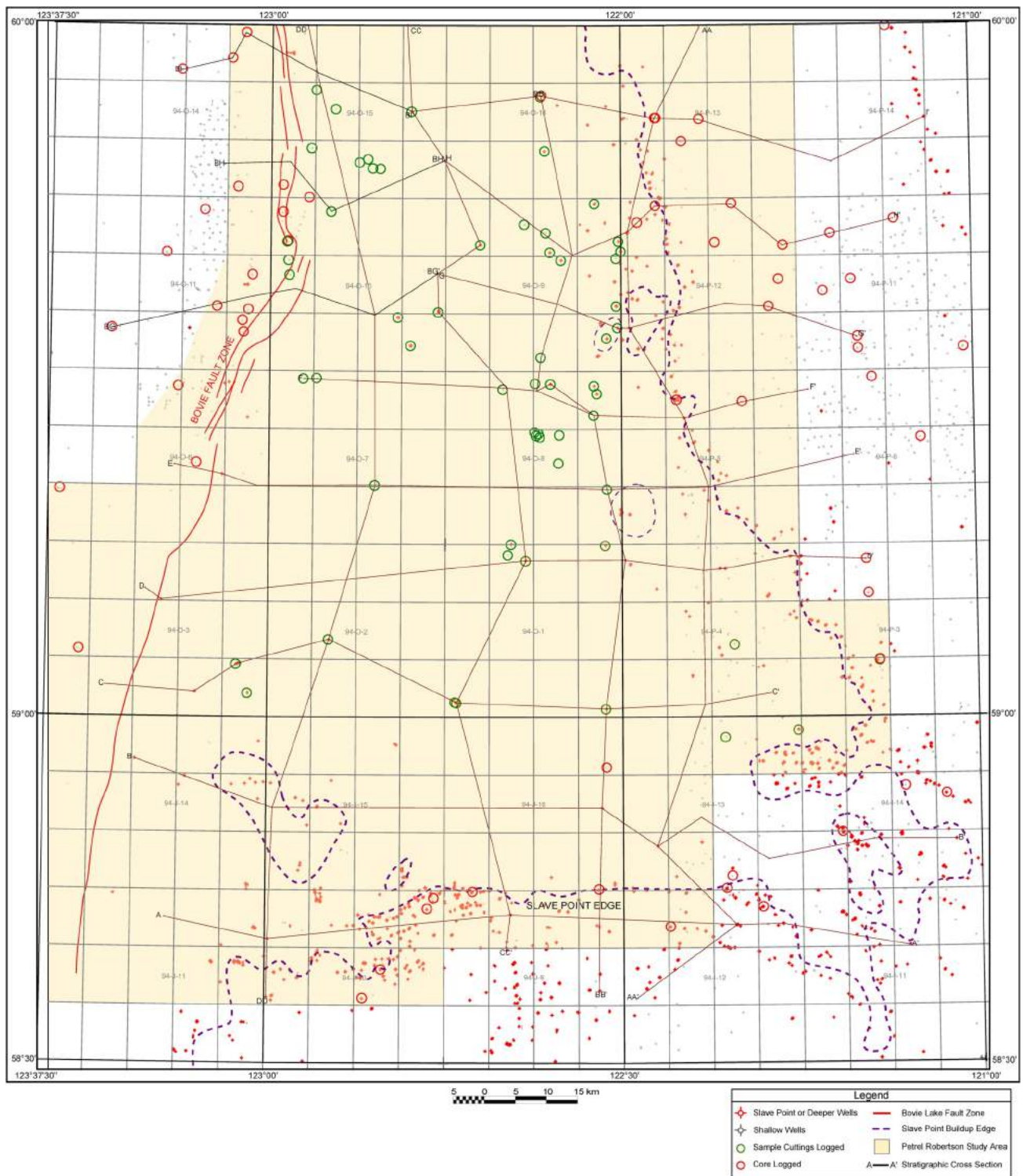


Figure 3. Locations of cross-sections, core logs and sample cuttings logs, Horn River Basin, northeastern British Columbia.

examined; however, very few cores were cut in Mississippian carbonate rocks within the HRB proper, and there is essentially no representation of the uppermost carbonate sections. Core coverage of Mattson Formation reservoirs to the west is similarly scanty.

A project was therefore commissioned to systematically examine and document drill cuttings from Mississippian carbonate rocks throughout the HRB, and from Mattson Formation sandstone sections near HRBPG lands in the west. JC Consulting Inc. examined cuttings across the pro-

spective section in relevant wells, and performed semiquantitative estimates of reservoir porosity and permeability. JMS Geological Consulting prepared samples for standard petrography, scanning electron microscope (SEM) imaging and X-ray diffraction (XRD) analysis, to provide additional reservoir characterization information.

Regional hydrostratigraphy and flow characteristics were examined by Canadian Discovery Ltd., which compiled available well test data, including flow and injectivity test data supplied by HRBPG members on their new water-source wells within the basin.

Incorporating all these data and interpretations, PRCL produced regional maps of key stratigraphic surfaces and intervals throughout the aquifer section. Core and sample data were tied to logs to estimate reservoir quality, which was also systematically mapped. Finally, reservoir maps were combined with hydrogeological interpretations to generate a basin-scale aquifer characterization of each key unit.

Preliminary Results

Project results are scheduled for release to HRBPG members in late 2009, and will be held confidential for a period of time to protect the confidentiality of data supplied to the project. However, a few general observations can be made at this point:

Mississippian platform carbonate rocks (Debolt Formation/Rundle Group) show good aquifer potential in many areas of the Horn River Basin. The best and most continuous reservoir quality is found immediately beneath the pre-Cretaceous unconformity, where solution and dolomitization is most consistently developed. There are clear stratigraphic controls on the distribution of these aquifer rocks.

Uppermost Mississippian clastic rocks of the Mattson Formation thicken rapidly west of the Bovie fault zone

on the western flank of the Horn River Basin, and provide locally good aquifer potential in that area.

Cretaceous valley fill (Gething Formation) and shoreface (Bluesky Formation) sandstone units exhibit lower grade aquifer potential along the eastern and southeastern flanks of the basin. Similarly, basal Cretaceous Chinkeh Formation sandstone units on the western side of the Bovie fault zone offer lower grade aquifer potential.

References

- Leckie, D.A. and Potocki, D.J. (1998): Stratigraphy and petrography of marine shelf sandstones of the Cretaceous Scatter and Garbutt formations, Liard Basin, northern Canada; *Bulletin of Canadian Petroleum Geology*, v. 46, p. 30–50.
- Leckie, D.A., Potocki, D.J. and Visser, K. (1991): The Lower Cretaceous Chinkeh Formation: a frontier type play in the Liard Basin of western Canada; *Bulletin of the American Association of Petroleum Geologists*, v. 75, p. 1324–1352.
- Monahan, P. (1999): Stratigraphy and potential hydrocarbon objectives of Mississippian to Lower Cretaceous strata in the eastern Liard Basin area; unpublished report, BC Ministry of Energy, Mines and Petroleum Resources, 14 p.
- Moore, P.F. (1993): Devonian, Subchapter 4D; *in* Sedimentary Cover of the Craton in Canada, D.F. Stott and J.D. Aitken (ed.), Geological Survey of Canada, *Geology of Canada*, no. 5, p. 150–201.
- Richards, B.C., Bamber, E.W., Higgins, A.C. and Utting, J. (1993): Carboniferous, Subchapter 4E; *in* Sedimentary Cover of the Craton in Canada, D.F. Stott and J.D. Aitken (ed.), Geological Survey of Canada, *Geology of Canada*, no. 5, p. 202–271.
- Stott, D.F. (1982): Lower Cretaceous Fort St. John Group and Upper Cretaceous Dunvegan Formation of the Foothills and Plains of Alberta, British Columbia, District of Mackenzie and Yukon Territory; Geological Survey of Canada, *Bulletin* 328, 124 p.

Biostratigraphic and Sedimentological Studies of Natural Gas-Bearing Triassic Strata in the Halfway River Map Area (NTS 094B), Northeastern British Columbia: Progress Report

M.L. Golding, University of British Columbia, Vancouver, BC, mgolding@eos.ubc.ca

F. Ferri, Resource Development and Geoscience Branch, Oil and Gas Division, British Columbia Ministry of Energy, Mines and Petroleum Resources, Victoria, BC

J.K. Mortensen, University of British Columbia, Vancouver, BC

J-P. Zonneveld, University of Alberta, Edmonton, AB

M.J. Orchard, Geological Survey of Canada Pacific, Natural Resources Canada, Vancouver, BC

Golding, M.L., Ferri, F., Mortensen, J.K., Zonneveld, J-P. and Orchard, M.J. (2010): Biostratigraphic and sedimentological studies of natural gas-bearing Triassic strata in the Halfway River map area (NTS 094B), northeastern British Columbia: progress report; *in* Geoscience BC Summary of Activities 2009, Geoscience BC, Report 2010-1, p. 249–258.

Introduction

The western part of the Western Canada Sedimentary Basin (WCSB) in northeastern British Columbia includes one of the most complete sections of Triassic strata found anywhere in the world (e.g., Gibson and Barclay, 1989; Gordey et al., 1991; Davies, 1997). This sequence represents an important source of hydrocarbons, and is thought to contain more than 37% of BC's conventional gas reserves. Although there is currently a high level of industry interest in the Triassic package in northeastern BC, much of this region remains significantly underexplored due to difficulties in accessibility and a lack of available infrastructure. The current exploitation success of unconventional natural gas reservoirs within the lower part of the Triassic succession is expected to significantly increase recoverable resources and further enhance the economic importance of this package within the province. In comparison to other hydrocarbon reservoir or source sequences within the WCSB, the Triassic has received very little study, and the nature and depositional setting of much of the Triassic section is not well understood.

A detailed study of Triassic strata in the Halfway River map area (NTS 094 B) in northeastern BC (Figure 1) was started with the goal of better understanding the stratigraphic and sedimentological framework, together with the paleotectonic setting of this economically important succession. This work represents a Ph.D. study by M. Golding, based at the University of British Columbia, and is being carried out

in conjunction with a multiyear BC Ministry of Energy, Mines and Petroleum Resources (MEMPR) geological mapping project in the Foothills of the Halfway River map area where the bulk of surface exposures are of Triassic age (Ferri, 2009). The current study has two main components: 1) detailed biostratigraphic characterization of the Triassic sequence, mainly using conodonts to provide age constraints; and 2) provenance studies of the Triassic units, employing both field-based sedimentology and chemical and isotopic analysis. Geoscience BC has provided funding for a one-year reconnaissance-level study of key portions of the Triassic section in the Halfway River map area. The focus of an additional two years of fieldwork, which are planned for this project, will be based in part on results of the initial scoping study.

Two weeks of fieldwork were carried out by M. Golding and F. Ferri in August of 2009. A section of Lower and Middle Triassic rocks south of the Halfway River was examined. This section was chosen by BC MEMPR to characterize Montney and Doig formations equivalent strata (the Toad and Grayling formations) in hopes of better understanding subsurface exposures of these rocks along the eastern Foothills. BC MEMPR collected samples for geochemical and geophysical testing. Vitrinite reflectance will be determined to delineate thermal maturity and several other geochemical analyses (e.g., total organic carbon, etc., by Rock Eval™) will be undertaken to determine hydrocarbon potential. Gamma-ray measurements were taken along the length of the section to allow correlation between the section and other sections in the subsurface. A detailed description of the section, local geology, and geochemical and geophysical results will be available in a BC MEMPR report later in 2010. Collected samples will also be processed for conodonts and detrital zircon geochronology to better constrain the depositional age of these units and the

Keywords: *Triassic, Western Canada Sedimentary Basin, conodont, detrital zircon, sediment provenance, Halfway River*

This publication is also available, free of charge, as colour digital files in Adobe Acrobat® PDF format from the Geoscience BC website: <http://www.geosciencebc.com/s/DataReleases.asp>.

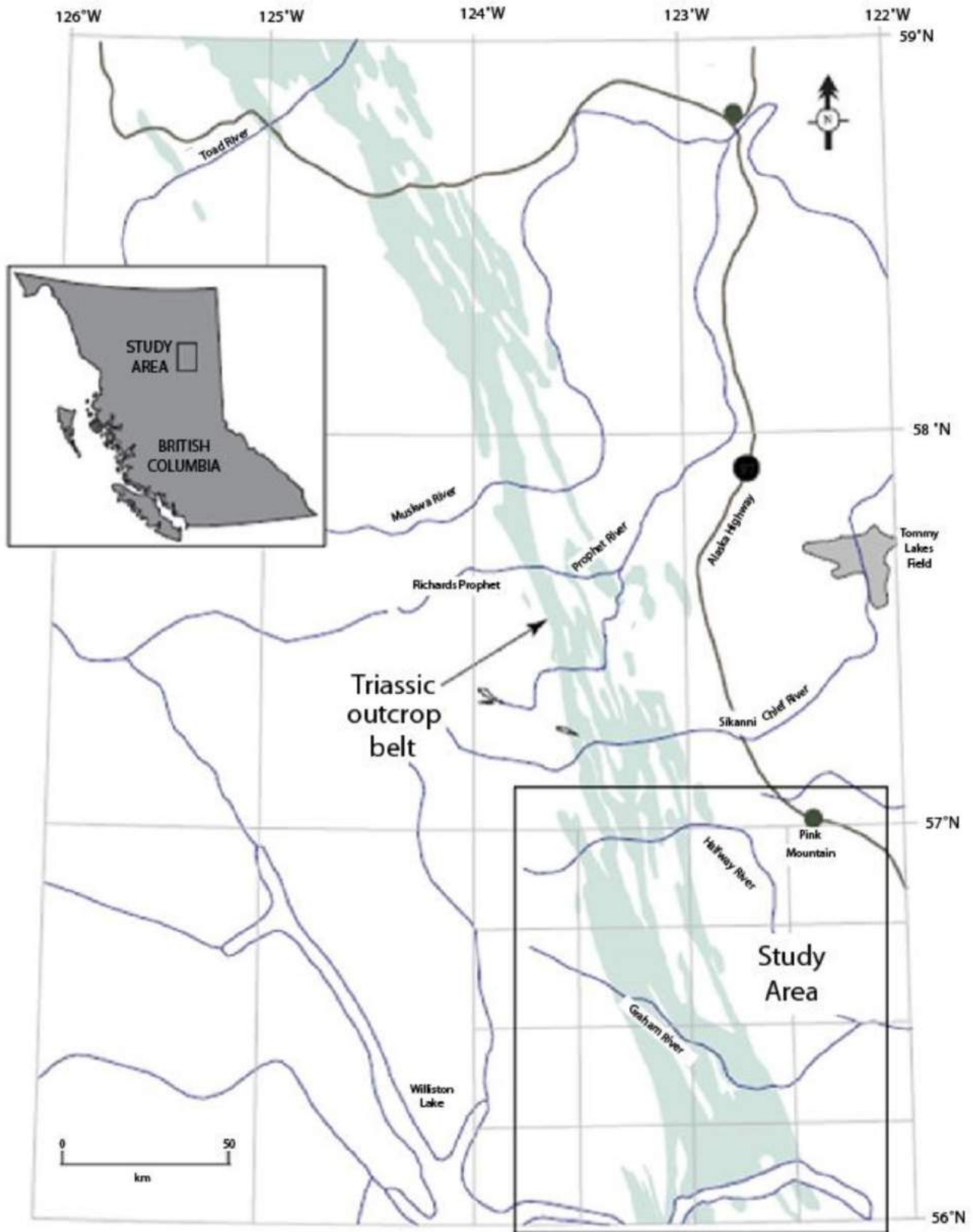


Figure 1. Location of the Halfway River study area and the distribution of economically important, potentially gas-bearing Triassic strata (pale blue) in part of northeastern British Columbia.

provenance of clastic sources. This report summarizes the progress of that investigation.

Regional Patterns of Tectonism and Sedimentation in the Triassic in the Northern Canadian Cordillera

Triassic strata in the western part of the WCSB have been shown to represent easterly derived, off-shelf sediments that were deposited along the western margin of ancestral North America (ANA; e.g., Gibson and Barclay 1989; Gordey et al., 1991; Gibson, 1993). Recent and ongoing work along the westernmost margin of ANA (representing the outer fringes of the WCSB) in northern BC and Yukon document mid to late Paleozoic extension of the margin associated with arc and back-arc development (Figure 2; Colpron et al., 2006, 2007). Geological evidence from the Yukon portion of the Cordilleran margin indicates that the Slide Mountain Ocean formed between latest Devonian and Middle Permian time as a back-arc basin east of a west-facing Yukon-Tanana Japanese-type magmatic arc (Figure 2). Pre-Late Devonian links between Yukon-Tanana and ANA have been demonstrated (Mortensen et al., 2006; Piercey and Colpron, 2009). A reversal of subduction polarity under the Yukon-Tanana arc led to the consumption of the Slide Mountain Ocean and construction of a short-lived, mainly Late Permian arc sequence that was built on the Yukon-Tanana Terrane. Final closure of the Slide Mountain Ocean in the northern Cordillera occurred in latest Permian time, at which time the pericratonic Yukon-Tanana Terrane, together with fragments of the oceanic Slide Mountain Terrane, collided with and overrode the western edge of ANA (e.g., Colpron et al., 2006; Nelson et al., 2006; Mortensen et al., 2007). Recent dating and sediment provenance studies of Triassic clastic strata in the western edge of the WCSB in the Yukon by Beranek (2009) have shown that Early to early Middle Triassic strata in this region are mainly derived from the west. These units yield detrital zircon and mica age signatures, which together with litho-geochemical and isotopic signatures, that indicate they were derived largely from erosion of the uplifted composite Yukon-Tanana/Slide Mountain block that formed the hinterland of a latest Permian to earliest Triassic collisional orogen. The Early and early Middle Triassic clastic units are interpreted to have been deposited within a foreland basin that was built on attenuated continental crust along the western edge of ANA, and were sourced dominantly from the west. By late Middle Triassic time the highland that had existed in the hinterland of this collisional orogen had largely disappeared, and Late Triassic strata were deposited as an overlap sequence that extended across both the earlier foreland and hinterland components of the collisional orogen (Mortensen et al., 2007; Beranek, 2009).

This interpretation for the Yukon portion of the WCSB is fundamentally different from previous models for the Tri-

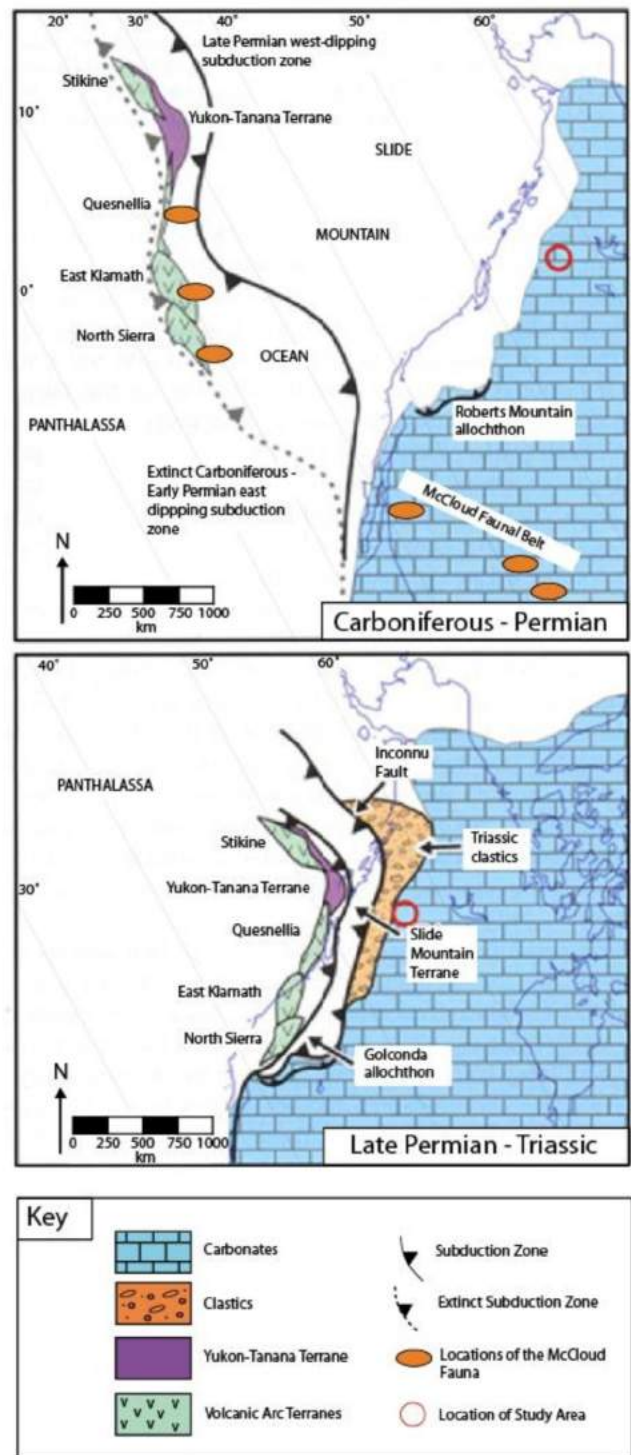


Figure 2. Tectonic interpretation of the Carboniferous to Triassic evolution of the northwestern margin of Laurentia (now northeastern British Columbia; modified from Colpron et al., 2007). Location of the Halfway River study area shown by the red circle.

assic in the northern Cordillera. The Triassic sequence is now considered to consist of two very distinct components: 1) an Early to early Middle Triassic foreland basin deposit with sediments shed mainly from a hinterland block to the west; and 2) a late Middle to Late Triassic overlap sequence

that reflects a return to a west-facing, off-shelf setting, with sediments shed mainly from the east.

The Triassic sequence in northeastern BC, which is the main focus of the current project, has received somewhat less study thus far from a paleotectonic standpoint, and it is not yet clear that the tectonic model presented above for this package also applies farther to the south. The total thickness of Triassic strata in northeastern BC is in excess of 1.5 km (e.g., Gordey et al., 1991). Paleocurrent information for the Triassic in the WCSB is limited; however, data from the eastern part indicates dominantly westerly paleoflow in at least some of the units (Gordey et al., 1991). Pelletier (1960, 1961, 1963) has recorded paleocurrents from the north and northwest within the Foothills of northeastern BC. In northeastern BC, the Triassic sequence is currently interpreted as a westward, prograding clastic-carbonate succession that was deposited, in part, on a Carboniferous to Permian rift sequence represented by the Fort St. John graben system. Sedimentological and stratigraphic studies by Zonneveld and coworkers (Zonneveld et al., 1997a, b, 2003, 2004; Zonneveld and Orchard, 2002; Zonneveld and Gingras, 2003) show anomalous thicknesses and facies distributions within Early and parts of the Middle Triassic in this region that appear to indicate that a highland lay to the west of the main depocentre and was likely the source for at least some of the sediments. Early Mississippian detrital zircon grains from early Middle Triassic strata in this area is also supportive of a western source as no igneous activity of this age is found in underlying WCSB sedimentary rocks to the east (Ferri, 2009). It is therefore considered likely that the Triassic sequence in northeastern BC reflects the same two-stage depositional history as has been documented farther north, with a change from mainly westerly derived foreland basin sedimentation to mainly easterly derived off-shelf deposition occurring somewhere in Middle Triassic time. If correct, this interpretation would be fundamentally important for assessing the regional Triassic stratigraphic framework in northeastern BC and would have implications for the ultimate gas potential of Triassic rocks in this area.

Stratigraphic and Sedimentological Relationships in the Triassic in Northeastern BC

Obduction of a composite Yukon-Tanana/Slide Mountain terrane hinterland block onto the western edge of ANA would have depressed the continental crust and led to foredeep development. Restoration of Cretaceous–Tertiary strike-slip faults in the Cordillera would place late Paleozoic ophiolite complexes and arc rocks of the Sylvester allochthon (Nelson, 1993) orthogonal to the embayment defined by Triassic rocks of the WCSB in northeastern BC, suggesting that this depositional feature may be an expression of this crustal loading. Evidence for a concurrent

forebulge may be found in the Peace River area of the western Foothills, where temporally significant unconformities in outboard settings and anomalous sediment thickness trends occur. In this area, Lower and Middle Triassic strata consist of organic-rich shale and siltstone deposited in a distal offshore depositional setting. Conodont data indicate that sedimentation rates were relatively consistent through the Early and early Middle (Anisian) Triassic.

However, there is an abrupt and profound change during the Ladinian (late Middle Triassic) when sedimentation rates drop dramatically, followed by a temporally extensive unconformity. Ladinian successions immediately to the east are significantly overthickened and comprise some of the thickest Middle Triassic successions in North America. The Middle–Upper Triassic boundary is characterized by an erosional unconformity, a switch to carbonate-dominated deposition and a dramatic increase in sedimentation rates (by at least an order of magnitude above Lower–Middle Triassic rates). Upper Triassic sedimentary rocks demonstrate an inverse relationship to that exhibited by Middle Triassic successions (i.e., grossly overthickened in the west and dramatically thinner towards the east).

The Ladinian decrease in sedimentation rates and subsequent unconformity in western Peace River localities are interpreted to reflect deposition on an early forebulge. During the Late Triassic, this forebulge is interpreted to have migrated eastwards, resulting in a thick deepwater succession of carbonate strata deposited in the west and a thin shallow-water succession of carbonate strata deposited in a proximal carbonate ramp setting farther to the east.

The dark, basinal shale, represented by the Triassic Montney, Toad and lower Sulphur Mountain formations, is interpreted to represent initial foredeep deposition prior to onset of coarser clastic sedimentation. Sedimentological constraints suggest that only eastern-sourced, continentally derived clastic rocks are preserved within the Triassic succession in northeastern BC. Indications of westerly derived clastic rocks are rare and are a reflection of poor preservation in the west. Chert granules and pebbles in coarse, Halfway Formation-equivalent sandstone within the western Foothills of the Peace River area suggest a local source. The fact that these coarse clasts are larger and more abundant towards the west may support the hypothesis that these sediments were derived from a western source.

Sediment Provenance Studies

A growing number of recent studies focus on the provenance of various sedimentary rock units within the WCSB (e.g., Garzzone et al., 1997; Ross et al., 1997; Gehrels and Ross, 1998; Mortensen et al., 2007; Beranek, 2009). Most of these studies utilize U-Pb dating of detrital zircon grains and, to a lesser extent, Ar-Ar dating of detrital mica grains (Beranek, 2009). The U-Pb age information for detrital zir-

con and monazite grains provides direct information on the age(s) of igneous rock units from which the clastic detritus was eroded, or in the case of polycyclic sediments, the ages of provenance for earlier sedimentary units that were themselves eroded and reworked. In addition, the whole rock geochemistry and Nd isotopic compositions of some rock units have been determined, and these data constrain the composition and to some extent the tectonic setting of the source rocks (e.g., magmatic arc versus rift versus ophiolite). The resulting data help constrain the general provenance of the sedimentary sequences being studied, and also provide key evidence for the regional tectonic controls on sedimentation, including nature and timing of tectonic uplift within the source area(s) as well as the nature of continent-scale drainage patterns. Results from Mesozoic and younger rock units within the Cordillera also yield important constraints on the nature and timing of terrane accretion that affected the western margin of Laurentia.

The study of Triassic clastic sedimentary units in the Yukon and adjacent parts of northern BC and eastern Alaska by Beranek (2009) also used extensive U-Pb dating of detrital zircon grains and Ar-Ar dating of detrital mica grains together with whole rock geochemical and Nd isotopic studies. In addition, conodont biochronology was used to provide biostratigraphic depositional ages. Results from this multidisciplinary study provide clear evidence for initial accretion of the inboard pericratonic terranes in this part of the Cordilleran margin in earliest Triassic time, some 60 m.y. earlier than had previously been thought (Monger and Price, 2002). These results support the earlier hypotheses of Nelson et al. (2006) and Colpron et al. (2006). A western source is evidenced by the abundance of Late Devonian to Early Mississippian and Late Permian detrital zircon grains, which can only have been derived from the middle and late Paleozoic arc assemblages in the Yukon-Tanana Terrane, as well as by the presence of a geochemical component in the fine-grained clastic units that must have come from a mafic source terrane (most probably the Slide Mountain Terrane). In the absence of definitive paleocurrent evidence, which is only rarely preserved within the Triassic clastic units, provenance information such as described above is the only way to demonstrate the source(s) from which a sedimentary unit was derived. Initial detrital zircon dating studies for the lower part of the Triassic succession by Ferri (2009) also appear to suggest a partial source from accreted terranes to the west.

Current Study

A detailed provenance study of Triassic clastic strata in the Halfway River map area in northeastern BC is being undertaken with the goal of evaluating the two-stage depositional model described above for Triassic units in this region. This study includes detailed conodont biostratigraphic work that will build on previous research by M. Orchard and co-

workers (e.g., Orchard et al., 2001, 2002; Orchard, 2006). The biochronology component is critical in order to provide the required temporal framework for the rock units being investigated. A total of 15 samples for conodont dating were collected from the section that was examined in 2009. The study will also include U-Pb dating of detrital zircon grains from biochronologically well dated units throughout the Triassic section in the Halfway River study area, with particular attention being paid to units for which paleocurrent information is available. Five samples were collected for this U-Pb dating of detrital zircon grains. The detrital zircon age patterns that are obtained, together with careful petrographic analysis of the samples, will provide critical information concerning the provenance of the Lower and Middle Triassic section in the Halfway River area. This will allow the comparison and contrasting of the provenance and paleotectonic setting of Triassic units of the WCSB in northeastern BC with age-equivalent rock units that have been studied by Beranek (2009) farther to the north. It is anticipated that results of this study will provide valuable stratigraphic information for industry concerning the regional depositional environment of the various parts of the economically important Triassic section (particularly the lower portion, which is presently considered to have the best gas potential). An improved understanding of the Triassic stratigraphy will be critical for assessing the nature and extent of possible source and reservoir units within the section.

Triassic Stratigraphy of the Halfway River Map Area

This study will focus on the Lower and lower Middle Triassic, which in the Halfway River map area is represented by the Grayling, Toad and Liard formations (Figure 3). Stratigraphic nomenclature is somewhat complicated in this area because different formation names are applied to some units in subsurface studies than are applied in surficial geology maps. The stratigraphy will be discussed in terms of surficial geology map units, but will include correlations with the subsurface rock units.

The Grayling Formation is the lowermost formation of the Triassic in northeastern BC, where it unconformably overlies the Permian Fantasque Formation (Gibson, 1971). It consists of a succession of dolomitic siltstone, silty shale and minor amounts of calcareous siltstone, silty limestone, dolomite and fine-grained sandstone (Thompson, 1989). The maximum thickness reached in the Halfway River map area is 35 m. It is the surface equivalent of the lower Montney Formation and contains ammonites indicative of a Griesbachian–Smithian age (Zonneveld and Gingras, 2000).

In many parts of the foreland, it is difficult to differentiate the Grayling Formation from the overlying Toad Forma-

Stratigraphic Age		Foothills - Halfway to Pine Rivers	Peace River Subsurface	Subsurface, Alberta/BC	Foothills - Bow/Sukunka Rivers
Jurassic		Ferne Formation			
Triassic	Rhaetian	Bocock Fm			
	Late	Norian	Pardonet Fm	Pardonet Fm	Pardonet Fm
		Carnian	Baldonnel Fm	Baldonnel Fm	Baldonnel Fm
	Middle	Ladinian	Liard Fm	Halfway Fm	Halfway Fm
		Anisian	Toad Fm	Doig Fm	Doig Fm
	Early	Grayling Fm	Montney Fm	Montney Fm	
Permian		Fantasque/Ishbel			

Figure 3. The formations of the Halfway River map area, northeastern British Columbia, and their correlations with other formations both in the subsurface and in southern Alberta. Modified from Ferri (2009). Abbreviations: Ck, creek; Fm, formation; Gp, group; Lk, Lake; Mtn, Mountain.

tion. In some cases the two units are therefore mapped as the Toad-Grayling Formation (Gibson, 1971). The Toad Formation itself conformably overlies the Grayling Formation, and comprises a thick sequence of argillaceous to calcareous siltstone, silty shale, silty limestone and dolomite, as well as very fine grained sandstone (Thompson, 1989). The formation achieves a maximum thickness of approximately 825 m in the Halfway River area. Its equivalents in the subsurface are the upper Montney and lower Doig formations, and pelecypods and ammonites suggest an age from Smithian to Ladinian (Zonneveld and Gingras, 2000).

The Liard Formation unconformably overlies and interfingers with the Toad Formation. It consists primarily of fine to coarse sandstone, calcareous and dolomitic siltstone and sandy to silty dolomite and limestone (Thompson, 1989). The formation shows a wide variation in thickness, from approximately 30 m in the Halfway River area, up to 300 m to the north and over 500 m in the south. The upper contact with the Charlie Lake Formation is conformable and in some areas hard to place, further complicating the measurement of unit thicknesses. The Liard Formation is the surface equivalent of the upper Doig and Halfway formations in the subsurface. A wide range of fossils suggest deposition of the formation during the Ladinian (Zonneveld and Gingras 2000).

Stratigraphy of the Lower and Middle Triassic South Halfway River Section

The stratigraphic section logged in the summer of 2009 is located to the south of the Halfway River in northeastern

BC, with the base of the section at 473870E 6311694N (Zone 10, NAD 83). The oldest unit present is the Toad Formation, located on the western side of a steep ridge. The Liard Formation is present higher up the ridge (Figure 4a). The section continues over the top of the ridge and down the eastern flank, where the Charlie Lake, Baldonnel and Pardonet formations are present, together with outcrops of the Jurassic Fernie Formation and the Jurassic-Cretaceous Minnes Group. The section appears to correspond with section GK-68-5 of Gibson (1971).

The total thickness of the measured section is 643 m. The Grayling Formation was not observed and the base of the measured section lies within the Toad Formation. The measured thickness of 604 m for the Toad Formation is therefore a minimum for this area. A structural section in this area suggests between 150 and 200 m of unexposed rocks of the Toad and Grayling formations below the base of the measured section. The Liard Formation overlies the Toad Formation and only 39 m of its lower part was measured. Outcrops of the Liard Formation continue above the measured section, but are inaccessible.

Fourteen conodont samples were collected from the Toad Formation and one from the Liard Formation. Three detrital zircon samples were collected from the Toad Formation and two from the Liard Formation. Macrofossils, primarily ammonoids and pelecypods, were collected throughout the section. Seven ammonites were recovered, along with 18 samples of pelecypods. Macrofossils that could not be extracted were photographed in situ.

A schematic graphic log of the section, along with the positions where samples were collected, is shown in Figure 5.

The Toad Formation at this section consists primarily of flaggy-weathering, calcareous siltstone, interbedded with lesser amounts of recessive, carbonaceous, silty shale (Figures 4b, c). Higher in the section, the amount of argillaceous material is reduced and very fine grained sand begins to appear (Figure 4c). This change is also exhibited by the relative decrease in gamma-ray values in the upper part of the section's geophysical log. The amount of carbonate present in the rock remains high throughout the section.

The lower part of the Toad Formation appears to have been deposited in relatively quiet, offshore conditions. It shows similarities to lithofacies A2 of Zonneveld and Gingras (2000), although the proportion of silt is higher than that of

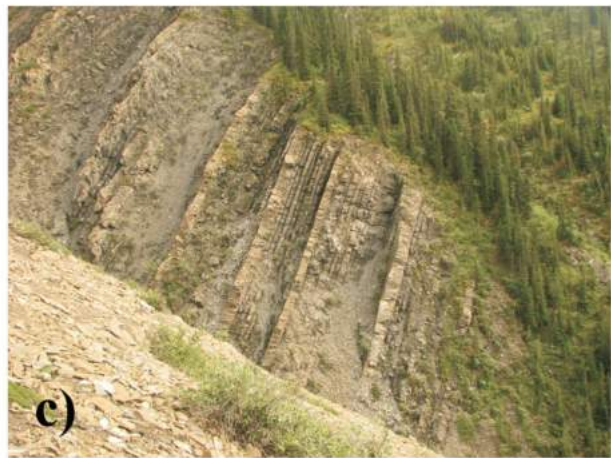
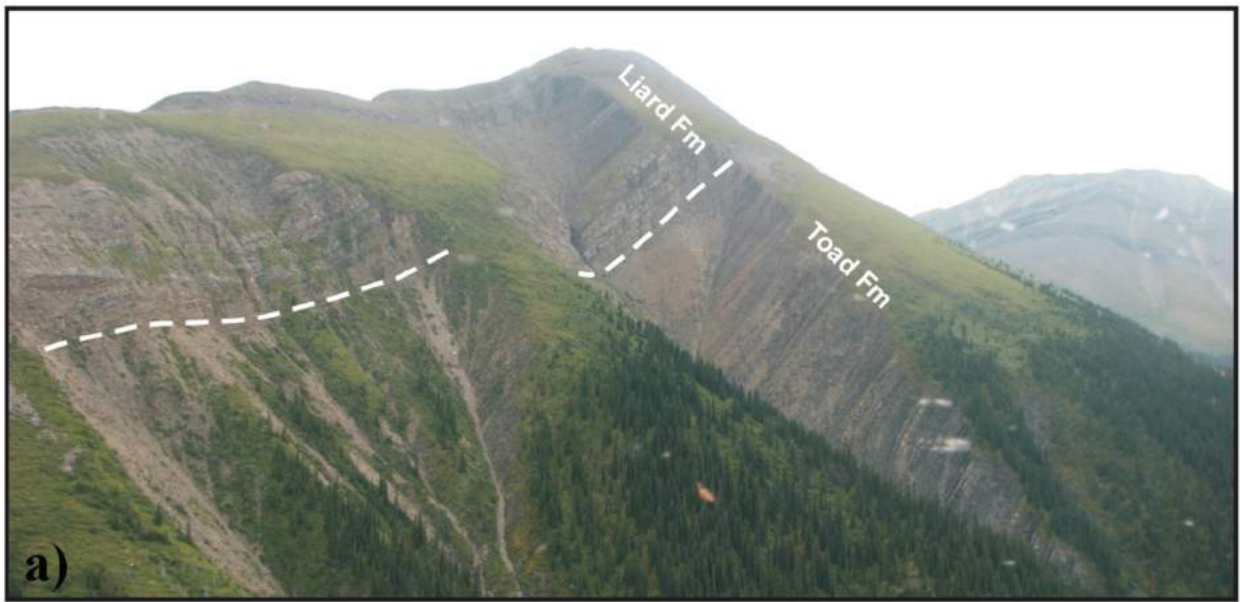


Figure 4: a) View south to the measured section containing exposures of Toad and Liard formations, south of Halfway River, north-eastern British Columbia. b) Recessive and fissile, dark grey calcareous siltstone within the lower part of the Toad Formation (approximately 145 m from the base of the section). This grades upwards into more resistive and cleaner, buff-weathering siltstone. c) Ribbed, buff-weathering, calcareous to dolomitic siltstone and recessive, calcareous siltstone from approximately the 160 m level of the section. d) Thin-bedded, graded turbidites (some with ball and pillow structures) at the 510 m level of the section. e) Bedding-parallel bioturbation within the basal Liard Formation at approximately the 611 m level of the section. Large burrows are approximately 3–5 cm in width.

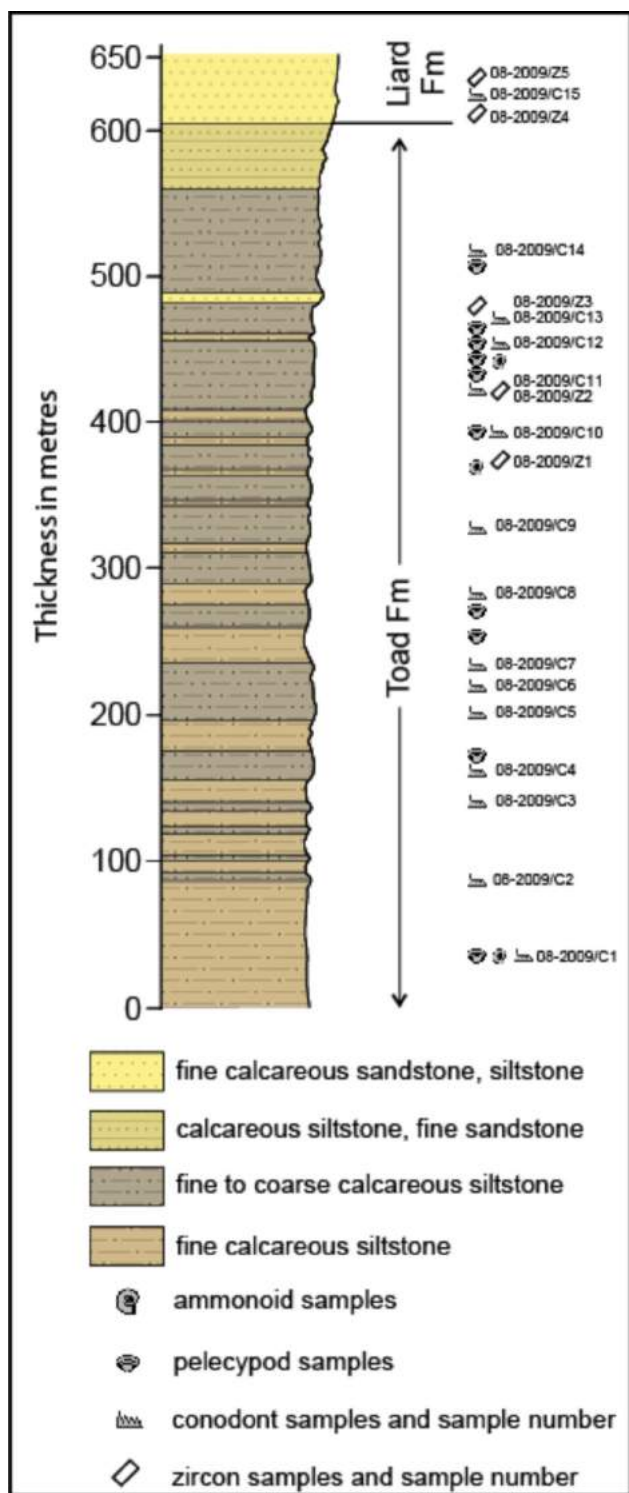


Figure 5. Schematic graphic log of the south Halfway River section, northeastern British Columbia, showing locations of samples collected. Abbreviation: Fm, formation.

shale. Higher up in the sequence, there is a greater proportion of very fine grained sandstone. There are also sedimentary structures, such as ripple and parallel lamination, convoluted bedding and possible tool marks, on the base of some beds that suggest turbiditic deposition (Figure 4d).

The upper part of the Toad Formation shows distinct similarities to lithofacies C of Zonneveld and Gingras (2000), indicating deposition on the continental shelf or slope. Fossils are rare, and consist mainly of ammonoids and pelecypods, although a crinoid and a belemnite were also found. No trace fossils were observed in this formation.

The lower boundary of the Liard Formation is drawn at the transition from dark siltstone to uniform, beige, very fine grained sandstone. Siltstone beds persist for a few metres above this horizon, before giving way to a more uniform succession of calcareous, very fine grained sandstone and siltstone. The Liard Formation is much cleaner than the underlying Toad Formation and consists entirely of calcareous sandstone and lesser siltstone at this section. The presence of limestone boulders in the talus suggests that this rock type is present higher in the sequence, above the measured section.

The coarser clastic material that comprises the Liard Formation indicates deposition in a relatively shallow-water setting compared to the Toad Formation. Similarities exist between rocks of the Liard Formation and those assigned to lithofacies E by Zonneveld and Gingras (2000), but, unlike lithofacies E, sedimentary structures in the rocks at this section are rare. The lowest part of the Liard Formation in this area likely formed in the offshore transition zone. Fossils are relatively common, although rarely found in situ. Terebratulid brachiopods are by far the most dominant body fossils present, although pelecypods were recovered as well. An ammonite and an ophiuroid were found in boulders that appear to be from the Liard Formation. Trace fossils are abundant and show a variety of forms (Figure 4e).

The section as a whole records an overall shallowing trend, from deposition on the distal shelf or slope to proximal deposition close to or above the storm wave base.

Further Work

The focus of current work is the processing and analysis of the zircon and conodont samples that were collected from the measured section. It is hoped that these will constrain the age and provenance of the sediments at this section, while helping to further refine the correlation between the conodont and ammonoid time scales for the Early and Middle Triassic. In future field seasons, other sections in the Halfway River map area will be logged and sampled. Future work will also include collection of samples for whole rock geochemistry and Nd isotopic analysis. Combining this data with that obtained from the detrital zircon grains will help to further constrain the provenance of Triassic sediments in the WCSB. In addition to work in the Halfway River map area, the project may be expanded in subsequent years to encompass other areas depending on the suitability of sections for study. This will also provide the opportunity to correlate between these sections, as well as those previ-

ously studied, to obtain an improved understanding of regional facies change and sediment transport. This in turn will allow better characterization of the Triassic gas reservoirs of northeastern BC and lead to continued production from the subsurface.

Acknowledgments

The authors thank the BC Ministry of Energy, Mines and Petroleum Resources for providing field support. Funding for analyses is being provided by Geoscience BC. L. Beranek reviewed an earlier draft of this submission, and his comments helped to improve the final product.

References

- Beranek, L. (2009): Provenance, paleotectonic setting, and depositional framework of North American Triassic strata in Yukon: the sedimentary record of pericratonic terrane accretion in the northern Canadian Cordillera; Ph.D. thesis, University of British Columbia, 324 p.
- Colpron, M., Nelson, J.L. and Murphy, D.C. (2006): A tectonostratigraphic framework for the pericratonic terranes of the northern Cordillera; *in* Paleozoic Evolution and Metallogeny of Pericratonic Terranes at the Ancient Pacific Margin of North America, Canadian and Alaskan Cordillera, M. Colpron and J.L. Nelson (ed.), Geological Association of Canada, Special Paper 45, p. 1–23.
- Colpron, M., Nelson, J.L. and Murphy, D.C. (2007): Northern Cordilleran terranes and their interactions through time; *GSA Today*, v. 17, no. 4/5, p. 4–10.
- Davies, G.R. (1997): The Triassic of the Western Canada Sedimentary Basin: tectonic and stratigraphic framework, paleogeography, paleoclimate and biota; *in* Triassic of the Western Canada Sedimentary Basin, T.F. Moslow and J. Wittenberg (ed.), *Bulletin of Canadian Petroleum Geology*, v. 45, p. 434–460.
- Ferri, F. (2009): Geology of the Jones Peak area (NTS 94B/02 and 07), Halfway River map sheet (94B); *in* Geoscience Reports 2009, BC Ministry of Energy, Mines and Petroleum Resources, p. 5–24.
- Garzzone, C.N., Patchett, P.J., Ross, G.M. and Nelson, J.L. (1997): Provenance of Paleozoic sedimentary rocks in the Canadian Cordilleran miogeocline: a Nd isotopic study; *Canadian Journal of Earth Sciences*, v. 34, p. 1603–1618.
- Gehrels, G.E. and Ross, G.M. (1998): Detrital zircon geochronology of Neoproterozoic to Permian miogeoclinal strata in British Columbia and Alberta; *Canadian Journal of Earth Sciences*, v. 35, p. 1380–1401.
- Gibson, D.W. (1971): Triassic stratigraphy of the Sikanni Chief River – Pine Pass region, Rocky Mountain Foothills, northeastern British Columbia; Geological Survey of Canada, Paper 70-31, 105 p.
- Gibson, D.W. (1993): Triassic, subchapter 4G; *in* Sedimentary Cover of the Craton in Canada, D.F. Stott and J.D. Aitken (ed.), Geological Society of America, The Geology of North America, v. D-1, p. 294–320.
- Gibson, D.W. and Barclay, J.E. (1989): Middle Absaroka sequence: the Triassic Stable Craton; *in* Western Canada Sedimentary Basin – A Case History, B.D. Ricketts (ed.), Canadian Society of Petroleum Geologists, p. 219–231.
- Gordey, S.P., Geldsetzer, H.H.J., Bamber, E.W., Henderson, C.M., Richards, B.C., McGugan, A., Gibson, D.W. and Poulton, T.P. (1991): Part A: ancestral North America; *in* Upper Devonian to Middle Jurassic Assemblages, Chapter 8 of Geology of the Cordilleran Orogen in Canada, H. Gabrielse and C.J. Yorath (ed.), Geological Survey of Canada, Geology of Canada, no. 4, p. 219–327.
- Monger, J.W.H. and Price, R.A. (2002): The Canadian Cordillera: geology and tectonic evolution; Canadian Society of Exploration Geophysicists Recorder, February, p. 17–36.
- Mortensen, J.K., Beranek, L. and Murphy, D.C. (2007): Permo-Triassic orogeny in the northern Cordillera: Sonoma North?; Geological Society of America, Cordilleran Section.
- Mortensen, J.K., Dusel-Bacon, C., Hunt, J.A. and Gabites, J. (2006): Lead isotopic constraints on the metallogeny of middle and late Paleozoic syngenetic base-metal occurrences in the Yukon-Tanana and Slide Mountain/Seventymile terranes and adjacent portions of the North American miogeocline area; *in* Paleozoic Evolution and Metallogeny of Pericratonic Terranes at the Ancient Pacific Margin of North America, Canadian and Alaskan Cordillera, M. Colpron and J.L. Nelson (ed.), Geological Association of Canada, Special Paper 45, p. 261–279.
- Nelson, J.L. (1993): The Sylvester allocthon: Upper Paleozoic marginal-basin and island-arc terranes in northern British Columbia; *Canadian Journal of Earth Sciences*, v. 30, p. 631–643.
- Nelson, J.L., Colpron, M., Piercey, S.J., Dusel-Bacon, C., Murphy, D.C. and Roots, C.F. (2006): Paleozoic tectonic and metallogenic evolution of the pericratonic terranes in Yukon, northern British Columbia and eastern Alaska; *in* Paleozoic Evolution and Metallogeny of Pericratonic Terranes at the Ancient Pacific Margin of North America, Canadian and Alaskan Cordillera, M. Colpron and J.L. Nelson (ed.), Geological Association of Canada, Special Paper 45, p. 323–360.
- Orchard, M.J. (2006): Late Paleozoic and Triassic conodont faunas of Yukon Territory and northern British Columbia and implications for the evolution of the Yukon-Tanana terrane; *in* Paleozoic Evolution and Metallogeny of Pericratonic Terranes at the Ancient Pacific Margin of North America, Canadian and Alaskan Cordillera, M. Colpron and J.L. Nelson (ed.), Geological Association of Canada, Special Paper 45, p. 229–260.
- Orchard, M.J., Tozer, E.T. and Zonneveld, J-P. (2002): Some preliminary observations on the association of ammonoids and conodonts about the Ladinian-Carnian boundary in North America; *Albertiana*, v. 27, p. 8–11.
- Orchard, M.J., Zonneveld, J.P., Johns, M.J., McRoberts, C.A., Sandy, M.R., Tozer, E.T. and Carrelli, G.G. (2001): Fossil succession and sequence stratigraphy of the Upper Triassic and Black Bear Ridge, northeast B.C., and a GSSP prospect for the Carnian-Norian boundary; *Albertiana*, v. 25, p. 10–22.
- Pelletier, B.R. (1960): Triassic stratigraphy, Rocky Mountain Foothills, northeastern British Columbia; Geological Survey of Canada, Paper 60-2, 32 p.
- Pelletier, B.R. (1961): Triassic stratigraphy of the Rocky Mountain and Foothills, northeastern British Columbia; Geological Survey of Canada, Paper 61-8, 32 p.
- Pelletier, B.R. (1963): Triassic stratigraphy of the Rocky Mountain and Foothills, Peace River District, British Columbia; Geological Survey of Canada, Paper 62-26, 43 p.

- Piercey, S.J. and Colpron, M. (2009): Composition and provenance of the Snowcap assemblage, basement to the Yukon-Tanana terrane, northern Cordillera: implications for Cordilleran crustal growth; *Geosphere*, v. 5, p. 439–464.
- Ross, G.M., Gehrels, G.E. and Patchett, P.J. (1997): Provenance of Triassic strata in the Cordilleran miogeocline, western Canada; *Bulletin of Canadian Petroleum Geology*, v. 45, p. 461–473.
- Thompson, R.I. (1989): Stratigraphy, tectonic evolution and structural analysis of the Halfway River map area (94B), northern Rocky Mountains, British Columbia; *Geological Survey of Canada, Memoir 425*, 119 p.
- Zonneveld, J-P. and Gingras, M.K. (2000): Triassic depositional framework and sequence stratigraphy, Williston Lake, northeastern British Columbia; Geological Association of Canada–Mineralogical Association of Canada, Joint Annual Meeting (GeoCanada 2000), field trip guide, 156 p.
- Zonneveld, J-P. and Gingras, M.K. (2003): The Triassic of northeastern British Columbia: constructing a depositional and stratigraphic framework; *Canadian Society of Petroleum Geologists–Canadian Society of Exploration Geophysicists Joint Convention*, 159 p.
- Zonneveld, J-P. and Orchard, M.J. (2002): Stratal relationships of the Baldonnel Formation (Upper Triassic), Williston Lake, northeastern British Columbia; *in Current Research 2002-A8*, Geological Survey of Canada, 15 p.
- Zonneveld, J-P., Carrelli, G.G. and Riediger, C. (2004): Sedimentology of the Upper Triassic Charlie Lake, Baldonnel and Pardonet formations from outcrop exposures in the southern Trutch region, northeastern British Columbia; *in Central Foreland NATMAP: Stratigraphic and Structural Evolution of the Cordilleran Foreland - Part 1*, L.S. Lane (ed.), *Bulletin of Canadian Petroleum Geology*, v. 52, p. 343–375.
- Zonneveld, J-P., Moslow, T.F. and Gingras, M.K. (1997a): Sequence stratigraphy and sedimentary facies of the Lower and Middle Triassic of northeastern British Columbia: progradational shoreface associations in a mixed carbonate siliciclastic system; *Sedimentary Events-Hydrocarbon Systems, 1997*, Canadian Society of Petroleum Geologists–Society for Sedimentary Geology (SEPM) Joint Convention, Calgary, field trip guide, 118 p.
- Zonneveld, J-P., Moslow, T.F. and Henderson, C.M. (1997b): Lithofacies associations and depositional environments in a mixed siliciclastic-carbonate depositional system, upper Liard Formation, Triassic, northeastern British Columbia; *Bulletin of Canadian Petroleum Geology*, v. 45, p. 553–575.
- Zonneveld, J-P., Beatty, T.W., Blakney, B.J., Gingras, M.K. and Orchard, M.J. (2003): Reservoir architecture of mixed siliciclastic-carbonate shallow marine strata: outcrop exposures of the Triassic Baldonnel Formation; *American Association of Petroleum Geologists, Annual Convention*, Salt Lake City, Utah, May 11–14, 2003.

Tectonic History, Biostratigraphy and Fracture Analysis of Upper Paleozoic and Lowest Triassic Strata of East-Central British Columbia (NTS 093I, O, P): Preliminary Report

C.M. Henderson, Department of Geoscience, University of Calgary, Calgary, AB,
charles.henderson@ucalgary.ca

K. Zubin-Stathopoulos, Department of Geoscience, University of Calgary, Calgary, AB

G. Dean, Department of Geoscience, University of Calgary, Calgary, AB

D. Spratt, Department of Geoscience, University of Calgary, Calgary, AB

Y.P. Chau, Department of Geoscience, University of Calgary, Calgary, AB

Henderson, C.M., Zubin-Stathopoulos, K., Dean, G., Spratt, D. and Chau, Y.P. (2010): Tectonic history, biostratigraphy and fracture analysis of upper Paleozoic and lowest Triassic strata of east-central British Columbia (NTS 093I, O, P): preliminary report; *in* Geoscience BC Summary of Activities 2009, Geoscience BC, Report 2010-1, p. 259–270.

Introduction

The British Columbia portion of the Western Canada Sedimentary Basin (WCSB) is far less developed than the Alberta portion. During the past decade, however, this area has experienced tremendous growth, particularly in natural-gas exploration. Pennsylvanian and Permian strata are among BC's important reservoir intervals (Bird et al., 1994), as they are underexplored and have considerable potential to yield new natural-gas supplies in addition to the already-discovered producing fields. One area that has been identified as having particularly high potential for undiscovered conventional natural-gas resources is the southern Foothills and adjacent Deep Basin in the Sukunka-Kakwa area (Figure 1; National Energy Board, 2006). Despite strong industry interest in Pennsylvanian and Permian strata (Hanington, Ksituan, Belcourt, Fantasque and Belloy formations, including the Ksituan Member of the Belloy Formation), no detailed stratigraphic and sedimentological studies of upper Paleozoic strata have been conducted in the Sukunka-Kakwa area. This study seeks to address this gap by developing detailed predictive sedimentary-facies and diagenetic models within a sequence biostratigraphic framework for known and potential reservoir intervals in upper Paleozoic and Lower Triassic strata within the Sukunka-Kakwa area (Figure 1) of east-central BC (1:250 000 NTS areas 093I, O and P; latitude 54–55.75°N; longitude 120–122°W). Data from outcrop sections will be integrated with all available subsurface data; in particular,

wireline logs will be compared to gamma-ray scintillometer curves generated at each outcrop location.

Fieldwork was conducted in August 2009, so the results provided in this report are very preliminary. Additional fieldwork is planned in 2010. This paper will also identify some of the essential objectives, methods and expected outcomes, and provide an initial assessment of how this research will benefit the exploration community.

Geological Setting

The strata in question were deposited on what has generally been interpreted as a relatively passive western North American cratonic margin during the Pennsylvanian to Early Triassic, with possible far field and relatively minor effects associated with the Antler (latest Devonian to earliest Mississippian) and Sonoman (latest Permian and earliest Triassic) orogenies (Henderson et al., 1994; Richards et al., 1994). However, increasing evidence (Fossenier, 2002; Dunn, 2003) is demonstrating that this region experienced significant tectonism in the form of block faulting and possible foreland-basin development similar to northern Nevada (Trexler et al., 2004).

The key to unravelling upper Paleozoic tectonostratigraphic history is the identification of unconformities that separate genetically related stratigraphic successions developed by a combination of eustatic and tectonic influences. These tectonostratigraphic events have been identified in Nevada as C1–C6, P1–P5 and Tr1 (Snyder et al., 2002; Trexler et al., 2004), and they mostly correlate with unconformities in Western Canada (Figure 2). Since standard lithostratigraphy and low-resolution biostratigraphy are insufficient to identify these discrete packages, high-resolution biostratigraphy and geochemical tools are required to reveal the position and duration of the uncon-

Keywords: Pennsylvanian, Permian, Lower Triassic, stratigraphy, biostratigraphy, conodonts, structure, fractures, petroleum exploration

This publication is also available, free of charge, as colour digital files in Adobe Acrobat® PDF format from the Geoscience BC website: <http://www.geosciencebc.com/s/DataReleases.asp>.

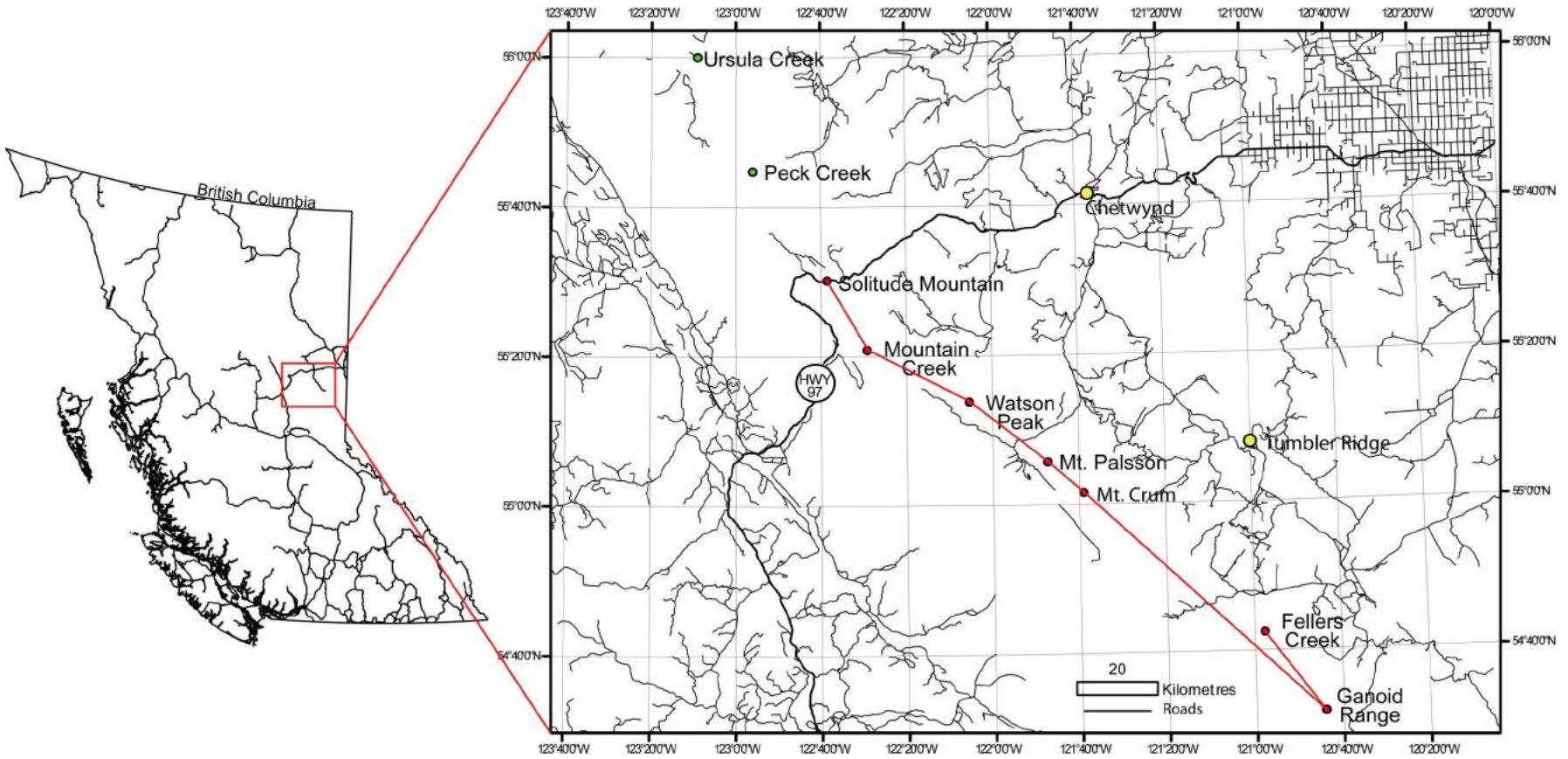


Figure 1. Sukunka-Kakwa study area of east-central British Columbia, showing sections measured and line (red) of cross-section depicted in Figure 3.

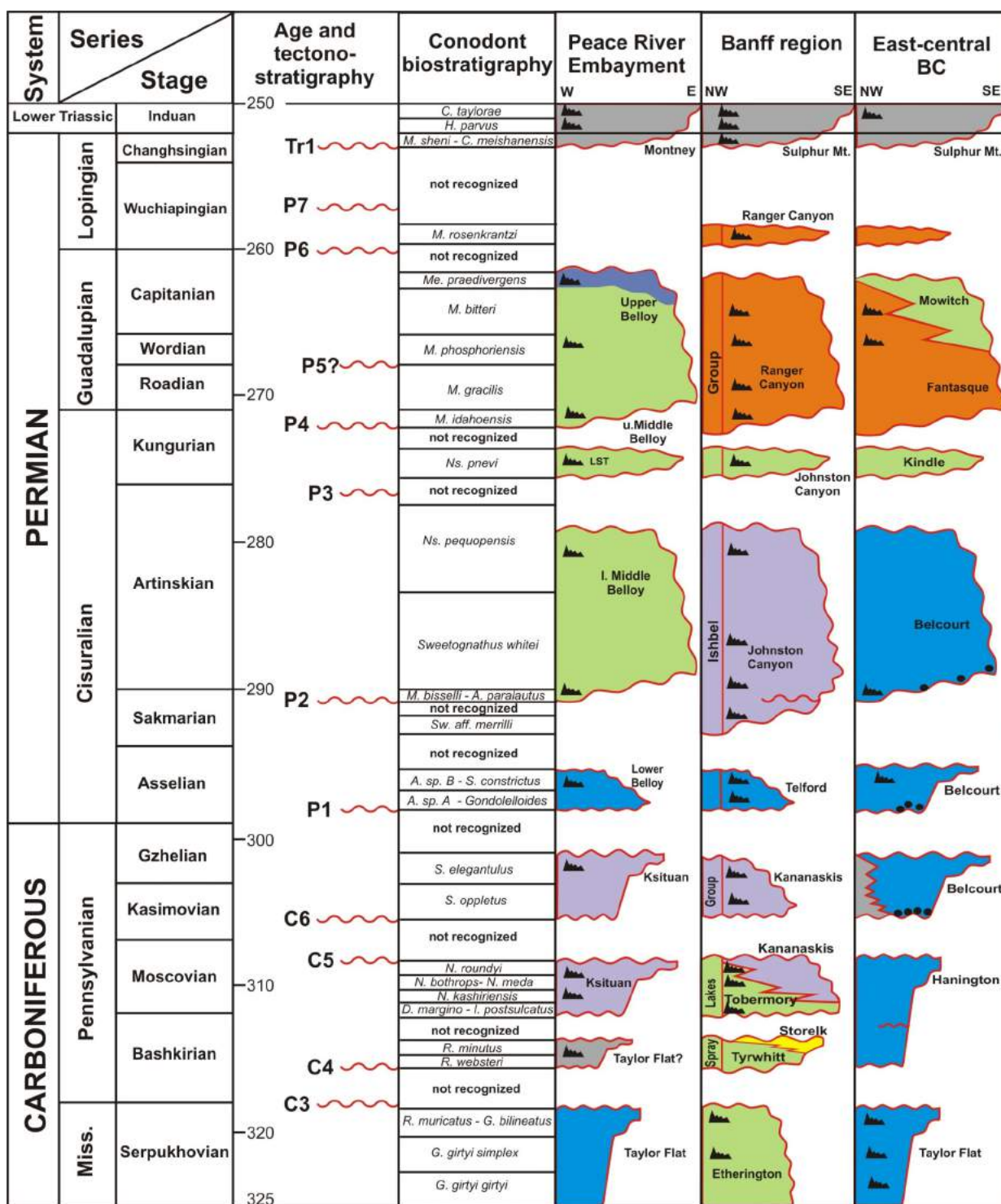


Figure 2. Stratigraphy and tectonostratigraphic sequences correlated among the southwestern Alberta Rocky Mountains, the Peace River Embayment of west-central Alberta and northeastern British Columbia, and the study area in east-central BC. Tectonostratigraphic sequences C1–C6, P1–P5 and Tr1 are after Snyder et al. (2002) and Trexler et al. (2004); P6 and P7 are new. Ages are from the 2009 International Commission on Stratigraphy Time Scale, with some modifications based on new ages (Henderson et al., 2009). Stratigraphy is modified from Henderson et al. (2002). Conodont symbols indicate control points in correlations: *G.*, *Gnathodus*; *R.*, *Rhachistognathus*; *D.*, *Declinognathodus* (including *D. marginodosus*); *I.*, *Idiognathoides*; *N.*, *Neognathodus* (including *N. medadulimus*); *S.*, *Streptognathodus*; *A.*, *Adetognathus*; *Sw.*, *Sweetognathus*; *M.*, *Mesogondolella*; *Ns.*, *Neostreptognathodus*; *Me.*, *Merrillina*; *C.*, *Clarkina*; *H.*, *Hindeodus*. The Hanington Formation is comparable to the Belcourt Formation in facies and there has been a recommendation to abandon the term; however, there is a distinct Moscovian age unit in the area and the name has been retained in this study. The basal conglomerate of the Belcourt has Upper Pennsylvanian and Lower Permian above and mid-Pennsylvanian (Moscovian) or Mississippian below. The upper Belloy Formation carbonate is primarily a caliche (Dunn, 2003). Colours depict dominant generalized lithology, including limestone (blue), dolostone (purple), chert (orange), quartz arenite (yellow), bioturbated and bioclastic sandstone (green), and silty shale (grey).

formities. Based on previous work (Higgins et al., 1991; Henderson et al., 2002) and preliminary results from this study, the authors have interpreted 10 unconformity-bound sequences from Serpukhovian to Induan (Figure 2). The succession of these discrete phases of sedimentary-basin development has resulted in variable preservation of the different stratigraphic units and compartmentalization of reservoir units.

Description and Geological Significance of Units (Pennsylvanian to Lowest Triassic)

Hanington Formation or Ksituan Member of the Belloy Formation

The Mountain Creek and Solitude Mountain sections might be the only outcrop locations studied that contain signifi-

cant Pennsylvanian strata, although their presence is postulated at Fellers Creek (Figures 3, 4). Solitude Mountain contains similar facies and is correlative with the Mountain Creek section (Figure 3). Although the Mountain Creek section contains several discrete units, including the Belcourt and Fantasque formations, in its upper portion, most of it may represent the Ksituan Member of the Belloy Formation described by Fossenier (2002) as shallow- to open-marine shoaling-upward cycles. In outcrop, this succession is equivalent to the Hanington Formation (Bamber and Macqueen, 1979) and represents the most important reservoir target in the subsurface immediately to the east of the studied sections. Detailed conodont biostratigraphy, based on the numerous samples collected during fieldwork, will be necessary to resolve questions about age, thickness (0–100 metres in the study area) and distribution of this unit.

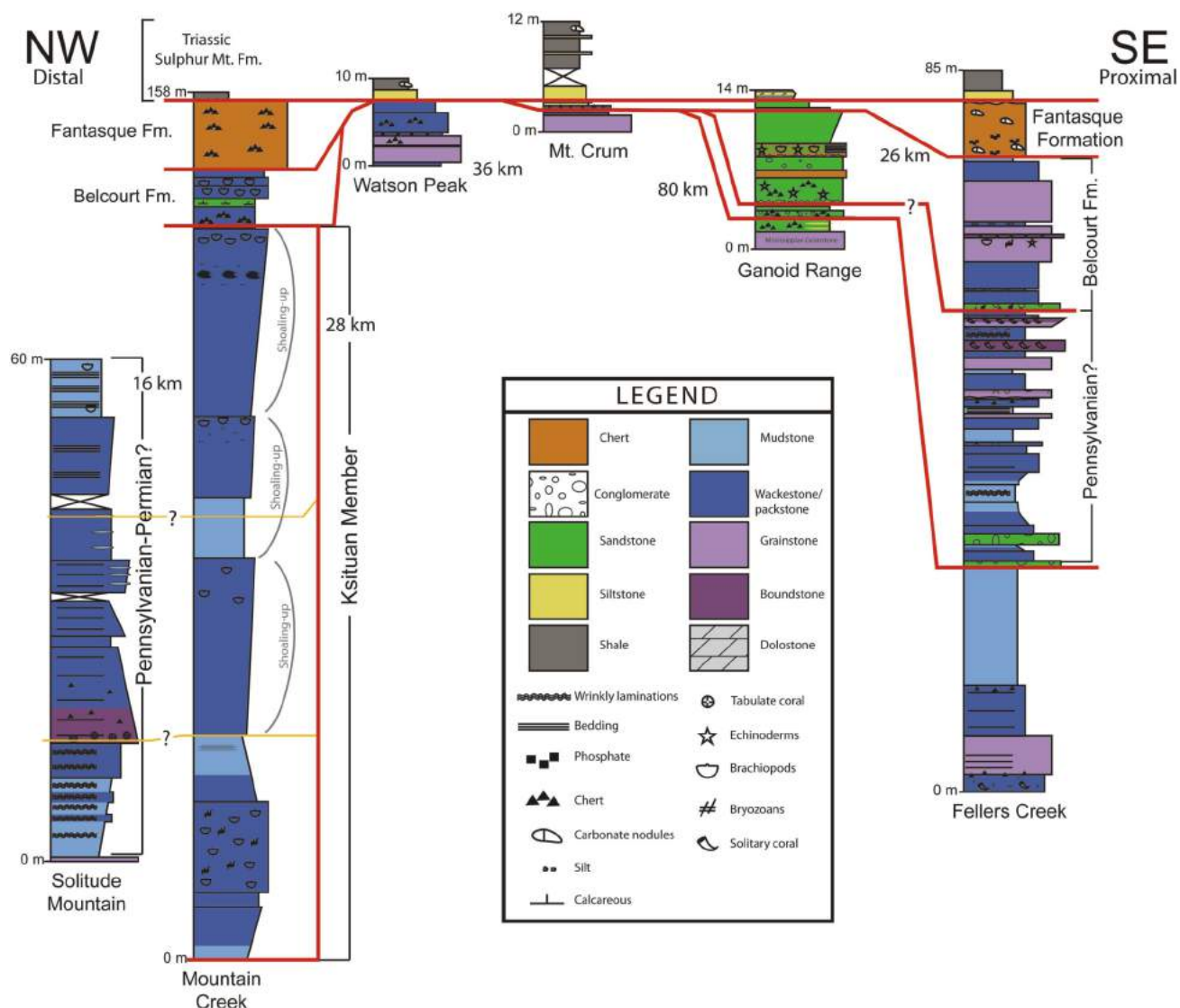


Figure 3. Cross-sections showing stratigraphic relationships in the Sukunka-Kakwa study area, east-central British Columbia. Stratigraphic units, in ascending order, are Mississippian (below lowest red line), Pennsylvanian Ksituan Member (Belloy Formation) or Hanington Formation, latest Pennsylvanian to Lower Permian Belcourt Formation, and Middle to Upper Permian Fantasque Formation. Base of the Triassic Sulphur Mountain Formation (Montney Formation in the subsurface) represents the datum.

The units at the Mountain Creek section are predominantly laminated mudstone and wackestone, with some brachiopod packstone representing the shallowest facies (Figure 5). The Solitude Mountain section consists of wackestone to packstone with some occasional coarser material (coral boundstone) in shoaling-upward packages (Figure 3). Assuming this is equivalent to the Mountain Creek section, it probably represents a shallower water facies.

Belcourt Formation

The Belcourt Formation is easily identified by a basal conglomerate in the Fellers Creek and Ganoid Range sections. This conglomerate consists of poorly sorted, subangular to rounded clasts in a carbonate matrix (Figures 3, 5) and has previously been described only as Permian in age (Bamber and Macqueen, 1979). The Belcourt Formation regionally contains some Pennsylvanian (part of Kasimovian and Gzhelian). Several conglomerate horizons were identified, and the exact age relationships at the Fellers Creek section will be determined by detailed conodont biostratigraphy. Each of these conglomerate levels may represent the product of erosion associated with discrete uplift events. Regionally, the sub-lower Kasimovian unconformity is the most significant. Several shoaling-upward cycles deposited on a gentle ramp occur at the Fellers Creek section. These consist initially of packstone to dolomitic mudstone. Up-section, these cycles grade into grainstone containing brachiopods, bryozoans, crinoids and, in some cases, coral boundstone (Figures 3, 5). The Belcourt Formation at the Ganoid Range is predominantly fine- to coarse-grained calcareous sandstone (Figure 5). The same basal conglomerate is identified, although it is much thinner than at Fellers Creek (Figures 3, 5). This succession represents a much shallower environment compared to Fellers Creek, and the siliciclastic sediments may have been delivered by erosion of uplifted portions of the Sukunka High, across which Pennsylvanian and Permian units thin or disappear in the area (Richards, 1989); the Belcourt Formation ranges in thickness from 0 to 50 m in the current study area.

Fantasque Formation

The Fantasque Formation is identified in four of the six sections described in this study, recognizable by the strong gamma kick at the base. At Fellers Creek, the Fantasque Formation is a 10 m thick unit with abundant phosphate and chert nodules at the base. It thins to approximately 1.2 m at Ganoid Range, where there are some phosphate and chert clasts, although the unit still appears nodular. The Fantasque at Mount Crum is represented by approximately 50 cm of nodular chert and phosphate. The formation may also be present at the Mountain Creek section, where there is an 18 m thick unit of nodular chert, although no apparent gamma kick exists (Figure 3). This is a condensed unit that is equivalent to the Ranger Canyon Formation in south-

western Alberta (Henderson et al., 1994). The Fantasque Formation is absent at Watson Peak.

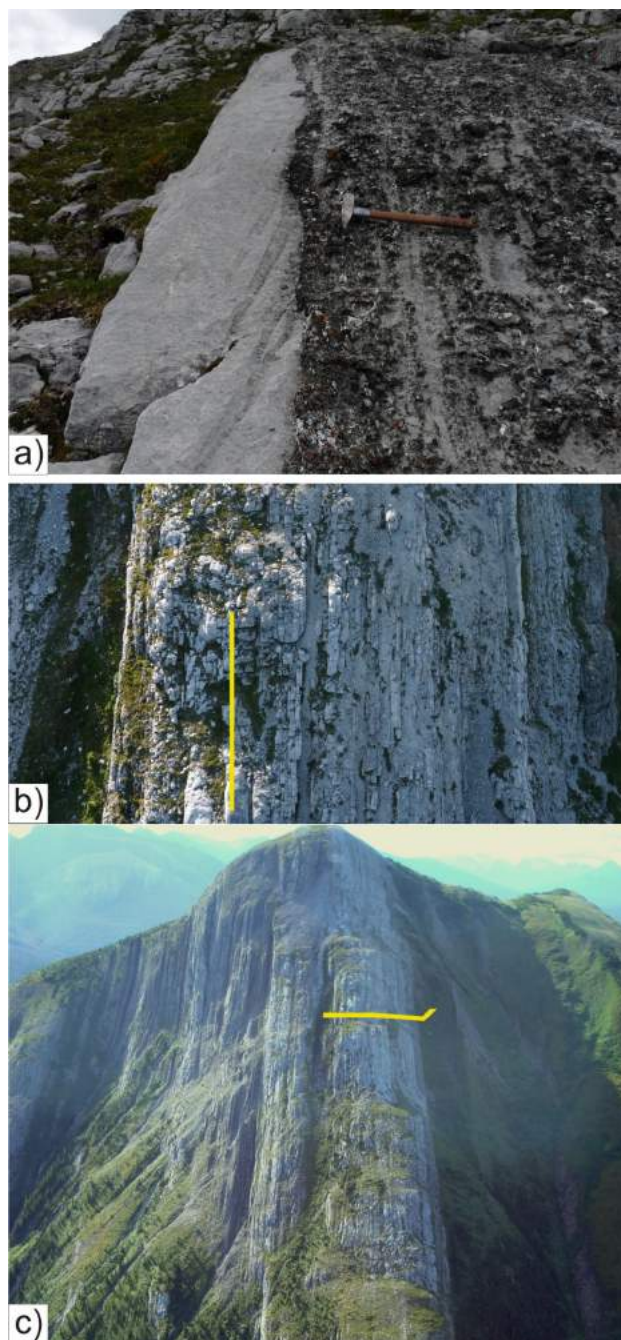


Figure 4. Photographs of Fellers Creek section, Sukunka-Kakwa area, east-central British Columbia: a) conglomerate unit representing the contact (just below 45 cm long hammer) between the Mississippian below and the Ksituan Member (Belloy Formation) and/or Belcourt Formation above; b) close-up aerial view of section; yellow line marks the contact between the Mississippian on the left and the Pennsylvanian–Permian Ksituan Member (Belloy Formation) and/or Belcourt Formation to the right; c) aerial view of section looking south; yellow line marks the measured section depicted in Figure 3 (section is 85 m thick).

Lower Sulphur Mountain (Montney) Formation

Shale and siltstone of the Lower Triassic Montney Formation and surface equivalents in BC were deposited in a ramp setting on the margin of the North American craton (Davies, 1997). Samples were collected from Fellers Creek, Ganoid Range, Mount Crum, Watson Peak and Mount Palsson; however, only the basal part of the formation was measured, so thicknesses are not available. The most significant sampling was at Mount Crum, where approximately 50 m of mainly shale was sampled sequentially at intervals of about 1 m. In addition, gamma-ray scintillometer readings were run on the same section at 0.5 m intervals. The following analyses are currently planned on this suite of samples: 1) total organic carbon analysis, 2) carbon isotope analysis, 3) carbon and oxygen isotope analysis on limestone nodules, 4) x-ray diffraction on shale samples, 5) Sr isotope analysis on conodont elements, 6) thin-section petrology of siltstone and limestone nodules, and 7) detrital zircon analysis of sandy/silty interbeds.

Total organic carbon analysis will be used to determine the values and range of total organic carbon in shale of the basal Triassic as a potential source rock. X-ray diffraction will be used to determine the bulk mineralogy of the shale, as well as any deep-burial diagenesis effects. Thin-section petrology will also aid in the determinations of composition and diagenetic process. Zircon analysis may determine the source of siliciclastic sediment in siltstone beds. Carbon isotopic analysis to determine ^{13}C shift in carbon isotopic signature across the Permian–Triassic boundary and Sr isotopes in conodont elements are important tools to facilitate correlation. The results of the latter analyses will be compared to the global secular Sr isotope curve to obtain an approximate age. The same analysis will be applied to conodont elements collected from the Middle to Upper Permian section (Fantasque Formation) in an attempt to establish the regional time break between the top of the Paleozoic and the basal Triassic, which is essential for recognizing the position of uplifted blocks and the diachronism of the latest Permian to lowest Triassic transgression.

Upper Paleozoic Tectonics

Trexler et al. (2004) documented a number of tectonic events in northern Nevada. Their C3 event represents the development of the Ely Basin and a transition from siliciclastic-dominated to carbonate-dominated deposition without a major break in sedimentation near the Mississippian–Pennsylvanian boundary. Preliminary results from the current study and previous studies (Henderson et al., 2002) suggest that this event in east-central BC coincides with the base of the Ksituan Member (Belloy Formation) or Hanington Formation. The schematic cross-section in Figure 6 suggests possible early foreland-basin development at this time in east-central BC, with a separate sub-basin de-

veloped to the east of the Sukunka High. The C6 event of Trexler et al. (2004) appears to correlate with the major conglomerate that typically forms the base of the Belcourt Formation, although multiple conglomerate units at Fellers Creek are problematic. These correlations suggest that the tectonics affecting northern Nevada extended at least as far

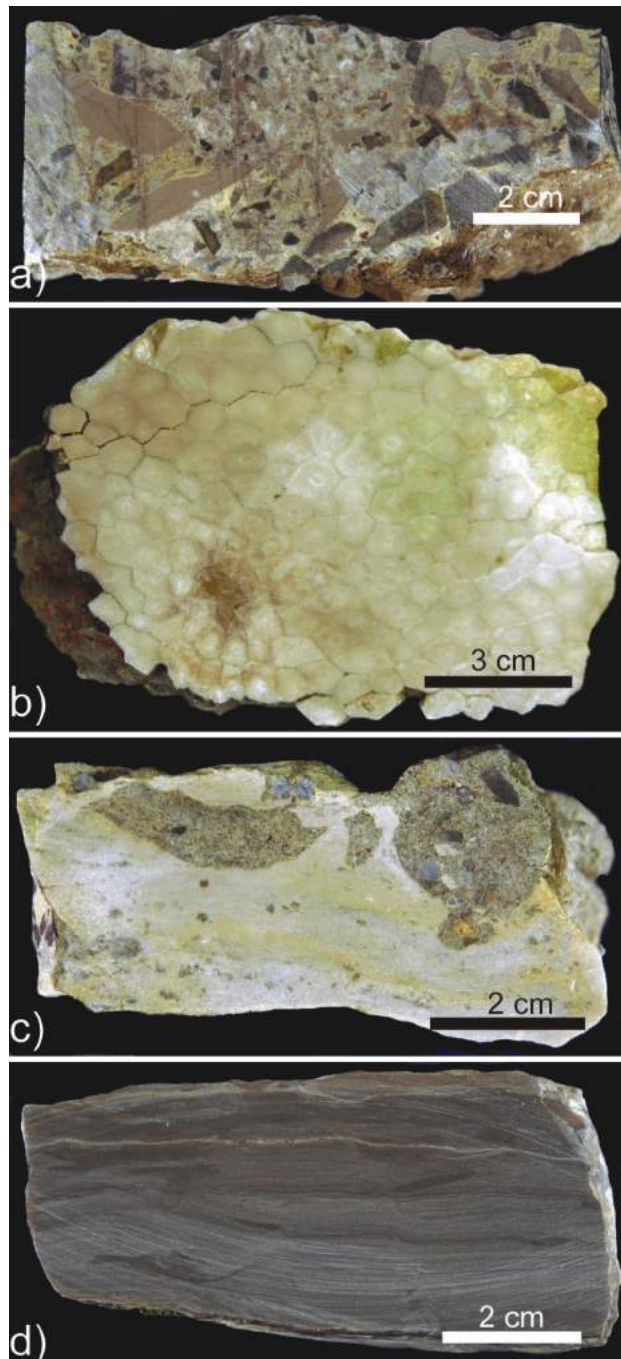


Figure 5. Selected rocks from Sukunka-Kakwa study area, east-central British Columbia: a) Belcourt Formation conglomerate from Ganoid Range at 3.5 m above base; b) coral boundstone from Fellers Creek at 66 m above base; c) fine-grained calcareous sandstone mixed with coarse sand from Ganoid Range at 1.7 m above base; d) laminated mudstone from Mountain Creek at 35.3 m above base.

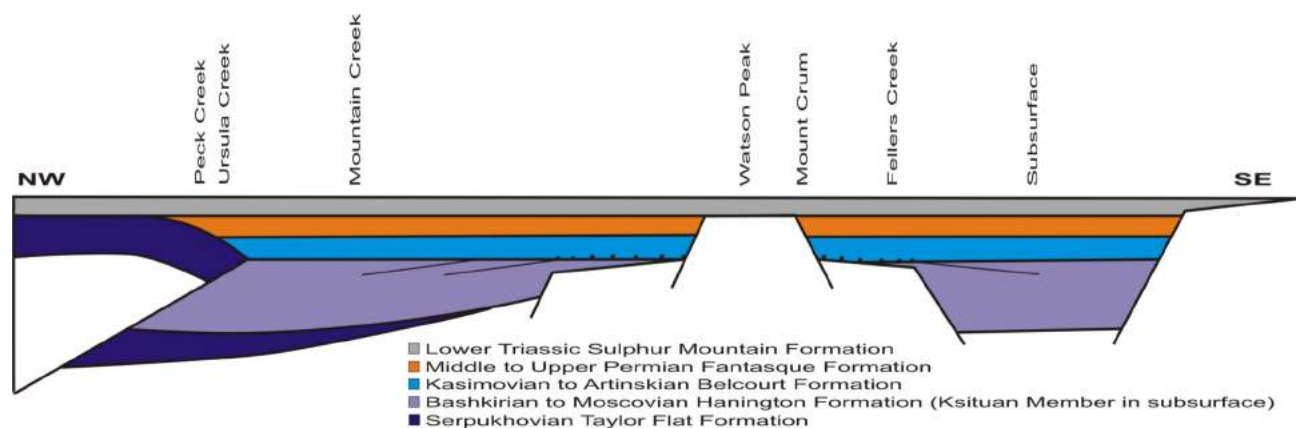


Figure 6. Schematic cross-section of the Sukunka-Kakwa, east-central British Columbia that suggests possible early foreland-basin development during the early Pennsylvanian. The high to the northwest is recognized only as a profound uniformity, with the Middle Permian Fantasque Formation overlying the Serpukhovian Taylor Flat Formation (actual fault relationships and origin are unknown). East of this area, there is a thick Pennsylvanian section that thins dramatically toward the Sukunka Uplift, where, at Watson Peak, Lower Triassic strata overlie mid-Mississippian strata. This high area acts somewhat like a peripheral bulge and probably saw several episodes of differential uplift, especially at level C6 (see Figure 2), indicated by truncation and basal conglomerate. Evidence of postulated erosion from this high and proximity to it is provided by the siliciclastic succession at the Ganoid Range (see Figure 3). East of this area, in the subsurface, is a sub-basin in which Ksituan Member rocks are thick and represent the primary exploration target.

north as east-central BC, and that these events are therefore intimately linked to large-scale structural events on the North American margin. Evidence indicates that Pennsylvanian block faulting led to thickness variations and preferential preservation of reservoir facies in local sub-basins (Figure 3). For example, the Moscovian interval is absent or restricted to a feather-edge (Hanington Formation) throughout much of the outcrop belt, especially adjacent to the Sukunka Uplift, whereas this unit is thick (>200 m) and gas prone in the subsurface to the east. The Fantasque Formation and equivalent units are the most widespread strata in the area that presumably point to a stable setting at a time when the Slide Mountain Ocean was at its widest and most distant from the North American margin (Nelson et al., 2006; Orchard, 2006 for ages).

Laramide Orogeny Structural Interpretation

Upper Paleozoic and Lower Triassic strata in the area were subjected to several discrete syndepositional tectonic events, as indicated above. However, the major structures that represent the structural traps in the subsurface were generated by thin-skinned thrusting during the latest Cretaceous and early Paleogene. In addition, it is very probable that some of these ancient block faults have affected the position of later Laramide-age structures (Dunn, 2003); certainly, individual thrust sheets display very different stratigraphic successions, with thick Pennsylvanian in westernmost sections studied (Mountain Creek), dramatic thinning of Pennsylvanian and Permian in a range to the east (Mount Crum, Watson Peak), and then thickening again of the upper Paleozoic in a range even farther east (Ganoid Range and Fellers Creek).

Understanding the influence of fractures generated within this Laramide-age fold-and-thrust belt on reservoir quality is of vital significance. Fractures are the representation of a surface or zone of failure by any non-sedimentary mechanical discontinuity. The use of outcrop data (orientation, size, density and intensity) for analysis of these features aids in their characterization (Dershowitz and Einstein, 1988).

Preliminary fracture results from linear scanlines show domination by six main fracture sets in the Ganoid Range (Figures 7–11). Set 1 is oriented parallel to the regional fold-axis trend (154°) and the local fold-axis trend (162°), implying that these fractures are Stearns Type 2 and formed as a result of increased curvature of bedding during folding. Set 2, oriented oblique to set 1, may have formed as a conjugate to the first set. Fracture sets 4 and 5 are conjugate to the principal stress direction (σ₁) and oriented perpendicular to the regional fold axis, implying that these are Stearns Type 1 fractures and formed as a result of regional compression. Fracture sets 4 and 5 (Stearns Type 1) generally appear in the hinge zones of the folds, whereas sets 1 and 2 (Stearns Type 2) dominate in the limbs. Set 3 fractures formed as conjugates to the dominant set 1 fractures at the Ganoid Range. Fracture sets 2 and 6 also formed as a conjugate pair, oblique to the fold-axis trend (Feltham, 2005).

Fracture density and intensity were calculated from circular window scanlines using equations derived from Mauldon et al. (2001). The fracture density is highest in the hinge zone of the folds, where bedding curvature is greatest (GR2–CSL2), and decreases on the limbs of the structure away from the hinge. The Terzaghi correction was applied to the data from linear scanlines to calculate the true fracture density and normalized against densities from circular

window scanlines. The same analysis will be completed for fracture data collected at the remaining field sites to find dominant sets and calculate fracture properties.

Fracture data collected from east-central BC will be of vital significance to hydrocarbon exploration. Analyzing the fractures will aid in refining the tectonic history and calculating optimal drilling directions for reservoir units. Creating a regional fracture model for the area will lead to en-

hanced methods of recovery in addition to more efficient exploration techniques in this upper Paleozoic gas play.

The small-scale structures observed at Mountain Creek (Figure 12) are disharmonic folds that may have developed as leading-edge structures above a thrust that dies out beneath them. These folds are disharmonic because the lower unit (Mississippian package) is more susceptible to deformation than the overlying units.

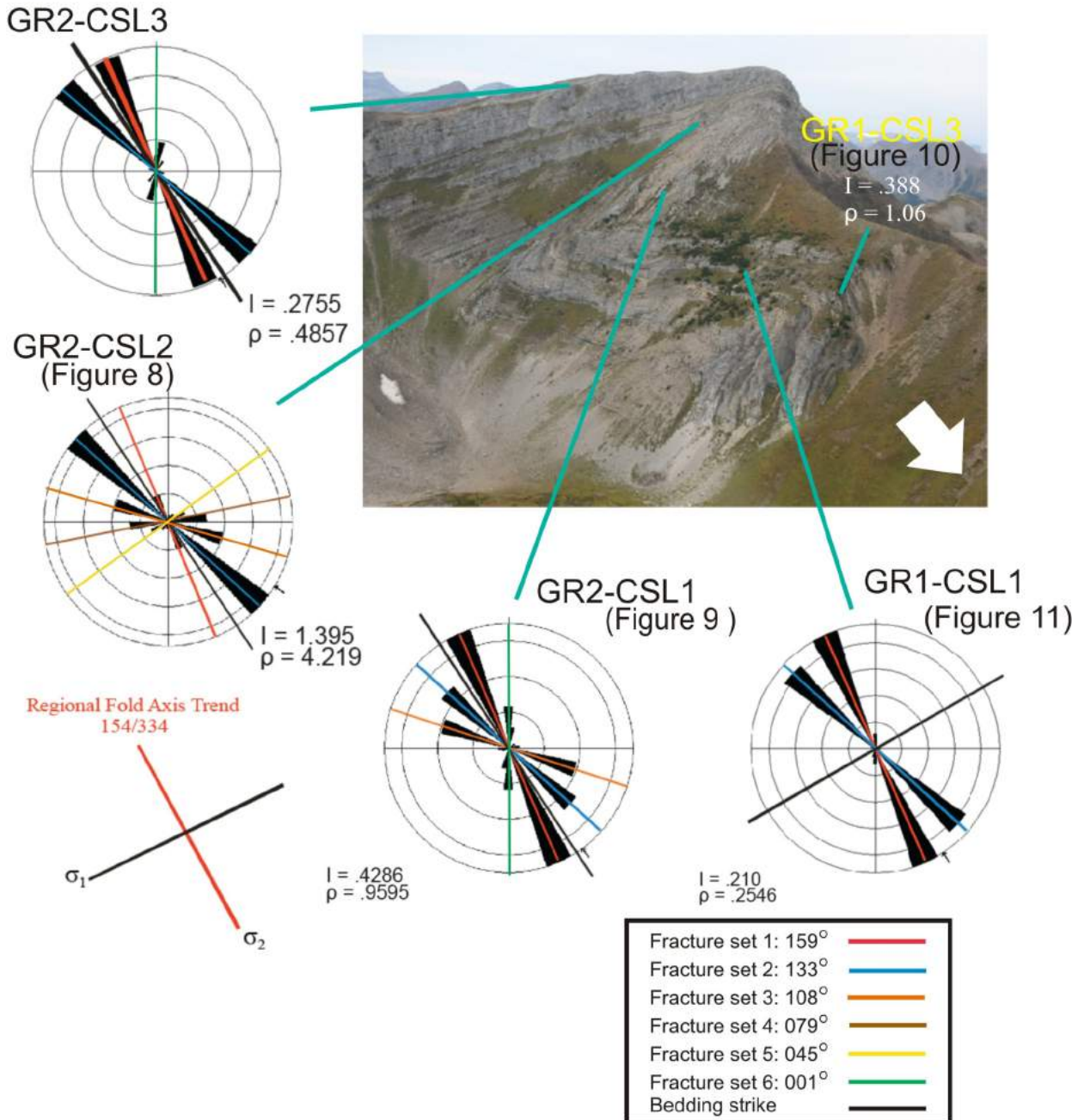


Figure 7. Ganoid Range, Sukunka-Kakwa area, east-central British Columbia: photograph of structure in the field area (white arrow points north), with orientations of linear scanline fractures and circular-window scanline calculated densities. Note the regional fold-axis trend of 154 and the principal stress direction of 064.

Tectonostratigraphic Implications for Petroleum Exploration

The Ksituan Member (Belloy Formation) in east-central BC has the greatest potential as a reservoir unit for this area because of the distribution of hydrocarbon-bearing lithofacies and structural traps (Fossenier, 2002). There are several major Pennsylvanian, Permian and Triassic gas fields (i.e., Brassey, Brazion, Bullmoose-Sukunka, Grizzly, Ojay) within the study area (Barss and Montandon, 1981; BC Oil and Gas Commission, 2001). Despite the size and quality of these reservoirs, it was believed until recently that much of the upper Paleozoic and Triassic interval in the study area was too ‘tight’ (i.e., too low in permeability) to allow economic production of hydrocarbons. Recent drilling, combined with the use of new technologies, has shown this to be incorrect. In the view of the authors, the complex nature of the stratigraphy and deformation, and the paucity of detailed geological studies in these intervals have delayed the discovery of new pools and hindered the accurate delineation of resources in discovered pools. Most of the study area is characterized by widely spaced wells and a paucity of available core.

A major problem for hydrocarbon exploration in Pennsylvanian, Permian and Lower Triassic strata in the Sukunka-Kakwa region is the absence of an existing integrated

lithostratigraphic and biostratigraphic framework. The study interval encompasses up to 500 m of stratigraphic section and spans approximately 75 million years (ca. 325–250 Ma) of Earth history. Regionally consistent unit subdivision and mapping are essential for effective hydrocarbon exploration. Preliminary studies have shown that optimum reservoir horizons occur in discrete chronostratigraphic units in the study interval (e.g., Moscovian for Ksituan Member). Throughout much of the study interval, these units are laterally inconsistent on a regional scale owing to numerous erosional unconformities and regional tectonism coeval with sediment accumulation. Thus, the production of an accurate, integrated chronostratigraphic-sequence stratigraphic framework for this succession is essential to develop effective exploration models for conventional and ‘tight gas’ resources.

Dolomitized shallow-water carbonate is the primary reservoir facies in the late Paleozoic (Pennsylvanian–Permian) and Belloy Formation, including the Ksituan Member. These units have proven to be highly important but exceptionally elusive reservoir successions in the Sukunka-Kakwa region. Major shifts in depositional setting and climate throughout the evolution of this succession signifi-

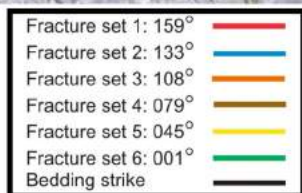
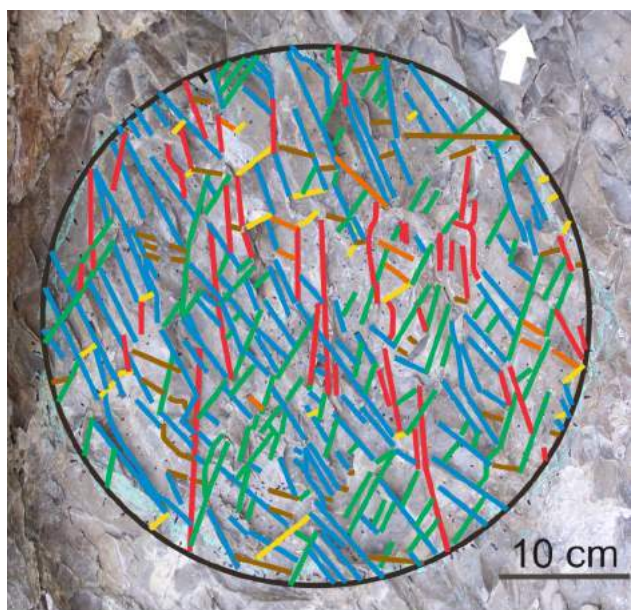


Figure 8. Ganoid Range, Sukunka-Kakwa area, east-central British Columbia: circular-window scanline 2-2 (GR2-CSL2), with fracture orientations; white arrow points north.

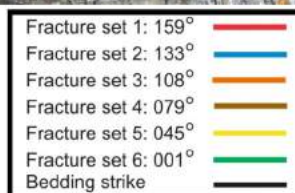


Figure 9. Ganoid Range, Sukunka-Kakwa area, east-central British Columbia: circular-window scanline 2-1 (GR2-CSL3), with fracture orientations; white arrow points north.

cantly complicate facies distribution. Furthermore, controls on dolomitization and other diagenetic changes are poorly constrained.

The Montney Formation represents a major shale-gas target in northeastern BC because it consists of very fine to fine-grained turbidite sandstone successions encased in organic-rich silty shale. Preliminary analyses, including conodont biostratigraphy, suggest that the turbidite facies are similar in age across the region. However, the age of the base of the Montney Formation varies regionally, probably because of onlap onto late Paleozoic highs; grain size also varies around these structures. This diachronism at the base of the Montney Formation will help in the mapping of late Paleozoic structures and may have some bearing on distribution of reservoir facies. Age differences between the underlying Permian section and the earliest Triassic, determined using strontium isotope analysis of conodonts, tied to the secular strontium isotope curve may provide insights into the degree of erosion and structural elevation of upper Paleozoic strata prior to Triassic deposition, and/or provide evidence of the influence of the Sukunka High on Early Triassic and even Middle Triassic (Caplan and Moslow, 1997) sedimentation.

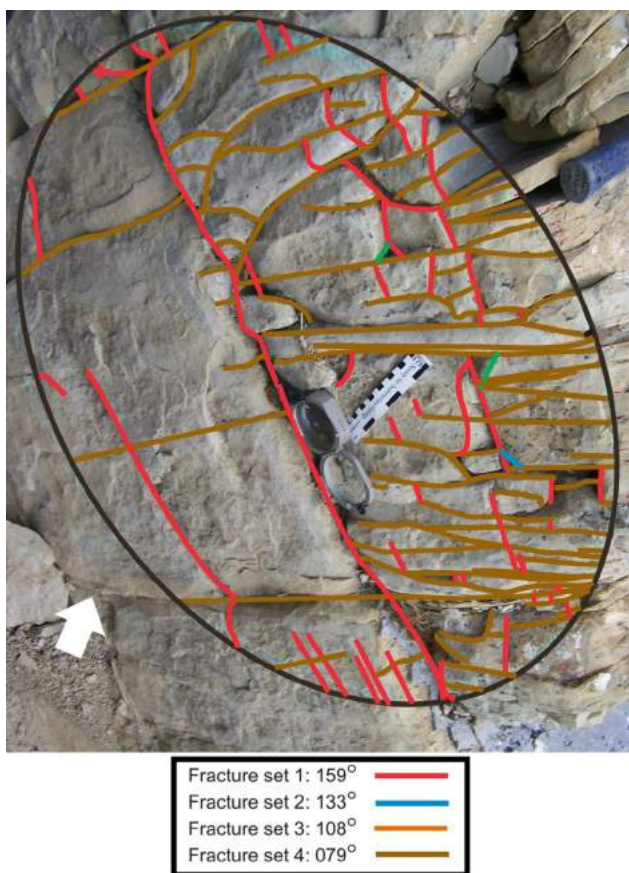


Figure 10. Ganoid Range, Sukunka-Kakwa area, east-central British Columbia: circular-window scanline 3 (GR2-CSL3), with fracture orientations (photo taken oblique to scanline); white arrow points north.

As Western Canada Sedimentary Basin exploration continues to mature, the focus of many hydrocarbon exploration companies will expand to encompass stratigraphic intervals with moderate to low porosity and microdarcy permeabilities. Ideally these horizons contain organic-rich rocks to provide the gas, and either coarser sedimentary rock types or sufficient fractures to provide reservoir- and flow-conduits. Identifying these characteristics, as this research continues, is the primary goal of the project.

Acknowledgments

The authors thank B. Beauchamp for reviewing the paper and Geoscience BC and Talisman Energy for financial support. Thanks also go to C. Stevens for his ArcGIS expertise. This project was also supported by a Natural Sciences and Engineering Research Council of Canada (NSERC) Discovery Grant to the senior author. Finally, Highland Helicopters of Chetwynd, BC is acknowledged for safe flying in August 2009.

References

- Bamber, E.W. and Macqueen, R.W. (1979): Upper Carboniferous and Permian stratigraphy of the Monkman Pass and southern Pine Pass areas, northeastern British Columbia; Geological Survey of Canada, Bulletin 301, 26 p.
- Barss, D.L. and Montandon, F.A. (1981): Sukunka-Bullmoose gas fields: models for a developing trend in the southern Foothills of northeast British Columbia; Bulletin of Canadian Petroleum Geology, v. 29, p. 293–333.
- Bird, T.D., Barclay, J.E., Campbell, R.I. and Lee, P.J. (1994): Triassic gas resources of the Western Canada Sedimentary Basin; Geological Survey of Canada, Bulletin 483, 96 p.

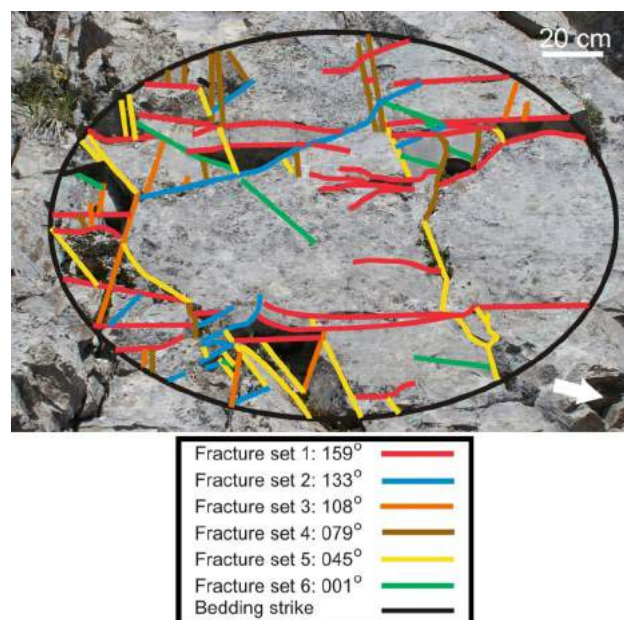


Figure 11. Ganoid Range, Sukunka-Kakwa area, east-central British Columbia: circular-window scanline 1 (GR1-CSL1), with fracture orientations; white arrow points north.

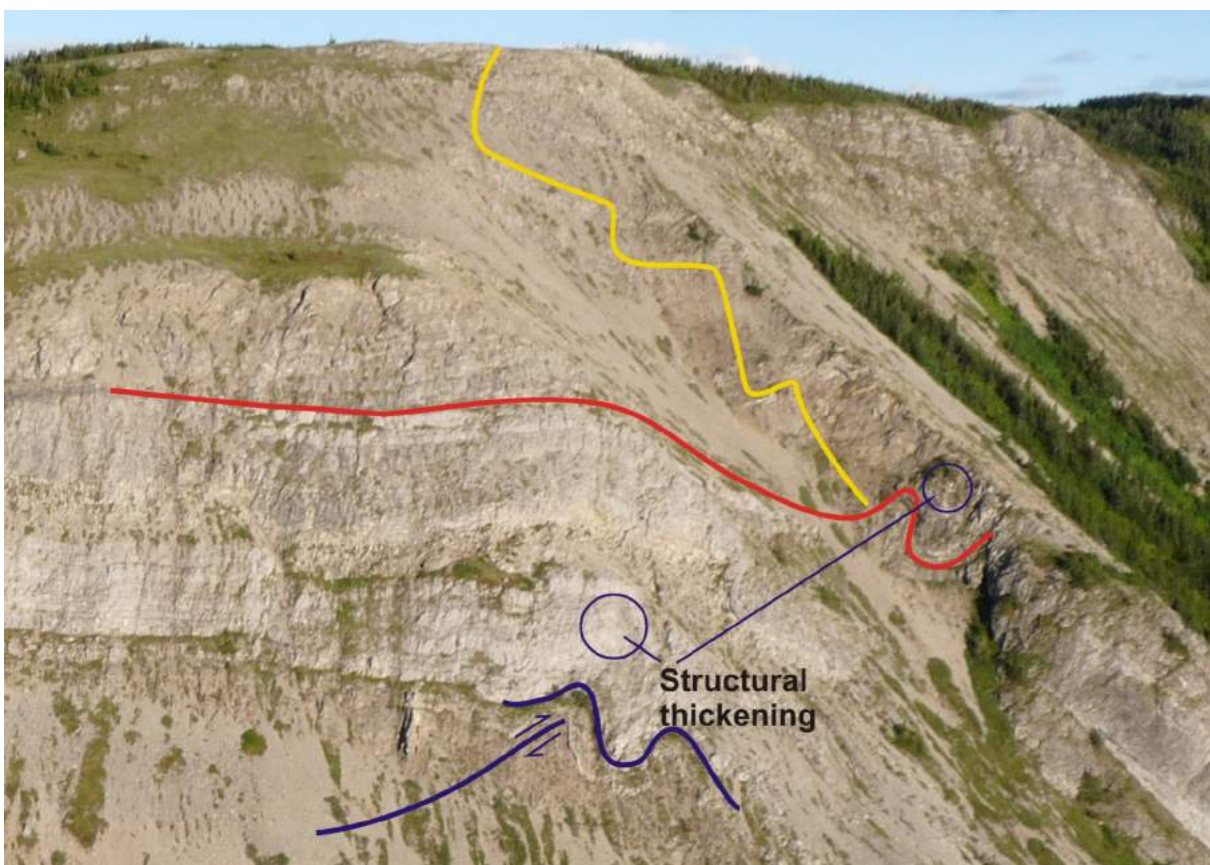


Figure 12. Small-scale disharmonic folding in the Mississippian at the Mountain Creek section, Sukunka-Kakwa area, east-central British Columbia. Red line represents approximate top of Mississippian. Purple lines depict structural features. Yellow line represents approximate line of section for the Hanington and Belcourt formations; jogs in the line of section are near cycle boundaries in the succession. Most of the Pennsylvanian and Permian succession does not display any folding.

- BC Oil and Gas Commission Engineering and Geology (2001): Hydrocarbon and by-product reserves in British Columbia 2001; BC Oil and Gas Commission, Engineering and Geology, 435 p.
- Caplan, M.C. and Moslow, T.F. (1997): Tectonic controls on preservation of Middle Triassic Halfway reservoir facies, Peejay Field, northeastern British Columbia: a new hydrocarbon exploration model; *in* Triassic of the Western Canada Sedimentary Basin, T.F. Moslow and J. Wittenberg (ed.), Bulletin of Canadian Petroleum Geology, v. 45, p. 595–614.
- Davies, G.R. (1997): The Triassic of the Western Canada Sedimentary Basin: tectonic and stratigraphic framework, paleogeography, paleoclimate and biota; *in* Triassic of the Western Canada Sedimentary Basin, T.F. Moslow and J. Wittenberg (ed.), Bulletin of Canadian Petroleum Geology, v. 45, p. 434–460.
- Dershowitz, W.S. and Einstein H.H. (1988): Characterizing rock joint geometry with joint systems models; *Rock Mechanics and Rock Engineering*, v. 21, p. 21–51.
- Dunn, L.A. (2003): Sequence biostratigraphy and depositional modeling of the Pennsylvanian to Permian Belloy Formation, northwest Alberta and northeast British Columbia; Ph.D. thesis, University of Calgary, 212 p.
- Feltham, G.R. (2005): Fold-related fractured reservoir analysis of the Pennsylvanian Ksituan Member of the Belloy Formation, Monkman Pass, northeastern British Columbia: optimal drilling directions determined from image log and outcrop studies; M.Sc. thesis, University of Calgary, 183 p.
- Fossenier, K. (2002): Stratigraphic framework of the Pennsylvanian to Permian Belloy Formation in the Peace River Embayment of northeastern British Columbia: a multi-disciplinary approach; M.Sc. thesis, University of Calgary, 292 p.
- Henderson, C.M., Richards, B.C. and Barclay, J.E. (1994): Permian strata of the Western Canada Sedimentary Basin; *in* Geological Atlas of the Western Canada Sedimentary Basin, G.D. Mossop and I. Shetsen (comp.), Canadian Society of Petroleum Geologists and Alberta Research Council, Special Report 4, pages 251–258, URL <http://www.ags.gov.ab.ca/publications/wcsb_atlas/atlas.html> [November 2009].
- Henderson, C.M., Dunn, L., Fossenier, K. and Moore, D. (2002): Sequence biostratigraphy and paleogeography of the Pennsylvanian–Permian Belloy Formation and outcrop equivalents in Western Canada; *in* Carboniferous and Permian of the World, L.V. Hills, C.M. Henderson and E.W. Bamber (ed.), Canadian Society of Petroleum Geologists, Memoir 19, p. 934–947.
- Henderson, C.M., Schmitz, M., Crowley, J. and Davydov, V. (2009): Evolution and geochronology of the *Sweetognathus* lineage from Bolivia and the Urals of Russia: biostratigraphic problems and implications for Global Stratotype Section and Point (GSSP) definition; *in* Permophiles 53,

- Supplement 1, abstracts of the International Conodont Symposium, C. Henderson and C. MacLean (ed.), p. 20–21.
- Higgins, A.C., Richards, B.C. and Henderson C.M. (1991): Conodont biostratigraphy and paleoecology of the uppermost Devonian and Carboniferous of the Western Canada Sedimentary Basin; *in* Ordovician to Triassic Conodont Paleontology of the Canadian Cordillera, M.J. Orchard and A.D. McCracken (ed.), Geological Survey of Canada, Bulletin 417, p. 215–251.
- Mauldon, M., Dunne, W.M. and Rohrbaugh, M.B. (2001): Circular scanlines and circular windows: new tools for characterizing the geometry of fracture traces; *Journal of Structural Geology*, v. 23, p. 247–258.
- National Energy Board (2006): Northeast British Columbia's ultimate potential for conventional natural gas; National Energy Board Report 2006-A, produced in co-operation with BC Ministry of Energy Mines and Petroleum Resources.
- Nelson, J.L., Colpron, M., Piercy, S.J., Dusel-Bacon, C., Murphy, D.C. and Roots, C.F. (2006): Paleozoic tectonic and metallogenetic evolution of pericratonic terranes in Yukon, northern British Columbia, and eastern Alaska; *in* Paleozoic Evolution and Metallogeny of Pericratonic Terranes at the Ancient Pacific Margin of North America, M. Colpron and J.L. Nelson (ed.), Geological Association of Canada, Special Paper 45, p. 323–360.
- Orchard, M.J. (2006): Late Paleozoic and Triassic conodont faunas of Yukon Territory and northern British Columbia and implications for the evolution of the Yukon-Tanana terrane; *in* Paleozoic Evolution and Metallogeny of Pericratonic Terranes at the Ancient Pacific Margin of North America, Canadian and Alaskan Cordillera; M. Colpron and J.L. Nelson (ed.), Geological Association of Canada, Special Paper 45, p. 229–260.
- Richards, B.C. (1989): Upper Kaskaskia Sequence: uppermost Devonian and Lower Carboniferous; *in* Western Canada Basin, a Case History, B.C. Ricketts (ed.), Canadian Society of Petroleum Geologists, p. 165–201.
- Richards, B.C., Barclay, J.E., Bryan, D., Hartling, A., Henderson, C.M. and Hinds, R.C. (1994): Carboniferous strata of the Western Canada Sedimentary Basin; *in* Geological Atlas of the Western Canada Sedimentary Basin, G.D. Mossop and I. Shetsen (comp.), Canadian Society of Petroleum Geologists and Alberta Research Council, Special Report 4, p. 221–250.
- Snyder, W.S., Trexler, J.H., Jr., Davydov, V.I., Cashman, P., Schiappa, T.A. and Sweet, D. (2002): Upper Paleozoic tectonostratigraphic framework for the western margin of North America; American Association of Petroleum Geologists (AAPG), Tulsa, Hedberg Research Conference, 4 p.
- Trexler, J.H., Jr., Cashman, P.H., Snyder, W.S. and Davydov, V.I. (2004): Late Paleozoic tectonism in Nevada: timing, kinematics, and tectonic significance; *Geological Society of America Bulletin*, v. 16, no. 5–6, p. 525–538.